



Water Environment Research Foundation
Collaboration. Innovation. Results.

Decentralized Systems



**FINAL
REPORT**

Quantitative Tools to Determine the Expected Performance of Wastewater Soil Treatment Units

GUIDANCE MANUAL

Co-published by



DEC1R06a

QUANTITATIVE TOOLS TO DETERMINE THE EXPECTED PERFORMANCE OF WASTEWATER SOIL TREATMENT UNITS

GUIDANCE MANUAL

by:

**John McCray
Mengistu Geza
Kathryn Lowe
Maria Tucholke
Assaf Wunsch
Sarah Roberts
Jörg Drewes**

Colorado School of Mines

**Jose Amador
Janet Atoyan
David Kalen
George Loomis
Thomas Boving**

University of Rhode Island

David Radcliffe
University of Georgia

2010



The Water Environment Research Foundation, a not-for-profit organization, funds and manages water quality research for its subscribers through a diverse public-private partnership between municipal utilities, corporations, academia, industry, and the federal government. WERF subscribers include municipal and regional water and wastewater utilities, industrial corporations, environmental engineering firms, and others that share a commitment to cost-effective water quality solutions. WERF is dedicated to advancing science and technology addressing water quality issues as they impact water resources, the atmosphere, the lands, and quality of life.

For more information, contact:
Water Environment Research Foundation
635 Slaters Lane, Suite G-110
Alexandria, VA 22314-1177
Tel: (571) 384-2100
Fax: (703) 299-0742
www.werf.org
werf@werf.org

This report was co-published by the following organization.

IWA Publishing
Alliance House, 12 Caxton Street
London SW1H 0QS, United Kingdom
Tel: +44 (0) 20 7654 5500
Fax: +44 (0) 20 7654 5555
www.iwapublishing.com
publications@iwap.co.uk

© Copyright 2010 by the Water Environment Research Foundation. All rights reserved. Permission to copy must be obtained from the Water Environment Research Foundation.

Library of Congress Catalog Card Number: 2010921681

Printed in the United States of America

IWAP ISBN: 978-1-84339-395-5/1-84339-395-6

This report was prepared by the organization(s) named below as an account of work sponsored by the Water Environment Research Foundation (WERF). Neither WERF, members of WERF, the organization(s) named below, nor any person acting on their behalf: (a) makes any warranty, express or implied, with respect to the use of any information, apparatus, method, or process disclosed in this report or that such use may not infringe on privately owned rights; or (b) assumes any liabilities with respect to the use of, or for damages resulting from the use of, any information, apparatus, method, or process disclosed in this report.

Colorado School of Mines

The research on which this report is based was developed, in part, by the United States Environmental Protection Agency (EPA) through Cooperative Agreement No. X-83085101-0 with the Water Environment Research Foundation (WERF). However, the views expressed in this document are not necessarily those of the EPA and EPA does not endorse any products or commercial services mentioned in this publication. This report is a publication of WERF, not EPA. Funds awarded under the Cooperative Agreement cited above were not used for editorial services, reproduction, printing, or distribution.

This document was reviewed by a panel of independent experts selected by WERF. Mention of trade names or commercial products or services does not constitute endorsement or recommendations for use. Similarly, omission of products or trade names indicates nothing concerning WERF's or EPA's positions regarding product effectiveness or applicability.

ACKNOWLEDGMENTS

This research was funded by the Water Environment Research Foundation.

Project Team

Principal Investigator:

John McCray, Ph.D.
Colorado School of Mines

Co-Principal Investigators:

Jörg Drewes, Ph.D.
Mengistu Geza, Ph.D.
Kathryn Lowe
Colorado School of Mines

Project Team:

Sarah Roberts
Maria Tucholke
Assaf Wunsch
Colorado School of Mines

David Radcliffe, Ph.D.
Ken Bradshaw
University of Georgia

Thomas Boving, Ph.D.
Jose Amador, Ph.D.
Janet Atoyan, Ph.D.
David Kalen
George Loomis
University of Rhode Island

Issue Area Team

Steven Berkowitz
North Carolina Department of Environment & Natural Resources

Matt Byers, Ph.D.
Zoeller Company

Bob Freeman, P.E.
U.S. Environmental Protection Agency

Anish Jantrania, Ph.D., P.E.
NCS Wastewater Solutions

Charles McEntyre, P.E., CHMM
Tennessee Valley Authority

Eberhard Roeder, Ph.D.
Florida Department of Health

Robert Rubin, Ed.D.
McKim Creed

Edwin Swanson, P.E.
Arizona Dept. of Environmental Quality

George Tchobanoglous, Ph.D.
Tchobanoglous Consulting

Water Environment Research Foundation Staff

Director of Research:	Daniel M. Woltering, Ph.D.
Senior Program Director:	Amit Pramanik, Ph.D., BCEEM

ABSTRACT AND BENEFITS

Abstract:

Onsite wastewater treatment systems (OWTS) are an important part of water management infrastructure in the United States. Thus, proper OWTS selection, design, installation, operation and management are essential. To aid this life-cycle, a toolkit was developed to enable evaluation and design of expected STU performance. The toolkit is comprised of this Guidance Manual, a companion Toolkit User's Guide, individual tools, and supplemental information. This framework provides detailed information to less experienced user's while enabling more experienced users to start directly with STUMOD or other tool implementation referring to limited sections of the Guidance Manual or User's Guide.

The toolkit was developed for a wide range of users faced with different needs of varying complexity when evaluating treatment of nitrogen, microbial pollutants (bacteria and virus), and organic wastewater contaminants (OWCs). Progressing through simple to more complex tools ultimately guides the user to the simplest tool that is appropriate, but discourages using a tool that is too simple for the decision at hand. The simplest tools include look-up tables and cumulative frequency distributions (CFDs) to direct the user to available pertinent information. Nomographs enable initial screening and quick insight into expected nitrogen removal based on the predicted output from STUMOD. Cumulative probability graphs illustrate modeling results in a risk-based framework while numerical model simulations demonstrate the usefulness of complex tools. Finally, two spreadsheet tools were developed, N-CALC and STUMOD, allowing the user to evaluate a range of STU operating conditions, soil hydraulics, and/or treatment parameters, as well as the relative influence of these factors on performance.

Benefits:

- ◆ Provides an explanation of soil treatment processes for design-of-performance based onsite wastewater treatment systems.
- ◆ Tools in the toolkit were developed with a basis in rigorous experimental data.
- ◆ Toolkit is hierarchical in nature and diverse with regard to breadth of tools provided.
- ◆ Uses decision diagrams to illustrate the frequent steps incurred during the STU design and guides the user to appropriate tools and input parameter selection.
- ◆ Provides tools within the toolkit that incorporate a risk-based approach to evaluate the uncertainty in STU performance compared to treatment goals.
- ◆ Provides hundreds of visual-graphic tools (nomographs, cumulative probability graphs, and scenario illustrations).
- ◆ Provides STUMOD and N-CALC as Microsoft™ Excel files.

Keywords: Soil treatment unit, onsite wastewater design, treatment, and performance.

TABLE OF CONTENTS

Acknowledgements.....	iii
Abstract and Benefits.....	v
List of Tables.....	viii
List of Figures.....	ix
List of Acronyms.....	xi
Executive Summary.....	ES-1
1.0 Introduction.....	1-1
1.1 Background and Motivation.....	1-1
1.2 Project Objectives and Approach.....	1-2
1.3 Using This Guidance Manual and Toolkit.....	1-3
1.3.1 Toolkit Components.....	1-3
1.3.2 Using Tools for Decision Making.....	1-4
1.3.3 Guidance Manual Organization.....	1-6
2.0 Tool Description.....	2-1
2.1 Tool Development.....	2-3
2.2 Tool Description.....	2-4
2.2.1 Spreadsheet Tools.....	2-4
2.2.1.1 N-CALC.....	2-4
2.2.1.2 STUMOD.....	2-5
2.2.2 Visual Graphic Tools.....	2-7
2.2.2.1 Look-Up Tables.....	2-7
2.2.2.2 Cumulative Frequency Distribution Diagrams.....	2-8
2.2.2.3 Nomographs.....	2-9
2.2.2.4 Model Output (Scenario) Illustrations using HYDRUS.....	2-12
2.2.3 Supplemental Information.....	2-14
2.2.3.1 Decision Protocol.....	2-15
2.2.3.2 Literature Review.....	2-15
2.2.3.3 Laboratory and Field Experimental Results.....	2-16
2.2.3.4 Other Materials.....	2-16
3.0 STU Design and Tool Implementation.....	3-1
3.1 Conceptual Design.....	3-2
3.1.1 Identify Objectives and Treatment Goals.....	3-3
3.1.2 Analyze Existing Information.....	3-3
3.1.3 Make Informed Assumptions.....	3-3
3.2 Delineate Operational Conditions.....	3-6
3.2.1 Assess Soil Characteristics.....	3-6
3.2.2 Assess Effluent Characteristics.....	3-8
3.2.3 Assess Daily Flow.....	3-12
3.2.4 Assess Soil Hydraulic Loading Rate and Application Method.....	3-12
3.3 Delineate Parameters Affecting Treatment.....	3-13
3.3.1 Parameters Affecting Nitrogen Attenuation.....	3-14

3.3.2	Parameters Affecting Microorganism Attenuation	3-15
3.3.3	Parameters Affecting Organic Wastewater Contaminant Attenuation ..	3-17
3.4	Guidance for Tool Selection and Use	3-19
3.4.1	Hypothetical Example 1: Conventional STU Performance	3-19
3.4.2	Hypothetical Example 2: Nitrified Effluent with Low Available Carbon	3-26
3.4.3	Hypothetical Example 3: Estimating STU Mass Loading	3-31
3.4.4	Hypothetical Example 4: Up-scaling STU Density	3-34
3.4.5	Hypothetical Example 5: Qualitative Scenario Comparison	3-37
4.0	Summary	4-1
	References	R-1
Supplemental Files		
	Toolkit User's Guide	
	Visual-Graphic Tools	
	N-CALC	
	STUMOD	
	Literature Review	

LIST OF TABLES

1-1	Type and Complexity of Tools	1-5
2-1	Diversity of Tools Developed.....	2-2
2-2	Example of Look-Up Table Illustrating Factors Influencing Ammonium Sorption	2-8
3-1	OWC Groups and Examples of Common Contaminants	3-12
3-2	Summary of STUMOD Outputs for Different Initial Ammonium-nitrogen Concentrations	3-26
3-3	Summary of STUMOD Output for HLRs shown in Figure 3-26	3-32
3-4	Nitrogen Mass Loading Estimates for Example #3	3-33
3-5	Comparison of Scenario Simulation Outputs for Estimated “Equivalent” Design.....	3-43

LIST OF FIGURES

1-1	Toolkit Framework for STU Performance.....	1-7
2-1	Illustration of N-CALC User Interface Showing Inputs and Outputs for Clay Soil.....	2-5
2-2	Illustration of STUMOD User Interface Showing Default Input and Outputs for Clay Soils.....	2-6
2-3	Example CFD Illustrating cBOD ₅ Concentrations in STE.....	2-9
2-4	Nomograph Illustrating Fraction of Nitrogen Remaining with Depth in Different Temperature Regions.....	2-10
2-5	Nomograph of Percent Nitrogen Removal at 60 cm Depth in Four Different Temperature Regions due to Different Effluent Concentrations.....	2-11
2-6	Example Cumulative Probability Graph of Monte Carlo Simulation for Three Different Soil Depths.....	2-12
2-7	Description of the Scenario Output for Trench System Simulations.....	2-13
2-8	Description of the Scenario Output for Drip System Simulations.....	2-14
3-1	Conceptual Design Decision Diagram.....	3-2
3-2	Making Informed Assumptions to Reduce Uncertainty Decision Diagram.....	3-5
3-3	Delineate Operational Conditions Decision Diagram.....	3-6
3-4	Assess Soil Characteristics Decision Diagram.....	3-7
3-5	Assess Effluent Characteristics Decision Diagram.....	3-10
3-6	Assess Effluent Characteristics for Nitrogen Reduction Decision Diagram.....	3-11
3-7	Assess Nitrogen Attenuation Decision Diagram.....	3-14
3-8	Assess Microorganism Removal/Inactivation Decision Diagram.....	3-17
3-9	Assess OWC Attenuation Decision Diagram.....	3-18
3-10	Nomograph Most Closely Illustrating Example 1 Conditions.....	3-20
3-11	Monte Carlo Cumulative Probability Graph for Three Different Soil Depths for Example 1 Conditions.....	3-21
3-12	STUMOD Output Graph Illustrating Nitrogen Concentrations Assuming Example 1 Initial Conditions.....	3-22
3-13	STUMOD Output Graph Illustrating the Fraction of Nitrogen Remaining in the STU Assuming Example 1 Initial Conditions.....	3-23
3-14	STUMOD Output Graph Illustrating Nitrogen Concentrations for Example 1 at a HLR of 1 cm d ⁻¹	3-24
3-15	STUMOD Output Graph Illustrating the Fraction of Nitrogen Removed for Example 1 at a HLR of 1 cm d ⁻¹	3-24
3-16	STUMOD Output Graph Illustrating Nitrogen Concentrations for Example 1 at a Soil Depth of 120 cm.....	3-25
3-17	STUMOD Output Graph Illustrating the Fraction of Nitrogen Removed for Example 1 at a Soil Depth of 120 cm.....	3-25
3-18	STUMOD Output for Example 2 Initial Conditions.....	3-27
3-19	STUMOD Output for Example 2 Assuming Advanced Treatment Prior to the STU ...	3-27
3-20	STUMOD User Input Interface for Example 2.....	3-28
3-21	STUMOD Output for Example 2 Assuming Conditions Illustrated in Figure 3-20.....	3-29
3-22	CFD of Denitrification Rates Assimilated from the Literature.....	3-29

3-23	Comparison of Cumulative Probability Graph to Evaluate Uncertainty for Example 2 STUMOD Outputs	3-30
3-24	STUMOD Output for Mass Flux of Nitrogen for Example #3.....	3-31
3-25	Graph Illustrating the Mass Flux of Nitrogen for Different HLRs with Depth Below the Trench	3-32
3-26	Determination of Media per Capita Water Use	3-33
3-27	Nitrogen Mass Flux Comparisons	3-35
3-28	Comparison of Nitrogen Mass Flux at Different HLRs.....	3-36
3-29	Comparison of Nitrogen Mass Flux from Six Homes to Equal Distribution Over a Given Area	3-37
3-30	Example Comparison of Trench System Scenario Outputs.....	3-38
3-31	Example Comparison of Drip System Scenario Outputs.....	3-39
3-32	Example Trench and Drip Comparison of Equivalent Mass	3-40
3-33	Illustration of Comparable Scenario “Footprints”	3-41
3-34	Mass Flux Response to Plant Uptake.....	3-44
3-35	Total Nitrogen Mass Flux as Affected by Rain Events	3-44

LIST OF ACRONYMS

BOD	biochemical oxygen demand
BOD ₅	biochemical oxygen demand, five-day test
C	carbon
CaCO ₃	calcium carbonate
CFD	cumulative frequency distribution
CO ₂	carbon dioxide
CSM	Colorado School of Mines
CW2D	Constructed Wetlands 2D model
HLR	hydraulic loading rate
N	nitrogen
N ₂	dinitrogen gas
N-CALC	Nitrogen Calculator (spreadsheet tool)
NRCS	Natural Resources Conservation Service
OWC	organic wastewater contaminants
OWTS	onsite wastewater treatment systems
SSURGO	Soil Survey Geographic
STATSGO	State Soil Geographic (soil database)
STE	septic tank effluent
STU	soil treatment unit
STUMOD	Soil Treatment Model (spreadsheet tool)
TMDL	total maximum daily load
UCR	University of California at Riverside
UGA	University of Georgia
URI	University of Rhode Island
USDA	United States Department of Agriculture
U.S. EPA	United States Environmental Protection Agency
USGS	United States Geological Survey
WERF	Water Environment Research Foundation

EXECUTIVE SUMMARY

Onsite wastewater treatment systems (OWTS) are an important part of water management infrastructure in the United States. Thus, proper OWTS selection, design, installation, operation and management are essential. While these systems vary widely in their design and implementation, the most prevalent type of system is a conventional OWTS that utilizes the soil for wastewater constituent treatment, hydraulic capacity, and eventually recharge to water resources. The soil treatment unit (STU) within an OWTS provides an effective and sustainable means for wastewater reclamation, but occasional water quality degradation has been experienced. While there is considerable concern about potential water quality degradation associated with OWTS, current permitting and design focus remains primarily on ensuring that hydraulic loading is not excessive. Furthermore, the lack of available simple tools for assessing the performance of the STU has limited assessment of treatment performance during OWTS design based on scientific principles.

The overall goal of this project was to provide a toolkit to assess STU performance. This toolkit enables evaluation and design of expected STU performance for important wastewater constituents over a relevant range of OWTS operating conditions. The toolkit was developed for a wide range of users faced with different needs of varying complexity. Within the toolkit framework, specific objectives were to:

- 1) identify the current best practices and tools utilized in STU design and performance,
- 2) develop and test tools to aid system designers and decision-makers assess the expected STU performance, and
- 3) provide decision diagrams (protocol) for selection and use of the different tools.

The first objective above was addressed in a comprehensive literature review submitted as a separate WERF report (McCray et al., 2009). To achieve the second objective, results from the literature review were combined with laboratory and field experimentation for development of simple tools that are based on known scientific principles. Finally, to aid the user during performance based STU design and treatment performance, a protocol consisting of flow charts and decision steps was prepared. This project was completed by a multi-university team from the Colorado School of Mines (CSM), the University of Rhode Island (URI), the University of Georgia (UGA), and the University of California at Riverside (UCR).

The toolkit was designed to evaluate treatment of nitrogen, microorganisms (bacteria and virus), and organic wastewater contaminants (OWCs). These pollutants are currently of primary concern, or are projected to be of high concern, to nearly every county and state in the United States. While phosphorus is of concern in some cases (e.g., shallow ground water in the vicinity of small lakes or sensitive waterways), in general soils have a high affinity for phosphorus attenuation via chemical-precipitation mechanisms and the available literature and relevant data was relatively sparse. Thus efforts were focused on developing the most effective tools possible for nitrogen, bacteria and virus, and OWCs. The literature review on phosphorus treatment and modeling, however, is a useful tool for OWTS professionals on its own merits.

The toolkit is hierarchical in nature and includes tools that are diverse with regard to their ability to incorporate complexity, user sophistication, and appropriateness for use. The complexity of the tools in the toolkit depends on the following considerations:

- ◆ relative importance of the pollutant of interest in the practical and regulatory arena,
- ◆ availability of existing data from which to build a solid theoretical foundation of the treatment processes,
- ◆ degree of complexity that is intended to be included in the problem analysis, and
- ◆ sophistication, technical resources, and treatment goals of the user.

Ideally, the simplest tools are the first to be used. These tools are best used as screening tools to decide if further action is needed and require little user sophistication, but cannot incorporate many of the complexities associated with different OWTS sites or pollutant treatment processes (see additional discussion related to existing models in the supplemental Literature Review). Examples of these tools include charts or tables that direct the user to the general best practice to optimize treatment for certain pollutants, simple spreadsheet solutions that predict concentrations at depth but that do not incorporate many of the important complexities associated with OWTS treatment processes, or written materials that describe a process or set of experimental results that lend insight to pollutant treatment. Such simple tools may not be appropriate for decision making, particularly if the health, regulatory, or legal risks associated with the decision are high. The tools developed for OWCs are less sophisticated and not as quantitative as the tools developed for nitrogen. Intermediate to nitrogen and OWCs are microbial pollutants. Bacteria and virus are important regulated pollutants, but the available data regarding treatment in OWTS or other similar systems is relatively sparse, and the processes associated with transformation and soil transport are very complex. Thus, it was not possible to develop tools that could rigorously incorporate the uncertainty of important processes.

The diversity in the toolkit depends on the pollutant of interest, primarily due to the information available related to treatment of that pollutant. A highly diverse toolkit is provided for nitrogen because considerable data are available, it is often the most important OWTS pollutant in the regulatory arena, and treatment considerations in OTWS designs are usually intended to mitigate nitrogen release. Conversely, little diversity is provided in the toolkit for important OWCs because there is very little data available, the fundamental understanding of OWC treatment processes is in the early stages, and most OWCs are not regulated. Again relative to nitrogen and OWCs, the diversity of the tools for microbial pollutants are intermediate consisting of generalized recommendations as well as diagrams developed from complex numerical models that depict treatment effectiveness for various relevant scenarios.

The components of the toolkit are:

- ◆ Guidance Manual
 - discussion of tools and their use
 - decision diagrams for tool selection and performance design
- ◆ User's Guide
 - assumptions and governing principles
 - tool and model development

- parameter selection
 - look-up tables
 - cumulative frequency distributions (CFDs) of important treatment parameters
- laboratory and field experimental results
- ◆ Tools
 - visual-graphic illustrations of expected soil treatment
 - N-CALC (Nitrogen Calculator)
 - STUMOD (Soil Treatment Unit Model)
- ◆ Supplemental Information
 - literature review
 - outreach materials

Spreadsheet tools enable estimation of treatment for user-specified conditions, but are presented in a simple-to-use format that does not require prior modeling knowledge or lengthy model run times. Of course, achieving these advantages requires that the incorporated treatment processes and operating conditions are simplified. Two spreadsheet tools were developed: N-CALC and STUMOD. Both of these spreadsheet tools allow the user to evaluate a range of STU operating conditions, soil hydraulics, and/or treatment parameters, as well as the relative influence of these factors on performance (i.e., determine which parameters are expected to exert the greatest influence on STU performance).

N-CALC (Nitrogen Calculator) can be used to investigate steady-state treatment effectiveness based on soil type (i.e., long-term performance for a relatively mature system). N-CALC accounts for removal processes such as adsorption, nitrification and denitrification and is intended as a screening level tool that can be used where input data is limited or as an initial step to determine the impacts from OWTS under worst-case scenarios (no mixing or attenuation). It can be used with minimal technical expertise, and may also be helpful as a field calculator, although it is not theoretically appropriate for shallow water tables and does not include a biozone or account for soil layering in the subsurface. Thus, N-CALC could be used to determine whether more resources should be devoted to data gathering or implementation of a more rigorous model such as STUMOD or HYDRUS.

STUMOD (Soil Treatment Unit Model) is relatively simple to use for personnel trained in the natural sciences or engineering, and is also rigorous enough to include most relevant hydraulic and nitrogen-transformation processes. STUMOD was developed based on existing fundamental principles of water movement and contaminant transport. An analytical solution is used to calculate profile of pressure and moisture content in the unsaturated STU. The chemical transport component is based on simplification of the general advection dispersion equation, which is based on chemical mass-balance. STUMOD is not theoretically appropriate for shallow water tables and does not explicitly account for any soil layering in the subsurface. The model requires a significant level of user sophistication with regard to using the appropriate input parameters. Because the sophistication of STUMOD may preclude many practitioners from using it, hundreds of visual-graphic illustrations of treatment for a variety of conditions relevant to OWTS were developed.

STUMOD could also be used for other OWTS pollutants. However, sufficient information was not available in the literature to provide detailed guidance on model development for either phosphorus or OWCs. STUMOD may become increasingly useful as additional research into quantitative assessments of removal for these constituents become available. This is particularly true of OWCs, because degradation of these compounds also depend on the aeration (i.e., water content) in the STU. With regard to microbial pollutants, a considerable variety of tools for virus transport in aquifers is already available from the U.S. EPA models website. While bacterial removal is less effective, simple tool development does not enable inclusion of the fundamental processes necessary to adequately quantify bacterial transport.

Visual-graphic tools provide an indication of whether treatment goals are likely or unlikely to be met for specific technical assumptions, site conditions, and OWTS operating factors. Three types of visual-graphic tools are included in the toolkit: nomographs, cumulative probability graphs, and scenario illustrations. Nomographs provide insight into the range of STU performance that can be expected for a given set of conditions. Cumulative probability graphs illustrate the likely range of treatment outcomes and the probability associated with any particular treatment effectiveness, or provides an understanding of key parameter variability based on reported values. These cumulative probability graphs help planners and regulators make decisions based on their willingness to accept an agreed-upon level of quantified risk. Scenario illustrations are based on selected HYDRUS-2D model simulations of different OWTS scenarios to visually demonstrate the usefulness of such a numerical model while showing the impacts of different scenarios on subsurface nitrogen concentrations, spatial treatment distributions, and mass-flux below a specified boundary.

For all of the visual-graphic illustrations, treatment information provided by these tools is based on data generated by numerical models that can incorporate complex and robust treatment and operating conditions. Because the choices for representative OWTS conditions are limited, the user must decide how their OWTS system fits within the limited treatment estimations displayed by the graphics. As the complexity of the STU increases, a numerical model such as HYDRUS-2D, should be used because it can incorporate any level of sophistication regarding subsurface heterogeneity, trench geometry, large multiple-trench systems, drip systems, water table position, or climate.

Look-up tables or charts and CFDs are also visual-graphic tools that aid users in selecting appropriate parameters for specific conditions or numerical modeling (i.e., denitrification rate in HYDRUS). CFDs are based on statistical evaluation of actual OWTS data from the literature or laboratory data.

All tools were developed with a basis in rigorous scientific understanding building from the current knowledge as presented in the literature supplemented with numerical modeling. The literature review uncovered some critically important aspects of the nitrogen transformation process that are not included in any existing numerical model capable of simulating a range of OWTS conditions. Thus, HYDRUS-2D was modified to include the important effects of temperature and the impact of aeration (via moisture content) on nitrogen transformations. This modified version of HYDRUS-2d is not currently available to the public, but may be available in the future (<http://www.pc-progress.com/en/Default.aspx?hydrus-3d>). In addition, the CW2D model, which has a wide range of complex biochemical processes for nitrogen transformation and is utilized by the most sophisticated modeler, was evaluated. While the CW2D model accurately predicted water movement and pressure heads, it underestimated nitrate

concentrations in the soil. Thus, HYDRUS-2D was used for numerical modeling conducted in support of tool development.

During tool development, laboratory and field experimentation was also conducted to fill in data gaps. For example, available data for clay soils is very sparse such that tool development based on literature data alone was not feasible. To address this data gap, field experiments in clay soils in Georgia were conducted. The results indicated that pressure heads were slightly positive to slightly negative in the zone around each trench in a range that may allow both nitrification and denitrification to proceed simultaneously. Nitrate concentrations in the soil beneath the trenches were low, but above background, and increased with time during the seven months of sample collection. Similarly, although considerable information exists in the literature regarding the fundamental mechanisms involving bacterial and virus transport, most of the studies were conducted in sandy soils with very little information available regarding other soil conditions. To address this considerable data gap, laboratory-scale mesocosms were designed to provide tool calibration data describing the removal of bacteria and virus from STUs. Thus, laboratory and field data from the team field sites in Rhode Island (sandy soils), Georgia (clay), and Colorado (silt and loam soils) were all used to corroborate the developed quantitative tool outputs.

In summary, selection and use of a tool in the toolkit depends on the pollutant of interest, the nature of the problem at hand, the desire to incorporate specific complexities in OWTS operation or in soil or climate conditions, the sophistication of the user, the resources available to the user, the relative complexity of the problem, and the relative risk associated with an improper design. Because both STU decision making and design are highly interrelated processes, a decision protocol was developed to guide the user through tool selection and use. This protocol is simply a series of flow charts and decision steps that walk the user through the process and directs them to where the information can be obtained (e.g., CFD) or in when additional data collection may be warranted (e.g., numerical modeling).

CHAPTER 1.0

INTRODUCTION

1.1 Background and Motivation

Throughout the United States, wastewater management incorporates a variety of centralized and decentralized approaches for protection of public health and the environment. Nearly 21% of the United States' population is served by decentralized wastewater systems, with a substantial portion of all new development also being supported by these systems (Lowe et al., 2007). Onsite wastewater treatment systems (OWTS) are an important part of the overall wastewater management plan. Thus, proper selection, design, installation, operation and management of OWTS are essential to ensure protection of the water quality and the public served by that water source.

While OWTS vary widely in their design and implementation, conventional OWTS rely on septic tanks for retention and digestion of solids in raw wastewater followed by discharge of wastewater effluent to the soil treatment unit (STU) for eventual recharge to underlying groundwater (Metcalf and Eddy, 1991; U.S. EPA, 1997; Crites and Technobanoglous, 1998; Siegrist, 2001; Siegrist et al., 2001; U.S. EPA, 2002). In many areas advanced treatment (e.g., sand filters, textile media filters) may be implemented where site conditions are not suitable for conventional systems, or to produce a higher quality effluent delivered to the STU in sensitive areas such as those with nitrogen loading concerns.

In conventional systems, where local conditions permit, the septic tank effluent (STE) (or higher quality effluent if additional treatment is employed) may still contain high concentrations of pollutants that are further treated by the STU. A STU may be comprised of a series of subsurface trenches or beds for infiltration or through a shallow network such as in a drip dispersal system. In both of these cases, effluent percolates through an underlying unsaturated zone (vadose zone) with ultimate recharge to ground water. An unsaturated flow regime is expected to result in longer travel times through the STU allowing for more extensive contact between percolating effluent and the soil (Beach and McCray, 2003). In an unsaturated system, water is retained first in the finer pore spaces adjacent to soil grains and not in large pores. Thus, an understanding of flow, transport, and chemical reactions in unsaturated soil is critical for optimal design of OWTS and predicting STU performance. Often, unsaturated flow can be achieved within the STU by constraining the design hydraulic loading rate (HLR) to a fraction of the soil's saturated hydraulic conductivity with effluent delivery to the STU by gravity flow or dosed to the infiltrative surface. At the soil infiltration surface, a biozone evolves which may have a biomat (also called a clogging layer) resulting in ponding of effluent on the infiltrative surface of a trench (McKinley, 2008). This biozone formation with subsequent ponding allows for more uniform infiltration both spatially and temporally (Siegrist and Boyle, 1987).

Historically, OWTS design and regulation has been based primarily on ensuring that wastewater can be successfully infiltrated into the soil, preventing backup of the effluent to the ground surface or into the associated dwelling or business. However, it is now widely recognized

that this approach does not consider potential nutrient or pollutant treatment and mass loading to a receiving environment (soil, ground water, surface water) on a range of scales (single lot, subdivision, watershed). In areas of growth, decisions are often made related to lower density suburban development served by OWTS compared to higher density urbanized development served by centralized treatment plants. In the past, lower density prescriptive design and siting requirements were often based on the presumption that the OWTS was performing to meet target goals, but due to budget and staffing limitations, field systems were rarely monitored to verify that the performance was as expected with respect to wastewater constituents. Unfortunately, problems are typically highlighted only after a gross failure is observed (e.g., surfacing of effluent, detection of bacteria, nutrients, or other pollutants in nearby drinking water wells or surface waters, etc.). Decentralized cluster/community systems are now being recognized to offer higher density development options combined with the desired benefits of green space preservation, sustainable water resources, and lower infrastructure costs while maintaining high performance standards. In both low- and high-density development scenarios, simple tools are needed to evaluate whether the specified treatment performance can be achieved with assurance that the performance objective can be reliably met.

1.2 Project Objectives and Approach

The goal of this project is to provide a toolkit for assessment of STU performance. The toolkit is appropriate for a wide range of users evaluating STU performance for a varying range of complexity. This Guidance Manual describes the tools developed for the toolkit and provides a decision protocol to enable evaluation and design of expected STU performance for important wastewater constituents over a relevant range of OWTS operating conditions. A comprehensive literature review supplements this Guidance Manual and has been published as a separate WERF report (McCray et al., 2009).

This project was a joint effort between Colorado School of Mines (CSM), the University of Rhode Island (URI), the University of Georgia (UGA), and the University of California at Riverside (UCR). This multi-university team provided the expertise needed in nutrient transformations, organic wastewater contaminants (OWCs), microbial pollutants, mathematical modeling, and OWTS training and outreach. In addition, this collaboration enabled incorporation of information from laboratory and field studies representing a wide range of soil and climate settings.

The tools contained in the toolkit are based on the scientific principle that the soil-water system (i.e., the STU) provides treatment via physical, chemical, and biological transformation processes using information in the science and engineering literature. The tools are intended for technical professionals who wish to optimize STU design for particular soil and hydraulic conditions as well as non-technical stakeholders and planners who hope to increase their understanding of, or implement performance-based STU design.

The tools range from very simple to complex for evaluation of STU performance under a range of design and soil conditions. The tools primarily address the most common operating conditions associated with trench and drip dispersal. The tools themselves do not provide STU designs. Rather they provide insight into the behavior of STUs and quantitative estimations of treatment as affected by a range of conditions. These insights and outcomes then aid decisions during STU design and/or planning through better understanding of the influence of operating conditions and site conditions on STU performance. However, many complex processes and

less-common operating conditions can be addressed by some of the more complex models (see additional discussion related to existing models in the supplemental Literature Review).

Finally, the focus of the toolkit is on treatment of wastewater constituents that are typically of concern with respect to environmental degradation: nitrogen reduction, virus removal, and OWC transformations. Because the toolkit is based on existing knowledge, data, and models, the associated tools for various pollutants are not similarly rigorous. For example, the tools for nitrogen performance are most robust and rigorous, while the tools associated with OWCs are insightful, but not as detailed because of the general lack of information in the technical literature and additional research is warranted.

1.3 Using This Guidance Manual and Toolkit

1.3.1 Toolkit Components

The toolkit focuses on simple tools such as visual-graphic illustrations and spreadsheets that estimate STU treatment with depth below the infiltrative surface. The components of the toolkit are:

- ◆ Guidance Manual
 - discussion of tools and their use
 - decision diagrams for STU tool selection and performance design
- ◆ User's Guide
 - assumptions and governing principles
 - tool and model development
 - parameter selection
 - look-up tables
 - cumulative frequency distributions (CFDs) of important treatment parameters
 - laboratory and field experimental results
- ◆ Tools
 - visual-graphic illustrations of expected soil treatment
 - N-CALC (Nitrogen Calculator)
 - STUMOD (Soil Treatment Unit Model)
- ◆ Supplemental Information
 - literature review

This Guidance Manual provides an introduction to each tool, describes how the tool was prepared, and highlights the specific assumptions/limitations of the tool. The user can use this Guidance Manual to assess the appropriateness of the individual tool for their application as well as identify where additional supplemental information exists.

Visual-graphic tools provide an indication of whether treatment goals are likely or unlikely to be met for specific technical assumptions, site conditions, and OWTS operating factors. Look-up tables summarize important model input parameters based on values reported in the literature such as effluent concentrations and denitrification rates. CFDs provide an understanding of key input parameter variability based on statistical evaluation of actual reported OWTS values. Nomographs provide insight into the range of STU performance that can be expected for a given set of conditions. Cumulative probability graphs illustrate the likely range of treatment outcomes and the probability associated with any particular treatment effectiveness. In both the nomographs and cumulative probability graphs, treatment information provided by these tools is based on data generated by numerical models that can incorporate complex and robust treatment and operating conditions. Numerical model simulations of different OWTS scenarios visually demonstrate the usefulness of such a numerical model while showing the impacts of different scenarios on subsurface nitrogen concentrations, spatial treatment distributions, and mass-flux below a specified boundary. Because the choices for representative OWTS conditions are limited, the user must decide how their OWTS system fits within the limited treatment estimations displayed by the graphics.

Spreadsheet tools enable estimation of STU treatment for user-specified conditions, but presented in a simple-to-use format that does not require prior modeling knowledge or lengthy model run times. Of course, achieving these advantages requires that the incorporated treatment processes and operating conditions are simplified. Two spreadsheet tools were developed: N-CALC and STUMOD. Both of these spreadsheet tools allow the user to evaluate a range of STU performance based on likely variations in operating conditions, soil hydraulics, and/or treatment parameters, as well as the relative influence of these factors on performance (i.e., determine which parameters are expected to exert the greatest influence on STU performance). Thus, the spreadsheet tools can help the user decide if the uncertainty in STU performance is acceptable or if additional information should be collected to assess the expected STU performance with more confidence or numerical modeling is required.

Supplemental information provides either guidance on tool selection or additional technical detail on literature review or experimental findings. The information gained during the literature review aided in the design of laboratory and field experiments, and development of the design tools to assess STU performance. The complete literature review can be found at www.werf.org. Both laboratory and field experimentation was also conducted to fill in identified data gaps with data from the experiments used to corroborate the developed tool outputs for a range of soil and climate conditions. Finally, the decision diagrams and a worksheet helps direct the user through the implementation logic referring to applicable tools or parameter tabulations.


1.3.2 Using Tools for Decision Making

Selection and use of the tools in this toolkit require making informed assumptions. This does not suggest agreement or consensus on the assumption, but rather that the assumption, basis of knowledge, and certainty/uncertainty are clear, such that the tool selection/use is defensible. Simplifying assumptions are not in and of themselves bad, but the associated uncertainty and the affect on the output (e.g., decision, spreadsheet model output) are important.

A range of tools provided in the toolkit enable the user to start with simple tools that provide some general insight (Table 1-1). Higher complexity tools can then be used if more specific site data are available, or if more accuracy in the predictions is desired. In cases where limited information is available the simplest graphical tools can be used. If more information is available or can be collected, then more complex spreadsheet tools can be utilized. If additional

data is collected, a more complex/rigorous tool might be helpful or required. Progressing through simple to more complex tools will ultimately guide the user to the simplest tool that is appropriate, but discourage using a tool that is too simple for the decision at hand. In all cases, a clear understanding of the site is of utmost importance, whether the user of the tools is interested in the performance of an existing system or is looking to design a new system.

Table 1-1. Type and Complexity of Tools.

Type of Tool					
Look-Up Tables	CFDs	Nomographs, Cumulative Probability Graphs, Scenario Illustrations	N-CALC	STUMOD	HYDRUS
Location of Tool					
User's Guide, Chapter 3.0	User's Guide, Chapter 3.0	Visual-Graphic Tools file	Microsoft™ Excel Workbook	Microsoft™ Excel Workbook	Not Provided
Complexity of Tool					
Simple					Complex
Skill/knowledge Required to Use Tool					
None to a basic understanding of the descriptive statistics (median, standard deviation, percentile).	Understanding of a risk-based approach for selecting input parameter values.	Ability to interpret graphical representations of numerical relationships for a set of conditions.	Minimal technical expertise. Understanding of underlying principles and assumptions. Ability to select appropriate input parameters.	Relatively sophisticated user. Understanding of underlying principles and assumptions. Ability to select appropriate input parameters.	Technical proficiency in and resources to support numerical modeling.
Tool Application					
Provide understanding of factors affecting attenuation. Selection of input parameters for individual conditions.	Provide the basis for selection of input parameters based on the estimation of a proportion of a population whose measured values are greater than or less than some stated level.	Initial screening and evaluation of STU nitrogen attenuation based on defined conditions.	Field calculator to estimate nitrogen removal when input data is limited or based on worse-case conditions (i.e., no mixing or attenuation).	Sophisticated spreadsheet tool to estimate STU nitrogen attenuation for a wide range of user-specified input. Allows flexibility for input of different parameters and can be calibrated to site-specific data.	Development of STUMOD and scenario illustrations. Evaluation of complex STU conditions.
Information Obtained from Tool					
Summary of model input parameters based on values reported in the literature. Information to enable evaluation of specific conditions and corresponding input parameter values.	Greater understanding of assimilated data from the literature. Enables selection of input parameter values which incorporate uncertainty.	Visual representation of expected nitrogen attenuation with depth. Insight into the uncertainty of a particular model output due to individual input data. Effect on STU attenuation from key operating conditions.	Screening level representation of STU nitrogen attenuation under steady-state conditions.	Numerical and graphical representation of STU nitrogen attenuation with depth for user-specified conditions.	Numerical and graphical representation of STU attenuation for wide range of complex user-specified conditions.

For example, during initial planning of a single site or subdivision development, a decision maker may first utilize look-up tables and nomographs which will show expected nitrogen concentrations at specific depths based on general soil characteristics and median treatment factors (e.g., denitrification rates, ammonium sorption, virus deactivation, etc). Reference to these visual-graphic tools illustrates the relative probability that the concentration will be lower or higher than a specified treatment goal. Use of more complex tools may then be warranted if these simple tools suggest that: 1) concentrations are likely to exceed set treatment goals, 2) the likelihood of exceeding the specified treatment goals is not acceptable, or 3) the user desires a broader understanding of treatment under uncertain conditions. For example, spreadsheet tools can then be used to evaluate a wider range of potential soil or operating conditions and the expected performance.

Both the visual-graphic tools and the spreadsheet models give the user some indication of the uncertainty in the treatment predictions (e.g., the median “best estimate” for treatment with confidence intervals around this best estimate). For example, STUMOD is linked with a risk-simulation software so that the probability of nitrogen removal can be evaluated based on the uncertainty in the relevant hydraulic, transport and nitrogen transformation parameters. In this manner, the user can make better-informed decisions that account for the uncertainty in the treatment predictions as well as the stakeholders’ collective willingness to accept or deny risk under uncertainty. The breadth of tools in the toolkit provides:

- ◆ understanding of key processes critical to STU performance,
- ◆ insight into the variability of parameters influencing STU performance, and
- ◆ guidance for obtaining the best assessment of STU performance for different levels of knowledge.

1.3.3 Guidance Manual Organization

This manual is organized into four Chapters. Chapter 1.0 describes the overall framework and toolkit components. Chapter 2.0 provides descriptions of the tools. Chapter 3.0 guides the user through the assessment of parameters relevant to treatment performance including examples for tool selection and how to use those tools. Chapter 4 provides a summary of the toolkit.

A companion User’s Guide must be used in conjunction with this Guidance Manual. The User’s Guide includes the fundamental assumptions that were incorporated into the development of the tools in this toolkit (Chapter 1.0). A detailed description of the tool development is provided in Chapter 2 and detailed guidance on parameters that affect STU treatment performance and how to select specific values are provided in Chapter 3. Chapter 4 provides a summary. Relevant general reference material such as the USDA soil textural triangle with grain size distributions and conversions for common parameters is presented in Appendix A. Appendix B includes a worksheet form that may help guide the user through the different decision-making steps while keeping all relevant information in a compact format. Appendix C provides the results from field experiments conducted in Georgia coupled with the 2D modeling using HYDRUS. Column experiments conducted in Rhode Island on the fate and transport of bacteria and virus and 2D modeling using HYDRUS are described in Appendix D.

Tools are provided as separate files. Visual-graphic tools including nomographs, cumulative probability graphs, and scenario illustrations are compiled into a separate pdf file. N-CALC and STUMOD are separate Microsoft™ Excel files.

The framework of the toolkit including this Guidance Manual is outlined in Figure 1-1.

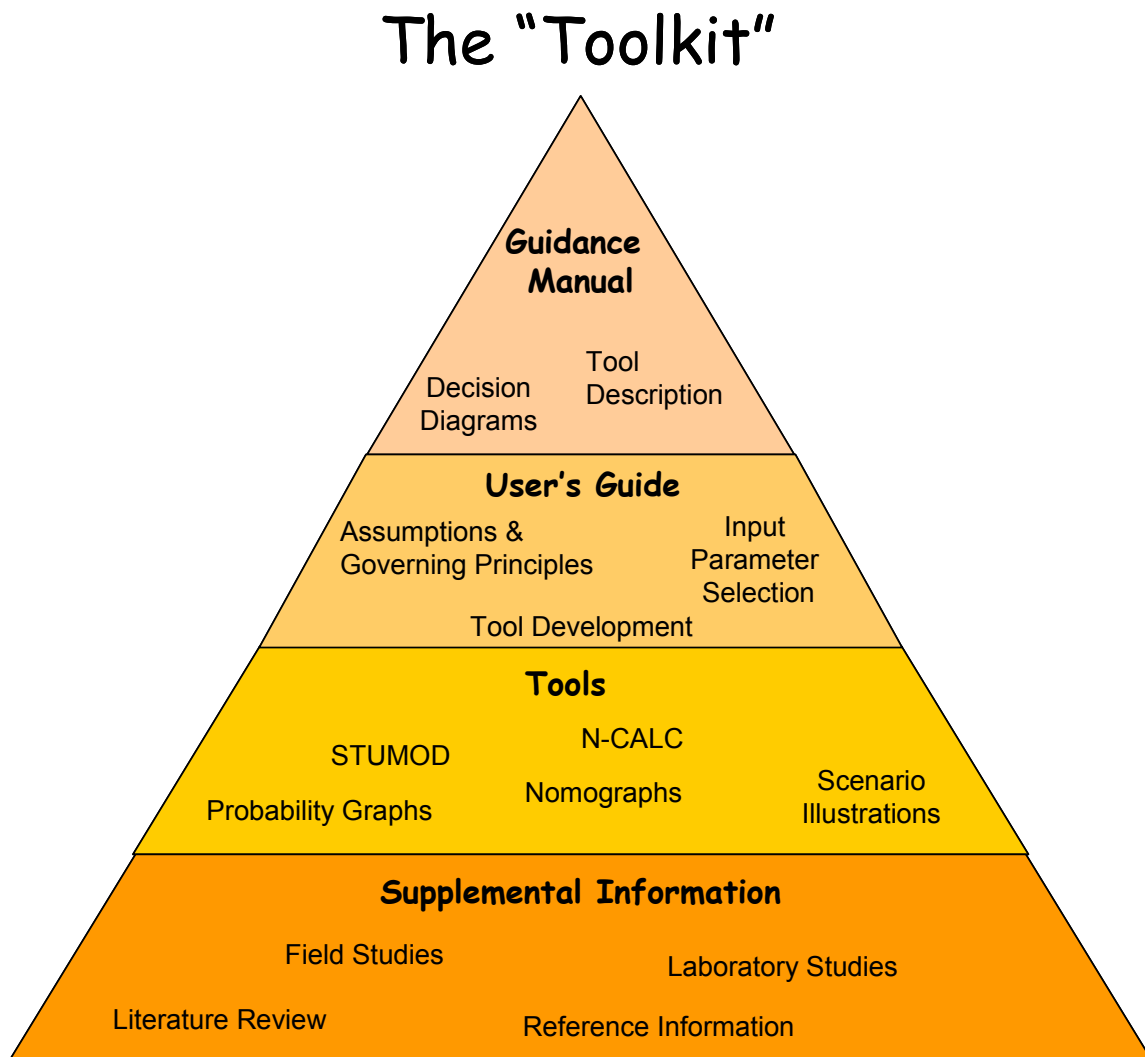


Figure 1-1. Toolkit Framework for STU Performance.

CHAPTER 2.0

TOOL DESCRIPTION

All of the tools presented in the toolkit were developed with a basis in rigorous experimental data. The quantitative tools or models were evaluated using data from the literature, from experiments conducted by the project team, or from scientific knowledge of operating OWTS treatment performance. The complexity of the various tools in the toolkit depends on the:

- ◆ Relative importance of the pollutant of interest in the practical and regulatory arena.
- ◆ Availability of existing data from which to build a solid theoretical foundation of these treatment processes.
- ◆ Degree of complexity that is intended to be included in the problem analysis.
- ◆ Sophistication, technical resources, and treatment goals of the user.

The toolkit is hierarchical in nature and includes tools that are diverse with regard to their ability to incorporate complexity, user sophistication, and appropriateness for use. Ideally, the simplest tools are the first to be used. These tools are best used as screening tools to decide if further action is needed and require little user sophistication, but cannot incorporate many of the complexities associated with different OWTS sites or pollutant treatment processes. Examples of these tools include charts or tables that direct the user to the general best practice to optimize treatment for certain pollutants, simple spreadsheet solutions that predict concentrations at depth but that do not incorporate any of the important complexities associated with OWTS treatment processes, or a description of a process or set of experimental results that lend insight to pollutant treatment. Such simple tools may not be appropriate for decision making, particularly if the health, regulatory, or legal risks associated with the decision are high.

An example of a more complex tool is a mathematical model that is simple enough that it can be implemented using a spreadsheet, but complex enough to include the most important complexities associated with relevant treatment processes (e.g., nitrification, and denitrification, and the dependence of these processes on relevant soil properties such as soil moisture or soil type), and can translate the effect of uncertainty in important soil or treatment parameters on to the uncertainty of treatment prediction. Such a model can be used directly by a relatively sophisticated user. Alternatively, nomographs summarize results for a variety of conditions for users who do not wish to embark on learning how to use and implement a mathematical model. The nomograph, can be readily used for decision making, but only for standard OWTS operating conditions, and only with due considerations of the limitations of the model. If a user wishes to consider specific complexities or alternate scenarios (e.g., different OWTS designs, spatial distribution of treatment in the subsurface, or seasonal effects of use or climate), then a powerful but highly sophisticated numerical mathematical model must be used. Such a tool requires

considerable resources to implement, but may be appropriate for considering complexity of the problem or when the relative risk associated with a poor design is high.

A highly diverse toolkit is provided (Table 2-1) because the amount of data and fundamental understanding of treatment processes varies between the OWTS pollutants. For example, the current state of knowledge regarding nitrogen fate and transport in soils receiving wastewater points at four major processes: 1) nitrification, 2) denitrification, 3) ammonium sorption to soil particles, and 4) uptake or assimilation of nitrogen species by plants or microbes. Conversely, for OWCs there is little data available, the fundamental understanding of treatment processes is in the early stages, and most OWCs are not regulated. Thus, the tools developed for OWCs are less sophisticated and not as quantitative as the tools developed for nitrogen. Intermediate to nitrogen and OWCs are microbial pollutants. Virus and bacteria are important regulated pollutants, but the available data regarding treatment in OWTS or other similar systems is relatively sparse, and the processes associated with transformation and soil transport are very complex. Thus, the tools for microbial pollutants are generalized recommendations as well as diagrams developed from complex numerical models that depict treatment effectiveness for various relevant scenarios.

Table 2-1. Diversity of Tools Developed.

Parameter	Look-up Table	CFD	Visual Graphic Illustration	Spreadsheet Tool	Supplemental Information
Nitrogen	Factors affecting attenuation. Reported input parameter values (ammonium sorption, nitrification, denitrification).	Concentration range in effluent. Reported input parameter values (sorption coefficients, transformation rates).	Nomographs. Cumulative probability graphs. Scenario illustrations.	N-CALC STUMOD	Literature search. Field study results.
Bacteria	Factors affecting attenuation.	Concentration range in effluent. Reported removal in soil.	None	None	Literature search. Laboratory study results.
Virus	Factors affecting attenuation.	Concentration range in effluent. Reported removal in soil.	None	None	Literature search. Laboratory study results.
OWCs	Factors affecting attenuation.	None	None	None	Literature search. Laboratory study results.
General	Soil texture properties. Regional temperatures. Effluent quality. Hydraulic loading rates.	Effluent quality ranges.	None	None	Literature search.

While there is an abundance of scientific knowledge on phosphorus, very little data related to phosphorus in STUs is reported in the literature. The largest gaps in the understanding of the fate and transport of phosphorus in STUs that are not considered in quantitative tools, are centered around two important issues: 1) phosphorus behavior in high ionic strength solutions, and 2) parameterization of functions that describe kinetic sorption and precipitation in STUs (most sorption and precipitation data in the literature is from equilibrium batch tests but field studies at CSM suggest that precipitation is not an equilibrium process). In addition, phosphates are subject to biological assimilation, sorption or precipitation, but some of these processes are reversible and depend greatly on the reduction-oxidation state of the soil, soil mineralogy, presence of other ions in STE, and hydraulic loading rate. Furthermore, the few reports in the literature have conflicting results regarding the amount of phosphorus removed in STUs, ranging from complete removal to development of distinct phosphorus plumes in groundwater beneath STUs. Thus, only supplemental information (compilation of knowledge from the literature,

McCray et al., 2009) is provided for phosphorus that should help practitioners make better decisions related to STU performance.

2.1 Tool Development

Simple tools must be defensible. Two types of defensible tools are presented in the toolkit: 1) tools based on statistical analysis of data available in the literature, and 2) tools that honor the current understanding of the scientific principles associated with the physical, chemical, and microbial treatment processes. The tools were also evaluated against measured data with no attempt to consider processes or design elements when the treatment theory is not well understood or where corroborative data is not readily available in the literature. For this reason, tool development did not rely solely on common understanding, which is often deficient with regard to the above criteria, and is thus not defensible. In addition, the tools must bridge the gap between incorporating biophysicochemical processes known to be relevant, and the ability to corroborate such tools versus measured data. Thus, development of “simple”, user-friendly tools that represent complex systems requires certain assumptions. A complete discussion of the scientific principles and governing assumptions for the toolkit is provided in the User’s Guide (Chapter 1.0).

Simple tools can be very helpful for a wide range of common OWTS scenarios. Because sufficient understanding, data, and project schedule do not exist to completely represent the wide range of STU conditions that occur, there are certain conditions where the developed tools are not sufficient to adequately predict performance, or the uncertainty in these predictions may be unacceptable for certain high-risk scenarios. In these cases, it must be recognized that more rigorous numerical modeling is required. It is up to the user to decide if the simple tools provided in this toolkit are appropriate or if more rigorous modeling/tools are required.

Empirical tools developed based on statistical evaluation of the available literature data provided insight into treatment and the factors influencing treatment, but the data sets were generally not sufficiently robust to enable development of empirical tools that were statistically reliable. Thus, the tools developed for this toolkit are based on current scientific understanding of the dominant soil processes influencing treatment, while avoiding theory too complex to allow evaluation of tools versus practically measurable data.

The visual-graphic illustrations (nomographs, cumulative probability graphs, scenario illustrations) of STU treatment are based on synthetic data sets obtained using the HYDRUS model software package (HYDRUS 1D, 2D, and 3D). HYDRUS simulates unsaturated transport of multiple species in saturated/unsaturated soils. It also has the ability to simulate a variety of pollutant reactions and transformations, geochemical reactions, kinetic and equilibrium reactions, as well as ponding and variable loading rates. HYDRUS has been used for various applications in OWTS by members of this research team (McCray et al., 2000; Beach and McCray, 2003; Doyle et al., 2005; Radcliffe et al., 2005; Pang et al., 2006; Bumgarner and McCray, 2007; Heatwole and McCray, 2007; Radcliffe and West, 2007; Finch et al., 2008) and by other researchers outside the project team (Beal et al., 2008). Specific for this project, HYDRUS was modified to account for the effect of water filled porosity, carbon content, and temperature on treatment to improve its ability to simulate nitrogen transformation under a variety of OWTS loading conditions. Based on an evaluation of many different numerical models, the newly modified version of HYDRUS was deemed to be the most robust model for examining OWTS STU performance.

N-CALC is a spreadsheet model to investigate steady-state treatment effectiveness based on soil type. N-CALC accounts for removal processes such as adsorption, nitrification and denitrification that can be used with minimal technical expertise. Initial screening with N-CALC may aid the user in determining whether more resources should be devoted to data gathering or implementation of a more rigorous model such as STUMOD or HYDRUS is required. The assumptions and limitations associated with HYDRUS, STUMOD, and N-CALC are described in the companion User's Guide (Chapter 1.0).

STUMOD is an easy-to-use spreadsheet model that estimates treatment performance with depth based on user-specified input for soil hydraulic parameters, loading rate, and soil-treatment parameters. STUMOD is relatively sophisticated with respect to the soil-hydraulic and treatment processes (incorporates many of the complex hydraulic and biochemical transformation processes found in HYDRUS) and can be calibrated to site data. However, the spreadsheet implementation requires simplification of OWTS operating conditions (e.g., constant loading rate, one-dimensional infiltration and treatment, etc).

2.2 Tool Description

2.2.1 Spreadsheet Tools

Two spreadsheet tools that use simplified transport models (e.g., for nitrogen transformation) were developed. These spreadsheet tools provide reasonable representations of more rigorous numerical models (e.g., HYDRUS 2D).

2.2.1.1 N-CALC

A simple spreadsheet tool, termed "N-CALC", can be used to investigate steady-state treatment effectiveness based on soil type (i.e., long-term performance for a relatively mature system). N-CALC is a screening level tool that can be used when input data is limited, or as an initial step to determine whether impacts from OWTS are likely under worst-case scenarios (no mixing or attenuation). It can be used with minimal technical expertise, and would also be helpful as a field calculator. The model could also be used to determine whether more resources should be devoted to data gathering or implementation of a more rigorous model such as STUMOD or HYDRUS is required. Thus, N-CALC can provide a cost-effective means to evaluate OTWS strategies before more expensive models are employed for a specific site.

N-CALC is relatively simple and requires few input data (Figure 2-1). The input parameters include effluent concentrations, hydraulic loading rates, porosity, soil depth, and parameters for nutrient transformation (sorption, first order nitrification and denitrification rates). N-CALC accounts for removal processes such as adsorption, nitrification and denitrification, but does not account for the effect of soil moisture or temperature on nitrogen treatment processes. Default values are recommended for each input parameter; however, users can use values specific to their site if available. The output is the expected performance illustrated as nitrogen concentrations and mass flux at a specified depth. Some examples of how the N-CALC can be used by OWTS practitioners include:

- ◆ Initial screening to evaluate if OWTS impacts are of potential concern based on model runs that consider a range of possibilities for treatment results. If "impact" is a reasonable concern, then models with increasing complexity and implementation cost may be used

in a sequential manner until the decision makers are comfortable with the uncertainty in the predictions, and the relative risk associated with those decisions.

- ◆ Users can obtain predictions on the fraction of ammonium, nitrate or total nitrogen removed at a particular depth below the infiltrative surface. An estimate of total nitrogen loading along the trench center line is calculated based on concentration and flow rate.
- ◆ A preliminary evaluation of treatment for different scenarios, such as lower nitrogen concentrations in effluent (e.g., due to various levels of pretreatment), soil type, and loading rates.
- ◆ A training tool to help promote a better understanding about how fundamental factors or processes influence OWTS treatment.

The screenshot shows the Ncalc software interface with the following parameters and values:

Category	Parameter	Value
Soil types	Clay	<input checked="" type="radio"/>
	Clay Loam	<input type="radio"/>
	Loam	<input type="radio"/>
	Loamy Sand	<input type="radio"/>
	Sand	<input type="radio"/>
	Sandy Clay	<input type="radio"/>
	Sandy Clay Loam	<input type="radio"/>
	Sandy Loam	<input type="radio"/>
	Silt	<input type="radio"/>
	Silty Clay	<input type="radio"/>
Hydraulic params	HLR	2
	n	0.46
Rates	Kr-nit	0.5
	V-dnt	0.2
Soil	Depth	60
	ρ	1.50
Adsorption params	kd	1.46
	fr	0.00
Effluent concentration	Co-NH4	60.0
	Co-NO3	1.0
Outputs at Max depth	C- NH4	1
	C- NO3	1
	C- TN	1
	C/Co TN	1
	Flux NO3	1
	Flux TN	1
Outputs at Half Max Depth	C- NH4	1
	C- NO3	1
	C-TN	1
	C/Co TN	1
	Flux NO3	1
	Flux TN	1

Buttons: Run Ncalc, Close

Figure 2-1. Illustration of N-CALC User Interface Showing Inputs and Outputs for Clay Soil.

2.2.1.2 STUMOD

STUMOD estimates treatment performance with depth based on user-specified input, but enables the user flexibility for input of soil hydraulic parameters, loading rate, and soil-treatment parameters. STUMOD is relatively sophisticated with respect to the soil-hydraulic and treatment processes, and can be calibrated to site-specific data (User's Guide, Section 2.2.4). STUMOD incorporates the same nitrification/denitrification equations used in HYDRUS, which are built into a spreadsheet, thus allowing users with no previous modeling knowledge to evaluate likely

STU performance. However, the spreadsheet implementation requires simplification of OWTS operating conditions (e.g., constant loading rate, one-dimensional infiltration and treatment, etc) and input parameters which are described in detail in the User's Guide (Chapters 1.0 and 2.0).

The input parameters include operational parameters (effluent concentrations, loading rates) and parameters for nutrient transformation (sorption, zero order nitrification and denitrification rates). Default values are provided in the user interface to aid the user during selection of inputs (Figure 2-2). The model requires a significant level of user sophistication with regard to using the appropriate input parameters. To supplement these default values, additional reference information is provided in the literature review (McCray et al., 2009) as well as look-up tables, and CFDs (User's Guide, Chapter 3.0). The output is expected performance such as constituent concentrations and fraction of nitrogen removed at user-selected depths (Figure 2-2).

The screenshot shows the STUMOD software interface with the following default values:

Category	Parameter	Value
Soil types	Clay	<input checked="" type="radio"/>
	Clay Loam	<input type="radio"/>
	Loam	<input type="radio"/>
	Loamy Sand	<input type="radio"/>
	Sand	<input type="radio"/>
	Sandy Clay	<input type="radio"/>
	Sandy Clay Loam	<input type="radio"/>
	Sandy Loam	<input type="radio"/>
	Silt	<input type="radio"/>
	Silty Clay	<input type="radio"/>
Biomat params	Kb	0.4
	BT	2
Carbon function	α	0.00
Hydraulic params	HLR	2
	α_1	0.025
	α_2	0.015
	Ks	14.75
	θ_1	0.098
	θ_2	0.459
	n	1.26
	m	0.206
	l	0.5
	ho	5.063
Effluent concentration	Co-NH4	60.0
	Co-NO3	1.0
Nitrification params	Kr-max	56.00
	Km-nit	5.00
	e2	2.267
	e3	1.104
	β_1	0.347
	fs	0.0
	fwp	0.0
	swp	0.154
	sl	0.665
	sh	0.809
Temperature	T	15.00
	Topt1	25.00
	Topt2	26.0
Denitrification params	Vmax	2.56
	Km-dnt	5.00
	e-dnt	3.774
	β_2	0.347
Adsorption params	sdn	0.0
	kd	1.46
	fr	0.00
Soil depth	ρ	1.50
	D	60
Outputs	C/Co NH4	1
	C/Co TotN	1

Buttons: Run STUMOD, Close

Figure 2-2. Illustration of STUMOD User Interface Showing Default Input and Outputs for Clay Soils.

Based on the complementary literature review (McCray et al., 2009), available data is very sparse and tool development based on literature data alone was not feasible. STUMOD was developed based on existing fundamental principles of water movement and contaminant transport. An analytical solution is used to calculate profile of pressure and moisture content in the unsaturated STU. The chemical transport component is based on simplification of the general

advection dispersion equation, which is based on chemical mass-balance. The model calculates change in moisture content with depth; thus, the effect of soil moisture content on nitrification and denitrification rate can be determined. It also has provisions to account for the effect of temperature. The model is linked with a risk-simulation software so that the uncertainty in nitrogen removal can be evaluated based on the uncertainty in the relevant hydraulic, transport and nitrogen transformation parameters. The model is not theoretically appropriate for shallow water tables, and does not explicitly account for any soil layering in the subsurface. Examples of how STUMOD can be used by OWTS practitioners are:

- ◆ Quantitative assessments of nitrogen concentration for STUs. Users can obtain predictions on the fraction of ammonium, nitrate or total nitrogen removed versus depth below trench, and nitrogen loading along the trench center line.
- ◆ Scenario Evaluation. Practitioners can perform rapid evaluations of scenarios that may influence nitrogen treatment such as the influence of nitrogen concentrations in effluent, soil properties, loading rates, and temperature.
- ◆ System design. Hydraulic loading rates, effluent quality, trench size, or loading area can be evaluated in light of nitrogen treatment goals.
- ◆ Rigorous system design. STUMOD can be calibrated to site data (e.g., removal rates) and subsequently used to optimize operation of OWTS or to design new OWTS in a similar soil setting.

It is recognized that the sophistication of STUMOD may preclude practitioners from using the tool. In this case, hundreds of visual-graphic illustrations for treatment were developed for a variety of conditions relevant to OWTS, including different loading rates, climates/geographic regions, soil types, and nitrogen concentration ranges. The visual-graphic tools provide a likely range of treatment outcomes and a probability associated with any particular treatment effectiveness. This output enables planners and regulators to make decisions based on their willingness to accept an agreed-upon level of quantified risk. These visual-graphic tools are provided in a separate file “Visual-Graphic Tools” and include nomographs, cumulative probability graphs, and scenario illustrations.

2.2.2 Visual Graphic Tools

The simplest tools developed are visual-graphic tools including look-up tables, CFDs, nomographs, cumulative probability graphs, and scenario illustrations. Look-up tables and CFDs aid input parameter selection when using N-CALC, STUMOD or HYDRUS. Nomographs, cumulative probability graphs, and scenario illustrations all enable initial screening of expected STU performance based on the predicted output from either STUMOD or HYDRUS.

2.2.2.1 Look-Up Tables

Look-up tables are reference tables that provide values or ranges for specific conditions. Primarily, look-up tables summarize important model input parameters based on values reported in the literature such as ammonium sorption isotherms, denitrification rates, effluent concentrations, etc. Look-up tables also capture specific factors that play a role the physical, chemical, or biological process, but insufficient information is available to quantify. In this case, an understanding of the relative behavior is intended help users select appropriate values from CFDs or from other sources. Table 2-2 illustrates a look-up table for guidance when selecting ammonium sorption rate (K_d) values. For example, in the case of ammonium sorption, if the

cation exchange capacity is very low, sorption is expected to be very low as well and the user may want to choose a smaller K_d value from the CFD or reduce the default value in STUMOD. In contrast if the concentration of chemical oxygen demand in STE is very high, sorption is expected to increase and a higher K_d value should be considered. Look-up tables are presented by parameter in the User's Guide (Chapter 3.0).

Table 2-2. Example of Look-up Table Illustrating Factors Influencing Ammonium Sorption.

Factors	Units	Expected Field Condition	Resulting Ammonium Sorption
Ammonium-nitrogen concentration of the effluent	mg-N L ⁻¹	Low	High
		High	Low
Chemical oxygen demand of the effluent	mg L ⁻¹	Low	Low
		High	High
Cation exchange capacity of the soil	meq 100g ⁻¹	Low	Low
		High	High
Calcium and magnesium mineral content of the soil	mg L ⁻¹	Low	High
		High	Low
Clay content of the soil	relative %	Low	Low
		High	High
Water filled porosity of the soil	%	Low	High
		High	Low

2.2.2.2 Cumulative Frequency Distribution Diagrams

When sufficient data are available, CFD diagrams are provided to enable better understanding of the assimilated data. CFDs are useful to estimate the proportion of a population whose measured values are greater than or less than some stated level (Snedecor and Cochran, 1980). The cumulative frequency as a percentage is presented on the y-axis and the reported values are presented on the x-axis (Figure 2-3).

In the case of summarizing literature values, the CFD also illustrates the uncertainty or “risk” in the reported data. The amount of available data (or lack of) is shown by the individual data points used to generate the distribution curves. Symbols represent values and lines represent trends. Increasing the number of data values (e.g., number of symbols illustrated) for a specific parameter, better represents the cumulative distribution and provides greater certainty in the reported range of values. The slope of the curve is also insightful. A steeper slope represents less variability in the range of data values (e.g., the 75th and 25th percentile values are not much different from the median value) which minimizes the uncertainty of selecting a parameter value. Alternative, a flatter slope indicates a wider range of values (where the 75th and 25th percentile values are much different from the median value) where more precise estimation of the parameter is difficult and may result in greater error.

Cumulative percent values selected from the CFD plots are interpolated from given points and should be used as approximate values. In Figure 2-3 the literature reported values for cBOD₅ in STE are summarized. A value that corresponds to the 75th percentile means that 75% of the cBOD₅ values reported in the literature were lower than this specific value. Similarly, the 50th percentile value means that 50% of the cBOD₅ values reported in the literature are higher and 50% of the reported values reported are lower than this value. In other words, the 50th percentile value is the median value.

The CFD enables the user to select a value from a range of actual reported data that incorporates an acceptable uncertainty for a specific condition. For example, a look-up table may provide the median ammonium sorption isotherm (K_d) based on reported conditions for key

conditions (e.g. soil type, laboratory or field test, etc.) while the complementary CFD shows all of the reported data and the distribution of the full range of values. In a sensitive location, a lower K_d value may be selected from the CFD to minimize the estimated ammonium sorption resulting in prediction of higher concentrations of mobile nitrogen in the STU. Alternatively, as a first estimate, perhaps the median value is used and the resulting nitrogen concentrations assessed for acceptable performance or not. Most importantly, a CFD provides the reported range of values which helps ensure that the user-selected values are realistic. CFDs are presented by parameter in the User's Guide (Chapter 3.0).

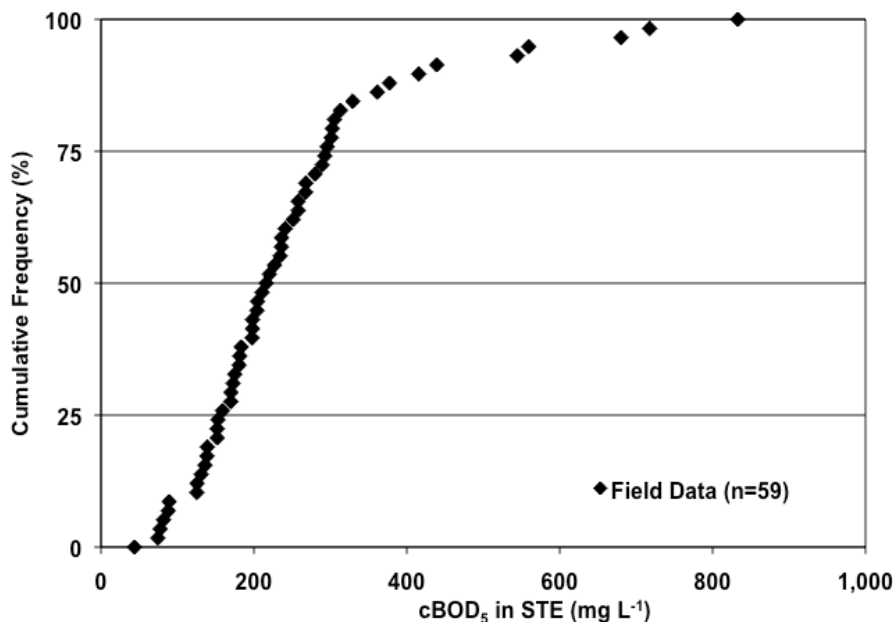


Figure 2-3. Example CFD Illustrating cBOD₅ Concentrations in STE (adapted from Lowe et al. 2009).

2.2.2.3 Nomographs

A nomograph is a graphical representation of a numerical relation based on a set of conditions. Two types of nomographs were developed for the toolkit: 1) nomographs that illustrate nitrogen removal in the soil with depth for specific conditions; and 2) cumulative probability graphs that illustrate the likelihood that a specific removal will be observed at different depths.

The first type of nomograph illustrating nitrogen concentration with depth for specific conditions was generated based on STUMOD (Figures 2-4 and 2-5). These nomographs represent the expected worse case condition of the maximum steady-state concentration directly below the center of the point of infiltration. Because STUMOD is a relatively simple spreadsheet program (compared to HYDRUS), each simulation runs quickly and nomographs were made illustrating the fraction of nitrogen remaining with depth for the following conditions (additional description of the nomograph conditions is provided in the Users Guide):

- ◆ Soil Type: clay, clay loam, loam, loamy sand, sand, sandy clay, sandy clay loam, sandy loam, silt, silty clay, silty clay loam, silty loam
- ◆ HLR: 2 cm d⁻¹ or 5% of saturated hydraulic conductivity (K_{sat}) (varied by soil texture)

- ◆ Effluent Concentration: STE represented by 60 mg-N L⁻¹ as ammonium-nitrogen and 1 mg-N L⁻¹ as nitrate-nitrogen or nitrified effluent represented by 15 mg-N L⁻¹ as nitrate-nitrogen
- ◆ Temperature Region: hyperthermic, thermic, mesic, frigid/cryic

These nomographs are presented in a separate “Visual-Graphics Tools” file. A total of 240 comparative curves on 60 nomographs are provided. These nomographs quickly provide insight into expected nitrogen removal (based on the assumptions incorporated in STUMOD). For example, Figure 2-4 suggests that if the desired treatment goal is 50% nitrogen reduction for the listed conditions, then in very warm soil conditions (hyperthermic) ~45cm of unsaturated soil is expected to be required compared to >120 cm of unsaturated soil in very cold soil conditions (frigid/cryic). Alternatively, Figure 2-5 suggests that for an initial concentration of 150 mg-N L⁻¹ as ammonium, in moderate temperature conditions (mesic) ~20% nitrogen is expected to be removed compared to 60% removal in a warm climate (hyperthermic). Note, soil temperature regimes for the contiguous United States are provided in Users Guide, Figure 3-9.

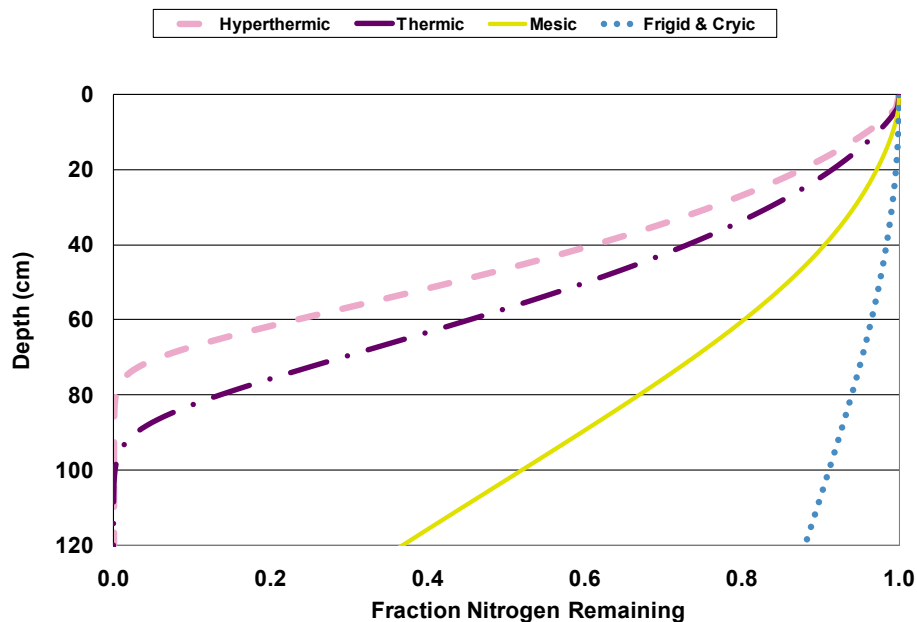


Figure 2-4. Nomograph Illustrating Fraction of Nitrogen Remaining with Depth in Different Temperature Regions. Assuming soil type = sandy loam shown, standard effluent, HLR = 2 cm d⁻¹ (other STUMOD input parameters are shown in the Visual-Graphic Tools, Table VG-1).

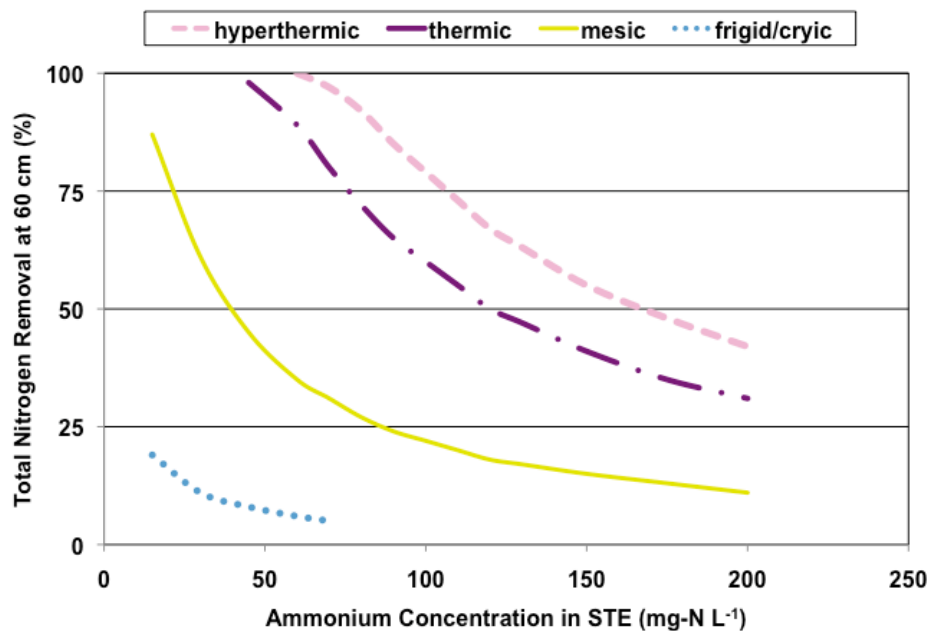


Figure 2-5. Nomograph of Percent Nitrogen Removal at 60 cm Depth in Four Different Temperature Regions due to Different Effluent Concentrations. Assuming soil type = clay loam, HLR = 2 cm d-1 (other STUMOD input parameters are shown in the Visual-Graphic Tools, Table VG-1).

The second type of nomograph, referred to as “cumulative probability graph”, was generated through use of a visual basic code added to STUMOD to allow Monte Carlo simulations. Monte Carlo simulations rely on random selection of input values for model runs producing a method for statistically quantifying the uncertainty of a model outcome. A model is run numerous times with the input parameters selected randomly from ranges of expected values. The output of the model runs is then statistically analyzed and the probability of realizing any one particular outcome can be quantified, thus allowing the modeling results to be viewed as a nomograph in a risk-based framework (the same as a CFD) by displaying the cumulative uncertainty of a particular model output due to individual input data. These cumulative probability graphs are ideal for modeling processes such as nitrogen attenuation in a STU where large ranges of uncertainty exist or where certain data parameters are unknown or highly variable.

Input values were generated according to built-in probability density functions that can be selected based on the available or expected data for a given input parameter. Up to 2000 Monte Carlo simulations were then incorporated into histograms and cumulative probability plots of the model outputs for a given set of conditions. These resulting cumulative probability graphs allow the user to determine the percentile of an outcome as well as illustrate “best”, “most likely”, and “worst” case outputs. Specifically, the Monte Carlo analyses based on STUMOD inputs provide the probability of the occurrence of a value (Figure 2-6).

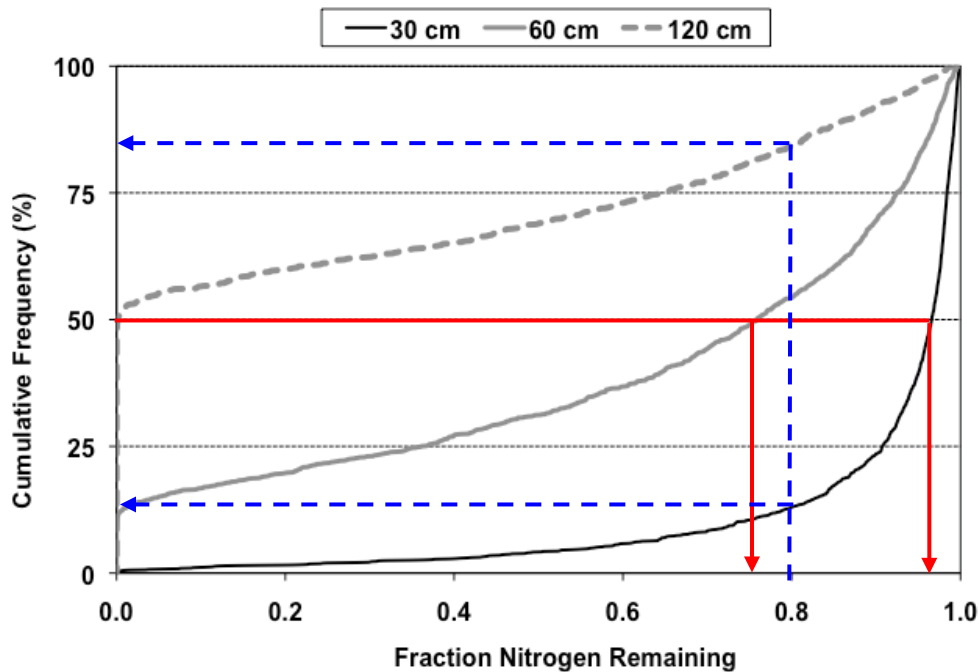


Figure 2-6. Example Cumulative Probability Graph of Monte Carlo Simulation for Three Different Soil Depths. Assuming soil texture = clay, temperature region = mesic, standard effluent quality, HLR = 5% of K_{sat} (other STUMOD input parameters are shown in the Visual-Graphic Tools, Table VG-1).

Rather than a single output that may or may not be accurate, this approach gives the probability of realizing any one specific outcome, based on the cumulative uncertainty of all model input parameters. For example, in Figure 2-6, a horizontal line through a given probability value of 50% suggests that there is a 50% likelihood that the fraction nitrogen remaining at 60 cm is ~0.75 and at 30 cm is ~0.95 (solid arrows in Figure 2-6). Alternatively, a vertical line through the 0.8 fraction nitrogen remaining value enables the user to estimate the associated probability (likelihood) of 20% nitrogen removal at the 30 cm depth (15%), compared to at 120 cm depth (80%) (dashed arrows in Figure 2-6).

2.2.2.4 Model Output (Scenario) Illustrations using HYDRUS

A flexible tool capable of complex scenarios is necessarily quite complex. The best approach is a numerical model that can incorporate any level of sophistication regarding subsurface heterogeneity, trench geometry, large multiple-trench systems, drip systems, water table position, or climate. For toolkit users who do not wish to implement a complex model, a series of colorful illustrations are provided that show the impacts of different scenarios on subsurface nitrogen concentrations, spatial treatment distributions, and mass-flux below a specified boundary. These visual-graphic tools illustrate the power of a numerical model, as well as provide some end-member treatment evaluations for the selected scenarios. A description of the scenario development is provided in User's Guide (Section 2.4)

The HYDRUS-2D scenario simulations also add a new type of information that is usually not available through conventional grab-sample techniques, which is an estimated mass flux at different depths below a trench or drip system. Mass flux provides understanding of the footprint from an STU rather than just an expected nitrogen concentration below the infiltrative surface.

The total mass load to the environment may be of more concern than a specific concentration in some locations. For example, this information is especially useful when setting total maximum daily loads (TMDLs) for a watershed, or for assessing the total nitrogen-contamination impact of cluster units. In this case the load over an area can be estimated through mass flux. Such information can then be used to back calculate how many trenches could be utilized at a site without exceeding the desired treatment goal.

The results from the scenarios allow comparison of STU performance. Each scenario output illustrates: 1) the moisture content distribution, 2) the corresponding nitrogen concentration distribution, 3) mass flux estimates at 60 and 120 cm below the point of infiltration, and 4) a nomograph of the center maximum concentration below the point of infiltration. Example scenario output data sheets for the trench and drip simulations are shown in Figures 2-7 and 2-8.

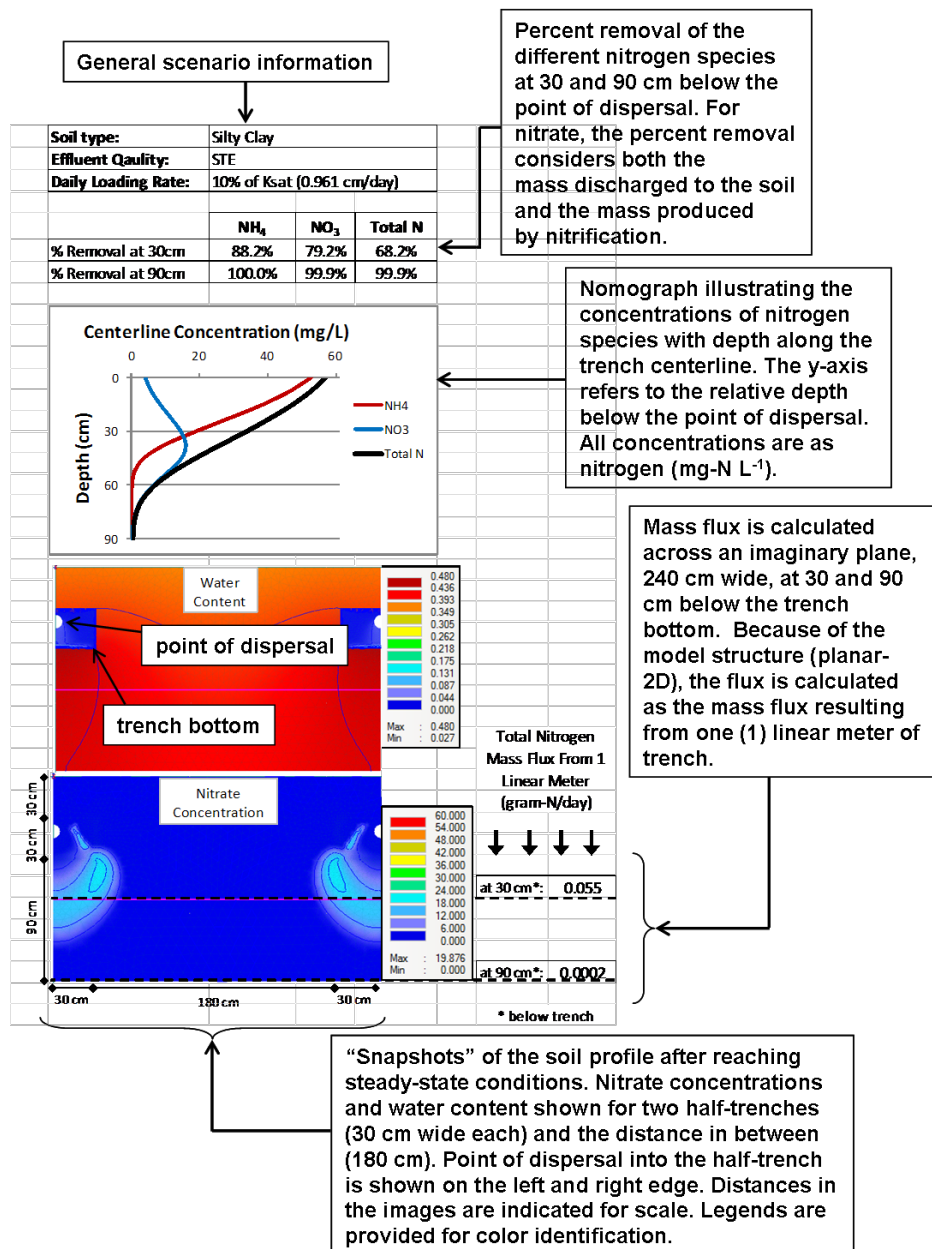
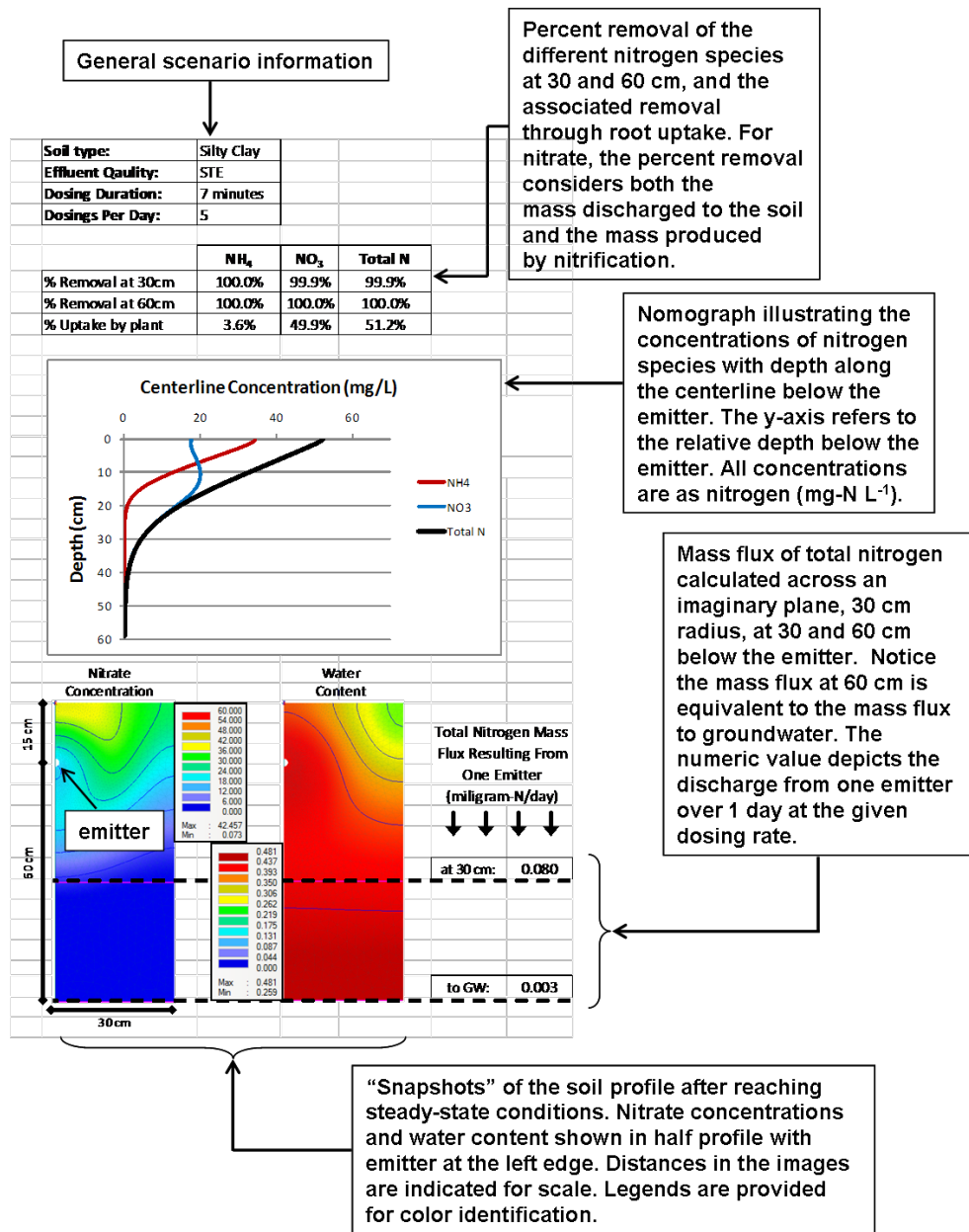


Figure 2-7. Description of the Scenario Output for Trench System Simulations.



Percent removal of the different nitrogen species at 30 and 60 cm, and the associated removal through root uptake. For nitrate, the percent removal considers both the mass discharged to the soil and the mass produced by nitrification.

Nomograph illustrating the concentrations of nitrogen species with depth along the centerline below the emitter. The y-axis refers to the relative depth below the emitter. All concentrations are as nitrogen (mg-N L⁻¹).

Mass flux of total nitrogen calculated across an imaginary plane, 30 cm radius, at 30 and 60 cm below the emitter. Notice the mass flux at 60 cm is equivalent to the mass flux to groundwater. The numeric value depicts the discharge from one emitter over 1 day at the given dosing rate.

Figure 2-8. Description of the Scenario Output for Drip System Simulations.

2.2.3 Supplemental Information

Supplemental information is also available that aids users in understanding key STU processes. Decision diagrams guide the user through selection of key input parameters and tool selection during the STU design process and are incorporated in this Guidance Manual (Chapter 3.0). Detailed information related to transport processes incorporated during tool development and input parameter selection for simple tools can be found in the comprehensive literature review (McCray et al., 2009) conducted as part of this project. During the literature review, several data and informational gaps were identified. To address these gaps, laboratory and field

studies were conducted. Laboratory experiments were carried out at URI to study the transport and fate of a model bacterium and virus and at CSM to assess fate and transport parameters of selected organic wastewater constituents. Field testing was conducted at the UGA to assess hydraulic performance and nitrogen movement in clayey soil. Results from the field and laboratory studies are described in the User's Guide (Appendix C and D).

2.2.3.1 Decision Protocol

A series of flow diagrams is provided to guide the user through the steps most often incurred during the STU design decision process. These flow diagrams serve as a decision protocol that prompts the user to choices important to evaluating or modeling performance treatment. The diagrams are also intended to guide the user to appropriate tools as well as selection of tool input parameters. This decision protocol is presented in Chapter 3.0 of this Guidance Manual. Several hypothetical examples are also provided to illustrate tool selection and refining performance risk based on available information. Finally, a worksheet form was developed to walk the user through key design decision steps (User's Guide, Appendix B).

2.2.3.2 Literature Review

A comprehensive literature review supplements this guidance document and has been previously published as a separate WERF report (McCray et al., 2009). Based on the findings reported in the literature, several conclusions were drawn related to modeling tools applicable to OWTS:

- ◆ No single model existed that was appropriate for modeling all wastewater constituents considered in this study. However, it may be possible to develop simple nitrogen models for STUs that predict the effect of different soil types (texture, structure, and drainage class) by adapting existing numerical models to OWTSs.
- ◆ The biggest question in modeling OTWS nitrogen fate is – “To what extent does denitrification occur?”
- ◆ Several studies indicate that differences in soil texture, structure or drainage class are likely to affect denitrification, largely through the effect of soil water content and oxygen availability.
- ◆ The review of existing public domain and commercial models demonstrate that simulation of microbial characteristics in OWTSs is still largely uncharted territory.
- ◆ The primary removal mechanism for bacterial pathogens and protozoa is mechanical filtration. This process is governed by soil texture, treatment depth, and the presence of unsaturated conditions below the infiltrative surface.
- ◆ In contrast, neither soil texture nor treatment depth appears to control the removal of virus particles. Virus removal is primarily determined by the interplay of virus isoelectric point, pH, clay mineralogy, and the level of dissolved organic matter in STE.
- ◆ Several studies have been conducted to model organic wastewater contaminants (OWC) fate and transport. However, OWCs form a broad class of compounds and it is unlikely that a single model or modeling approach will be appropriate for all OWCs.
- ◆ OWC attenuation in the STU is affected by several different factors. A single treatment method does not exist that can reduce the concentrations of all different compounds.

2.2.3.3 Laboratory and Field Experimental Results

The information gained during the literature review aided in the design of laboratory and field experiments conducted at URI and UGA to address data gaps and provide information for the development of the tools within the toolkit. Results from these studies are described in the User's Guide (Appendix C and D).

Laboratory experiments were carried out at URI to study the transport and fate of a model bacterium (*E.coli*) and virus (*MS-2* coliphage) using three types of soils obtained from sites in Rhode Island, Colorado, and Georgia. HYDRUS was then used to simulate microbial transport and fate processes, such as the transport of viruses, colloids, and/or bacteria by either attachment/detachment theory or filtration theory. The primary objective of these laboratory experiments and HYDRUS simulations was to provide the practitioner with guidelines to estimate bacteria and virus removal efficiencies for OWTSs based on a trench design and pulsed loading. The experiments and simulations indicate that the design of OWTSs should focus primarily on bacteria removal. Second, even prior to the formation of a mature biofilm, bacteria removal was quantitative at depths exceeding 70 cm. The removal effectiveness varied only slightly under variably high stress conditions, with changes in the HLR having the comparably greatest impact. Even though the structured clay loam soil from GA efficiently removed bacteria from the aqueous phase, further work is needed to better understand the potential influence of preferential flow transport in structured materials.

The field test site at the UGA was established to conduct OWTS experiments in clayey soil while measuring hydraulic performance and nitrogen movement. These results were then used to develop a 2Dimensional model of water and nitrogen movement and compare the model predictions to the data obtained at the experimental site. Nitrate concentrations in the soil beneath the trenches were generally low, but above background concentrations, and increased with time during the 6 months in which samples were collected. Ammonium concentrations were very low, except immediately below the trench on the last two sampling dates. The CW2D model accurately predicted water movement and pressure heads, but underestimated nitrate concentrations in the soil as observed at the UGA experimental site.

2.2.3.4 Other Materials

Relevant general reference materials (USDA soil textural triangle, conversions for common parameters HLR) are also provided in the User's Guide (Appendix A). This toolkit incorporates the scientific principles as currently understood. However, as research and the behavior of STUs advances, improved tools are expected to be available.

Outreach materials will continue to be developed in support of this toolkit. A range of materials will be considered including conference presentations, journal publications, informational fliers, web-based seminars, and training workshops. Users should view the following websites for updates: www.werf.org, <http://smallflows.mines.edu>, <http://www.uri.edu/ce/wq/OWT/index.htm>, and <http://www.cropsoil.uga.edu/extension/index.html>.

CHAPTER 3.0

STU DESIGN AND TOOL IMPLEMENTATION

While OWTS vary widely in their design and implementation, conventional OWTS rely on septic tanks for retention and digestion of solids in raw wastewater followed by discharge of wastewater effluent to the STU. Like an OWTS, the STU design also varies widely, but generally relies on unsaturated flow for further treatment and eventual recharge to underlying groundwater. In environmentally sensitive areas or where site conditions are not suitable for conventional systems, advanced treatment (e.g., sand filters, textile media filters) may be implemented to decrease constituents of concern (e.g., BOD, total suspended solids, total nitrogen). To select, design, and implement a properly functioning OWTS, it is thus important to assess the operational conditions and parameters that affect treatment performance relevant to the site of interest. This must be done in context of the current knowledge of the site conditions, scientific principles, and treatment and performance goals.

The tools within the toolkit were developed to help the user decide if the uncertainty in STU performance is acceptable based on the specific target goals. In some cases, the tools may suggest additional information should be collected to assess the expected STU performance with more confidence. In all cases, a clear understanding of the site is of utmost importance, whether the user of the tools is interested in the performance of an existing system or is looking to design a new system. In addition, the importance of a soil scientist or other qualified person to describe the soil or other site conditions should not be over looked. The information presented here is intended to aid in choosing the best possible simplifying assumptions for selection and use of tools presented in this toolkit rather than to estimate actual field conditions. In this manner, the enlightened user can make better-informed decisions that account for the uncertainty in the treatment predictions as well as the stakeholders' collective willingness to accept or deny risk under some level of uncertainty. The tools enable the user to start with simple tools that provide some general insight and then use more complicated tools if more data are available, or if more insight into the uncertainty of the predictions is desired. Progressing through simple to more complex tools ultimately guides the user to the simplest tool that is appropriate, but discourages using a tool that is too simple for the decision at hand.

A protocol, in the form of a series of flow charts is provided to guide the user through the series of steps most often incurred during the design decision process. These flow diagrams are intended to aid in the identification of the important steps as well as guiding the user to appropriate tools helpful in aiding selection of tool parameters. Reference within the flow diagrams to look-up tables, CFDs and other information directs the user to the available pertinent information. For a more experienced user, they may wish to start directly with STUMOD or other tool implementation referring to only limited sections of this guidance manual. Alternatively, a worksheet form is provided (User's Guide, Appendix B) that directs the user through parameter selection during use of the tools. Guidance for parameter selection is provided in Chapter 3.0 of the User's Guide.

3.1 Conceptual Design

The first step in assessing OWTS implementation is to develop a conceptual design (Figure 3-1). This process consists of analyzing various approaches to develop a site specific design, including: 1) identifying objectives and treatment goals; 2) analyzing existing information; and 3) making informed assumptions to quickly narrow the range of likely options. Typically general information about the site is gained such as topography, landscape, depth to water table, available STU area, potential set-back limitations, etc. Additional information related to the wastewater source is also obtained such as residential or commercial and expected flow (e.g., the size of the residence, how many occupants reside there). Based on this initial information, an iterative conceptual design process may continue to reduce uncertainty to acceptable limits as warranted by individual conditions. In some situations the conceptual design may be straight forward based on prescriptive guidelines. For example, in a remote location with low OWTS density, adequate soil conditions, residential effluent, and no environmental or public risk, a trench design based on an estimated flow and long-term acceptance rate may be all that is required. However, in other situations, the conceptual design may be a more detailed process of screening several input conditions with several treatment approaches to ultimately optimize the reduction of risk to a sensitive environment. In some situations, advanced treatment should be considered. For the purposes of this toolkit, “advanced treatment” is viewed as pre-treating the STE before discharging to the soil in order to supplement the soil’s ability to remove contaminants.

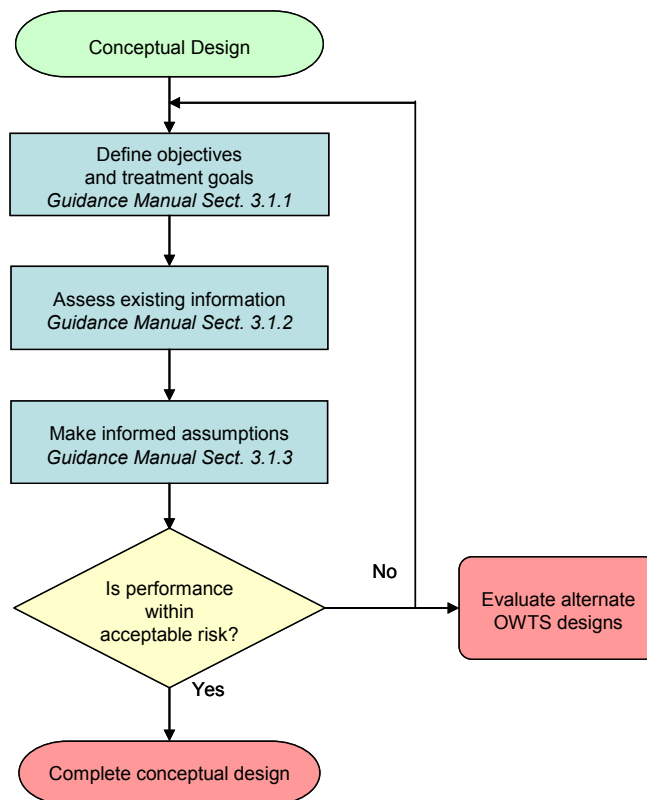


Figure 3-1. Conceptual Design Decision Diagram.

3.1.1 Identify Objectives and Treatment Goals

Specific objectives and treatment goals may vary due to: 1) local regulations (e.g., depth from infiltration zone to water table, nitrogen discharge limits etc.); 2) sensitive areas where protection of the environment is of utmost importance; or 3) significant growth and development. In the past, prescriptive design and siting requirements were often based on the presumption that the system was being maintained such that it is performing to meet implied objectives or treatment goals (e.g., protect groundwater). However, due to budget and staffing limitations, field systems are rarely monitored to verify that the STU is indeed maintained and performing as expected with respect to treatment of wastewater constituents. Furthermore, treatment goals are often specified only after a problem has been identified (e.g., elevated nitrogen concentrations in receiving waters, bacterial detection in drinking water wells, etc.). In these cases, the associated corrective measures can be costly, difficult to implement, and face stakeholder resistance. Decisions are also often made related to lower density suburban development served by OWTS compared to higher density urbanized development served by centralized treatment plants without evaluation of various scenarios based on treatment performance improvement. Thus, it is critical to identify and have a clear understanding of the treatment goals prior to final OWTS design.

3.1.2 Analyze Existing Information

All conceptual designs start with some level of existing knowledge and information. This knowledge and information may be a result of professional experience, specific data collected, or a statistical summary of a range of data. When specific data cannot be obtained, the median value is often a good place to start. When sufficient data are available, look-up tables highlight factors important for consideration and CFD diagrams provide understanding of assimilated data. It is up to the user to assess if existing information or literature data is sufficient or if additional data gathering is required. In all cases, a clear understanding of the site is of utmost importance, whether the user is interested in the performance of an existing system or is looking to design a new system.

3.1.3 Make Informed Assumptions

In order to develop a conceptual design, informed assumptions must be made. Making informed assumptions often requires an iterative process of re-evaluating existing information (Guidance Manual, Section 3.1.2) in the context of treatment objectives (Guidance Manual, Section 3.1.1) (Figure 3-2). To increase the risk of meeting treatment objectives, the uncertainty in the key operational and treatment parameters must be reduced. In some cases, professional experience may provide acceptable certainty to ensure treatment objectives are met. However, in other cases, one outcome may be the requirement to collect specific field data while another outcome may be the implementation of tools within this toolkit to improve the understanding of the expected STU behavior, and yet another outcome may be the need to consider an alternative OWTS design.

Making informed assumptions does not necessarily mean that there is agreement or consensus on the assumption, but rather that the assumption, basis of knowledge, and certainty/uncertainty are clear. In this regard, the assumptions must be defensible. Assumptions

based solely on common understanding are often deficient and may not be defensible. Alternatively, certain scientific principles may underlie common understanding. For example, selection of a higher loading rate may be assumed to lead to higher saturation of the soil, which is linked to higher denitrification, which is theoretically good. However, higher saturation is also associated with faster travel times through the soil reducing the treatment time in the vadose zone. Because the reaction dependencies on soil saturation, and response of soil unsaturated hydraulic conductivity to saturation, are non-linear functions, prediction by intuition alone is difficult. Simplifying assumptions are not in and of themselves bad, but the associated uncertainty and the affect on the output (e.g., decision, spreadsheet model output) are important.

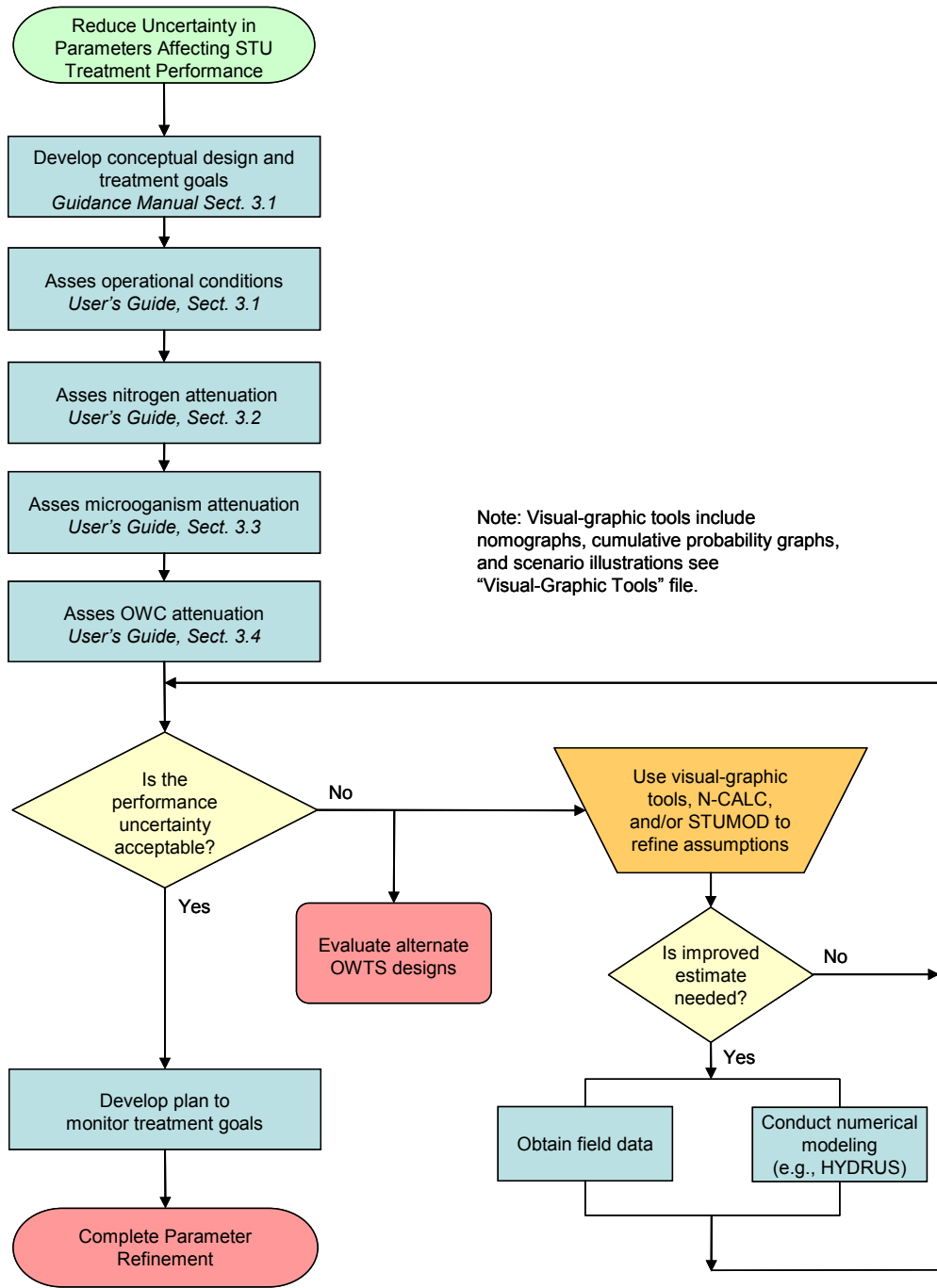


Figure 3-2. Making Informed Assumptions to Reduce Uncertainty Decision Diagram.

3.2 Delineate Operational Conditions

After the initial conceptual design has been developed and assessed delineation of operational conditions continues in order to reduce uncertainty of risk and/or increase the likelihood of meeting defined objectives. In some cases, no further delineation of conditions may be required. However, in other cases additional information may be beneficial to better assess expected treatment performance. Key operational conditions include but are not limited to, gaining a clear understanding of the soil properties, effluent quality characteristics, the expected flows, and potential HLRs (Figure 3-3). Guidance for parameter selection is provided in the User's Guide, Chapter 3.0. Alternatively, a worksheet form is provided (User's Guide, Appendix B) that directs the user through parameter selection during use of the tools.

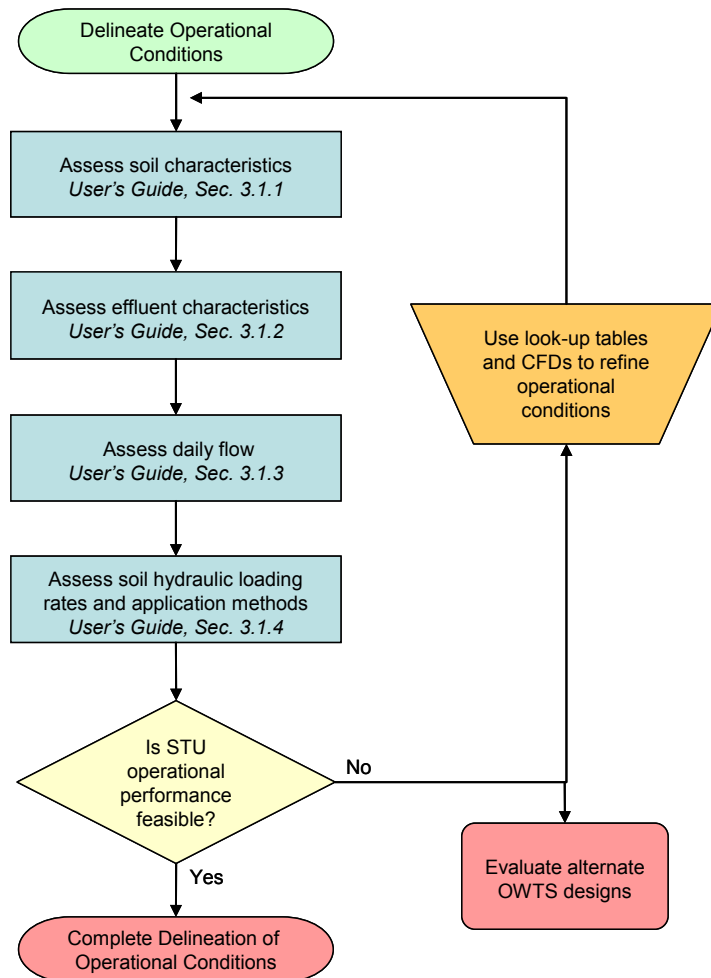


Figure 3-3. Delineate Operational Conditions Decision Diagram.

3.2.1 Assess Soil Characteristics

Specific knowledge of the soil is important prior to using this toolkit because the simple tools are based to a high degree on soil specific properties (Figure 3-4). Soil texture is one of the most important initial operating conditions to be estimated as it influences subsequent hydraulic

and treatment properties. During conceptual design and initial delineation of operating conditions, soil texture may be easily obtained from existing databases (e.g., State Soil Geographic (STATSGO), Soil Survey Geographic (SSURGO), or Natural Resources Conservation Service (NRCS)). Information obtained from a database may also be adequate when a numerical model, such as HYDRUS, is used. However, actual soil samples from the site are especially necessary to finalize OWTS design or if the uncertainty in performance is high (e.g., environmentally sensitive areas). Furthermore, there will be greater confidence in any model output if site-specific information can be obtained.

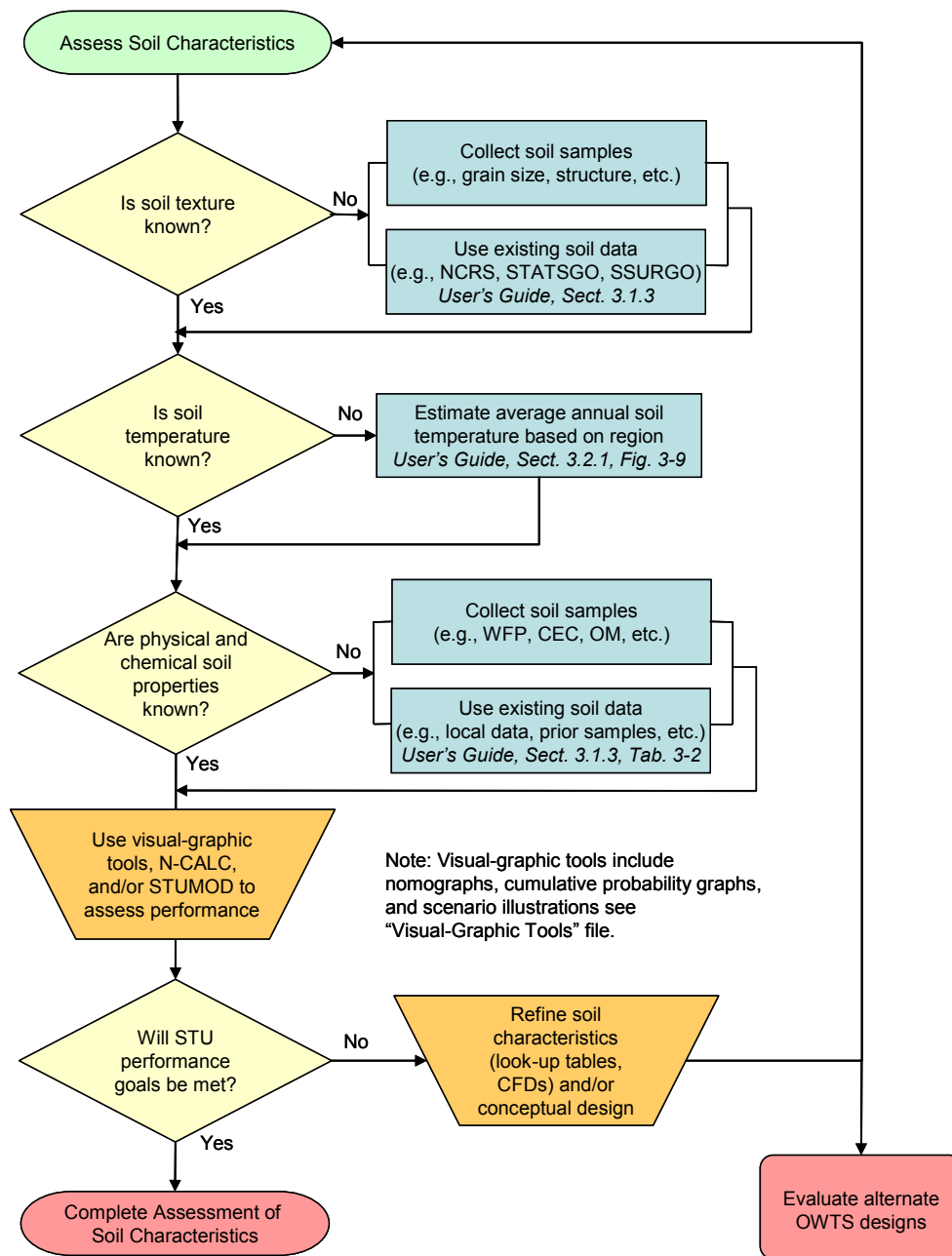


Figure 3-4. Assess Soil Characteristics Decision Diagram.

Soil temperature is also an important soil characteristic that has a direct effect on microbial activity, fate and transport, and plays an important role in nitrogen transformation processes. Soil temperatures at depths relevant to OWTS (0.1 to 3 m below surface) can vary significantly geographically. The average annual soil temperature in the regions of interest can be used as an initial estimate for assessing treatment performance.

Further field assessment is generally necessary to obtain site-specific measurements of physical and chemical soil properties. Physical properties, such as texture, soil profile with depth, soil moisture content with depth, K_{sat} , and depth to groundwater all affect hydraulic behavior and performance. Chemical properties such as seasonal temperature extremes (e.g., frost depth), organic carbon content, and pH may also be important for treatment performance. Site assessment should also identify hydrogeology and climatic conditions that are critical to treatment performance. For example, impediments to unsaturated flow may include restrictive layers in the subsurface, highly heterogeneous soils, seasonal water table fluxuations, or perched water zones. Extreme climatic conditions (drought, seasonal high and low temperatures, precipitation) may also impact soil conditions. These types of information are typically required to run even simple models with even more specific data such as residual and saturated soil moisture (θ_r and θ_s respectively), nitrification and denitrification rates, or van Genuchten parameters (α and n) required for numerical modeling or more rigorous estimates of STU performance.

3.2.2 Assess Effluent Characteristics

The effluent quality applied to the STU is a principle design parameter effecting performance due to mass loading to the STU and the physical, chemical, and microbial requirements for transformation processes. Historically, the effluent quality was often based on BOD_5 and TSS loadings to the soil related to soil clogging concerns (Siegrist, 1988; U.S. EPA, 2002). While these parameters are important for soil clogging, they do not adequately describe the effluent for other objectives such as nitrogen reduction or OWC prevalence. Specific knowledge of the effluent characteristics is important when using this toolkit to understand the effect of effluent quality has on meeting treatment goals (Figure 3-5).

In the case of nitrogen reduction treatment goals, not only is the total nitrogen concentration of interest, but also alkalinity, pH and carbon (Figure 3-6). Alkalinity buffers the pH produced during nitrification with approximately 7 mg L^{-1} of alkalinity (as CaCO_3) required for the nitrification of 1 mg-N L^{-1} (as ammonium-nitrogen). Sufficient alkalinity generally exists in effluent for nitrification, although concentrations can vary. The pH of the effluent will impact the magnitude of nitrification, as the nitrifying microbes are highly sensitive to low pH levels. Although the pH is normally within optimum levels for the microbes, low pH levels may be encountered in some nitrifying systems if the alkalinity is limited. The minimum carbon to nitrogen (C:N) ratio to facilitate denitrification is in the range of 4:1 to 7:1 depending on the form of carbon. If the C:N ratio is lower than 4:1, then sufficient carbon may not be present for denitrification. For residential STE, the C:N ratio is likely within the range of 4:1 to 7:1. Alternatively, for nitrified effluent if the carbon is reduced and nitrate-nitrogen remains high, these conditions may limit subsequent denitrification. Indeed, nitrate contaminated groundwater has occurred, and in such instances it can be assumed that one or more of the requirements for denitrification are not met.

In the case of microorganisms, a wide range of human-pathogenic microorganisms (enteric viruses, enteropathogenic bacteria, and protozoa) are found in STE at concentrations

ranging from not present (e.g., specific virus) to $>10^8$ organism per 100 mL of effluent with infectious doses as low as 1 organism (McCray et al., 2009). The large differences in physicochemical properties among these organisms influence their fate in a STU. Thus, clear differences in factors controlling the fate of pathogenic organisms present in STE pose a challenge for optimization of removal of these organisms in STUs. For example, in principle, the use of soils with a sufficient amount of appropriate clay minerals would increase the probability of removal of viruses, bacteria and protozoa; however, soils with these properties are not evenly distributed in space, either requiring the use of engineered soils using imported clays minerals, or foregoing the benefits of virus removal in areas that lack appropriate clay minerals. Alterations in these design parameters are also likely to affect biogeochemical processes involved in removal of other parameters of interest (e.g., phosphorus and nitrogen) which rely on a particular set of environmental conditions and/or sequence of events to take place. It is generally assumed that the soil provides robust treatment conditions for microorganism removal due to physical straining and filtration. However, if preferential pathways in the STU are known to occur (e.g., fractured bedrock) with potential to contaminate drinking water sources, further assessment of microorganism removal for site-specific soil conditions should be evaluated rather than estimating differences in the effluent quality.

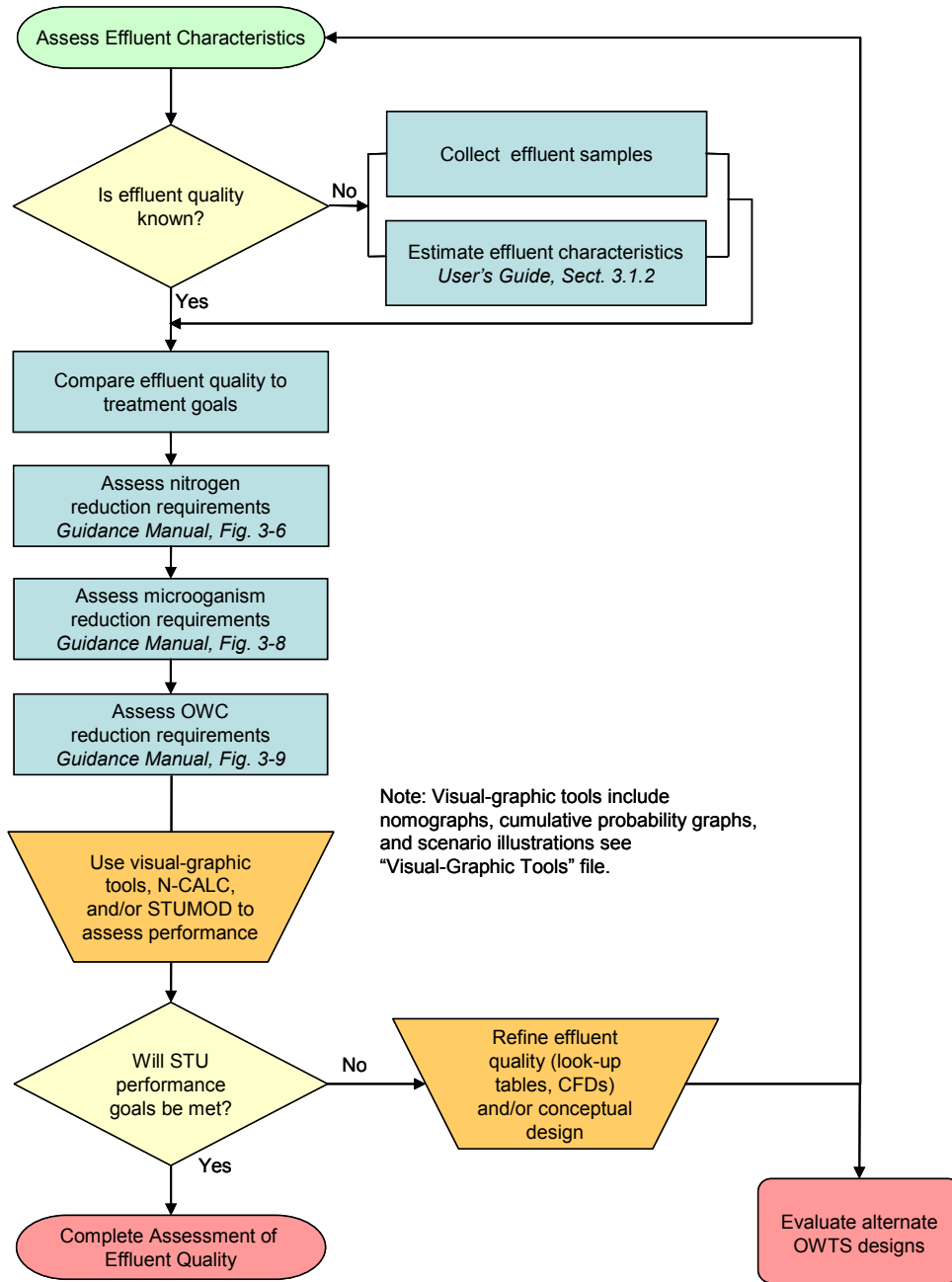


Figure 3-5. Assess Effluent Characteristics Decision Diagram.

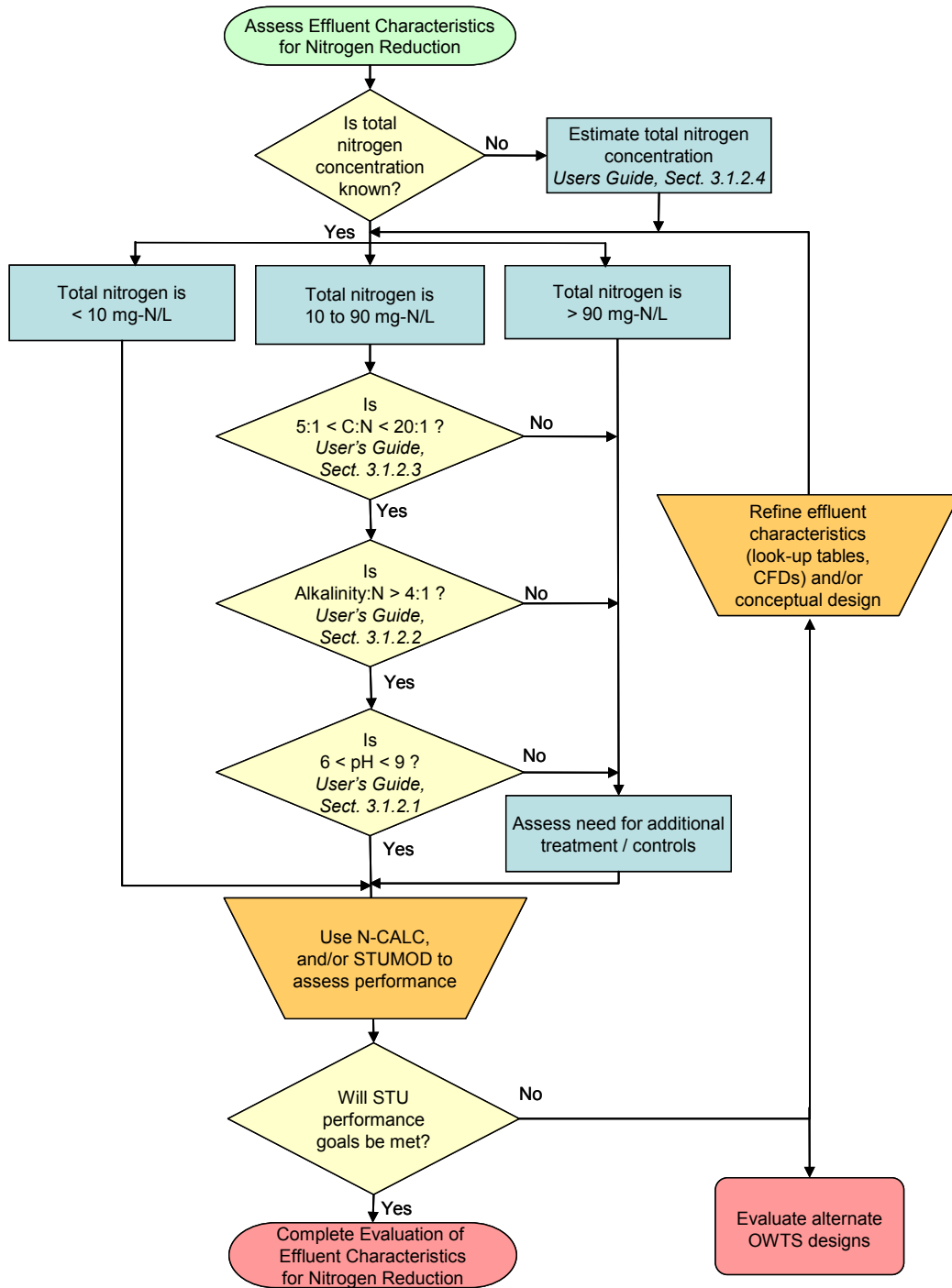


Figure 3-6. Assess Effluent Characteristics for Nitrogen Reduction Decision Diagram.

In the case of organic wastewater constituents, the compounds expected to occur are largely based on the type of onsite source being serviced. While many compounds (detergents, antimicrobials) are fairly ubiquitous in all onsite wastewater sources, the occurrence of some compounds (such as pharmaceutical drugs) depends on the profile of the people contributing to the wastewater stream. The magnitude of concentration may also depend on source type. For

example, a convenience store with scheduled bathroom cleaning times may have higher concentrations of solvents and surfactants at certain times.

Pharmaceuticals, antimicrobials, and other OWCs are often grouped into compound classes based on their function (i.e., antibiotics or cholesterol reducers). However, this grouping does not account for similarities or differences in treatment characteristics. For this toolkit, four common types of OWCs that may require treatment consideration are: 1) detergent/surfactant metabolites; 2) reproductive hormones; 3) phenolic antimicrobials; and 4) acid pharmaceutical compounds (Table 3-1). A comprehensive report on OWCs can be found in “*State-of-the-Science Review of Occurrence and Physical, Chemical and Biological Processes Affecting Biosolids-borne Trace Organic Chemicals in Soils*”, WERF Project SRSK5T09 (Higgins et al., 2010).

Table 3-1. OWC Groups and Examples of Common Contaminants.

Surfactant Metabolites	Reproductive Hormones	Acid OWCs	Phenolic Antimicrobials
Nonylphenols	Estrone	NSAIDs	Triclosan
Nonylphenol Ethoxylates	17β-Estradiol	Salicylic acid	Triclocarbon
	17α-Ethynylestradiol	Gemfibrozil	
	Estriol	Diclofenac	

It is presumed that for new systems, the expected effluent quality must be estimated. However, if the OWTS is already installed, a field sample of the effluent can be obtained. While generally agreed that flow-weighted samples are the most representative, a simple grab sample is often sufficient as changes in constituent concentrations are normalized due the effluent holding time in the septic tank (Van Cuyk et al., 2005; Lowe et al., 2009). In either case, the sample should be collected at a point in the system just prior to discharge into the STU.

3.2.3 Assess Daily Flow

Estimated daily flow is a critical OWTS operation and design parameter typically based on an estimated per capita occupancy of the bedrooms and some expected median per capita water use value. A conservative peak factor may be used (e.g., 1.5 times the average design flow) to ensure performance during high flow periods. Such an approach may be required by local regulations, but may also lead to oversized tanks and/or hydraulic loading of effluent to the STU at a fraction of the design HLR. A clear understanding of actual interior water use may enable OWTS designers and decision makers to evaluate various potential designs and performance implications.

3.2.4 Assess Soil Hydraulic Loading Rate and Application Method

The soil HLR is one of the principle design parameters for OWTS that effects STU performance. Based on the soil type, daily flow, and effluent quality, the appropriate HLR and the distribution method are determined. For conventional STU configurations, HLR is defined in units of length per time (e.g., cm d⁻¹), which is the same as volume per time over area (e.g., gal ft⁻² d⁻¹). For drip dispersal systems, each emitter delivers a nominal rate of 2.3 to 2.5 L hr⁻¹ (0.61 to 0.65 gal/hr) +/- 5% at 7 to 60 psi. For drip dispersal systems, the HLR is a function of the frequency and duration of doses each day for a given length of dispersal tubing (i.e., number of drip emitters).

An estimation of HLR typically begins with a percolation test or textural analysis of the soil (U.S. EPA, 2002), assuming a specific daily flow of STE based on number of bedrooms, occupants and a peaking factor (Guidance Manual, Section 3.2.3). Theoretically, a HLR can be

as high as the K_{sat} of the native soil. However, soil acceptance rates will decline over time even with the addition of potable water (Driscoll, 1987; Van Cuyk et al., 2005). The design HLR, or long term acceptance rate, commonly used in the United States ranges between 1-5 cm d^{-1} (~ 0.2 - $1.2 \text{ gpd ft}^{-2} \text{ d}^{-1}$) (Bouma, 1975; Jenssen and Siegrist, 1990; U.S. EPA, 2002; Beal et al., 2005; Siegrist, 2006).

The soil's ability to transmit water is only one aspect of HLR design, the other is the nutrient loading associated with the effluent. A high HLR results in high nutrient loading on the receiving soil, which creates increased oxygen demand by the microorganisms degrading the wastewater and anaerobic conditions are created when the applied oxygen demand exceeds what diffusion through the soil is able to supply (Otis, 1985; Siegrist, 1988; Tyler and Converse, 1989; Erickson and Tyler, 2001; Van Cuyk et al., 2005). Consequently, the accumulating solids and the metabolic by-products may cause soil clogging and loss of infiltrative capacity (McKinley, 2008).

The range of HLRs is nearly infinite based on soil conditions, effluent quality, and daily flows. Development of visual-graphic illustrations in this toolkit focused on two comparable HLRs; 2 cm d^{-1} and 5% of K_{sat} for all soil textures, climatic conditions and effluent qualities (note scenario illustrations conducted for 10% of K_{sat}). This enables comparison across soil types to highlight key behaviors. For more refined estimation of HLR impacts, one of the spreadsheet models can be used. Both N-CALC and STUMOD, as well as HYDRUS, allow the user to specify the HLR. However, both N-CALC and STUMOD assume a constant steady state HLR (see User's Manual, Chapter 1.0). For more complex loading rates (sidewall infiltration, timed dosing rates, etc.), numerical models such as HYDRUS 2D can be used to simulate these operating conditions.

3.3 Delineate Parameters Affecting Treatment

Based on the initial conceptual design and refined estimates of operational conditions, the feasibility of STU performance to achieve specific goals can be reassessed. Again in some cases a wide range of STU designs may be appropriate and no further evaluation is warranted. In other cases, the need for alternative technologies may need to be re-visited and/or better estimates may be critical to reduce uncertainty in the expected performance. In these later cases, more complex tools may be employed which require additional evaluation of key parameters affecting treatment.

If additional evaluation is required, the parameters affecting treatment performance need to be assessed. Treatment performance in the STU is controlled by several factors, including operational characteristics and physical, chemical and biological properties that ultimately affect the fate and transport of nitrogen, microorganisms and OWC in a STU. While other factors (such as soil mineralogy, microbial population, etc.) may also play an important role in attenuation of different compounds, they are not included in this toolkit as either insufficient information was available for the incorporation of the processes in the tools or simplifying conditions could not be quantified. Specifically, a flexible tool capable of complex scenarios is necessarily quite complex (Users Manual, Chapter 1.0).

3.3.1 Parameters Affecting Nitrogen Attenuation

Relevant key parameters can be identified depending on the defined treatment goals. For nitrogen attenuation, key treatment parameters include but are not limited to, sorption, nitrification and denitrification parameters (Figure 3-7). Guidance for parameter selection is provided in the User’s Guide Chapter 3.0. Alternatively, a worksheet form is provided (User’s Guide, Appendix B) that directs the user through parameter selection during use of the tools.

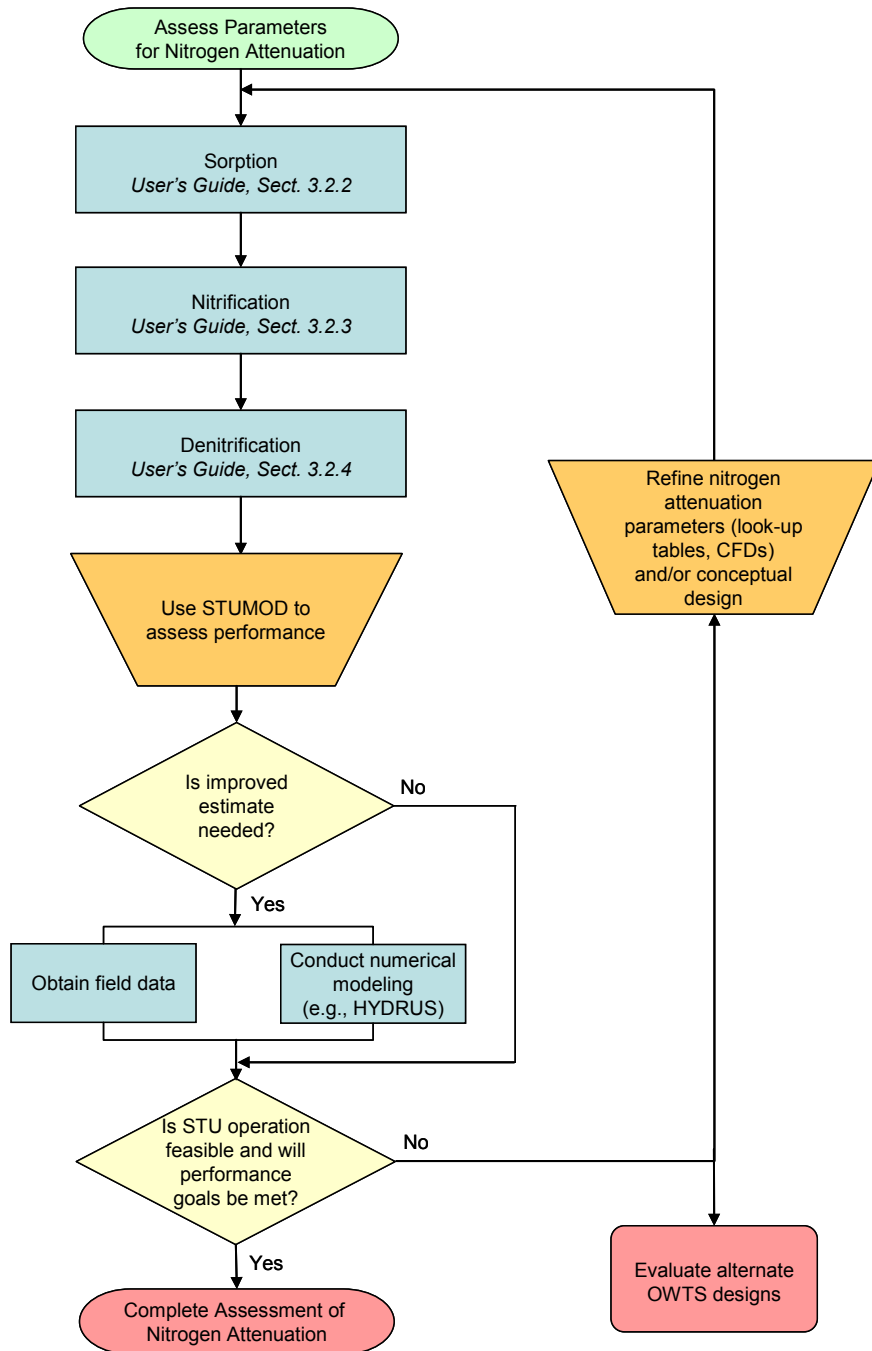


Figure 3-7. Assess Nitrogen Attenuation Decision Diagram.

The basis of nitrogen attenuation is that ammonium-nitrogen is converted to nitrate-nitrogen (nitrification) and nitrate-nitrogen is converted to nitrogen gas (denitrification). Other processes (e.g., ammonification, anammox) may affect nitrogen attenuation, but are not incorporated into the tools as either insufficient information was available or simplifying conditions could not be quantified. Nitrification requires somewhat aerobic conditions while denitrification requires anaerobic conditions. However, both processes depend on the oxygen diffusion rates to and from nitrogen sites which effect kinetic transformation rates in the STU.

Ammonium association with soils is an important process in nitrogen transformation. The sorption process is thought to be controlled by cation exchange processes, which depend on the ionic composition of the soil, as well as the ionic makeup of the effluent. To select an appropriate ammonium sorption coefficient, several factors should be considered including the concentration of ammonium-nitrogen in the effluent, the cation exchange capacity of the soil, the abundance of calcium and magnesium minerals, the abundance of clay minerals, the water filled porosity. See Section 2.1.1 and Section 3.2.2 in the User's Manual for additional information on ammonium sorption and specific parameter selection.

Nitrification is the process where ammonium ions are oxidized to nitrite then to nitrate by autotrophic bacteria. The nitrification rate is an expression of consumption of ammonium and formation of (ultimately) nitrate. To select an appropriate nitrification rate, several factors should be considered including the concentration of ammonium-nitrogen in the effluent, abundance of alkalinity (consumed in the reaction), the pH, the water filled porosity (as a surrogate for oxygen diffusion), and temperature. See Section 2.1.3 and Section 3.2.3 in the User's Manual for additional information on nitrification rates and specific parameter selection.

Denitrification is the process where nitrate is reduced to elemental nitrogen (either as nitrous oxide or nitrogen gas). The denitrification rate is an expression of the consumption of nitrate and formation of nitrogen gas. To select an appropriate denitrification rate, the key factors to consider include available carbon (consumed in the reaction) and the water filled porosity (as a surrogate for oxygen diffusion). See Section 2.1.4 and Section 3.2.4 in the User's Manual for additional information on denitrification rates and specific parameter selection.

3.3.2 Parameters Affecting Microorganism Attenuation

In general, pathogens carried with the percolating STE are most likely to be attenuated in subsurface (Lance and Gerba, 1984). Factors influencing the transport and fate of microorganisms in the subsurface include the nature of the soil, microorganism type, attachment/detachment rates, filtration, temperature, microbial activity including the presence of other microorganism, inactivation, moisture content, pH, organic matter content, and hydraulic conditions including advection-dispersion (Jin and Flury, 2002) (Figure 3-8). In the case of viruses, the inactivation rate is considered the single most important parameter in groundwater systems (John and Rose, 2005), which is often slower than the rate of die-off of other pathogens, such as infectious bacteria (Faulkner et al., 2003). However, there is not yet a consensus on which factor(s) have the greatest impact on eliminating microbial matter in general.

In the study of the transport and fate of microbial matter, mathematical models in combination with direct observation, can be useful tools for the quantitative assessment of microbial transport and fate in the subsurface. To develop guidelines for practitioners to estimate bacteria and virus removal efficiencies in STUs, laboratory experiments were carried to study the

transport and fate of a model bacterium (*E.coli*) and virus (*MS-2* coliphage) in three soils: sandy soil (from Rhode Island), sandy loam (from Colorado), and structured clay loam (from Georgia). Removal efficiency was then simulated, based on a trench design with dosed loading under variable HLRs, precipitation patterns, initial microbe concentrations and other environmental stresses. These simulations suggest that the removal of *E.coli*: 1) decreased with decreasing HLR, 2) was independent of initial *E.coli* concentration, and 3) increased with precipitation or irrigation events (although the increase was relatively short termed). Simulations were not conducted for the removal of *MS-2* because the laboratory results indicated that the removal of *MS-2* (viruses) was much more effective relative to *E.coli* (bacteria)). Complete results of the laboratory testing and simulations are provided in the User's Manual, Appendix D. Results from the laboratory experiments coupled with numerical modeling using HYDRUS-2D suggest high removal could be attained in the STU. However, specific simple tools could not be developed to address microorganism attenuation in the STU because attenuation relies on difficult to obtain field parameters (User's Guide, Appendix D).

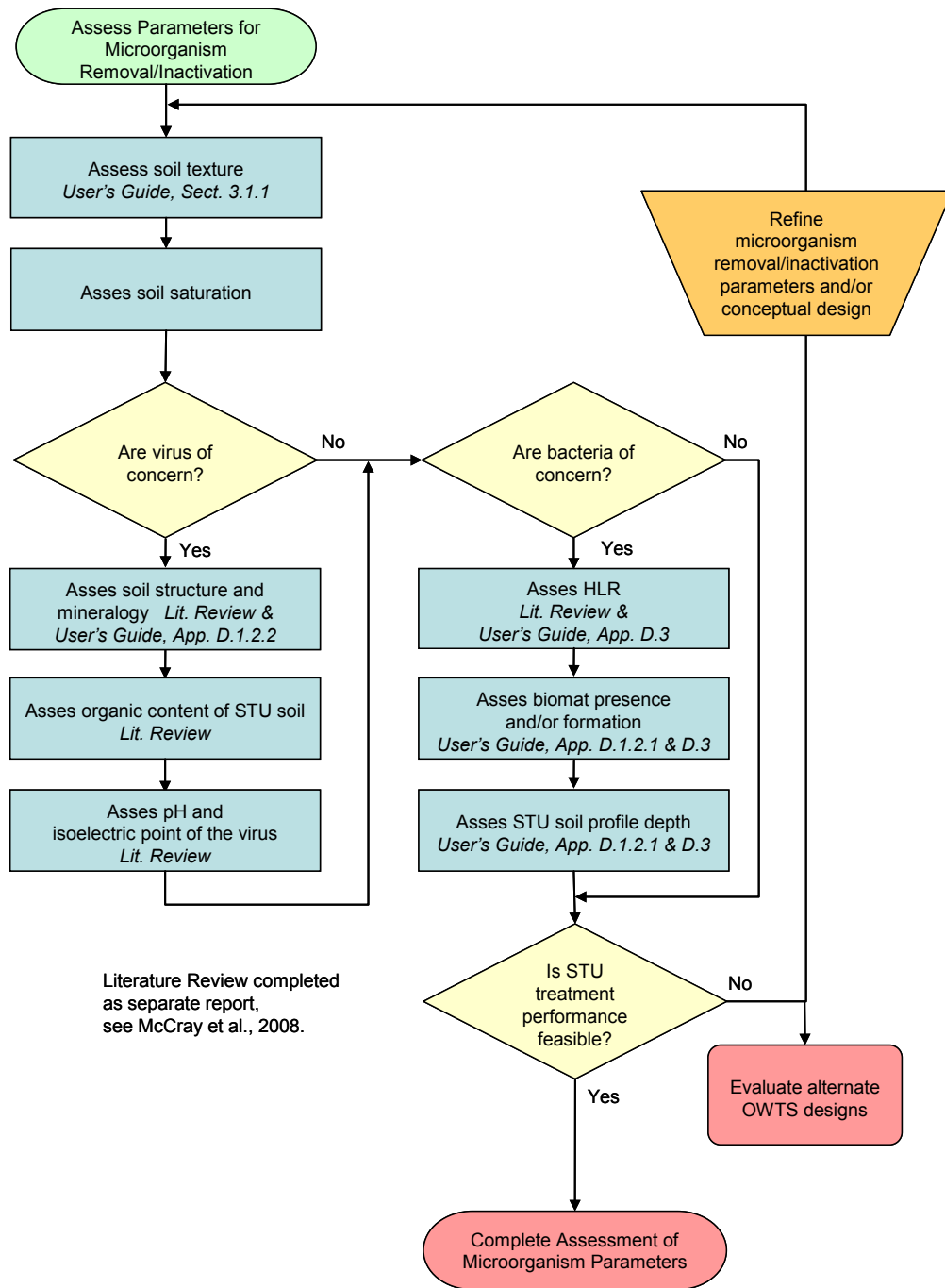


Figure 3-8. Assess Microorganism Removal/Inactivation Decision Diagram.

3.3.3 Parameters Affecting Organic Wastewater Contaminant Attenuation

OWCs, often referred to as emerging contaminants, pharmaceuticals and personal care products, or organic micro-pollutants, are being detected in surface water and groundwater influenced by OWTSs (Drewes et al., 2003; Zimmerman, 2004). Where OWTS sources are concerned, these compounds may be released into the STU from the effluent of the septic tank or

other treatment units. Based on the mechanisms for removal that are characteristic of many of these compounds, a well designed STU has the potential to reduce concentrations to negligible amounts for most OWCs, although the responsible microbiological, chemical, and physical mechanisms are not yet well understood.

OWCs form a broad class of compounds, and thus no single model or tool is appropriate. Because of the variety of compounds, estimating treatment efficiencies for a specific STU includes a high degree of uncertainty at this time. However, known fate and transport mechanisms important for estimating treatment of OWCs include, but are not limited to, biodegradation, sorption, and abiotic degradation (Figure 3-9). Based on the characteristics of different OWCs, limiting STU treatment conditions include: 1) shallow depth to water table or confining layer, 2) low organic carbon content in soil, 3) anoxic soil conditions, and 4) high effluent pH. The depth to groundwater or a confining layer is important for conditions where OWCs do not strongly sorb to soils with low organic carbon and for soils that drain relatively quickly. The carbon content is important as the primary sorption mechanism for most of the targeted OWCs is hydrophobic partitioning to organic matter, while in other cases, pH-dependent organic matter partitioning may play a role (Higgins et al., 2010). Anoxic soil conditions are also important as many OWC compounds biodegrade aerobically, although some OWCs have been shown to undergo anaerobic biodegradation at lower rates. Finally, high pH effluent may affect the ability of acidic OWC compounds to sorb to soil particles.

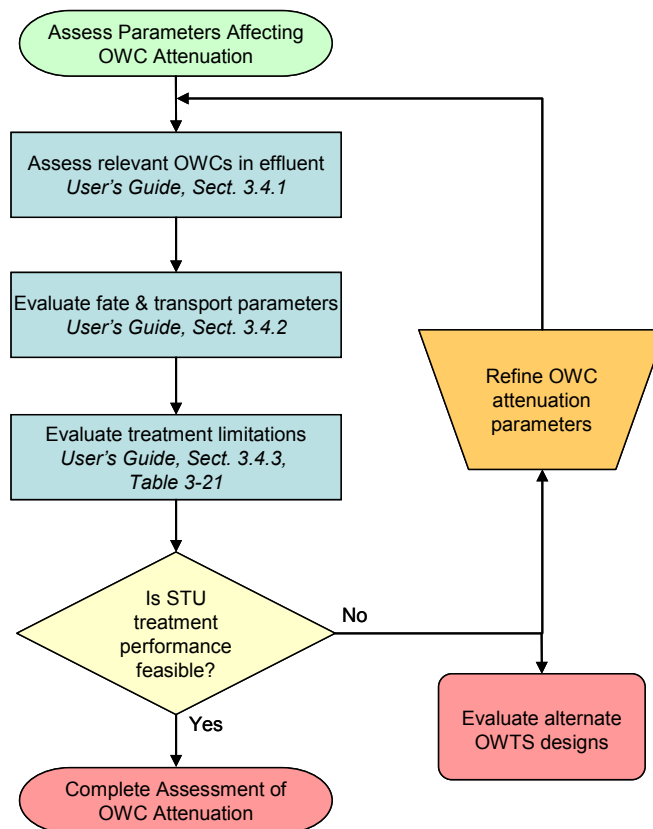


Figure 3-9. Assess OWC Attenuation Decision Diagram.

3.4 Guidance for Tool Selection and Use

The toolkit has been designed to be hierarchical in nature with tools that are diverse with regard to their ability to incorporate complexity, user sophistication, and appropriateness for use. During initial planning and conceptual design through detained design, the tools within this toolkit can be used to further refine key parameter selection thereby reducing the uncertainty of the STU performance assessment (Guidance Manual, Section 1.3.2). Selection and use of the appropriate tool depends on the: technical expertise of the user, the objectives and treatment goals, and the compound of interest. In context of the objectives and treatment goals, ideally the simplest tools are the first to be used. The simplest tools serve as screening tools to aid decision making as to whether further action is needed. However, simple tools cannot incorporate many of the complexities associated with different OWTS sites or pollutant treatment processes. If more detail is needed, spreadsheet tools can be used which are rigorous enough to include most relevant hydraulic and nitrogen-transformation processes, but still simplify the processes incorporated in numerical models. Finally, if more complex processes and/or less-common operating conditions need to be evaluated, a numerical model such as HYDRUS should be used.

For less experienced or non-technical users, visual graphic tools such as look-up tables and CFDs can be used to guide parameter selection (e.g., median value from a CFD, some arbitrary value within the parameter range based on relative conditions described in a look-up table). Alternatively visual-graphic tools illustrating STU performance for specific conditions can be compared to identify how key parameters are expected to affect STU performance. N-CALC and STUMOD are spreadsheet tools that are relatively simple to use for personnel trained in the natural sciences or engineering. Both of these spreadsheet tools allow the user to evaluate ranges of STU performance based on likely variations in operating conditions, soil hydraulics, and/or treatment parameters. N-CALC is based on a simplification of the general advection dispersion equation and is intended as a screening level tool that can be used where input data is limited. STUMOD was developed based on existing fundamental principles of water movement and contaminant transport, but is not theoretically appropriate for shallow water tables and does not explicitly account for any soil layering in the subsurface. Again, for more complex environmental or operating conditions, a numerical model such as HYDRUS should be used.

The following examples illustrate selection and use of tools provided in the toolkit to refine assumptions while reducing the uncertainty in the estimated outputs. In these hypothetical cases, treatment goals are evaluated for different conditions. The described cases are hypothetical to illustrate selection and use of the tool and not intended to necessarily represent a “real-world” case. It is up to the user to define the individual case of interest, but it is important that appropriate selection of the tools and limitations of the outputs are understood to minimize misuse of the toolkit.

3.4.1 Hypothetical Example 1: Conventional STU Performance

In this hypothetical case, conventional STU performance is evaluated for a location in Iowa, receiving “standard” effluent, with the treatment goal of achieving 50% reduction of total nitrogen at 60 cm below the trench bottom. The following steps outline selection and use of the tools.

- 1) **Determine the soil texture at the site:** Based on local NRCS maps for central Iowa, the soil texture is assumed to be sandy loam. It is also assumed that there are no limiting or unfavorable conditions (e.g., restrictive soil layers, high groundwater table, etc.).

- 2) **Determine the expected effluent quality:** Based on the CFD for nitrogen concentrations (User’s Manual, Figure 3-4) the median value of 54 mg-N L⁻¹ as ammonium is assumed.
- 3) **Choose a preferred HLR:** Because of the uncertainty in the daily flow, effluent quality, soil texture and structure, an average HLR of 0.4 gal ft⁻² d⁻¹ (~2 cm d⁻¹) is chosen for sandy loam from the “Tyler Table” (U.S. EPA, 2002).
- 4) **Determine the average annual soil temperature:** Based on the regional soil temperature map (User’s Manual, Figure 3-9) Iowa is located in the “mesic” soil temperature region.
- 5) **Summary of Example 1 initial conditions are:**
Treatment Goal: 50% reduction of nitrogen at 60cm
Soil Texture: Sandy loam
HLR: 2 cm d⁻¹
Effluent Nitrogen Concentration: 54 mg-N as ammonium
Location: Iowa, mesic temperature region (annual mean soil temperature = 11.5°C)
- 6) **Use nomographs for initial screening:** First, the appropriate nomograph to assess treatment at the desired soil depth (in this case 60 cm below the trench bottom) must be located. Based on the above assumptions, the nomograph that most closely represents the hypothetical conditions is for sandy loam soil, receiving standard effluent (60 mg-N L⁻¹) at a rate of 2 cm d⁻¹ (Visual-Graphic Tools, Figure VG-29). As illustrated in Figure 3-10 (red circle), the nomograph suggests ~20% of total nitrogen is expected to be removed at 60 cm depth in a “mesic” temperature region. This outcome does not meet the target goal of 50% nitrogen reduction with 60 cm of soil.

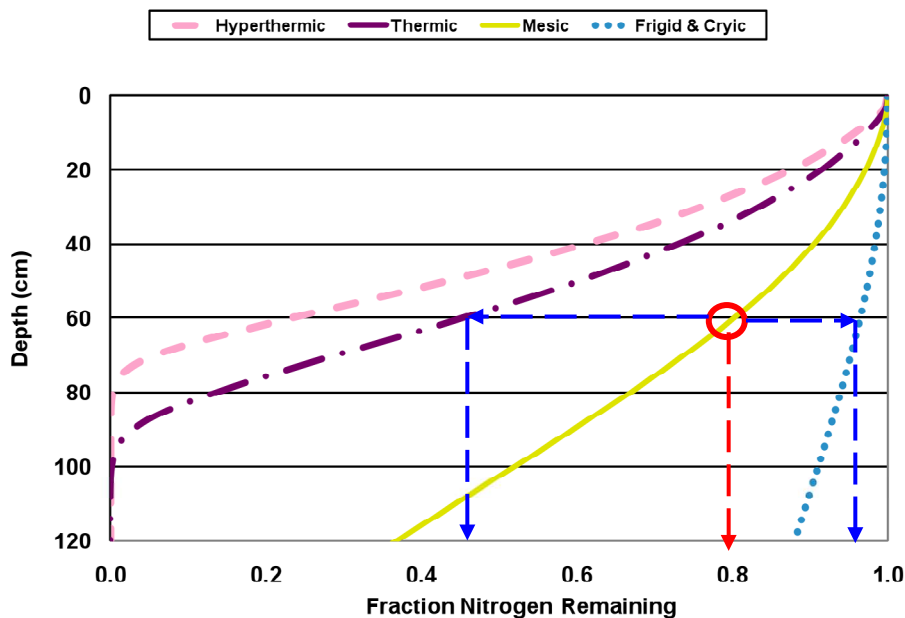


Figure 3-10. Nomograph Most Closely Illustrating Example 1 Conditions.

Note, actual conditions of nomograph are: sandy loam soil, HLR = 2 cm d⁻¹, 60 mg-N L⁻¹ as ammonium effluent concentration.

- a. It is important to note that Figure 3-10 illustrates the expected behavior of different temperatures on nitrogen removal for the defined conditions (sandy loam soil, 2 cm d^{-1} HLR, 60 mg-N L^{-1} as ammonium effluent concentration). Specifically, as temperature varies such as winter in Iowa (blue dashed line to the right) a higher fraction of nitrogen will remain in the soil (~ 0.95) while in warmer temperatures such as summer in Iowa (blue dashed line to the left) a lower fraction of nitrogen will remain in the soil (~ 0.45). In this manner, assuming the same Example 1 initial conditions (sandy loam soil, 2 cm d^{-1} HLR, 54 mg-N L^{-1} as ammonium effluent concentration), but in Wisconsin (frigid/cryic climate) the treatment goals are less likely to be achieved and additional refinement with the tools is necessary. Alternatively these same initial conditions, but in Arkansas (thermic climate) the treatment goals will likely be achieved and no further refinement is necessary.
- b. Because there is uncertainty in the input parameters used to generate the nomographs, a complementary cumulative probability graph can be used to assess this uncertainty or underlying risk of achieving the treatment outcome. After selecting the complimentary cumulative probability graph (Visual-Graphic Tools, Figure VG-177), first find the fraction nitrogen remaining from Figure 3-10 (red solid arrow = 0.8). Now go to the cumulative probability graph (Figure 3-11), locate this same fraction of nitrogen remaining on the x-axis and go up vertically (red solid arrow) until you intersect the soil depth of interest (red circle). From this intersection now go left horizontally (red solid arrow) to the y-axis and determine the associated uncertainty of the nomograph condition (0.8 Fraction Nitrogen Remaining, 60 cm depth), which is $\sim 30\%$ in this case.

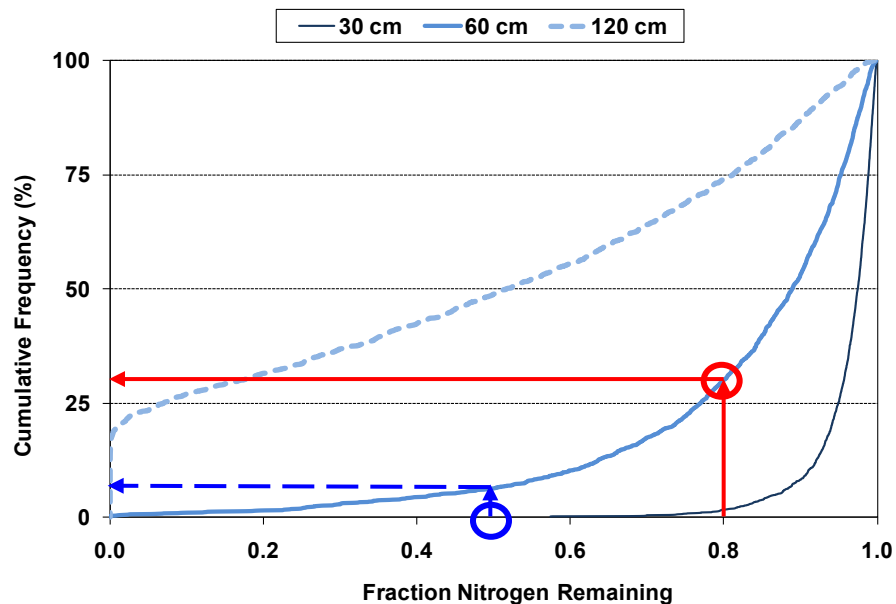


Figure 3-11. Monte Carlo Cumulative Probability Graph for Three Different Soil Depths for Example 1 Conditions.
 Note, actual conditions of the cumulative probability graph are: sandy loam soil, thermic temperature region, $\text{HLR} = 2 \text{ cm d}^{-1}$, 60 mg-N L^{-1} as ammonium effluent concentration.

- c. In this example, the cumulative probability graph suggests there is a 30% probability that the output condition (Fraction of Nitrogen Remaining) will be less than 0.8. Alternatively there is a 70% probability that the fraction of nitrogen remaining in the soil will be greater than 0.8. Another way to express the same finding is that the fraction of nitrogen remaining at 60 cm is expected to be less than 0.8 (20% nitrogen removal) 30% of the time.
 - d. Another way of using the cumulative probability graph (Figure 3-11) is to locate the treatment goal on the y-axis (blue circle), go vertically up to the 60 cm soil depth line (blue dashed line), then horizontally over to the x-axis to determine the percent likelihood of achieving that goal. In this case the probability of achieving a 50% removal at 60 cm is only ~10% which may be insufficient and further evaluation is warranted.
 - e. In some cases this treatment outcome with associated uncertainty may be sufficient. However, for this example, the estimated treatment at 60 cm does not achieve the treatment goal of 50% removal of total nitrogen (0.5 fraction of nitrogen remaining) within comfortable uncertainty limits and further delineation of conditions and parameter inputs are warranted.
- 7) **Run spreadsheet tools to reduce uncertainty:** If more accurate results are required beyond the nomographs to reduce uncertainty, N-CALC or STUMOD spreadsheet tools can be used. For this example, STUMOD simulation based on the Example 1 initial operational conditions illustrates that the total nitrogen was reduced from 54 mg-N L⁻¹ to ~42 mg-N L⁻¹ (Figure 3-12). This evaluation results in 30% removal (Figure 3-13), which does not meet target goal of 50% nitrogen removal. This output is expected and in agreement with the nomograph evaluation.

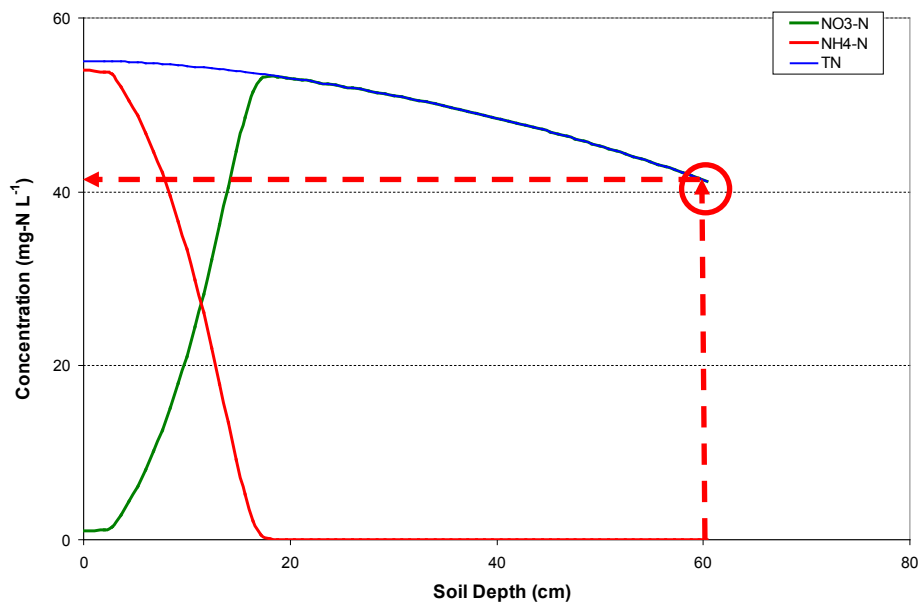


Figure 3-12. STUMOD Output Graph Illustrating Nitrogen Concentrations Assuming Example 1 Initial Conditions.

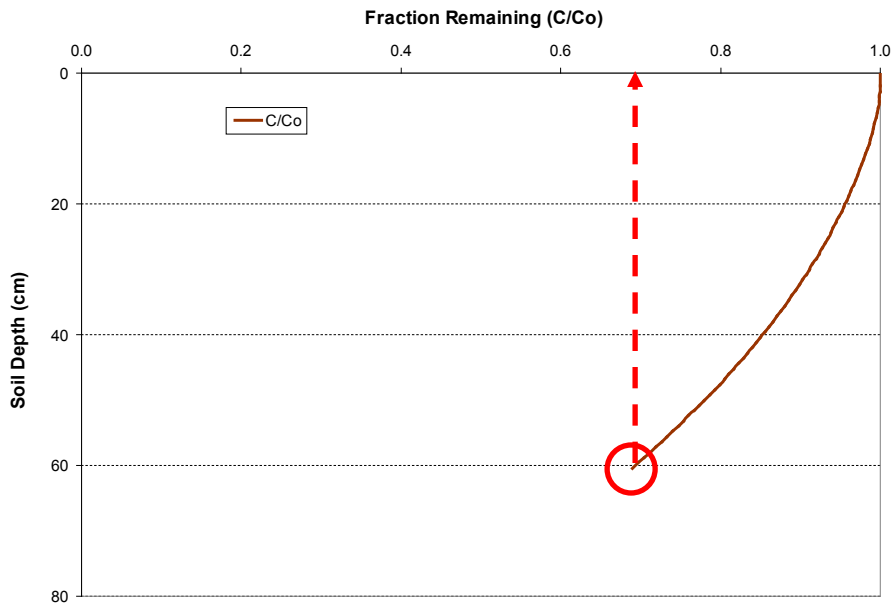


Figure 3-13. STUMOD Output Graph Illustrating the Fraction of Nitrogen Remaining in the STU Assuming Example 1 Initial Conditions.

- 8) **Refine initial conditions to achieve treatment goals:** To achieve the 50% removal goal, further refinement in operational conditions can now be assessed. For this example, further refinement of operational conditions is done using STUMOD.
- a. If the HLR is changed to 1 cm d^{-1} and no other parameters are changed, the STUMOD output suggests no improvement in treatment performance. Further evaluation of HLR using STUMOD suggests that for these initial conditions, the HLR does not control performance. For example, even reducing the HLR to an unreasonably low value (e.g., 0.01 cm d^{-1}) results in similar treatment performance. However, a similar type of evaluation where only the temperature is varied and no other parameters are changed, suggests that at higher soil temperatures (e.g., 17°C) total nitrogen was reduced from 54 mg-N L^{-1} to $\sim 26 \text{ mg-N L}^{-1}$ (Figure 3-14) or $\sim 50\%$ removal (Figure 3-15). This result may suggest that in warmer summer months the treatment goal is likely to be met, but during the remainder of the year the target goal may not be met. The user can then determine if this would be an appropriate field condition, if further STUMOD refinement is warranted, or a field evaluation should be conducted.

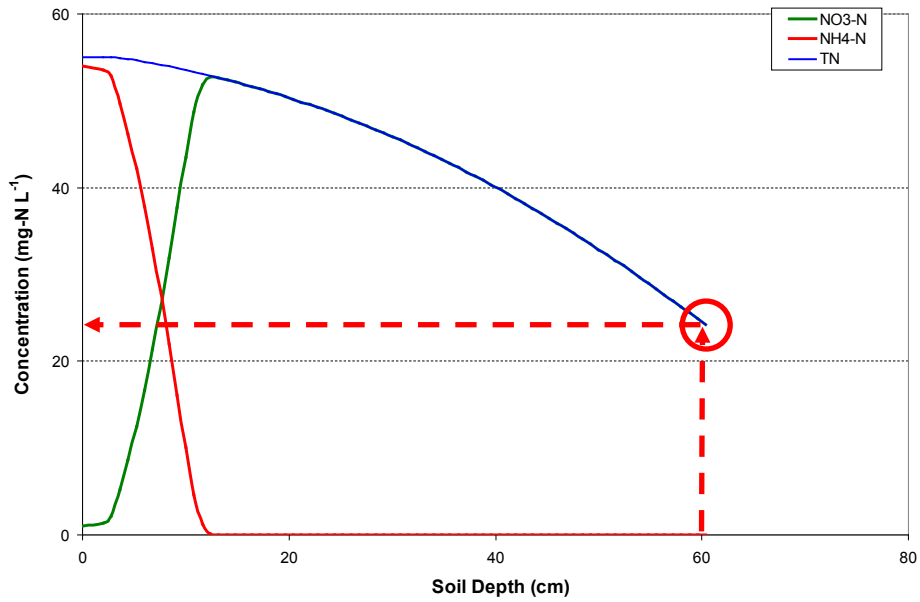


Figure 3-14. STUMOD Output Graph Illustrating Nitrogen Concentrations for Example 1 at Temperature = 17°C.

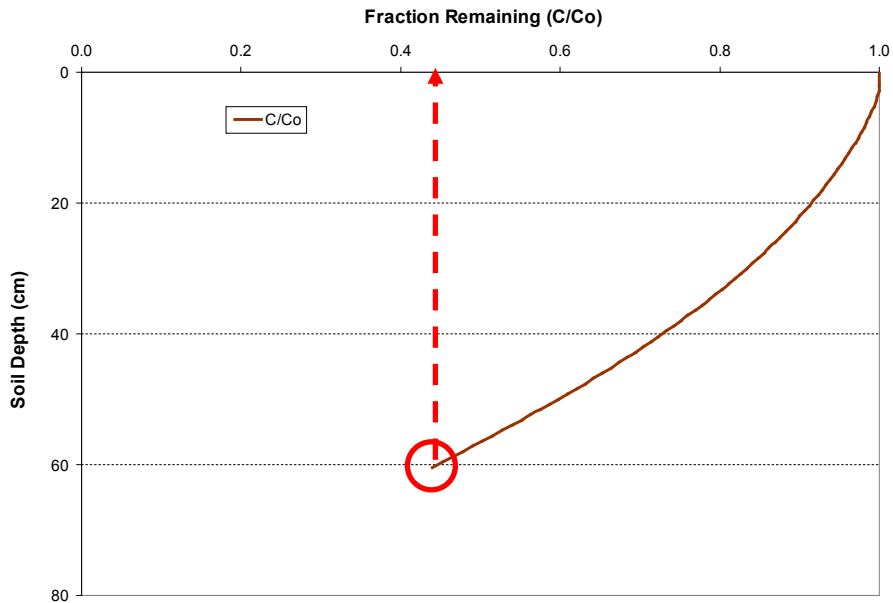


Figure 3-15. STUMOD Output Graph Illustrating the Fraction of Nitrogen Removed for Example 1 at Temperature = 17°C.

- b. If it is unreasonable to alter the HLR (e.g., expected daily flow, a limit to the design area, regulatory limitations, etc.) removal with depth can be evaluated to determine if the treatment goal can be achieved at greater soil depths. In this case the target depth in STUMOD is changed to 120 cm. Now evaluation of the nitrogen concentration

indicates the initial concentration of 54 mg-N L^{-1} has been reduced to $\sim 13 \text{ mg-N L}^{-1}$ (Figure 3-16), which is $\sim 75\%$ nitrogen removal (Figure 3-17).

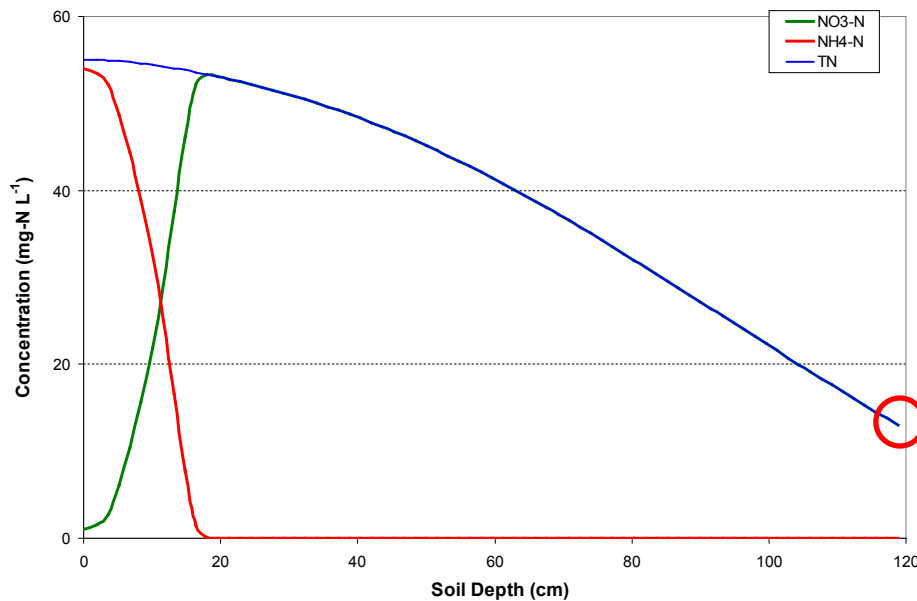


Figure 3-16. STUMOD Output Graph Illustrating Nitrogen Concentrations for Example 1 at a Soil Depth of 120 cm.

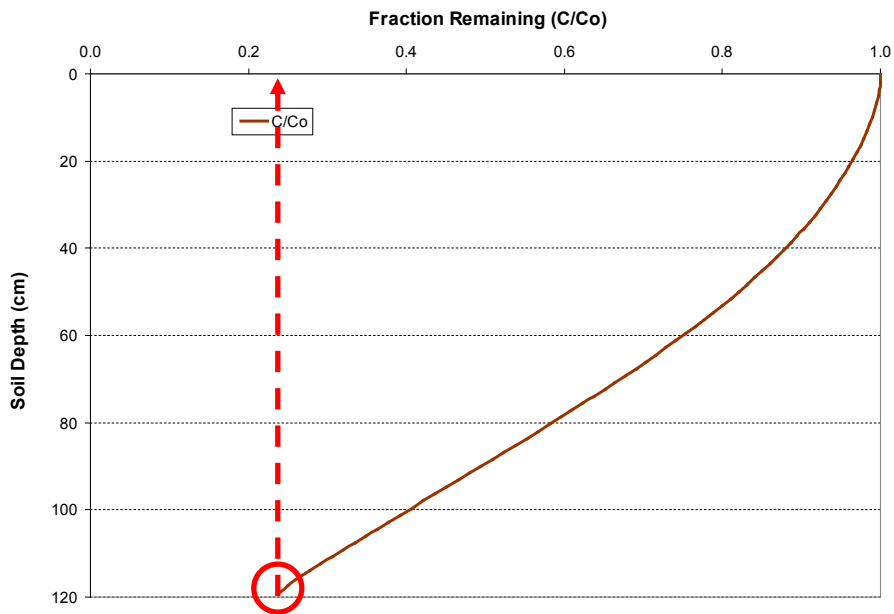


Figure 3-17. STUMOD Output Graph Illustrating the Fraction of Nitrogen Removed for Example 1 at a Soil Depth of 120 cm.

- c. Further refinements may include changing other input parameters within STUMOD such as denitrification rates, half-saturation constants or effluent concentration to continue to evaluate the limits of the operating and environmental conditions able to

achieve the treatment goals. However, the accuracy of the model output depends on whether better information is available than the values initially used. In either case, this exercise provides the user with the sense of which parameters have the greatest effect on STU treatment performance. This information in turn enables better understanding of the limiting conditions and enables the user to evaluate the likelihood of realizing those conditions at the site.

- d. In the case of effluent quality, it could be assumed that additional treatment would be employed to produce effluent with ammonium concentrations of 10, 20, or 30 mg-N L⁻¹. When STUMOD is run for these three different initial effluent concentrations, the resulting nitrogen concentration with depth can be evaluated (Table 3-2).

Table 3-2. Summary of STUMOD Outputs for Different Initial Ammonium-nitrogen Concentrations.

Initial Ammonium-nitrogen Concentration (mg-N L ⁻¹)	Nitrate-nitrogen Concentration (mg-N L ⁻¹) at Soil Depth Below Trench			
	0 cm	30 cm	60 cm	90 cm
10	10	7.2	2.2	<1
20	20	16.5	8.9	1.6
30	30	26.3	17.5	6.6

- 9) **Revisit treatment goals and operational constraints:** Following the refinement of parameter selection using STUMOD, the achievability of the initial treatment objectives can be re-assessed with the stakeholders and a revised conceptual design developed as appropriate.

3.4.2 Hypothetical Example 2: Nitrified Effluent with Low Available Carbon

Nitrified effluent can be evaluated in STUMOD (e.g., initial effluent concentration as nitrate-nitrogen rather than ammonium-nitrogen); however, the underlying assumption is that sufficient carbon is present for denitrification. In some cases, STE may be aerobically treated transforming the ammonium to nitrate while also reducing carbon concentrations. Because STUMOD does not incorporate a carbon function, Example #2 evaluates the effect of low carbon content by reducing the denitrification rate. In this example the STU performance is evaluated for a location in Southern Missouri, with silty clay soil texture and a target treatment goal of achieving 50% reduction of total nitrogen at 30 cm below the trench bottom.

- 1.) **Example 2 initial conditions:**

Soil Texture: Silty Clay

HLR: 2 cm d⁻¹

Effluent Nitrogen Concentration: 70 mg-N L⁻¹ as ammonium-nitrogen and 1 mg-N L⁻¹ as nitrate-nitrogen

Location: Southern Missouri, thermic temperature region (annual mean soil temperature = 18.5°C)

Treatment Goal: 35 mg-N L⁻¹ (50% reduction of nitrogen) at 30 cm

- 2.) **Run STUMOD with default conditions for base case:** The STUMOD simulation based on the initial operational conditions and the default input parameters, illustrates that the total nitrogen was reduced from 71 mg-N L⁻¹ to ~45 mg-N L⁻¹ at 30 cm (Figure 3-18). The STUMOD output suggests that while the target goal of 50% nitrogen removal at 30 cm is not met, it could be met with an additional 10 cm of soil depth.

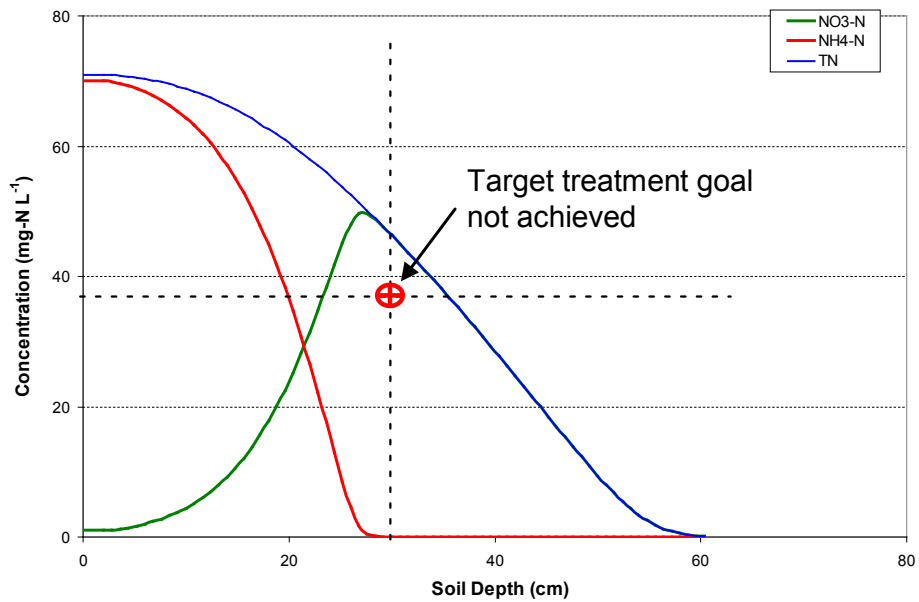


Figure 3-18. STUMOD Output for Example 2 Initial Conditions.

- 3.) **Run STUMOD assuming pretreatment to reduce nitrogen:** Next STUMOD is again run, but this time assuming that some form of advanced treatment prior to the STU will be employed achieving 25% nitrogen reduction. In this case, the STUMOD simulation is based on an initial effluent concentration of 52.5 mg-N L⁻¹ as nitrate-nitrogen and 1 mg-N L⁻¹ as ammonium-nitrogen, again using the default input parameters. The STUMOD output now suggests that the target goal is achieved (Figure 3-19). However, if it is expected that the carbon content may limit denitrification, the effect of a lower denitrification rate on the STUMOD output can be evaluated.

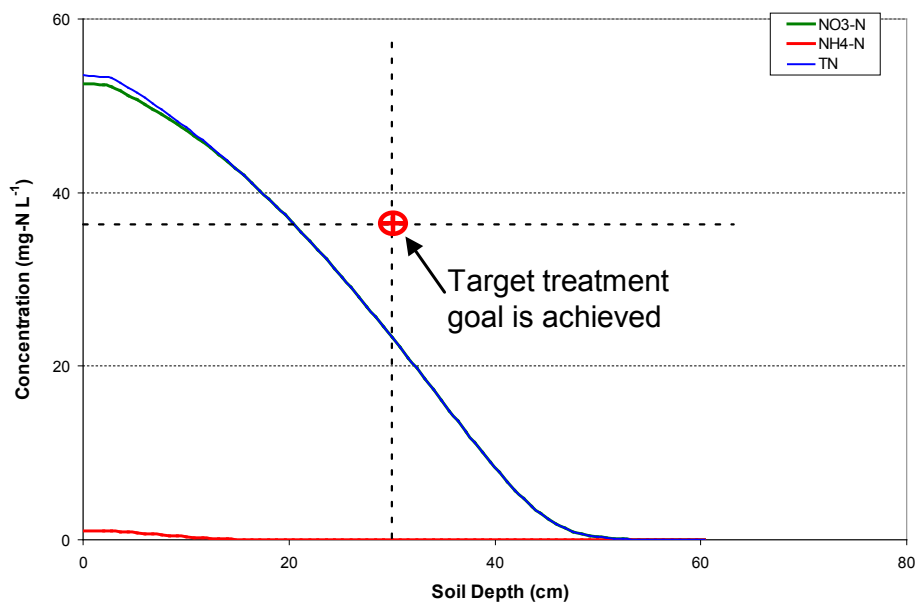


Figure 3-19. STUMOD Output for Example 2 Assuming Advanced Treatment Prior to the STU.

4.) **Evaluate denitrification rate effect:** Iterative runs of the same initial conditions, but changing only the denitrification rate, suggests that a minimum denitrification rate of $1.8 \text{ mg-N L}^{-1} \text{ d}^{-1}$ is required to achieve the target treatment goal, assuming advanced treatment resulted in a nitrified effluent with 25% nitrogen reduction (i.e., 52.5 mg-N L^{-1} as nitrate-nitrogen for input condition) (Figures 3-20 and 3-21). Comparing this denitrification rate to the CFD compiled from reported literature values (User's Guide, Figure 3-18), indicates that approximately 43% of the maximum denitrification rates reported in the literature were below the value of $1.8 \text{ mg-N L}^{-1} \text{ d}^{-1}$ (Figure 3-22).

This is a more conservative assumption than the STUMOD default condition, but an even more conservative estimate may be warranted. For example, choosing the 25th percentile rate on the CFD would be indicative of even less available carbon. After running STUMOD with the 25th percentile value ($0.29 \text{ mg-N L}^{-1} \text{ d}^{-1}$), the fraction nitrogen remaining at 30 cm is 0.95, i.e., the initial nitrogen concentration was only lowered 5% ($\sim 47.4 \text{ mg-N L}^{-1}$ remaining at 30 cm).

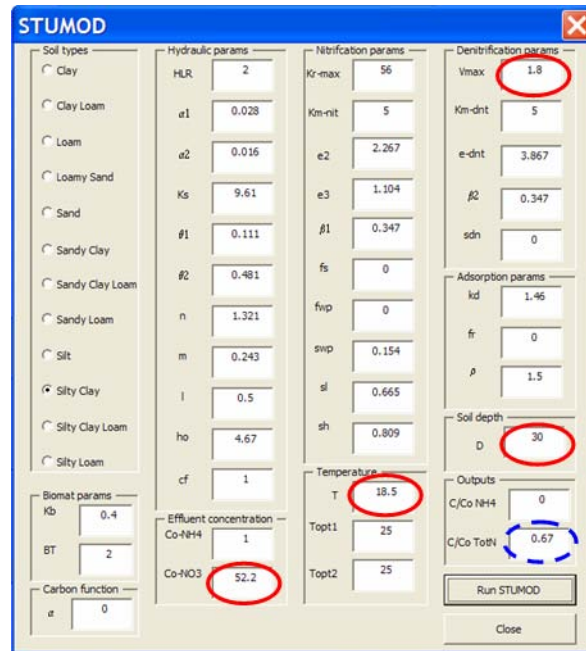


Figure 3-20. STUMOD user input interface for Example 2. Red (solid) circles illustrate changes in input values. Blue (dashed) circle highlights the simulated fraction of nitrogen remaining at the selected soil depth.

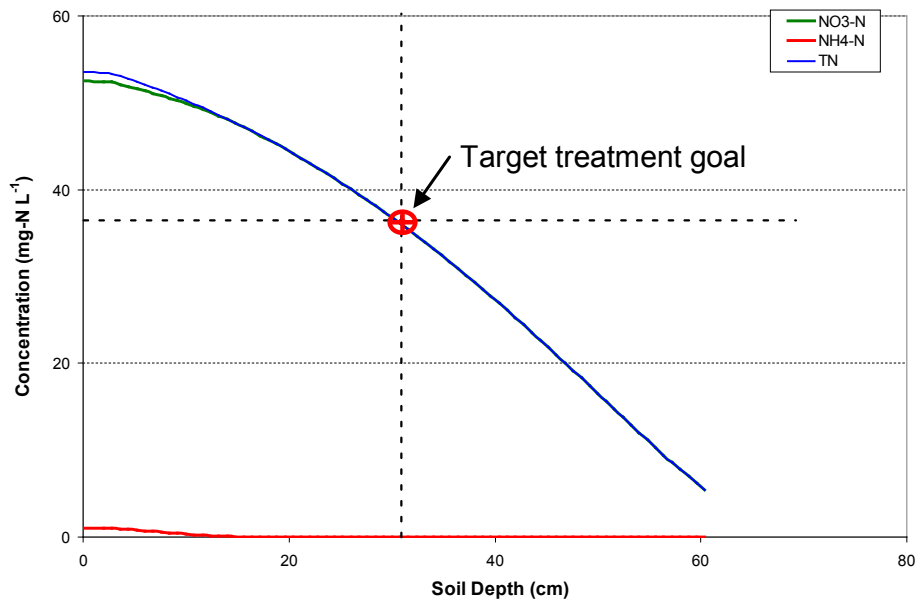


Figure 3-21. STUMOD Output for Example 2 Assuming Conditions Illustrated in Figure 3-20.

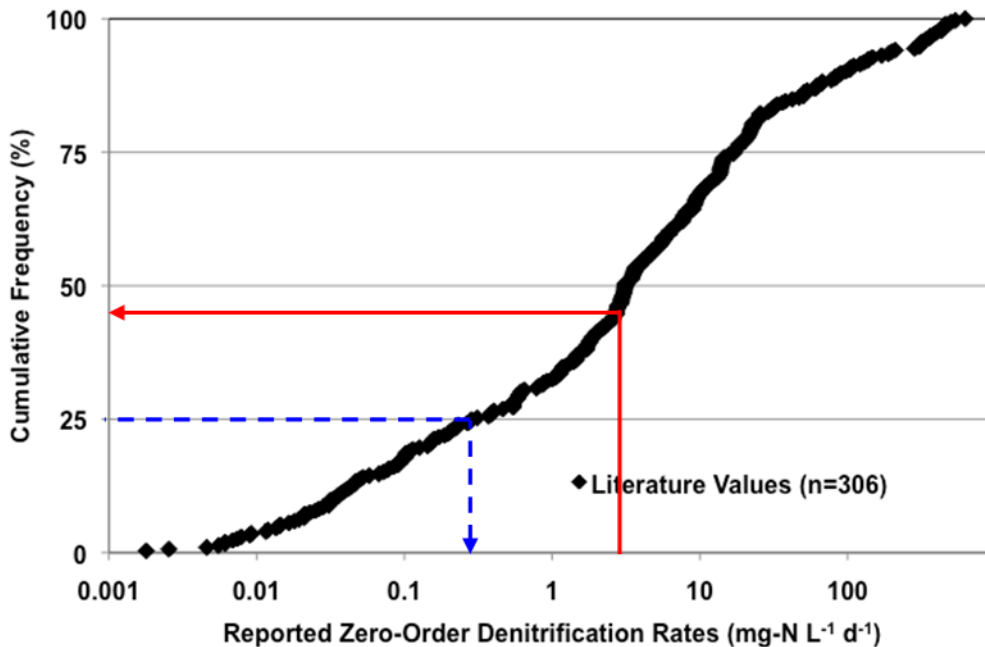


Figure 3-22. CFD of Denitrification Rates Assimilated from the Literature.

Red (solid) lines show estimation of the frequency of 1.8 mg-N L⁻¹ d⁻¹.
 Blue (dashed) lines show the 25th percentile rate of 0.29 mg-N L⁻¹ d⁻¹.

- 5.) **Evaluate the associated uncertainty with the output:** The user can now assess the uncertainty for the various conditions described above. It may be that the user is comfortable accepting the uncertainty within effluent concentration and expected advanced treatment nitrogen reduction, while the carbon availability is largely unknown. From this outcome, perhaps interim limits, such as 25 mg-N L⁻¹ at 30 cm, are established

and monitoring conducted. If the interim limit is exceeded it may then trigger the need for further evaluation and/or decision making. Alternatively, the cumulative probability nomographs can be used to assess this uncertainty or underlying risk of achieving the treatment outcome. Evaluation of the cumulative probability graphs that most closely resemble the Example 2 conditions (Figure 3-23) suggests there is >95% probability that the output condition (Fraction of Nitrogen Remaining) will be less than 0.67. However, the user is cautioned that while the Monte Carlo simulation incorporates a range of input parameters (including denitrification rates), the underlying assumption is that sufficient carbon is available and the initial nitrate concentration was $\ll 52 \text{ mg-N L}^{-1}$.

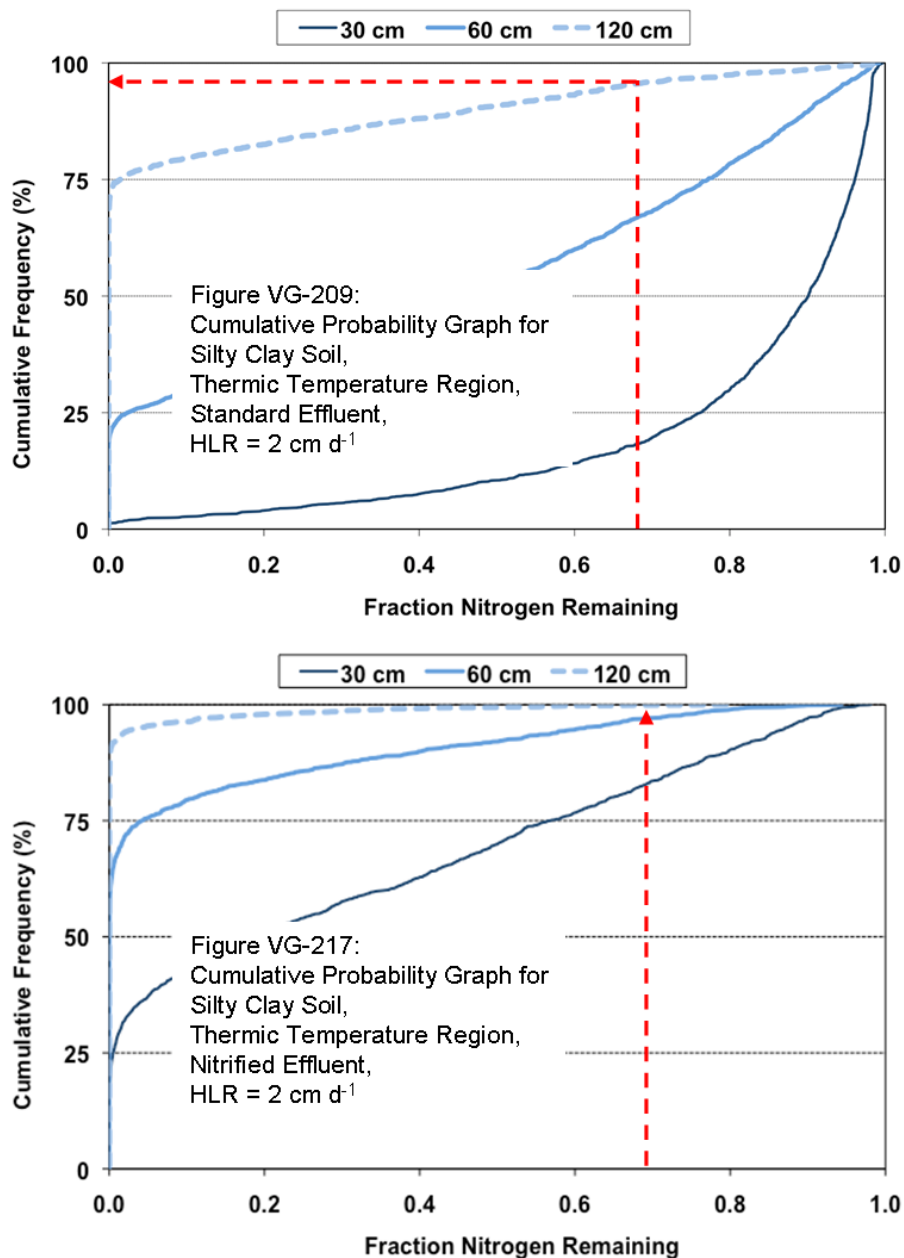


Figure 3-23. Comparison of Cumulative Probability Graph to Evaluate Uncertainty for Example 2 STUMOD Outputs.

3.4.3 Hypothetical Example 3: Estimating STU Mass Loading

Estimating the mass of nitrogen percolating from the STU may be an important evaluation criterion, especially in environmentally sensitive areas and/or when evaluating larger scale impacts (e.g., new developments, watershed, etc.). For example, although the treatment goal specified for Example #1 has been achieved based on nitrogen concentration (see Figure 3-16), perhaps additional development in the area is planned and local regulators hope to minimize the overall nitrogen load to the groundwater by evaluating lot size. Example #3 evaluates the estimated mass of nitrogen reaching a specific depth from a 3-bedroom home with 6 occupants. In this example, the initial conditions are the same as in hypothetical Example #1.

1) **Example 3 initial conditions:**

Soil Texture: Sandy loam

HLR: 2 cm d⁻¹

Effluent Nitrogen Concentration: 54 mg-N L⁻¹ as ammonium

Location: Iowa, mesic temperature region (annual mean soil temperature = 11.5°C)

Treatment Goal: 27 mg-N L⁻¹ (50% reduction of nitrogen) at 90 cm

- 2) **Estimate mass flux from STU:** Using the above initial conditions, Figure 3-24 illustrates the STUMOD output for nitrogen mass flux. The estimated mass flux at 90 cm is ~ 0.24 g-N m⁻² d⁻¹ (green dashed circle). To assess the likely range of operating conditions, the HLR can be altered and the resulting mass flux of nitrogen evaluated. Figure 3-25 illustrates a summary of the expected mass flux of nitrogen for different HLRs at different depths below the trench for Example #3. The STUMOD output is summarized in Table 3-3.

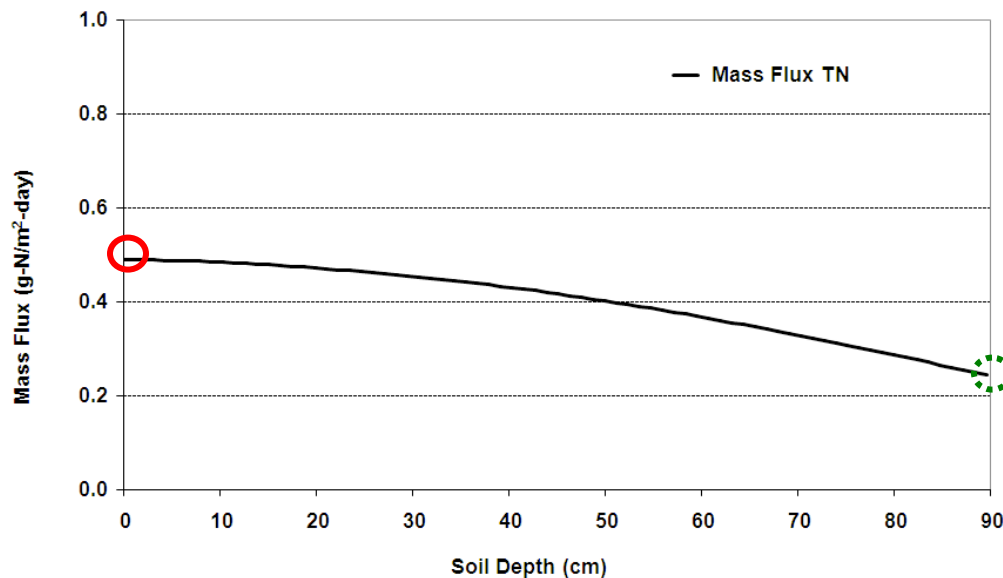


Figure 3-24. STUMOD Output for Mass Flux of Nitrogen for Example #3. Red (solid) circle depicts mass flux (0.5 g-N m⁻² d⁻¹) at the infiltrative surface and the green (dashed) circle depicts mass flux at 90 cm below trench (0.24 g-N m⁻² d⁻¹).

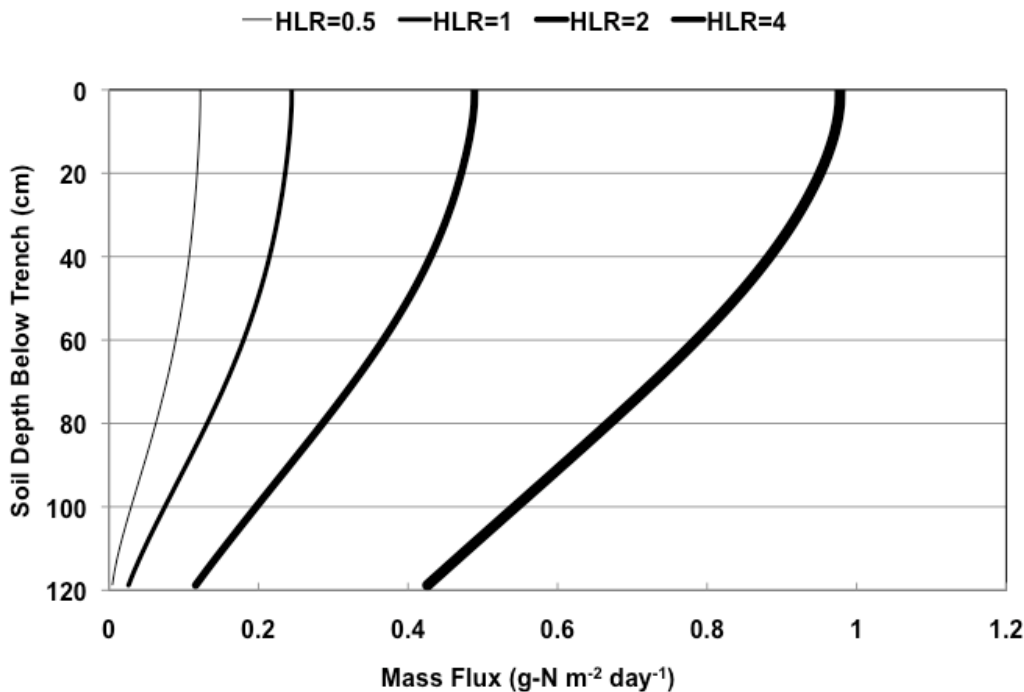


Figure 3-25. Graph Illustrating the Mass Flux of Nitrogen for Different HLRs with Depth Below the Trench.

Table 3-3. Summary of STUMOD Output for HLRs shown in Figure 3-26.

HLR cm d ⁻¹	Nitrogen Mass Flux (g-N m ² d ⁻¹) at Soil Depth Below Trench			
	0 cm	30 cm	60 cm	120 cm
0.5	0.12	0.11	0.09	0.005
1	0.24	0.23	0.18	0.03
2	0.49	0.45	0.37	0.12
4	0.98	0.92	0.79	0.43

- 3) **Determine area requirements for STU:** Next the required STU infiltrative area can be estimated based on per capita flow and an assumed HLR.
 - a. Per capita water use may be estimated from local regulation requirement or from literature data. Figure 3-26 illustrates the CFD for daily flow (User's Guide, Figure 3-8). Based on the median value of 171 L capita⁻¹ d⁻¹, then the total expected flow would be 1,026 L d⁻¹ for the household (6 occupants × 171 L capita⁻¹ d⁻¹). (Recall that 1 gallon capita⁻¹ d⁻¹ is approximately 3.8 L capita⁻¹ d⁻¹.)
 - b. Next, the infiltrative area of the STU can be estimated by dividing the daily flow by the HLR. Assuming a HLR of 2 cm d⁻¹ (equivalent to 20 L m⁻² d⁻¹), approximately 52 m² of trench bottom is required.
 - c. Multiplying the mass flux by the required trench bottom area yields a mass of nitrogen percolating from the STU. First the mass flux at 90 cm is estimated at 0.24 g-N m⁻² d⁻¹ (Table 3-3, at HLR of 2 cm d⁻¹ → 0.37 g-N m⁻² d⁻¹ + 0.12 g-N m⁻² d⁻¹) / 2 = 0.245 g-N m⁻² d⁻¹). Multiplying the mass flux at 90 cm below the trench (0.24 g-N

$\text{m}^{-2} \text{d}^{-1}$) by the required trench bottom area (52 m^2) yields a mass of nitrogen percolating daily from the STU of $\sim 12.3 \text{ g}$ or $\sim 4.5 \text{ kg-N year}^{-1}$ ($\sim 10 \text{ lbs year}^{-1}$).

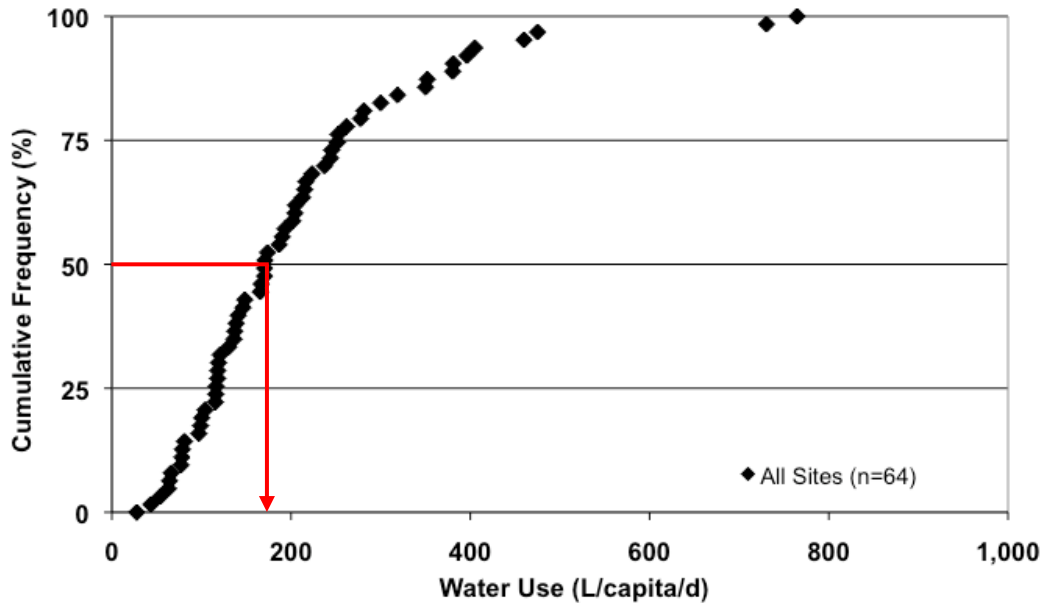


Figure 3-26. Determination of Media per capita Water Use. Red lines depict the median value of $171 \text{ L capita}^{-1} \text{ d}^{-1}$.

- 4) **Optimize total mass loading:** Using the same calculations as described in step 3 above, the user can estimate the mass of nitrogen from each household if different HLRs are used, assuming of course that different HLRs require different infiltration areas. Table 3-4 summarizes the mass of nitrogen that is expected to percolate from the STU in this case.

In this example the output shows little difference in nitrogen mass loadings between the HLRs at shallow depths; however, at deeper depths ($> 90 \text{ cm}$) the higher HLR yields a greater nitrogen loading. This phenomenon is important to understand because as the effluent is dispersed over a larger area, it may have longer contact time with the underlying soil and lower soil pore saturation which ultimately will effect nitrogen removal.

A similar approach can be used to evaluate the nitrogen mass loading impact of a range of daily flows (presumed to be correlated to number of household occupants).

Table 3-4. Nitrogen Mass Loading Estimates for Example #3
(single house with 6 people and total daily flow of 1,025 L).

HLR (cm d^{-1})	Required STU Infiltration Area (m^2)	Total Nitrogen Mass Percolating from the STU (g-N d^{-1}) at Soil Depth Below Trench				
		0 cm	30 cm	60 cm	90 cm	120 cm
0.5	205.2	24.6	22.6	18.5	10.3	1.0
1	102.6	24.6	23.6	18.5	10.4	3.1
2	51.3	25.1	23.1	19.0	12.3	6.2
4	25.65	25.1	23.6	20.3	15.6	11.0

3.4.4 Hypothetical Example 4: Up-scaling STU Density

As shown in hypothetical Example #3, estimating the mass of nitrogen percolating from the STU may provide additional insight while evaluating large scale impacts (e.g., new developments, watershed, etc.). In Example #4, the goal is to illustrate up-scaling the estimated nitrogen mass loading from one residence to two, or increasing the number of residents in one house. The lot size is assumed to be the same. For this example, again a 3-bedroom home with 6 occupants is assumed with the same operational conditions delineated in Example #1 and the nitrogen mass loading estimated in Example #3.

5) **Example 4 initial conditions:**

Soil Texture: Sandy loam

HLR: 2 cm d^{-1}

Effluent Nitrogen Concentration: 54 mg-N L^{-1} as ammonium

Location: Iowa, mesic temperature region (annual mean soil temperature = 11.5°C)

Residence: 6 occupants with a daily household flow of $1,026 \text{ L d}^{-1}$

STU Configuration: $\text{HLR} = 2 \text{ cm d}^{-1}$, 52 m^2 infiltrative area

Estimated Nitrogen Mass Flux at 90 cm: 12.3 g-N d^{-1}

- 6) **Estimate mass flux for multiple homes:** Using the above initial conditions and estimated mass flux at 90 cm of $\sim 12.3 \text{ g-N d}^{-1}$ from Example #3, the effect of multiple homes is a simple task of multiplication. In this case the number of homes is multiplied by the estimated daily mass flux. The mass flux is calculated in the same manner and does not change for one or more homes. For example, for two homes the expected flow has now doubled and the STU infiltrative area doubles as well, resulting in a total mass load of nitrogen of 24.6 g-N d^{-1} for two homes (Figure 3-27).

Similarly, for multiple occupants in the home, the per capita loading rate does not change. For ten occupants the flow has increased by a factor of 10 (to $10,260 \text{ L d}^{-1}$) and the discharge area must increase to 520 m^2 . The resulting mass flux ($0.24 \text{ g-N m}^{-2} \text{ d}^{-1}$) does not change, but the mass load of nitrogen at 90 cm increases to 123 g d^{-1} (Figure 3-27).

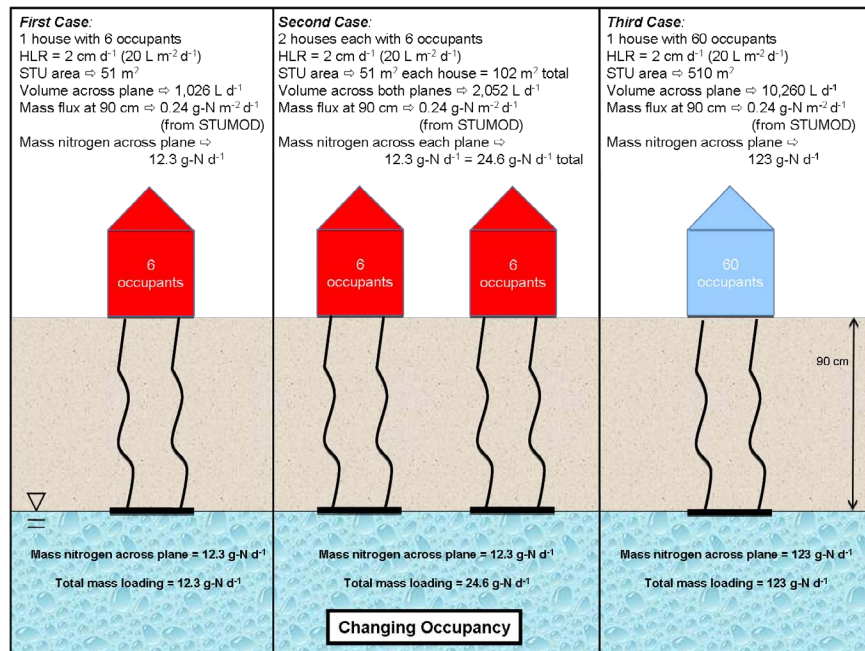


Figure 3-27. Nitrogen Mass Flux Comparisons.

- 7) **Effect of HLR on mass flux:** When evaluating the total mass loading to a given area such as a housing development or watershed, it is important to understand the effect of HLR on mass flux. Specifically, simply dividing the total mass load by a given area is not appropriate as this would fundamentally assume equal distribution of that mass across the given area. In reality, the total mass will still be loaded onto a small fraction of the given area.

Figure 3-28 illustrates this effect by comparing the nitrogen mass flux at 90 cm at HLRs of 2 cm d⁻¹ and 1 cm d⁻¹, assuming all other operating conditions remain the same. By decreasing the HLR, the infiltration surface increases to account for the flow. In this case for a daily flow of 1040 L d⁻¹, the infiltrative surface increases to 104 m² (right illustration in Figure 3-28). Again, the mass flux of nitrogen crossing the plane at 90 cm is 12.3 g-N d⁻¹ (left illustration in Figure 3-28) for the initial conditions in Example #3 (see step 1 of this example). Alternatively, for a HLR of 1 cm d⁻¹, STUMOD yields a mass flux of 0.1 g-N m⁻² d⁻¹. Thus, the mass flux of nitrogen crossing the 90 cm depth is decreased to 10.4 g-N d⁻¹ (right illustration in Figure 3-28). However, it is now clear that this mass flux is approximately 25% less rather than a 50% decrease as would be estimated without consideration of the HLR. Again, as noted in step 4 of Example #3, as the effluent is dispersed over a larger area, longer contact time with the underlying soil and lower soil pore saturation result which ultimately effect nitrogen transformation rates (e.g., ammonium sorption, nitrification, denitrification).

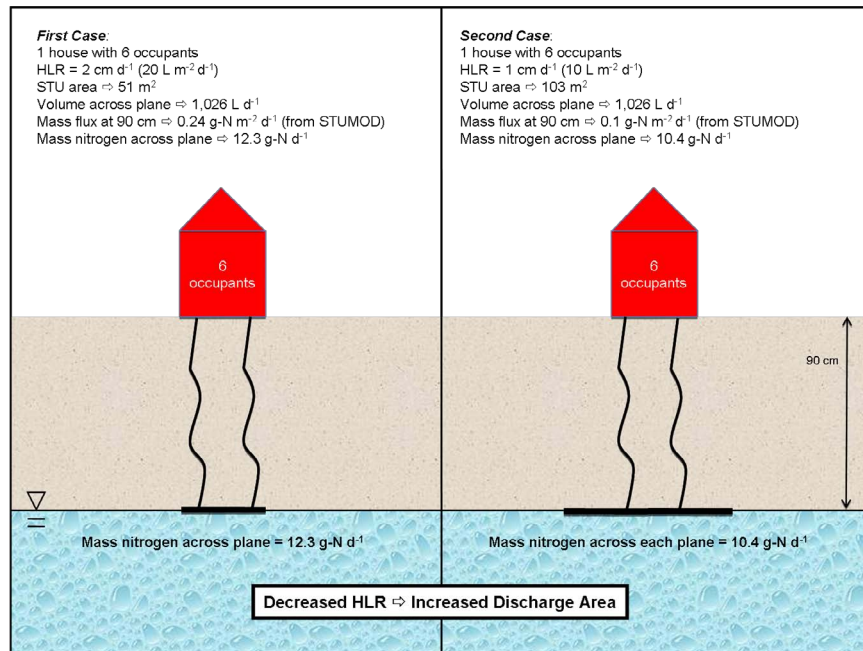


Figure 3-28. Comparison of Nitrogen Mass Flux at Different HLRs.

Figure 3-29 compares the total mass load assumed to be equally distributed over a given area. In this case the mass flux of nitrogen at 90 cm below the infiltrative surface from six homes is compared to the assumption that the effluent is distributed over the entire lot size. For this comparison the total area is 10,000 m² (~2.5 acres) with the same initial conditions described in step 1 resulting in a total daily flow of 6,156 L. Again, the estimated mass flux at 90 cm is ~ 12.3 g-N d⁻¹ per home which yields a total mass flux of 73.8 g-N d⁻¹ (left illustration in Figure 3-29) for 6 homes.

If the same daily volume of 6,156 L is equally distributed over the entire 10,000 m² area, the effective HLR becomes 0.062 cm d⁻¹ (right illustration in Figure 3-29) and STUMOD yields a mass flux at 90 cm of 0.0056 g-N m⁻² d⁻¹. Multiplying this mass flux by the total lot area, results in a total mass flux of nitrogen of 56 g-N d⁻¹. Of course this is not reasonable as the “discharge area” increased from 312 m² to 10,000 m². Furthermore, it is interesting to note that the mass of nitrogen percolating from the STU only decreased 25% from the six individual homes to the equal distribution (from 73.8 g d⁻¹ to 56 g d⁻¹).

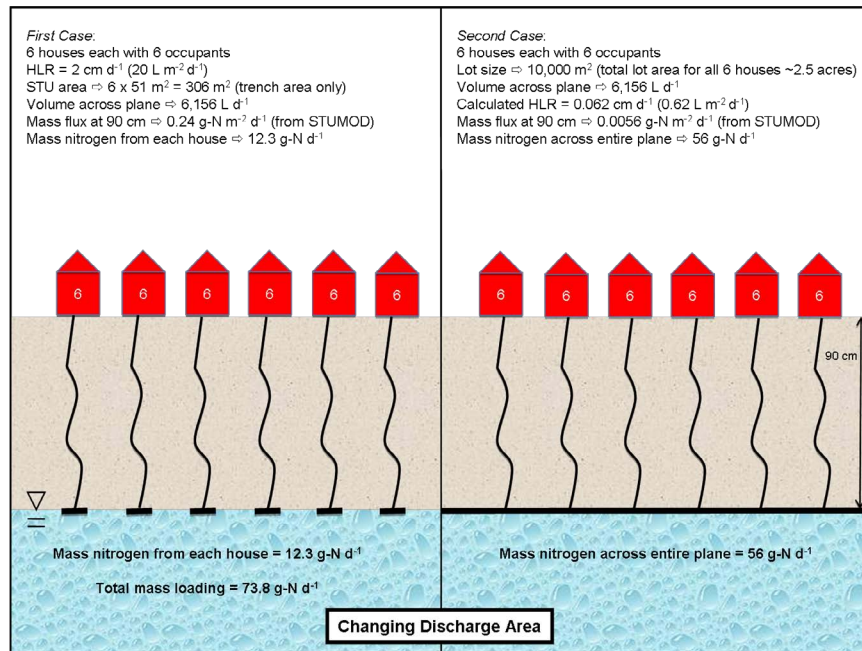


Figure 3-29. Comparison of Nitrogen Mass Flux from Six Homes to Equal Distribution Over a Given Area.

3.4.5 Hypothetical Example 5: Qualitative Scenario Comparison

Obviously, all possible design and environmental conditions could not be realistically covered by numerical simulations, because of time and system resources required to run such simulations. For toolkit users who do not wish to implement a complex model to assess the impacts of these conditions on STU performance, a series of different “scenarios” were simulated using HYDRUS-2D with model outputs generated for subsurface nitrogen concentrations, spatial treatment distributions, and mass-flux below a specified boundary illustrated. These scenarios were chosen because they represent typical systems under a range of conditions providing insight into different outcomes that might result from different scenarios. More importantly, the simulation outputs show the difference in nitrogen removal between two systems that have some common features, yet differ by a certain parameter, such as soil texture, effluent quality, HLR, or depth to groundwater. In this manner, comparison of the scenario outputs provides qualitative assessment of the expected STU performance.

Comparison of the scenario outputs illustrates behaviors that can be expected to occur for different operating and environmental conditions. For example, Figure 3-30 illustrates a trench simulation in sandy loam where the trench system receives STE at 2 cm d⁻¹ (Visual-Graphic Tools, Figure VG-255) and the same HYDRUS domain, but with a HLR of 3.825 cm d⁻¹ (equal to 10% of the soil’s saturated hydraulic conductivity) (Visual-Graphic Tools, Figure VG-258). Comparison of the illustrations indicates that the total nitrogen mass flux at 90 cm below the trench is estimated as 0.39 g d⁻¹ (left portion of Figure 3-30) and 0.89 g d⁻¹ (right portion of Figure 3-30) for one linear meter of trench length. In this comparison, an increase in loading rate by a factor of 1.9 resulted in an increased nitrogen flux of 2.3 suggesting improved nitrogen removal at lower HLR which is not linearly correlated with the mass applied.

In another example (Figure 3-31), comparison of simulations of drip systems in sandy soil with water tables at 60 cm below drip line receiving 19 minute doses, five times each day can be compared. Again the same HYDRUS domain was used for both simulations other than the effluent quality applied. STE is illustrated by Visual-Graphic Tools, Figure VG-262 and nitrified effluent is illustrated Visual-Graphic Tools, Figure VG-264. In this case, 4 times more total nitrogen was introduced into the soil from the STE system compared to the nitrified effluent system (60 mg-N L^{-1} STE vs. 15 mg-N L^{-1} nitrified effluent). However, the total mass flux to the water table was ~ 7 times higher suggesting improved nitrogen removal with higher effluent quality which is not linearly correlated with the mass applied (red circles on Figure 3-31). Thus, when all the conditions are equal except effluent concentration, simple scaling between systems to estimate nitrogen removal may not be accurate (4x in does not equal 4x out).

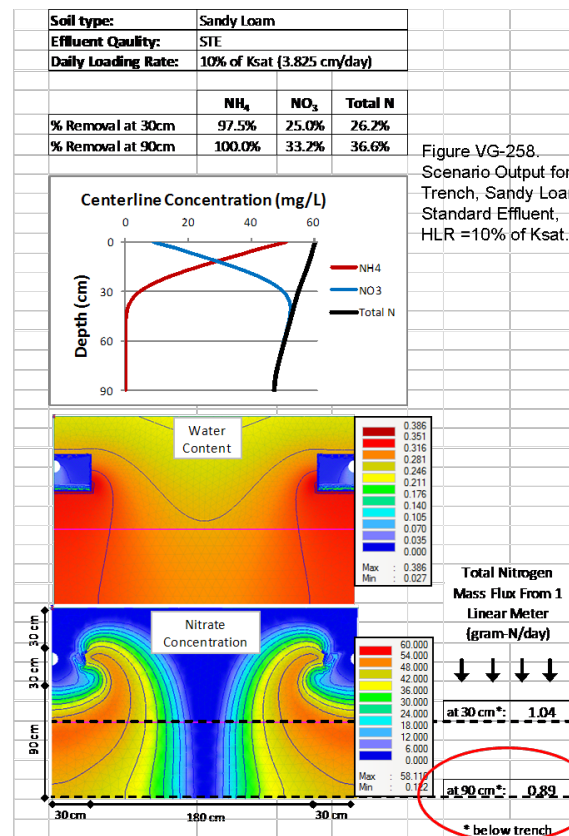
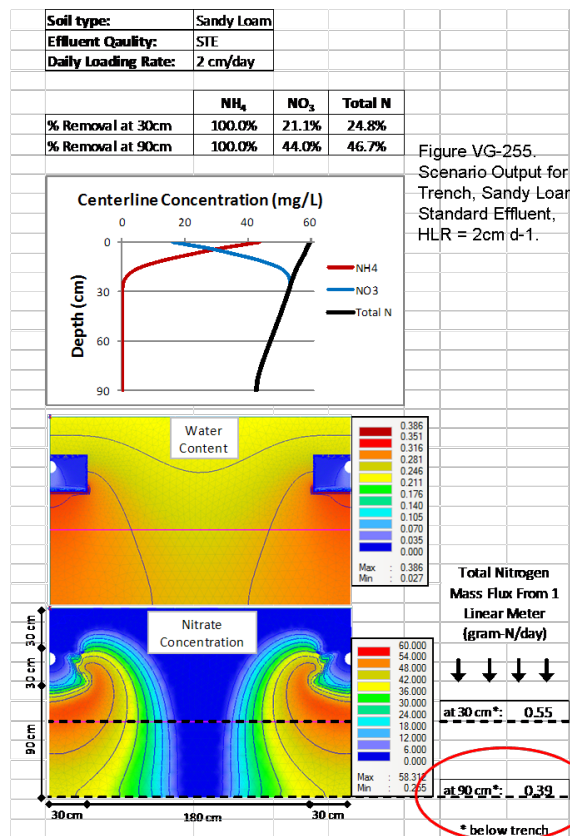


Figure 3-30. Example Comparison of Trench System Scenario Outputs.

Figure VG-262
Scenario Output for
Drip Dispersal, Sandy Soil,
Standard Effluent, HLR = "High".

Figure VG-264
Scenario Output for
Drip Dispersal, Sandy Soil,
Nitrified Effluent, HLR = "High".



Figure 3-31. Example Comparison of Drip System Scenario Outputs.

The output from the scenario simulations can also be extrapolated such that comparison of some arbitrary assumed equivalent conditions (such as a specific design or operating condition for a given site) can provide a general expectation of nitrogen removal. To use the scenario results for this type of comparison, the user must first define a given HLR, STU area, or delivery volume. Similar to when using the nomographs or cumulative probability plots, the equivalent condition to be evaluated must be within a reasonable range of the initial conditions, in this case the scenario model domain. The following examples illustrate an equivalent extrapolation for: 1) a given STU area or “footprint” and, 2) a given daily flow to a STU. Figure 3-32 illustrates the two individual scenario outputs for trench (left portion of Figure 3-32) and drip (right portion of Figure 3-32) for sandy soil receiving STE.

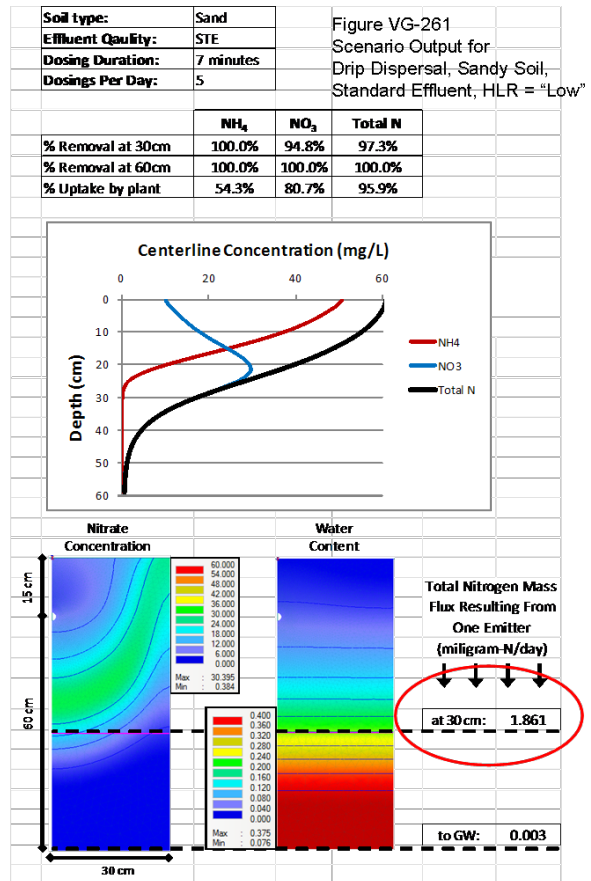
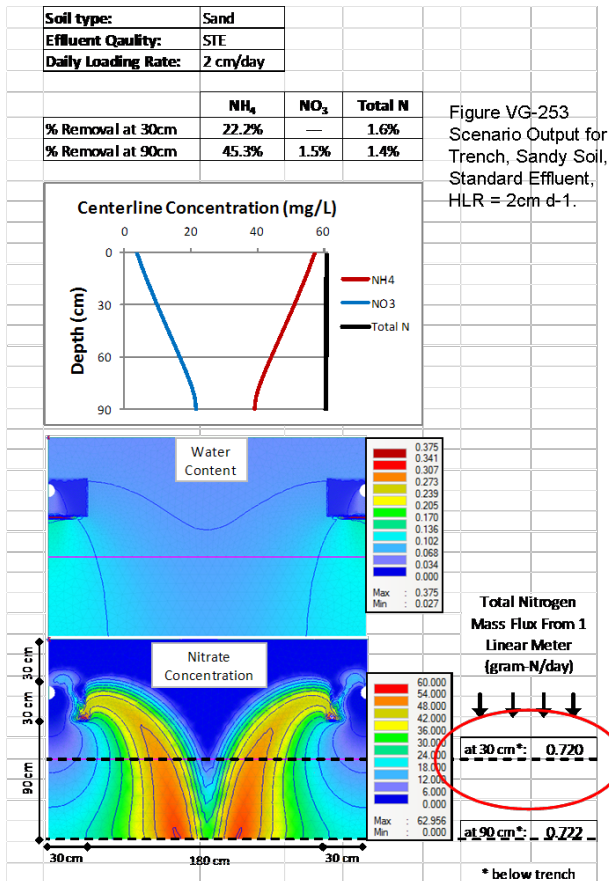


Figure 3-32. Example Trench and Drip Comparison of Equivalent Mass.

The first example extrapolates the model results to some equivalent STU length (10 m) such that the mass flux can be estimated. Equivalent trench and drip footprints are illustrated in Figure 3-33. In this example, the mass flux at the shallow 30-cm depth for a trench is estimated by multiplying the mass flux per linear meter of trench by 10. Because the mass flux values for the scenario illustrations are for a specific footprint area (width x length where width = 30 cm + 180 cm + 30 cm = 240 cm = 2.4 m cross sectional area, and length = 1m linear meter of trench), the mass flux is simply multiplied by the linear length. For these assumptions, the “equivalent 10 m footprint” estimation for a trench (left portion of Figure 3-32) is:

$$[0.72 \text{ g-N d}^{-1} \text{ m}^{-1}] \times [10 \text{ m}] \approx 7.2 \text{ g-N d}^{-1}$$

A drip system footprint is overlaid on the trench system footprint on Figure 3-33 with the radial influence of each emitter shown as a circle. By counting the number of circles within the trench mass flux area, more than 6.5 but less than 6.75 emitters are estimated to fit (for the purposes of this example, it will be assumed that 6.67 emitters lay within the one linear meter of trench as shown on Figure 3-33). Now the mass flux can be estimated by multiplying the number of emitters (each receiving the estimated number of 5 doses per day) by 10. Note, the drip system mass flux is in milligrams rather than grams and must be converted. For these assumptions, the “equivalent” estimation for a drip system (right portion of Figure 3-32) would be:

$$[1.86 \text{ mg-N d}^{-1} \text{ emitter}^{-1}] \times [6.67 \text{ emitters per linear meter}] \times [10 \text{ m}] \approx 0.12 \text{ g-N d}^{-1}$$

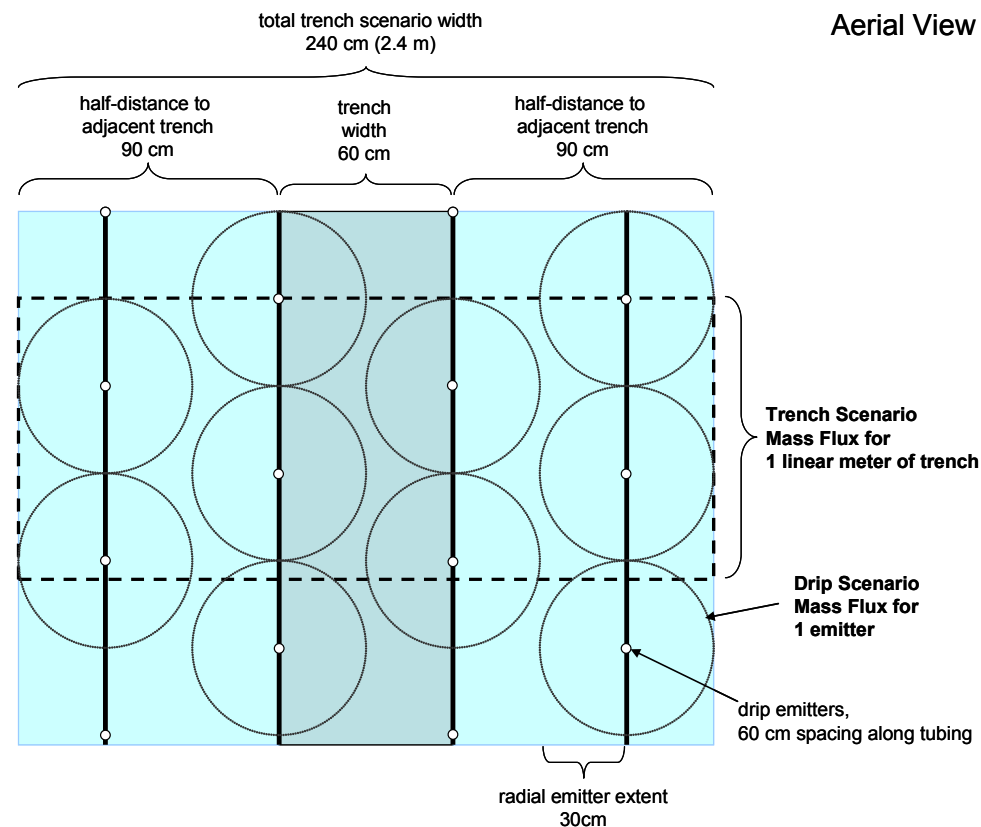


Figure 3-33. Illustration of Comparable Scenario "Footprints".

The second example extrapolates the model results to some expected operating daily flow, such that the mass flux can be estimated. In this example comparison of an equivalent daily flow of 400 L (~106 gallons) to the STU requires estimation of the length required for a given HLR or estimation of a HLR required for a given length. The HLR and emitter dosing rates are assumed "fixed" rates based on the model conditions, specifically 2 cm d^{-1} for a trench and either 7 or 19 minute doses for the drip dispersal system. Based on these assumptions (daily flow of 400 L at a soil HLR of 2 cm d^{-1}), the trench length required can be estimated using the model trench width (two 30 cm half trenches = 60 cm) and then multiplied by the mass flux. The estimated trench mass flux at 30cm for this daily flow would be:

$$\begin{aligned}
 & ([400 \text{ L d}^{-1}] \times [1000 \text{ cm}^3 / \text{L}]) / [2 \text{ cm d}^{-1}] \approx 200,000 \text{ cm}^2 = 20 \text{ m}^2 \text{ of trench bottom area} \\
 & [20 \text{ m}^2] / [0.6 \text{ m width}] = 33.3 \text{ linear m of trench required for a HLR of } 2 \text{ cm d}^{-1} \\
 & [33.3 \text{ m}] \times [0.72 \text{ g-N d}^{-1} \text{ m}^{-1}] \approx 23.6 \text{ g-N d}^{-1}
 \end{aligned}$$

A comparable drip system estimate can be made by dividing the daily volume by the recommended linear loading rate to estimate the tubing length required and the associated number of emitters. Recommended linear loading rates of 6.34 L m^{-1} (0.5 to $0.6 \text{ gal LF}^{-1} \text{ d}^{-1}$) for sand, 4.04 L m^{-1} (0.3 to $0.4 \text{ gal LF}^{-1} \text{ d}^{-1}$) for sandy loam, and 2.31 L m^{-1} ($<0.2 \text{ gal LF}^{-1} \text{ d}^{-1}$) for silty clay are typical manufacturer recommendations. However, these linear loading rates incorporate the tubing volume necessary for pressurization to ensure equal distribution through all emitters. It should be noted that the linear tubing length (and the resulting estimate of number of emitters) can also be estimated for pressurization of 8x, 5x, and 3x for high, medium and low

soil loading rates. Because the emitter orifice controls the rate of flow to the STU ($2.46 \text{ L hr}^{-1} = 0.65 \text{ gal hr}^{-1}$), after the number of emitters is estimated, the actual volume distributed to the soil must be checked by multiplying the number of emitters by the emitter rate to get the total volume and the dose duration may need adjustment. Based on these assumptions (daily flow of 400 L dispersed to the soil in 5 doses per day, at a sand linear loading rate of 6.34 L m^{-1}), the associated calculations are:

Total tubing length required to disperse the effluent:

$$[400 \text{ L d}^{-1}] / [6.34 \text{ L m}^{-1}] = 63.1 \text{ m length} \approx 103 \text{ emitters,}$$

Hourly discharge rate from the total length:

$$[103 \text{ emitters}] \times [2.46 \text{ L hr}^{-1}] \approx 253 \text{ L hr}^{-1} \text{ delivered to the STU by 103 emitters.}$$

For the scenario modeled (5 daily doses lasting 7 minutes each), the total duration of effluent delivery is:

$$35 \text{ min d}^{-1} = 0.58 \text{ hr d}^{-1}.$$

The total volume delivered to the STU for this condition is:

$$[253 \text{ L hr}^{-1}] \times [0.58 \text{ hr d}^{-1}] \approx 146.7 \text{ L d}^{-1} \text{ which is 37\% or about one third of the target volume (400 L d}^{-1}\text{).}$$

Because the dosing regime affects the mass flux (as previously described in this section), it would not be accurate to simply multiple the number of emitters by the mass flux by 3. Rather the dose duration for 5 doses d^{-1} can be checked to determine which scenario best represents the defined example conditions:

$$[400 \text{ L d}^{-1}] / [253 \text{ L hr}^{-1}] = 1.58 \text{ hr d}^{-1} \text{ of dosing required,}$$

$$\text{for 5 equal doses } \text{d}^{-1} = 0.32 \text{ hr dose}^{-1} \approx 19 \text{ min doses}$$

This suggests that the scenario that best represents the conditions required to deliver 400 L of STE to the STU via a drip dispersal system in sandy soil would be VG-262 which illustrates the scenario output for drip dispersal, sandy soil, standard effluent (STE), and a “high” HLR = 5 doses d^{-1} at 19 min dose^{-1} (left side of Figure 3-31). Now multiplying the mass flux for the comparable conditions (86.8 mg-N d^{-1} at 30 cm, green dashed circle on left side of Figure 3-31), the “equivalent” drip estimation would be:

$$[103 \text{ emitters}] \times [86.8 \text{ mg-N d}^{-1} \text{ emitter}^{-1}] \approx 8.9 \text{ g-N d}^{-1}$$

In this comparison, the trench system is estimated to have a mass flux of 23.6 g-N d^{-1} and a comparable drip dispersal is estimated to have a mass flux of 8.9 g-N d^{-1} highlighting the plant uptake in the drip system (see green box on left side of Figure 3-31).

Table 3-5 summarizes the comparable mass flux for these two examples (for a given 10 m linear length and for a given daily flow of 400 L). It is important to note that these examples allow evaluation of comparable estimates and do not reflect what may be actual OWTS designs. The user can follow similar calculations to estimate comparable values for specific conditions. However, with comparable estimates, trends within the scenarios become evident. Specifically, in both trench and drip systems there is increased nitrogen removal due to soil texture (i.e., lower mass fluxes with finer soil texture) and HLR (i.e., lower mass fluxes at lower HLRs). There appears to be little additional nitrogen removal with depth in the trench systems (with the exception of the finer textured silty clay soil), but additional soil depth did increase nitrogen removal in the drip systems. The mass flux was lower when the trench spacing was decreased and is probably due to the increased saturation between trenches which may promote

denitrification (note, the ammonium profiles are not significantly different suggesting the difference is related to nitrate). Finally, in the drip systems there is an apparent increased nitrogen mass removal based on higher quality effluent. A complete description of the scenario development is provided in the User's Guide, Section 2.4.

Table 3-5. Comparison of Scenario Simulation Outputs for Estimated "Equivalent" Design Conditions¹.

Scenario Figure	Soil Texture	Effluent Quality	HLR	Scenario Mass Flux (g-N d ⁻¹) [*]		10 m linear length		400 L d ⁻¹ flow	
				Shallow	Deep	Shallow	Deep	Shallow	Deep
Trench System Scenarios									
VG-253	sand	low	low	0.72	0.72	0.3	0.3	24.0	24.1
VG-254	sand	low	high	23.4	23.5	9.8	9.8	24.3	24.4
VG-255	sandy loam	low	low	0.55	0.39	0.2	0.2	18.3	13.0
VG-256	sandy loam	low	low	0.36	-	0.2	-	12.0	-
VG-257	sandy loam	low	low	0.28	0.22	0.1	0.1	9.3	7.3
VG-258	sandy loam	low	high	1.04	0.89	0.4	0.4	18.1	15.5
VG-259	silty clay	low	high	0.37	0.1	0.2	<0.1	12.3	3.3
VG-260	silty clay	low	low	0.055	0.0002	<0.1	<0.1	3.8	<0.1
Drip System Scenarios									
VG-261	sand	low	low	1.861	0.003	0.1	<0.1	8.3	6.7
VG-262	sand	low	high	86.8	69.4	5.2	4.2	8.3	6.7
VG-263	sand	high	low	0.318	0.001	<0.1	<0.1	1.8	0.9
VG-264	sand	high	high	18.8	9.6	1.1	0.6	1.8	0.9
VG-265	sandy loam	low	low	0.434	0.04	<0.1	<0.1	na	na
VG-266	sandy loam	low	high	83.2	68.3	5.0	4.1	na	na
VG-267	sandy loam	high	low	0.03	0.002	<0.1	<0.1	na	na
VG-268	sandy loam	high	high	22.8	20.4	1.4	1.2	na	na
VG-269	silty clay	low	low	0.08	0.003	<0.1	<0.1	<0.1	<0.1
VG-270	silty clay	low	high	11.7	2.8	0.7	0.2	<0.1	<0.1
VG-271	silty clay	high	low	0.0036	0.0002	<0.1	<0.1	<0.1	<0.1
VG-271	silty clay	high	high	0.51	0.03	<0.1	<0.1	<0.1	<0.1

¹ See Table VG-3 (Visual Graphic Tools) for actual simulation conditions

² Mass flux for drip simulations in mg d⁻¹

na = example condition not analyzed, scenario conditions and hypothetical conditions are not comparable

Effluent Quality: low = STE, high = nitrified effluent

HLR: low = 2 cm d⁻¹ (trench) and 7 min dose (drip), high = 10% of K_{sat} (trench) and 19 min dose (drip). Note, for silty clay trench systems, 10% of K_{sat} is actually the lower HLR.

Mass Flux: shallow = 30 cm, deep = 90 cm (trench) and 60 cm (drip)

Figure 3-34 displays the change in nitrogen mass flux to the water table for drip dispersal systems when plant uptake ceases (due to change of seasons or frost), assuming a sandy loam soil, receiving 7 minute doses 5 times a day. It can be seen that without plant uptake the total nitrogen mass flux to the water table is much higher, as well as the concentration in the soil profile. Figure 3-35 shows the result of a disturbance to the system in the form of rain events. Rain enhances soil saturation, decreases solute travel times through the soil and "flushes" out contaminants, yet is also leads to dilution of contaminants in the soil. In Figure 3-35, nitrogen mass flux is plotted from two rain events; a daylong event of 5 cm d⁻¹ and a two-hour event of 1 cm. Notice the difference in the recovery time or the time it takes the system to regain steady-state conditions. It is also apparent that the mass flux decreases to below steady-state levels after the initial peak rain event flush. Again, these graphs and scenario illustrations show the power of a numerical model that can not be included in a simple spreadsheet tool.

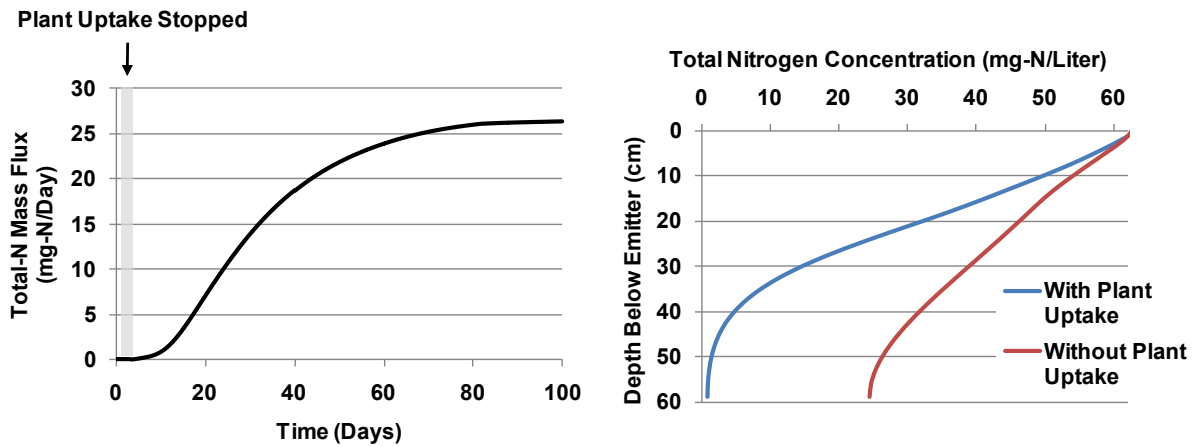


Figure 3-34. Mass Flux Response to Plant Uptake.

Left: Total-N mass flux into the water table from one drip emitter. Plant uptake in the simulation ceased on day 2.
 Right: Depth profile of the total-N concentration in the soil beneath the emitter, at steady-state conditions (day 0 and day 100 of simulation).

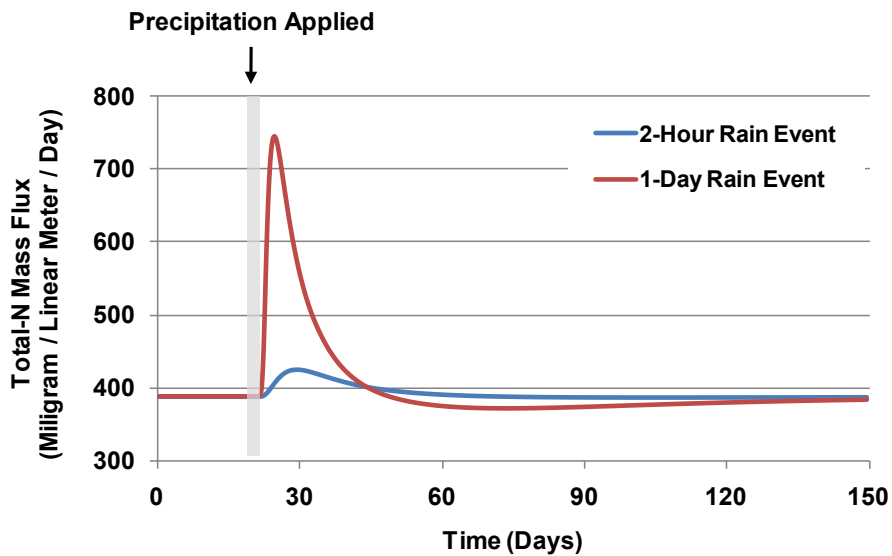


Figure 3-35. Total Nitrogen Mass Flux as Affected by Rain Events.
 Mass flux determined at the plane 90 cm below trench bottom.

CHAPTER 4.0

SUMMARY

This toolkit enables evaluation and design of expected STU performance for important wastewater constituents over a relevant range of OWTS operating conditions. The toolkit is comprised of this Guidance Manual, a companion Toolkit User's Guide, individual tools, and supplemental information. This Guidance Manual provides an introduction to each tool, describes how the tool was prepared, and highlights the specific assumptions/limitations of the tool. The User's Guide includes the fundamental assumptions that were incorporated into the development of the tools, detailed description of the tool development, guidance on input parameter selection, results from field and laboratory studies, and general reference material. Visual-graphic tools (nomographs, cumulative probability graphs, and scenario illustrations) are provided in a separate file. STUMOD and N-CALC are provided as Microsoft™ Excel files. This framework provides detailed information to less experienced user's while enabling more experienced users to start directly with STUMOD or other tool implementation referring to limited sections of the Guidance Manual or User's Guide.

All of the tools presented in the toolkit were developed with a basis in rigorous experimental data. The quantitative tools or models were evaluated using data from the literature, from experiments conducted by the project team, or from scientific knowledge of operating OWTS treatment performance. The toolkit was developed for a wide range of users faced with different needs of varying complexity when evaluating treatment of nitrogen, microbial pollutants (bacteria and virus), and organic wastewater contaminants (OWCs).

The toolkit is hierarchical in nature and diverse with regard to breadth of tools provided. Appropriate tool selection depends on the relative importance of the pollutant in the practical and regulatory arena, the degree of problem complexity, and user sophistication, technical resources, and treatment goals. Ideally, the simplest tools will be used first. Progressing through simple to more complex tools ultimately guides the user to the simplest tool that is appropriate, but discourages using a tool that is too simple for the decision at hand. A series of flow diagrams is provided to guide the user through the steps most often incurred during the STU design decision process. These flow diagrams identify the important steps as well as guiding the user to appropriate tools helpful in selection of tool parameters.

The simplest tools include look-up tables and CFDs. Both of these tools direct the user to available pertinent information. Nomographs enable initial screening and quick insight into expected nitrogen removal based on the predicted output from STUMOD. Cumulative probability graphs illustrate modeling results in a risk-based framework by displaying the cumulative uncertainty of a particular model output due to individual input data. Selected numerical model simulations are also provided to visually demonstrate the usefulness of such a numerical model while showing the impacts of different scenarios on STU behavior. Finally, two spreadsheet tools were developed, N-CALC and STUMOD, allowing the user to evaluate a range of STU operating conditions, soil hydraulics, and/or treatment parameters, as well as the relative influence of these factors on performance.

The tools within the toolkit were developed to help the user decide if the uncertainty in STU performance is acceptable based on the specific target goals. In some cases, the tools may suggest additional information should be collected to assess the expected STU performance with more confidence. The importance of a soil scientist or other qualified person to describe the soil or other site conditions should not be over looked. The information presented here is intended to aid in choosing the best possible simplifying assumptions for selection and use of tools presented in this toolkit. To select, design, and implement a properly functioning OWTS, it is important to assess the operational parameters, evaluate field conditions, manage and maintain the system, and monitor performances. This must be done in context of the current knowledge of the site conditions, scientific principles, and treatment and performance goals. In this manner, the enlightened user can make better-informed decisions that account for the uncertainty in the treatment predictions as well as the stakeholders' collective willingness to accept or deny risk under some level of uncertainty.

REFERENCES

- Beach, D.N. and J.E. McCray. 2003. Numerical modeling of unsaturated flow in wastewater soil absorption systems. *Ground Water Monitoring Remediation* 23 (2):64-72.
- Beal, C.D., E.A. Gardner, and N.W. Menzies. 2005. Process, performance and pollution potential: A review of septic tank-soil absorption systems. *Australian Journal of Soil Research* 43:781-802.
- Beal, C.D., D.W. Rassam, E.A. Gardner, G. Kirchhof, and N.W. Menzies. 2008. Influence of Hydraulic Loading and Effluent Flux on Surface Surcharging in Soil Absorption Systems. *Journal of Hydrologic Engineering* 13 (8):681-692.
- Bouma, J. 1975. Unsaturated flow during soil treatment of septic tank effluent. *Journal of Environmental Engineering* 101 (6):967-983.
- Bumgarner, J.R. and J.E. McCray. 2007. Estimating biozone hydraulic conductivity in wastewater soil-infiltration systems using inverse numerical modeling. *Water Research* 41 (11):2349-2360.
- Crites, R.C. and G. Technobanoglous. 1998. *Small and Decentralized Wastewater Management Systems*. McGraw-Hill, New York, NY.
- Doyle, S., J.E. McCray, K.S. Lowe, and G.D. Thyne. 2005. *Modeling phosphorus reaction and transport at an experimental onsite wastewater site*. Proceedings of the National Onsite Wastewater Recycling Association (NOWRA) Annual Meeting, Cleveland, OH. NOWRA, Laurel, MD.
- Drewes, J.E., T. Heberer, T. Rauch and K. Reddersen (2003). Fate of pharmaceuticals during ground water recharge. *Ground Water Monitoring and Remediation* 23(3): 64-72.
- Driscoll, F.G. 1987. *Groundwater and Wells, Second Edition*. U.S. Filter / Johnson Screens Publisher, St. Paul, MN. 1089 pgs.
- Erickson, J. and E. Tyler. 2001. A model for soil oxygen delivery to wastewater infiltration surfaces. Proceedings of the On-Site Wastewater Treatment - Ninth National Symposium on Individual and Small Community Sewage Systems, March 11-14, in Fort Worth, TX. American Society of Agricultural Engineers (ASAE), St. Joseph, MI.
- Faulkner, B.R., W.G. Lyon, F.A. Khan and S. Chattopadhyay. 2003. Modeling leaching of viruses by the Monte Carlo method. *Water Research* 37(19): 4719-4729.
- Finch, S.D., D.E. Radcliffe, and L.T. West. 2008. Modeling trench sidewall and bottom flow in on-site wastewater systems. *Journal of Hydrologic Engineering* 13 (8):693-701.
- Heatwole, K.K. and J.E. McCray. 2007. Modeling potential vadose-zone transport of nitrogen from onsite wastewater systems at the development scale. *Journal of Contaminant Hydrology* 91 (1-2):184-201.

- Higgins, C., J. Sharp, J. Sepulvado, B. Littrell, G. O'Connor, E. Snyder, and D. McAvoy. 2010. *State-of-the-Science Review of Occurrence and Physical, Chemical and Biological Processes Affecting Biosolids-borne Trace Organic Chemicals in Soils*. Project No. SRSK5T09. Prepared for Water Environment Research Foundation (WERF), Alexandria, VA by Colorado School of Mines (CSM), Golden CO.
- Jenssen, P.D. and R.L. Siegrist. 1990. Technology assessment of wastewater treatment by soil infiltration systems. *Water Science & Technology* 22 (34):83-92.
- Jin, Y. and M. Flury. 2002. Fate and transport of viruses in porous media. *Advances in Agronomy* 77:39-102.
- John, D.E. and J.B. Rose. 2005. Review of factors affecting microbial survival in groundwater. *Environ. Sci. Technol.* 39 (19):7345-7356.
- Lance, J.C. and C.P. Gerba. 1984. Virus movement in soil during saturated and unsaturated soil. *Applied and Environmental Microbiology* 47 (2):335-337.
- Lowe, K., N. Rothe, J. Tomaras, K. DeJong, M. Tucholke, J. Drewes, J. McCray, and J. Munakata-Marr. 2007. *Influent Constituent Characteristics of the Modern Waste Stream from Single Sources: Literature Review*. Project No. 04-DEC-1. Prepared for WERF, Alexandria, VA by CSM, Golden CO.
- Lowe, K., M. Tucholke, J. Tomaras, K. Conn, C. Hoppe, J. Drewes, J. McCray, and J. Munakata-Marr. 2009. *Influent Constituent Characteristics of the Modern Waste Stream from Single Sources: Final Report*. Project No. 04-DEC-1. Prepared for WERF, Alexandria, VA by CSM, Golden CO.
- McCray, J., D. Huntzinger, S. Van Cuyk, and R. Siegrist. 2000. Mathematical modeling of unsaturated flow and transport in soil-based wastewater treatment systems. WEFTEC 2000, Water Environment Federation. October, Anaheim, CA.
- McCray, J., K. Lowe, M. Geza, J. Drewes, S. Roberts, A. Wunsch, D. Radcliffe, J. Amador, J. Atoyan, T. Boving, D. Kalen, and G. Loomis. 2009. *Development of Quantitative Tools to Determine the Expected Performance of Wastewater Soil Treatment Units: Literature Review*. Report No. DEC1R06. Prepared for WERF by CSM, Golden CO.
- McKinley, J. 2008. *Occurrence and Environmental Behavior of Humic Substances and Polysaccharides Accumulating in Soil Wastewater Treatment Units*. Ph.D. Dissertation, Environmental Science & Engineering Division, CSM, Golden, CO.
- Metcalf, E. and H. Eddy. 1991. *Wastewater Engineering: Treatment, Disposal and Reuse*. Singapore: McGraw-Hill.
- Otis, R.J. 1985. Soil clogging mechanisms and control. Proceedings of the On-Site Wastewater Treatment - Fourth National Symposium on Individual and Small Community Sewage Systems. ASAE, St. Joseph, MI. p 238-250.
- Pang, L., C. Nokes, J. Simunek, H. Kikkert, and R. Hector. 2006. Modeling the Impact of Clustered Septic Tank Systems on Groundwater Quality. *Vadose Zone J.* 5 (2):599-609.
- Radcliffe, D.E. and L.T. West. 2007. Modeling long term acceptance rates for OWMSs. Proceedings of the Eleventh National Symposium on Individual and Small Community Sewage Systems, October 20-24, 2007, in Warwick, RI. American Society of Agricultural and Biological Engineers (ASABE), St. Joseph, MI.

- Radcliffe, D.E., L.T. West, and J. Singer. 2005. Gravel effect on wastewater infiltration from septic system trenches. *Soil Science Society of America Journal* 69:1217-1224.
- Siegrist, R.L. 1988. Hydraulic loading rates for soil absorption systems based on wastewater quality. Proceedings of the 5th National Symposium on Individual and Small Community and Sewage Treatment. ASAE, St. Joseph, MI, pp 232-241.
- Siegrist, R.L. 2001. Perspectives on advancing the science and engineering of onsite wastewater systems. *Small Flows Quarterly* 2 (4):8-13.
- Siegrist, R.L. 2006. Evolving a rational design approach for sizing soil treatment units: Design for wastewater effluent infiltration. *Small Flows Quarterly* 7 (5):16-24.
- Siegrist, R.L. and W.C. Boyle. 1987. Wastewater-induced soil clogging development. *Journal of Environmental Engineering* 113 (3).
- Siegrist, R.L., E.J. Tyler, and P.D. Jensen. 2001. *Design and Performance of Onsite Wastewater Soil Absorption Systems*. EPRI Report No 1001446. Prepared for Electric Power Research Institute, Palo Alto, CA.
- Snedecor, G.W. and W.G. Cochran. 1980. *Statistical Methods*. 7th ed. Iowa State University Press.
- Tyler, J.E. and J.C. Converse. 1989. Hydraulic loading based upon wastewater effluent quality. Proceedings of the 6th Northwest On-site Wastewater Treatment Short Course, in Seattle, WA. pp 163-172.
- U.S. EPA. 1997. *Response to Congress on Use of Decentralized Wastewater Treatment Systems*. U.S. EPA, Office of Water. Cincinnati, OH.
- USEPA. 2002. *Onsite Wastewater Treatment Systems Manual*. Report No. 625/R-00/008. U.S. EPA, Office of Water. Cincinnati, OH.
- U.S. EPA. 2002a. *A homeowner's guide to septic systems*. EPA-832-B-02-005. U.S. EPA, Office of Water. Cincinnati, OH.
- Van Cuyk, S., R. Siegrist, K. Lowe, J. Drewes, J. Munakata-Marr, and L. Figueroa. 2005. *Performance of Engineered Treatment Units and Their Effects on Biozone Formation in Soil and System Purification Efficiency*. Project No. WU-HT-03-36. Prepared for National Decentralized Water Resources Capacity Development Project. Washington University, St. Louis, MO by CSM, Golden, CO.
- Zimmerman, M.J. 2004. *Occurrence of Organic Wastewater Contaminants, Pharmaceuticals, and Personal Care Products in Selected Water Supplies, Cape Cod, Massachusetts*. Review of 3106. U.S. Geological Survey Scientific Open-File Report 2005 1206:16.



Water Environment Research Foundation

635 Slaters Lane, Suite G-110 ■ Alexandria, VA 22314-1177

Phone: 571-384-2100 ■ Fax: 703-299-0742 ■ Email: werf@werf.org

www.werf.org

WERF Stock No. DEC1R06a

Co-published by

IWA Publishing

Alliance House, 12 Caxton Street

London SW1H 0QS

United Kingdom

Phone: +44 (0)20 7654 5500

Fax: +44 (0)20 7654 5555

Email: publications@iwap.co.uk

Web: www.iwapublishing.co

IWAP ISBN: 978-1-84339-395-5/1-84339-395-6



Nov 2010



Water Environment Research Foundation
Collaboration. Innovation. Results.

Decentralized Systems



**FINAL
REPORT**

Quantitative Tools to Determine the Expected Performance of Wastewater Soil Treatment Units

TOOLKIT USER'S GUIDE

Co-published by



DEC1R06b

QUANTITATIVE TOOLS TO DETERMINE
THE EXPECTED PERFORMANCE OF
WASTEWATER SOIL TREATMENT UNITS

TOOLKIT USER'S GUIDE

2010



The Water Environment Research Foundation, a not-for-profit organization, funds and manages water quality research for its subscribers through a diverse public-private partnership between municipal utilities, corporations, academia, industry, and the federal government. WERF subscribers include municipal and regional water and wastewater utilities, industrial corporations, environmental engineering firms, and others that share a commitment to cost-effective water quality solutions. WERF is dedicated to advancing science and technology addressing water quality issues as they impact water resources, the atmosphere, the lands, and quality of life.

For more information, contact:

Water Environment Research Foundation
635 Slaters Lane, Suite G-110
Alexandria, VA 22314-1177
Tel: (571) 384-2100
Fax: (703) 299-0742
www.werf.org
werf@werf.org

This report was co-published by the following organization.

IWA Publishing
Alliance House, 12 Caxton Street
London SW1H 0QS, United Kingdom
Tel: +44 (0) 20 7654 5500
Fax: +44 (0) 20 7654 5555
www.iwapublishing.com
publications@iwap.co.uk

© Copyright 2010 by the Water Environment Research Foundation. All rights reserved. Permission to copy must be obtained from the Water Environment Research Foundation.

Library of Congress Catalog Card Number: 2010937541

Printed in the United States of America

IWAP ISBN: 978-1-84339-537-9/1-84339-537-1

This report was prepared by the organization(s) named below as an account of work sponsored by the Water Environment Research Foundation (WERF). Neither WERF, members of WERF, the organization(s) named below, nor any person acting on their behalf: (a) makes any warranty, express or implied, with respect to the use of any information, apparatus, method, or process disclosed in this report or that such use may not infringe on privately owned rights; or (b) assumes any liabilities with respect to the use of, or for damages resulting from the use of, any information, apparatus, method, or process disclosed in this report.

Colorado School of Mines

The research on which this report is based was developed, in part, by the United States Environmental Protection Agency (EPA) through Cooperative Agreement No. X-83085101-0 with the Water Environment Research Foundation (WERF). However, the views expressed in this document are not necessarily those of the EPA and EPA does not endorse any products or commercial services mentioned in this publication. This report is a publication of WERF, not EPA. Funds awarded under the Cooperative Agreement cited above were not used for editorial services, reproduction, printing, or distribution.

This document was reviewed by a panel of independent experts selected by WERF. Mention of trade names or commercial products or services does not constitute endorsement or recommendations for use. Similarly, omission of products or trade names indicates nothing concerning WERF's or EPA's positions regarding product effectiveness or applicability.

ACKNOWLEDGMENTS

This research was funded by the Water Environment Research Foundation.

Project Team

Principal Investigator:

John McCray, Ph.D.
Colorado School of Mines

Co-Principal Investigators:

Jörg Drewes, Ph.D.
Mengistu Geza, Ph.D.
Kathryn Lowe
Colorado School of Mines

Project Team:

Sarah Roberts
Maria Tucholke
Assaf Wunsch
Colorado School of Mines

David Radcliffe, Ph.D.
Ken Bradshaw
University of Georgia

Thomas Boving, Ph.D.
Jose Amador, Ph.D.
Janet Atoyan, Ph.D.
David Kalen
George Loomis
University of Rhode Island

Issue Area Team

Steven Berkowitz
North Carolina Department of Environment & Natural Resources

Matt Byers, Ph.D.
Zoeller Company

Bob Freeman, P.E.
U.S. Environmental Protection Agency

Anish Jantrania, Ph.D., P.E.
NCS Wastewater Solutions

Charles McEntyre, P.E., CHMM
Tennessee Valley Authority

Eberhard Roeder, Ph.D.
Florida Department of Health

Robert Rubin, Ed.D.
McKim Creed

Edwin Swanson, P.E.
Arizona Dept. of Environmental Quality

George Tchobanoglous, Ph.D.
Tchobanoglous Consulting

Water Environment Research Foundation Staff

Director of Research:	Daniel M. Woltering, Ph.D.
Senior Program Manager:	Amit Pramanik, Ph.D., BCEEM

ABSTRACT AND BENEFITS

Abstract:

Onsite wastewater treatment systems (OWTS) are an important part of water management infrastructure in the United States. Thus, proper OWTS selection, design, installation, operation and management are essential. To aid this life-cycle, a toolkit was developed to enable evaluation and design of expected STU performance. The toolkit is comprised of this Guidance Manual, a companion Toolkit User's Guide, individual tools, and supplemental information. This framework provides detailed information to less experienced user's while enabling more experienced users to start directly with STUMOD or other tool implementation referring to limited sections of the Guidance Manual or User's Guide.

The toolkit was developed for a wide range of users faced with different needs of varying complexity when evaluating treatment of nitrogen, microbial pollutants (bacteria and virus), and organic wastewater contaminants (OWCs). Progressing through simple to more complex tools ultimately guides the user to the simplest tool that is appropriate, but discourages using a tool that is too simple for the decision at hand. The simplest tools include look-up tables and cumulative frequency distributions to direct the user to available pertinent information. Nomographs enable initial screening and quick insight into expected nitrogen removal based on the predicted output from STUMOD. Cumulative probability graphs illustrate modeling results in a risk-based framework while numerical model simulations demonstrate the usefulness of complex tools. Finally, two spreadsheet tools were developed for nitrogen transport, N-CALC and STUMOD, allowing the user to evaluate a range of STU operating conditions, soil hydraulics, and/or treatment parameters, as well as the relative influence of these factors on performance.

Benefits:

- ◆ Provides an explanation of soil treatment processes for design-of-performance based onsite wastewater treatment systems.
- ◆ Tools in the toolkit were developed with a basis in rigorous experimental data.
- ◆ Toolkit is hierarchical in nature and diverse with regard to breadth of tools provided.
- ◆ Uses decision diagrams to illustrate the frequent steps incurred during the STU design and guides the user to appropriate tools and input parameter selection.
- ◆ Provides tools within the toolkit that incorporate a risk-based approach to evaluate the uncertainty in STU performance compared to treatment goals.
- ◆ Provides hundreds of visual-graphic tools (nomographs, cumulative probability graphs, and scenario illustrations).
- ◆ Provides STUMOD and N-CALC as Microsoft™ Excel files.

Keywords: Soil treatment unit, onsite wastewater design, treatment, and performance.

TABLE OF CONTENTS

Acknowledgments.....	iii
Abstract and Benefits.....	v
List of Tables.....	ix
List of Figures.....	x
List of Acronyms.....	xii
Executive Summary.....	ES-1
1.0 Scientific Principles and Governing Assumptions.....	1-1
1.1 OWTS Design and Operating Conditions.....	1-1
1.1.1 Daily Flow.....	1-1
1.1.2 Effluent Delivery Method.....	1-2
1.1.3 OWTS Geometry.....	1-2
1.1.4 Hydraulic Loading Rate.....	1-3
1.1.5 Subsurface Heterogeneity.....	1-3
1.1.6 Subsurface Soil Hydraulic Properties.....	1-3
1.1.7 Interactions Between the STU and the Water Table.....	1-4
1.1.8 Cumulative Impacts of OWTSs.....	1-4
1.2 Effluent Quality.....	1-4
1.2.1 Nitrogen.....	1-4
1.2.2 Carbon.....	1-5
1.2.2.1 Background.....	1-6
1.2.2.2 Carbon in OWTS Effluents.....	1-7
1.2.2.3 Carbon in STUs.....	1-8
1.2.2.4 Summary.....	1-9
1.3 Nitrogen Transport and Transformation Assumptions.....	1-10
1.3.1 Sufficient Alkalinity and pH Exist for Nitrogen Transformations.....	1-10
1.3.2 Nitrogen Transformation Parameters.....	1-11
1.3.3 Soil Temperatures Impact Nitrogen Transformations.....	1-12
1.3.4 Ammonium Sorption is a Linear Process.....	1-13
1.3.5 Nitrogen Transformation Rates Follow Monod Kinetics.....	1-13
1.3.6 Nitrogen Transformations are a Function of Soil Water Content.....	1-14
1.4 Microorganism Transport and Transformations.....	1-15
1.5 OWC Transport and Transformations.....	1-15
1.6 Other Considerations.....	1-16
2.0 Tool Development.....	2-1
2.1 HYDRUS Description.....	2-3
2.1.1 Ammonium Sorption.....	2-3
2.1.2 Ammonification.....	2-5
2.1.3 Nitrification.....	2-6
2.1.3.1 Nitrification Half-Saturation Constants.....	2-7
2.1.3.2 Temperature Effects on Nitrification.....	2-7
2.1.3.3 Maximum Nitrification Rates.....	2-9
2.1.3.4 Soil Moisture Dependency.....	2-10
2.1.4 Denitrification.....	2-13

	2.1.4.1	Denitrification Half-Saturation Constants	2-16
	2.1.4.2	Temperature Effects on Denitrification	2-17
	2.1.4.3	Maximum Denitrification Rates	2-18
	2.1.4.4	Soil Moisture Dependency	2-18
2.2		STUMOD Description and Development.....	2-22
	2.2.1	Nitrogen Attenuation Calculation.....	2-24
	2.2.1.1	Hydraulics	2-24
	2.2.1.2	Contaminant Transport	2-25
	2.2.1.3	Nitrification Rate	2-26
	2.2.1.4	Denitrification Rate.....	2-26
	2.2.2	Parameter Sensitivity Analysis	2-26
	2.2.2.1	Uncertainty Analysis Using Monte Carlo Approach.....	2-29
	2.2.3	Benchmarking of STUMOD and HYDRUS.....	2-29
	2.2.4	STUMOD Calibration.....	2-32
2.3		N-CALC – Description and Development.....	2-33
2.4		Scenario Development using HYDRUS.....	2-38
	2.4.1	Trench Systems.....	2-39
	2.4.2	Drip Systems.....	2-40
	2.4.3	Calculating Nitrogen Removal	2-43
2.5		CW2D Model Development	2-44
	2.5.1	Discussion.....	2-46
	2.5.2	Conclusions.....	2-48
3.0		Parameters Affecting Treatment Performance.....	3-1
	3.1	Parameters Relevant to Operational Conditions.....	3-1
	3.1.1	Soil Texture.....	3-2
	3.1.2	Effluent Quality	3-4
	3.1.2.1	pH.....	3-5
	3.1.2.2	Alkalinity	3-5
	3.1.2.3	Carbon.....	3-5
	3.1.2.4	Nitrogen	3-7
	3.1.3	Daily Flow	3-10
	3.1.4	Hydraulic Loading Rate.....	3-12
	3.2	Parameters Relevant to Nitrogen Attenuation	3-14
	3.2.1	Soil Temperature.....	3-16
	3.2.2	Ammonium Sorption Coefficient	3-17
	3.2.3	Nitrification Parameters	3-20
	3.2.3.1	Nitrification Rate	3-22
	3.2.3.2	Half-Saturation Constant for Ammonium	3-24
	3.2.4	Denitrification Parameters	3-25
	3.2.4.1	Denitrification Rate.....	3-27
	3.2.4.2	Half-Saturation Constant for Nitrate.....	3-29
	3.3	Parameters Relevant to Microorganism Attenuation.....	3-30
	3.3.1	Virus.....	3-30
	3.3.2	Bacteria	3-31
	3.4	Parameters Relevant to OWC Attenuation	3-33
	3.4.1	OWC Compounds.....	3-34

3.4.2	Fate and Transport Parameters.....	3-34
3.4.2.1	Estimation of the Relevant Transformation Parameters	3-35
3.4.2.2	Parameter Estimation Example: Estrogenic Hormones	3-36
3.4.3	Treatment Limitations.....	3-37
3.4.3.1	Shallow Depth to Groundwater or Confining Layer Conditions	3-38
3.4.3.2	Low Organic Carbon Content Conditions	3-38
3.4.3.3	Anoxic Soil Conditions.....	3-38
3.4.3.4	High pH Conditions	3-38
3.4.3.5	Additional Treatment Considerations.....	3-39
Appendix A: General Reference Information.....		A-1
Appendix B: Worksheet Form		B-1
Appendix C: Field Testing For Tool Development		C-1
Appendix D: Microbial Fate and Transport.....		D-1
References.....		R-1

Supplemental Files Also on Disk:

Guidance Manual
Visual-Graphic Tools
N-CALC
STUMOD
DEC1R06 Literature Review: State of the Science – Review of Quantitative Tools to
Determine Wastewater Soil Treatment Unit Performance

LIST OF TABLES

1-1	Concentrations of Nitrogen and Organic Constituents Found in STE.....	1-7
2-1	Summary of Ammonium Sorption Coefficients for Clay-Rich and Clay-Poor Soils as Reported in the Literature	2-5
2-2	Results of 1-way ANOVA to Determine the Effect of Soil Texture on Nitrification Rates	2-10
2-3	Correlation Matrix for the Curves Shown in Figure 2-4.....	2-12
2-4	Fitted Parameters for the Nitrification Moisture Dependency Function	2-13
2-5	Fitted Parameters for the Denitrification Moisture-Dependency Function for the Three Different Soil Groups.....	2-21
2-6	STUMOD Input Parameters	2-23
2-7	Summary of Conditions for Comparison of STUMOD and HYDRUS-2D	2-30
2-8	Denitrification Rates used During Benchmarking of STUMOD and HYDRUS-2D	2-30
2-9	Comparison of STMOD Estimated Nitrogen Removal to Reported Measured Data	2-33
2-10	N-CALC Input Parameters	2-34
3-1	Summary of Soil Texture Properties.....	3-2
3-2	Summary of Soil Texture Hydraulic Properties.....	3-3
3-3	Summary of Typical Constituents Found in STE.....	3-4
3-4	Measured Indoor Daily Flow Summary Statistics ($L \text{ capita}^{-1} \text{ d}^{-1}$).....	3-11
3-5	Summary of HLR Used in STU Design	3-12
3-6	Summary of Key Factors Influencing the LTAR and Design HLR Values	3-13
3-7	Nitrogen Transformation Parameters Reported in the Literature	3-15
3-8	Citations for Reported Nitrogen Transformation Parameters.....	3-15
3-9	Annual Average Temperatures by Climate Region	3-17
3-10	Summary of Factors Influencing Ammonium Sorption	3-19
3-11	Summary of Factors Influencing Nitrification.....	3-22
3-12	Summary of Half Saturation Constants for Ammonium Reported in the Literature	3-24
3-13	Summary of Factors Influencing Denitrification.....	3-27
3-14	Summary of Half Saturation Constants for Nitrate Reported in the Literature	3-29
3-15	Summary of Factors Influencing the Magnitude of Virus Removal.....	3-31
3-16	Summary of Factors Influencing the Magnitude of Bacteria Removal	3-32
3-17	Characteristics for Selected OWCs.....	3-34
3-18	OWC Groups and Examples of Common Contaminants	3-34
3-19	Summary of Fate and Transport Properties for Four Different OWC Groups	3-35
3-20	Summary of Factors Influencing OWC Removal.....	3-38
3-21	Potential Design Options to Overcome Limiting Conditions	3-39

LIST OF FIGURES

1-1	Trench and Drip Domains as Represented in HYDRUS	1-2
1-2	Effect of pH on the Maximum Nitrification Rate Using Equation 1.3.1-1.....	1-11
1-3	Distribution of NRCS Soil Temperature Stations in the U.S., Puerto Rico, and Antarctica	1-13
1-4	Graphical Representation of the Monod Function.....	1-14
2-1	Decrease in Sorption Coefficient with Increase in Ammonium Concentration	2-4
2-2	Nitrification Temperature-Dependency Function.....	2-8
2-3	Fitted Temperature Functions to Soil Nitrification Data	2-9
2-4	Best Fit of Experimental Data to the Moisture-dependency Function	2-12
2-5	Nitrification Moisture Dependency Function Developed from Existing Data	2-13
2-6	Results of Using Model Input Parameters Developed by Wang et al. (2005).....	2-14
2-7	Visual Representation of the Functions Incorporated into HYDRUS-2D.....	2-16
2-8	Denitrification Rates as Function of Soil Temperature	2-17
2-9	Comparison of Denitrification Rates as Function of Soil Temperature	2-18
2-10	Conceptual Model for Denitrification Moisture Dependency	2-19
2-11	Example of Reported WFPs from Denitrification Experiments in “Silty” Soils.....	2-20
2-12	Reported Denitrification Rates and Average Rates based on Lumping as a Function of WFP.....	2-20
2-13	Fitted Denitrification Moisture-dependency Functions to Literature Data for the Three Different Soil Groups.....	2-21
2-14	Flowchart of Nitrogen Attenuation Procedures Incorporated into STUMOD.....	2-24
2-15	Sensitivity of Soil Moisture Content to Input Parameters	2-27
2-16	Sensitivity of Ammonium-nitrogen Concentration to Input Parameters (STE)	2-28
2-17	Sensitivity of Fraction Nitrogen Removed to Input Parameters (STE).....	2-28
2-18	Sensitivity of Fraction Nitrogen Removed to Input Parameters (nitrified effluent).....	2-29
2-19	Benchmarking Results for Sandy Loam at 15°C	2-30
2-20	Benchmarking Results for Silty Loam at 15°C	2-31
2-21	Benchmarking Results for Silt at 15°C.....	2-31
2-22	First Order Nitrification Rates Reported in the Literature.....	2-36
2-23	First Order Denitrification Rates Reported in the Literature	2-36
2-24	Example Concentration Profile for Ammonium (NH ₄ -N), Nitrate (NO ₃ -N) and Total Nitrogen (TN) using N-CALC.....	2-37
2-25	Example Removal Efficiency of Total Nitrogen using N-CALC.....	2-38
2-26	Example Mass Flux Prediction with Depth for Ammonium (NH ₄ -N), Nitrate (NO ₃ -N), and Total Nitrogen (TN) Using N-CALC.....	2-38
2-27	Three-Dimensional Visualization of the Two-Dimensional Trench Model.....	2-39
2-28	Representation of Axis-Symmetrical Domain as Used in the Drip Simulations	2-40
2-29	Graphical Representation of the Feddes Root-Uptake Water-stress Function	2-42
2-30	Spatial Distribution of the Root Density in the Drip Simulations	2-43
2-31	Finite Element Mesh for HYDRUS Model (dimensions in cm).....	2-44
2-32	Soil Layers in HYDRUS Model	2-45
2-33	Pressure Heads in cm Predicted by the HYDRUS Model After 100 Days	2-46
2-34	Nitrate Concentrations in mg-N L ⁻¹ Predicted by HYDRUS After 100 Days.....	2-47

2-35	Ammonium Concentrations in mg-N L ⁻¹ Predicted by HYDRUS After 100 Days.....	2-47
2-36	Dinitrogen Gas Concentrations in mg-N L ⁻¹ Predicted by HYDRUS After 100 Days .	2-48
3-1	Alkalinity Concentrations Measured in STE	3-5
3-2	COD Concentrations Measured in STE.....	3-6
3-3	cBOD ₅ Concentrations Measured in STE.....	3-7
3-4	Total Nitrogen Concentrations Measured in STE.....	3-8
3-5	Ammonium-Nitrogen Concentrations Measured in STE	3-8
3-6	Nomograph Illustrating Percent Nitrogen Removal at 60 cm Depth in Different Temperature Regions with Different Initial Effluent Concentrations	3-9
3-7	Nitrate-Nitrogen Concentrations Measured in STE.....	3-10
3-8	Measured Daily Indoor Flows	3-11
3-9	Average Soil Temperatures in the United States	3-16
3-10	Decision Diagram for Estimating the Ammonium Sorption Coefficient	3-18
3-11	Cumulative Frequency Distribution of Ammonium Sorption Coefficient (K _d) Values as Reported in the Literature.....	3-19
3-12	Cumulative Frequency Distribution of Ammonium Sorption Coefficient (K _d) Values for Clay-Rich versus Clay-Poor Soil as Reported in the Literature	3-20
3-13	Decision Diagram for Determining Nitrification Parameters.....	3-21
3-14	Zero-order Nitrification Rates Reported in the Literature	3-23
3-15	Maximum Zero-order Nitrification Rates Reported in the Literature	3-23
3-16	Decision Diagram for Determining Nitrification Parameters	3-26
3-17	Zero-order Denitrification Rates Reported in the Literature	3-28
3-18	Zero-order Denitrification Rates at 100% WFP for Three Different Soil Groups	3-28
3-19	Virus Removal as Reported in the Literature	3-31
3-20	Fecal Coliforms in STE as Reported in the Literature.....	3-33
3-21	Bacteria Removal as Reported in the Literature.....	3-33
3-22	Fate and Transport Dependence on K _d Value.....	3-36
3-23	K _d Values for Estrogenic Hormones for Associated Fraction of Soil Organic Carbon	3-37

LIST OF ACRONYMS

ANOVA	analysis of variance
APHA	American Public Health Association
BDL	below detection limit
BOD	biochemical oxygen demand
BOD ₅	biochemical oxygen demand, five-day test
cBOD	carbonaceous biochemical oxygen demand
C	carbon
CaCO ₃	calcium carbonate
CEC	cation exchange capacity
CFD	cumulative frequency distribution
cfu	colony forming unit
CO ₂	carbon dioxide
COD	chemical oxygen demand
CSM	Colorado School of Mines
CW2D	Constructed Wetlands 2D model
DOC	dissolved organic carbon
ET	evapotranspiration
GFP	green fluorescent protein
HLR	hydraulic loading rate
IQR	inter-quartile range
LB	lysogeny broth
LTAR	long term acceptance rate
N	nitrogen
N ₂	dinitrogen gas
N-CALC	Nitrogen Calculator (spreadsheet tool)
NH ₄ ⁺	ammonium ion
NO ₃ ⁻	nitrate-nitrogen
NRCS	Natural Resources Conservation Service
OWC	organic wastewater contaminants
OWTS	onsite wastewater treatment systems
PBS	phosphate-buffered saline
pfu	plaque forming unit

PO ₄ ⁻³	phosphate
POC	particulate organic carbon
RT	retention time
SSURGO	Soil Survey Geographic
STATSGO	State Soil Geographic (soil database)
STE	septic tank effluent
STU	soil treatment unit
STUMOD	Soil Treatment Model (spreadsheet tool)
TDR	time domain reflectometry water content sensors
TMDL	total maximum daily load
TOC	total organic carbon
UCR	University of California at Riverside
UGA	University of Georgia
URI	University of Rhode Island
USDA	United States Department of Agriculture
U.S. EPA	United States Environmental Protection Agency
USGS	United States Geological Survey
WERF	Water Environment Research Foundation
WFP	water filled porosity

EXECUTIVE SUMMARY

The overall goal of this project was to provide a toolkit to assess the soil treatment unit (STU) performance. This toolkit enables evaluation and design of expected STU performance for important wastewater constituents over a relevant range of onsite wastewater treatment systems (OWTS) operating conditions. The toolkit was developed for a wide range of users faced with different needs of varying complexity. The toolkit was designed to evaluate treatment of nitrogen, microorganisms (bacteria and virus), and organic wastewater contaminants (OWCs). These pollutants are currently of primary concern, or are projected to be of high concern, to nearly every county and state in the United States. The components of the toolkit are: Guidance Manual, User's Guide, Visual-graphic tools, and Spreadsheet tools.

The Guidance Manual provides a general introduction and overview to the toolkit while the User's Guide provides the technical details important to tool development and use. This User's Guide is a separate document that must be used in conjunction with the Guidance Manual. The fundamental assumptions that were incorporated into the development of the tools in this toolkit are provided in Chapter 1.0. A detailed description of the tool development is provided in Chapter 2.0 and detailed guidance on parameters that affect STU treatment performance and how to select specific values during tool use are provided in Chapter 3.0. Relevant general reference material such as the USDA soil textural triangle with grain size distributions and conversions for common parameters is presented in Appendix A. Appendix B includes a worksheet form that may help guide the user through the different decision-making steps while keeping all relevant information in a compact format. Appendix C provides the results from field experiments conducted in Georgia coupled with the 2D modeling using HYDRUS. Column experiments conducted in Rhode Island on the fate and transport of bacteria and virus are provided in Appendix D.

The companion Guidance Manual is organized into four chapters. Chapter 1.0 provides an introduction to the toolkit. Chapter 2.0 provides description of the tools. Chapter 3.0 guides the user through the decision process for assessment of parameters relevant to treatment performance including examples on tool selection and how to use those tools. Chapter 4.0 provides a summary of the toolkit.

Tools are provided as separate files. Visual-graphic tools (nomographs, cumulative probability graphs, and scenario illustrations) are compiled into a separate pdf file. STUMOD and N-CALC are separate Microsoft™ Excel files.

CHAPTER 1.0

SCIENTIFIC PRINCIPLES AND GOVERNING ASSUMPTIONS

Simple tools can be very helpful for a wide range of common onsite wastewater treatment system (OWTS) scenarios. Because sufficient understanding, data, and project schedule do not exist to completely represent the wide range of soil treatment unit (STU) conditions that occur, there are certain conditions where the developed tools are not sufficient to adequately predict performance, or the uncertainty in these predictions may be unacceptable for certain high-risk scenarios. In these cases, it must be recognized that more rigorous numerical modeling is required. It is up to the user to decide if the simple tools provided in this toolkit are appropriate or if more rigorous modeling/tools are required.

During the literature review, some empirical tools were developed based on statistical evaluation of the available data. However, while these tools provided insight into treatment and the factors influencing treatment, the data sets were generally not sufficiently robust to enable development of empirical tools that were statistically reliable. Thus, the focus of this User's Guide is describing the tools that were developed based on current scientific understanding of the dominant soil processes influencing treatment, while avoiding theory too complex to allow evaluation of tools versus practically measurable data. The basic philosophy and fundamental assumptions that are inherent in the technical development of the tools is discussed in this chapter. Descriptions of HYDRUS and STUMOD and the relevant parameter selection used for tool development are provided in Chapter 2.0.

1.1 OWTS Design and Operating Conditions

The possible combinations of OWTS design and operation are nearly infinite. In addition, tools based on sparse information are no more defensible than tools based on common knowledge without adequate data. Therefore, this toolkit focuses on a subset of the most common systems for which sufficient data are available to develop reliable tools. The design and operating assumptions for tool development are described below.

1.1.1 Daily Flow

Daily flow is an important parameter used for design of OWTS and is normally based on an estimated per capita occupancy of the bedrooms in a residence and some expected median per capita water use value. While such a calculation may be sufficient in many situations, knowledge of actual flow is often more useful. In recent research by Lowe et al. (2009), daily flow was measured at 16 single family homes in three different regions. Look-up tables and cumulative frequency distribution (CFD) graphs from that work are provided in Section 3.1.3 of this User's Guide to aid in making daily flow estimations if the water use is not known. However, use of this

toolkit does not require estimation of daily flow, but rather is based on assumed hydraulic loading rates (HLRs) (User's Guide, Section 3.1.4).

1.1.2 Effluent Delivery Method

The focus of this toolkit is on two general types of OWTS design: a subsurface trench and a drip dispersal system installed in the shallow subsurface. Figure 1-1 illustrates the domain as represented by HYDRUS. The science and engineering literature, theory, and data are not in agreement regarding the relative performance of soil infiltrative surface and therefore are not explicitly considered. Rather, it was assumed that the STU performs similarly for each infiltrative surface. Furthermore, the shallow drip dispersal system was assumed to have a grass cover to account for the associated flux of nitrogen upward. Additional scenarios illustrate differences in nitrogen mass flux due to various growing season length (Visual-Graphic Tools, Chapter VG-3.0).

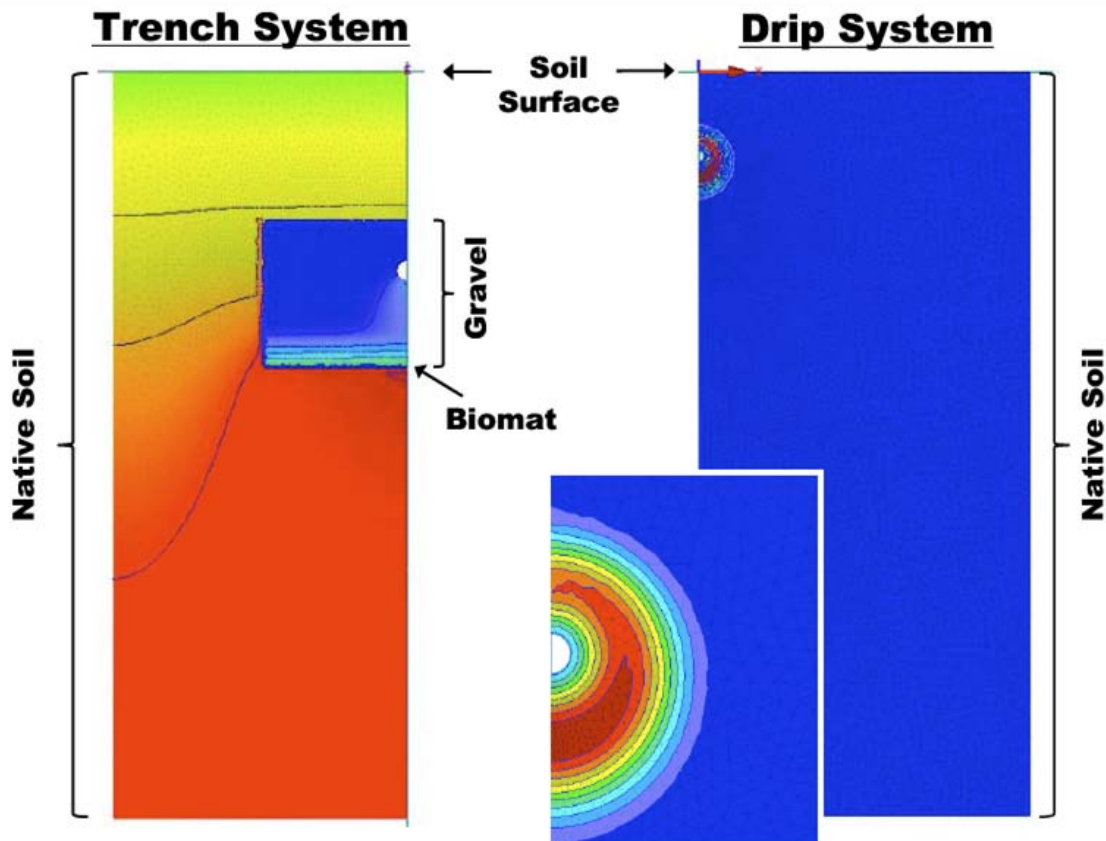


Figure 1-1. Trench and Drip Domains as Represented in HYDRUS.
(The colors show general wetting pattern of the soil.)

1.1.3 OWTS Geometry

Although HYDRUS can be used to simulate virtually any subsurface geometry for trench or drip systems, 2D cross sections were utilized in this project. The details on HYDRUS geometry are described in Section 2.4 of this User's Guide. STUMOD is limited to a 1D vertical system and is thus most appropriate for estimating treatment along the centerline directly below an infiltrative surface. In this regard, STUMOD will tend to underestimate the nitrogen removal

(over estimate nitrogen concentrations in the STU) compared to HYDRUS and provide a more conservative assessment (User's Guide, Section 2.2.3).

1.1.4 Hydraulic Loading Rate

HYDRUS can simulate constant or time-dependent loading at various rates. For development of the simple tools, two loading rates were used to represent a range of those expected. For the subsurface trench, HLRs of 2 cm d⁻¹ or 10% of the hydraulic conductivity (K_{sat}) for a given soil textural class was used for scenario illustrations. For the drip dispersal system, both low and high rates were used based on typical manufacturer recommendations. The low rate is consistent with rates applicable to clay soils while the high rate is consistent with rates applicable to sandy soils. Each of these conditions illustrate a range of loading rates and enable the user to visualize the impact of HLR on different soil textures.

The nomographs were developed using STUMOD and a HLR of 2 cm d⁻¹ or 5% of K_{sat} . When using STUMOD, the user can specify any HLR less than the saturated hydraulic conductivity of the receiving soil. STUMOD accepts a constant loading rate so an average constant rate is used. This assumption may be reasonable given that biozone formation can cause ponding and result in quasi-steady rates even for dosed systems.

1.1.5 Subsurface Heterogeneity

Although HYDRUS can consider subsurface heterogeneity, an infinite number of combinations of subsurface heterogeneities are possible. Thus, the visual-graphic tools developed from HYDRUS consider an average homogeneous subsoil layer overlain by a lower permeability biozone. This is a reasonable approach given that nearly all the literature data that was used to obtain tool and model input described the soil using a single soil classification, and did not report the heterogeneity of the soil, even though all soil is generally heterogeneous.

STUMOD currently assumes a homogeneous soil profile, other than the hydraulic presence of a biozone. Similar to HYDRUS, it is possible to enable STUMOD to account for a layered soil profile, but that enhancement becomes impractical.

1.1.6 Subsurface Soil Hydraulic Properties

Hydraulic properties of the different soil textural classes were taken from the statistical database by Schaap et al. (2001). This database provides hydraulic properties (saturated hydraulic conductivity, porosity, residual moisture content, and other parameters related to soil suction and capillarity) based on statistical evaluation of thousands of samples. Hydraulic parameters are provided in Section 3.1.1 of this User's Guide for each of 12 soil textures designated in the United States Department of Agriculture (USDA) soil triangle (User's Guide, Appendix A, Figure A-1).

Biozone hydraulic properties are based on a literature review conducted by Beach (2001), as well as recent studies (Beach and McCray, 2003; Beal et al., 2005; Bumgarner and McCray, 2007; Radcliffe and West, 2007; Beal et al., 2008; Finch et al., 2008; McKinley, 2008; Radcliffe and West, 2009). It was not possible to quantify and account for any influence of the biozone on treatment, as very little information was available in the literature; however, some treatment enhancement for nitrogen, virus, and organic wastewater compounds (OWCs) is anticipated. Ignoring the potential treatment enhancements of the biozone will lead to a conservative prediction.

1.1.7 Interactions Between the STU and the Water Table

HYDRUS can simulate nearly any realistic subsurface flow scenario associated with the water table, including impacts of shallow water tables on soil moisture in the STU (and thus on treatment) and mounding of the water table. However, the possibilities are again nearly infinite, and thus representative conditions have been defined. A shallow water table depth (60 cm below the drip-line) is assumed in the simulations of drip-systems, while a deep water table (greater than 90 cm) is assumed in the select trench dispersal systems. This is consistent with some regulatory statutes, as well as an alternate case that assumes free drainage (i.e., no impact from a deep water table on flow or soil moisture). If the user desires information on the interactions between STUs and the water table at specific water table depths, then a professional hydrologic modeler would need to be hired to implement HYDRUS, or some other numerical model.

STUMOD assumes that flow is steady and that drainage occurs freely (i.e., the water table is far below the infiltrative surface such that it does not impact soil moisture in the infiltrating region). STUMOD should not be used if the influence of a shallow water table on treatment or the influence of the STU on the water table is to be investigated. However, a screening estimate can be identified based on the centerline concentration for a given depth below the infiltrative surface.

1.1.8 Cumulative Impacts of OWTSs

HYDRUS can simulate single or multiple OWTS with essentially any geometric arrangement. As it was not feasible to simulate all the possible OWTS configurations, again simplifying assumptions were made and only a single OWTS is represented by the tools. HYDRUS was used to illustrate select scenarios that show the impacts of precipitation, shallow versus deep water table, and different HLRs, which show the impacts of different moisture regimes. STUMOD does not implicitly account for cumulative impacts or OWTS density, however; an example of how to use STUMOD to conduct such an evaluation is presented in Section 3.4 of the Guidance Manual.

1.2 Effluent Quality

To develop the visual-graphic tools two general effluent qualities were considered: 1) typical septic tank effluent (STE) obtained after primary treatment in the septic tank; and 2) a nitrified effluent such as would be obtained from aerobic treatment prior to discharge into the STU. The effectiveness of nitrogen removal during aerobic treatment varies widely based on individual site conditions and the overall treatment train configuration; hence an attempt was not made to account for specific performance, but rather to recognize that a nitrified effluent applied to the soil may affect the expected STU performance. Knowledge of the total nitrogen and carbon concentrations are important, as the ratio of carbon to nitrogen determines if nitrification and denitrification is likely to occur.

1.2.1 Nitrogen

It is generally assumed that about 85 to 90% of the organic nitrogen in raw wastewater is converted to ammonium-nitrogen in the septic tank (APHA, 2005). In fact, Lowe et al. (2009) confirmed that the mass of organic nitrogen was reduced by 85% in the septic tank with less than 10% of the total nitrogen in STE as organic nitrogen. The remaining organic nitrogen is likely transformed to ammonium-nitrogen in the STU, assimilated into the cells of certain

microorganisms, or remains as organic nitrogen in soil solution. As no information on the fate and transport of organic nitrogen is available, the impact of this small amount of organic nitrogen in the soil system was not included in tool development. Furthermore, HYDRUS and STUMOD do not incorporate organic nitrogen. Thus, the total nitrogen concentration in STE was assumed to be in the form of ammonium-nitrogen, which is a conservative assumption.

The concentration of total nitrogen in STE is typically assumed to range between 25-90 mg-N L⁻¹ (Crites and Tchobanoglous, 1998; U.S. EPA, 2002). Based on field monitoring completed in WERF 04-DEC-1 (Lowe et al., 2009) concentrations ranged from 25 to 125 mg-N L⁻¹ with total nitrogen concentrations less than 90 mg-N L⁻¹ 90% of the time and the median total nitrogen concentration of ~60 mg-N L⁻¹ (median literature value = 58 mg-N L⁻¹, median value from field monitoring = 64 mg-N L⁻¹, Lowe et al., 2007 and 2009). Lowe et al. (2009) found the inter-quartile range of ammonium-nitrogen to be between 45 mg-N L⁻¹ and 70 mg-N L⁻¹, with a median concentration of 53 mg-N L⁻¹. Very little nitrate-nitrogen is typically present in STE. The anaerobic conditions that prevail in a septic tank do not allow for oxidation (nitrification) of ammonium to nitrate, which result in a median nitrate-nitrogen value of 1 mg-N L⁻¹ (Lowe et al., 2009). Thus for the simple tool development, the concentration of total nitrogen in STE was assumed to be 60 mg-N L⁻¹ of ammonium-nitrogen with 1 mg-N L⁻¹ of nitrate-nitrogen.

For the nitrified effluent, it was assumed that all ammonium-nitrogen had been converted to nitrate-nitrogen and that sufficient carbon was present to enable denitrification. For simple tool development, the nitrified effluent was assumed to have no ammonium-nitrogen but 15 mg-N L⁻¹ of nitrate-nitrogen.

The spreadsheet tools STUMOD and N-CALC can accept any range of ammonium-nitrogen and nitrate-nitrogen concentrations. More complex tools may require that the user have some knowledge of the actual concentrations of ammonium-nitrogen and nitrate-nitrogen in the effluent. In these cases, the user can estimate concentrations from the CFDs provided in Section 3.1.2.4 of this User's Guide or refer to Lowe et al, 2007 and 2009 for complete WERF 04-DEC-1 findings.

1.2.2 Carbon

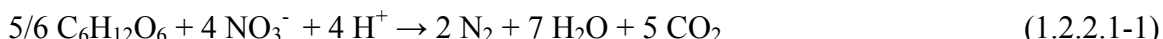
Nitrification is the process where ammonium ions are oxidized by autotrophic bacteria (bacteria that obtain their energy from carbon dioxide gas [CO₂] rather than organic matter). Because soil gas is known to have high concentrations of CO₂ (Jury and Horton, 2004), it was assumed that sufficient carbon was always present for nitrification, providing that gas diffusion was not inhibited due to high soil water contents. In contrast, a carbon source is necessary for biological denitrification as the denitrifying organisms obtain their energy from the oxidation of organic compounds. A lack of organic carbon has been shown to be a factor limiting denitrification (Smith and Duff, 1988; Starr and Gillham, 1993; DeSimone and Howes, 1998; Devito et al., 2000; Pabich et al., 2001) and several studies have shown that denitrification increases when ample amounts of organic carbon are present in the soil (Stanford et al., 1975; Beauchamp et al., 1980; Groffman and Tiedje, 1989; Brettar and Höfle, 2002). Denitrification has been correlated to total organic carbon (TOC) in soil (Anderson, 1998; Brettar and Höfle, 2002); however, Tucholke et al. (2007) showed that no relationship could be established between organic carbon and denitrification.

While numerous soil denitrification studies have been conducted, few have investigated how the magnitude of denitrification in an STU is influenced by available carbon in OWTS

effluents. Rather the assumption is typically made that sufficient carbon for the denitrification process is applied to the STU such that numerical models that do not account for the affect of carbon limitation on denitrification are still assumed to be representative. This assumption is valid if both the carbon in the effluent and the soil is biologically active and available at a C:N ratio greater than stoichiometric requirements. The following provides further detail into the assumption of sufficient carbon in OWTS for tool development.

1.2.2.1 Background

The process of denitrification is primarily enzyme-catalyzed by heterotrophic facultative anaerobic microbes (i.e., microbes that obtain their energy from an organic carbon source). The electrons needed typically originate from the microbial oxidation of organic carbon. Various stoichiometric equations may be written for the denitrification process relating organic carbon and nitrate, but the process is often expressed using the following equation:



The above stoichiometry implies that 1.25 mols of carbon are required to denitrify 1 mol of nitrate-nitrogen to nitrogen gas (+231 mV) (i.e., C:N = 1.25:1). Thus, if 20 mg-N L⁻¹ (1.43 mmol) is mobile in the STU pore water, then 25 mg-C L⁻¹ (1.79 mmol) is required for denitrification. It is important to realize that the above equation does not take into account the amount of carbon that is oxidized in the soil or the amount of carbon necessary for microbial respiration. Finally, the equation assumes carbon in the form of glucose (C₆H₁₂O₆), which is a generalized way to depict organic carbon in a wastewater. However, this example equates to a carbon content that is much less than a typical soil (~0.001%), assuming all the organic carbon in the soil is water-soluble.

Because organic carbon tends to be oxidized preferentially with the electron acceptor that supplies the most energy (specifically free oxygen O₂, +334mV) (Rivett et al., (2008) adapted from Korom (1992)), 1 mol of organic carbon must first be converted to O₂, which requires 2.7 mols of carbon. Therefore, up to ~4 mg-C L⁻¹ may be required to denitrify 1 mg-N L⁻¹. In otherwords, 2.7 mols of carbon is first utilized to convert O₂, then 1.25 mols of carbon are utilized to denitrify 1 mole of nitrate-nitrogen (2.7 + 1.25 = 3.95 → C:N = 4:1).

Alternatively, the C:N may be determined using chemical oxygen demand (COD). COD is a measure of the oxygen equivalent of the organic matter content that is susceptible to oxidation by a strong chemical oxidant. The oxygen equivalent of nitrate-nitrogen is 2.86 mg O₂ mg⁻¹ nitrate-nitrogen (or -2.86 mg COD mg⁻¹ nitrate-nitrogen), which means 1 mg nitrate-nitrogen denitrified to nitrogen gas (N₂) has the same electron accepting capacity as 2.86 mg O₂ (or the same electron donor capacity as -2.86 mg COD). The C:N (in units of mg COD) is obtained using the following relationship:

$$C : N = \frac{2.86}{(1 - Y_H)} \quad (1.2.2.1-2)$$

where Y_H is the mg biomass COD formed per mg COD removed calculated from experiments or typically assumed to be 0.60 (Henze et al., 1987), which yields a C:N of 7.2. Finally, although the assumptions for the basis are not clear, U.S. EPA (2004) recommends a minimum ratio of 5:1 for denitrification.

The bioavailability of the carbon is also critical to consider. In general, as the molecular weight of the organic carbon increases (high molecular weight compounds), the carbon becomes more “humified” and is less biologically reactive (i.e., available as an electron donor for denitrification). However, humic substances are not recalcitrant and still provide a carbon source albeit less biologically reactive compared to lower molecular weight carbon compounds (e.g., sugars, acetate). Fractions of TOC are also operationally defined by the XAD resin fractionation analysis method:

- ◆ hydrophobic acids – mainly composed of humic substances (humic acid, fulvic acid) which are removed more slowly, but still degrade;
- ◆ hydrophilic – sugars, proteins, alcohols, and low molecular weight acids which are easily digested;
- ◆ colloidal OM – undegraded sugars and microbial colloids which are typically very easily removed carbon sources and likely to be quickly degraded during subsequent soil treatment; and
- ◆ hydrophobic neutrals – polysaccharides.

1.2.2.2 Carbon in OWTS Effluents

Reported and measured ranges of nitrogen and carbon in residential STE are provided in Table 1-1. Based on these values, the C:N ratio ranges from 1:1 to 9:1 depending on the form of nitrogen and carbon. While some research has shown that well-oxidized effluent contains only small amounts of carbon that can act as an electron donor (Robertson et al., 1991; MacQuarrie et al., 2001), other work has shown that sufficient organic carbon is available to support denitrification (Lance, 1972; Spalding et al., 1993).

Table 1-1. Concentrations of Nitrogen and Organic Constituents Found in STE.

	TN	NH ₄ -N	cBOD ₅	COD	TOC	DOC
Literature Values						
Number of Values	42	80	94	34	6	4
Median	mg L ⁻¹ 55	36	156	330	85	55
Range	mg L ⁻¹ 26-124	nd-96	38-861	157-1931	41-147	32-94
C:TN ratio			2.8	6.0	1.5	1.0
C:NH ₄ ratio			4.3	9.2	2.4	1.5
Measured Values						
n	65	65	63	64	63	64
Median	mg L ⁻¹ 63	53	216	389	105	66
Range	mg L ⁻¹ 27-119	25-112	44-833	201-944	50-243	22-140
C:TN ratio			3.4	6.2	1.7	1.0
C:NH ₄ ratio			4.1	7.3	2.0	1.2

Data taken from Lowe et al., 2009

Nitrified effluent is typically obtained by aerobic treatment of STE prior to discharge to the soil. The specific STE treatment goal (i.e., nitrate-nitrogen concentration achieved) varies based on the initial nitrogen concentration in STE, the individual site conditions, the advanced treatment employed, and the overall treatment train. If the cBOD₅ is reduced to <25 mg L⁻¹ and the total nitrogen is reduced by say 50%, C:N ratios could be well below 4:1 and denitrification would be limited. For example, an initial STE nitrogen concentration of 55 mg-N L⁻¹ reduced by 50% and completely nitrified would yield a nitrate-nitrogen concentration of 27.5 mg-N L⁻¹. If

the BOD₅ was also reduced to < 25mg L⁻¹, the resulting nitrified effluent C:N ratio would be 0.9:1 suggesting that denitrification may be limited in the absence of an additional carbon source.

Evaluation of the molecular weight distribution of the organic matter in STE and textile filter effluent (i.e., nitrified effluent) conducted at the Colorado School of Mines (CSM) suggests a shift from polysaccharides and humic acids in STE to a build-up of humic and fulvic-like material in the textile filter effluent (Rauch, 2004; Van Cuyk et al., 2005; Lowe et al., 2008). Additional bulk organic fractionation was also evaluated and suggests a higher percentage of hydrophobic organic carbon in the nitrified effluent compared to STE. Both of these results suggest that the carbon remaining in the nitrified effluent is relatively less available for denitrification compared to the carbon in STE. Rivett (2008) also suggested that nitrified effluent has little remaining carbon, and the carbon that is remaining is the least bioavailable. While the effluent analysis at CSM has confirmed this, additional carbon sources in the STU (e.g., particulate organic carbon, cell mass, soil organic carbon) are not considered.

1.2.2.3 Carbon in STUs

Organic carbon concentrations in soil normally range from non-detectable to 15% (by dry weight soil), although most soils contain levels less than 1%. It is important to realize that the amount of available organic carbon in the soil varies greatly with depth. Levels are usually highest in the topsoil (Morris et al., 1988; Ryan, 1998), and generally decrease rapidly further into the sub-surface, which may cause a decrease in denitrification (Fang and Moncrieff, 2005). However, high denitrification rates have been observed at great depths if the soil is amended with additional carbon (McCarty and Bremner, 1992; Jarvis and Hatch, 1994; McCarty and Bremner, 1995), which is assumed to be the case during the application of carbon rich effluent to STUs.

In addition, the contribution of different components of soil organic carbon is not well understood. Dissolved organic carbon (DOC) is typically assumed to be an indicator of the carbon available to soil microorganisms as it serves as a substrate for microbial respiration (Brye et al., 2000). While the rate of soil denitrification is frequently related to the amount of DOC in the pore water, rather than the total amount of solid organic carbon present (Burford and Bremner, 1975; Lundquist et al., 1999; Cannavo et al., 2004), Lundquist et al. (1999) reported that changes in DOC and respiration rates were not correlated and that DOC was not a good indicator of organic carbon availability to microorganism. The ability of DOC to serve as a predictor of microbial respiration is also limited due to the complexity in DOC production and consumption within soils (Fang and Moncrieff, 2005). Furthermore, because the mobility of DOC in the soil profile is strongly affected by sorption to mineral constituents and by the drainage capability of the soil, a decrease in DOC concentrations with depth can be expected in the soil (Jardine et al., 1989).

Soil biomass activity measurements have been conducted at the field test site at CSM (Van Cuyk et al., 2005). Total viable biomass (measured using phospholipid extraction of the organic bound phosphorus expressed as nmol PO₄⁻³ g⁻¹ dry soil) in the soil quantified all viable microbial cells that are potentially, but not necessarily active in soil. Background biomass concentrations in the soil were on the order of 1-15 nmol phosphate per g dry soil in the first 2 m of soil with decreasing biomass with depth. In soils receiving STE, a significant growth of soil biomass was observed in the upper 50 cm of the soil profile of the test cells with the total viable biomass increased by about a factor of 10 near the infiltrative surface and decreasing exponentially with depth. This biomass depth profile is an indication that most of the biological

processes causing organic and inorganic nutrient removal are occurring in the first 50 cm of the vadose zone.

Soil cores collected at the same time as the viable biomass analysis were also analyzed for polysaccharide and humic substances (McKinley, 2008). A similar trend of decreasing concentration of fulvic acid, humic acid, and polysaccharides with depth below the infiltrative surface was observed. In these soil cores, the carbon accumulations above background were confined to the top 2-4 cm of the soil. Additionally, humic substances composed the majority (80%) of TOC in the soil while polysaccharides composed a small percentage (20%). Again, these findings confirm that carbon limiting conditions for denitrification increase with depth either attributed to lower abundance or dominance of less bioavailable carbon compounds.

Organic carbon in the soil solution below the infiltrative surface has also been analyzed at CSM to determine the fate of carbon in the vadose zone (Tackett et al., 2004; Dimick, 2005; Lowe et al., 2007b). Since the nominal pore size of the suction lysimeter used to sample the soil pore water is 0.2 μm , it was assumed that the soil solution measurement represented DOC ($<0.45 \mu\text{m}$ filter normally employed for measuring DOC). After 3 years of effluent delivery, DOC ranged from 4-6 mg-C L^{-1} and TN ranged from 15 to 50 mg-N L^{-1} for STE and was $\sim 10 \text{ mg-N L}^{-1}$ for nitrified effluent at 60 cm below the infiltrative surface. In addition, the DOC concentrations were similar at 120 cm below the infiltrative surface, but up to 20% additional TN removal was observed (Lowe et al., 2007b). In this study, the stoichiometric C:N ratio (as DOC:TN) suggested that denitrification would be limited with depth. However, additional nitrogen removal was observed (even for nitrified effluents with an initially low C:N ratio). Particulate organic carbon which is a source of DOC, but not measured as DOC was not accounted for as well as other long term carbon sources such as microbial cells that die off and filtered solids. These observations indicate available carbon (e.g., microbial cell recycling and other particulate organic carbon that is not included in DOC) may be present in the STU such that denitrification is observed with depth, even though the C:N ratio based on effluent quality suggests denitrification may be limited.

1.2.2.4 Summary

The minimum C:N ratio to facilitate denitrification is in the range of 4:1 to 7:1 depending on the form of carbon. The C:N ratio for residential STE is likely often within this range although the C:N ratio for nitrified effluent may suggest conditions that limit denitrification. Certainly, nitrate contaminated groundwater has been documented and it can be assumed that one or more of the requirements for denitrification are not met, or that the nitrate loading into the STU exceeds the denitrification capacity. However, there is strong evidence for the occurrence of adequate organic carbon (including particulate organic carbon) to facilitate denitrification in STUs even with the effluent applied may have low carbon with optimum conditions for denitrification likely to occur in the top few centimeters of the STU (2-50 cm). Thus, the assumption that sufficient carbon for the denitrification process is applied to the STU is expected to be representative. Finally, it is important to note in situations where effluent is nitrified and/or the carbon is removed, less denitrification is expected to occur resulting in less nitrogen removal in the STU.

1.3 Nitrogen Transport and Transformation Assumptions

Volumes of literature address the scientific concepts of nitrogen transformation and attenuation in soils. The processes of nitrification and denitrification are very complex, with a consortium of microorganisms responsible for the transformations. Some of these organisms operate under anaerobic conditions, some under aerobic conditions, and some can operate under both conditions. These microorganisms also need nutrients and a carbon source, which can be different for the various organisms. Considering all the relevant processes would require simulation of many complex processes including: microbial growth, metabolism, transport and death for several different types of microbes; and diffusion, transport, microbial uptake, and biochemical transformation of nutrients including carbon, hydrogen, oxygen, nitrogen, phosphorus, and sulfur. The Constructed Wetlands (CW2D) module of HYDRUS (Langergraber and Šimůnek, 2005) is the only known model that attempts to simulate most of these relevant processes. However, because CW2D has more than 50 relevant model-input parameters for the nitrogen transformations alone, excluding spatial heterogeneities in properties, the model cannot be calibrated uniquely. CW2D was used successfully with field results from the University of Georgia (UGA) field test site, which was designed for model calibration (User's Guide, Appendix C). However, insufficient information exists in the scientific literature to parameterize a defensible model based on literature values alone. Thus, the relevant processes have been simplified to enable development of a defensible numerical model that can then be used to produce data needed for the simple tools. The following describes all nitrogen transport and transformation assumptions used in the tool development.

1.3.1 Sufficient Alkalinity and pH Exist for Nitrogen Transformations

During tool development it was assumed that sufficient alkalinity was present and that the pH was in a range for sufficient nitrification and denitrification to occur. Sufficient alkalinity is required for nitrification, most of which is associated with the neutralization of the hydrogen ions released during the nitrification process. STE is known to be alkaline, with concentrations of alkalinity typically exceeding 300 mg L⁻¹ as calcium carbonate (User's Guide, Figure 3-1). In contrast, the process of denitrification destroys hydrogen ions while producing CO₂, hence causing an increase in alkalinity. In fact, sufficient alkalinity has been measured at depths of up to 8 feet in soils below the dispersal of STE at the Mines Park Test Site at CSM (Tillotson, 2009), and experimental data from laboratory columns show that alkalinity is not depleted below the infiltrative surface (Beach, 2001; Tackett et al., 2004; Walsh, 2006).

While most bacteria grow poorly outside a pH range of 6-8, nitrifying bacteria, especially *Nitrosomonas*, are particularly sensitive to pH. Research has shown that the growth rate reach a maximum at a pH between 7 and 8, and declines at lower or higher pH levels (Quinlan, 1984). Because the pH in STE typically range between 7.1 and 7.7 (Lowe et al., 2009), it is not expected to significantly impact the nitrification rate. The pH was therefore assumed to have little impact on the rate of nitrification in development of the simple tools. However, it is important to realize that if the pH is found to be significantly lower than the typical range, the rate of nitrification will decrease. If that is the case then the maximum nitrification rate used in the provided tools should be adjusted accordingly. Siegrist and Gujer (1987) modeled the effect of lower pH levels on the nitrification rate (μ) using Equation (1.3.1-1):

$$\mu = \frac{\mu_{\max}}{1 + 10^{(6.5-pH)}} \quad (1.3.1-1)$$

where μ_{\max} is the max rate at optimum pH. The results agree with those found by Suzuki et al. (1974) and Laudelout et al. (1976). Of note, this equation only predicts the decline in rate at lower pH levels, which should not be a problem as the hydrogen ions released during nitrification depress the pH so that values rarely exceed 8.5. Figure 1-2 depicts the expected reduction in nitrification based on Equation 1.3.1-1.

In contrast, the denitrifying bacteria are not very sensitive to pH within expected ranges below the infiltrative surface and can handle most environmental conditions (Tucholke, 2007). Consequently, changes in pH and consumption or production of alkalinity during the nitrogen transformation process are not considered. It is reasonable to believe that denitrifiers in acidic soils produce a denitrification optimum at the soil's pH. However, Šimek and Cooper (2002) showed that when soil pH changes, such as due to a constant flux of nutrients at a certain pH, the pH optimum for denitrification is shifted as well to match the new conditions. In other words, the microbial population adapts to the new conditions, regardless of the condition itself, as soon as 12 hours after the change. When the shift is towards a neutral pH (as is the case with typical STE), the denitrification rate is at its highest. Therefore, pH was not considered an inhibiting factor for denitrification during tool development.

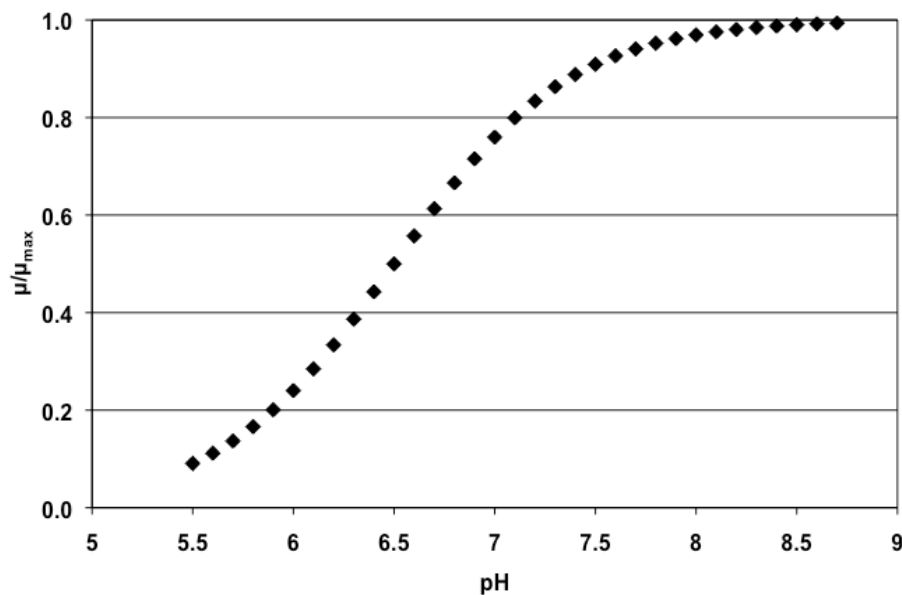


Figure 1-2. Effect of pH on the Maximum Nitrification Rate Using Equation 1.3.1-1.

1.3.2 Nitrogen Transformation Parameters

Treatment estimates were based on statistical distributions of the most important parameters developed from data obtained in the literature. All relevant data for different parameters (e.g., nitrogen transformation rate constants, ammonium sorption constants, hydraulic parameters such as hydraulic conductivity, etc.) were compiled from the literature. From these data, mean values with standard deviations or median values with quartiles, and/or the cumulative frequency of parameter values were calculated. CFDs were produced to evaluate the frequency of occurrence of measured values. The 50th percentile value is the median value. The 38th percentile value (for example) indicates that 38% of all the data in the literature are less

than this value, and 62% are greater than this value. Where possible, the CFDs or statistical analyses are produced for each of the three soil groups represented in the visual-graphic tools; however, scarcity of data precluded this approach for all parameters (e.g., for ammonium sorption constants). In these cases, look-up tables provide guidance for parameter selection or other conditions that might warrant using a higher or lower value than the reported median. For example, ammonium sorption is larger in clay soils, so using a value greater than the suggested median would be appropriate (the converse is true for sandy soils).

1.3.3 Soil Temperatures Impact Nitrogen Transformations

There are numerous studies that indicate nitrogen transformation rates generally increase with temperature to a maximum value of about 25°C and decline with additional increasing temperature (Malhi and McGill, 1982; Grundmann et al., 1995; Avrahami et al., 2003). Because soil temperature at depths relevant to OWTS (0.1 to 3 m below surface) can range between 3°C and 25°C (Brady and Weil, 2002) with significant geographical variation, the average annual soil temperature in different regions of the U.S. were taken into account during tool development.

The USDA divides the contiguous U.S. into five sub-regions based on soil annual average temperatures and seasonal variations (Figure 3-2 in Chapter 3.0). According to the USDA classification, most of U.S. soils are considered “mesic” or “thermic”. Soils have a mesic temperature regime if the mean annual temperature is between 8°C and 15°C, whereas thermic soils have a mean annual temperature between 15°C and 22°C (USDA, 1999). Table 3-1 in Chapter 3.0 presents the low and high annual averages for each soil temperature regime (USDA, 1999), with the overall annual mean. Because both “frigid” and “cryic” regions have the same annual mean soil temperature, those regions were combined into one region during tool development. As a result, the nomograph tools are divided not only into soil textural class, but also into temperature region.

Because the entire nation is not monitored at the county level, and much of the assumed soil temperatures are assigned by interpolation between stations or by extrapolation, a user who wishes to dive further into the data can refer to the Natural Resources Conservation Service (NRCS) webpage: <http://www.wcc.nrcs.usda.gov/scan/>, which contains an interactive map (shown in Figure 1-3), illustrating the nation-wide real-time and non-real-time soil temperature readings (alongside other data such as soil moisture). The soil temperatures are taken in these stations at various depths, and a specific legend is provided in the website for each location.

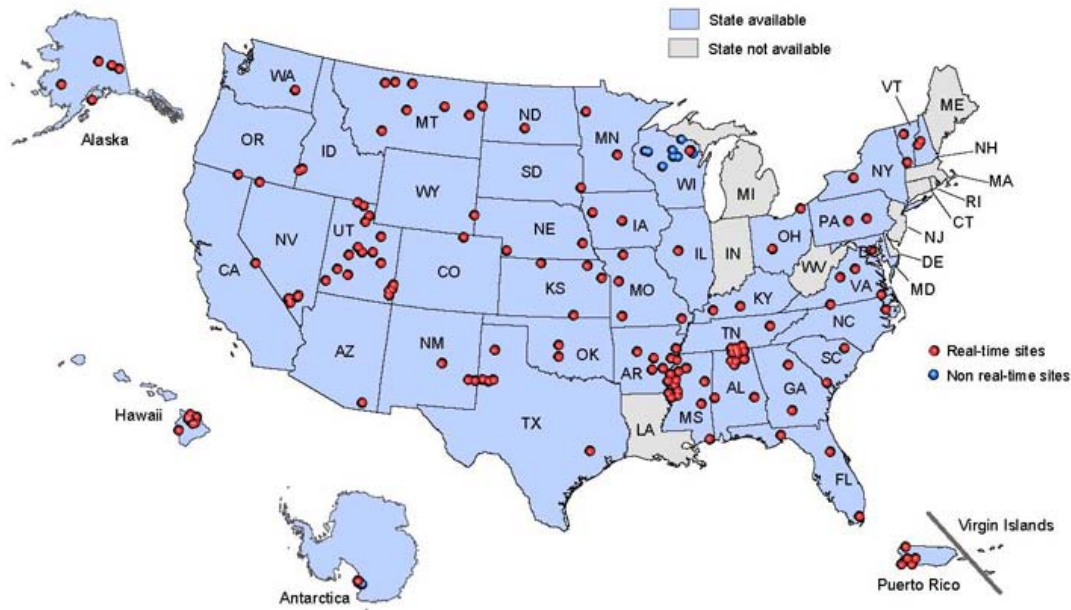


Figure 1-3. Distribution of NRCS Soil Temperature Stations in the U.S., Puerto Rico and Antarctica.
 Source: http://www.wcc.nrcs.usda.gov/scan/scan_map.jpg

1.3.4 Ammonium Sorption is a Linear Process

Ammonium association with soils is an important process in nitrogen transformation. Specifically, ammonium adsorbed during the wetting pulse of effluent application is held on the soil and can be nitrified when the soil becomes dry (in between pulses). The sorption process is thought to be controlled by cation exchange processes, which depend on the ionic composition of the soil, as well as the ionic makeup of the effluent. The cation exchange process is typically assumed to be reversible; however, most of the data in the literature report sorption constants for ammonium that assume linear, equilibrium, reversible sorption, which does not consider the details of cation exchange. Thus, the cation exchange of ammonium was assumed to be a linear, equilibrium, reversible process. Furthermore, ammonium was assumed to be the only nitrogen species that adsorb to soil colloids based on the range of pH in STE-amended soil. The literature on conversion of organic nitrogen to ammonium is very sparse; hence it was not considered during tool development.

1.3.5 Nitrogen Transformation Rates Follow Monod Kinetics

Most enzyme-catalyzed biological reactions follow Monod kinetics, where the reaction rate of is controlled by the availability of substrate. The kinetics of nitrogen transformations can thus be represented mathematically by the following relationship:

$$\mu = \mu_{\max} \left(\frac{C}{K_m + C} \right) \quad (1.3.5-1)$$

where μ_{\max} is the maximum reaction rate, C is the substrate concentration, and K_m is the half-saturation constant, which is the substrate concentration at which the growth rate is half the maximum growth rate. The transition between zero and first order kinetics is set by the half-

saturation constant (K_m). When K_m is much greater than C (i.e., at low concentrations of substrate) the rate becomes almost proportional to the substrate concentration, thereby approximating first-order kinetics, conversely when C is much greater than K_m , μ becomes independent of the concentration (i.e., $\mu = \mu_{max}$) and approximates zero-order kinetics (Hemond and Fechner-Levy, 2000). Thus, Monod kinetics enables first order kinetics at lower values of nitrogen concentrations, and zero-order kinetics at higher values of nitrogen concentrations (Figure 1-4). Further discussion on the selected K_m value is provided in Section 2.1.3.1.

It follows that for nitrogen concentrations in the STU that produce elevated nitrogen concentrations in groundwater; the transformation rates are expected to be zero order. Nonetheless, both STUMOD and HYDRUS (as modified for this project, see Chapter 2.0 of this User's Guide) can simulate Monod kinetics for nitrification (conversion of ammonium-nitrogen to nitrate-nitrogen, the conversion of nitrite-nitrogen to nitrate-nitrogen is known to be very fast) and for denitrification (conversion of nitrate-nitrogen to molecular nitrogen); hence the actual reaction order becomes irrelevant.

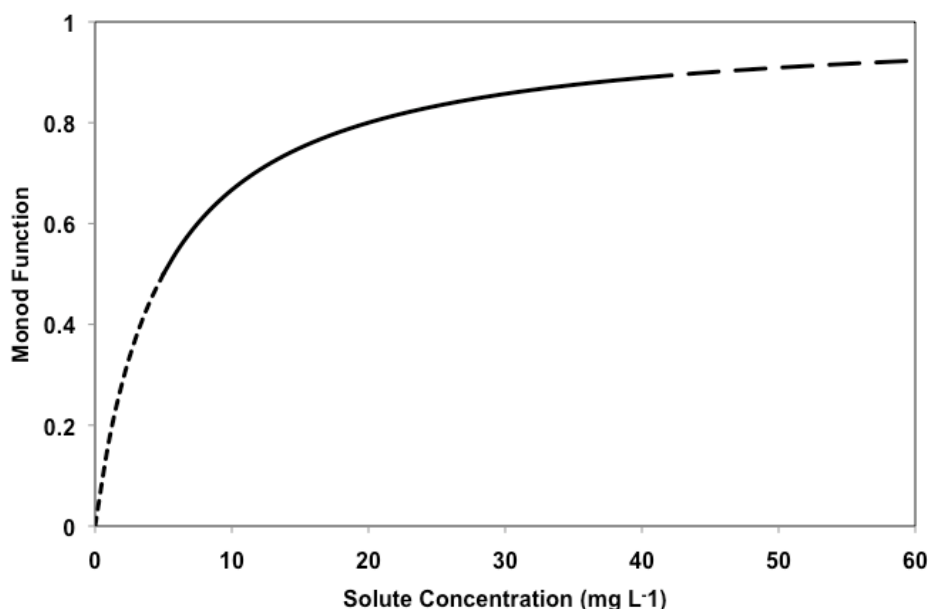


Figure 1-4. Graphical Representation of the Monod Function.

The fine dashed line shows the concentration range at which the function acts as first-order kinetics, and the coarse dash shows the concentration range at which the function acts as zero-order kinetics.

1.3.6 Nitrogen Transformations are a Function of Soil Water Content

All tool development was based on the assumption that ammonium-nitrogen is converted to nitrate-nitrogen, and nitrate-nitrogen is converted to nitrogen gas, based on Monod kinetics, and that the transformations are a function of water content in the STU. Nitrification requires aerobic conditions, and denitrification requires anaerobic conditions. Both processes depend on the oxygen diffusion rates to and from nitrogen transformation sites compared to the kinetic uptake rate of oxygen. These processes are too complex to model based on available information in the literature. However, oxygen diffusion depends upon the soil tortuosity and the water content (Millington and Quirk, 1960). Thus, soil texture and water content were used as

surrogates for the many parameters that control oxygen diffusion and uptake (Tucholke, 2007). Others have also suggested that nitrification and denitrification are functions of water content (Grant, 1995; Bollman and Conrad, 1998; Schjonning et al., 2003). For example, nitrification cannot occur at relatively large water saturations because insufficient oxygen can diffuse to the nitrifying microbes. On the other hand, nitrification cannot occur at very low water contents because nutrient diffusion to the microbes is limited. Thus, a non-linear function that modifies the maximum nitrification rate for a particular soil type was used.

Denitrification requires anaerobic conditions that, in turn, require that the soil saturation be greater than a value to limit oxygen diffusion (about 70%). Denitrification is maximized when soils are saturated to limit oxygen diffusion in the gas phase and when soils have sufficient tortuosity to limit diffusion in the aqueous phase. Tortuosity is correlated to soil texture (e.g., clays have considerable tortuosity that limits oxygen diffusion in the aqueous phase, and sands have less tortuosity which enables more effective oxygen diffusion). Consequently, maximum denitrification rates are associated with soil textures and are reduced using non-linear functions of water content. The maximum rate values for each soil texture and functions are based on an exhaustive review of reported nitrogen transformation rates in the literature (Tucholke 2007; McCray et al., 2005).

1.4 Microorganism Transport and Transformations

A wide range of human-pathogenic microorganisms, which include enteric viruses, enteropathogenic bacteria, and protozoa are found in STE. In soil-based OWTS, the STU is expected to remove and/or inactivate these biological contaminants, preventing their transport to surface or ground water. Removal and inactivation of pathogens depends on system design parameters and soil properties and the dynamic interaction between these.

Among the most important OWTS design parameters are the distance to ground or surface water, HLRs, and/or dosing regimes. Most onsite wastewater codes require a minimum separation distance between the infiltration zone of the STU and the seasonal high water table or saturated zone irrespective of soil characteristics (U.S. EPA, 2002). However, the effectiveness of these separation distances can be significantly influenced by the HLR, dosing regime, and soil properties, which are not necessarily designed for optimal removal of all types of pathogens.

The interplay of virus isoelectric point, pH and clay mineralogy is an important factor in determining virus removal, as are the level of dissolved organic matter in STE and the presence of unsaturated conditions below the infiltrative surface. Neither soil texture nor treatment depth appears to be important controls on viral fate. Removal of bacterial pathogens and protozoa, on the other hand, takes place primarily by mechanical filtration, a process that is governed by soil texture, treatment depth, and the presence of unsaturated conditions below the infiltrative surface. By contrast, HLR does not appear to have a consistent effect on bacterial removal.

1.5 OWC Transport and Transformations

Organic wastewater contaminants (OWCs) can have a wide array of ecotoxicological effects and negative impacts. Endocrine disrupting compounds are a subclass of OWCs that negatively influence reproductive development and hormone production and response in some organisms. This has been shown to cause “gender-bender” effects in some species of fish and

amphibians causing populations to become predominantly female or male organisms to exhibit female qualities (Brown et al., 2003). Some OWCs affect other internal systems such as the renal system, which can lead to kidney failure in some organisms (Oaks et al., 2002). Other compounds have been shown to be carcinogenic and/or mutagenic (Robertson, 1994). Antimicrobial compounds may contribute to the evolution of resistant strains of bacteria (Glaser, 2004; Singh, 2007; Suarez et al., 2007). Due to the wide array of compounds, five OWCs were selected based on the assessment of the compounds that are most likely to be associated with environmental implications and most likely to be regulated, and represent the diversity of compounds considered OWCs. The five contaminants are triclosan, 4-nonylphenol, 1,4-dichlorobenzene, 17 β -estradiol, and diclofenac.

1.6 Other Considerations

Although a user may not be comfortable with the assumptions described above, the simple tools developed may still be useful. For example, N-CALC, STUMOD, and HYDRUS all allow the user to select parameters (e.g., the nitrogen transformation rates, ammonium sorption, hydraulic parameters, etc) based on individual site conditions and user expertise. While median values represent the best engineering estimate based on available data, estimates of treatment can be obtained by selecting values that are considered less than optimal or that provide more than median treatment, based on the statistical distributions of the data representing model-input parameters (i.e., the 25th or 75th percentile values for each parameter). To aid the user in parameter selection, CFDs and look-up tables are provided in Chapter 3.0. In addition, rigorous sensitivity analyses and Monte Carlo simulations to determine the 25th, median, and 75th percentile values for treatment can be conducted in STUMOD. For HYDRUS, these values are not true 25th and 75th percentile estimates because treatment simulations are time-consuming and preclude Monte Carlo simulations or similar statistical methods. When using the simple tools such as N-CALC or STUMOD, the user can select parameter values that better represent their understanding or risk. For example, if the user believes that his OWTS scenario should provide more treatment than the assumptions allow, he could choose an optimistic treatment prediction, such as a 75th percentile value. On the other hand, if the user believes that her site or operating conditions are less conducive to treatment than suggested by the assumptions, then she could choose a conservative estimate (e.g., the 25th percentile) for parameter values.

It should also be noted that a technical consultant can be hired to conduct site-specific simulations using HYDRUS. This is especially true if the user wishes to include different or more specific soil conditions, loading regimes, or OWTS geometries. The version of HYDRUS that was used to develop the tools provided in this toolkit incorporates the relevant processes associated with OWTS treatment. A technical consultant can also be hired to consider more detail in certain processes by using a model other than HYDRUS. An example is using a geochemical model to incorporate more detailed processes regarding ammonium cation exchange or phosphorus precipitation.

CHAPTER 2.0

TOOL DEVELOPMENT

The tools developed for this toolkit are based on the scientific principle that the soil-water system (i.e., the STU) provides treatment via physical, chemical, and biological transformation processes (see User's Guide, Chapter 1.0). The tools range from very simple to complex and are structured to build off existing knowledge to evaluate the variations in STU performance under a range of the most common design, operating, and soil conditions. Models are valuable tools for predicting the behavior of a system. They can range in complexity from a simple equation that describes the main process in a system under ideal conditions to a complex numerical model that solves non-linear equations and generates results from time and space-varying inputs. Field data, statistical analyses, and mathematical modeling are used to develop and implement the simple tools.

Some complex processes and interactions preclude incorporation into a simple tool (User's Guide, Chapter 1.0). However, many of these complex processes as well as less-common operating conditions can be addressed by more complex models. Several existing models that are capable of simulating nitrogen attenuation in STUs were evaluated prior to selection of HYDRUS for tool development. Of these models, two stood out, each for different reasons: HYDRUS-2D CW2D, and DRAINMOD-N2.

HYDRUS-2D (Šimůnek et al., 1999) is a variably-saturated water flow and solute transport program, that was proven to successfully simulate various small scale to agricultural and watershed scale hydrological processes. In 2005, an extension to HYDRUS-2D, called CW2D module (Langergraber and Šimůnek, 2005), was released. The CW2D module was based on activated sludge models, and was originally developed to simulate wastewater treatment in constructed wetlands. It was the only model that was found to consider most of the processes and components that are relevant to wastewater treatment in soils. The components include oxygen, three organic matter fractions (readily available, slowly degradable and inert), four nitrogen species (ammonium, nitrite, nitrate, and dinitrogen gas), inorganic phosphorous and three microbial populations (heterotrophs, autotrophic *Nitrobacter* and autotrophic *Nitrosomonas*). The model also considers oxygen diffusion, water-dependency functions and heat-dependency functions. Because CW2D has more than 50 relevant model-input parameters for the nitrogen transformations alone, excluding spatial heterogeneities in properties, the model could not be calibrated uniquely. Furthermore, insufficient information exists in the scientific literature to parameterize a defensible model based on literature values alone. While the model did manage to produce realistic growth of microbes that resembles a biomat, other outputs were questionable and difficult to explain. A complete description of CW2D is provided in Section 2.5 of this User's Guide.

The second model evaluated was DRAINMOD-N2 (Youssef et al., 2005). This model is an agricultural model, which takes into account nitrogen transformations and their dependencies

on water content, temperature and carbon content. DRAINMOD-N2 is a 1D model, and as such it is simple to run, yet engineering aspects of STUs cannot be simulated (trench systems versus drip, and other designs).

The benefits of both models were combined such that the equations that are used in DRAINMOD-N2 were programmed into a HYDRUS-2D module specifically for this project. The coupling of HYDRUS-2D with the DRAINMOD-N2 equations allowed tool development using the already-proven water and solute flow functions and design flexibility of HYDRUS-2D, with the relative simplicity of the DRAINMOD-N2 nitrogen transformation equations. The number of input parameters for this module is less than half of the number of input parameters that are needed for CW2D. Thus, the modified numerical model HYDRUS-2D was used to develop the spreadsheet tools in the toolkit. (Note, the modified version of HYDRUS-2D used for this project is not publicly available at this time. Users interested in a modified version of HYDRUS should direct their interest to the HYDRUS developer.) Spreadsheet models are a simplification of numerical models enabling estimation of treatment based on user-specified conditions presented in a simple-to-use format that does not require prior modeling knowledge or lengthy model run times. Two spreadsheet tools developed for this toolkit are N-CALC and STUMOD.

N-CALC is a spreadsheet model based on a further simplification of the general advection dispersion equation, which can be used to investigate steady-state treatment effectiveness based on soil texture (i.e., long-term performance for a relatively mature system). In N-CALC, the calculated nitrogen removal is influenced by the loading rate, certain soil properties, and nitrification and denitrification rates (that are associated with soil texture). STUMOD is a spreadsheet model developed based on existing fundamental principles of water movement and contaminant transport. An analytical solution is used to calculate profile of pressure and moisture content in the unsaturated STU. The chemical transport component is based on simplification of the general advection dispersion equation, which is based on chemical mass-balance. Because STUMOD has more accurate formulation for flow and the biochemical nitrogen transformations (based on water content) it provides a more robust answer for different soil types and moisture conditions. STUMOD should generally be used when the User is comfortable with the complexity of this model compared to N-CALC.

To enable development of the nomograph tools and scenario outputs, numerous STUMOD and HYDRUS simulations were run to evaluate and illustrate various conditions. Prior to preparation of these tools, STUMOD was benchmarked against HYDRUS and the models were calibrated to field data. Benchmarking was done to ensure that both models produced similar and comparable STU performance output. Calibration of HYDRUS and STUMOD to field data was done to ensure that the model outputs match actual observed data. The models, HYDRUS and STUMOD, were calibrated using data from laboratory tests and field test sites where extensive monitoring was conducted that is not feasible in practice. However, data for model calibration is very limited to do rigorous calibration. For STUMOD, model results were compared to literature data for sandy soil (Whelan, 1988). The HLR and the effluent concentration in this study were 2.69 cm d^{-1} and 96 mg L^{-1} respectively. A comparison with measured data for total nitrogen showed that there was a good match between observed and model predicted values ($R^2 = 0.92$).

Descriptions of HYDRUS, STUMOD, and N-CALC are presented below. In addition, available information related to specific parameters and the rationale for parameter selection

utilized during tool development is also described. These parameters are first discussed in the description of HYDRUS (Section 2.1). Any differences in the parameter selection between the models are described in the appropriate STUMOD or N-CALC sections (Section 2.2 and 2.3 respectively).

2.1 HYDRUS Description

As mentioned previously, HYDRUS-2D (Šimůnek et al., 1999) is a variably saturated water flow and solute transport program. During tool development, the numerical stability of HYDRUS-2D was improved especially with regard to high reaction rates and drip system simulations. It was critical to make sure that HYDRUS was not only parameterized correctly, but that it also produced realistic results. For example, operational scenarios that are typical to STUs, such as frequent wetting-drying periods, are computationally demanding as the soil system is almost constantly away from steady-state conditions. In addition, under certain conditions the reaction rates are very high (mostly nitrification), which creates numerical fluctuations in instabilities. An improvement implemented during tool development was the ability to track several solute mass fluxes at several depths (the original software allows tracking mass fluxes of only one solute) which added another dimension of simulation evaluation – in addition to the actual solute concentration at a specific depth. In this regard, the mass flux across a boundary or at a specific depth gives a more direct estimate of the mass percent removed during STU percolation. Finally, initial domain set-up in HYDRUS revealed that a half-space model with a horizontal distance equal to one half the typical distance between trench center lines will account for any interactions that occur between trenches.

The best available data from the science and engineering literature was used as input to HYDRUS for both visual graphic and simple spreadsheet tool development.

2.1.1 Ammonium Sorption

Both HYDRUS and STUMOD incorporate ammonium sorption (K_d). Several factors control the ammonium sorption capacity of the soil. For example, an increase in organic matter increases the preference for ammonium sorption (Fernando et al., 2005). Sorption is also expected to increase at higher temperatures (Rodriguez et al., 2005), and in dry soils versus wet soils. In fact, an inverse linear relationship has been observed between the amount of ammonium adsorbed on clay and the water content in the clay independent of clay mineralogy and cation exchange capacity (CEC) (Mortland and Raman, 1968; Dontsova et al., 2005), suggesting that the adsorbed water inhibits ammonium adsorption.

Furthermore, other cations present in wastewater (e.g., Na^+ , K^+ , Ca^{2+} and Mg^{2+}) will compete for sorption sites, hence lowering the effective capacity for the ammonium ion. The selectiveness of these ions relative to ammonium is not clear; although it is typically assumed that the ions with the highest charge will have the highest affinity for cation exchange sites (Jorgensen and Weatherley, 2003). The following series of relative selectivity has been suggested in order of decreasing affinity for cation exchange sites: $\text{Al}^{3+} > \text{Ca}^{2+} > \text{Mg}^{2+} > \text{NH}_4^+ > \text{K}^+ > \text{H}^+ > \text{Na}^+$ (Buss et al., 2005).

Research has also shown that ammonium sorption typically follows a linear isotherm in field soils where the concentrations of ammonium are relatively low ($<22 \text{ mg-N L}^{-1}$) (DeSimone and Howes, 1998), while a nonlinear adsorption relationship is typically assumed under high

concentration conditions (van Raaphorst and Malschaert, 1996; Laima et al., 1999; Fernando et al., 2005) (Figure 2-1). While this phenomenon may impact the magnitude of sorption in the STU, a constant K_d value was used in the tool development efforts. Of note, the sorption coefficient is not expected to vary much with soil depth (van Raaphorst and Malschaert, 1996).

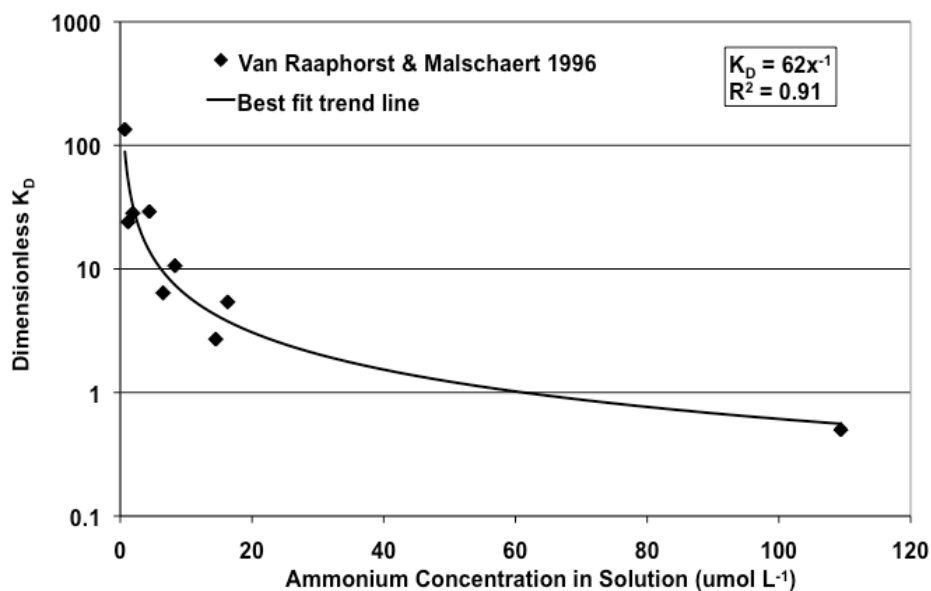


Figure 2-1. Decrease in Sorption Coefficient with Increase in Ammonium Concentration. Data obtained from van Raaphorst and Malschaert (1996).

Although a CFD serves as an excellent tool for making risk based decisions on the selection of appropriate K_d values to be used in the predictive tools, a few factors should be taken into account. For example, the magnitude of the CEC, which is the sum of cations a soil can absorb, depends on soil texture, types of minerals in the soil and the amount of organic matter. Because sand typically has a very low CEC (2-10 meq per 100 g), while clay-rich soils have a high CEC (20-40 meq per 100 g), the clay content in any given soil will control ammonium sorption (Buss et al., 2005).

In total, 43 K_d values were found in the literature. While the values ranged greatly, minimum of 0.025 to a maximum of 150 L kg⁻¹ (User's Guide, Figure 3-11), the median value was 0.6 L kg⁻¹, and the inter-quartile range (IQR) 0.23 to 1.5 L kg⁻¹ for all soils. However, because the CEC greatly influences the sorption capacity of the soils, two soil groups were created to summarize the assimilated K_d values (User's Guide, Figure 3-12): 1) the clay-poor group (soils with less than 30% clay); and 2) the clay-rich group (soils with more than 30% clay). Of note, the USDA soil triangle (User's Guide, Appendix A, Figure A-1) can be used as a guide to determine which textures are considered clay-rich versus clay-poor. The ammonium sorption values are summarized in Table 2-1.

Table 2-1. Summary of Ammonium Sorption Coefficients for Clay-Rich and Clay-Poor Soils as Reported in the Literature.

	n	Ammonium Sorption Coefficient K_d (L kg ⁻¹)		
		Minimum	Median	Maximum
All soils	43	0.025	0.6	8.7*
Clay-rich	9	0.18	1.46	8.7
Clay-poor	34	0.025	0.35	3.5

* One value of 150 L kg⁻¹ excluded

It is useful to note that one clay rich value was excluded from any statistical analysis. This value was 150 L kg⁻¹, which is much larger than the next largest value (8.7 L kg⁻¹). The latter agrees with the U.K. Environment Agency study (Buss et al., 2005), which indicated a largest value for K_d of 6.5 L kg⁻¹ among clay-rich soils. It should also be noted that the Buss et al. (2005) study values were not used in this analysis if the values were reported with “low confidence” for a particular soil.

To include sorption in the uncertainty analysis, a representative “average” value with minimum and maximum values was required. Because the distribution of K_d values is log-normal (User’s Guide, Figure 3-11), the use of normal statistics (i.e., calculation of mean and standard deviation) was precluded. Instead, the median values for the clay-rich and clay-poor soils were used to determine best representative values, and the 5th and 95th percentiles were used to show expected ranges in K_d values for the uncertainty analysis.

For hydraulic simulations during tool development, the clay-poor K_d values were used for the following groups: sand, loamy sand, sandy loam, loam, silt loam, and silt. For the remaining soil groups, the clay-rich values were used. However, as stated previously, other factors may also be important for consideration for individual specific cases. For example if the CEC is very low (20 meq per 100 g), sorption is expected to be very low as well and selection of a smaller K_d value from the CFD may be warranted. In contrast if the effluent is high in COD, sorption is expected to increase and a higher K_d value should be chosen. Table 3-10 in this User’s Guide summarizes the factors that play a role in ammonium sorption and may aid in the decision making of choosing an appropriate K_d value.

2.1.2 Ammonification

HYDRUS was modified for the transformation of organic nitrogen to ammonium (ammonification). However, because the tools developed for this toolkit were based on the application of ammonium-nitrogen and nitrate-nitrogen only, the ammonification process is not considered. The following discussion is provided for completeness related to modifications made to HYDRUS.

$$\mu_{amm} = \mu_{amm,max} \left(\frac{C_{org}}{K_{m,org} + C_{org}} \right) f_t f_{sw} \quad (2.1.2-1)$$

where μ_{amm} is the calculated zero-order ammonification rate, $\mu_{amm,max}$ is the maximum (optimum) ammonification rate, C_{org} is the organic-nitrogen concentration, and $K_{m,org}$ is the half-saturation constant, which is the organic-nitrogen concentration at which the ammonification rate is half its maximum value. f_t and f_{sw} are temperature-dependency and saturation-dependency functions, respectively, and are defined as:

$$f_t = \exp \left[-0.5\beta T_{opt} + \beta T \left(1 - \frac{0.5T}{T_{opt}} \right) \right] \quad (2.1.2-2)$$

where f_t is the temperature-dependency function (given values between 0 and 1), T is the temperature, T_{opt} is the optimum temperature for nitrification, and β is a fitting parameter.

$$f_{sw} = \begin{cases} f_s + (1 - f_s) \left(\frac{1-s}{1-s_h} \right)^{e_2} & s_h < s \leq 1 \\ 1 & s_l \leq s \leq s_h \\ f_{wp} + (1 - f_{wp}) \left(\frac{s-s_{wp}}{s_l-s_{wp}} \right)^{e_3} & s_{wp} \leq s < s_l \end{cases} \quad (2.1.2-3)$$

where f_{sw} is the saturation-dependency function (given values between 0 and 1), f_s is the value of f_{sw} at full saturation, f_{wp} is the value of f_{sw} at the wilting point, s_h is the upper saturation boundary for optimal ammonification, s_l is the lower saturation boundary for optimal ammonification, s_{wp} is the saturation level at the wilting point, s is the actual soil saturation, and e_2 and e_3 are fitting exponents.

2.1.3 Nitrification

During nitrification, ammonium-nitrogen is transformed to nitrite-nitrogen and nitrate-nitrogen through biological aerobic oxidation, by specific autotrophic microbes (*Nitrosomonas* & *Nitrobacter*). These organisms use oxygen as a terminal electron acceptor, with *Nitrosomonas* oxidizing ammonium-nitrogen to nitrite-nitrogen, and *Nitrobacter* converting nitrite-nitrogen to nitrate-nitrogen. The process is assumed to occur relatively fast in the STU. The following equation describes the nitrification rate equation implemented in STUMOD and HYDRUS:

$$\mu_{nit} = \mu_{nit,max} \left(\frac{C_{NH_4}}{K_{m,NH_4} + C_{NH_4}} \right) f_t f_{sw} \quad (2.1.3-1)$$

where μ_{nit} is the calculated nitrification rate, $\mu_{nit,max}$ is the maximum (optimum) nitrification rate, C_{NH_4} is the ammonium-nitrogen concentration, and K_{m,NH_4} is the half-saturation constant, which is the ammonium-nitrogen concentration at which the nitrification rate is half its maximum value. f_t and f_{sw} are the temperature-dependency (equation 2.1.2-2) and saturation-dependency functions (equation 2.1.3-2).

$$f_{sw} = \begin{cases} f_s + (1 - f_s) \left(\frac{1-s}{1-s_h} \right)^{e_2} & s_h < s \leq 1 \\ 1 & s_l \leq s \leq s_h \\ f_{wp} + (1 - f_{wp}) \left(\frac{s-s_{wp}}{s_l-s_{wp}} \right)^{e_3} & s_{wp} \leq s < s_l \end{cases} \quad (2.1.3-2)$$

where f_{sw} is the saturation-dependency function (given values between 0 and 1), f_s is the value of f_{sw} at full saturation, f_{wp} is the value of f_{sw} at the wilting point, s_h is the upper saturation boundary for optimal nitrification, s_l is the lower saturation boundary for optimal nitrification, s_{wp} is the saturation level at the wilting point, s is the actual soil saturation, and e_2 and e_3 are fitting exponents.

2.1.3.1 Nitrification Half-Saturation Constants

Half-saturation constants for ammonium transformation (K_{m,NH_4}) reported in the literature generally range between 0.06 and 12 mg-N L⁻¹ (Jenkins and Kemp, 1984; Lotse et al., 1992; Sheibley et al., 2003), with the majority of the values between 1 and 5 mg-N L⁻¹ (Sheibley et al., 2003). A commonly accepted value is 1.0 mg-N L⁻¹ (Rittmann and Snoeyink, 1984; Henze et al., 1987). These values essentially result in zero-order rates for relevant nitrogen concentrations in onsite wastewater problems (i.e., nitrogen concentrations above natural background of a few mg-N L⁻¹). However, a value of 5 mg-N L⁻¹ was chosen as it still simulates zero-order reaction rates, but also because the numerical formulations in HYDRUS and STUMOD were more stable when K_{m,NH_4} values were greater than 1. Furthermore, sensitivity analyses showed that predicted treatment does not change measurably for a range of K_{m,NH_4} values between 1 and 5.

2.1.3.2 Temperature Effects on Nitrification

Nitrification rates are a non-linear function of temperature. The general shape of the function is a Gaussian-type bell-curve, with a peak corresponding to the optimum temperature for nitrification (T_{opt}) and width of curve determined by β (Figure 2-2). To determine the impact any given soil temperature has on the magnitude of nitrification, equation 2.1.2-2 was used. Because most researchers only report temperature response of nitrifying bacteria in ranges lower than T_{opt} , the attempt to parameterize T_{opt} and β from curve fitting was virtually impossible. Specifically, the available data had a large peak at ~25 to 26°C (room temperature) with limited data at temperatures above and below. In addition, past research typically report microbial response to only three fixed temperatures, which is not sufficient for robust curve fitting. Thus, similar to nitrification curve fitting, Excel Solver was used to back-calculate the T_{opt} .

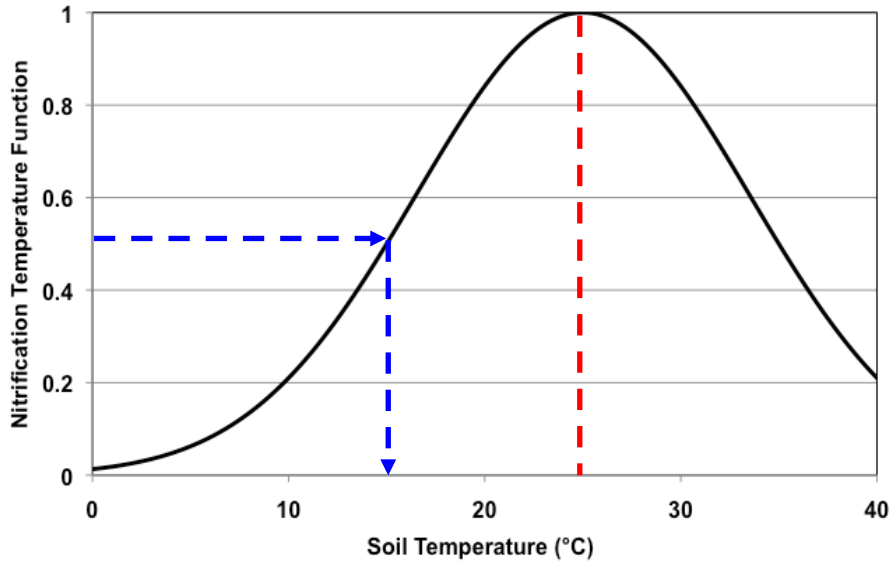


Figure 2-2. Nitrification Temperature-Dependency Function.

The function retrieves a maximum value at 25°C (red dashed line) and at 15°C the temperature function yields a value of 0.5 (blue dashed lines).

Q_{10} is a measure of the factor of increase or decrease of microbial activity when temperature is changed by 10°C. While Q_{10} values can range significantly, research has shown that $Q_{10} = 2$ is typical for nitrification (Addiscott, 1983; Campbell et al., 1984). With an optimum temperature of 25°C and Q_{10} of 2, the temperature function implemented in HYDRUS and STUMOD should yield a value of 0.5 at 15°C (Figure 2-2), which was obtained by using a fitted β value of 0.34 in the temperature function (Equation 2.1.2-2).

Malhi et al. (1990) showed that the optimal temperature for nitrification changes from region to region based on the average annual air temperature: nitrifying microbes in cold climate will have a lower optimum temperature than nitrifying microbes in warm climates. This phenomenon is shown in Figure 2-3 through curve fitting to several data sets from several locations with different climatic zones. It can be seen that microbes from a cold climate (e.g., Alberta, Canada, with an average annual air temperature of 2.5°C) are exhibiting maximum nitrification at ~19°C (Malhi and McGill, 1982), whereas nitrifying microbes in more temperate regions (e.g., Germany and France), perform best at ~25°C (Grundmann et al., 1995; Avrahami et al., 2003). Although the optimum temperature may vary slightly between regions, the compilation of the reported rates from the literature yielded an optimum temperature of 25°C (Figure 2-3).

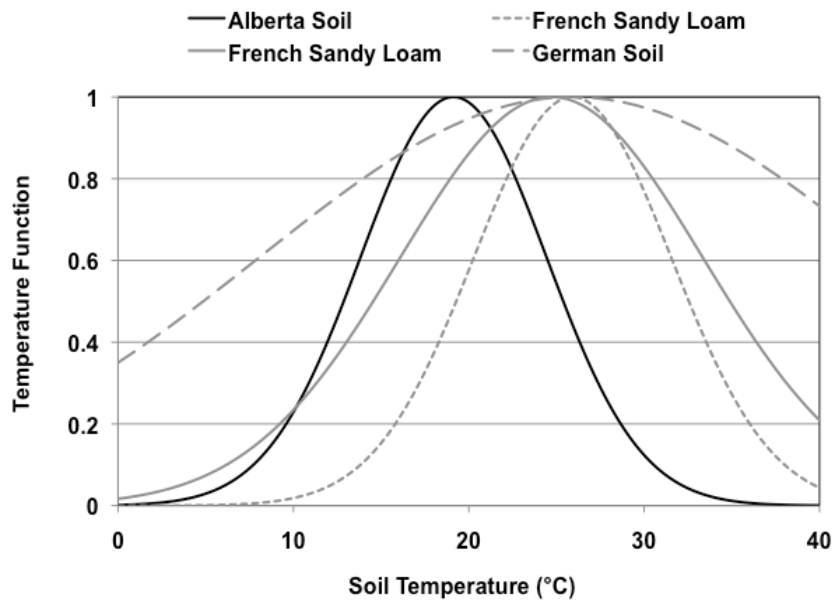


Figure 2-3. Fitted Temperature Functions to Soil Nitrification Data.

2.1.3.3 Maximum Nitrification Rates

To determine appropriate maximum nitrification rates ($\mu_{nit,max}$) for Equation 2.1.3-1 as input values in STUMOD and HYDRUS, 20 maximum nitrification rates from twelve different studies were compiled. Several studies reported the rates as first order (d^{-1}); however, those rates were not used because the input parameters in the numerical models required rates reported as $mg\ N\ L^{-1}\ d^{-1}$. When the rates were reported as $mg\ N\ kg^{-1}\ d^{-1}$, the rates were converted to $mg\ N\ L^{-1}\ d^{-1}$ using bulk density, porosity and soil moisture. Because the nitrification rates are expected to reach a maximum at 25°C, and to enable a comparison of the reported rates, they were first temperature corrected to 25°C using the Arrhenius equation (2.1.3.3-1).

$$\ln\left(\frac{k_1}{k_2}\right) = \frac{E_a}{R} \left(\frac{1}{T_2} - \frac{1}{T_1} \right) \quad (2.1.3.3-1)$$

where k_1 is the reaction rate ($mg-N\ L^{-1}\ d^{-1}$) at 298.15 K, and k_2 is the reaction rate at the reported temperature (T_2), E_a is the activation energy ($J\ mol^{-1}$), R is the gas constant ($8.31\ J\ mol^{-1}\ K^{-1}$) and T_1 is the temperature when nitrification is maximum (298.15 K). It is necessary to know the activation energy before temperature correcting the rates. The activation energy is a function of Q_{10} , which is typically assumed to equal 2 when normalizing reaction rates to a set temperature that fall in the narrow range of temperatures (5-28 °C) that normally occur in the soil (Stark, 1996). It follows, from Equation 2.1.3.3-1, that if $T_2 = 308.15\ K$, $T_1 = 298.15\ K$, and $k_2 = 2 \times k_1$, the activation energy becomes $E_a = 53\ kJ\ mol^{-1}$. The reported rates could thus be temperature corrected to 25°C. Of note, the Arrhenius equation is fundamentally an empirical equation based on the linear relationship obtained from a plot of the natural logarithm of the reaction rate versus the inverse of the temperature. Virtually all rate constants can be written in the Arrhenius form (Hill, 1977); hence it is a useful relationship to use whether zero-order or first-order reaction rates are expected. The range in the reported nitrification rates was quite large

(4 orders of magnitude), with a minimum value of 0.5 mg-N L⁻¹ d⁻¹, a maximum value of 574 mg-N L⁻¹ d⁻¹, and a median value of 56 mg-N L⁻¹ d⁻¹ (User's Guide, Figure 3-14). With such highly skewed data, the IQR of 4 to 87 mg N L⁻¹ d⁻¹ better portrays the expected range in rates.

To conduct uncertainty analysis of the reported rates, the minimum and maximum values, along with the mean and standard deviation are required; however such analysis cannot be done unless the data are normally distributed (typically not the case with environmental data). If the data set is log-normally distributed, it can first be log-transformed, after which select statistical analysis (e.g., mean and standard deviation) can be conducted. A normality test of the reported rates confirmed that the distribution of the data was lognormal. The IQR serves as the basis for identifying suspected outliers in a data set, where an observation may be an outlier if it falls more than 1.5×IQR above the third quartile or below the first quartile in a normally distributed data set. After transforming the data, the data were first screened for outliers using the 1.5×IQR test. Upon close examination of the compiled and transformed data, no outliers were found to exist.

Because the magnitude of nitrification is expected to vary depending on soil texture, the reported rates were separated into three textural groups (sandy soil, silty soil and loam) to allow for further statistical analysis. These groups were arbitrarily chosen as they are similar to the three soil groups present for denitrification (of note, clay-rich soils were omitted as none were reported in the literature). A 1-way analysis of variance (ANOVA) test was deemed appropriate, as the transformed data were normally distributed. The ANOVA test showed that the means between the different soil groups were not statistically different at alpha = 0.05 (Table 2-2). As a result, the reported nitrification rates for all soil textures were lumped together to obtain the median expected rate.

Table 2-2. Results of 1-way ANOVA to Determine the Effect of Soil Texture on Nitrification Rates.

Source of Variation	Sum of Squares	Degrees of Freedom	Mean Square	F-Test	P
Soil texture	7.01	2	3.51	0.85	0.45
Residual	70.4	17	4.14		
Total	77.4	19			

2.1.3.4 Soil Moisture Dependency

Soil moisture content has a large influence on the diffusivity of gases and therefore on the availability of oxygen to the nitrifying microbes. Research has shown that a water filled porosity (WFP) around 60% offers the most suitable conditions for aerobic bacteria (Linn and Doran, 1984; Del Grosso et al., 2000), because the diffusion of oxygen is not restricted (Parton et al., 1996). At a WFP below 60% nitrifying activity is inhibited due to limited substrate diffusion and limited water availability for microbial activity (Stark and Firestone, 1995), while at a WFP above 60% conditions favor anoxic bacteria as oxygen diffusion into the soil is inhibited. While little research has been conducted as to the influence of soil texture on the magnitude of nitrification, coarse-textured soils have been found to have a maximum nitrification rate at 45-50% WFP while fine-textured soils have a max rate at 55-65% WFP (Bollman and Conrad, 1998; Del Grosso et al., 2000). But, maximum nitrification activity has also been found at greater WFP. In fact Schjonning et al. (2003) showed that soils with high porosity (0.5) and large fraction clay (35%) may see maximum nitrification rates at 82% WFP, and in soils with low porosity (0.4) and low fraction of clay (11%) the maximum nitrification rates were at 63% WFP. Although the expected maximum nitrification rate has been found to occur at higher WFP in fine-textured soils compared to in coarse-textured soils, the magnitude of the rate is typically

greater in the latter. The above research may suggest that substrate diffusion is inhibited in fine-textured soils at lower soil moisture contents; and although ample oxygen is present in the soil for the nitrifying bacteria there is not enough substrate. In contrast, as the soil moisture content increases and sufficient substrate becomes available, anoxic conditions prevail resulting in a lower maximum nitrification rates in fine-textured soils compared to in coarse-textured soils.

It is well understood that nitrification is an aerobic process; hence nitrification is unlikely to occur in nearly saturated soils, providing the oxygen has been consumed. Diffusion to nitrification sites is often too slow to enable sufficient nitrification (depending on soil texture). Furthermore, at low moisture contents the substrate (ammonium and aqueous CO₂) diffusion between soil pores is limited because of poor connectedness of “wet” soil pores. Thus, low moisture contents limits or disables nitrification as well.

The conceptual model for nitrification soil moisture function is thus a function with a peak nitrification at intermediate water contents, where both oxygen diffusion and ammonium diffusion reach an optimal balance, and low nitrification at low and high water contents is described by equation 2.1.2-3. Parameterization of this equation was completed using available literature data. Data points were extracted from several articles that reported nitrification rates as a function of WFP, and were fitted with equation above using the Excel Solver tool (Figure 2-4). As expected, different soils were parameterized with different values, yet the overall fits to data were very good (all better than $R^2 = 0.9$).

Because the available data did not cover all existing soil textures, an attempt was made to combine the existing data into groups that could be used as indicator for soil textures for which data was not available. A correlation matrix was compiled for the 6 curves that are shown in Figure 2-4. The fitted curves were checked for correlation (i.e., how much do the moisture-dependency curves in clay or silt look alike, or how much do they differ from the moisture-dependency curves of sandy soils) to determine if combining the different curves was possible (i.e., assume similarity of moisture-dependent curves between different soils). In this process, the correlation between each two fitted curves is calculated, and represented by an R^2 value (Table 2-3) with correlations of $R^2 > 0.7$ highlighted.

It can be seen that there is a clear correlation between the moisture-dependency curves of soils with high silt content, and a good correlation between the sandy loam and the silt-rich soils. On the other hand, the two curves for clay-rich soils do not correlate well with any other soils, but only with each other. Clearly, clay-rich soils (>30% clay content) tend to have a narrow-peaked shape at high water-filled porosities, whereas clay-poor soils (<30% clay content) tend to have a broad peak at intermediate water-filled porosities. However, due to the limited number of studies reporting moisture dependency for clay-rich soils, it was deemed necessary to combine the results from all reported studies, resulting in one moisture-dependency curve (Figure 2-5). The parameters for the nitrification water-dependency equation could then be obtained.

Table 2-4 summarizes the numerical values for the parameters that make up the nitrification water-dependency equation. Because the number of fitted curves was not high enough to reliably calculate standard deviations for each parameter, the minimum and maximum values are shown instead.

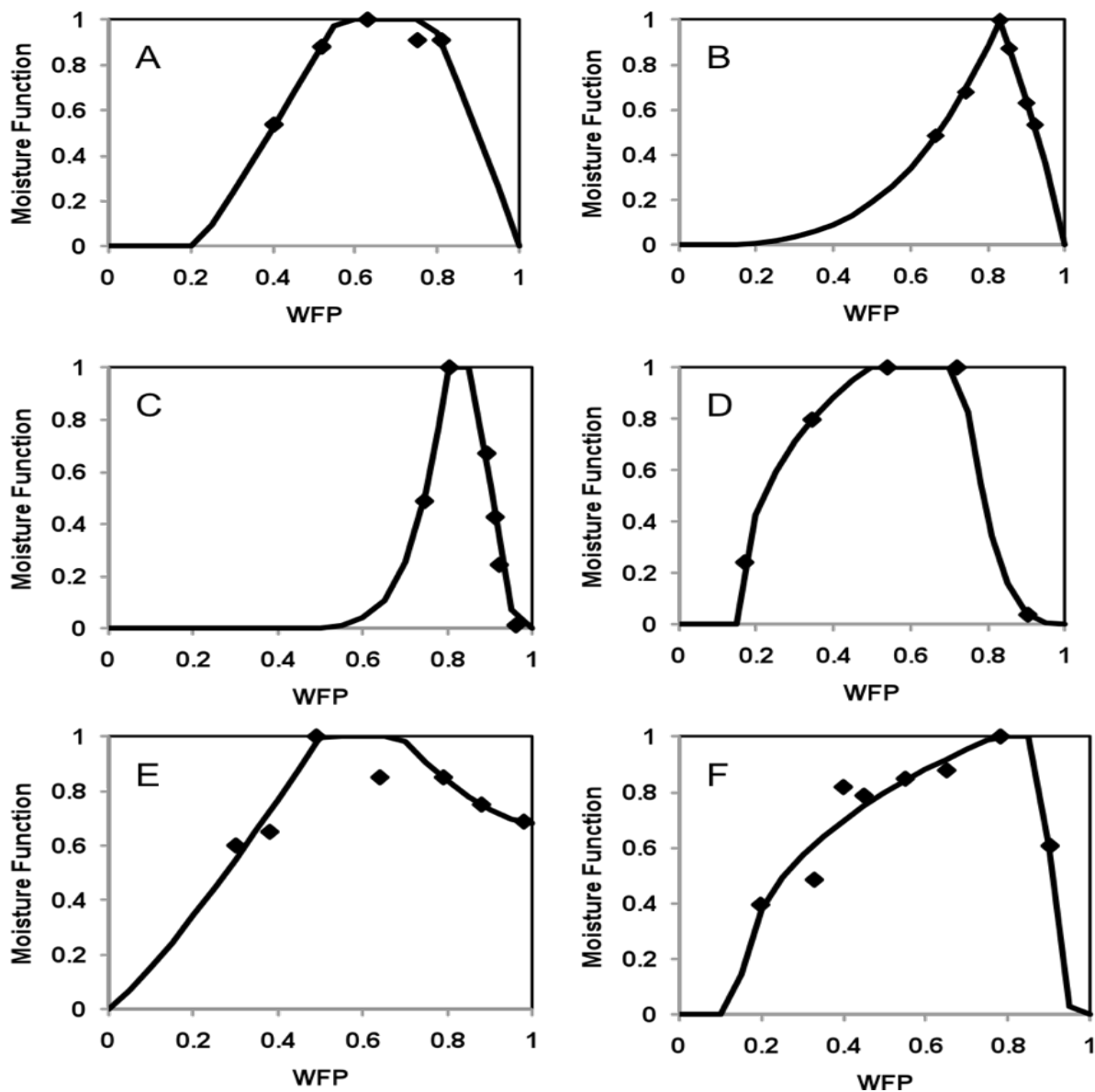


Figure 2-4. Best Fit of Experimental Data to the Moisture-dependency Function.

A) Sandy loam (Schjonning, 2003); B) Sandy clay loam (Schjonning, 2003); C) Sandy clay loam / sandy clay (Schjonning, 2003); D) Silty loam (Grant, 1995); E) Silt (Bollman and Conrad, 1998); F) Silty loam (Bollman and Conrad, 1998).

Table 2-3. Correlation Matrix for the Curves Shown in Figure 2-4.

	Sandy Loam	Sandy Clay Loam	Sandy Clay	Silt Loam	Silt	Silt Loam 2
Sandy Loam	x	x	x	x	x	x
Sandy Clay Loam	0.695	x	x	x	x	x
Sandy Clay	0.443	0.887	x	x	x	x
Silt Loam	0.674	0.018	-0.186	x	x	x
Silt	0.924	0.592	0.293	0.720	x	x
Silt Loam 2	0.873	0.602	0.520	0.728	0.821	x

R² values > 0.7 are highlighted.

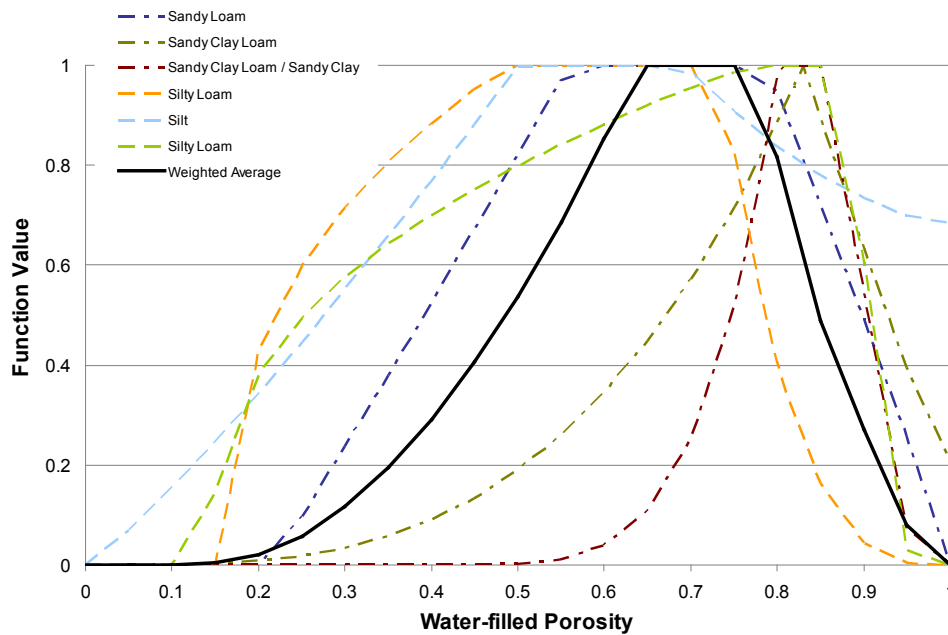


Figure 2-5. Nitrification Moisture Dependency Function Developed from Existing Data.

Table 2-4. Fitted Parameters for the Nitrification Moisture Dependency Function.

Parameters	Minimum	Median	Maximum
fwp	0.000	0.000	0.029
fs	0.000	0.000	0.000
swp	0.000	0.154	0.378
sl	0.488	0.665	0.829
sh	0.690	0.809	0.888
e2	0.841	2.267	4.341
e3	0.393	1.104	5.007

2.1.4 Denitrification

Denitrification rates and soil characteristics were obtained from Tucholke (2007). In total, over 600 denitrification rates were assimilated and analyzed. While both first order and zero order rates were reported, only zero order rates were used, because denitrification is assumed to follow Monod kinetics (User's Guide, Section 1.3.5) such that when concentrations are high (such as the case in wastewater systems), the rate become zero order. Most rates reported in the literature are zero order. The use of principal component analysis helped determine that WFP was the most important controlling soil characteristics. The results showed that variations in denitrification rates were strongly related to soil textural classes. Three principal groups were identified that coincided with soil textural classes: 1) sandy soils – those with >50% sand content; 2) silty soils – those with >50% silt content; and 3) clayey soils – those with <50% sand and <50% silt content. It should be noted that the clayey soils do not necessarily mean high clay content. For example, a soil can have 45% sand, 45% silt and only 10% clay, while still falling into the clayey group (see User's Guide, Appendix A, Figure A-1).

Most of the denitrification rates reported in the literature are associated with agricultural studies, and thus the denitrification rates were typically reported in terms of mass nitrogen per

area per time, which is analogous to the flux over the ground surface area. To use HYDRUS for visual-graphic tool development, and for the development of the spreadsheet models, the units were converted to mass nitrogen per volume per time, where the volume is the pore volume, not the bulk soil volume, and the soil was fully saturated. The conversion from area to volume of pore water required making some assumptions. To convert from area to volume of bulk soil, a representative soil depth value had to be considered. The meaning of this soil depth value was that most denitrification, reported as flux from the surface of a field-plot or test column, occurred between the soil surface and that depth. Because the process of denitrification is dependent on carbon, the assumed soil depth translates indirectly to the thickness of the organic-rich topsoil. Although regional variations exist in topsoil thickness, a representative value of 20 cm was chosen. By using the carbon function (Equation 2.1.4-1) and the model input parameters determined by Wang et al. (2005), it can be shown that when the soil depth is greater than 20 cm, little denitrification is expected (Figure 2-6). The carbon function can be written as:

$$f_z = e^{-az} \quad (2.1.4-1)$$

where a is a fitting parameter, and z is depth below the soil surface.

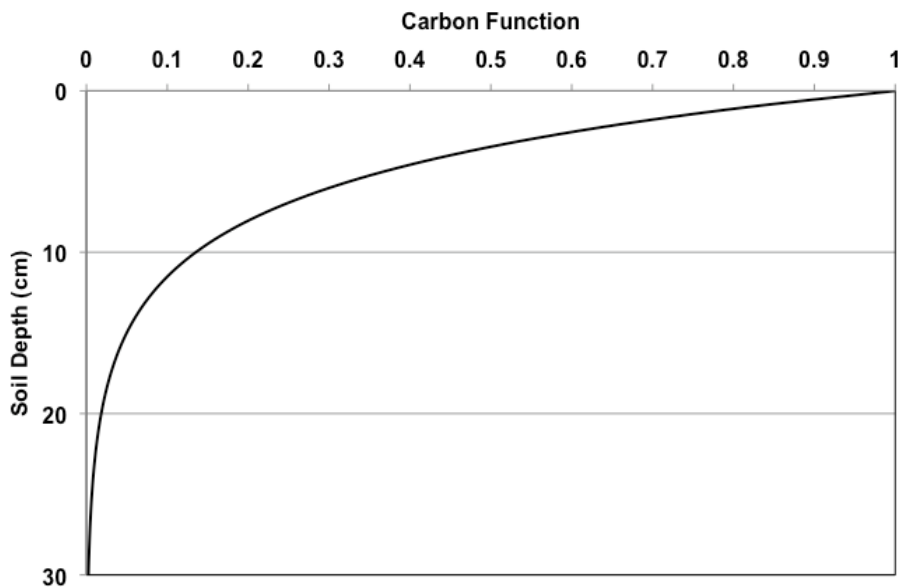


Figure 2-6. Results of Using Model Input Parameters Developed by Wang et al. (2005).

The carbon function provides the fraction by which the denitrification rate can be multiplied in a typical soil.

Using the carbon function and an assumed 20 cm soil depth for converting the denitrification rates from flux rates to mass nitrogen per volume per time was deemed justifiable because most of the assimilated denitrification data came from studies conducted on agricultural or forest soils. The carbon content for agricultural/forest soils is well known and assumed to be a limiting factor, whereas the carbon distribution with the STU beneath a trench or drip system is not well known. The carbon function was not used in the development of the spreadsheet tools (STUMOD and N-CALC) as it was assumed that sufficient carbon exist in the STE to promote denitrification (User's Guide, Section 1.2.2).

It is reasonable to assume that denitrification does not occur within the soil grains, and that the process is confined to the pore space (including the surface of soil grains). The conversions of denitrification rates from volume of bulk soil to volume of pore water were done by using the porosity. While the porosity varied between different soils, a value of 0.4 was used in the calculations. It is important to realize that all denitrification parameters were developed prior to this last conversion.

Because literature-review findings (McCray et al., 2005; Tucholke, 2007) suggest that denitrification rates are zero order at higher concentrations and first-order at lower concentrations, Monod kinetics were utilized when modeling nitrate-nitrogen transformations. The following equation describes the denitrification rate equation implemented in STUMOD and HYDRUS:

$$\mu_{denit} = \mu_{denit,max} \left(\frac{C_{NO3}}{K_{m,NO3} + C_{NO3}} \right) f_t f_{sw,dn} f_z \quad (2.1.4-2)$$

where μ_{denit} is the calculated denitrification rate, $\mu_{denit,max}$ is the maximum (optimum) denitrification rate, C_{NO3} is the nitrate-nitrogen concentration, and $K_{m,NO3}$ is the half-saturation constant, which is the nitrate-nitrogen concentration at which the denitrification rate is half its maximum value. f_t , f_{sw} , and f_z are temperature-dependency, saturation-dependency, and carbon-dependency functions, respectively. f_t is defined in Equation 2.1.2-2, while f_z is defined by Equation 2.1.4-1 and f_{sw} is defined as:

$$f_{sw,dn} = \begin{cases} 0 & s < s_{dn} \\ \left(\frac{s - s_{dn}}{1 - s_{dn}} \right)^e & s \geq s_{dn} \end{cases} \quad (2.1.4-3)$$

where $f_{sw,dn}$ is the saturation-dependency function (given values between 0 and 1), s_{dn} is a threshold saturation value for denitrification, s is the actual soil saturation, and e is a fitting exponent. Figure 2-7 provides a visualization of these denitrification functions.

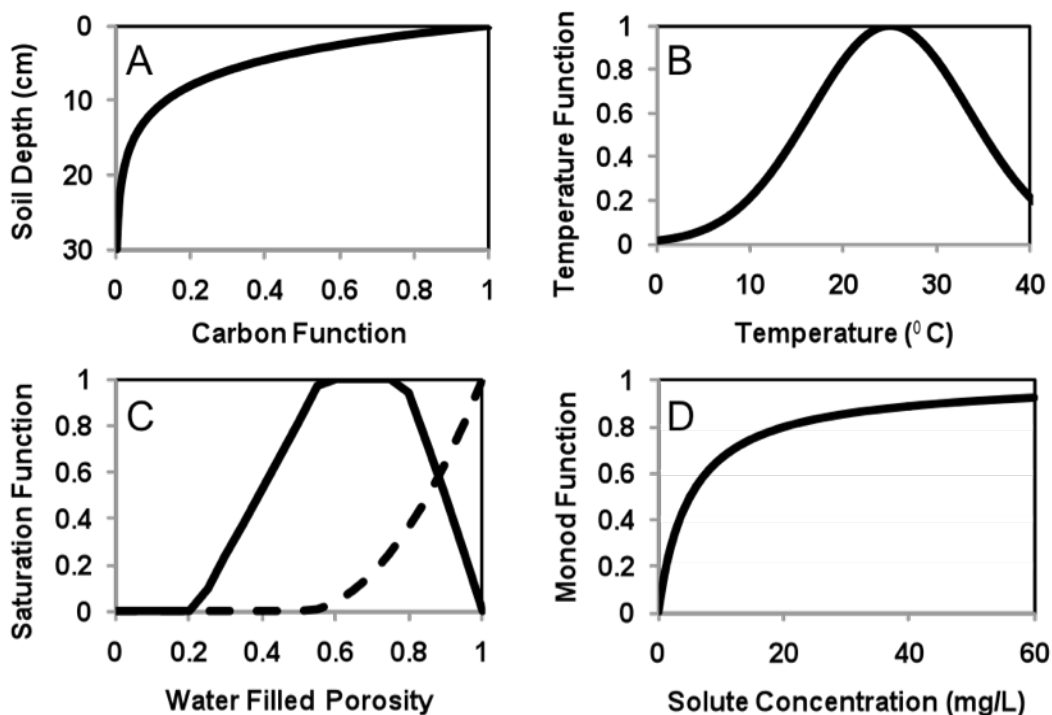


Figure 2-7. Visual Representation of the Functions Incorporated into HYDRUS-2D.

A) Carbon-dependency function (equation 2.1.4-1), B) the temperature-dependency function (equation 2.1.2-2), C) the saturation-dependency functions for, nitrification (solid line), and denitrification (dashed line) (equations 2.1.2-3 and 2.1.4-3), and D) the Monod (reaction dependency on available nutrients for Equations 2.1.3-1 and 2.1.4-2).

2.1.4.1 Denitrification Half-Saturation Constants

Half-saturation values for nitrate-nitrogen transformations (K_{m,NO_3}) based on actual measurements are sparsely reported in the literature, but have been found to range from 0.76 to 10 mg-N L⁻¹ (Abdul-Talib et al., 2002). While a half-saturation constant of 1 mg L⁻¹ is commonly used when modeling nitrogen transformations in most natural soil systems, both STUMOD and HYDRUS were unstable with such a low value (division by low K_{m,NO_3} values resulted in high values in the calculation matrixes). Instead, a half-saturation constant of 5 mg L⁻¹ was used in the tool development (as discussed for nitrification). Because the concentration of nitrate-nitrogen in the nitrified effluent is typically much greater than K_{m,NO_3} , zero-order denitrification rates are expected except for at depths where the concentration of nitrate-nitrogen has decreased significantly. Although use of first-order rates may be more appropriate at such depths, the soil moisture content will be the limiting factor; thus little to no denitrification is expected to occur.

2.1.4.2 Temperature Effects on Denitrification

The optimal temperature for denitrification was determined based on 306 data points from the literature (Tucholke, 2007). Only rates reported as $\text{mg-N L}^{-1} \text{d}^{-1}$ were used when determining the optimal temperature, as any potential errors from doing rate conversions from flux rates were omitted. The distribution of the reported data as function of temperature is depicted in Figure 2-8. Although the magnitude of denitrification varied greatly at all temperatures, the largest rates were reported when the soil temperature was between 20 and 30°C. Based on the apparent “bell-shape” present in Figure 2-8, it seemed reasonable to assume that the optimal temperature for denitrification is 25°C.

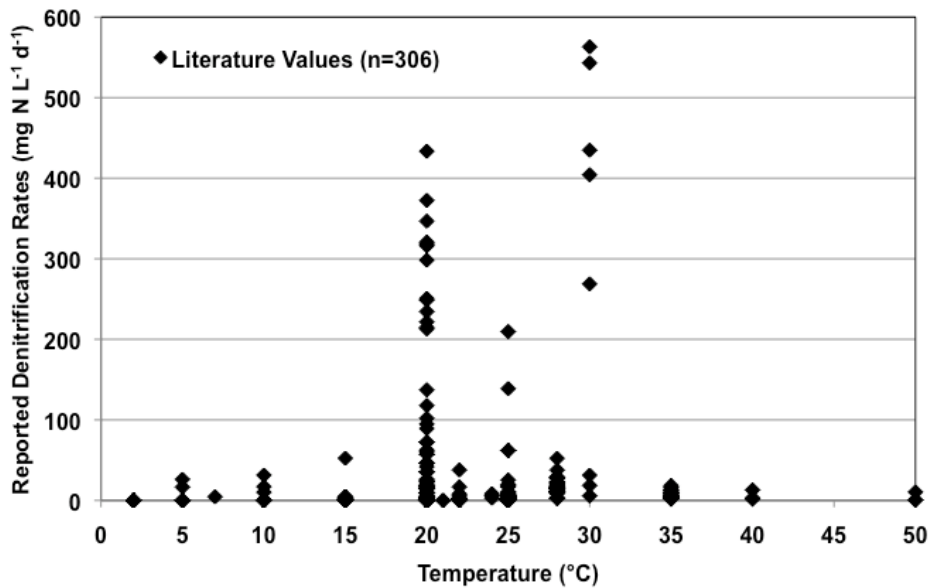


Figure 2-8. Denitrification Rates as Function of Soil Temperature.
Plot contains 306 data points assimilated from the literature (data from Tucholke, 2007).

The temperature function for denitrification is the same as for nitrification (Equation 2.1.2-2). While the optimum temperature could be determined from Figure 2-8, the β value, which determines the shape of the temperature function, could not be fitted due to the high scatter of the data. However, because the β value is related to Q_{10} , and Q_{10} is assumed to be 2, the β value for denitrification was set to be equal to the β value from the nitrification temperature-dependency function, which was 0.34 (User’s Guide, Section 2.1.3.4). The assumption that $Q_{10}=2$ when converting reaction rates to 25°C is a common assumption in most microbial systems. However, it is interesting to note that if a $Q_{10}=4$ is used when converting the reported data, little overall difference is noticeable in the CFD (Figure 2-9).

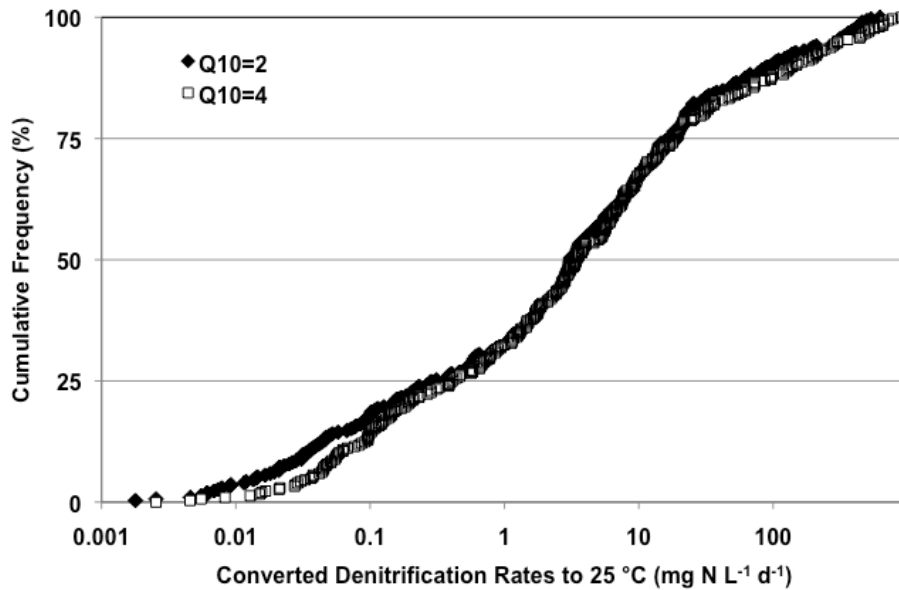


Figure 2-9. Comparison of Denitrification Rates as Function of Soil Temperature.
(306 data points assimilated from the literature adapted from Tucholke, 2007).

2.1.4.3 Maximum Denitrification Rates

Denitrification is expected to reach a maximum value at fully saturated conditions (i.e., when the WFP is 100%). Because the reported experiments were conducted at different temperatures, the rates were first normalized to 25°C using the Arrhenius expression (Equation 2.1.3.3-1) as described earlier (User’s Guide, Section 2.1.3.3). The maximum denitrification rates used as input values in STUMOD and HYDRUS were compiled from the rates reported as mg-N L⁻¹ d⁻¹ in the literature when the WFP was 100%. The rates were separated into the three different soil groups described earlier (Figure 2-10). In total, 165 maximum denitrification rates were used.

2.1.4.4 Soil Moisture Dependency

Unlike nitrification, denitrification takes place under anaerobic circumstances. Most denitrifying microbes are facultative, which means they can utilize different compounds for respiratory processes. When oxygen is depleted, microbes turn to nitrate-nitrogen as an electron acceptor, and convert nitrate-nitrogen to nitrogen gas. Soil moisture is highly correlated to the ability of oxygen to diffuse into soil pores. During high microbial activity, saturated soil leads to the creation of anaerobic conditions and enhances denitrification. The conceptual model for the soil moisture dependency of denitrification consists of a threshold WFP, below which there is no denitrification, and an exponential increase in denitrification with an increase in WFP.

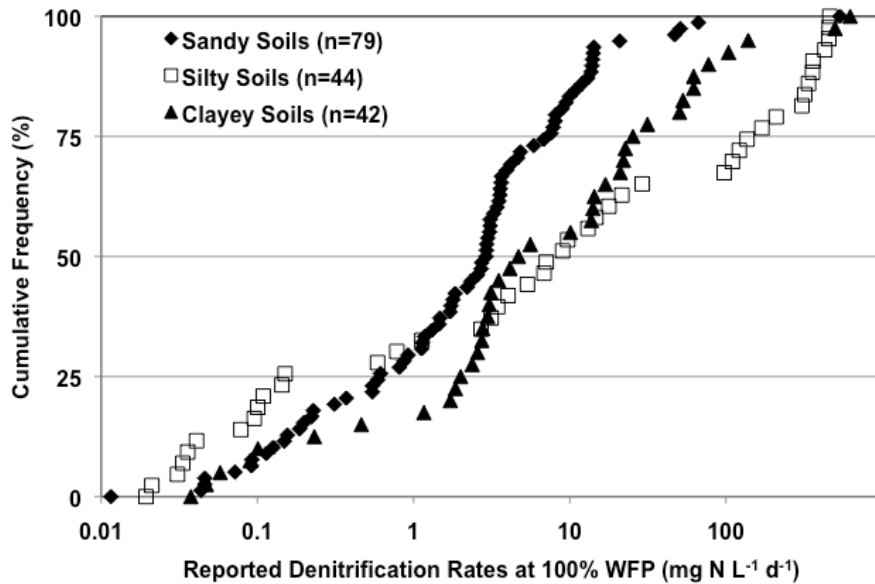


Figure 2-10. Maximum Denitrification Rates by Soil Group.
 (165 data points assimilated from the literature, adapted from Tucholke, 2007)

The denitrification saturation-dependency function implemented into HYDRUS and STUMOD is described by Equation 2.1.4-3. As with nitrification, water-dependency functions were fitted to data reported in the literature. However, while nitrification water-dependency functions were fitted to data sets from a few individual studies, a previous literature review and analysis (Tucholke, 2007) enabled a fit of denitrification curves to data values from several studies. In fact, sufficient data were reported to allow three separate water-dependency curves for the three prominent soil groups. However, positioning data points from many articles side-by-side led to great scatter in the data, which made curve-fitting difficult. These data points capture the effect of WFP on denitrification; yet do not imply other factors, which may have influenced the actual rate. The scatter in the data led to unrealistic optimized curves. For example, the rates reported for 100% WFP ranged from 0.012 to 624 mg-N L⁻¹ d⁻¹. It is obvious that a denitrification rate of 624 mg-N L⁻¹ d⁻¹ is far too high to be realistic, yet receives great importance when using a standard normalizing routine. Hence, it was deemed necessary to normalize the rates on a scale from 0 to 1 (1 being equivalent to the highest recorded value) using the following equation:

$$NR = \frac{R - MinR}{MaxR - MinR} \quad (2.1.4.4-1)$$

where NR is the normalized rate (scale of 0-1), R is a specific rate, and MinR and MaxR are the lowest and highest reported rates, respectively. To eliminate the biased effect of the extremely high or low reported rates, a “lumping” technique was applied to the data. This technique, while being somewhat subjective, is a good way of assigning an average value to a set of reported rates for similar WFPs, as the “lumping” is based not on the rates themselves, but on the distribution of WFP data (Figure 2-11). First, the reported WFPs were ranked by soil group from high to low (or vice-versa), and plotted against a “running tally” x-axis. Such plotting

emphasizes the distribution of WFPs and the number of reported rates in similar WFPs. Next, the average rates were calculated for similar WFPs based on the distribution of data. Although this results in fewer data points, each is more meaningful than each data point of the bulk data because they represent an average value (Figure 2-12).

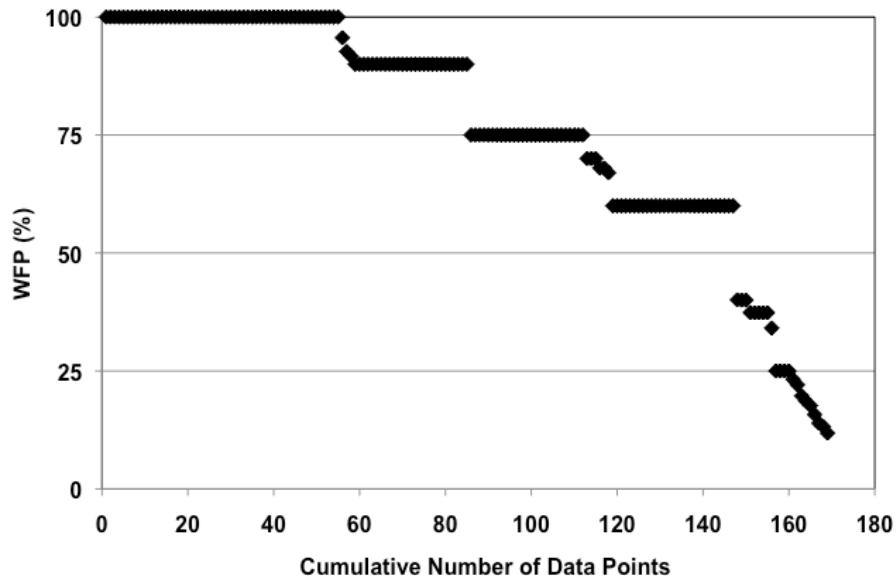


Figure 2-11. Example of Reported WFPs from Denitrification Experiments in “Silty” Soils.

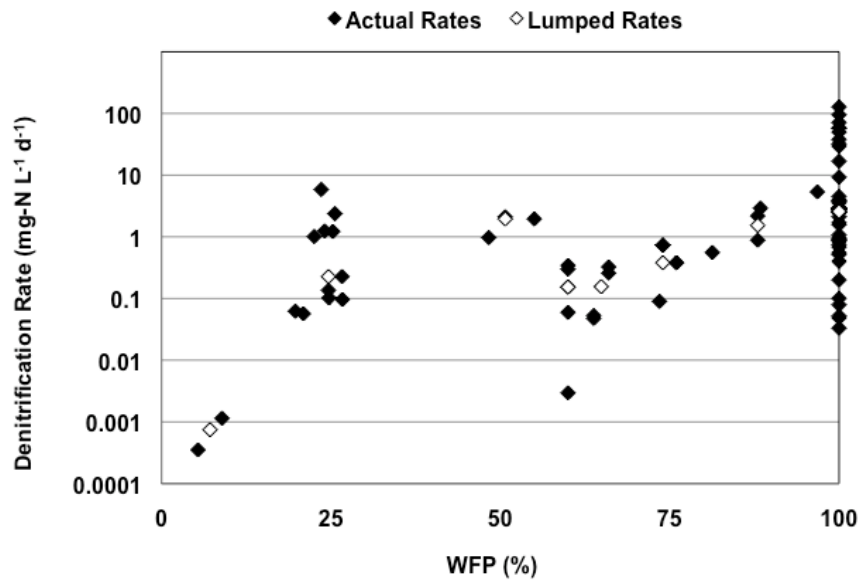


Figure 2-12. Reported Denitrification Rates (solid black diamonds) and Average Rates Based on Lumping (open squares) as a Function of WFP.

The optimized threshold values (Figure 2-13, Table 2-5) may seem too low, as most researchers place the threshold moisture content for denitrification in the 50%-80% WFP range (Grundmann and Rolston, 1987; Bergstrom and Beauchamp, 1993; Machefert and Dise, 2004; Wang et al., 2005); however, visual inspection of the optimized curves reveals that denitrification moisture curves with low threshold values and large exponent values are similar to curves with mid-ranged threshold moisture values and small exponent values. Furthermore, it is apparent from the reported denitrification rates (Figure 2-13) that some denitrification occurs when the WFP is below 50%. A phenomenon that can be explained by the presence of micro-sites in soils, which enable creation of local anaerobic conditions even as the bulk soil moisture content is low. These micro-sites can be related to: 1) physical restriction of oxygen diffusion into small soil pores (Arah, 1990; Klemmedtsson et al., 1997); 2) local increased aerobic activity where carbon “hot spots” exist (e.g., dead beetles, dead leaves and roots) (Parkin, 1987; Arah, 1990); and 3) the ability of some microbes to utilize nitrate-nitrogen as an electron acceptor even in the presence of oxygen (Robertson and Kuenen, 1984).

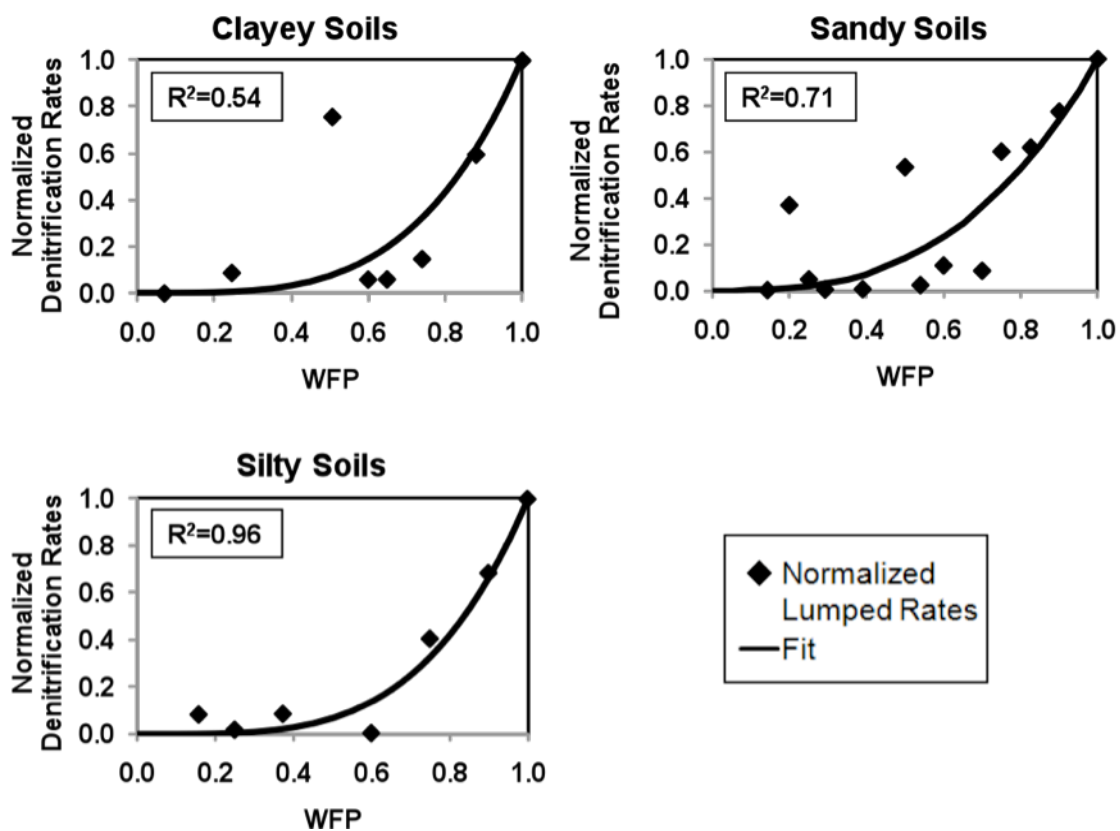


Figure 2-13. Fitted Denitrification Moisture-Dependency Functions to Literature Data for the Three Different Soil Groups.

Table 2-5. Fitted Parameters for the Denitrification Moisture-Dependency Function for the Three Different Soil Groups

Parameter	“Sandy” Soil Group	“Silty” Soil Group	“Clayey” Soil Group
S_{dn}	0	0	0
e_1	2.86	3.86	3.77

2.2 STUMOD Description and Development

A simple spreadsheet model, STUMOD, was developed incorporating the same nitrification and denitrification equations used in HYDRUS. This tool is relatively simple to use but detailed enough to account for important fate and transport processes such as adsorption, biodegradation (for organics), nitrification, and denitrification. STUMOD calculates change in moisture content with depth; thus, the effect of soil moisture on denitrification rate can be determined. In STUMOD, an analytical solution is used to calculate the depth profile of pressure and moisture content based on Darcy's law. The chemical transport component is based on a mass balance for advective transport with reactions. The STUMOD input parameters include operational parameters (effluent concentrations, HLRs) and calibration parameters for hydraulics and nutrient transformation. The output is the expected steady-state performance (i.e., constituent concentration) at the center under the point of effluent application. Input parameters required for STUMOD are listed in Table 2-6.

STUMOD was developed for transport in the unsaturated zone, which is assumed to be predominantly vertical flow with contaminants transported mainly by advection and the effect of dispersion ignored. Continuous, steady state infiltration is assumed. When the effluent application rate is constant, the infiltration reaches steady state and the pressure profile or soil moisture profile does not change with time. Thus, a steady state pressure profile is predicted and a steady state concentration with depth is computed. A biomat and transitional biozone is incorporated. STUMOD can accept ammonium-nitrogen or nitrate-nitrogen effluent concentrations or both. If the effluent is ammonium, nitrogen can be removed through both adsorption and denitrification. If the effluent is nitrate, then nitrogen is removed through denitrification. The effect of moisture content on nitrification and denitrification is calculated based on soil moisture profile. STUMOD accounts for the effect of temperature on nitrification and denitrification.

Default values are provided in the spreadsheet to aid the user during selection of inputs. However, additional reference information is also provided in the look-up tables and parameter sensitivity analysis.

Table 2-6. STUMOD Input Parameters.

Parameter	Units	Definition
Biomat Parameters		
Kb	cm d ⁻¹	Biomat hydraulic conductivity
BT	cm	Biomat thickness
Carbon Parameters		
α	-	An empirical exponent for carbon content adjustment (also referred to as α_C)
Hydraulic Parameters		
HLR	cm d ⁻¹	Hydraulic loading rate
α_1	-	Parameter α in Gradner's analytical equation for pressure distribution (also referred to as α_G)
α_2	-	Parameter α in the soil water retention function (also referred to as α_{VG})
K _s	cm d ⁻¹	Saturated hydraulic conductivity (also referred to as K _{sat})
θ_1	-	Residual soil moisture (also referred to as θ_r)
θ_2	-	Saturated soil moisture (also referred to as θ_s)
n	-	Parameter n in the soil water retention function
m	-	Parameter m in the soil water retention function
l	-	Tortusity parameter
ho	cm	Pressure head at the infiltrative surface
cf	-	Calibration coefficient for pressure distribution (a multiplier from 0 to 1.5)
Effluent Quality Parameters		
Co-NH4	mg-N L ⁻¹	Effluent ammonium-nitrogen concentration
Co-NO3	mg-N L ⁻¹	Effluent nitrate-nitrogen concentration
Nitrification Parameters		
Kr-max	mg-N L ⁻¹ d ⁻¹	Maximum nitrification rate
Km-nit	mg-N L ⁻¹	Half-saturation constant for ammonium-nitrogen
e2	-	Empirical exponent for nitrification
e3	-	Empirical exponent for nitrification
β_1	-	Empirical coefficient for temperature function for nitrification (also referred to as β_{nit})
fs	-	Value of the soil water response function at saturation
fwp	-	Value of the soil water response function at wilting point
swp	-	Relative saturation at wilting point
sl	-	Relative saturation for biological process (lower limit)
sh	-	Relative saturation for biological process (upper limit)
Temperature Parameters		
T	°C	Soil temperature
Topt1	°C	Optimum soil temperature for nitrification (also referred to as Topt-nit(oC))
Topt2	°C	Optimum soil temperature for denitrification (also referred to as Topt-dnt(oC))
Denitrification Parameters		
Vmax	mg-N L ⁻¹ d ⁻¹	Maximum denitrification rate
Km-dnt	mg-N L ⁻¹	Half-saturation constant for nitrate-nitrogen
e-dnt	-	Empirical exponent for denitrification
β_2	-	An empirical coefficient for temperature function (also referred to as β_{dnt})
sdn	-	A threshold relative saturation (dimensionless)
Ammonium Sorption Parameters		
kd	L kg ⁻¹	Adsorption Isotherm
fr	-	Fraction of ammonium-nitrogen that remains sorbed on soil, calibration parameter (0 to 1)
ρ	kg L ⁻¹	Soil bulk density
Target Depth for Output Displays		
D	cm	Soil depth
Output Values at Target Depth		
C/Co NH4	mg-N L ⁻¹	Fraction of ammonium-nitrogen remaining at soil depth D
C/Co TotN	mg-N L ⁻¹	Fraction of total nitrogen remaining at soil depth D

2.2.1 Nitrogen Attenuation Calculation

The overall procedure used to calculate nitrogen attenuation in STUMOD is shown in Figure 2-14. First the pressure profile is calculated first. The soil moisture profile is then calculated using the pressure profile and soil water retention parameters. The soil water profile is also used to calculate the unsaturated hydraulic conductivity. The soil moisture profile is important to determine the correction factor for the effect of soil moisture on nitrification and denitrification. Further detail is given in subsequent sections.

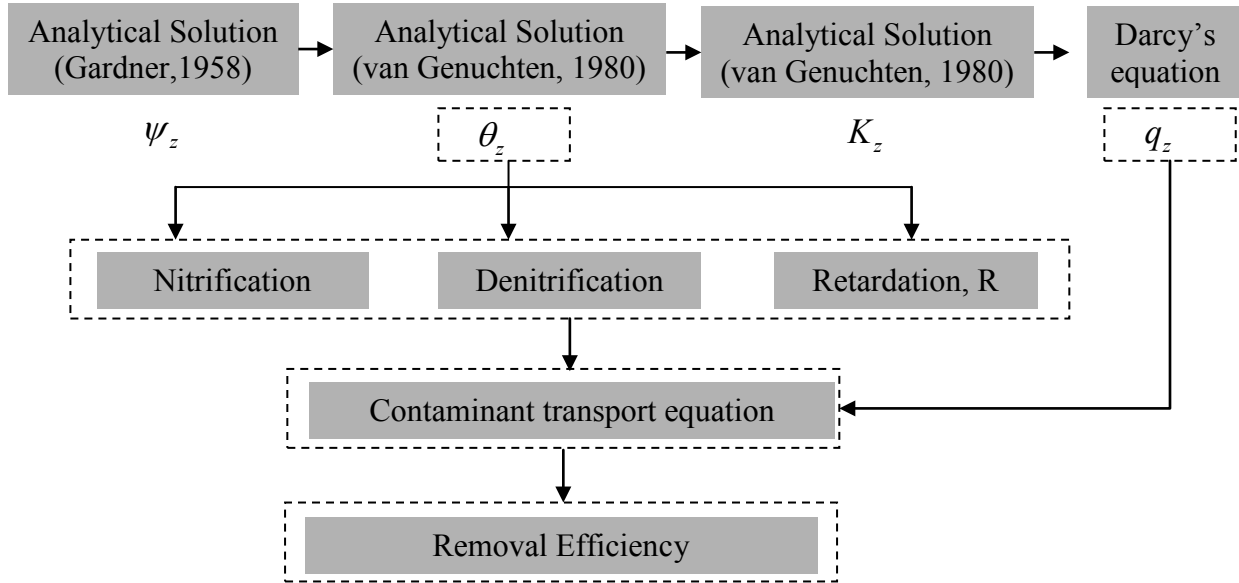


Figure 2-14. Flow Chart of Nitrogen Attenuation Procedures Incorporated into STUMOD.

2.2.1.1 Hydraulics

The STU hydraulic behavior is an important part of fate and transport of pollutants. For STUMOD development, it was assumed that after a period of time, effluent infiltration into the STU would reach steady state. When the effluent application rate is constant the infiltration also reaches steady state and the pressure profile or soil moisture profile will not change with time. Thus, a steady state pressure profile is predicted in STUMOD. The equation for pressure profile is developed by combining Darcy's equation and an exponential model introduced by Gardner (1958) (Equation 2.2.1.1-1):

$$\psi = c_f \left[\psi_o - z + \frac{1}{\alpha_G} \ln \left\{ \frac{v}{K_o} e^{-\alpha_G \psi_o} (e^{\alpha_G \psi_o} - 1) + 1 \right\} \right] \quad (2.2.1.1-1)$$

where ψ is the pressure head and α_G is an exponential parameter relating the unsaturated hydraulic parameter to suction head. Typically, α_G is about 0.01 cm^{-1} , and the range of values from 0.05 to 0.002 cm^{-1} likely covers most applications (Philip, 1969). K_o is hydraulic conductivity corresponding to $\psi = 0$.

The pressure profile is then used to predict the moisture profile as described by Equation 2.2.1.1-2. Then the pressure profile is then calculated on layer-by-layer basis in the soil. Two layers are included in STUMOD, the homogenous soil and an overlying less permeable biomat,

although additional layer can be added. STUMOD calculates the boundary condition (a pressure head) below the biomat based on the approach developed by Bouma (1975). The method assumes that the flux at the trench bottom through the biomat will be equal to the flux through the soil just beneath the biomat. Biomat thickness and hydraulic conductivities are inputs to the model. A correction factor (c_f) is introduced as a calibration parameter or a multiplier used to adjust profile estimated using the empirical equation. The above empirical equation can be used to solve for ψ at z . The suction head ψ is then used in the van Genuchten (1980) equation below to calculate the soil moisture profile.

$$\theta(\psi) = \left\{ \theta_r + \frac{\theta_s - \theta_r}{\left[1 + |\alpha_{vG}\psi|^n\right]^m} \quad \text{if } \psi < 0 \quad \text{and } \theta(\psi) = \theta_s \quad \text{if } \psi \geq 0 \right\} \quad (2.2.1.1-2)$$

where α_{vG} (cm^{-1}) and n (unit less) are fitted parameters, $\theta(\psi)$ is the volumetric water content ($\text{cm}^3 \text{cm}^{-3}$), θ_s is the saturated volumetric water content ($\text{cm}^3 \text{cm}^{-3}$), θ_r is the residual volumetric water content ($\text{cm}^3 \text{cm}^{-3}$), and $m = 1-1/n$. The soil moisture profile calculated using Equation 2.2.1.1-2 is then used to compute and the change in unsaturated hydraulic conductivity with depth and the soil moisture function for nitrification and denitrification discussed in subsequent sections. θ from the above equation is used to calculate, the effective water content, which is then used to calculate the unsaturated hydraulic conductivity. Thus, the unsaturated hydraulic conductivity is also a function of the water content of a layer. The flux in each layer is calculated using the unsaturated hydraulic conductivity and the pressure head gradient using Darcy's equation. The flux or velocity, v_z , in each layer, is used to calculate the removal rate. Thus, the slower the flow through a layer the greater the removal in that layer and vice versa.

2.2.1.2 Contaminant Transport

Nitrogen can be removed in the vadose zone through sorption or reaction. The approach used in STUMOD is based on simplification of the general advection dispersion equation. A simplified relationship given by Equation 2.2.1.2-1 was developed assuming steady state condition and that advection dominates dispersion.

$$c + k_m \ln(c) = c_o + k_m \ln(c_o) + R\mu_{\max} f_z f_t f_{sw} \frac{z}{v_z} \quad (2.2.1.2-1)$$

where C is the concentration of the dissolved constituent at a given soil depth (z), C_o is the concentration at the boundary, v_z is the vertical water velocity, k_m is the half saturation constant, R is the retardation factor, f_z , f_t and f_{sw} are reduction factors (between 0 and 1.0) for carbon, temperature and soil moisture dependency (discussed later), and μ_{\max} represents the maximum reaction rate ($\text{mg N L}^{-1} \text{d}^{-1}$). Concentration cannot be calculated explicitly from Equation 2.2.1.2-1, but rather the equation is solved iteratively. The vertical velocity, v_z , depends on the hydraulic loading and the soil properties, which affects how fast wastewater moves in the vadose zone and, thus, influences removal efficiency. Equation 2.2.1.2-1 is used for both nitrification and denitrification. However, for nitrification the retardation factor (R) and the carbon content function (f_z) are set to 1.0, because these factors have no effect on nitrate-nitrogen removal. The retardation factor is given by Equation 2.2.1.2-2:

$$R = 1 + \frac{\rho K_d}{\theta} \quad (2.2.1.2-2)$$

where ρ is the bulk density and K_d is the distribution coefficient, θ is the soil moisture content for each layer calculated using Equation 2.2.1.2-1. To predict the steady state concentration profile, the calculation is started from the top layer where C_o is known (septic effluent concentration). The calculated concentration on the bottom of the first layer is used as new C_o value for the second layer and so on. The K_d value used in STUMOD is based on reported literature values (User's Guide, Section 3.2.2).

Mass flux (mass/area/day) at the trench centerline is calculated as a product of centerline concentration and HLRs. However, using a centerline flux overestimates mass flux because centerline concentrations and flow rates are relatively high. To account for that, the concentration and flow rates were assumed to decline uniformly from the maximum value at centerline to zero at the trench boundary. Concentration and loading rate values at a distance one-third the trench width away from the centerline were used. Thus, the mass flux was calculated as a product of two-third of the concentration and two-third of the loading rates.

2.2.1.3 Nitrification Rate

The nitrification rate function in STUMOD is the same as described for HYDRUS as developed based on a modification of DRAINMOD-N2 (Skaggs, 1978; Youssef et al., 2005) (User's Guide, Section 2.1.3). In STUMOD, a Monod-kinetic term is used (User's Guide, Section 1.3.5). The Monod-kinetic term is multiplied by the temperature and soil moisture dependency functions f_t and f_{sw} to adjust for the effect of these factors on the reaction rate as defined in DRAINMOD equations.

2.2.1.4 Denitrification Rate

The denitrification rate function in STUMOD is the same as described for HYDRUS as developed based on a modification of DRAINMOD-N2 (Skaggs, 1978; Youssef et al., 2005) (User's Guide, Section 2.1.4). In the original DRAINMOD equation, a first-order maximum denitrification rate was used and then adjusted for the effect of temperature and soil moisture condition. In STUMOD, the first-order maximum denitrification rate was replaced by a Monod-kinetic term (User's Guide, Section 1.3.5). The Monod-kinetic term is then multiplied by the temperature and soil moisture dependency functions f_t and f_{sw} to adjust for the effect of these factors on the reaction rate as defined in DRAINMOD equations. An exponential depth function that describes the distribution of organic carbon (f_c , Equation 2.1.4-1), was not incorporated in STUMOD because of the complexity of the function with depth (dependent on nitrogen transformation, oxygen availability, carbon form, etc.) and insufficient data to model this process in the STU.

2.2.2 Parameter Sensitivity Analysis

A sensitivity analysis indicates which input parameters are critical to and which parameters have less influence on the final model output. This process allows evaluation of which model inputs are most important based on the greatest impact to a prediction. Ultimately this information allows the user to understand and focus on the parameters that will have the most affect on STU performance and to understand how potentially small changes in the parameter may produce a wide range of model outputs.

An automated sensitivity analysis tool was developed for the analysis of multiple STUMOD input parameters. One input parameter was selected and its value randomly picked from a distribution of the input parameter values (e.g., values obtained from a literature search)

while all other input parameters were held at their base case value. STUMOD was run several times with continued random selection of the input parameter value to produce a corresponding output distribution based on that particular input parameter. The process was then repeated for the other input parameters producing output distributions for each input parameter. To perform this sensitivity analysis the input parameters must be selected from either a uniform or normal distribution of parameter values. For a uniform distribution, the specified minimum, maximum, and base case values for each input parameter are required. For a normal distribution, the mean and standard deviation values for each input parameter are required. The standard deviation of each output distribution was then compared and used as an indicator of the sensitivity of the output to the variability of the input parameter. For the purpose of comparison, a ratio of the standard deviation of each parameter to the maximum standard deviation was calculated for each parameter. Thus, the ratio varies from 0 to 1 and reflects the sensitivity of a parameter relative to the parameter with the highest sensitivity.

The analysis for STUMOD input parameters was conducted for two different scenarios; one with ammonium-nitrogen effluent input and another with nitrate-nitrogen effluent input (assuming ammonium was completely nitrified before applied to STU). From these scenarios, the sensitivity of different outputs (soil moisture content, ammonium-nitrogen concentration, and fraction removed [C/C_0]) was evaluated. The soil moisture content was sensitive to identical sets of parameters regardless of the effluent type (Figure 2-15). Parameters relevant for ammonium concentration are shown in Figure 2-16 and Figures 2-17 and 2-18 show the sensitivity results for STE or nitrified effluent applied to STU, respectively. These graphs show that the fraction of nitrogen removed (C/C_0) is sensitive to a similar set of parameters; however, the order or level of importance was different. It is not surprising that for the case of STE (ammonium-nitrogen effluent), the model output is most sensitive to each of the parameters in the nitrification process (Figure 2-16) with the most sensitive (i.e., important) parameter being the maximum nitrification rate.

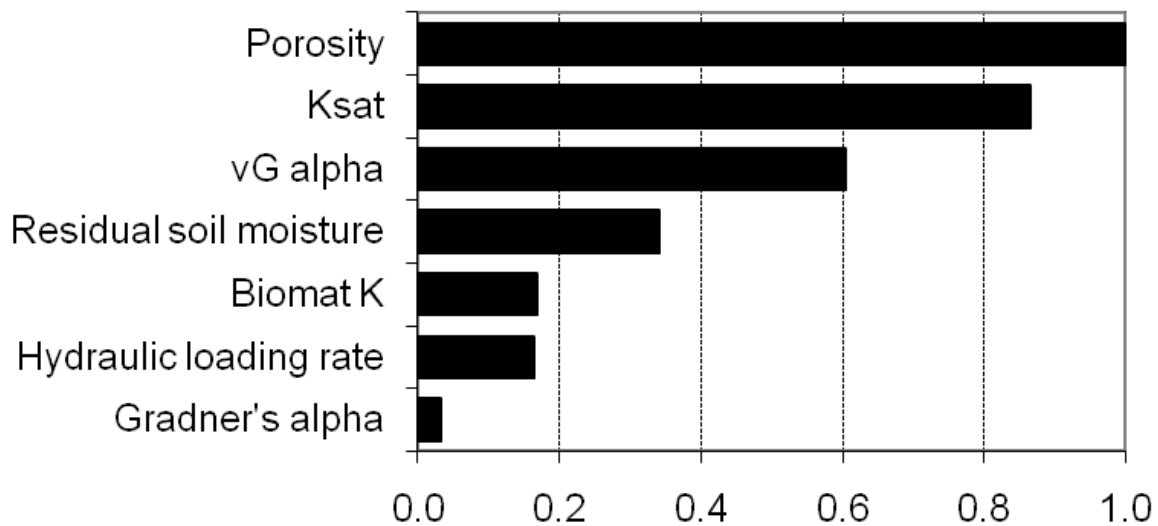


Figure 2-15. Sensitivity of Soil Moisture Content to Input Parameters.

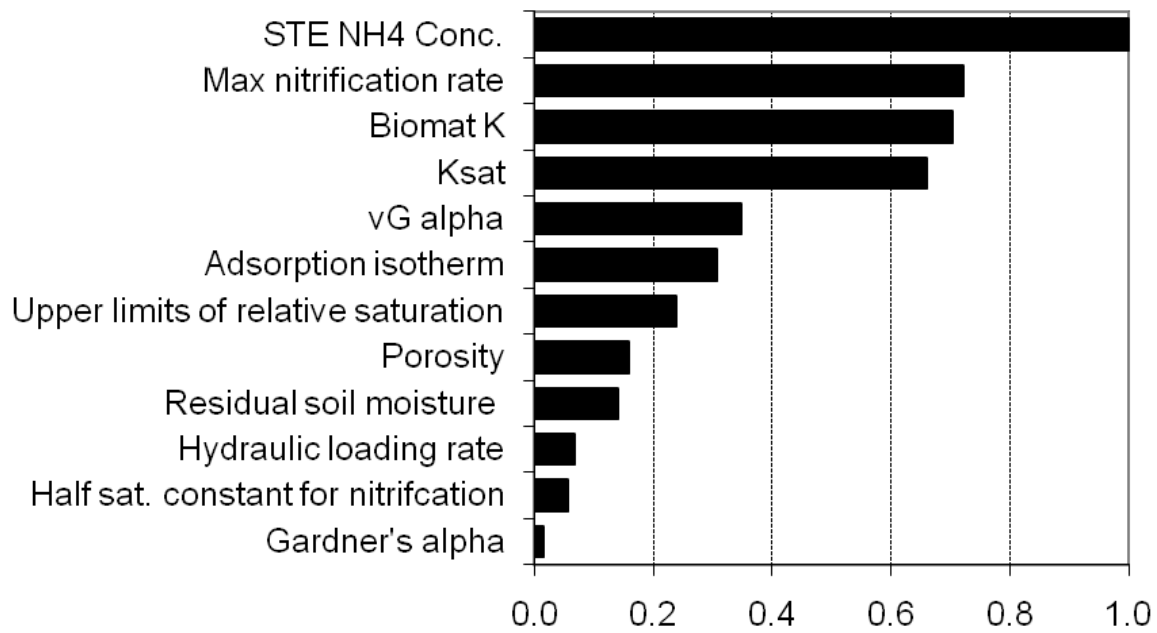


Figure 2-16. Sensitivity of Ammonium-nitrogen Concentration to Input Parameters (STE).

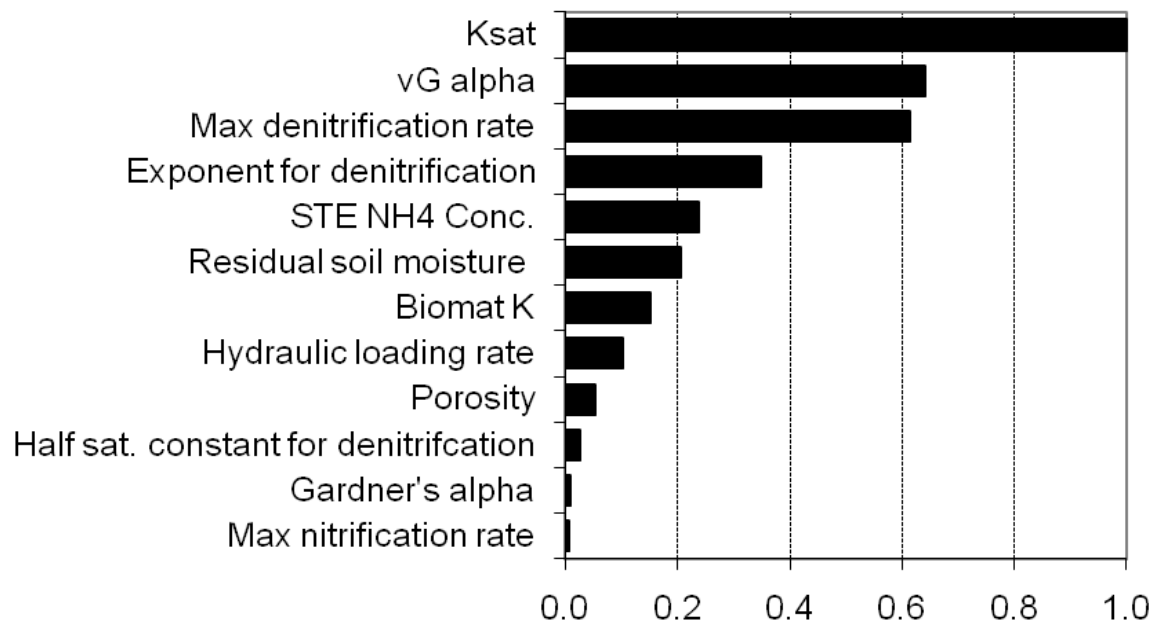


Figure 2-17. Sensitivity of Fraction Nitrogen Removed to Input Parameters (STE).

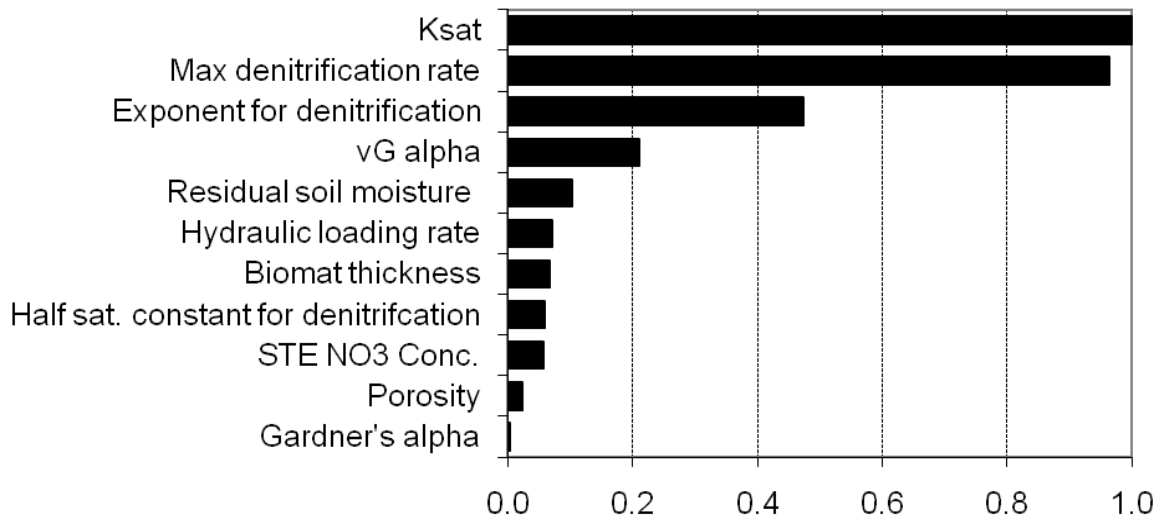


Figure 2-18. Sensitivity of Fraction Nitrogen Removed to Input Parameters (nitrified effluent).

2.2.2.1 Uncertainty Analysis using Monte Carlo Approach

Monte Carlo simulation was used to quantify the uncertainty of model outcome in STUMOD. The model was executed many times with the input parameter values randomly generated from ranges of values. By statistically analyzing thousands of model output results, the probability of realizing one particular outcome (concentration at a particular depth relative to effluent concentration [C/C_o]) was quantified. For this analysis a visual basic code was added to STUMOD to allow Monte Carlo simulation. The code allowed random number generation of multiple input parameters across user-specified ranges or from the distribution of the input parameters. The resulting model output can be viewed in a probabilistic framework allowing the user to determine which percentiles and outcomes are acceptable or unacceptable, or which outcomes represent “best,” and “worst” cases. Rather than a single output that may or may not be accurate, this approach gives the probability of realizing any one specific outcome, based on the cumulative uncertainty of all model input parameters. The probability of realizing C/C_o values was calculated for different soil depths (15, 30 and 60 cm), four different soil temperature zones (hyperthermic, thermic, mesic, and frigid/cryic), and 12 soil textures for two scenarios: 1) STE represented as 60 mg-N L^{-1} of ammonium, and 2) nitrified effluent represented as 15 mg-N L^{-1} of nitrate. In general, for both effluent qualities, higher C/C_o values (i.e., fraction of nitrogen remaining) were typical at shallow depths and less frequent under high soil temperature zones and clayey soil textures.

Results of these Monte Carlo simulations illustrate the differences in the cumulative probability of C/C_o values. The cumulative probability graphs are presented in a separate supplemental file “Visual-Graphic Tools”.

2.2.3 Benchmarking of STUMOD and HYDRUS

STUMOD was compared with HYDRUS-2D for the conditions summarized in Table 2-7. The hydraulic data was obtained from Rossetta soil database (Schaap et al., 2001). The effect of soil moisture and temperature was considered, but not the effect of carbon content.

Table 2-7. Summary of Conditions for Comparison of STUMOD and HYDRUS-2D.

Test	Soil type	Hydraulic Data	Nitrification Rate	Denitrification Rates	Effect of Moisture	Effect of Temp.	Effect of Carbon
2	silt	Rosetta	56 mg L ⁻¹ d	2.58 mg L ⁻¹ d	yes	yes	no
3	silty loam	Rosetta	56 mg L ⁻¹ d	3.32 mg L ⁻¹ d	yes	yes	no
6	sandy loam	Rosetta	56 mg L ⁻¹ d	3.32 mg L ⁻¹ d	yes	yes	no

The actual soil temperature was set to 15°C and the rate was then adjusted using the DRAINMOD temperature function. The optimum temperature was assumed to be 25°C (Figure 2-7). Because the rates are used for comparative purpose only, the actual rates used did not affect the results of this comparison. STUMOD and HYDRUS-2D were compared for removal rates (C/C₀). In summary, STUMOD and HYDRUS results matched well under the different conditions as shown in Table 2-8 and Figures 2-19, 2-20 and 2-21.

Table 2-8. Denitrification Rates used During Benchmarking of STUMOD and HYDRUS-2D.

Denitrification Condition	25°C (mg L ⁻¹ ·d ⁻¹)		15°C (mg L ⁻¹ ·d ⁻¹)	
	sand	silt	sand	silt
Low	0.9	0.074	0.45	0.037
Best	6.06	13.9	3.03	6.95
High	74.44	88.64	37.22	44.32

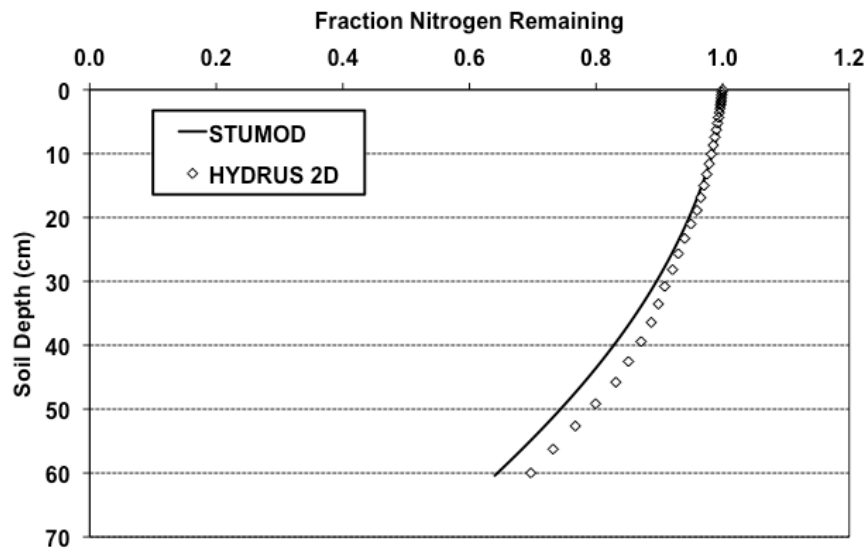


Figure 2-19. Benchmarking Results for Sandy Loam at 15°C.

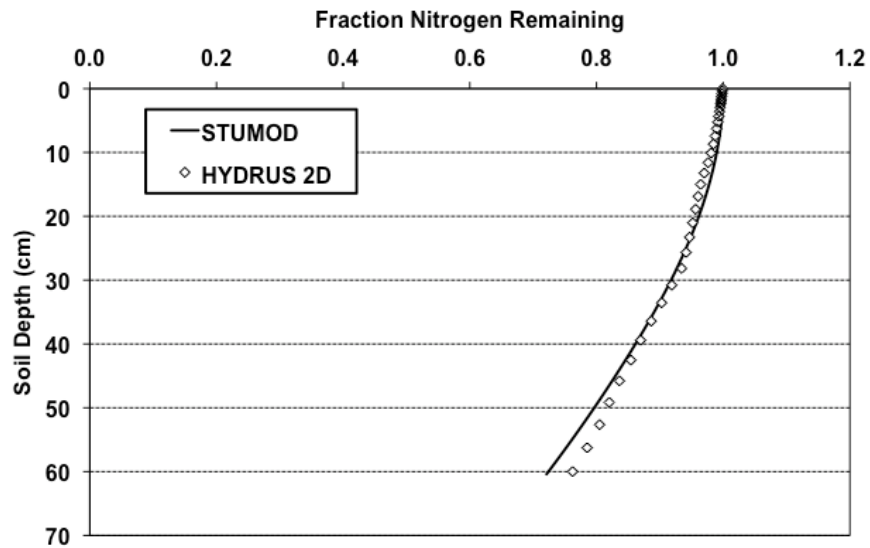


Figure 2-20. Benchmarking Results for Silty Loam at 15°C.

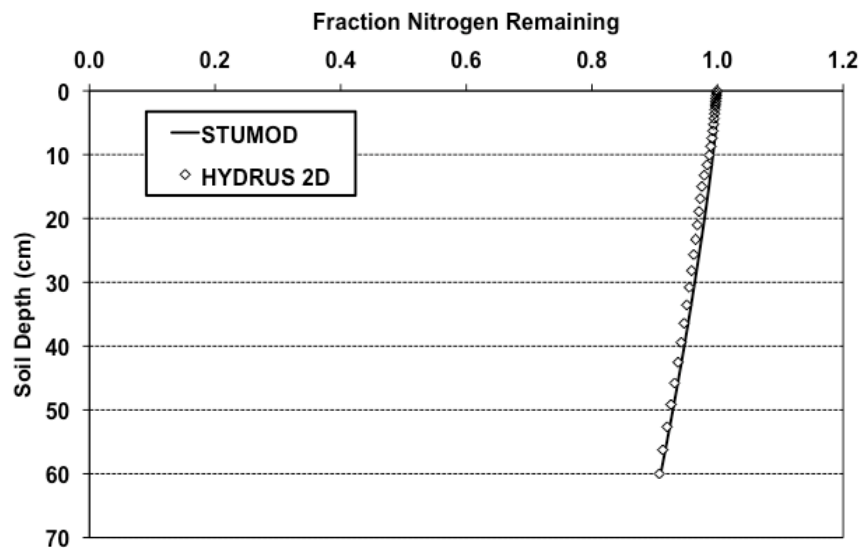


Figure 2-21. Benchmarking Results for Silt at 15°C.

STUMOD is a simple to use model, but has several parameters (both for hydraulics and nutrient transformation) providing flexibility for calibration with observed data. The comparison between HYDRUS and STUMOD showed that STUMOD easily matched HYDRUS. The two models use identical parameters for hydraulics and nutrient transformation. Thus, the hydraulic parameters were set to same value based on Rosetta database. HYDRUS uses numerical solution

for hydraulics while an analytical solution is used in STUMOD. Gardner's alpha (α_G) is used in STUMOD in the analytical solution for pressure head (parameter not used in HYDRUS-2D), however this parameter is not very sensitive. Typically, α_G is about 0.01 cm^{-1} , and the range of values 0.05 to 0.002 cm^{-1} seem likely to cover most applications (Philip, 1969). STUMOD and HYDRUS gave a better fit when α_G was set to recommended value of 0.01 or below. STUMOD and HYDRUS also gave a better fit when m was set to a value close to $1-1/n$. It is important to note that the fit between STUMOD and HYDRUS was very sensitive to this parameter with minor adjustment from the $1-1/n$ improving the fit. Another important parameter was the Van Genuchten α_{VG} . To get a good fit between HYDRUS and STUMOD, it is preferred that this parameter is set to a lower value. Values close to 0.01 were good for sandy soils and for silt and clay soils a value less than 0.01 should be used.

2.2.4 STUMOD Calibration

After STUMOD was benchmarked against HYDRUS, STUMOD was calibrated to ensure that the model outputs matched actual observed data. STUMOD was calibrated using data from laboratory tests and field test sites where extensive monitoring was conducted that is not feasible in practice. However, data for model calibration is very limited and a rigorous calibration could not be conducted. Rather, reported operational conditions (HLR, effluent quality, soil texture, and depth) were entered into STUMOD and the % removal estimated by STUMOD was compared to the observed values. Default model parameters provided in STUMOD were used based on the soil texture.

Numerous investigations on fate of nitrogen in STUs have shown that the percent removal is quite variable, even for sites that appear to have similar conditions. The effects of dispersion, dilution, spatial variability in soil properties, wastewater infiltration rates, and temperature impacts are few of the factors that attribute to this variability in removal rates (Otis, 2007). For example, laboratory column studies reported total nitrogen removal ranging from <1 to 84% under varied HLRs (5 to 215 cm d^{-1}) and influent concentrations (16 to 74 mg-N L^{-1}). In field studies performed on OWTSS installed in sandy soil, estimates of total nitrogen removal in ranged from 0 to 94% (Otis, 2007).

Results for the STUMOD calibration are shown in Table 2-9 including the operational conditions and the measured and estimated total nitrogen removals for different soils. In the process of identifying the inputs shown in Table 2-9, STUMOD removal rates were simultaneously evaluated for consistency in removal rates and trends among soil types reported in the literature for varying HLRs and effluent concentrations. The results show that STUMOD predictions are similar to measured values. It is useful to note that the outputs are good first estimates of removal rates under different conditions. However, further adjustments can be made to STUMOD input parameters to match measured data (when/if available) or to reflect actual field observations. For example, the denitrification rate was adjusted for data reported by Tackett (2004) which resulted in an improved STUMOD estimated percent removal from 38% to 44% (observed value = 43% removal).

Table 2-9. Comparison of STUMOD Estimated Nitrogen Removal to Reported Measured Data.

Soil Texture	HLR (cm d ⁻¹)	Effluent Conc. (mg-N L ⁻¹)	Depth (cm)	Measured (% removal)	STUMOD (% removal)	Experimental Setting	Reference
Sand	4.0	48.0	38	0.8	2.6	Laboratory	Potts et al., 2004
Sand	7.0	60.0	60	10.0	6.5	Laboratory	Beach, 2001
Sand	8.4	57	90	5.0	5.0	Laboratory	Van Cuyk et al., 2001
Sand	8.4	57	60	6.0	4.0	Laboratory	Van Cuyk et al., 2001
Sand	5.0	57	90	11.0	7.0	Laboratory	Van Cuyk et al., 2001
Sand	5.0	57	60	3.0	5.0	Laboratory	Van Cuyk et al., 2001
Sandy loam	2.16	61.3	61	36.0	21.0	Field	Andreoli et al., 1979
Sandy loam	2.16	61.3	122	38.0	62.0	Field	Andreoli et al., 1979
Sandy loam	4.0	82.3	60	43.3	37.7b, 43.7c	Field	Tackett, 2004
Sandy loam	2.0	14 ^a	60	87.74	86.8	Field	Conn et al., 2009
Sandy loam	2.0	14 ^a	120	99.37	100.0	Field	Conn et al., 2009
Sandy loam	2.0	14 ^a	240	90.57	99.8	Field	Conn et al., 2009
Sandy loam	8.0	14 ^a	60	69.5	68.7	Field	Conn et al., 2009
Loamy sand	1.2	44.25	170	97.0	98.0	Field	Cogger and Carlile, 1984
Sandy clay loam	2.9	47.5	170	98.0	100.0	Field	Cogger and Carlile, 1984
Sandy clay loam	4.1	43.5	170	93.0	98.0	Field	Cogger and Carlile, 1984
Clay	0.4	44.25	170	97.0	100.0	Field	Cogger and Carlile, 1984
Clay	0.4	44.25	170	98.0	100.0	Field	Cogger and Carlile, 1984
Clay	1.0	44.25	170	98.0	99.0	Field	Cogger and Carlile, 1984
Clay	3.7	31.1	60	99.3	99.8	Field	Radcliffe unpublished ^d
Clay	3.7	31.1	90	99.9	99.9	Field	Radcliffe unpublished ^d

^a Nitrified effluent as nitrate = 14 mg-NO₃ L⁻¹.

^b Denitrification rate = 2.58 mg L⁻¹ d⁻¹; default value provided in STUMOD.

^c Denitrification rate = 3 mg L⁻¹ d⁻¹; input parameter adjusted from default value.

^d Data from field testing, see User's Guide, Appendix C.

Both the measured data and STUMOD output show a relatively higher removal in clayey soils compared to sandy soils. Long (1995) reviewed studies of nitrogen transformation in STUs to develop a methodology for predicting nitrogen loading to the environment. Long (1995) indicated that STUs remove 23-100 % of the nitrogen and correlated greater removals with finer grained soils because anoxic conditions would be achieved more frequently, which would also preserve available organic carbon for denitrification.

In addition, for most soil STUMOD predicted ammonium conversion to nitrate within the first foot below the trench infiltrative surface (based on input data given in Table 2-6). STUMOD results showed that ammonium persisted relatively deeper below the trench in finer soils due to low nitrification rates caused by high predicted water content. These model output results agree with studies described in the literature. For example, studies conducted on nitrogen attenuation and transformation in soils showed that most ammonium present in wastewater is oxidized quite readily, and that nitrate is the dominant nitrogen species in soil pore water within few tens of cm below the STE infiltrative surface (Walker et al., 1973b; Kristiansen, 1981; Cogger et al, 1988; Fischer, 1999).

2.3 N-CALC – Description and Development

N-CALC is a spreadsheet tool developed for calculating nitrogen removal in STUs. It is simple to use while still including relevant removal processes such as adsorption, nitrification and denitrification. The input parameters are effluent concentration, HLR, porosity, and soil

depth with calibration parameters for nutrient transformation (sorption, nitrification and denitrification rates) (Table 2-10). The chemical transport component is based on advective transport only, without consideration of dispersion and diffusion. Similar to STUMOD, all computations are made for steady state conditions and effluent concentrations can be as ammonium-nitrogen and/or nitrate-nitrogen. If the nitrogen in the effluent is in the form of ammonium, then nitrogen is removed through adsorption, nitrification and denitrification. If the nitrogen in the effluent is only in the form of nitrate, then nitrogen is removed through denitrification. Users can choose any of the 12 soil textures based on USDA textural classification (User's Guide, Appendix A, Figure A-1). Default input values are provided based on literature values; however, users with sufficient knowledge of the site of interest can manually input values. The user interface displays the model output as ammonium-nitrogen, nitrate-nitrogen, total nitrogen and mass flux values at a user input soil depth (D) and at half the maximum simulation depth (D/2). N-CALC also produces concentration profiles for ammonium-nitrogen, nitrate-nitrogen, and total nitrogen.

Table 2-10. N-CALC Input Parameters.

Parameter	Units	Definition
Hydraulic Parameters		
HLR	cm d ⁻¹	Hydraulic loading rate
n	-	Porosity
Soil Parameters		
D	cm	Soil depth
ρ	kg L ⁻¹	Soil bulk density
Effluent Quality Parameters		
Co-NH4	mg-N L ⁻¹	Effluent ammonium-nitrogen concentration
Co-NO3	mg-N L ⁻¹	Effluent nitrate-nitrogen concentration
Nitrification/Denitrification Parameters		
Kr-nit	mg-N L ⁻¹ d ⁻¹	Maximum nitrification rate
V-dnt	mg-N L ⁻¹ d ⁻¹	Maximum denitrification rate
Ammonium Sorption Parameters		
kd	L kg ⁻¹	Adsorption Isotherm
fr	-	Fraction of ammonium-nitrogen that remains sorbed on soil, calibration parameter (0 to 1)

Chemicals can be removed in the vadose zone through biodegradation, sorption or reaction. The approach is based on simplification of the general advection dispersion equation. The source of ammonium-nitrogen is effluent, while the source of nitrate-nitrogen could be ammonium-nitrogen nitrified to nitrate-nitrogen in the effluent, in the STU or both. An exponential decay function is used in N-CALC for both ammonium and nitrate.

$$C(z) = C_0 \exp\left(-\frac{RK_r z}{v_z}\right) \quad (2.3-1)$$

where C is the concentration of the dissolved constituent at a given soil depth (z), C_0 is the initial concentration in the effluent, v_z is the vertical water velocity, K_r is first order reaction rate (nitrification or denitrification rate) and R is the retardation factor. The retardation factor (R) is the same as given by Equation 2.2.1.2-2. Default values are included in N-CALC for each soil texture based on literature. However, the user can input values that are appropriate to their site.

A constant seepage velocity (v_z) is used in N-CALC in the exponential decay function (Equation 2.3-1). The seepage velocity is computed by dividing the HLR by the porosity. By excluding the water filled porosity, the residence time in a given layer is overestimated. For clay

type soils and high loading the water filled porosity is close to 1 and the error is minimal. However, for sandy soils and low loading rates the seepage velocity may be overestimated. Consequently, the velocity in sand is higher than in clay, resulting in a lower removal fraction for a given depth in sand. The user can make minor adjustments in the porosity to account for this overestimation of seepage velocity at low loading rates. An elemental depth (Δz) is used. To predict the steady state concentration profile, the calculation is started from the top layer where C_o is known (e.g., STE). The calculated concentration from the bottom of the first layer is then used as the new C_o value for the second layer and so forth.

Nitrification and denitrification rates depend on the degree of saturation. An unsaturated zone is typically present under the biomat in STUs, and the degree of saturation is expected to vary based on soil texture, with a relatively higher degree of saturation in clay soils than in sandy soils. Some models use maximum rates (identical rates regardless of soil texture) and calculate actual rates based on soil moisture profile (e.g., STUMOD). However, in N-CALC actual rates are used instead of maximum rates based on the median first order nitrification / denitrification rates found in (McCray et al., 2005).

N-CALC was compared with STUMOD to qualitatively check the reasonableness of N-CALC output estimations. For this comparison it was assumed that nitrification occurs in the first 30 cm of soil below a STU, provided the water table is not present and unsaturated conditions exist (Brown, 2003) and N-CALC should be able to achieve this for a reasonable range of input parameters values such as nitrification, sorption and denitrification rates. The range of input nitrification rates was based on the CFD developed by McCray et al. (2005) for first order nitrification rates based on reported literature values ranging from 0.0768 to 211 d^{-1} , with a median rate of 2.9 d^{-1} (Figure 2-22). Complete conversion of ammonium-nitrogen to nitrate-nitrogen occurred within a depth range of 10 to 40 cm occurred using N-CALC and first order rates ranging from 0.15 d^{-1} (for clayey soils) to 1.0 d^{-1} (for sandy soils). These results are in agreement with the ammonium conversion rates obtained using STUMOD and zero order nitrification rates (note that the zero order nitrification rates used in STUMOD were obtained based on literature values as described in Section 3.2.3.1 of this User's Guide).

The first order denitrification rates were adjusted in N-CALC to yield an identical fraction removal with depth (C/C_o vs. depth) obtained using the zero order denitrification rates in STUMOD at a depth of 60 cm. These input denitrification rates ranged from 0.004 d^{-1} (for sandy soils) to 0.9 d^{-1} (for clayey soils), with a median rate of 0.025 (d^{-1}). Relatively higher rates were used for clayey soils compared to sandy soils to reflect the relatively high degree of saturation in clays. Again, these input parameters are in agreement with reported literature values, which show that actual rates are higher for clayey soils (Tucholke et al., 2007). N-CALC with first order denitrification rates produced identical results with STUMOD using zero order rates that were again within the range reported by McCray et al. (2005) (Figure 2-23).

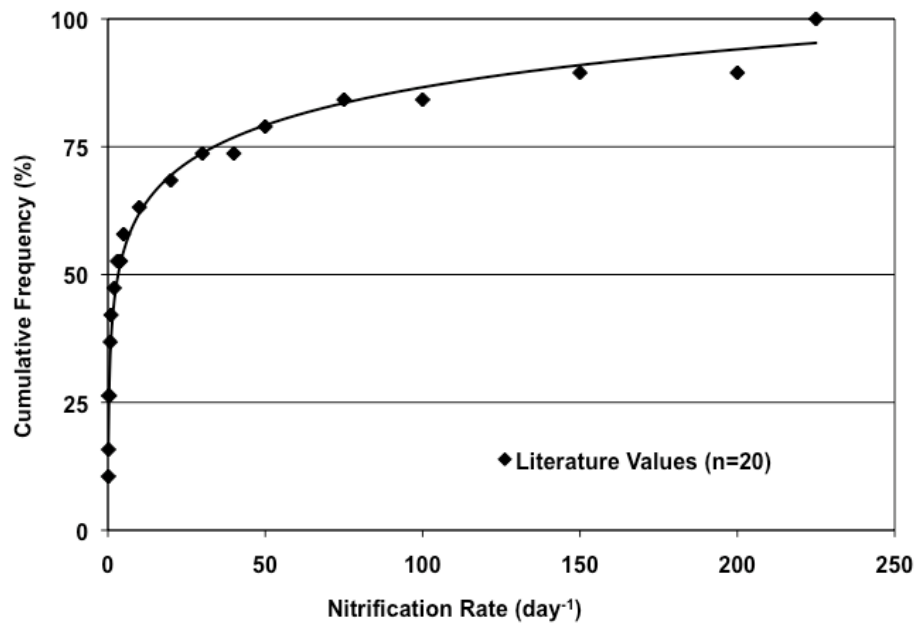


Figure 2-22. First Order Nitrification Rates Reported in the Literature (adapted from McCray et al., 2005).

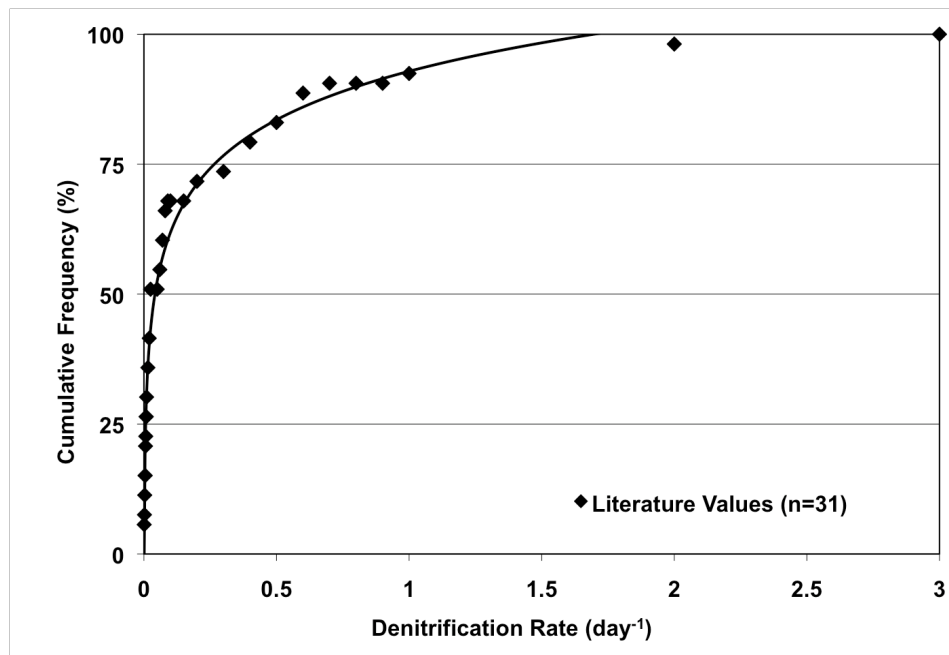


Figure 2-23. First Order Denitrification Rates Reported in the Literature (adapted from McCray et al., 2005).

Ammonium sorption (K_d) values used in N-CALC are the same as those used in STUMOD. As with other parameters, representative sorption values are provided as default values for each soil texture. However, users can input values appropriate to their specific site conditions or adjust the parameters if observed data on concentration of ammonium-nitrogen and

nitrate-nitrogen is available. It is up to the user of the model to estimate the most appropriate rate for their site conditions.

N-CALC output graphs illustrate the nitrogen concentration at the centerline of a trench (Figure 2-24), the fraction of nitrogen remaining with depth (Figure 2-25) and mass flux (Figure 2-26). Mass flux (mass/area/day) is calculated in N-CALC as a product of the centerline concentration and HLR. If a 1-D model is used to calculate the center line mass flux based on the centerline concentration for some trench cross-sectional area and relatively high flow rates, the mass flux will be overestimated and of course, provide a very conservative estimate. Since N-CALC is in one dimension (i.e., output is the centerline concentration), a vertical plane below the trench must be extrapolated to estimate mass flux. To account for this, the concentration and flow rates were assumed to decline uniformly from the maximum value at the centerline to zero at the trench boundary. This assumption is based on field observations as well as 2-D model simulations. This assumption leads to the estimation of the center of mass of the plume to be one third of the distance from the centerline to the “zero” concentration. This in turn yields a two thirds of the centerline concentration and water flux based on geometry. Thus, within N-CALC, concentration and loading rate values at a distance one-third the trench width away from the centerline were used and the mass flux is calculated as a product of two-thirds of the concentration (Figures 2-24, 2-25, and 2-26).

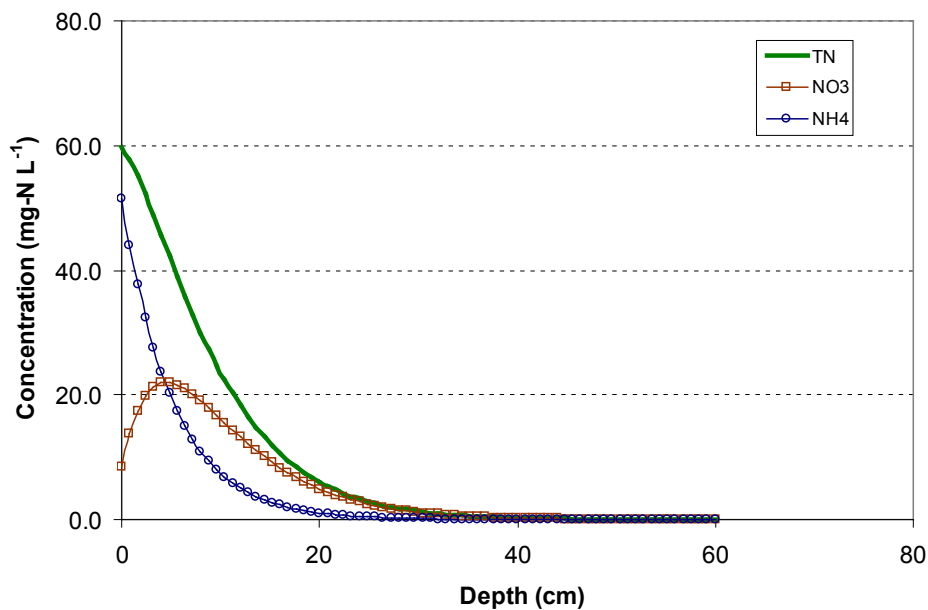


Figure 2-24. Example Concentration Profile for Ammonium (NH₄-N), Nitrate (NO₃-N) and Total Nitrogen (TN) using N-CALC.

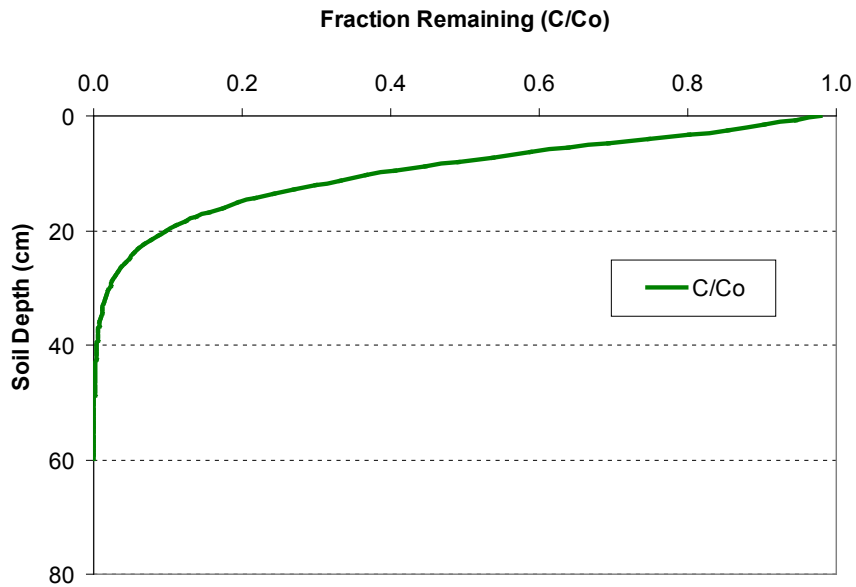


Figure 2-25. Example Removal Efficiency of Total Nitrogen Using N-CALC.

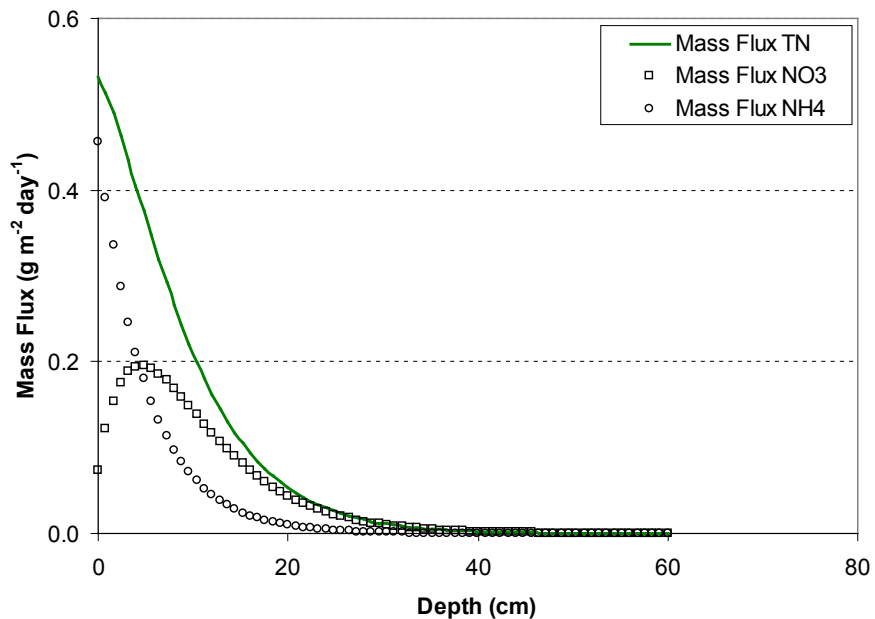


Figure 2-26. Example Mass Flux Prediction with Depth for Ammonium (NH₄-N), Nitrate (NO₃-N), and Total Nitrogen (TN) using N-CALC.

2.4 Scenario Development using HYDRUS

For toolkit users who do not wish to implement a complex model to assess the impacts of these conditions on STU performance, a series of different “scenarios” were simulated using HYDRUS-2D with model outputs for generated for subsurface nitrogen concentrations, spatial

treatment distributions, and mass-flux below a specified boundary illustrated. These qualitative scenario illustrations show the power of a numerical model, as well as provide some end-member treatment evaluations for the selected scenarios.

2.4.1 Trench Systems

The trench model domain was a planar-two-dimensional domain. It included two half-trenches (rather than one central trench) to better visually understand a possible water and solute overlap between two adjacent trenches. The domain geometry (Figure 2-27) considers a system with two 60 cm (2 feet) wide trenches that are 30 cm (1 foot) deep, with 30 cm of overburden and six feet of trench spacing. The bottom boundary of the domain is 3 feet below the infiltration surface, and is considered a “free-flow” boundary condition, which represents a deep water table. Three different “materials” are included in the domain: “gravel” (filling the trenches), “native soil” (surrounding the trenches) and a “biomat” (a 2 cm thick zone at the bottom of the infiltrative surface, extending 5 cm up the trench sidewall). The “biomat” was assigned hydraulic properties similar to those of the native soil, yet with a reduced hydraulic conductivity.

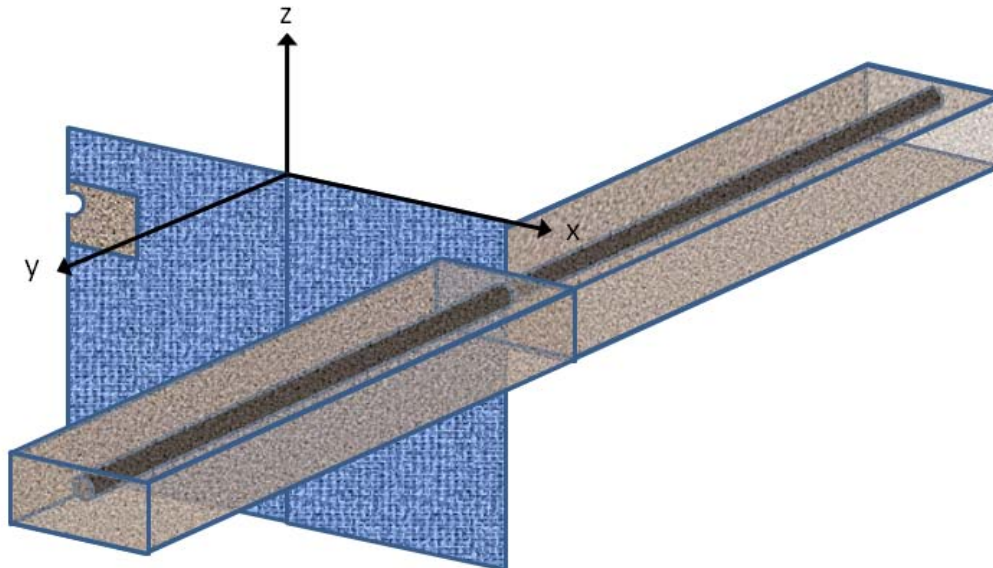


Figure 2-27. Three-Dimensional Visualization of the Two-Dimensional Trench Model.
The 2D-planar section represents the model domain boundaries.

The flow across the discharging pipe was assumed as constant which was equal to a 2 cm d⁻¹ HLR. While a HLR of 2 cm d⁻¹ may be low for sandy soils, it was important to maintain a constant loading rate for the different soils to enable suitable comparison. The mass flux across a certain depth in HYDRUS-2D is given in units of mass-N per unit-length, which is a result of the two-dimensional setup. The cumulative water flux across a boundary in a two-dimensional model has units of area (e.g., cm²). However, the concentration is still calculated as mass of solute over a volume (e.g., µg-N cm⁻³). Mass flux is typically calculated as the concentration times the volume across a certain boundary. The resulting mass flux in a two-dimensional model thus has units of mass per length (e.g., µg-N cm⁻¹) as shown in Equation 2.4.1-1:

$$\frac{\mu\text{g} - N}{\text{cm}^3} \times \text{cm}^2 = \frac{\mu\text{g} - N}{\text{cm}} \quad (2.4.1-1)$$

Because this type of expression is not very intuitive, the resulting mass flux was thus multiplied by another length unit representing a third dimension, which conceptually extends from the screen towards/away from the observer. The chosen length unit was 1 meter, which means the mass flux across the 30 cm plane and the domain's bottom boundary is calculated for a trench that is 60 cm wide and 1 meter long. To achieve an expected mass flux for an entire system, the provided mass flux has to be multiplied by the total length of the trenches in the system (in meters). The result and domain "snapshots" (i.e., scenario illustrations) represent steady-state conditions. The criteria for steady-state were a constant flux of each of the nitrogen species across the lower boundary, as well as a steady visual output.

2.4.2 Drip Systems

The drip model structure consists of a two-dimensional axi-symmetrical domain. In an axi-symmetrical domain, the flow out of a point source is calculated as if it is discharged into a three-dimensional space, using radial flow equations, yet the display given is of a two-dimensional vertical plane (Figure 2-28).

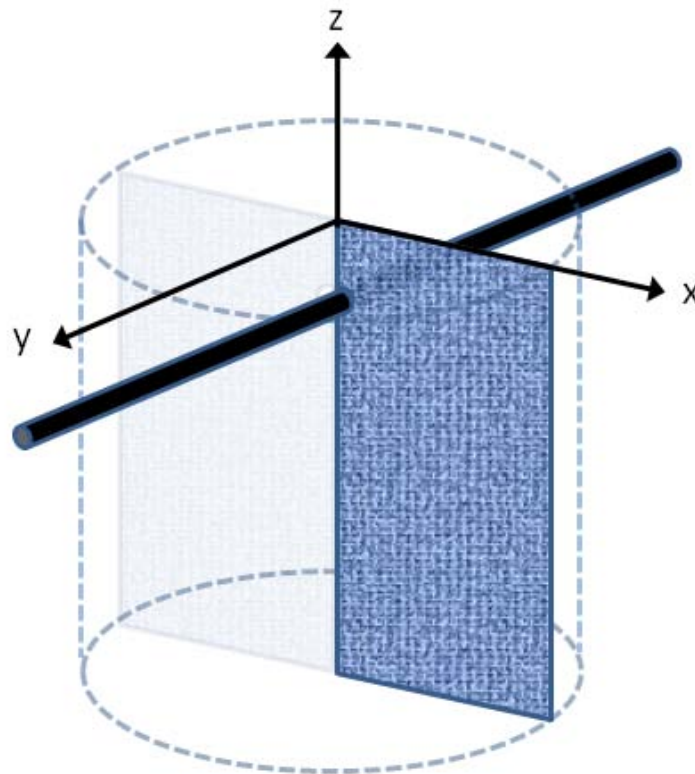


Figure 2-28. Representation of Axi-Symmetrical Domain as Used in the Drip Simulations.

The dark rectangle represents the domain boundaries.

The black narrow cylinder shows the conceptual location of a typical low-flow irrigation pipe.

Most drip systems today are equipped with orifices in the emitters, which are self cleaning and dictate a constant flow rate over a wide range of intra-pipe pressures. The manufacturer specifies this emitter rate of 0.64 to 0.68 mL sec⁻¹ (0.61 to 0.65 gal hr⁻¹) (+/- 5% at psi from 7 to 60 psi) with suggested loading rates to the soil of 2.5 to 7.4 L m⁻¹ d⁻¹ (0.2 to 0.6 gal linear foot (LF)⁻¹ d⁻¹). The actual loading rate to the soil is then balanced between the frequency of dosing, duration of dose, and tubing length (i.e., number of zones and individual zone length). Typically drip dispersal systems receive four doses per zone per day at standard run times from 4.5 to 15.5 min. To ensure equalized dosing between all emitters, the frequency and duration of dosing is also dependent on the volume of tubing length (0.16 L m⁻¹ = 0.013 gal LF⁻¹), which provides dosing under predominantly pressurized conditions. For the scenario simulations, a total of 183 m (600 ft) of tubing receiving a system flow rate of ~1500 L d⁻¹ (400 gal d⁻¹) was assumed. So, a 183 m zone has a volume of 29.5 L (7.8 gallons) and 300 emitters. Thus, a “low” dose of three times the tubing volume would result in a rate of 0.30 L (0.078 gal) emitter⁻¹ dose⁻¹ and a “high” dose of eight times the tubing volume would result in a rate of 0.79 L (0.208 gal) emitter⁻¹ dose⁻¹.

Based on these operating assumptions and constraints, for a low permeable soil such as clay, the recommended dose would be three times the tubing volume, which is 88.6 L (23.4 gallons) per dose cycle (0.30 L emitter⁻¹ dose⁻¹). For a daily flow of 1500 L of STE to the STU, 17 doses d⁻¹ are required. For a two-zone system, that is 8.5 doses d⁻¹ = 4.1 L m⁻¹ (0.33 gallons LF⁻¹) of the zone and for a four-zone system, that is 4.25 doses d⁻¹ = 2.1 L m⁻¹ (0.166 gallons LF⁻¹) of the zone. For a sandy soil, the recommended dose would be as high as eight times the tubing volume, which is 236 L (62.4 gallons) per dose cycle (0.79 L emitter⁻¹ dose⁻¹). Again, for a daily flow of 1500 L of STE to the STU, 6.4 doses d⁻¹ = 8.3 L m⁻¹ (0.67 gallons LF⁻¹) of the zone are required. For a two-zone system, that is 3.2 doses d⁻¹ = 4.1 L m⁻¹ of the zone and for a four-zone system, that is 4.25 doses d⁻¹ = 2.1 L m⁻¹ of the zone. All of these operating conditions are within typical recommendations from the manufacturers.

All scenario simulations included a constant flow rate into the soil, with varying dosing durations to demonstrate the effect of lower and higher loading rates on nitrogen removal. The different scenarios included the combined effect of varying dosing times (seven minutes versus 19 minutes, five doses per day), soil texture (sand, sandy loam, and silty clay) and effluent quality (STE represented as 60 mg-N L⁻¹ of ammonium and 1 mg-N L⁻¹ of nitrate; and nitrified effluent represented as 15 mg-N L⁻¹ of nitrate). An exception was made for silty-clay soils, where long pulses of effluent are not possible because of the low hydraulic conductivity of the soil. Due to this constriction, a high loading rate was implemented as 10 doses per day, each lasting seven minutes.

The domain geometry placed the emitter 15 cm (~6 inches) below the ground level, and the bottom limit of the domain at 60 cm (~2 feet) below the emitter. The width of the domain was 30 cm (~1 foot), which is a typical halfway distance between two emitters. The bottom boundary condition, at 60 cm below the emitter, was set to a constant-head of 0 cm; thus establishing the bottom boundary as the groundwater level in the model. Furthermore, each drip simulation was coupled with an assumed plant uptake. The choice of plant was turfgrass, being the typical “back yard” vegetation in many homes. Several fitting parameters are associated with plant uptake, including the potential evapotranspiration (ET) rate, the water stress function, and the root distribution with depth.

The potential ET rate for any crop depends on climate conditions such as temperature, relative humidity, wind speed, sunshine intensity, sunshine duration etc. (Bastug and Buyuktas, 2003). Turfgrass is quite unique in the sense that it almost uniformly covers the soil surface. Also, different types of turfgrass respond differently to different conditions. For example, warm-season turfgrass has greater water conservation power than cold-season turfgrass (Bastug and Buyuktas, 2003). However, several sources show that a rate of 5 mm d^{-1} is a generally acceptable daily ET rate for turfgrass (Kneebone et al., 1992; Beard, 1994; Bastug and Buyuktas, 2003). For more information regarding ET rates the user is referred to other source such as Huang and Fry (1999).

The plant uptake water stress function describes the actual plant water uptake based on the pressure potential or water content in the soil. Different function-shapes are used by different researchers, and both curves suggested by Feddes et al. (1978) and van Genuchten (1985) are implemented into HYDRUS-2D. HYDRUS-2D also contains a database of suggested values for parameterization of the Feddes root-uptake water-stress function, and default values for turfgrass were used in our simulations along with the “*Feddes*” function. The same parameters were used for all soil textures, except for the wilting-point pressure-head, which was adjusted to a lower value for pure sand, as recommended by the HYDRUS-2D manual. The water stress functions are plotted in Figure 2-29.

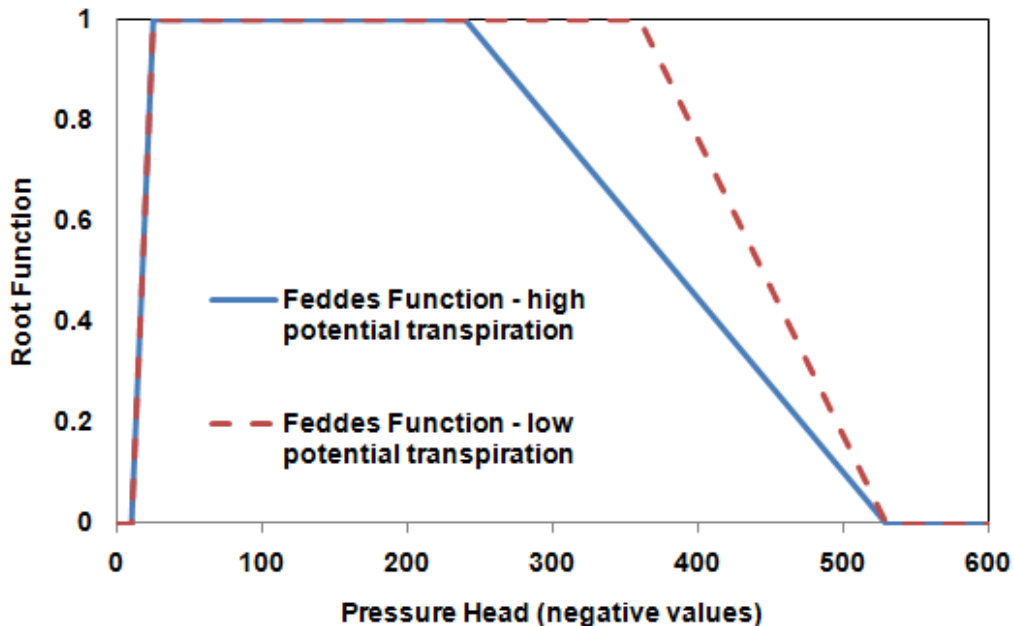


Figure 2-29. Graphical Representation of the Feddes Root-Uptake Water-Stress Function.

Water uptake by turfgrass is also affected by the root distribution in the soil. In general, turfgrass rooting depths are fairly shallow, averaging around 30 cm (Wu, 1985; Beard and Green, 1994; Huang and Fry, 1999). The root density typically decreases from the soil surface to the lowest extent of root distribution. However, under subsurface drip irrigation the maximum root density is affected by the depth of the drip system (Vrugt et al., 2001), thus a root density profile with a maximum root density at 15 cm was selected for the simulated scenarios (Figure 2-30).

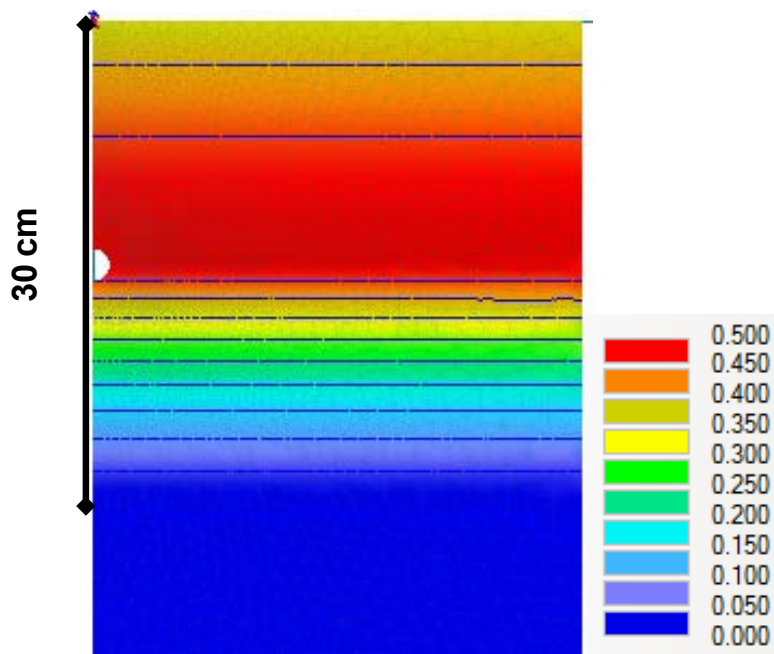


Figure 2-30. Spatial Distribution of the Root Density in the Drip Simulations.

The values in the legend are dimensionless, as they represent a density function (sum of root uptake distribution = 1).

HYDRUS-2D allows the user to specify a maximum turfgrass root water uptake concentration. If a certain solute's concentration in the root zone is higher than this threshold value, the simulated plant uptakes water as usual, but some solute mass is left behind in the soil. No values could be found in the literature for a maximum uptake concentration of nitrate-nitrogen and ammonium-nitrogen, and therefore the maximum uptake concentration for both solutes was set to the highest expected solute concentration during the simulation (60 mg-N L^{-1}).

2.4.3 Calculating Nitrogen Removal

The percent nitrogen removal was calculated by dividing the daily mass flux over the bottom boundary (or 30 cm depth) by the daily input into the system at steady-state conditions as shown in Equation 2.4.3-1:

$$\% \text{Removal} = 1 - \frac{\text{Mass across bottom boundary}}{\text{Mass in effluent} + \text{Mass converted}} \times 100 \quad (2.4.3-1)$$

where the numerator is the daily mass flux across the bottom boundary or 30 cm depth, "Mass in effluent" is the daily mass flux from the pipe into the domain, and the "Mass converted" is the daily addition of a solute to the system due to a reaction (relevant for nitrate-nitrogen only). In this context, it is important to note some bias in the calculation of nitrate-nitrogen removal; the HYDRUS output for mass introduced as a reaction daughter product is calculated for the entire domain. Therefore, it could not be distinguished between nitrate-nitrogen emerging as a transformation product above the 30 cm depth and below it. For some simulations, it has produced a largely skewed estimation of the amount of nitrate-nitrogen removed at 30 cm below the trench (for trench simulations) or emitter (for drip simulations). Where such a calculation resulted in a negative removal rate, the results were eliminated from the result sheets.

2.5 CW2D Model Development

A two-dimensional HYDRUS (Šimůnek et al., 2006) model for the conventional gravel trench established at the UGA experimental site was developed (see Appendix C of this User's Guide for full description of the test site and results). A finite element mesh that included the gravel space within the model domain was used (Figure 2-31). Half of the trench area was modeled assuming flow symmetry around the trench centerline axis. The soil surface was at the top of the model domain and the trench bottom was 72 cm below the soil surface. A variable flux boundary condition was applied at the perforated pipe circumference that produced a dose 3 times a day. An atmospheric boundary condition was used at the surface that allowed a small rain during each dose (to introduce dissolved oxygen) and a low potential evaporation rate for the remainder of the day. The bottom boundary was a deep drainage condition appropriate for a deep water table. All other boundaries were no flux. Three soil layers with depths and hydraulic properties including saturated hydraulic conductivity (K_{sat}) measured at the UGA experimental site were included in the model (Figure 2-32). A biomat was not included in the model due to the short time the UGA test site had been in operation.

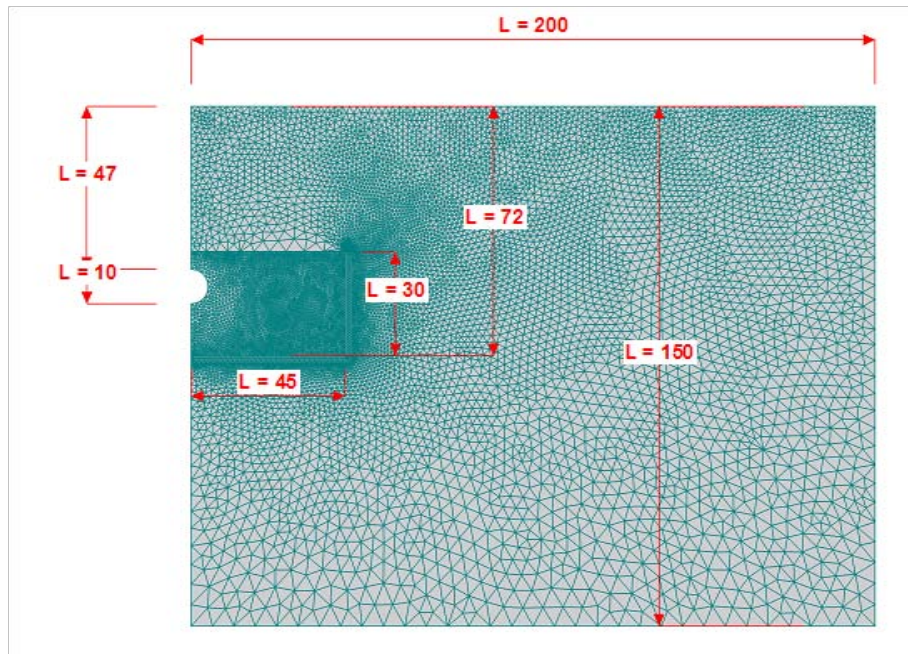


Figure 2-31. Finite Element Mesh for HYDRUS Model (dimensions in cm).

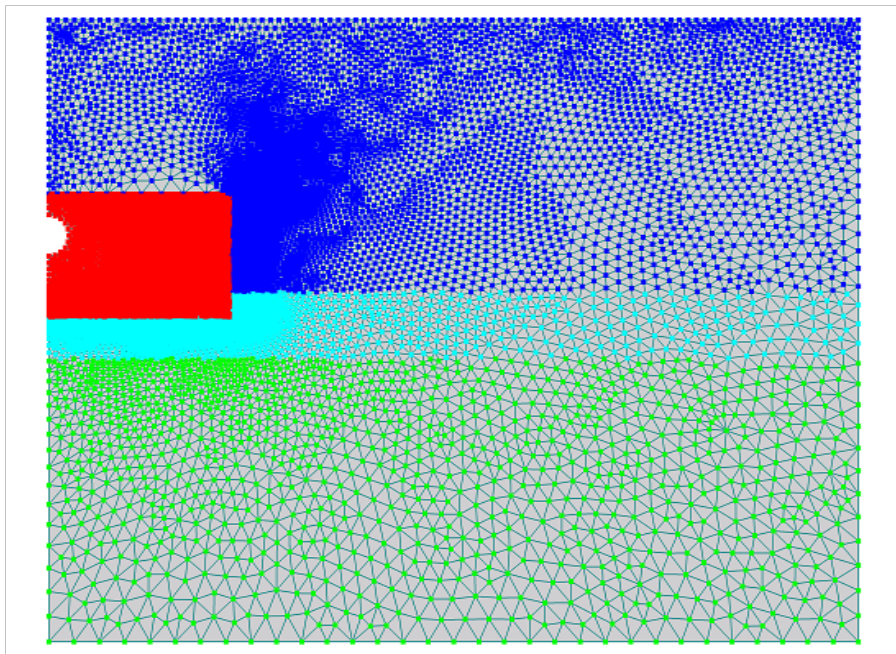


Figure 2-32. Soil Layers in HYDRUS Model: clay Bt1 horizon (blue, $K_{sat} = 1.4 \text{ cm d}^{-1}$), sandy clay Bt2 horizon (turquoise, $K_{sat} = 1.1 \text{ cm d}^{-1}$), clay loam BC horizon (green, $K_{sat} = 0.05 \text{ cm d}^{-1}$), and gravel trench (red, $K_{sat} = 1000 \text{ cm d}^{-1}$).

To model nitrogen fate and transport, the constructed wetlands two-dimensional option (Langergraber and Šimůnek, 2005) in HYDRUS was used. This code is a multi-component reactive transport model that simulates 12 components and 9 processes; thus making it a more robust model to use based on nitrogen removal processes. Three microbe populations are simulated: heterotrophic microorganisms, *Nitrosomonas*, and *Nitrobacter*. Concentrations of nitrogen (ammonium, nitrite, nitrate, dinitrogen), dissolved oxygen, and three forms of organic matter are predicted. It was assumed that the nitrogen entering the trench consisted entirely of ammonium at a concentration of 60 mg-N L^{-1} .

The model was run for 100 days. The distribution of pressure heads at the end of the model run is shown in Figure 2-33. Pressure heads were in the range of negative 20 to positive 10 cm in the region around the trench, which is similar to the range measured at the UGA experimental site (User's Guide, Appendix C, Figure C-5). The most positive values occurred immediately below the trench.

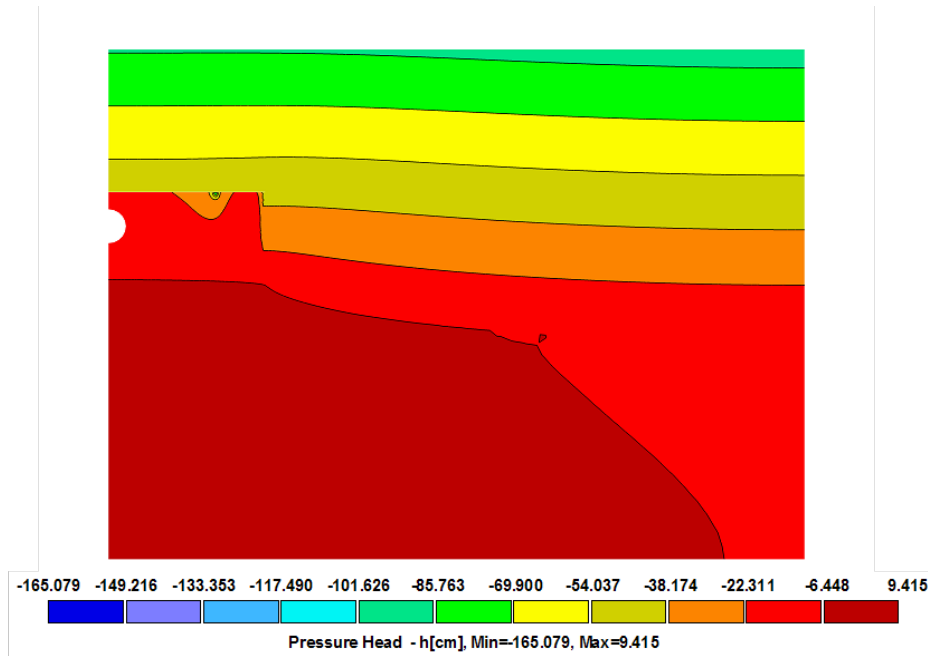


Figure 2-33. Pressure heads in cm predicted by the HYDRUS model after 100 days.

2.5.1 Discussion

Predicted concentrations of nitrate-nitrogen after 100 days are shown in Figure 2-34. Nitrate-nitrogen was present only within the trench. Ammonium-nitrogen in solution was only present in a band immediately below the trench (Figure 2-35). Adsorbed ammonium-nitrogen (not shown) was present in a band similar to that in Figure 2-35. These results indicate that in the model most of the ammonium-nitrogen was rapidly converted to nitrate-nitrogen within the trench. The ammonium-nitrogen that was not converted in the trench, sorbed to the soil in a narrow zone below the trench and this sorbed ammonium-nitrogen maintained elevated concentrations in this zone. The reason why nitrate-nitrogen did not appear outside of the trench was because it was rapidly converted to dinitrogen gas (N_2) through denitrification. This was shown by the predicted distribution of N_2 in Figure 2-36. Elevated concentrations occurred in the trench and surrounding the trench indicating denitrification was occurring in these areas.

Overall, the model predictions of nitrogen seemed to overestimate the denitrification observed in the UGA experimental site soil. It may be possible to adjust parameter values in the wetlands option in HYDRUS to get a model that is adequate for OWTS. For example the growth and lysis rates for the different microbial populations may need adjusting. The current values were developed for a constructed wetland and appropriate values for an OWTS trench and surrounding soil might be different.

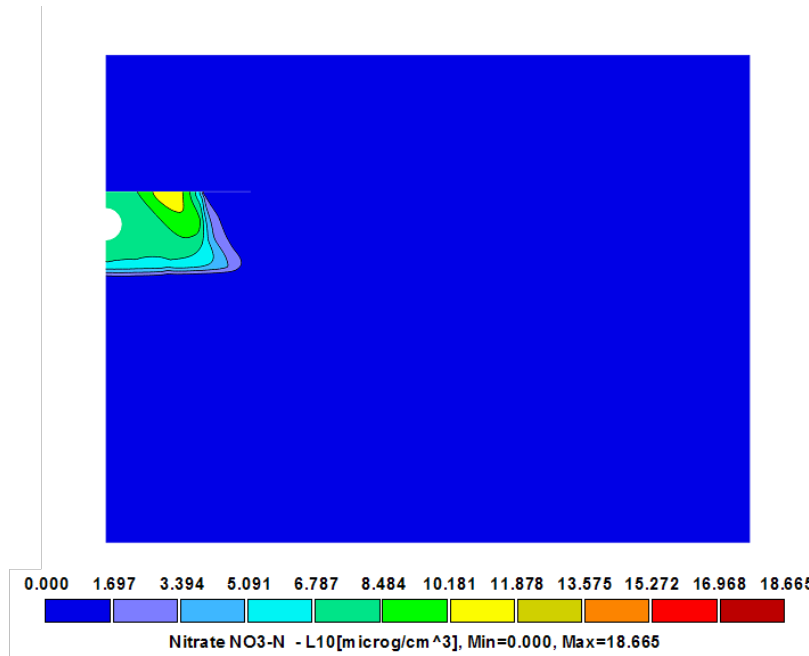


Figure 2-34. Nitrate-Nitrogen Concentrations in mg-N L⁻¹ Predicted by HYDRUS After 100 days.

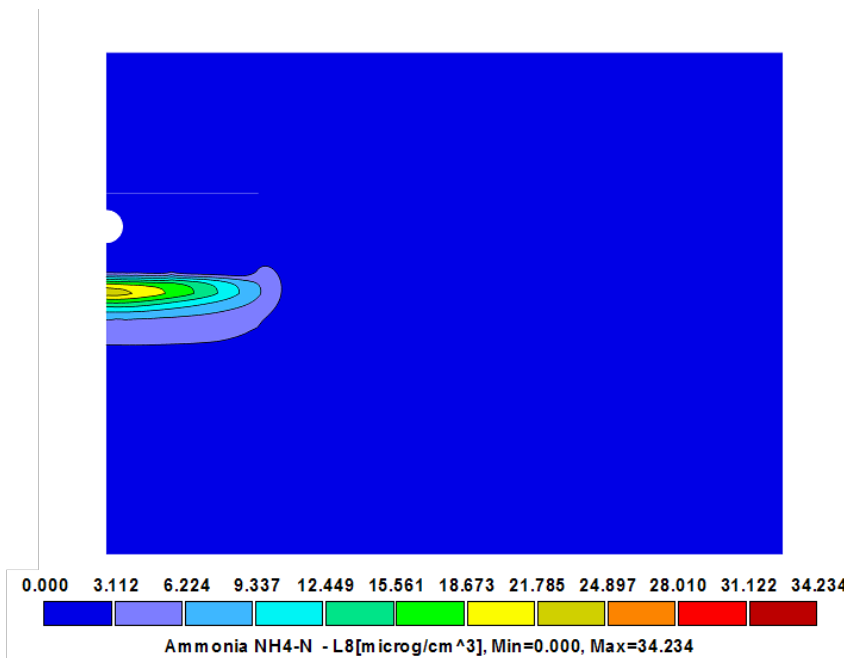


Figure 2-35. Ammonium Concentrations in mg-N L⁻¹ Predicted by HYDRUS After 100 days.

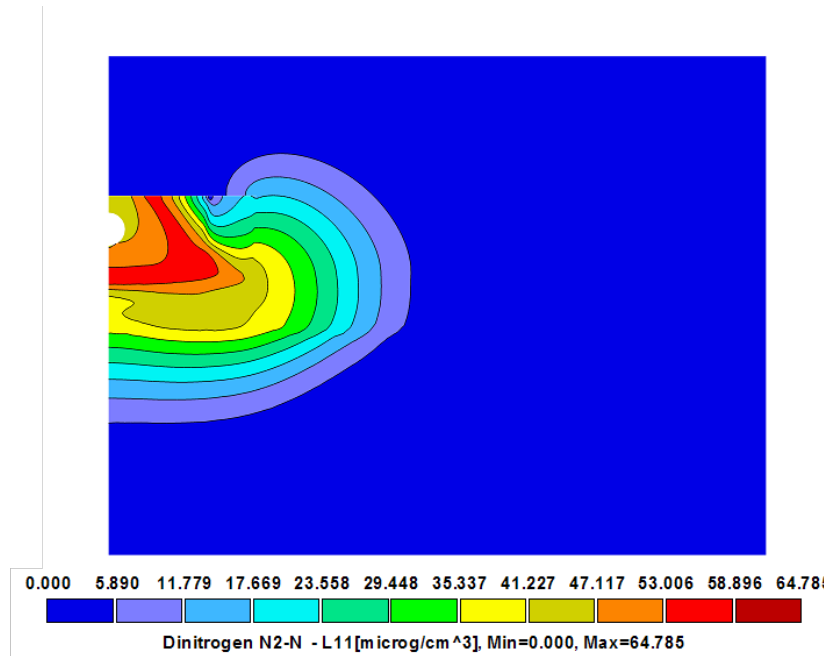


Figure 2-36. Dinitrogen Gas Concentrations in mg-N L⁻¹ Predicted by HYDRUS After 100 days.

2.5.2 Conclusions

The literature review of models for OWTSSs indicated that there is no state-of-the-art model available for modeling nitrogen in OWTSSs, but some existing models might be modified to simulate these processes. Denitrification and the soil and moisture conditions under which it would occur is a critical question in modeling nitrogen. The CW2D model accurately predicted water movement and pressure heads, but underestimated nitrate-nitrogen concentrations in the soil as observed at the UGA experimental site. While it may be possible to adjust the model processes to produce a state-of-the-art OWTSS model for water and nitrogen movement, the difficulty in obtaining a unique calibration and insufficient available information to parameterize the model precluded further use for tool development in this project.

CHAPTER 3.0

GUIDE FOR PARAMETER SELECTION

The tools within the toolkit were developed to help the user decide if the uncertainty in STU performance is acceptable based on the specific target goals. In some cases, the tools may suggest that additional information be collected to assess the expected STU performance with more confidence. In this manner, the user can make better-informed decisions that account for the uncertainty in the treatment predictions as well as the stakeholders' collective willingness to accept or deny risk under some level of uncertainty.

A protocol, in the form of a series of flow charts is provided in the Guidance Manual (Chapter 3.0) to lead the user through the series of steps most often incurred during the design decision process. These flow diagrams not only identify important steps during the design process, but also reference look-up tables, CFDs and other information to support informed decision making. This supplemental information for parameter selection is presented in this chapter. A more experienced user may wish to start directly with nomograph and cumulative probability graph evaluation or begin using the spreadsheet tools, N-CALC or STUMOD.

To aid in the compilation of the relevant information that is required and/or recommended in the decision diagrams prior to using the tools, an easy to use worksheet form was developed (User's Guide, Appendix B). The worksheet guides the user to systematically gather the information presented in the Guidance Manual and Chapter 3.0 of this User's Guide. A series of questions on the worksheet will guide the user to an appropriate look-up table and/or CFD where the relevant information can be obtained. Typically a choice will be made to either select a median value or use a more risk-based approach by selecting lower or higher values depending on expected site conditions, impact of parameter on performance, etc. Reference pages are provided where additional information on each topic can be attained.

3.1 Parameters Relevant to Operational Conditions

Key operational conditions include but are not limited to, gaining a clear understanding of the soil properties, effluent quality characteristics, the expected flows, and potential HLRs. A field assessment is generally necessary to obtain site-specific measurements of soil properties, such as texture, soil depth profile, and depth to groundwater. Additional information such as temperature, organic carbon content, pH, saturated hydrologic conductivity (K_{sat}), and soil moisture content may also be important for reducing the uncertainty in STU performance. While detailed information relevant to estimating operational conditions is presented here, the importance of a soil scientist or other qualified person to describe the soil should not be overlooked. The information presented here is intended to aid in choosing the best possible simplifying assumptions for selection and use of tools presented in this toolkit rather than to estimate actual field conditions. Based on the identified treatment goals, the understanding of and certainty of key parameters such as field capacity, WFP, or soil depth profile is critical to the STU performance.

3.1.1 Soil Texture

Soil texture describes the relative proportion of different grain sizes of mineral particles in a soil. Particles are grouped according to their size into what are called soil separates. These separates are typically named clay, silt, and sand. Soil textures are classified by the fractions of each soil separate (sand, silt, and clay) present in a soil. Classifications are typically named for the primary constituent particle size or a combination of the most abundant particles sizes, e.g., sandy clay or silty clay. A fourth term, loam, is used to describe a roughly equal concentration of sand, silt, and clay. The USDA defines twelve soil texture classifications which are represented by the relative fraction of soil separate on a triangle diagram. The USDA soil texture triangle is presented for reference in Appendix A, Figure A-1 of this User's Guide.

Soil texture is very important in a STU as it influences many other properties such as nitrogen transformations and ability to retain moisture. Generally speaking, sandy soils tend to be low in organic matter content and native fertility, low in ability to retain moisture and nutrients, low in cation exchange and buffer capacities, and highly permeable (i.e., they permit rapid movement of water and air). As the relative percentages of silt and/or clay particles become greater, properties of soils are increasingly affected. Finer-textured soils generally are more fertile, contain more organic matter, have higher cation exchange and buffer capacities, are better able to retain moisture and nutrients, and less permeable. Table 3-1 summarizes the relevant fraction of sand, silt and clay in USDA soil textural classes (STATSGO).

Table 3-1. Average Sand/Silt/Clay Fractions for Soil Texture.

Soil Texture	% Sand	% Silt	% Clay
Sand	92	5	3
Loamy Sand	82	12	6
Sandy Loam	58	32	10
Sandy Clay Loam	17	70	13
Loam	10	85	5
Silt Loam	43	39	18
Silt	58	15	27
Sandy Clay	10	56	34
Clay Loam	32	34	34
Silty Clay Loam	52	6	42
Silty Clay	6	47	47
Clay	22	20	58

It is important to note that because the tools in this toolkit evaluate STU performance, the tools highly dependent on soil specific properties. Thus, a soil scientist or other qualified person to describe the soil is often necessary to finalize OWTS design or to minimize the uncertainty of the tool outputs. In addition, more detailed information from an existing soils database may be adequate. These soil databases approximate soil textures between known data in order to develop generalized soils maps across the United States. A widely used database is the State Soil Geographic (STATSGO) database, with maps available for the entire United States. The STATSGO maps are produced by generalizing soil survey data; however, with a mapping scale of 1:250,000 they may be most appropriate for regional or watershed-scale planning or initial estimates during conceptual design. The Soil Survey Geographic (SSURGO) database has a mapping scale of 1:24,000 allowing it to be used on a local scale and for small watersheds. Although limited information is available in digital format, more data is becoming available every year. Both of these databases are managed by the NRCS and can be accessed at: www.soils.usda.gov. It must be understood that soil textures can (and do) vary significantly

within a relatively small area. It is up to the user to determine the level of accuracy required when estimating soil texture.

To use the spreadsheet tools N-CALC or STUMOD or when using a numerical model, such as HYDRUS, additional hydraulic parameters are important including residual and saturated soil moisture (θ_r and θ_s respectively), nitrification and denitrification rates, or van Genuchten parameters (α and n). Each of the 12 specific USDA soils textures can be hydraulically characterized by the response of the soil saturation to changes in pressure head (“suction”), often referred to as “retention curves” when plotted as soil moisture versus pressure head. Each of these curves can then be expressed mathematically by, among others, a series of parameters referred to as the “van-Genuchten parameters”. Average retention curves for each USDA soil texture have been suggested by (Carsel and Parrish, 1988), and more recently by Schaap et al. (2001) based on averages of hundreds of measured retention characteristics. These relevant parameters are summarized in Table 3-2. The full chart from Schaap et al. (2001), with average values and standard deviations per soil texture, can be found at: <http://www.ars.usda.gov/Services/docs.htm?docid=8953>.

Table 3-2. Summary of Soil Texture Hydraulic Properties (Schaap et al., 2001).

Soil Texture	Statistic	θ_r (cm ³ cm ⁻³)	θ_s (unitless)	K_{sat} (cm d ⁻¹)	α (cm ⁻¹)	n (unitless)
Sand	Mean	0.053	0.375	642.980	0.0353	3.180
	SD	0.029	0.055	477.784	0.0155	1.081
Loamy Sand	Mean	0.049	0.390	105.120	0.0347	1.747
	SD	0.042	0.070	81.021	0.0229	0.539
Sandy Loam	Mean	0.039	0.387	38.250	0.0267	1.448
	SD	0.054	0.085	29.875	0.0194	0.324
Sandy Clay Loam	Mean	0.063	0.384	13.190	0.0211	1.330
	SD	0.078	0.061	11.328	0.0170	0.321
Loam	Mean	0.061	0.399	12.040	0.0111	1.474
	SD	0.073	0.098	10.591	0.0090	0.382
Silt Loam	Mean	0.065	0.439	18.260	0.0051	1.663
	SD	0.073	0.093	14.941	0.0037	0.458
Silt	Mean	0.050	0.489	43.740	0.0066	1.677
	SD	0.041	0.078	20.244	0.0033	0.432
Sandy Clay	Mean	0.117	0.385	11.350	0.0334	1.207
	SD	0.114	0.046	9.888	0.0244	0.155
Clay Loam	Mean	0.079	0.442	8.180	0.0158	1.415
	SD	0.076	0.079	7.515	0.0126	0.341
Silty Clay Loam	Mean	0.090	0.482	11.110	0.0084	1.520
	SD	0.082	0.086	9.178	0.0062	0.393
Silty Clay	Mean	0.111	0.481	9.610	0.0162	1.321
	SD	0.119	0.080	7.022	0.0125	0.271
Clay	Mean	0.098	0.459	14.750	0.0150	1.253
	SD	0.107	0.079	12.976	0.0119	0.186

For the most part, the average values listed in Table 3-2 are a good starting place for modeling movement of water and solutes in soils. Again it is important to understand that these are only suggested values. The accuracy and reliability of these average values are directly related to the amount of existing measurements (i.e., greater confidence is expected in the average value with more measurements). In the analysis by Schaap et al. (2001), 476 different measurements were used to compile a series of average values for the van Genuchten parameters of sandy loam soils, but only 6 measurements were available to calculate average van Genuchten parameters for soils defined as “silt”. Therefore, a site-specific investigation may be required to improve the accuracy of these parameters before conducting numerical simulations of a specific

site. Moreover, the van Genuchten parameters do not take into account, in most cases, the structure of the soil (e.g., root channels, block structure, macropores, etc.).

3.1.2 Effluent Quality

The effluent quality applied to the STU is a principle design parameter effecting performance due to mass loading to the STU and the physical, chemical, and microbial requirements for transformation processes. Specific knowledge of the effluent characteristics is important when using this toolkit to understand the effect of effluent quality has on meeting treatment goals. In the case of nitrogen reduction treatment goals, not only is the total nitrogen concentration of interest, but also alkalinity, pH and carbon. In the case of microorganisms, a wide range of human-pathogenic microorganisms (enteric viruses, enteropathogenic bacteria, and protozoa) are found in STE at concentrations ranging over eight orders of magnitude. In the case of OWCs, the occurrence and magnitude again varies widely and is largely based on the OWTS source. Table 3-3 summarizes relevant constituents in STE.

Table 3-3. Summary of Typical Constituents found in STE (Lowe et al., 2009).

	Units	Literature Values			Measured Field Values		
		n	Median	n	25th Percentile	Median	75th Percentile
pH	-	29	7.1	61	7.1	7.3	7.7
Alkalinity	mg CaCO ₃ L ⁻¹	9	433	61	292	411	410
COD	mg L ⁻¹	36	325	60	320	389	444
cBOD ₅	mg L ⁻¹	98	158	59	156	216	294
Total Nitrogen	mg-N L ⁻¹	40	54	61	47	63	78
Ammonium-nitrogen	mg-N L ⁻¹	26	42	61	43	53	68
Nitrate-nitrogen	mg-N L ⁻¹	38	0.4	61	0.6	0.7	1.1
Total Suspended Solids	mg L ⁻¹	93	61	63	47	61	84
<i>E. coli</i>	cfu 100mL ⁻¹	6	2.6 × 10 ⁶	55	2.2 × 10 ⁴	6.4 × 10 ⁴	2.3 × 10 ⁵

The tools in this toolkit focus on residential wastewater sources. Specifically the nomographs and cumulative probability graphs were developed assuming effluent qualities representative of “typical effluent” (i.e., STE) or “nitrified effluent”. While these effluents are known to vary widely, a concentration of 60 mg-N L⁻¹ (as ammonium-nitrogen) was chosen to represent “typical effluent” and a concentration 15 mg-N L⁻¹ (as nitrate-nitrogen) was chosen to represent “nitrified effluent”. If the effluent concentrations are either much greater or lower than these concentrations, the nomographs and cumulative probability graphs should not be used. Both N-CALC and STUMOD allow the user to select any nitrogen concentration. However, it is important that the user understand the general assumptions and limitations of the tools (see Chapters 1.0 and 2.0 of this User’s Guide).

If a different waste stream is expected, the waste strength for various parameters is expected to vary greatly. Additional information on other waste streams and the general occurrence of constituents in wastewater can be found in Conn et al., 2006; Lowe et al., 2007; and Higgins et al., 2010.

3.1.2.1 pH

The effluent pH may impact the magnitude of nitrification, as the nitrifying microbes are highly sensitive to low pH levels. pH is normally at a level that is optimum for the microbes (7.1 to 7.7) and one can be reasonably confident it is sufficient for nitrification (User's Guide, Section 1.3.1). However, if low pH levels are of concern, the maximum nitrification rate should be adjusted as described in equation 3.1.2.1-1. This adjusted rate can be used in the spreadsheet tools (N-CALC or STUMOD) or numerical models.

$$\mu = \mu_{\max} \left[1 + 10^{(6.5 - \text{pH})} \right]^{-1} \quad 3.1.2.1-1$$

3.1.2.2 Alkalinity

Alkalinity is necessary to absorb or buffer the pH. In wastewater effluents pH is lowered during nitrification with approximately 7 mg L⁻¹ of alkalinity (as CaCO₃) consumed during the conversion of 1 mg-N L⁻¹ as ammonium-nitrogen to nitrate-nitrogen. Sufficient alkalinity generally exists in effluent for nitrification, with little impact of lowered pH on the microbial community responsible for nitrogen transformations (User's Guide, Section 1.3.1). Alkalinity is typically in the range of 300 to 500 mg L⁻¹ as CaCO₃ (Lowe et al., 2009), with a median value of approximately 410 mg L⁻¹ as CaCO₃ (Figure 3-1). Alkalinity may vary due to regional location, household activities, or use of water softeners.

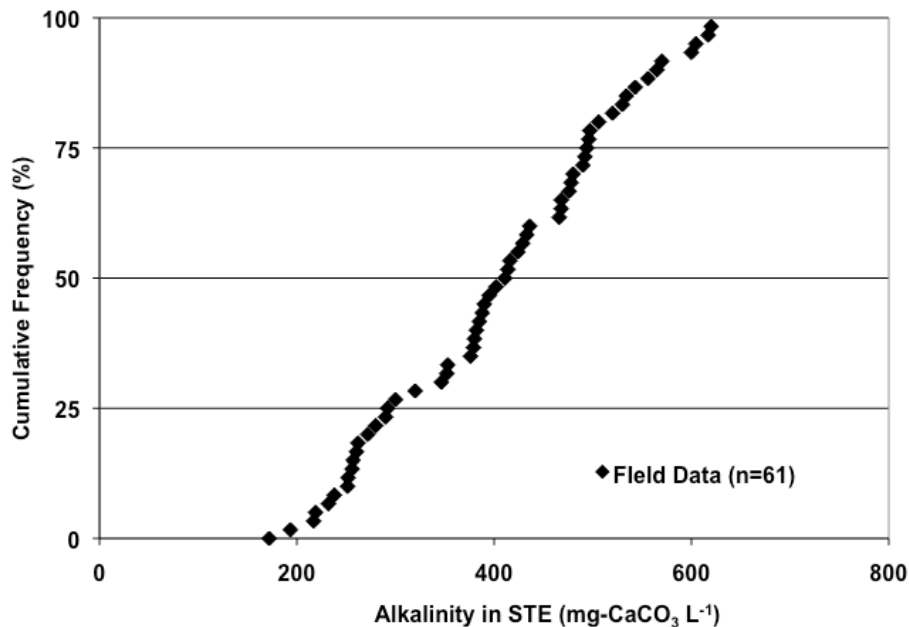


Figure 3-1. Alkalinity Concentrations Measured in STE (adapted from Lowe et al., 2009).

3.1.2.3 Carbon

Carbon concentration in the effluent is important as it may limit or facilitate attenuation processes for nitrogen and OWCs in the STU. Carbon is measured in many different forms

including, TOC, DOC, particulate organic carbon (POC) or indirectly through the BOD or COD tests. Both BOD and COD tests quantify an aggregate amount of organic matter comprising of organic constituents, provide insight into attenuation processes, and are commonly measured in wastewater effluents. The BOD test measures the aerobic biological decomposition of organic material comprised of carbonaceous and nitrogenous BOD. The five-day (BOD₅) test measures the difference in dissolved oxygen within the sample over a given time period. The COD test measures the oxygen equivalent of organic matter that is susceptible to oxidation (by a strong chemical oxidant) and provides insight into the total amount of organics present. Because the COD test can show the presence of organic materials that are not readily susceptible to attack by microorganisms, the COD values are typically higher than BOD₅ values for the same sample.

For nitrogen attenuation, a COD to nitrogen ratio of at least 5:1 is recommended by EPA for nitrogen removal in the STU (User’s Guide, Section 1.2.2). COD values are typically not measured; however, the expected COD concentration can be estimated from the CFD shown in Figure 3-2. Although the range in COD concentrations is quite large (201 to 944 mg L⁻¹), the IQR (25 to 75 percentile values) is relatively small (320 to 552 mg L⁻¹) suggesting little variability in concentration. Alternatively, the COD concentration can be estimated from the carbonaceous BOD (cBOD₅) concentration, using the following relationship established by Lowe et al. (2009) in measured effluents:

$$\text{COD} = 1.34 \text{ cBOD}_5 + 206 \tag{3.1.2.3-1}$$

Measured cBOD₅ values are illustrated in Figure 3-3.

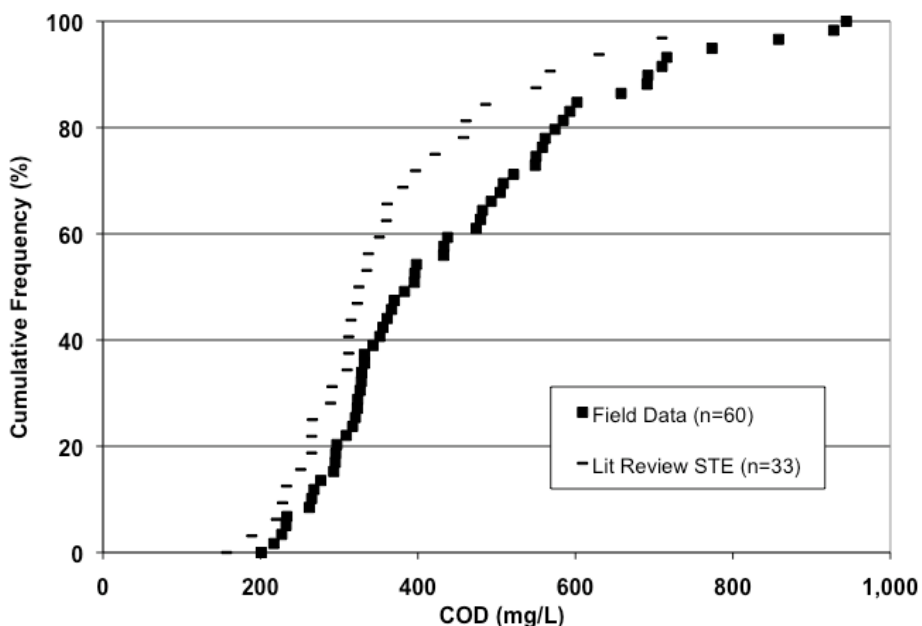


Figure 3-2. COD Concentrations Measured in STE (adapted from Lowe et al., 2009).

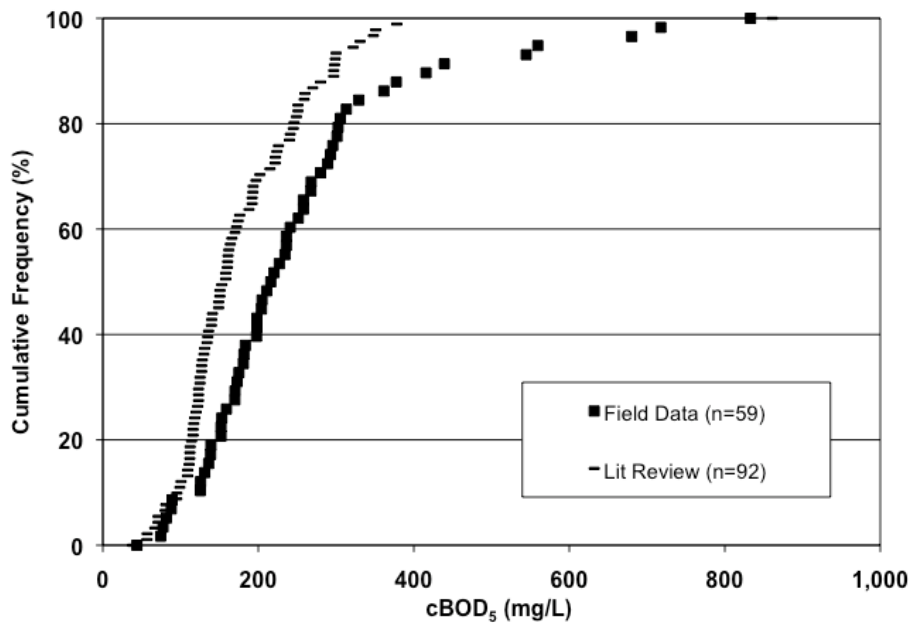


Figure 3-3. cBOD₅ Concentrations Measured in STE (adapted from Lowe et al., 2009).

The minimum C:N ratio to facilitate denitrification is in the range of 4:1 to 7:1 depending on the form of carbon (User’s Guide, Section 1.2.2). The C:N ratio for residential effluent is most likely within this range although nitrified effluents may remove carbon during the nitrification process resulting in insufficient carbon in the effluent for denitrification. Indeed, nitrate contaminated surface waters and ground waters have been documented suggesting that one or more of the requirements for denitrification were not met. Because the spreadsheet tools N-CALC and STUMOD assume that sufficient carbon is available, in cases where nitrogen attenuation is of great concern, caution should be used in evaluating the output from these simple tools (e.g., estimates will be aggressive – that is over assume removal – and lower denitrification rates may be advised).

3.1.2.4 Nitrogen

Knowledge of total nitrogen in effluent is primarily important for nitrogen attenuation. The total nitrogen concentration in STE can be estimated from the CFD shown in Figure 3-4. Lowe et al. (2009) noted that the measured total nitrogen concentration in STE was than 90 mg-N L⁻¹ 90% of the time. A similar CFD for nitrified effluent was not prepared due to the wide range of treatment systems and assessment of these systems was beyond the scope of this project. In cases where advanced treatment is employed (e.g., sand filters, textile filters, aerobic treatment, etc.), the ammonium-nitrogen concentration may be close to zero, while the concentration of nitrate-nitrogen is greater, keeping in mind the potential for carbon limitations.

Ammonium-Nitrogen. Ammonium-nitrogen concentrations found in typical STE can be quite large (Figure 3-5). If no information is available, the concentration can be estimated from the CFD (Figure 3-5), or from Table 3-1. Again, it should be noted that the CFD illustrates “typical effluent” (i.e., STE) with only primary treatment utilized. As discussed in Section 1.3 of this User’, alkalinity is required for the nitrification process and the alkalinity to ammonium-nitrogen

ratio should be estimated. If the ratio is below 7:1, then alternative treatment options may be required to achieve nitrogen reduction treatment goals. Similarly, if the ammonium-nitrogen concentration is significantly greater than 60 mg-N L⁻¹, advanced treatment of the STE may be necessary as the capacity of the certain soils to remove nitrogen is greatly reduced (Figure 3-6).

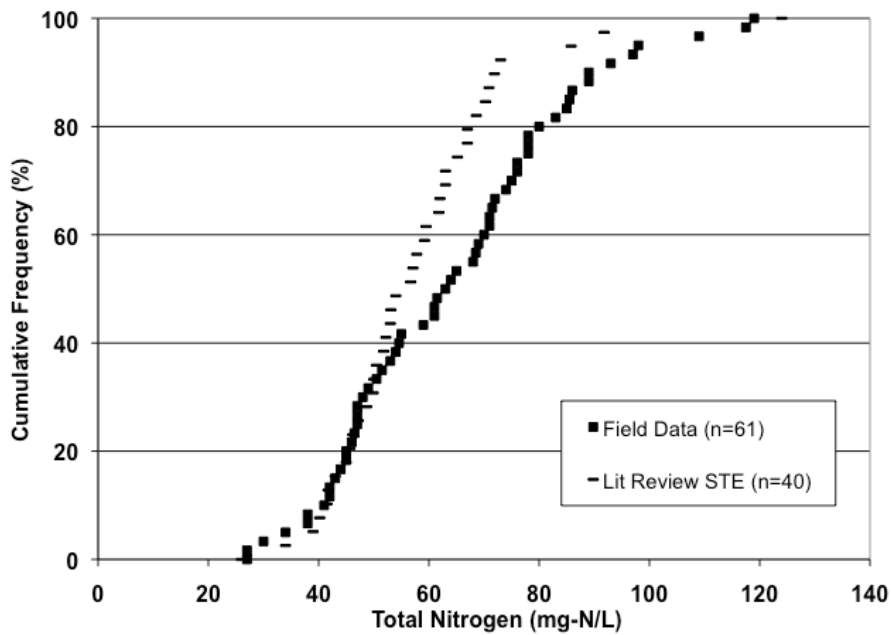


Figure 3-4. Total Nitrogen Concentrations Measured in STE (adapted from Lowe et al., 2009).

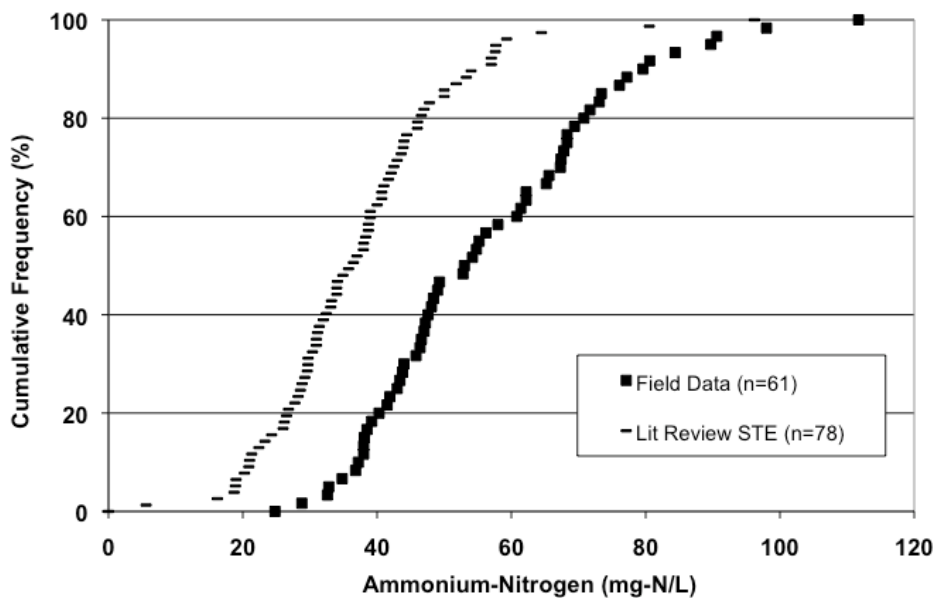


Figure 3-5. Ammonium-nitrogen Concentrations Measured in STE (adapted from Lowe et al., 2009).

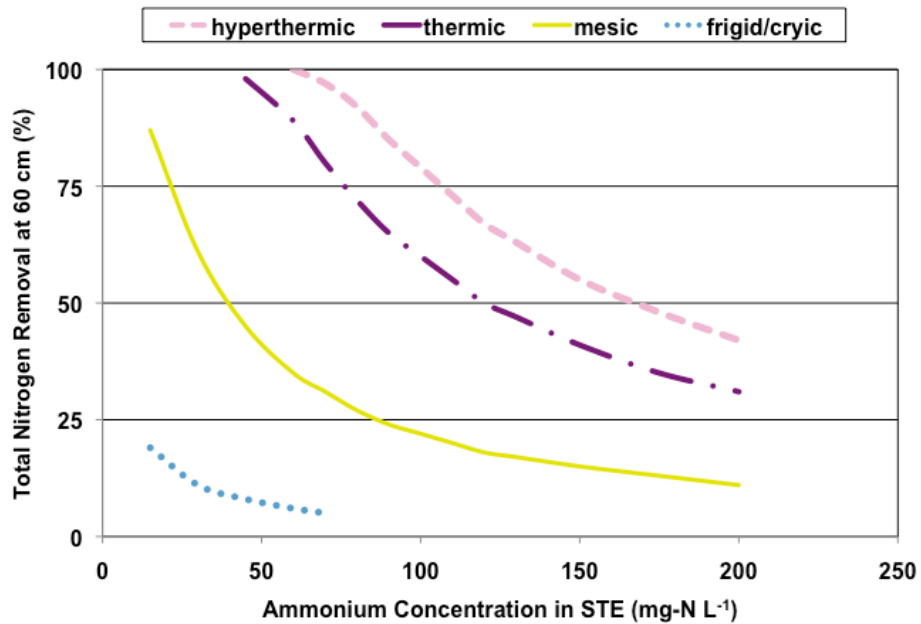


Figure 3-6. Nomograph Illustrating Percent Nitrogen Removal at 60 cm Depth in Different Temperature Regions with Different Initial Effluent Concentrations (x-axis). Note: soil texture = clay loam, HLR = 2 cm d⁻¹.

Nitrate-Nitrogen. OWTS effluents typically contain very little nitrate-nitrogen unless aerobic treatment has been utilized. In cases where advanced treatment is utilized, the concentration may be below the maximum concentration limit (10 mg-N L⁻¹) or achieve treatment goals. In fact, achievement of a target nitrate-nitrogen concentration is often why advanced treatment is employed. However, it should be noted that subsequent monitoring should be conducted to determine if the target treatment goals are met. In one recent study (Harden and Chanton, 2010), field monitoring of STUs receiving advanced treatment effluent indicated that target treatment goals were not met while in another study (Wren et al., 2004) old retrofitted systems may not meet treatment goals. The importance of monitoring to ensure treatment goals have been met is equally important for conventional OWTS. Figure 3-7 illustrates nitrate-nitrogen concentrations in STE for reference.

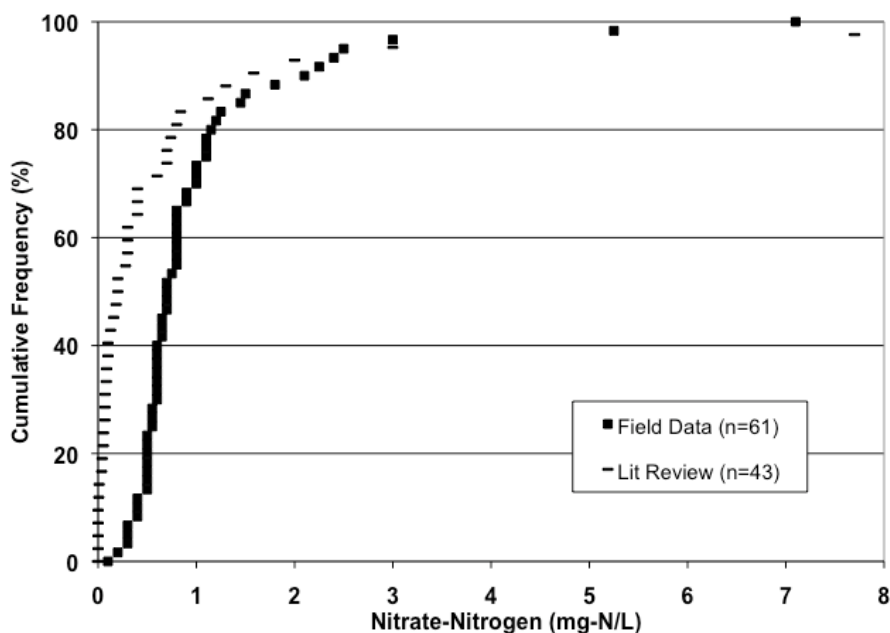


Figure 3-7. Nitrate-nitrogen Concentrations Measured in STE (adapted from Lowe et al., 2009).

3.1.3 Daily Flow

The estimated daily flow is a critical OWTS design parameter typically based on an estimated per capita occupancy of the bedrooms and some expected median per capita water use value. A conservative peak factor (e.g., 1.5 times the average design flow) is also often used to ensure performance during high flow periods. Such an approach may be required by local regulations, but may also lead to conservatively oversized tanks and STUs with associated additional costs. Understanding of actual interior water use may enable OWTS designers and decision makers to evaluate various potential designs and performance implications.

Daily water use from single sources is known vary significantly (Mayer et al., 1999; Anderson et al., 1993; Anderson and Siegrist, 1989; Brown and Caldwell, 1984; Lowe et al., 2009). A risk-based approach to estimation of daily flow can be utilized by using the CFD provided in Figure 3-8. For example, if a user plans for a maximum daily flow at the 50% cumulative frequency ($171 \text{ L capita}^{-1} \text{ d}^{-1}$) as measured in the field in 2008, they can be reasonably confident that the design will include half of the expected household flows (Lowe et al., 2009). By multiplying this median flow rate by an estimated household per capita such as 3, a daily household flow rate of 513 liters per day is estimated ($\sim 135 \text{ gpd}$). However, as the household occupancy increases, the average per capita water use declines due to common household activities such as washing clothes and dishes (Mayer et al., 1999). Alternatively, water conserving fixtures may suggest up to 20% or more water savings (Anderson et al., 1993; Anderson and Siegrist, 1989; Brown and Caldwell, 1984). In these cases (higher occupancy or water conserving fixtures), lower daily flows may be selected. However, OWTS designs are commonly based on expected bedroom occupancy of 2 persons per bedroom, and a 1.5 peaking factor. If a three bedroom house is assumed, this equates to a daily flow of 1539 liters per day or more than doubles the initial estimate above.

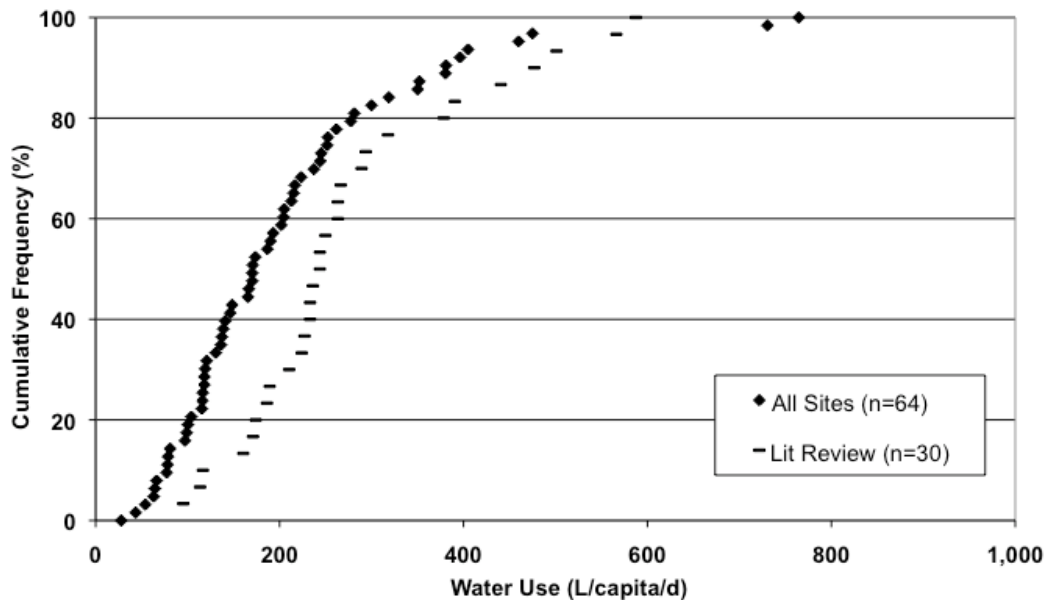


Figure 3-8. Measured Daily Indoor Flows (adapted from Lowe et al., 2009).

Comparison of measured daily flows in Figure 3-7 between the 2008 study (field data $n=64$) and the literature reported values (Lit Review $n=30$) suggests that indoor water use from single sources is less today than what has been previously reported in the literature (Lowe et al., 2007). Thus, a more conservative approach for estimating daily flow would be to use all values as reported in the literature. It is also interesting to note that observations during the 2008 field study suggested that daily flows were strongly correlated to the occupant's age and regional location. Specifically, occupants older than 65 had much greater water use and homes in the Western United States had higher water use compared to other regions.

A look-up table with statistical information provides additional guidance for estimating values that may not be easily interpreted from a CFD (Table 3-4). For example, a conservative estimate (i.e., an estimate reflecting a higher flow) would be to select the 75th percentile value of all reported flow values ($252 \text{ L capita}^{-1} \text{ d}^{-1}$) while a less conservative estimate (i.e., an estimate reflecting a lower flow) would be to select a regional 25th percentile value (e.g., $109 \text{ L capita}^{-1} \text{ d}^{-1}$ in the South). Table A-1 (Users Guide, Appendix A) summarizes this same information in units of gallons $\text{capita}^{-1} \text{ d}^{-1}$.

Table 3-4. Measured Indoor Daily Flow Summary Statistics ($\text{L capita}^{-1} \text{ d}^{-1}$) (adapted from Lowe et al., 2009).

Statistic	Literature	All Sites	Age		Mid-West	Region	
			Occupants >65	Occupants <65		South	West
n	30	64	40	24	20	24	20
Mean	278	207	148	297	207	184	234
Std Deviation	128	143	78	177	98	103	207
25 th Percentile	fill in	116	87	169	137	109	98
Median	244	171	137	248	173	171	154
75 th Percentile	fill in	252	196	381	235	226	254

3.1.4 Hydraulic Loading Rate

The HLR is one of the principle parameters key to STU performance. An estimation of HLR typically begins with a percolation test or textural analysis of the soil (U.S. EPA, 2002), assuming a specific daily flow of STE based on number of bedrooms, occupants and a peaking factor. Theoretically, a HLR can be as high as K_{sat} of the native soil. However, soil acceptance rates will decline over time even with the addition of potable water (Driscoll, 1987; Van Cuyk et al., 2005). The soil's ability to transmit water is only one aspect of HLR design, others include nutrient and organic loading associated with the effluent and treatment effectiveness. A high HLR results in high nutrient loading on the receiving soil.

The HLR is defined in units of length per time (e.g., cm d^{-1}), which is the same as volume per time over area (typically $\text{gallons ft}^{-2} \text{d}^{-1}$). The orthogonal shape of the trenches allows for a quick calculation of the HLR, where the volume per time is the expected daily flow from a residence (User's Guide, Section 3.1.3), and the area is the total area of the trench bottom:

$$\frac{\text{Daily_Flow} \left[\frac{L^3}{T} \right]}{\text{Area} [L^2]} = \text{HLR} \left[\frac{L}{T} \right] \quad (3.1.4-1)$$

where L is a length unit and T is a time unit. Varying the estimated daily flow or the trench area provides insight into the potential range of HLRs at a given site that may be reasonable while evaluating the associated nitrogen attenuation. The user may also want to consider peak flows in addition to estimated median daily flows.

Over the lifespan of the STU with formation of a biozone and/or clogging zone high HLRs are not advised (Siegrist, 2006). Instead it is recommended that the HLR does not exceed 10% of K_{sat} (Siegrist, 1987; Jenssen and Siegrist, 1990). A summary of select design HLRs (based on historical perspectives) with select design parameters that influence the HLR is provided in Table 3-5. Table A-3 (Users Guide, Appendix A) summarizes this same information in units of $\text{gallons ft}^{-2} \text{d}^{-1}$.

Table 3-5. Summary of HLR Used in STU Design.

Soil Texture	HLR used in OWTS design (cm d^{-1})					K (cm d^{-1})	
	Bouma, 1975	U.S. EPA, 1980	U.S. EPA, 2002	Siegrist, 2006	Radcliffe and West, 2009	K_{sat}	5% of K_{sat}
Sand	5	3.2-5	1.6-3.2	4	4.4	643	32
Loamy sand		3.2	1.6-3.2	4	3.7	105	5.2
Sandy loam	3	2.4	0.8-2.4	2	3.0	38	1.9
Loam		2	0.8-2.4		2.7	12	0.6
Silt loam	5	2	1.6-2.4	2	3.8	18	0.9
Silt					4.3	44	2.2
Sandy clay loam			0.8-1.6		2.0	13	0.6
Clay loam		0.8	0.8-1.6	0.5	2.0	8	0.4
Silty clay loam		0.8	0.8-1.6	0.5	2.8	11	0.6
Silty clay			0.8		1.9	10	0.5
Sandy clay			0.8		1.5	11	0.6
Clay	1		0.8		2.0	15	0.8
Notes:	Based on soil K-curves	Based on soil percolation test	Based on texture and structure, at $\text{BOD}=150 \text{ mg L}^{-1}$	Based on K_{sat} , soil class and effluent type, at $\text{BOD}=150 \text{ mg L}^{-1}$	Based on HYDRUS-2D and the Bouma Eqn.	Hydraulic conductivity is provided for reference. Soil texture specific K_{sat} values from Rosetta Database(Schaap et al., 2001)	

Of note, the soil's infiltrability is only one aspect of HLR design; the other is the organic loading associated with the effluent strength. When effluent is applied to a STU, oxygen demand is created by the microorganisms that breakdown the biodegradable materials in the wastewater. This oxygen demand must be satisfied by oxygen in the soil or the aerobic microorganisms cannot thrive. Anaerobic conditions are created when the applied oxygen demand exceeds what diffusion through the soil is able to supply (Otis, 1985; Erickson and Tyler, 2001). A high HLR forces a high organic loading on the receiving soil, which opens the way for anaerobic conditions, in which the utilization and degradation of organic matter by facultative and anaerobic microorganisms is much less efficient. Consequently, the accumulating waste materials and the metabolic by-products may cause soil clogging and loss of infiltrative capacity. The BOD in domestic STE can range significantly (Figure 3-3). Although a common BOD value used for OWTS design is 150 mg L⁻¹, recent work by Lowe et al., (2009) found the median BOD in domestic STE to be approximately 200 mg L⁻¹ as cBOD₅.

An understanding of the effluent quality is thus important when determining an appropriate design HLR and the user is advised to consider the potential for clogging. The HLR that can be sustained by the STU over long periods of time is referred to as and operationally defined as the long term acceptance rate (LTAR). The decision protocol in the Guidance Manual does not account for estimation of a LTAR; instead it is up to the user make informed decisions based on available information specific to their site. Table 3-6 provides a summary of the conditions to be considered when estimating the LTAR. The user is reminded that the expected treatment performance in STUs is directly correlated to the HLR, which is the one variable that can be adjusted (e.g., increase infiltration area for the same daily flow), unlike other variables that are cannot be manipulated such as soil texture, temperature, depth to water table, etc.

Table 3-6. Summary of Key Factors Influencing the LTAR and Design HLR Values (adapted from Siegrist, 2006).

Factors	Relative Importance	Attribute	LTAR	References
K _{sat} of natural soil	Minor-Moderate	Well-drained permeable soils (K _{sat} ~ 5- to 2,500 cm d ⁻¹)	Approaches 2 cm d ⁻¹	(Jenssen and Siegrist, 1990; Beal et al., 2005 and 2008)
Soil conditions	Moderate	High soil temp, low soil moisture, high aeration	Increased	(Siegrist et al., 2001)
Infiltrative surface	Moderate	Shallow narrow trenches, aggregate-free infiltrative surface	Increased	(Van Cuyk et al., 2001; Siegrist et al., 2004; Beach et al., 2005)
HLR	Major	High HLR → High mass loading	Decreased	(Siegrist, 1987; Siegrist and Boyle, 1987; Jenssen and Siegrist, 1990; Siegrist et al., 2001; Van Cuyk et al., 2005)
Effluent quality	Major	High strength effluent → High mass loading	Decreased	(Siegrist, 1988; Tyler and Converse, 1989; Van Cuyk et al., 2005)
Continuity of use	Major	Infrequent and/or intermittent with resting periods	Increased	(Siegrist et al., 2001)

Note: "→" should be read as "leads to".

When assessing the HLR, the method of application must also be considered. For the tools developed in this toolkit, two application methods were considered: "standard" trench design with continuous effluent delivery and drip dispersal. While many other approaches can be considered, differing geometries and dosed effluent application requires the use of more complex numerical models. Thus, the assumption of continuous, steady state infiltration results a pressure

profile or soil moisture profile that does not change with time and can be incorporated in simple tools. The nomographs, N-CALC and STUMOD are all based on continuous effluent delivery to trench systems. However, scenarios developed using HYDRUS-2D for select operational conditions illustrate drip dispersal system behavior (see Guidance Manual, Section 3.4.4 and/or Visual-Graphic Tools file).

Conventional trench systems are comprised of a network of trenches installed with a backhoe. Trench widths can range from with the trench bottom located 60-120 cm (2-4 feet) below ground surface. Advantages of trench systems include: 1) ease of installation, 2) robustness to wide range of daily flows including peak flows, and 3) low installation costs. Disadvantages of trench systems include: 1) construction impacts that effect infiltration such as embedment of gravel or compaction of the infiltrative surface, and 2) limitations of oxygen diffusion (e.g., large beds, deep trenches, etc.). Trench systems vary widely accommodating a wide range of effluent distributions, geometries, and porous media (U.S. EPA, 2002).

Drip systems are comprised of shallowly laid (typically 15-25 cm deep), small-diameter, flexible perforated pipes, similar to those used in drip irrigation. Advantages of drip dispersal includes: 1) shallow installation depths, 2) flexibility in design layout, and 3) uptake of nutrients. Disadvantages of drip systems include: 1) cost of operation (pumps required to pressurize the tubing length), and 2) maintenance to avoid clogging of the pipes and emitters. Drip dispersal systems have been installed in a range of climates with the greater concern for a system that is used on periodically over cold weather months allowing freezing within the systems.

Drip dispersal relies on flow-controlling orifices (emitters) which dictate a constant discharge rate out for a wide range of intra-pipe pressures. Because the discharge rate is fairly constant, the variation in HLR comes to play in the number of doses a system handles per day, and the duration of each dose. Typically, a system installed in a clay-rich soil will be programmed for more frequent shorter doses compared to a sandy soil that can accept less frequent longer doses. In addition, for a fixed daily flow, the optimum dosing regime (frequency and duration) can be achieved through the length of tubing installed (runs and zones). Additional guidance can be found at: <http://www.americanonsite.com/american/manuals/designguide1.html> and http://www.geoflow.com/design_w.html.

3.2 Parameters Relevant to Nitrogen Attenuation

The basis of nitrogen attenuation is that ammonium-nitrogen is converted to nitrate-nitrogen (nitrification) and nitrate-nitrogen is converted to nitrogen gas (denitrification). Other processes (e.g., ammonification, anammox) may affect nitrogen attenuation, but are not incorporated into the tools as either insufficient information was available or simplifying conditions could not be quantified. Nitrification requires somewhat aerobic conditions while denitrification requires anaerobic conditions. Both processes depend on the oxygen diffusion rates to and from nitrogen transformation sites compared to the kinetic uptake rate of oxygen. Thus for simple tool development, the transformations are a function of water content in the STU. The transformation rates are assumed to follow Monod kinetics, which allow the rate to be zero order at higher concentrations and first order at lower concentrations (see Chapters 1.0 and 2.0 in this User's Guide for additional information on nitrogen transformations and how they are incorporated into the spreadsheet models).

To use tools to estimate nitrogen attenuation, whether they are simple spreadsheet tools or numerical models, requires the selection of various parameters for sorption, nitrification and denitrification. A summary of the values reported in the literature for these parameters effecting nitrogen transformation is provided in Table 3-7. The references where these values were reported are provided in Table 3-8. The complete reference citation can be found in the References Section of the Guidance Manual.

Table 3-7. Nitrogen Transformation Parameters Reported in the Literature.

	Units	n	Mean	Standard Deviation	25 th Percentile	Median	75 th Percentile
Ammonium Sorption							
All soils	L kg ⁻¹	75	3.0	17.3	0.12	0.42	1.3
Clay-rich soil	L kg ⁻¹	9	2.5	2.7	0.21	1.46	7.1
Clay-poor soil	L kg ⁻¹	34	0.5	0.7	0.11	0.35	0.6
Nitrification Rates							
Zero-order	mg L ⁻¹ d ⁻¹	46	123	223	3.3	36	100
First-order	d ⁻¹	20	38	69	0.4	2.9	23
Maximum Nitrification Rates							
All soils	mg L ⁻¹ d ⁻¹	19	87	139	4.0	56	87
Denitrification Rates							
Zero-order	mg L ⁻¹ d ⁻¹	306	38	99	0.29	3.1	16.9
First-order	d ⁻¹	31	0.4	0.7	0.009	0.07	0.45
Maximum Denitrification Rates							
Sandy soil	mg L ⁻¹ d ⁻¹	168	12.3	50.6	0.16	1.8	7.8
Silty soil	mg L ⁻¹ d ⁻¹	58	84.9	141	0.26	11.7	107
Clayey soil	mg L ⁻¹ d ⁻¹	74	62.2	126	1.9	9.7	52

Note: Nitrification and denitrification zero- and first-order rates include all soils.

Table 3-8. Citations for Reported Nitrogen Transformation Parameters.

Nitrogen Attenuation Process	Literature Source
Sorption	Antonopoulos, 2001; Antonopoulos and Wyseure, 1998; Birkinshaw and Ewen, 2000; Booker et al., 1996; BGS, 2000; Buss et al., 2004; Butler et al., 2003; Ceazan et al., 1989; Chang and Donahue, 2007; Colley, 1991; Davison and Lerner, 1998; DeSimone and Howes, 1998; DeSimone and Howes, 1996; Dontsova et al., 2005; Buss et al., 2005; Buss et al., 2003; Erskine, 2000; Fernando et al., 2005; Fonstad, 2004; Hanson et al., 2006; Hongprayoon et al., 1991; Jackson, 1989; Jemison et al., 1994; Jenkins and Kemp, 1984; Kaluarachchi and Parker, 1988; Kunjikutty et al., 2007; Laima et al., 1999; Ling and El-Kadi, 1998; Lotse et al., 1992; Lumbanraja and Evangelou, 1994; Nommik and Vantras, 1982; van Raaphorst and Malschaert, 1996; Rao et al., 1984; Selim and Iskandar, 1981; Thornton et al., 2000; Thornton et al., 2001; Wang and Alva, 2000; Yamaguchi et al., 1996
Nitrification	Bollman and Conrad, 1998; Flowers and O'Callaghan, 1983; Garrido et al., 2000; Grant, 1995; Grundmann et al., 1995; Malhi and McGill, 1982; Müller et al., 2003; Schjonning et al., 2003; Sheibley et al., 2003; Stark and Firestone, 1995; Yamaguchi et al., 1996
Denitrification zero-order rates reported as M M ⁻¹ T ⁻¹ or M L ⁻³ T ⁻¹	Aulakh et al., 1991a; Aulakh et al., 2000a; Aulakh et al., 2000b; Bandibas et al., 1994; Bradley et al., 1992; Bateman and Baggs, 2005; Bollman and Conrad, 1997; Bremner and Shaw, 1958; Brettar and Höfle, 2002; Burford and Bremner, 1975; Cavigelli and Robertson, 2000; Christensen, 1980; Christensen and Tiedje, 1988; Cosandey et al., 2003; Craswell, 1974; Drury et al., 1991; Ekpete and Cornfield, 1964; Ekpete and Cornfield, 1965; Groffman and Tiedje, 1988; Günkör and Ünlö, 2005; Hall et al., 1998; Henault et al., 2001; Henrich and Haselwandter, 1997; Keeney et al., 1979; Maag and Vinther, 1996; McGarity, 1961; Powlson et al., 1988; Reddy et al., 1978; Saad and Conrad, 1993; Yamaguchi et al., 1990
Denitrification zero-order rates reported at M L ⁻² T ⁻¹	Aulakh et al., 1991; Avalakki et al., 1995a; Avalakki et al., 1995b; Barton et al., 1998; Clough et al., 1998; Davidson and Ståhl, 2000; de Klein and van Logtestijn, 1994; de Klein and van Logtestijn, 1996; Fedler et al., 2003; Groffman, 1984; Groffman and Tiedje, 1989a; Groffman and Tiedje, 1989; Henault et al., 2001; Hoffmann et al., 2000; Johns et al., 2004; Lowrance and Hubbard, 2001; Perez et al., 2003; Pinay et al., 1993; Ryden et al., 1987; Stanford et al., 1975a; Stanford et al., 1975; Vinther, 1992; Well and Myrold, 2002; Weier et al., 1993

3.2.1 Soil Temperature

Soil temperature has a direct effect on microbial activity, and thus plays an important role in nitrogen transformation processes as well as microorganism fate and transport. Nitrogen transformation rates generally increase with temperature to a maximum value at about 25°C, at which point they decline with continued increasing temperature (Malhi and McGill, 1982; Grundmann et al., 1995; Brady and Weil, 2002; Avrahami et al., 2003). Oxidation of ammonium ions by autotrophic bacteria is most efficient if the temperature is around 25°C compared to very inefficient (slow) in cold soil conditions. In contrast, denitrifying microbes adapt well to a range in temperature although the optimum temperature for denitrification is 25°C.

Because soil temperatures at depths relevant to OWTS (0.1 to 3 m below surface) can range between 3°C and 25°C (Brady and Weil, 2002), and the variation can be significant geographically, the average annual soil temperature in the regions of interest needs to be taken into account when determining treatment performance. Depending on treatment goals, it may be warranted to conduct a field assessment to obtain actual soil temperature recognizing that the soil temperature varies greatly between regions as well as seasonally. The average annual soil temperature in five different regions in the contiguous United States is provided to aid the user in selection of appropriate temperature conditions for a specific site.

Figure 3-9 illustrates the five different soil temperature regions in the contiguous United States. Soil temperatures are assigned by interpolation between stations or by extrapolation (User's Guide, Figure 1.3).

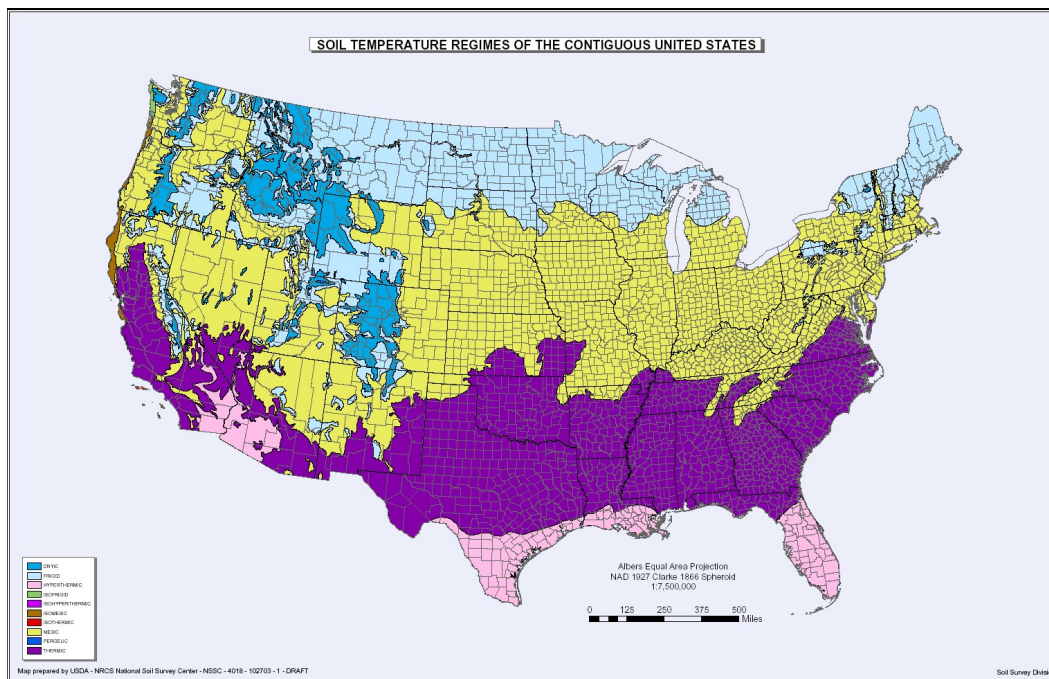


Figure 3-9. Average Soil Temperatures in the United States.

Used by permission from the USDA, http://soils.usda.gov/use/thematic/images/soil_temp_reg.jpg).

Table 3-9 presents the low and high annual averages and the overall annual mean temperature for each soil temperature regime (USDA, 1999). Because both “frigid” and “cryic” regions had the same annual mean soil temperature, the regions were combined into one region

for preparation of the nomographs, cumulative probability graphs and the spreadsheet tools N-CALC and STUMOD.

Table 3-9. Annual Average Temperatures (°C) by Climate Region.

Zone	Color	Annual Mean	Low	High
Hyperthermic		25.5	22	29
Thermic		18.5	15	22
Mesic		11.5	8	15
Frigid		4.5	0	8
Cryic		4.5	0	8

3.2.2 Ammonium Sorption Coefficient

Ammonium association with soils is an important process in nitrogen transformation. The sorption process is thought to be controlled by cation exchange processes, which depend on the ionic composition of the soil, as well as the ionic makeup of the effluent. To select an appropriate ammonium sorption coefficient (K_d), several factors should be considered including the concentration of ammonium-nitrogen and COD in the effluent, the CEC of the soil, the abundance of calcium (Ca^{2+}) and magnesium (Mg^{2+}) minerals, the abundance of clay minerals, and the WFP (Figure 3-10). As with all processes important for nitrogen attenuation, these ammonium sorption factors play a key role at both the macro and micro scale although the initial estimates are based on the general effluent quality and soil conditions. For example, the ammonium-nitrogen concentration is important at the soil pore space, but general estimates are based on the expected effluent quality applied to the soil.

It is likely that a combination of these factors illustrated in Figure 3-10 will attribute to the estimation of K_d with some factors suggesting high sorption capacity while other factors suggesting low sorption capacity at the site. General information on how these factors affect sorption is shown in Table 3-10. The user should have an understanding of these factors in combination with soil properties to select reasonable K_d values. Clearly, the more information that is available, the better the estimation will be of K_d for a specific site. Additional information on ammonium sorption can be found in Section 2.1.1 of this User's Guide.

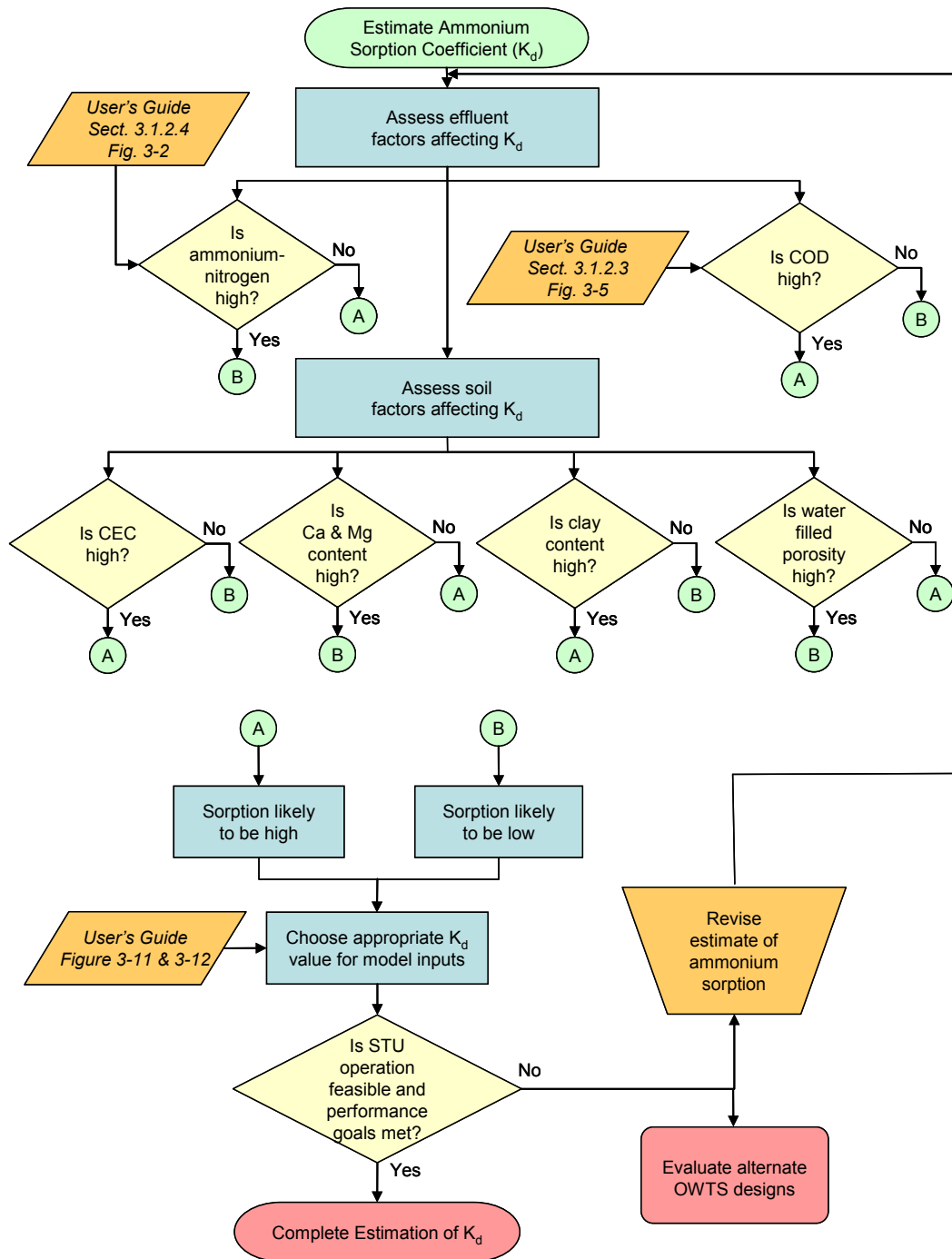


Figure 3-10. Decision Diagram for Estimating the Ammonium Sorption Coefficient.

Table 3-10. Summary of Factors Influencing Ammonium Sorption.

Factors	Units	Expected Field Condition	Resulting Ammonium Sorption
Ammonium-nitrogen concentration of the effluent	mg-N L ⁻¹	Low	High
		High	Low
Chemical oxygen demand of the effluent	mg L ⁻¹	Low	Low
		High	High
Cation exchange capacity of the soil	meq 100g ⁻¹	Low	Low
		High	High
Calcium and magnesium mineral content of the soil	mg L ⁻¹	Low	High
		High	Low
Clay content of the soil	relative %	Low	Low
		High	High
Water filled porosity of the soil	%	Low	High
		High	Low

A K_d value can be selected from the CFD (Figure 3-11) based on either the understanding of or assumptions for the key factors at the site (e.g., ammonium-nitrogen concentration, CEC, etc.). If little information is known, a median K_d value from the CFD may be a good starting point. If additional information is known, either a higher or lower K_d value can be selected.

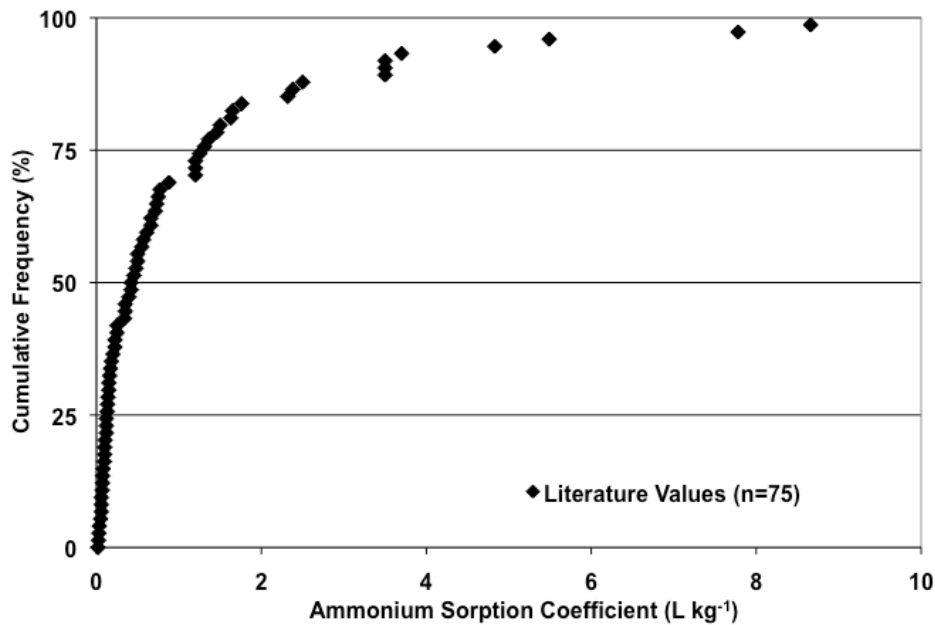


Figure 3-11. Cumulative Frequency Distribution of Ammonium Sorption Coefficient (K_d) Values as Reported in the Literature.

In the spreadsheet tools N-CALC and STUMOD, there are two sorption default values based on clay content described as clay-rich or clay-poor. After the soil texture at the site has been determined, the USDA soil triangle (User's Guide, Appendix A, Figure A-1) can be used to determine if the soil would be considered clay-rich or clay-poor. For example, if the soil of interest is a loam, then it is clear from the soil triangle that the soil has less than 30% clay and would be considered a clay-poor soil. In another example, if the soil of interest is sandy clay loam, the distinction is not quite as clear the textural class splits the clay-rich / clay-poor

division. In this case, if nitrogen attenuation is the treatment goal, additional information may be warranted. Figure 3-12 illustrates clay-rich and clay-poor K_d values reported in the literature.

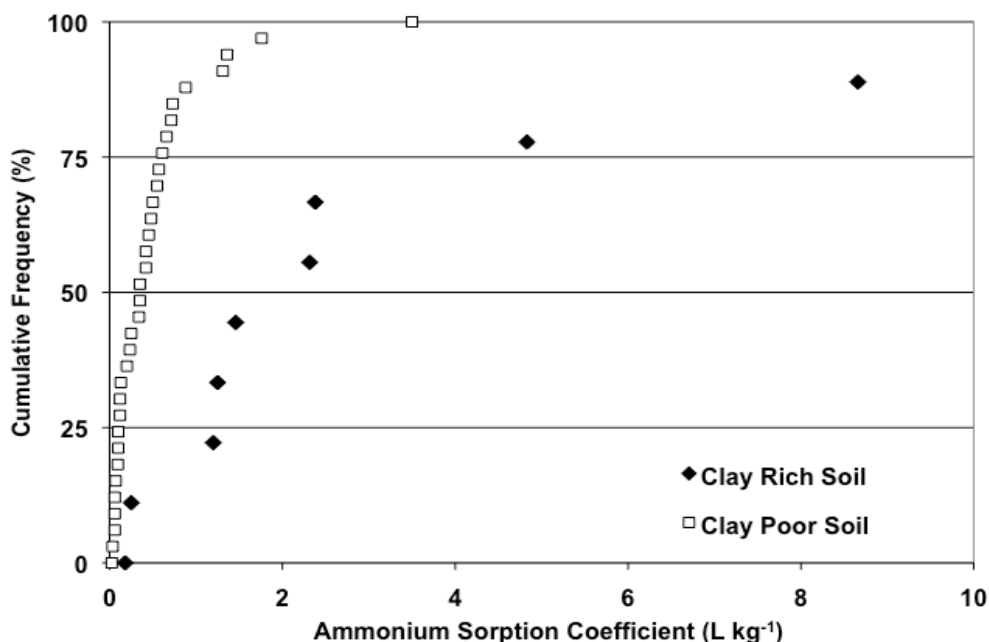


Figure 3-12. Cumulative Frequency Distribution of Ammonium Sorption Coefficient (K_d) Values for Clay-Rich versus Clay-Poor Soil as Reported in the Literature.

3.2.3 Nitrification Parameters

Nitrification is the process where ammonium ions are oxidized by autotrophic bacteria (bacteria that obtain their energy from CO_2 rather than organic matter). Because soil gas is known to have high concentrations of CO_2 (Jury and Horton, 2004), sufficient carbon and oxygen is assumed to exist for nitrification. This transformation process occurs relatively fast (e.g., $mg\ L^{-1}\ d^{-1}$) in the STU. To select appropriate nitrification parameters, several factors should be considered including the effluent pH, the effluent ratio of alkalinity to ammonium-nitrogen, the soil moisture content or WFP, and soil temperature (Figure 3-13). As with sorption processes important for nitrogen attenuation, these factors play a key role at both the macro and micro scale although the initial estimates are based on the general effluent quality and soil conditions. For example, the ratio of alkalinity to ammonium-nitrogen is important at the soil pore space, but general estimates are based on the expected effluent quality applied to the soil.

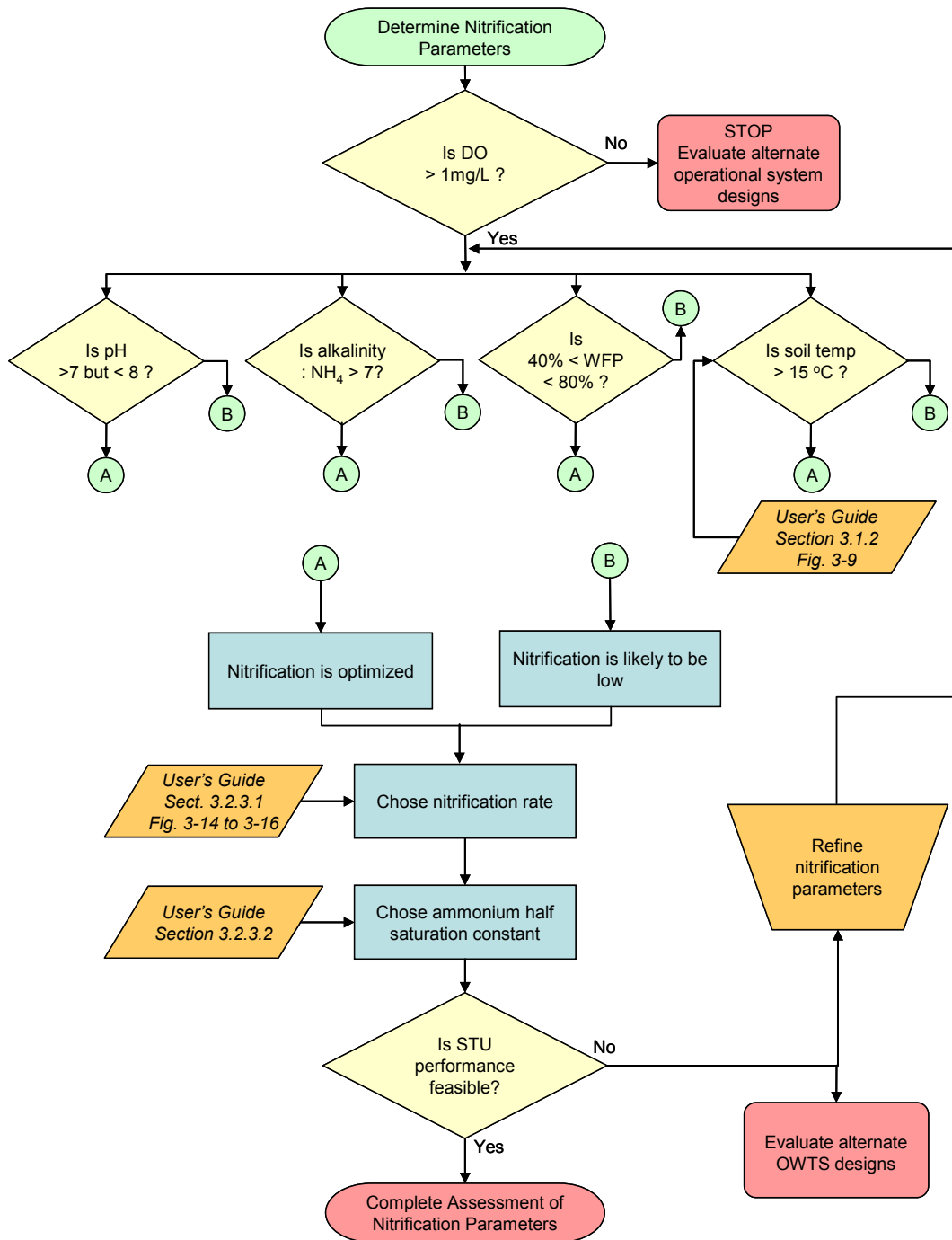


Figure 3-13. Decision Diagram for Determining Nitrification Parameters.

Each of these factors illustrated in Figure 3-13 ultimately impact the nitrifying microorganisms (*Nitrosomonas* and *Nitrobacter*) resulting in either higher or lower nitrification rates. The pH of the effluent will impact the magnitude of nitrification, as the nitrifying microbes are highly sensitive to low pH levels. Although the pH is normally at a level that is optimum for the microbes, low pH levels may be encountered. Sufficient alkalinity is required for nitrification, most of which is associated with the neutralization of the hydrogen ions released

during the nitrification process. If sufficient alkalinity is not available, the pH will decrease during the nitrification process resulting in decreased microbe growth rates (i.e., lower nitrification rates). For soils with high water content (i.e., soil moisture content or WFP), carbon availability to the microorganisms may be inhibited due to gas diffusion (specifically CO₂ diffusion). Finally, soil temperature also affects the rate of nitrification with optimum kinetics reported at temperatures of ~20-30°C.

It is likely that a combination of these factors will attribute to the estimation of nitrification in the STU with individual factors suggesting either more or less nitrification. General information on how these factors affect nitrification is shown in Table 3-11. The user should have an understanding of these factors in combination with soil properties to select reasonable nitrification values. Clearly, the more information that is available, the better the estimation will be for a specific site. Additional information on nitrification can be found in Sections 1.3 and 2.1.3 of this User's Guide.

Table 3-11. Summary of Factors Influencing Nitrification.

Factors	Units	Expected Field Condition	Resulting Effect on Nitrification
pH concentration of the effluent	-	<7	Decreased
		>7 but <8	Optimal
Alkalinity : ammonium-nitrogen ratio of the effluent	-	<7	Decreased
		>7	Optimal
Temperature of the soil	°C	5	Rate is ¼ of optimal
		15	Rate is ½ of optimal
		25	Optimal
		<40 or >80	Decreased
Water filled porosity of the soil	%	60	Optimal

3.2.3.1 Nitrification Rate

The rate in which nitrification occurs can be selected from a CFD based on either the understanding of or assumptions for the key factors at the site (e.g., soil temperature, WFP, etc.). The range in the reported nitrification rates was quite large (4 orders of magnitude), with a minimum value of 0.5 mg-N L⁻¹ d⁻¹, a maximum value of 574 mg-N L⁻¹ d⁻¹, and a median value of 56 mg-N L⁻¹ d⁻¹ (Figure 3-14). With such highly skewed data, the inner quartile range of 4 to 87 mg N L⁻¹ d⁻¹ better portrays the expected range of rates. If little information is known, a median value from the CFD may be a good starting point; however, either a higher or lower nitrification rate may be appropriate based on site conditions. In cases where pH is outside the optimum range, the maximum nitrification rate may be adjusted by multiplying it with a reduction factor (User's Guide, Section 1.3.1).

Based on the units required by individual tools, nitrification rates may be expressed as either zero- or first-order rates or a maximum rate may be required. The zero-order rate is independent of the initial ammonium-nitrogen concentration while a first order rate is dependent on the initial ammonium-nitrogen concentration. However, most enzyme-catalyzed biological reactions, such as nitrification, follow Monod kinetics where the reaction rate of is controlled by the availability of substrate or ammonium-nitrogen in the case of nitrification (User's Guide, Section 1.3.5). The CFD for reported zero-order nitrification rates is shown in Figure 3-14. The CFD for maximum reported zero-order nitrification rates is shown in Figure 3-15.

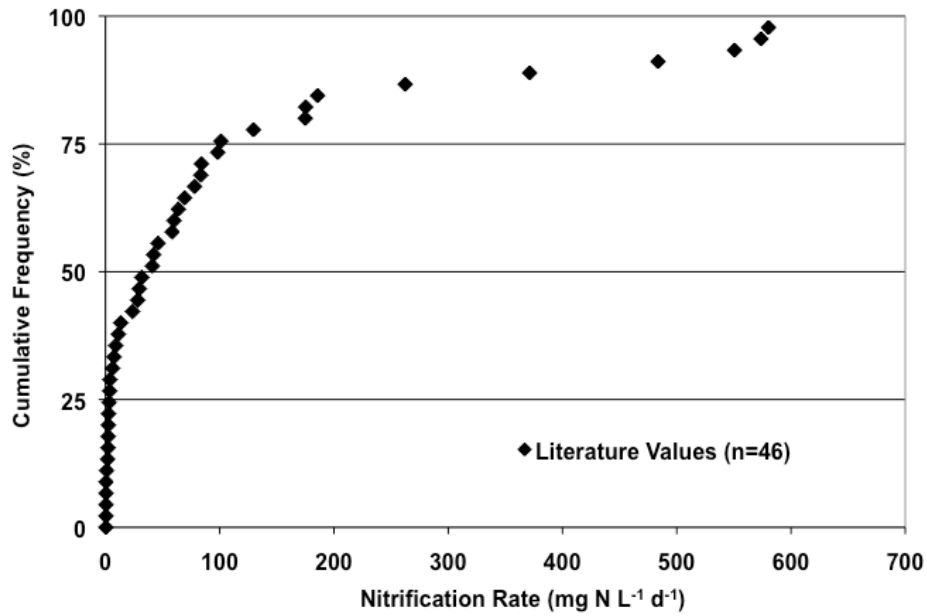


Figure 3-14. Zero-Order Nitrification Rates Reported in the Literature. Temperature Corrected to 25°C.

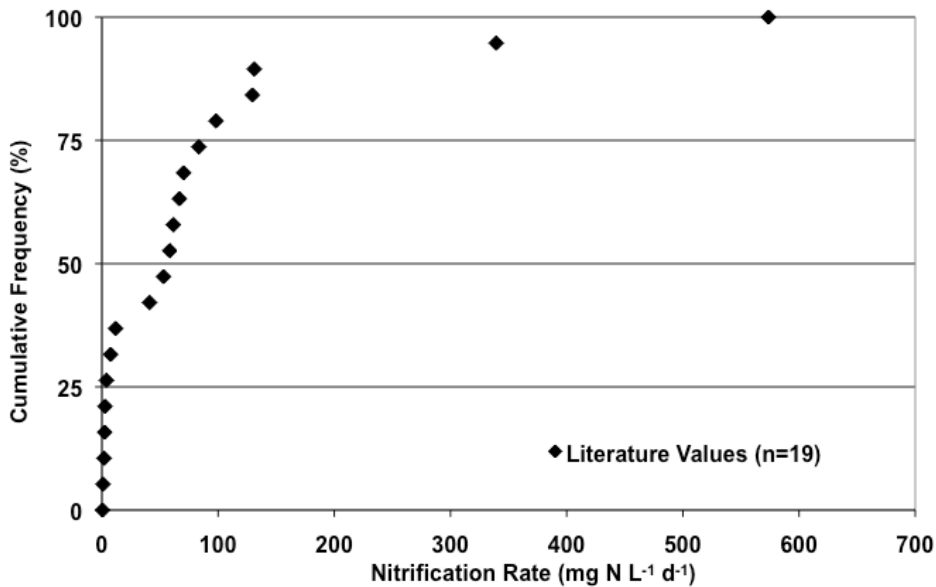


Figure 3-15. Maximum Zero-Order Nitrification Rates Reported in the Literature. Temperature Corrected to 25°C.

N-CALC uses first order nitrification rates (User's Guide, Section 2.3) and values should be selected from Figure 2-22. In contrast, STUMOD uses a Monod function to describe nitrification which allows the actual transformation rate to vary from zero- to first-order based on the half saturation constant of ammonium (User's Guide, equation 1.3.5-1). Because both STUMOD and HYDRUS incorporate Monod kinetics, the optimum nitrification rate (maximum

rate) is required to implement either tool (Figure 3-15). The user is also reminded that the nomographs were generated using STUMOD and the scenario illustrations were generated using HYDRUS-2D and thus incorporate use of the Monod function.

3.2.3.2 Half-Saturation Constant for Ammonium

The half-saturation constant for ammonium is the substrate (ammonium-nitrogen) concentration at which the microbial growth rate is half the maximum growth rate (User's Guide, Section 1.3.5). When Monod kinetics are used, the transition between zero-order (i.e., fixed regardless of concentration) and first-order (i.e., the reaction is faster as concentration increases) reactions is set by the half-saturation constant. Theoretical and physical evidence exist for both, but quantification of the different ranges is problematic. In short, use of a large half-saturation constant in a model will result in faster nitrification, because the maximum nitrification rate will be used for a wide range of concentrations. When a small half-saturation value for ammonium is used, one should expect slower nitrification. The bottom line is, the use of high half-saturation values will result in more removal of nitrogen in model output, because nitrate-nitrogen will be produced farther up in the soil profile and will be available earlier for denitrification.

Half-saturation constants for ammonium transformation (K_{m,NH_4}) generally range between 0.06 and 12 mg L⁻¹, with the majority of the values between 1 and 5 mg-N L⁻¹ (Table 3-12). These values essentially result in zero-order rates for relevant nitrogen concentrations in STUs (i.e., nitrogen concentrations above natural background of a few mg-N L⁻¹). A value of 5 mg L⁻¹ is the default value in STUMOD as it simulates zero-order reaction rates, but also because the numerical formulations were more stable when K_{m,NH_4} values were greater than 1. If the user has the technical expertise to determine a more appropriate value for the half-saturation constant, then such a value can be used in the spreadsheet tools.

Table 3-12. Summary of Half Saturation Constants for Ammonium Reported in the Literature.

Reported Value(s)	Units	Comment	Reference
1-180	µg/g	Assumed value range for modeling	Wang et al., 2005
3.1-6.1	mg N/L	Pilot scale experiments with wastewater	Kapagiannidis et al., 2006
7.2-12.6	mg N/L	Authors obtained constants from the literature	Jenkins and Kemp, 1984
0.5-25	mg N/L	Assumed value range for modeling	Langergraber, 2007
0.21	mg N/L	Reported in Sheibley et al., 2003	Stark and Firestone, 1996
0.7	mg N/L	Reported in Sheibley et al., 2003	Gee et al., 1990
0.76	mg N/L	Reported in Sheibley et al., 2003	Drtil et al., 1993
1.1	mg N/L	Reported in Sheibley et al., 2003	Knowles et al., 1965
1.1	mg N/L	Reported in Sheibley et al., 2003	McLaren, 1970
0.05	mg N/L	Calibrated value to 11°C	Choubert et al., 2005
0.04	mg/L	Adjusted to 20°C, it is unknown if the value is reported as nitrogen, experiments with wastewater	Poduska and Andrews, 1974
0.2	mg/L	Unknown if value is reported as nitrogen, experiments with wastewater	Downing et al., 1964
0.6	mg/L	Adjusted to 20°C, unknown if value is reported as nitrogen, experiments with wastewater	Gujer, 1977
1.0	mg/L	Unknown if value is reported as nitrogen, experiments with wastewater	Lijklema, 1973
1.5-4	mg N/L	Wastewater experiments	Goel and Gaudy, 1969
0.2-5.0	mg N/L	Reported in (Buss et al., 2004)	U.S. EPA, 1993
0.3-0.7	mg N/L	Wastewater	Henze et al., 2002

3.2.4 Denitrification Parameters

Denitrification is the reduction of nitrate-nitrogen to elemental nitrogen through an enzyme-catalyzed process by heterotrophic facultative anaerobic microbes (i.e., microbes that obtain their energy from an organic carbon source). The electrons needed typically originate from the microbial oxidation of organic carbon. Because the microbes responsible for denitrification are very tolerant and adaptable to environmental changes, the pH of the effluent is not of primary importance in the denitrification process. In fact, research has shown that pH has little influence on the process (Simek and Cooper, 2002).

To select appropriate denitrification parameters, several factors should be considered including the carbon to total nitrogen ratio in the effluent, soil texture, soil temperature, and the soil moisture content or WFP (Figure 3-16). As with other processes important for nitrogen attenuation, these factors play a key role at both the macro and micro scale although the initial estimates are based on the general effluent quality and soil conditions. For example, for denitrification to occur, the carbon to total nitrogen ratio is important at the soil pore scale, but initial estimates are based on the expected effluent quality applied to the soil.

A good measure of the availability of carbon for denitrification is the COD in the effluent (User's Guide, Sections 1.2.2 and 3.1.2.3). It is typically assumed that a COD:TN ratio greater than 4:1 is sufficient. The soil texture is an important factor as with finer textured soils the water retention in the pore spaces is increased which promotes anaerobic conditions resulting in higher denitrification. Similarly, for soils with high water content (i.e., soil moisture content or WFP), oxygen availability to the microorganisms is inhibited due to gas diffusion and anaerobic conditions are favored. Finally, soil temperature also affects the rate of nitrification with optimum kinetics reported at temperatures of ~20-30°C (Figure 2-8). It is likely that a combination of these factors will attribute to the estimation of denitrification in the STU with individual factors suggesting either more or less denitrification. General information on how these factors affect denitrification is shown in Table 3-13. The user should have an understanding of these factors in combination with soil properties to select reasonable denitrification values. Clearly, the more information that is available, the better the estimation will be for a specific site. Additional information on denitrification can be found in Sections 1.3 and 2.1.4 of this User's Guide.

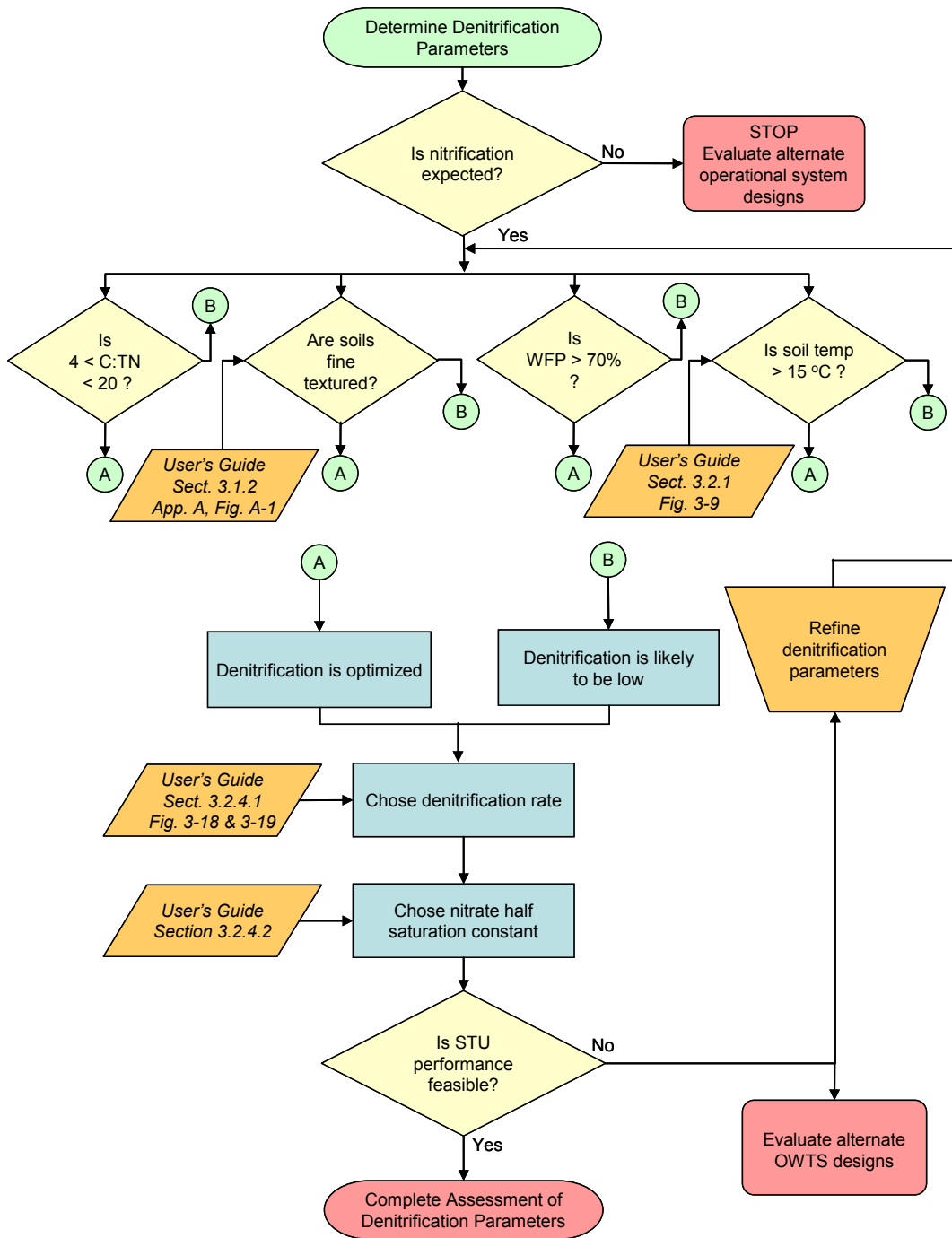


Figure 3-16. Decision Diagram for Determining Denitrification Parameters.

Table 3-13. Summary of Factors Influencing Denitrification.

Factors	Units	Expected Field Condition	Resulting Effect on Denitrification
Soil texture		Sandy	Low
		Silty	High
		Clayey	High
Soil temperature	°C	5	Rate ¼ of optimal
		15	Rate ½ of optimal
		25	Optimal
Water filled porosity	%	<70	Decreased
		>70	Optimal
Carbon : total nitrogen ratio		<4 as COD:TN	Decreased
		>4 as COD:TN	Optimal

3.2.4.1 Denitrification Rate

The rate in which denitrification occurs can be selected from a CFD based on either the understanding of or assumptions for the key factors at the site (e.g., soil temperature, WFP, etc.). Over 600 denitrification rates were identified in the literature (Figure 3-17) and while denitrification is known to follow both zero-order and first-order kinetics, only zero-order reaction data are presented here because the majority of the literature suggested the denitrification rate was not a function of nitrate concentration (Tucholke, 2007). If little information is known, a median value from the CFD may be a good starting point; however, either a higher or lower denitrification rate may be appropriate based on site conditions. Specifically, Tucholke (2007) found that the denitrification rates were strongly related to soil textural class. Three principal groups were identified that coincided with soil textural classes: 1) sandy soils – those with >50% sand content; 2) silty soils – those with >50% silt content; and 3) clayey soils – those with <50% sand and <50% silt content. The user should refer to the USDA soil texture triangle (User’s Guide, Appendix A, Figure A-1) as all clayey soils do not necessarily have high clay content. For example, a soil can have 45% sand, 45% silt and only 10% clay, while still falling into the clayey group. The CFD for reported zero-order denitrification rates by soil group is shown in Figure 3-18.

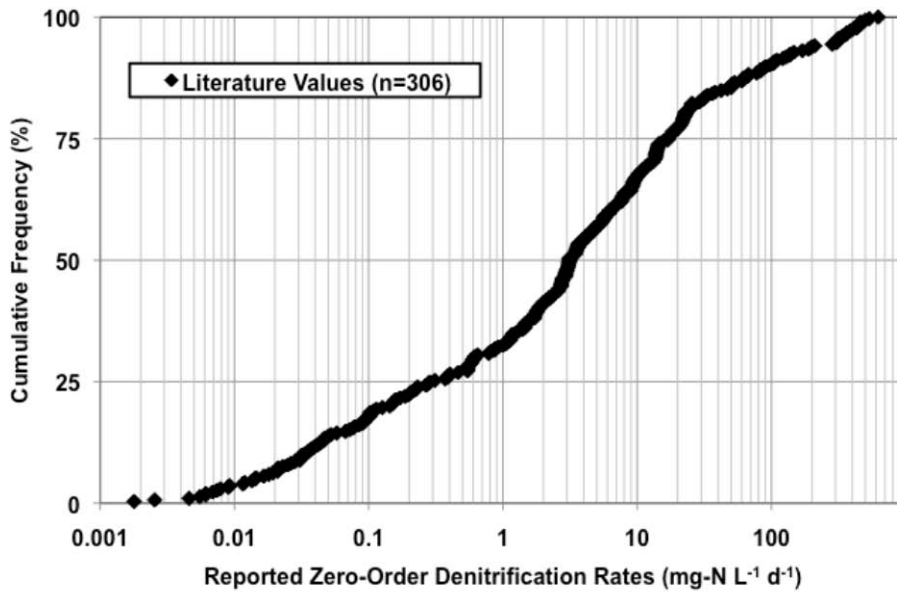


Figure 3-17. Zero-order Denitrification Rates Reported in the Literature (data from Tucholke, 2007).
Temperature corrected to 25°C.

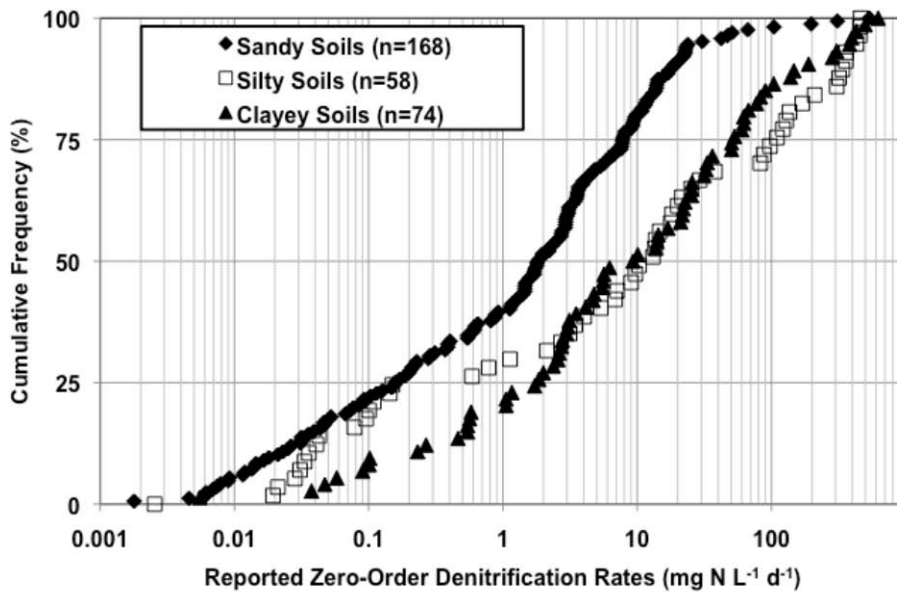


Figure 3-18. Zero-order Denitrification Rates for Three Different Soil Groups (data from Tucholke, 2007).
Temperature corrected to 25°C.

Similar to nitrification rates, the denitrification rate may be expressed as either zero- or first-order rates or a maximum rate may be required. Again, literature findings (McCray et al., 2005; Tucholke, 2007) suggest that denitrification rates are zero order at higher concentrations and first-order at lower concentrations. Thus, Monod kinetics were utilized when modeling nitrate-nitrogen transformations. However, as with nitrification, N-CALC uses first order

denitrification rates (User's Guide, Section 2.3) and values should be selected from Figure 2-23. In contrast, STUMOD uses a Monod function to describe denitrification which allows the actual transformation rate to vary from zero- to first-order based on the half saturation constant of nitrate-nitrogen (User's Guide, equation 1.3.5-1). Again, the user is reminded that the nomographs were generated using STUMOD and the scenario illustrations were generated using HYDRUS-2D and thus incorporate use of the Monod function.

3.2.4.2 Half-Saturation Constant for Nitrate

The half-saturation constant for nitrate is the substrate (nitrate-nitrogen) concentration at which the microbial growth rate is half the maximum growth rate (User's Guide, Section 1.3.5). When Monod kinetics are used, the transition between zero-order (i.e., fixed regardless of concentration) and first-order (i.e., the reaction is faster as concentration increases) reactions is set by the half-saturation constant. Use of a large half-saturation constant in a model will result in faster denitrification, because the maximum denitrification rate will be used for a wide range of concentrations. When a small half-saturation value for nitrate is used, one should expect slower denitrification. As with nitrification, again the bottom line is, the use of high half-saturation values will result in more removal of nitrogen in model output.

Half-saturation values for nitrate transformations (K_{m,NO_3}) based on actual measurements are sparsely reported in the literature, but have been found to range from 0.76 to 10 mg-N L⁻¹ (Table 3-14). It should be noted that both STUMOD and HYDRUS were unstable when using a half-saturation constant for nitrate of 1 mg-N L⁻¹ (division by low K_{m,NO_3} values resulted in high values in the calculation matrixes). A value of 5 mg-N L⁻¹ is the default value in STUMOD as it simulates zero-order reaction rates, but also because the numerical formulations were more stable when K_{m,NO_3} values were greater than 1. If the user has the technical expertise to determine a more appropriate value for the half-saturation constant, then such a value can be used in the spreadsheet tools.

Table 3-14. Summary of Half Saturation Constants for Nitrate Reported in the Literature.

Reported Value(s)	Units	Comment	Reference
1-60	mg /L	Assumed range for modeling, unknown if values are reported as nitrogen	Wang et al., 2005
<<<<1	mg N/L	Pilot scale experiments with wastewater	Kapagiannidis et al., 2006
4.06	mg N/L	Reported in (Sheibley et al., 2003)	Kohl et al., 1976
3.06	mg N/L	Reported in (Sheibley et al., 2003)	Messer and Brezonik, 1983
0.21-1.26	mg N/L	Reported in (Sheibley et al., 2003)	Maag et al., 1997
0.1-0.2	mg/L	Unknown if value is reported as nitrogen, experiments with wastewater	Christensen, 1977
0.1-0.2	mg/L	Unknown if value is reported as nitrogen	Engberg and Schroeder, 1975
0.76	mg N/L	Wastewater experiments	Abdul-Talib et al., 2002
10	mg/L	Assumed value for modeling, unknown if value is reported as nitrogen	Lotse et al., 1992
10	mg/L	Assumed value for modeling, unknown if value is reported as nitrogen	Kunjikutty et al., 2007
0.8-1.2	mg N/L	Wastewater	Henze et al., 2002
120-1400	μM	Conversion to concentration can only be made if soil properties are known	Klemetsson et al., 1991
130-2100	μM	Conversion to concentration can only be made if soil properties are known	Myrold and Tiedje, 1986

3.3 Parameters Relevant to Microorganism Attenuation

Key parameters for microorganism attenuation include but are not limited to, gaining a clear understanding of the soil properties (e.g., texture, STU profile depth, WFP), operational conditions (e.g., biozone formation, HLR), and effluent quality characteristics (e.g., bacteria, virus, pH). Additional information is also important for attenuation of specific microorganisms in the STU including temperature, filtration, organic matter content, microorganism type, attachment/detachment rates, inactivation, and microbial activity including the presence of other microorganisms. Specific simple tools could not be developed to address microorganism attenuation in the STU because the attenuation relies on difficult to obtain field parameters. However, mathematical models in combination with direct observation can be useful for the quantitative assessment of microbial transport and fate in the STU. The information presented here is intended to aid the user in choosing the best possible simplifying assumptions. Detailed information and results from laboratory studies are provided in Appendix D of this User's Guide. As with other parameters important for estimating STU performance, understanding of the factors affecting microorganism attenuation and better estimations of STU performance is directly linked to the initial information available and understanding for a specific site. Additional information on microbial attenuation can be found in Section 1.4 of this User's Guide and the supplemental literature review (McCray et al., 2008).

3.3.1 Virus

Human viruses are not part of the normal fecal flora, but occur in infected persons between 10^6 and 10^{10} viral particles per gram of feces (Kowal, 1982; Feachem et al., 1983). Removal of viruses in the STU is mainly attributed to removal/inactivation through adsorption (i.e., pH, soil mineralogy, and presence of organic matter), extent of water saturation (i.e., WFP or soil saturation), and the particular strain of virus. The inactivation rate of a virus, which depends on the strain of virus, is considered the single most important parameter in attenuation of virus. Adsorption of the virus to the soil is more efficient when the pH of the soil is below the isoelectric point (pI) of the virus. Alternatively high fractions of colloidal and soluble organic material may compete with viruses for adsorption on clay particles. Soil saturation is also important for virus removal with unsaturated conditions favorable due to more contact of virus particles with soil particle surfaces or to partitioning of the virus to the air-water interface. Data reported in the literature show that neither texture nor depth of soil, which may be important for the removal of larger particles, correlate particularly well with virus removal (McCray et al., 2008). However, soil texture and structure will influence virus attenuation with finer soil textures and/or less structured soils increasing the expected virus removal.

General factors that affect virus attenuation in the STU are summarized in Table 3-15. A combination of these factors will attribute to virus attenuation in the STU with individual factors suggesting either more or less attenuation. Because the range and interaction of factors controlling virus attenuation is diverse, it is difficult to pinpoint which factors are most important. In addition, these factors play a key role at both the macro and micro scale although the initial estimates are based on the general effluent quality and soil conditions.

Table 3-15. Summary of Factors Influencing the Magnitude of Virus Removal.

Factors	Expected Field Condition	Resulting Virus Attenuation
pH of the effluent	pH >> 7	Decreased
	pH << 7	Decreased
	pH > pI *	Decreased
Soil mineralogy	Clay > 15%	Increased
	Low Ca ²⁺ & Mg ²⁺	Increased
Amount of organic matter in the STU **	Low	Increased
	High	Decreased
Soil saturation	Unsaturated	Increased
	Saturated	Decreased

* Isoelectric point (pI) of the virus

** Dissolved and colloidal organic matter

Figure 3-19 illustrates virus removal in STUs based on values reported in the literature. The assimilated data includes results from several different soil depths and in soils with different texture. The CFD suggests that 60% of the time there is greater than 1-log removal (again, independent of soil texture or depth). However, it is important that this data be taken in context with infectious dose (i.e., as low as 1 organism) and the potential public health risk as STUs may be expected to achieve 6-log (99.9999%) virus removals.

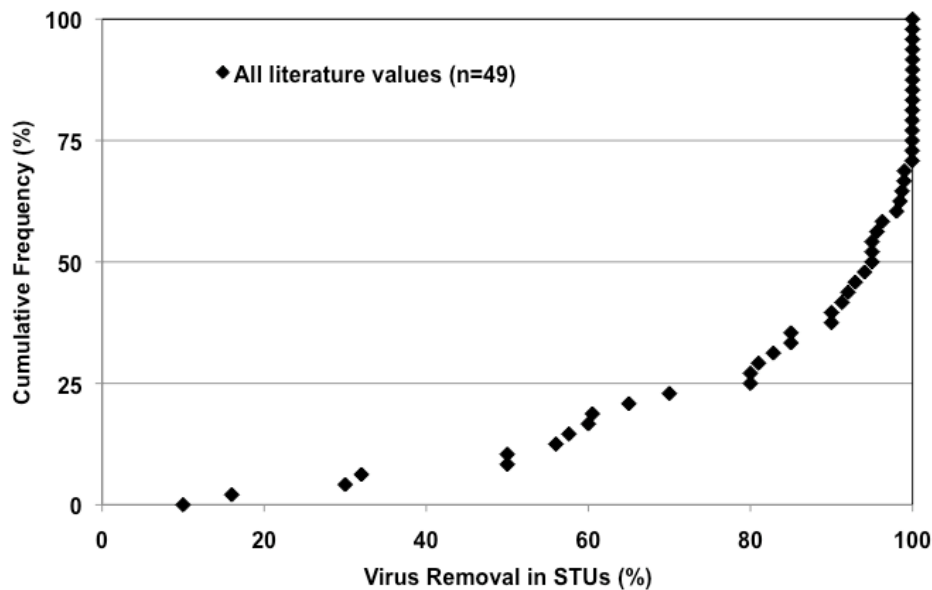


Figure 3-19. Virus Removal as Reported in the Literature.

3.3.2 Bacteria

There are about 10¹³ bacteria in the human digestive tract, with members from 500 to 1000 species present (Sears, 2005). The infectious dose for bacterial species covers a wide range, but infections can be caused by as few as 10 cells. Important factors for bacteria attenuation in the STU include mechanical filtration (i.e., soil texture, soil depth profile, biozone/biomas formation), adsorption (i.e., WFP or soil saturation), and predation resulting from adverse

temperatures or the inability to compete with indigenous bacteria. Filtration within the biomat and/or in the underlying unsaturated zone plays an important role in the removal of bacteria due to the comparatively greater size of bacteria (compared to virus). Filtration is affected by the soil texture and depth. Coarser textured soils are much less efficient at removing bacteria than finer textured soils; however, the depth of unsaturated soil is more important. Adsorption is primarily influenced by soil saturation (which may be controlled through HLR) with unsaturated soils increasing bacteria attenuation due to increased soil retention time and contact. Soil saturation may be controlled by HLR with lower HLRs promoting unsaturated conditions and increasing the expected bacteria removal.

General factors that affect bacteria attenuation in the STU are summarized in Table 3-16. Again, it is likely that a combination of these factors will attribute to bacteria attenuation in the STU with individual factors suggesting either more or less attenuation. In addition, these factors play a key role at both the macro and micro scale although the initial estimates are based on general soil conditions.

Table 3-16. Summary of Factors Influencing the Magnitude of Bacteria Removal.

Factors	Expected Field Condition	Resulting Bacteria Attenuation
Soil texture	Fine	Increased
	Coarse	Decreased
Depth of STU soil profile	Deep (>60cm)	Increased
	Shallow (<30cm)	Decreased
Soil saturation	Unsaturated	Increased
	Saturated	Decreased
Biozone formation	Biomat present	Increased
	Biomat not present	Decreased

Figure 3-20 illustrates fecal coliform concentrations in STE while Figure 3-21 illustrates total bacteria removal in STUs based on values reported in the literature. Much of the current understanding of bacteria in STU soils stems from studies using fecal coliforms, *E. coli*, and fecal enterococci. These organisms are used as indicators of human fecal contamination in ground and surface waters, but because bacterial species vary widely in their ecology and physicochemical properties, the fate of these organisms is likely not representative of all enteropathogenic bacteria found in STE.

The assimilated data in Figure 3-21 includes results from different organisms, soil depths and soils textures. No removal values of less than 60% were reported in the literature, while 46 reported values were greater than 1-log removal, 31 reported values were greater than 2-log removal, and 21 of the reported values were greater than 3-log removal (total number of reported values = 55), independent of soil texture or depth. Although seemingly small, the differences in removal rates can translate into large differences in bacterial numbers because they are often present in STE at high concentrations. For example, Figure 3-20 illustrates of the presence of 10^3 - 10^8 fecal coliforms per 100 mL of STE. At the higher occurrence of fecal coliforms, a removal rate of 99% would still leave up to 10^6 per 100 mL. In comparison, the EPA's National Primary Drinking Water Standards call for a maximum contaminant level goal for fecal coliforms of zero per 100 mL (U.S. EPA, 2008).

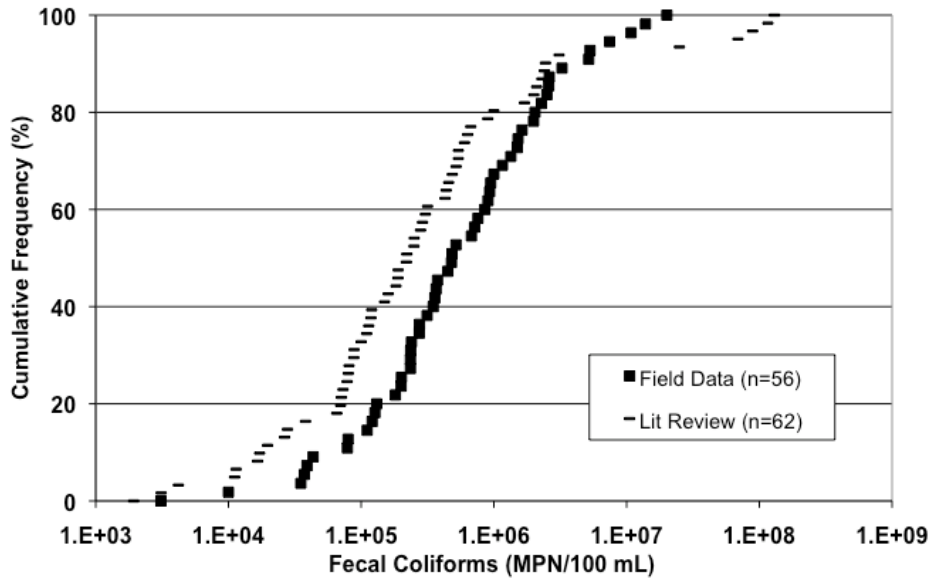


Figure 3-20. Fecal Coliforms in STE as Reported in the Literature (adapted from Lowe et al., 2009).

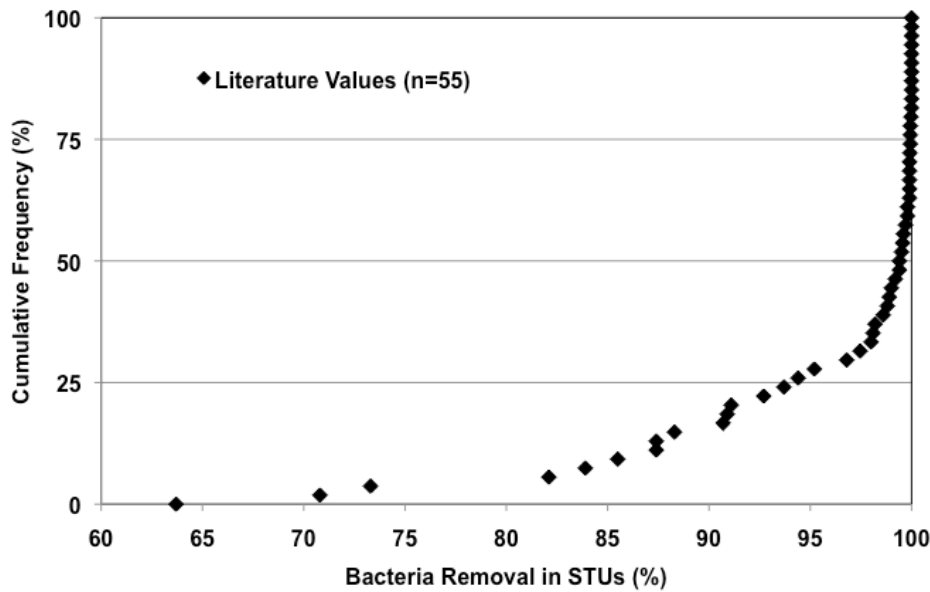


Figure 3-21. Bacteria Removal as Reported in the Literature.
Removals <60% Where Not Reported.

3.4 Parameters Relevant to OWC Attenuation

Key factors for OWC attenuation include but are not limited to, the target compound or class of compounds, compound properties affecting fate and transport, and potential treatment limitations. For specific OWCs of interest, additional information such as partitioning coefficients, organic carbon content, degradation rates, sorption, etc. will be important for

assessing OWC attenuation in STUs (Table 3-17). Specific simple tools could not be developed to address OWC attenuation in the STU because of the wide range of OWC compounds and the corresponding limited information available related to removal mechanisms in the soil. As with other parameters important for estimating STU performance, understanding of the factors affecting OWC attenuation is directly linked to the initial information available and understanding for a specific site. Additional information on OWC attenuation can be found in the supplemental literature review (McCray et al., 2008) and Higgins et al., 2010.

The information presented here is intended to walk the user through the process of choosing the best possible simplifying assumptions. Due to the wide array of compounds, five OWCs were selected based on the assessment of the compounds that are most likely to be associated with environmental implications and most likely to be regulated, and represent the diversity of compounds considered OWCs (Table 3-17).

Table 3-17. Characteristics for Selected OWCs.

Compound	Class	Toxicity/Risk	Persistence in Environment	Appearance in Onsite Wastewater
Diclofenac	analgesic	high	high	moderate
Triclosan	antimicrobial	high	moderate	very high
1,4-dichlorobenzene	deodorant	high	moderate	high
17- β estradiol	hormone	high	high	moderate
Estrone	hormone	high	moderate	moderate

3.4.1 OWC Compounds

OWC are often grouped into compound classes based on their function (e.g., antibiotics, surfactants, personal care products, etc.). However, grouping compounds in this basis does not account for similarities or differences in STU treatment characteristics. In addition, many compounds (detergents, antimicrobials) are ubiquitous in onsite wastewater effluents, while the appearance of some compounds (such as pharmaceutical drugs) may depend on specific activities or residents contributing to the wastewater effluent. Because of the wide variety of OWCs expected in onsite wastewater (i.e., STE), four common groupings based on treatment considerations are: 1) detergent/surfactant metabolites; 2) reproductive hormones; 3) phenolic antimicrobials; and 4) acid pharmaceutical compounds (Table 3-18).

Table 3-18. OWC Groups and Examples of Common Contaminants.

Surfactant Metabolites	Reproductive Hormones	Acid OWCs	Phenolic Antimicrobials
Nonylphenols	Estrone	NSAIDs	Triclosan
Nonylphenol Ethoxylates	17 β -Estradiol	Salicylic acid	Triclocarbon
	17 α -Ethinylestradiol	Gemfibrozil	
	Estriol	Diclofenac	

3.4.2 Fate and Transport Parameters

Fate and transport mechanisms important for OWCs attenuation include biodegradation, sorption, and abiotic degradation. The relative importance of these mechanisms is dependent on the specific OWC. Little research has targeted the investigation of the fate and transport parameters for many pertinent OWC compounds in soil environments, and no information is currently available for actual removal rates of these compounds in various soils or STU conditions. Some studies have investigated the phase partitioning coefficients and degradation rate constants in selected scenarios, but characterization of these mechanistic constants is

currently insufficient for estimating treatment efficiencies in a variety of scenarios. Thus, estimating treatment efficiencies for a specific system involves a high degree of uncertainty and general knowledge of fate and transport behaviors can be best used to identify STU scenarios where treatment may be insufficient or where additional treatment options may be warranted. The best currently available information on fate and transport parameters for OWC treatment in STUs is summarized in (Table 3-19). As research of the behavior of OWCs advances, improved estimations of the removal rates of these compounds may be attained using sorption and degradation constants.

Table 3-19. Summary of Fate and Transport Properties for Four Different OWC Groups.

Fate & Transport Property	Surfactant/Detergent Metabolites	Reproductive Hormones	Acid OWCs	Phenolic Antimicrobials
Sorption to organic carbon in soil	Significant	Possible	Wastewater pH dependent	Significant
Plant uptake	Observed	Possible	Possible	Observed
Photodegradation	Not observed	Not observed	Observed for select compounds	Observed for select compounds
Aerobic Biodegradation	Significant	Possible	Possible	Significant
Anaerobic Biodegradation	Observed*	Not observed	Not observed	Not significant

* Observed when 1/2 life is approximately 10x corresponding aerobic 1/2 life

3.4.2.1 Estimation of the Relevant Transformation Parameters

Little research has targeted the fate and transport parameters for many pertinent OWCs in soil systems. However, it may be possible to estimate (with some uncertainty) the expected contaminant removal with an appropriate conceptual model for the fate and transport of OWC compounds in soil. For example, using partitioning coefficients, sorption rate coefficients and degradation rate constants, allows for assessment of certain processes as well as estimation of removal rates, although other processes may also affect OWC attenuation. This approach provides a more detailed estimation of treatment of a specific OWC or group of OWCs with minimal additional research requirements.

For example, to estimate the sorption coefficient (K_d), while maximizing the use of current information, it is first necessary to characterize the non-reactive solute fate and transport in system in terms of maximum concentration at point of interest and retention time. Second, it is necessary to characterize OWC in terms of K_d and 1st order degradation rate. In this example, the transport characteristics of a non-reactive solute are adjusted according to the effects of sorption and 1st order degradation.

Figure 3-22 relates K_d values to the effect on retention time (RT) and maximum concentration (C_{max}) for three biodegradation rates according to the Richards' equation (Richards, 1931) for saturated-unsaturated water flow and advection dispersion equations based on Fick's law for the transport of solutes. The model is used to simulate the unsaturated soil hydraulic properties of vadose zone gravity and capillary force driven transport (Šimůnek, 1998). The relationships illustrated in Figure 3-22, are then used to modify the fate and transport characteristics (C_{max} and RT) according to the transport parameters (K_d and biodegradation half life) of an OWC. Specifically, the known retention time of a tracer can be multiplied by RT/RT_{tracer} to estimate the retention time of an OWC. Likewise, the maximum concentration of a tracer can be multiplied by $C_{max}/C_{max-tracer}$ to estimate the maximum concentration of an OWC.

Finally it should be noted that current K_d information may be insufficient to use this approach without additional investigation for all OWCs based the current status of knowledge.

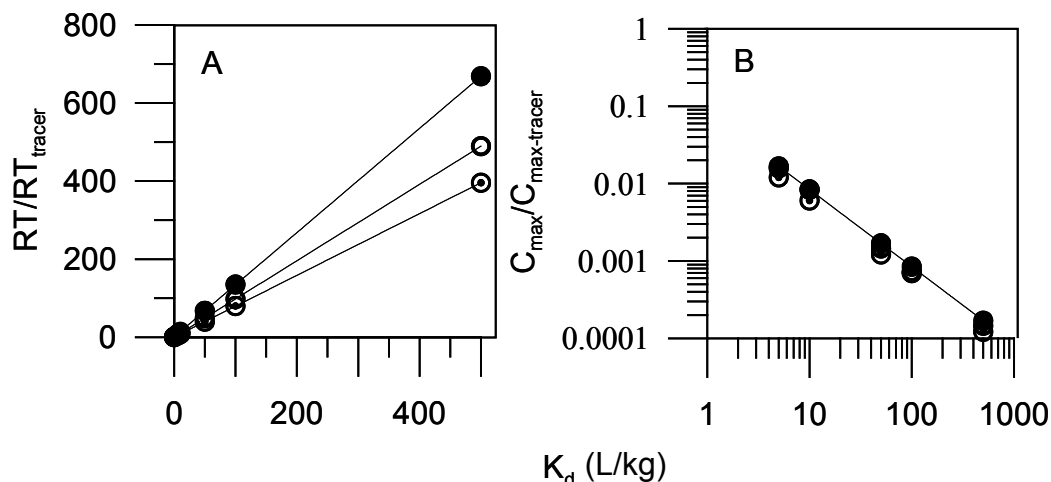


Figure 3-22. Fate and Transport Dependence on K_d Value.

A: Retention time (RT), normalized by the retention time of a non-reactive solute (RT_{tracer}) against K_d .

B: Maximum solute concentration (C_{max}) normalized by maximum solute concentration for a non-reactive solute ($C_{\text{max-tracer}}$) against K_d .

Three different solute half lives were included in simulations; ● = no degradation, ● = 1/2 life of 5 days, ⊖ = 1/2 life of 2 days.

3.4.2.2 Parameter Estimation Example: Estrogenic Hormones

The first step for estrogenic hormones (estrone, 17β -estradiol, and 17α -ethynylestradiol) is to estimate K_d based on the relationship of a range of K_d values to soil organic carbon content (Figure 3-23). Ideally, this range (defined by 95% confidence intervals for a linear regression) incorporates the variability associated with addition soil and solution characteristics by involving a number of various experimentally determined K_d values while not accounting for the variability or effect of soil characteristics other than the f_{oc} . In Figure 3-23, K_d values from this study and literature for estrone, 17β -estradiol, and 17α -ethynylestradiol are combined under the assumption that these chemicals, being similar in structure, demonstrate similar sorption characteristics. A regression was then fit between the K_d values and corresponding f_{oc} values and 95 and 99% confidence intervals displayed. This initial range provides a realistic indication of the effect of sorption on retardation of OWCs during infiltration without requiring extensive batch studies to characterize K_d values for variety of soil conditions.

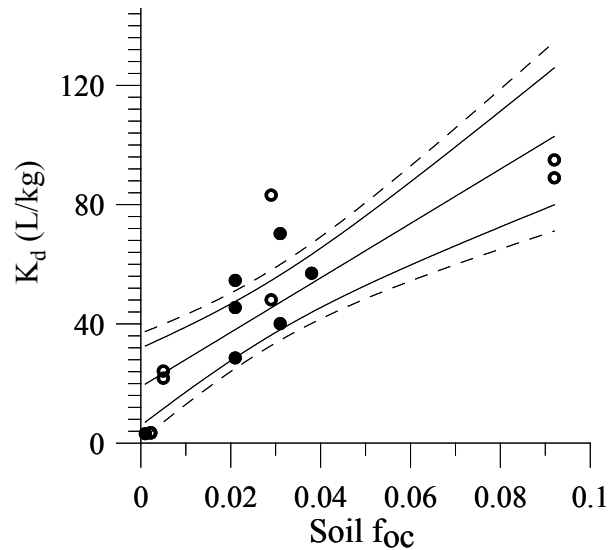


Figure 3-23. K_d Values for Estrogenic Hormones for Associated Fraction of Soil Organic Carbon. Isotherms with <20% variability from this study are denoted by solid data points. Literature reported values are denoted by open data points (estrone, 17 β -estradiol, and 17 α -ethynylestradiol) (Das et al., 2004; Ying et al., 2003). Middle solid line is the linear regression fit along with 95 (dashed lines) and 99% (outer solid lines) confidence intervals.

The second step is to estimate the half-life of the OWC. Again, few studies have investigated the biodegradation of estrogenic hormones in soil. However, Das et al. (2004) reported an average half-life of 2.0 days (+/- 2.6 standard deviation) for a variety of soil types. Ying et al. (2003) also estimated a half-life of two days while others have estimated half-lives between two and six days for estrogenic hormones. Considering this data, a degradation rate that corresponds with a half-life that ranges between two and six days may most appropriate. Using a value on the low end of this range may incorporate more risk (less OWC attenuation) into a treatment scenario than using a value on the high end of this range. Referring back to Figure 3-22, the relationship between C_{max} and $C_{max-tracer}$ can be considered for conditions of no biodegradation, biodegradation with a two-day half-life, and biodegradation with a five-day half-life.

3.4.3 Treatment Limitations

Published laboratory studies identify various mechanisms that aid in the removal of OWCs from infiltrating water in STUs. These include abiotic degradation, biodegradation, and sorption to solids (Heberer, 2002) (Boyd et al., 2003; Daughton and Ternes, 1999). Based on the characteristics of the different types of OWCs (Table 3-19), conditions that may limit the amount of treatment achieved by these mechanisms can be identified. For example, treatment limiting conditions include: 1) shallow depth to water table or confining layer; 2) low organic carbon content in soil; 3) anoxic soil conditions; 4) and high pH in the effluent. General factors important to OWC attenuation in STUs of these compounds are summarized in Table 3-20.

Table 3-20. Summary of Factors Influencing OWC Removal.

Factors	Expected Field Condition	Resulting OWC Attenuation
Unsaturated soil depth of STU	Shallow	Decreased
	Deep	Optimal
Amount of organic carbon in the STU	Low	Decreased
	High	Optimal
Amount of oxygen in the STU	Anaerobic	Decreased
	Aerobic	Optimal
Acid dissociation constant (pKa) of the OWC	pKa < pH	Decreased
	pKa > pH	Increased

3.4.3.1 Shallow Depth to Groundwater or Confining Layer Conditions

To ensure adequate soil treatment, the retention time of compounds in the unsaturated zone should be maximized. Ideally, greater unsaturated soil depths will maximize the retention time of the OWC enhancing treatment (e.g., degradation). A shallow depth to groundwater or confining layer is expected to be a most important issue in soils with low organic carbon content in combination with OWCs that do not strongly sorb. This may also be an issue for soils that drain relatively quickly.

3.4.3.2 Low Organic Carbon Content Conditions

Many organic compounds sorb strongly to the organic carbon in soil (Lee et al., 2003; Das et al., 2004; Yu et al., 2004; Duering et al., 2002). If sorption is irreversible, it can be considered as removal of the compound from the aqueous phase. If sorption is reversible, treatment may be enhanced because the retention time in the unsaturated zone is increased, thus allowing for increased degradation. Low organic carbon content is most limiting in STUs with shallow soil profile. High organic carbon contents in the biozone may provide potential organic carbon sorption sites with live and/or deceased cellular material (Siegrist, 1987; McKinley, 2008).

3.4.3.3 Anoxic Soil Conditions

Laboratory studies have demonstrated the ability of many of OWCs to biodegrade aerobically (Shah et al., 2001; Das et al., 2004; Ying and Kookana, 2007; Lucas and Jones, 2006; Zwiener and Frimmel, 2003). Some OWCs have been shown to be capable of anaerobic biodegradation at much lower rates than for aerobic conditions (Joss et al., 2006; Ying and Kookana, 2007). Anoxic conditions in the soil may be promoted by operational conditions (e.g., high HLRs, effluent application method). Site conditions, such as fine textured soils or poorly draining soil, may also contribute to anoxic soil conditions.

3.4.3.4 High pH Conditions

High pH effluent may affect the ability of acidic compounds to sorb to soil particles. The acid dissociation constant (pKa) of a compound can be used to assess whether a compound may be affected by pH. If the pKa of a compound is below the pH of the wastewater, sorption may be inhibited for the compound (Hari et al., 2005).

3.4.3.5 Additional Treatment Considerations

Considering the fate and transport processes of the OWC compound groups, additional treatment options may improve treatment for STUs with known limiting conditions. Table 3-21 summarizes some potential treatment options.

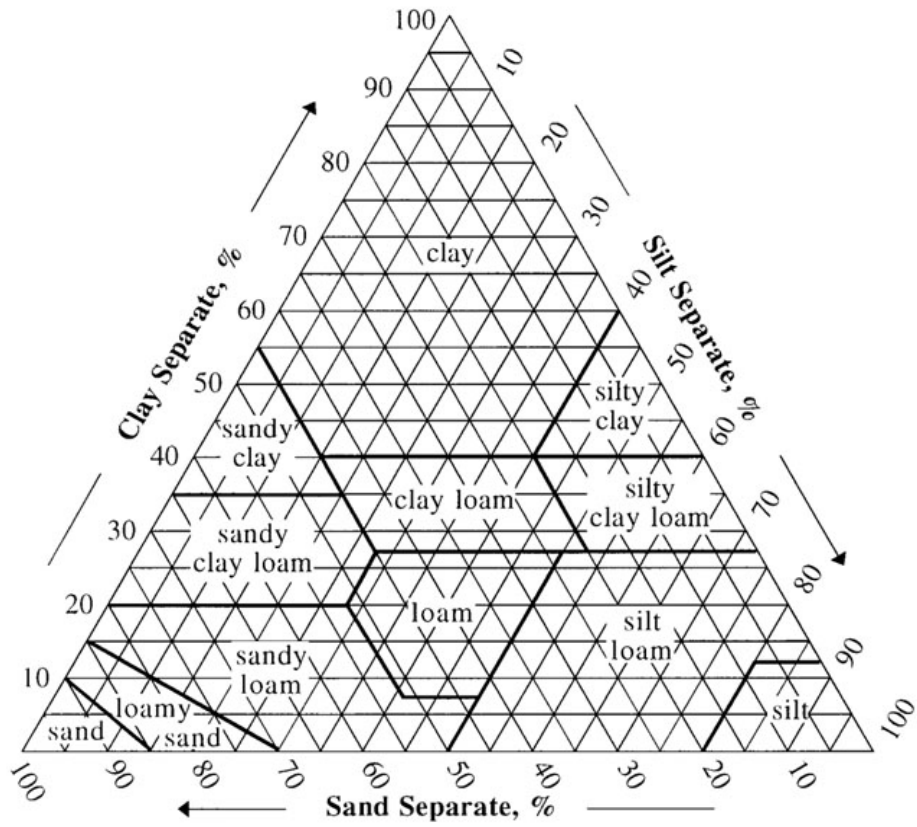
Table 3-21. Potential Design Options to Overcome Limiting Conditions.

Additional Treatment or Design Options	Shallow Soil Profile	Low Organic Carbon Content	Anoxic Soil Conditions	High pH Wastewater
Aerobic Treatment	X	X	X	X
UV Treatment	X			
Spray dispersal		X		
Timed dosing				
Continuous dosing				
Trench		X		
Infiltration bed	X			
Above-grade mound	X			
Constructed wetland	X	X	X	

"X" indicates potential to overcome limitation

APPENDIX A

GENERAL REFERENCE INFORMATION



COMPARISON OF PARTICLE SIZE SCALES

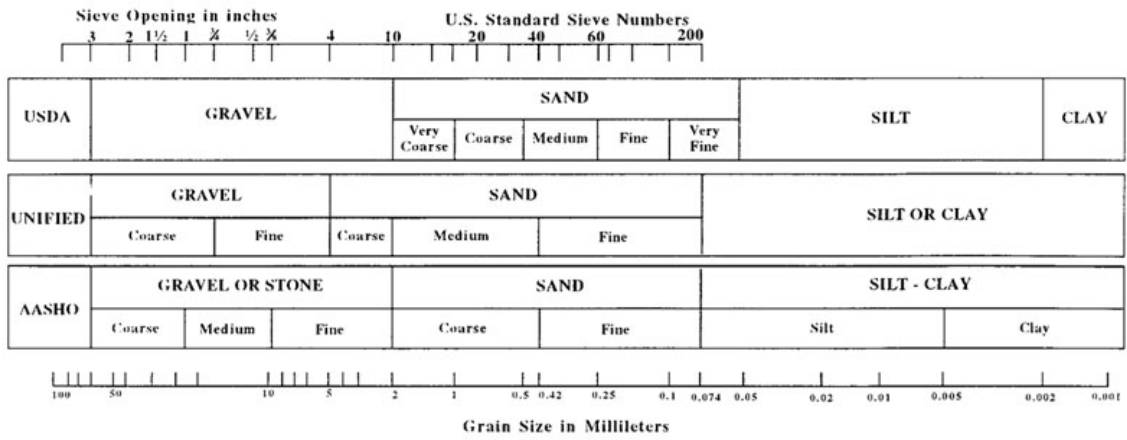


Figure A-1. USDA Soil Triangle and Particle Size Distribution.

Table A-1. Measured Indoor Daily Flow Summary Statistics (gallons capita⁻¹ d⁻¹) (adapted from Lowe et al., 2009).

Statistic	Literature	All Sites	Age		Mid-West	Region	
			Occupants >65	Occupants <65		South	West
n	30	64	40	24	20	24	20
Mean	73	55	39	78	55	49	62
Std Deviation	37	38	21	47	26	27	55
25 th Percentile	fill in	31	23	45	36	29	26
Median	64	45	36	66	46	45	41
75 th Percentile	fill in	67	52	101	62	60	67

Table A-2. Conversion Factors for HLR from cm d⁻¹.

cm d ⁻¹	L m ⁻² d ⁻¹	Gallons (U.S.) ft ⁻² d ⁻¹	Gallons (Imperial) ft ⁻² d ⁻¹
1	10	0.245	0.204
2	20	0.491	0.408
3	30	0.735	0.612
4	40	0.980	0.816
5	50	1.225	1.020
6	60	1.470	1.224
7	70	1.715	1.428
8	80	1.960	1.632
9	90	2.205	1.836
10	100	2.450	2.040

Note: 1 U.S. gallon = 3.785 liters; 1 Imperial gallon = 4.546 liters

Table A-3. Summary of HLR Used in STU Design.

Soil Texture	Bouma, 1975	HLR used in OWTS design (gallons ft ⁻² d ⁻¹)				K (ft d ⁻¹)	
		U.S. EPA, 1980	U.S. EPA, 2002	Siegrist, 2006	Radcliffe and West, 2009	K _{sat}	5% of K _{sat}
Sand	1.2	0.8-1.2	0.4-0.8	1	1.07	21	1.05
Loamy sand		0.8	0.4-0.8	1	0.9	3.4	0.17
Sandy loam	0.72	0.6	0.2-0.6	0.5	0.74	1.2	0.06
Loam		0.45	0.2-0.6		0.66	0.4	0.02
Silt loam	1.2	0.45	0.4-0.6	0.5	0.92	0.6	0.03
Silt					1.05	1.4	0.07
Sandy clay loam			0.2-0.4		0.5	0.4	0.02
Clay loam		0.2	0.2-0.4	0.12	0.5	0.3	0.01
Silty clay loam		0.2	0.2-0.4	0.12	0.69	0.4	0.02
Silty clay			0.2		0.46	0.3	0.02
Sandy clay			0.2		0.36	0.4	0.02
Clay	0.24		0.2		0.5	0.5	0.03
Notes:	Based on soil K-curves	Based on soil percolation test	Based on texture and structure, at BOD=150 mg L ⁻¹	Based on K _{sat} , soil class and effluent type, at BOD=150 mg L ⁻¹	Based on HYDRUS-2D and the Bouma Eqn.	Hydraulic conductivity (K) is provided for reference. Soil texture specific K _{sat} values from Rosetta Database (Schaap et al., 2001)	

APPENDIX B

WORKSHEET FORM

Step 1. Assess operational conditions

Step 1A. Develop a conceptual design

Step 1B. Deliniate hydraulic conditions

(a) What is the daily flow?

if known → Go to Box 1a
if unknown → Estimate from CFD
Obtain value from Table

Box 1a Daily Flow: L/capita/day

(b) What is the expected HLR?

if known → Go to Box 1b
if unknown → Estimate from daily flow & unit design
Obtain value from reference table

Box 1b HLR: cm/day

(c) Determine the application method of STE into the STU

Box 1c Method:

Is STU performance feasible?

yes → Go to Step 1C
no → STOP! Evaluate alternative treatment technologies

Step 1C. Assess effluent characteristics

(d) What is the alkalinity in the STE?

if known → Go to Box 1d
if unknown → Analyze effluent
Estimate from CFD
Obtain value from Table

Box 1d alkalinity: mg-CaCO₃/L

(e) What is the pH of the STE?

if known → Go to Box 1e
if unknown → Analyze effluent
assume sufficient for nitrification

Box 1e pH:

(f) Is pH assumed sufficient for nitrification?

- yes → Go to next step
- no → Calculate reduction factor for nitrification

Box 1f reduction factor:

(g) What is the concentration of COD in STE?

- if known → Go to Box 1g
- if unknown → Estimate from CFD
 - Obtain from Table
 - Calculate from Equation
 - analyze effluent if advance treatment units are utilized

Box 1g COD: mg/L

(h) What is the concentration of TN?

- if known → Go to Box 1h
- if unknown → Analyze effluent
 - Estimate from CFD
 - Obtain from Table

Box 1h TN: mg-N/L

(i) What is the COD:TN ratio?

Box 1i COD:TN ratio:

Is the ratio COD:TN > 4:1?

- yes → Go to next step
- no → STOP! Evaluate alternative treatment technologies

(j) What is the concentration of $\text{NH}_4^+ \text{-N}$?

- if known → Go to Box 1j
- if unknown → Estimate from CFD
 - Obtain from Table
 - analyze effluent if advance treatment units are utilized

Box 1j $\text{NH}_4^+ \text{-N}$: mg-N/L

(k) What is the alkalinity:NH4 ratio?

Box 1k alk:NH4 ratio:

Is the ratio alkalinity:NH4 > 7:1?

yes → Go to next step

no → STOP! Evaluate alternative treatment technologies

(l) What is the concentration of NO₃⁻-N?

if known → Go to Box 1l

if unknown → assume 1 mg/L if conventional septic tanks are utilized
analyze effluent if advance treatment units are utilized

Box 1l NO₃⁻-N: mg-N/L

(m) Determine if the effluent is considered standard or high quality

Box 1m effluent quality:

Step 2. Assess parameters affecting treatment performance

Step 2A. Assess soil characteristics

(a) What is the soil texture at the site?

if known → Go to Box 2a

if unknown → Collect soil samples or use database

Box 2a soil texture:

(b) What is the average soil temperature?

if known → Go to Box 2b

if unknown → Estimate average soil temp for site

Box 2b soil temp: °C

(c) Which temperature region is most appropriate for site?

Box 2c region:

(d) Obtain soil texture hydraulic properties

Box 2d

θ_r	θ_s	K_s	α	n
------------	------------	-------	----------	-----

Step 2B. Assess nitrogen removal parameters

Sorption:

(e) What is the ammonium sorption coefficient?

- if known → Go to Box 2e
- if unknown → use default value
- Estimate from CFD**
- Obtain from Table

Box 2e K_D : L/kg

**Adjustments may be needed if concentrations of COD and Ca^{2+} & Mg^{2+} , and CEC are high

Nitrification:

Is alkalinity sufficient and nitrification expected?

- yes → Go to the next step
- no → STOP! Evaluate alternative treatment technologies

(f) What is the max zero-order nitrification rate ($\mu_{nit,max}$)?

- if known → Go to Box 2f
- if unknown → Estimate from CFD
- Obtain from Table

Box 2f $\mu_{nit,max}$: mg-N L⁻¹ day⁻¹

(g) Does the rate need to be adjusted due to low pH level in the STE?

- yes → Multiply the rate with the reduction factor (Box 1f)
- Use of STUMOD is recommended
- no → Go to next step

Box 2g new rate: mg-N L⁻¹ day⁻¹

(h) What is the first order nitrification rate ?**

**only relevant if using N-calc

if known → Go to Box 2h
 if unknown → Estimate from CFD
 Obtain from Table

Box 2h day⁻¹

(i) Does the rate need to be adjusted due to low pH level in the STE?

yes → Multiply the rate with the reduction factor in Box 1f
 no → Go to next step

Box 2i new rate: day⁻¹

(j) What is the half saturation constant (K_m)?

if known → Go to Box 2j
 if unknown → Use default value

Box 2j K_m mg L⁻¹

Denitrification:

Is COD sufficient and denitrification expected?

yes → Go to the next step
 no → STOP! Evaluate alternative treatment technologies

(k) What is the max denitrification rate ($\mu_{dn,max}$)?

if known → Go to Box 2k
 if unknown → Estimate from CFD
 Obtain from Table

Box 2k $\mu_{dn,max}$ mg-N L⁻¹ day⁻¹

(l) Is the half saturation constant (K_m) known?

yes → Go to Box 2l
 no → Use default value

Box 2l K_m mg/L

APPENDIX C

FIELD TESTING FOR MODEL DEVELOPMENT

The field test site at the University of Georgia (UGA) was established to conduct onsite wastewater treatment system (OWTS) experiments in clayey soil while measuring hydraulic performance and nitrogen movement. These results were then used to develop a 2-dimensional model of water and nitrogen movement and compare the model predictions to the data obtained at the experimental site. Findings from the literature review included four major conclusions regarding modeling nitrogen attenuation in OWTS that were incorporated into the field design:

- ◆ little is known under what conditions and to what extent denitrification occur;
- ◆ differences in soil texture, structure or drainage class are likely to affect the magnitude of denitrification;
- ◆ the HYDRUS model framework including a nitrogen model for two-dimensional simulations of a constructed wetland (CW2D) have been used in several studies; and
- ◆ it may be possible to develop simple nitrogen models for soil treatment units (STUs) based on data generated from a HYDRUS model adapted to OWTSs.

C.2 Description of UGA Experimental Site

A conventional OWTS was installed and instrumented at the UGA experimental site in March 2009. The site is in typical Piedmont soil with three replicated trenches 10 m in length and 0.9 m in width (Figure C-1). Wastewater from a nearby sewage treatment plant providing service to a residential area was transported to the site and pumped to the septic tank three times a week (Figure C-2). The trenches were instrumented with water level sensors and the surrounding soil was instrumented with water content sensors (TDR), tensiometers, and suction lysimeters (Figures C-1 and C-3). Sensors were monitored continuously using data loggers. Lysimeter samples were collected monthly for analysis of nitrate and ammonium beginning in April 2009 and ending in October 2009.

Prior to wastewater delivery to the soil, a falling head experiment was conducted with water in each of the three trenches to determine hydraulic properties at the site. Water was ponded in each trench to a height of approximately 15 cm and then allowed to infiltrate, which took one to three days depending on the trench. While water was infiltrating, water levels in the trench and water contents and pressure heads in the soil surrounding the trench were measured using TDR and tensiometers. The data was used to run a HYDRUS model of the OWTS in an inverse mode to improve estimates of soil saturated hydraulic conductivity and water retention curve parameters for three horizons surrounding the trenches, thus ensuring that the model was capable of simulating the hydraulics of the experimental site.



Figure C-1. Experimental UGA Site Showing Storage Tank that Discharges to the Septic Tank and Three Trenches and Instrumentation. A Data Logger Housing, Rain Gauge, and Solar Panel is Also Shown.

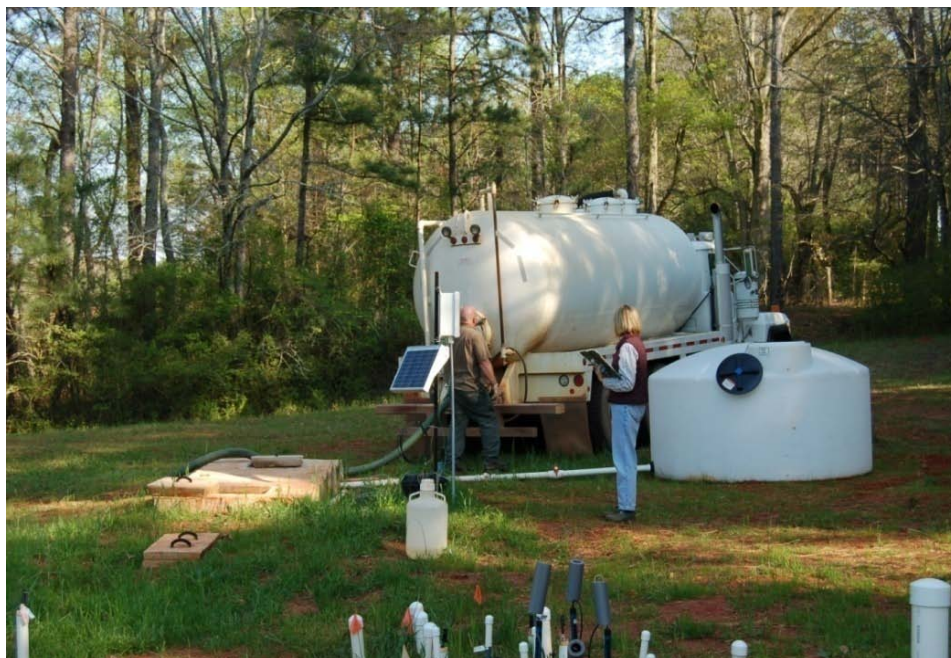


Figure C-2. Tanker Truck Used for Transporting Wastewater from the Local Sewage Treatment Plant to the UGA Experimental Site (pumped into a storage tank).



Figure C- 3. Trench During Installation of Sensors into the Underlying Soil.

C.3 Hydraulic Performance at the UGA Experimental Site

Water levels in the trenches are shown in Figure C-4 during two periods: April 10-11 and July 10-11, 2009. Three doses were applied each day at a rate of 3.7 cm/day, which is 1.5 times the recommended dose for this soil in Georgia (the higher rate was applied to speed the development of the biomat in the first year). These figures show a sharp rise in water level in response to each dose and a slow decline in water levels between doses. Minimum water levels varied between 2 and 10 cm of ponding, except in trench 2 in July when they reached zero just before each dose.

Pressure heads measured by tensiometers surrounding trench 1 over a four-hour period on July 24, 2009 are shown in Figure C-5. Pressure heads were relatively constant in time and varied from -45 cm in the soil to the side and near the top of the trench to 80 cm immediately below the trench at the deepest depth (60 cm below the trench bottom).

The effect of rainfall on trench water levels and soil pressure heads is shown in Figure C-6 during the period April 1 to August 1, 2009. Water levels clearly rose in the trench in late May and early June due to a period of frequent rainfall and in mid-July when there was a large storm.

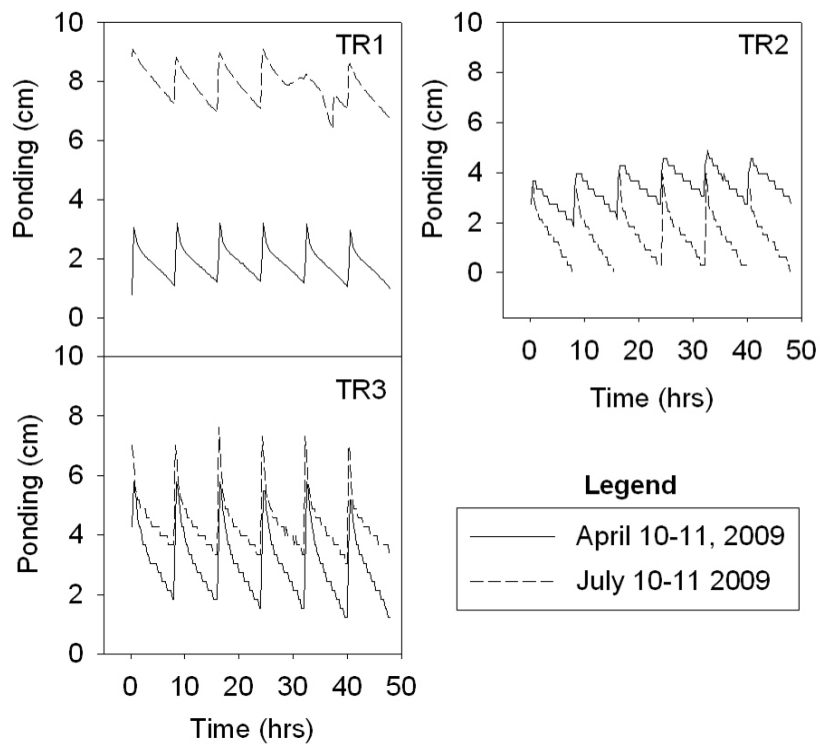


Figure C-4. Water levels in Trench 1 (TR1), Trench 2 (TR2), and Trench 3 (TR3) During April 10-11 and July 10-11, 2009.

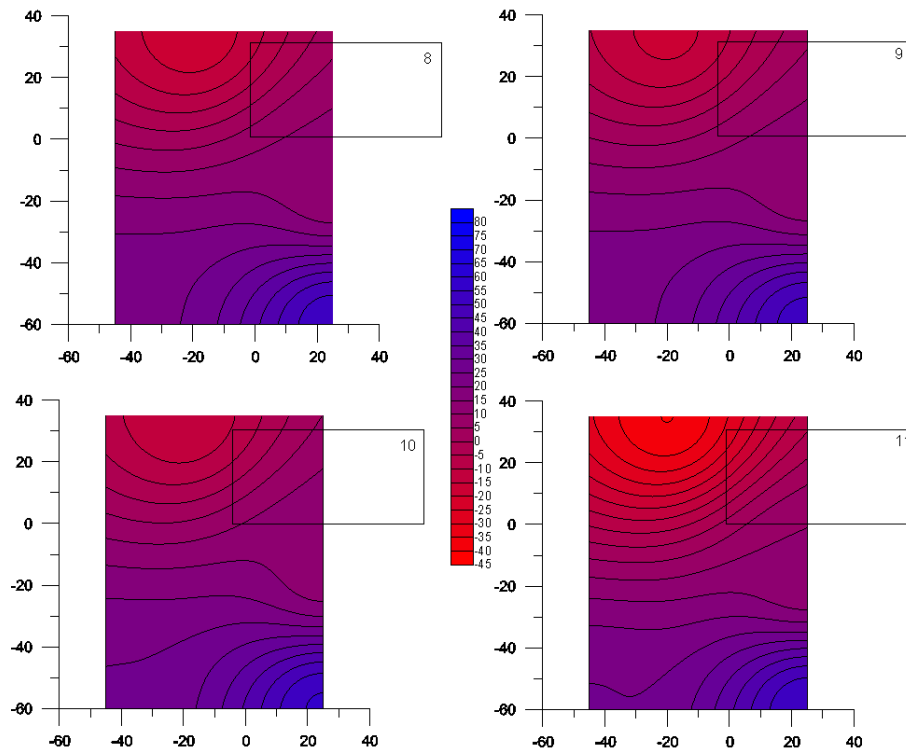


Figure C-5. Pressure Heads (in cm) around Trench 1. Clockwise from the upper left: 8, 9, 10, and 11am on April 24, 2009. Distance (cm) is shown on each axis relative to the lower left corner of the trench. The outline of the trench is shown in the upper right of each figure.

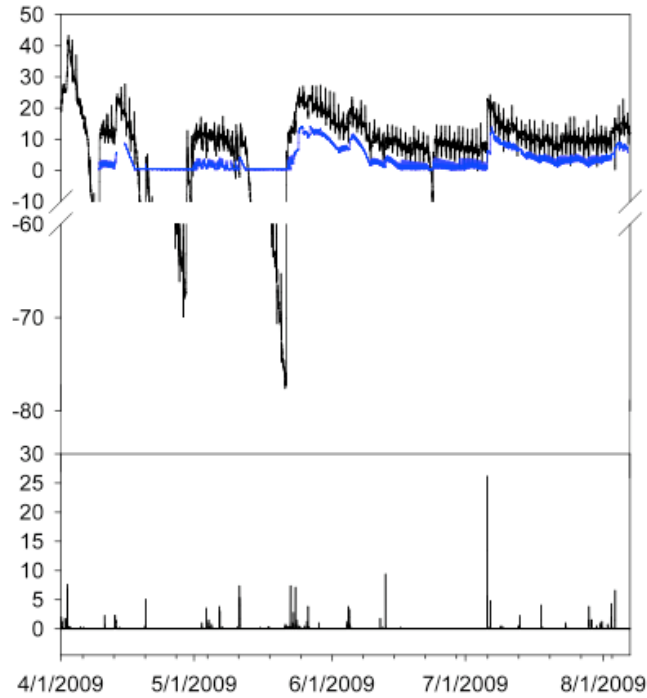


Figure C-6. Pressure Head (in cm) at Tensiometer Located 15 cm Below Trench 1.
 Pressure head is shown by the black line and the water level (cm) in the trench is shown by the blue line during the period April 1 to August 1, 2009 in the upper graph. Precipitation (mm) is shown in the lower graph.

C.4 Nitrogen Loss Results

The position of the suction lysimeters used to monitor nitrogen concentrations relative to each trench is shown in Figure C-7. There were four suction lysimeters immediately below the trench (at 15, 30, 60, and 90 cm below the trench bottom) and four more samplers at a distance of 30 cm down slope of the trench (at the same depths). An additional sampler was placed 90 cm down slope at the deepest depth. The lysimeter array was installed at two points along each of the three trenches: 3.3 m (Point A) and 6.6 m (Point B) from the end of the trench near the distribution box.

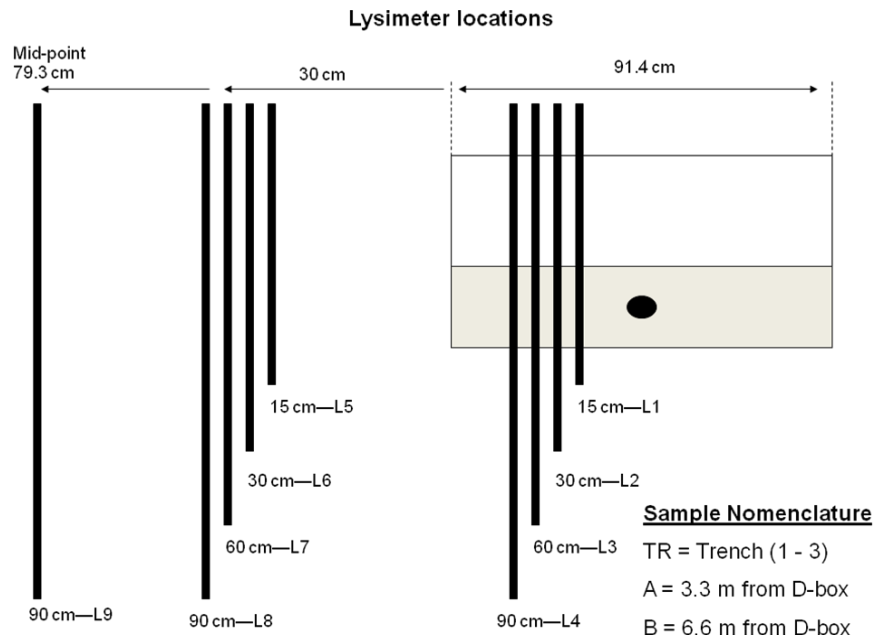


Figure C-7. Location of Suction Lysimeters Relative to Each Trench.

Two sampling points (A and B) were established at 3.3 and 6.6 m from the end of each trench near the distribution box. An outline of the trench and perforated pipe is shown in the upper right of the figure.

A summary of the concentrations of nitrate and ammonium from each lysimeter location on the eight sampling dates is presented in Tables C-1, C-2, and C-3. Concentrations of ammonium in the STE varied from the mid 20s to low 40s, while the concentrations of nitrate were near zero. Concentrations in the first compartment (ST-IN) and second compartment (ST-OUT) of the septic tank are also shown at the bottom of each table.

Lysimeter concentrations above 1 mg-N L^{-1} were considered above background as they exceeded the STE values and are highlighted in yellow in Tables C-1, C-2, and C-3. Most samplers had concentrations below 1 mg-N L^{-1} ; however, there was evidence that concentrations increased over time. For example, on April 2nd, only eight of the 54 lysimeters had nitrogen concentrations above 1 mg-N L^{-1} compared to August 12th where 21 of the lysimeters and October 23rd where 34 of the lysimeters had nitrogen concentrations above 1 mg-N L^{-1} . The lysimeter position that most frequently showed concentrations above 1 mg-N L^{-1} was L9, which was farthest down slope from the trench bottom (Figure C-7). Concentrations were above 1 mg-N L^{-1} in 17 of the 24 samples collected at this position (6 dates x 2 trench distances x 3 trenches). In addition, concentrations tended to be above background at L9 on all dates, however; these concentrations remained relatively low (less than 2 mg-N L^{-1} in most cases).

Table C-1. Nitrogen Concentrations (mg-N L⁻¹) in Samples Taken from April to May 2009.

April 2, 2009			May 6, 2009			May 27, 2009		
Sample	NH ₄ -N	NO ₃ -N	Sample	NH ₄ -N	NO ₃ -N	Sample	NH ₄ -N	NO ₃ -N
TR1A-L1	<0.04	0.07	TR1A-L1	<0.04	<0.02	TR1A-L1	<0.04	0.99
TR1A-L2	0.06	0.51	TR1A-L2	<0.04	0.52	TR1A-L2	<0.04	0.48
TR1A-L3	<0.04	0.54	TR1A-L3	<0.04	0.33	TR1A-L3	<0.04	0.11
TR1A-L4	0.05	0.55	TR1A-L4	<0.04	0.31	TR1A-L4	0.05	0.15
TR1A-L5	<0.04	0.46	TR1A-L5	<0.04	0.62	TR1A-L5	<0.04	0.60
TR1A-L6	<0.04	0.21	TR1A-L6	0.07	0.27	TR1A-L6	0.05	0.28
TR1A-L7	<0.04	0.31	TR1A-L7	0.04	0.73	TR1A-L7	<0.04	0.16
TR1A-L8	0.05	0.41	TR1A-L8	<0.04	0.21	TR1A-L8	<0.04	0.15
TR1A-L9	0.04	1.29	TR1A-L9	0.04	1.65	TR1A-L9	<0.04	2.57
TR1B-L1	<0.04	0.39	TR1B-L1	<0.04	0.96	TR1B-L1	0.04	4.57
TR1B-L2	<0.04	0.90	TR1B-L2	<0.04	0.85	TR1B-L2	<0.04	1.08
TR1B-L3	<0.04	0.36	TR1B-L3	<0.04	0.43	TR1B-L3	<0.04	0.36
TR1B-L4	<0.04	0.24	TR1B-L4	0.08	0.28	TR1B-L4	0.04	0.13
TR1B-L5	<0.04	2.60	TR1B-L5			TR1B-L5	<0.04	0.63
TR1B-L6	<0.04	2.58	TR1B-L6	<0.04	2.92	TR1B-L6	<0.04	3.28
TR1B-L7	<0.04	0.79	TR1B-L7	<0.04	1.40	TR1B-L7	<0.04	0.80
TR1B-L8	<0.04	1.65	TR1B-L8			TR1B-L8		
TR1B-L9	<0.04	1.44	TR1B-L9	<0.04	2.53	TR1B-L9	<0.04	2.30
TR2A-L1	<0.04	0.04	TR2A-L1	<0.04	<0.02	TR2A-L1	<0.04	3.66
TR2A-L2	<0.04	0.89	TR2A-L2	<0.04	0.94	TR2A-L2	0.05	0.59
TR2A-L3	0.04	0.61	TR2A-L3	<0.04	0.26	TR2A-L3	<0.04	0.43
TR2A-L4	0.04	0.79	TR2A-L4	<0.04	1.03	TR2A-L4	<0.04	0.68
TR2A-L5	0.04	<0.02	TR2A-L5	0.04	<0.02	TR2A-L5	<0.04	0.22
TR2A-L6			TR2A-L6	0.25	<0.02	TR2A-L6	<0.04	0.07
TR2A-L7	<0.04	0.20	TR2A-L7	0.07	0.25	TR2A-L7	<0.04	0.06
TR2A-L8	0.06	0.53	TR2A-L8	0.15	<0.02	TR2A-L8	0.04	0.74
TR2A-L9	0.07	0.39	TR2A-L9	0.09	<0.02	TR2A-L9	0.11	0.12
TR2B-L1	<0.04	<0.02	TR2B-L1			TR2B-L1	<0.04	7.63
TR2B-L2	0.05	0.37	TR2B-L2			TR2B-L2	<0.04	0.98
TR2B-L3	<0.04	0.57	TR2B-L3			TR2B-L3	<0.04	0.37
TR2B-L4			TR2B-L4			TR2B-L4	<0.04	0.24
TR2B-L5	<0.04	0.04	TR2B-L5			TR2B-L5	<0.04	0.15
TR2B-L6	<0.04	<0.02	TR2B-L6			TR2B-L6		
TR2B-L7	<0.04	0.86	TR2B-L7			TR2B-L7	<0.04	0.05
TR2B-L8	<0.04	0.06	TR2B-L8			TR2B-L8	0.05	0.07
TR2B-L9	<0.04	3.46	TR2B-L9			TR2B-L9	<0.04	0.36
TR3A-L1	<0.04	0.08	TR3A-L1	<0.04	<0.02	TR3A-L1	0.04	1.31
TR3A-L2	<0.04	<0.02	TR3A-L2	<0.04	<0.02	TR3A-L2	0.74	0.02
TR3A-L3	<0.04	0.47	TR3A-L3	<0.04	0.07	TR3A-L3	<0.04	0.02
TR3A-L4	<0.04	0.19	TR3A-L4	0.06	0.14	TR3A-L4	<0.04	0.10
TR3A-L5	<0.04	<0.02	TR3A-L5	0.11	<0.02	TR3A-L5	0.20	<0.02
TR3A-L6	<0.04	0.19	TR3A-L6			TR3A-L6		
TR3A-L7	<0.04	0.62	TR3A-L7	0.15	0.11	TR3A-L7	<0.04	0.04
TR3A-L8	<0.04	0.11	TR3A-L8			TR3A-L8	0.36	0.02
TR3A-L9	0.04	<0.02	TR3A-L9	0.44	0.55	TR3A-L9	<0.04	0.44
TR3B-L1			TR3B-L1	0.39	<0.02	TR3B-L1	<0.04	1.60
TR3B-L2	<0.04	0.80	TR3B-L2	0.10	0.58	TR3B-L2	<0.04	0.41
TR3B-L3	<0.04	0.95	TR3B-L3	0.05	0.55	TR3B-L3	<0.04	0.55
TR3B-L4	<0.04	0.67	TR3B-L4	0.05	0.30	TR3B-L4	<0.04	0.55
TR3B-L5	<0.04	0.80	TR3B-L5	<0.04	0.11	TR3B-L5	<0.04	0.49
TR3B-L6	0.04	<0.02	TR3B-L6	0.04	<0.02	TR3B-L6		
TR3B-L7	<0.04	0.49	TR3B-L7	0.08	0.27	TR3B-L7	0.08	1.09
TR3B-L8	<0.04	2.76	TR3B-L8	0.08	1.57	TR3B-L8	<0.04	1.76
TR3B-L9	<0.04	1.86	TR3B-L9	0.24	1.76	TR3B-L9	0.04	1.35
ST-IN	26.67	<0.02	ST-IN	28.19	<0.02	ST-IN	30.38	0.05
ST-OUT	28.21	<0.02	ST-OUT	28.39	<0.02	ST-OUT	33.55	0.04

Table C-2. Nitrogen Concentrations (mg-N L⁻¹) in Samples Taken from June to August 2009.

June 10, 2009			July 8, 2009			August 12, 2009		
Sample	NH ₄ -N	NO ₃ -N	Sample	NH ₄ -N	NO ₃ -N	Sample	NH ₄ -N	NO ₃ -N
TR1A-L1	0.04	0.13	TR1A-L1	<0.04	<0.02	TR1A-L1	0.22	<0.02
TR1A-L2	<0.04	0.39	TR1A-L2	0.05	0.07	TR1A-L2	0.06	<0.02
TR1A-L3	<0.04	<0.02	TR1A-L3	0.04	<0.02	TR1A-L3	0.07	<0.02
TR1A-L4	0.05	0.19	TR1A-L4	<0.04	0.06	TR1A-L4	0.05	<0.02
TR1A-L5	0.07	0.02	TR1A-L5	0.10	2.64	TR1A-L5		
TR1A-L6	0.19	<0.02	TR1A-L6	<0.04	<0.02	TR1A-L6	0.20	<0.02
TR1A-L7	<0.04	<0.02	TR1A-L7	0.07	<0.02	TR1A-L7	0.10	0.66
TR1A-L8	0.04	<0.02	TR1A-L8	<0.04	<0.02	TR1A-L8	0.06	<0.02
TR1A-L9	0.04	1.73	TR1A-L9	0.06	1.74	TR1A-L9	0.07	0.72
TR1B-L1	<0.04	3.13	TR1B-L1	<0.04	0.22	TR1B-L1	<0.04	<0.02
TR1B-L2	0.05	4.09	TR1B-L2	0.04	1.78	TR1B-L2	0.05	0.23
TR1B-L3	0.04	0.67	TR1B-L3	<0.04	0.31	TR1B-L3	0.08	0.12
TR1B-L4	0.07	0.80	TR1B-L4	0.05	8.59	TR1B-L4	0.06	14.70
TR1B-L5	0.05	0.11	TR1B-L5	0.06	3.47	TR1B-L5	0.08	9.55
TR1B-L6	<0.04	1.30	TR1B-L6	<0.04	1.52	TR1B-L6	0.04	2.17
TR1B-L7	0.05	0.58	TR1B-L7	0.06	0.50	TR1B-L7	0.05	0.55
TR1B-L8	<0.04	0.56	TR1B-L8	<0.04	3.82	TR1B-L8	0.05	1.92
TR1B-L9	<0.04	4.38	TR1B-L9	0.04	<0.02	TR1B-L9	<0.04	<0.02
TR2A-L1	<0.04	0.93	TR2A-L1	0.05	<0.02	TR2A-L1	0.12	<0.02
TR2A-L2	<0.04	0.43	TR2A-L2	0.04	<0.02	TR2A-L2	0.07	<0.02
TR2A-L3			TR2A-L3	<0.04	0.11	TR2A-L3	0.04	<0.02
TR2A-L4	<0.04	0.60	TR2A-L4	<0.04	0.24	TR2A-L4	0.05	<0.02
TR2A-L5	0.05	<0.02	TR2A-L5	<0.04	0.02	TR2A-L5	0.05	<0.02
TR2A-L6	0.05	<0.02	TR2A-L6	1.41	<0.02	TR2A-L6	1.02	0.09
TR2A-L7	0.06	<0.02	TR2A-L7	0.36	<0.02	TR2A-L7	2.57	<0.02
TR2A-L8	0.05	0.03	TR2A-L8	0.08	2.90	TR2A-L8		
TR2A-L9	0.48	<0.02	TR2A-L9	1.37	1.35	TR2A-L9	3.41	6.25
TR2B-L1	0.08	0.73	TR2B-L1	0.27	0.38	TR2B-L1	0.45	0.23
TR2B-L2	<0.04	1.90	TR2B-L2	<0.04	0.68	TR2B-L2	<0.04	0.44
TR2B-L3	<0.04	0.79	TR2B-L3	0.05	0.49	TR2B-L3	<0.04	0.09
TR2B-L4	0.07	0.18	TR2B-L4	0.04	2.30	TR2B-L4	0.09	2.95
TR2B-L5	<0.04	<0.02	TR2B-L5	<0.04	7.36	TR2B-L5	<0.04	8.35
TR2B-L6	<0.04	<0.02	TR2B-L6	0.04	7.10	TR2B-L6	0.08	11.81
TR2B-L7	0.04	<0.02	TR2B-L7	<0.04	4.90	TR2B-L7	0.04	9.35
TR2B-L8			TR2B-L8	<0.04	0.23	TR2B-L8	0.06	0.22
TR2B-L9	0.04	<0.02	TR2B-L9	<0.04	0.03	TR2B-L9	<0.04	0.14
TR3A-L1	0.04	0.18	TR3A-L1	0.26	<0.02	TR3A-L1	1.59	<0.02
TR3A-L2	1.20	<0.02	TR3A-L2	2.65	<0.02	TR3A-L2	10.09	<0.02
TR3A-L3	<0.04	<0.02	TR3A-L3	0.05	<0.02	TR3A-L3	0.04	<0.02
TR3A-L4	<0.04	<0.02	TR3A-L4	0.06	<0.02	TR3A-L4	0.05	<0.02
TR3A-L5	0.43	<0.02	TR3A-L5	0.99	1.60	TR3A-L5	2.81	1.88
TR3A-L6			TR3A-L6	3.28	<0.02	TR3A-L6	0.25	<0.02
TR3A-L7	0.05	<0.02	TR3A-L7	0.11	<0.02	TR3A-L7	5.53	<0.02
TR3A-L8	0.45	<0.02	TR3A-L8	0.45	0.11	TR3A-L8	0.50	0.05
TR3A-L9	0.04	1.12	TR3A-L9	<0.04	0.40	TR3A-L9	0.07	1.37
TR3B-L1	0.05	0.46	TR3B-L1	<0.04	0.06	TR3B-L1	0.09	7.49
TR3B-L2	0.04	0.35	TR3B-L2	0.06	0.36	TR3B-L2	0.04	0.15
TR3B-L3	<0.04	0.27	TR3B-L3	<0.04	0.13	TR3B-L3	0.06	0.09
TR3B-L4	0.05	0.06	TR3B-L4	<0.04	<0.02	TR3B-L4	0.05	<0.02
TR3B-L5	0.04	0.21	TR3B-L5	0.05	2.01	TR3B-L5	<0.04	1.96
TR3B-L6	<0.04	0.06	TR3B-L6	<0.04	1.95	TR3B-L6	0.05	1.96
TR3B-L7	0.07	0.98	TR3B-L7	0.04	1.61	TR3B-L7	0.07	3.46
TR3B-L8	<0.04	1.31	TR3B-L8	<0.04	0.73	TR3B-L8	<0.04	1.94
TR3B-L9	<0.04	0.08	TR3B-L9	<0.04	0.27	TR3B-L9	0.06	<0.02
ST-IN	32.62	<0.02	ST-IN	13.94	<0.02	ST-IN	46.44	<0.02
ST-OUT	29.57	<0.02	ST-OUT	23.06	<0.02	ST-OUT	40.74	<0.02

Table C-3. Nitrogen Concentrations (mg-N L⁻¹) in Samples Taken in September and October 2009.

September 11, 2009			October 23, 2009		
Sample	NH ₄ -N	NO ₃ -N	Sample	NH ₄ -N	NO ₃ -N
TR1A-L1	1.71	<0.02	TR1A-L1	2.81	0.20
TR1A-L2	0.02	<0.02	TR1A-L2	0.04	<0.02
TR1A-L3	0.07	<0.02	TR1A-L3	0.08	<0.02
TR1A-L4	0.05	<0.02	TR1A-L4	0.04	<0.02
TR1A-L5	0.17	1.69	TR1A-L5	0.18	1.94
TR1A-L6	0.43	<0.02	TR1A-L6	0.74	<0.02
TR1A-L7	0.21	2.49	TR1A-L7	0.20	2.18
TR1A-L8	0.08	1.20	TR1A-L8	0.04	7.54
TR1A-L9	0.08	1.54	TR1A-L9	0.06	3.49
TR1B-L1	0.03	3.88	TR1B-L1	0.05	2.03
TR1B-L2	0.02	14.13	TR1B-L2	0.04	4.84
TR1B-L3	0.04	0.18	TR1B-L3	0.04	1.12
TR1B-L4	0.05	26.25	TR1B-L4	0.04	18.80
TR1B-L5	0.06	13.83	TR1B-L5	0.03	3.57
TR1B-L6	0.02	1.38	TR1B-L6	0.02	7.62
TR1B-L7	0.03	0.41	TR1B-L7	0.03	0.64
TR1B-L8	0.02	1.14	TR1B-L8	0.09	3.78
TR1B-L9	0.02	<0.02	TR1B-L9	0.06	0.14
TR2A-L1	2.89	<0.02	TR2A-L1	11.25	1.05
TR2A-L2	0.06	<0.02	TR2A-L2	0.09	0.06
TR2A-L3	0.06	<0.02	TR2A-L3	0.21	<0.02
TR2A-L4	0.02	<0.02	TR2A-L4	0.04	0.08
TR2A-L5	0.05	<0.02	TR2A-L5	0.08	0.14
TR2A-L6	2.05	7.50	TR2A-L6	1.46	1.57
TR2A-L7	5.51	<0.02	TR2A-L7	9.58	2.53
TR2A-L8			TR2A-L8		
TR2A-L9	4.58	10.93	TR2A-L9	3.42	4.27
TR2B-L1	4.81	7.32	TR2B-L1	5.92	3.65
TR2B-L2	0.05	0.30	TR2B-L2	0.05	1.68
TR2B-L3	0.04	0.18	TR2B-L3	0.05	0.36
TR2B-L4	0.06	4.38	TR2B-L4	0.05	4.37
TR2B-L5	0.06	19.78	TR2B-L5	0.03	6.81
TR2B-L6	0.08	19.42	TR2B-L6	0.05	4.96
TR2B-L7	0.05	24.19	TR2B-L7	0.05	15.33
TR2B-L8	0.03	0.51	TR2B-L8		
TR2B-L9	0.09	0.27	TR2B-L9	0.06	0.65
TR3A-L1	17.88	<0.02	TR3A-L1	22.85	0.44
TR3A-L2	17.88	<0.02	TR3A-L2	17.63	0.79
TR3A-L3	0.06	<0.02	TR3A-L3	0.06	<0.02
TR3A-L4	0.08	<0.02	TR3A-L4	0.07	<0.02
TR3A-L5	4.32	4.79	TR3A-L5	3.84	4.17
TR3A-L6	13.51	<0.02	TR3A-L6	14.48	0.02
TR3A-L7	0.26	<0.02	TR3A-L7	0.24	<0.02
TR3A-L8	0.49	0.17	TR3A-L8	0.55	<0.02
TR3A-L9	0.05	4.81	TR3A-L9	0.05	7.25
TR3B-L1	0.20	20.88	TR3B-L1	0.17	15.25
TR3B-L2	0.04	0.93	TR3B-L2	0.03	3.19
TR3B-L3	0.05	0.44	TR3B-L3	0.06	1.25
TR3B-L4	0.03	0.13	TR3B-L4	0.04	0.53
TR3B-L5	0.05	27.53	TR3B-L5	0.05	11.99
TR3B-L6	0.03	9.13	TR3B-L6	0.04	11.80
TR3B-L7	0.05	9.54	TR3B-L7	0.05	8.54
TR3B-L8	0.04	3.87	TR3B-L8	0.03	9.66
TR3B-L9	0.04	0.08	TR3B-L9	0.01	0.47
ST-IN	50.00	<0.02	ST-IN	47.98	<0.02
ST-OUT	60.08	<0.02	ST-OUT	34.81	<0.02

One might expect the lysimeters at positions L1 and L2 immediately below the trench to most frequently show concentrations above background, but this was not the case. Only seven of 24 samples at L1 and 7 of 24 samples at L2 were above 1 mg-N L⁻¹. In most cases, the concentrations above 1 mg-N L⁻¹ at these positions occurred on the last 2 dates. These locations were among the few that showed ammonium concentrations above 1 mg-N L⁻¹. On the last two sampling dates, the lysimeters at position L4, the deepest depth immediately below the trenches frequently showed concentrations above 1 mg-N L⁻¹.

The lysimeters that frequently showed above background concentrations of nitrogen (aside from the position L9) were those located 30 cm down slope of the trench (L5-L8) (Figure C-7). L6 was the most common position to show concentrations above 1 mg-N L⁻¹ (13 of 24 times), followed by L5 and L8 (9 of 24 times), and L7 (8 of 24 times).

To illustrate these trends, nitrate concentrations are plotted in Figure C-8 as a function of position relative to the trenches on the last two sampling dates. Concentrations tended to be higher at lysimeter array point B (6.6 m along the trench, the lower row of plots in Figure C-8). The zone of high nitrate concentrations around lysimeters L5-L8, to the side and downslope of the trenches, is apparent on both dates. Comparison of the chloride and nitrate distribution indicates that chloride was present in most areas around the trench but nitrate only appeared in some areas. This trend may suggest that rather than preferential flow, denitrification may not be occurring in some areas (Figure C-9).

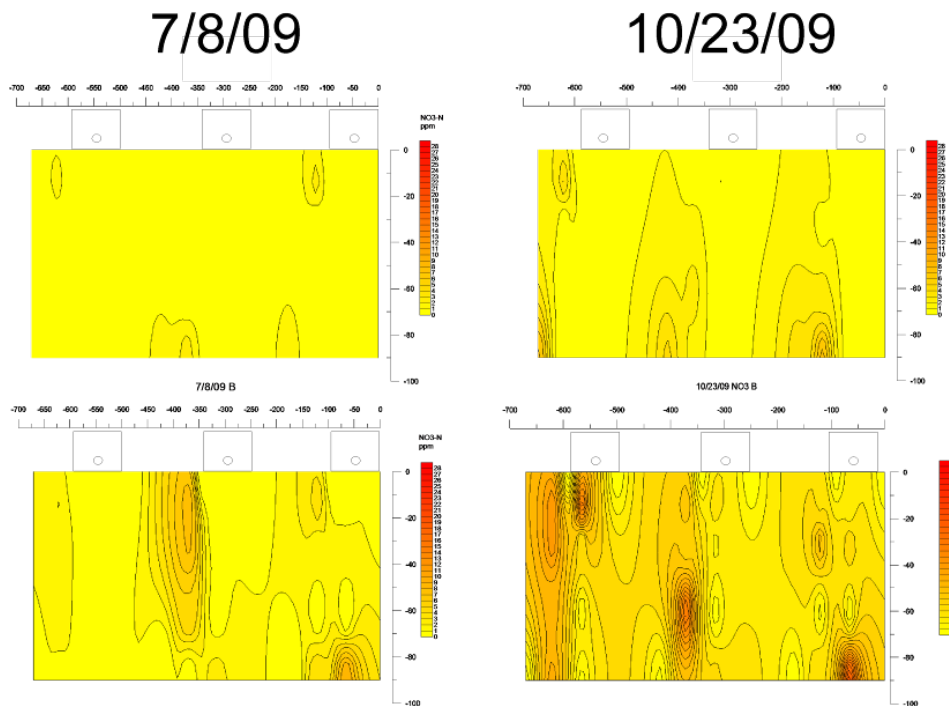
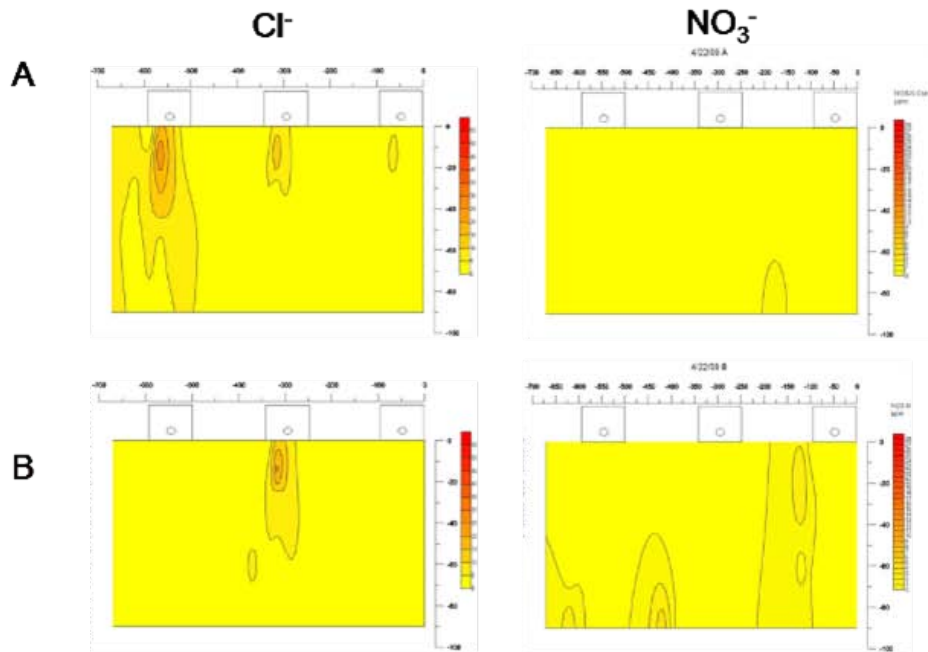


Figure C-8. Comparison of Nitrate Concentrations (mg-N L⁻¹) on July 8 and October 23, 2009 (the last two sampling dates) as a Function of Position Relative to the Three Trenches at Two Distances: 3.3 m (top row) and 6.6 m (bottom row). Distances are in cm and are measured from the lower right corner of the trench farthest up slope. Outlines of the trenches and perforated pipes are shown at top.

4/22/09



10/23/09

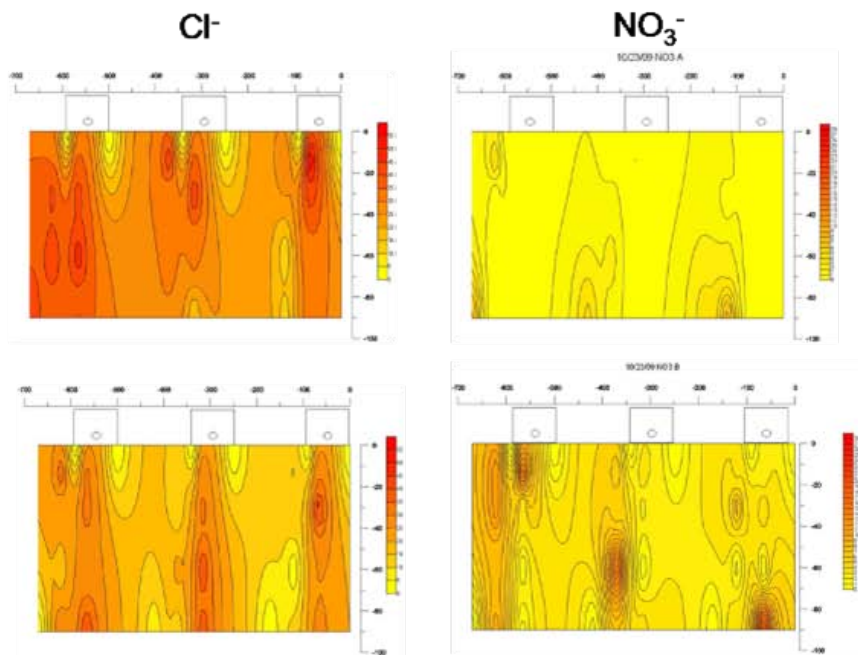


Figure C-9. Comparison of Chloride and Nitrate Concentrations (mg-N L^{-1}) in April and October 2009.

C.5 Discussion

Overall, the results indicated that some nitrate was moving away from the trenches in this clayey soil. There was a tendency for nitrate concentrations to increase over time so the final steady-state distribution of nitrate is not known. Most of the lysimeters indicated background concentrations, but some lysimeters consistently showed concentrations of nitrate above 1 mg-N L^{-1} . The absence of ammonium in the lysimeters, except for a few cases close to the trench indicated that ammonium was either converted to nitrate in or very near the trench, or adsorbed very near the trench. Nitrate concentrations may have been low immediately below the trench because this was the wettest area (Figure C-5) and denitrification was optimal. The zone of high nitrate that occurred between and below the trenches may have been due to the fact that this was a dryer area where denitrification was less optimal (Figure C-5). Another possible explanation is that preferential flow in this clayey soil produced nitrate plumes that were intersected by only a small number of our samplers.

The experimental site in a clayey soil has shown that water levels were ponding in the trench, even in a system that did not have a fully developed biomat. Pressure heads were slightly positive to slightly negative in the zone around each trench in a range that may allow both nitrification and denitrification to occur. Nitrate concentrations in the soil beneath the trenches were generally low, but above background concentrations, and increased with time during the 6 months in which samples were collected. Ammonium concentrations were very low, except immediately below the trench on the last two sampling dates.

The CW2D model accurately predicted water movement and pressure heads, but underestimated nitrate concentrations in the soil as observed at the UGA experimental site. It may be possible to adjust the model processes to produce a state-of-the-art OWTS model for water and nitrogen movement.

APPENDIX D

MICROBIAL FATE AND TRANSPORT

Laboratory experiments were carried to study the transport and fate of a model bacterium (*E. coli*) and virus (MS-2 coliphage). Three types of soils were obtained from sites in Rhode Island (RI), Colorado (CO), and Georgia (GA). These soils were sandy, sandy-loam, and structured clay loam, respectively. The primary objective of these laboratory studies was to provide the practitioner with guidelines to estimate bacteria and virus removal efficiencies for an OWTS based on a trench design and pulsed loading. The removal efficiency of such a system was simulated under variable hydraulic loading rates (HLRs), precipitation patterns, initial microbe concentrations and other environmental stresses. Guidelines were then developed based on the most significant results, which were typically based on the bacteria fate and transport results from the dosing experiments.

D.1 Laboratory Methods

D.1.1 Experimental Design

Replicate (n=3) segmented mesocosms were designed to provide authentic data for the calibration of models describing the removal of microbial pathogens in STUs. These mesocosms consisted of straight-sided polypropylene Nalgene jars (10.5 cm high, 6.5 cm i.d.) with sample ports between jars to allow for sampling of drainage water directly below the infiltrative surface (4 cm), and at succeeding 10.5-cm depths (14.5 cm, 25 cm, 35.5 cm), hereafter referred to as 4 cm, 14.5 cm, 25 cm, and 35.5 cm (Figure D-1). The mesocosms were packed with typical soils with soil treatment unit (STU) installations: 1) a sandy, B and C horizon soil from Kingston, RI; 2) a sandy loam soil from Golden, CO; or 3) a clay loam soil from GAs. The remaining space in the 4 cm mesocosm was packed with gravel. Mesocosms were maintained at room temperature (19-21°C) in the dark. STE was obtained approximately every 7-10 days from a residential dwelling house and stored at room temperature. STE was applied every 12 hr at a rate of 2.4 cm d⁻¹ (0.6 gal ft⁻² d⁻¹). The soil atmosphere at the mesocosm infiltrative surface mimicked that of a full-scale operating STU trench because the headspace of the first mesocosm (4 cm) was vented to a 30 cm column of dry soil. Vacuum pressure of -7 kPa was used to approximate the suction from underlying unsaturated soil. Water samples were collected periodically in UV-sterilized glass vials from sample ports below the mesocosms using vacuum. One to three mLs of water was collected from each mesocosm per sampling event.

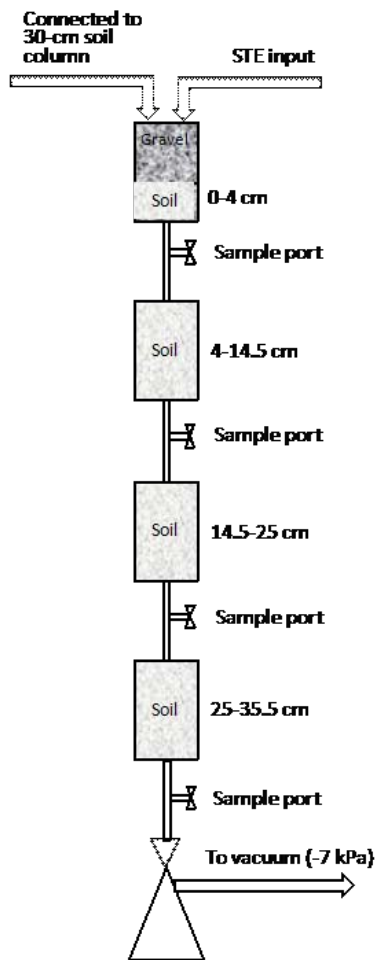


Figure D-1. Experimental Apparatus.

For each soil, column experiments were performed by dosing known quantities of either aqueous phase *E. coli* or MS-2 onto a gravel layer on top of the column. The aqueous phase, spiked with microbial matter, percolated downward through the gravel and the unsaturated soil. The gravel layer mimicked the aggregate fill of a typical onsite wastewater treatment system (OWTS) trench. Over time, a biofilm developed in the uppermost part of the soil column. Dosing experiments were carried out before and after the biofilm matured. Microbial concentrations were measured at three sample ports at 4 cm, 14.5 cm and 25 cm depth (see schematic of experimental apparatus in Figure D-1). Infiltration tests were performed on all three soil column systems to compare the infiltration rate of the various soils before and after biofilm formation. In addition, *E. coli* and MS-2 die-off experiments were conducted to determine the die-off rate constants for the various soil/microbe systems including die-off in the aqueous phase in the absence of any soil materials.

D.1.1.1 *E. coli* Tracer Experiment

A novel strain of *E. coli* (BTF 132) (Biomérieux, Hazelwood, MO) was used as a bacterial tracer in these systems. The strain has a gene for green fluorescent protein (GFP)

inserted into the chromosome. Because the gene is chromosomal and is not easily lost, this GFP-labeled *E. coli* strain is ideal for use as a bacterial tracer. Bacterial colonies formed on agar plates glow green under UV light; therefore, it is possible to differentiate between the bacteria that were added to the mesocosms and native fecal coliform bacteria, which do not fluoresce.

For each bacterial addition experiment, GFP *E. coli* were grown overnight at 37°C in lysogeny broth (LB) then diluted in phosphate-buffered saline (PBS) to $\sim 5 \times 10^6$ cfu mL⁻¹. Approximately 2 mL of the diluted GFP *E. coli* culture was added to each mesocosm over a 37-h period, coincident with each wastewater dose (4 doses total). GFP *E. coli* were enumerated using a standard membrane filtration method (APHA, 2005) with visualization under UV light.

D.1.1.2 Virus Tracer Experiment

For virus addition experiments, bacteriophage MS-2 was used as a tracer. MS-2 is a single-stranded RNA coliphage with a 25-nm diameter and an isoelectric point of 3.9 (Powelson, 1990). *E. coli* strain K12 was used as the host for this bacteriophage. For each addition experiment, MS-2 was diluted in PBS to $\sim 5 \times 10^6$ cfu mL⁻¹ and added as described above for the *E. coli* addition experiment. Bacteriophage were enumerated using the plaque-forming assay of Adams (1959) on LB agar plates, which were incubated for ~ 4 hr at 37°C and then overnight at room temperature before counting of plaques in the host lawn.

D.1.1.3 Bromide Tracer

STE used during the *E. coli* and virus tracer experiments was spiked with bromide (~ 20 mg/l) to determine whether bacterial movement was retarded relative to that of the STE. Bromide concentrations were measured using the method of Lepore and Barak (2009).

D.1.1.4 Survival in Soil and STE Experiment

Experiments were conducted to determine the survival of the tracer strains in soil and STE. For soil, 2 g (air-dry weight) of soil from each of the three soil types was placed in plastic scintillation vials, in triplicate and to allow for multiple sampling events. Prior to use, soil was either air-dried or sterilized (121°C for 60 min on 5 consecutive days). GFP *E. coli* or MS-2 bacteriophage were added to an approximate concentration of 2.4×10^5 cfu(pfu) per gram of soil in 200 μ L of sterile distilled water. Vials were tightly capped and placed in a humidified environment.

For enumeration, 20 mL of either sterile phosphate-buffered saline (for *E. coli*) (Turco, 1994) or sterile 1.5% beef extract, pH 8.7 (for MS-2) (Powelson, 1990) was added to each vial, and vials were placed on a reciprocal shaker for 10 min. GFP *E. coli* and MS-2 bacteriophage were then enumerated as described above.

To determine survival in STE, 4 250-mL polypropylene bottles containing 100 mL of effluent were amended with approximate concentrations of: 1) 4.8×10^2 cfu GFP *E. coli* mL⁻¹; 2) 5.2×10^6 cfu GFP *E. coli* mL⁻¹; 3) 2.3×10^2 pfu MS-2 coliphage mL⁻¹; or 4) 4.4×10^6 pfu MS-2 coliphage mL⁻¹. STE was then incubated at room temperature, in the dark. Samples were analyzed for *E. coli* and MS-2 as described above. Initial concentrations were determined by identical dilutions using PBS in place of STE followed by immediate enumeration. For replication, this experiment was repeated on 3 separate occasions.

D.1.1.5 STE Properties

STE samples were analyzed for dissolved oxygen using the azide modification of the Winkler titration method (APHA, 2005). The pH was determined using a combination pH electrode and a Model UB-10 pH meter (Denver Instruments, Denver, CO). STE was analyzed for fecal coliform bacteria using the standard membrane filtration method (APHA, 2005), and for virus capable of growing on *E. coli* (K12) using the plaque-forming assay of Adams (1959). BOD was determined following the 5-day BOD test (APHA, 2005). Total phosphorous and total nitrogen were measured in STE using the persulfate digestion method (APHA, 2005) followed by colorimetric analysis (Schoenau and Karamanos, 1993; Doane and Horwath, 2003). Results of the STE analyses are provided in Table D-1.

Table D-1. STE Properties for Laboratory Experiments.

Property	Mean (n=23-36)	Maximum	Minimum
BOD ₅ (mg L ⁻¹)	224	383	45
pH	6.82	7.20	6.43
Dissolved oxygen (mg L ⁻¹)	0	0	0
Total phosphorus (mg-P L ⁻¹)	5.8	8.4	1.7
Total nitrogen (mg-N L ⁻¹)	30	52	0
Fecal coliforms (cfu mL ⁻¹)	2.9 x 10 ³	8.7 x 10 ³	1 x 10 ²
Virus (pfu mL ⁻¹)	0	2	0

D.1.2 Experimental Results

D.1.2.1 Evaluation of the Fate of GFP-labeled *E. coli* in STU Mesocosms

Sandy Soil GFP-labeled *E. coli* were added to sandy soil mesocosms two weeks after dosing began at an initial concentration of 4 x 10⁵ cfu mL⁻¹ STE coincident with dosing over a 37-hr period (4 doses). GFP-bacteria levels in water draining from the 4 cm depth peaked at 5.6 x 10⁴ cfu mL⁻¹ at 41 hr and declined to below detection limits (BDL) of 1 cfu mL⁻¹ over approximately 672 hr. GFP-bacteria levels in water draining from 14.5 cm peaked at 3.6 x 10² cfu mL⁻¹ at 41 hr, reaching the detection limit after 360 hr. Water draining from 25 cm reached a maximum level of GFP-bacteria of 1.2 x 10¹ cfu mL⁻¹ at 41 hr, reaching the detection limit after 192 hr (Figure D-2). Tap water (3.9 cm) was added over 3.3 hr to simulate a heavy rainfall/irrigation event 672 hr after commencement of the GFP-labeled *E. coli* experiment. No GFP bacteria were detected in drainage water from the 14.5 cm and 25 cm soil depths during the event and for the subsequent 5 days, and <2 GFP bacteria mL⁻¹ were detected from the 4 cm depth (Figure D-2).

Twenty-six weeks after STE dosing began, GFP-*E. coli* were again added at an initial concentration of 5 x 10⁵ cfu mL⁻¹ STE to examine removal after the formation of a biomat. GFP-bacteria levels in water draining from the 4 cm depth peaked at 6.5 x 10⁴ cfu mL⁻¹ at 41 hr and declined to BDL over approximately 408 hr. GFP-bacteria levels in water draining from 14.5 cm peaked at 2.8 x 10¹ cfu mL⁻¹ at 41 hr, reaching the detection limit after 336 hr. Water draining from 25 cm had levels of GFP-bacteria BDL on all days (Figure D-3).

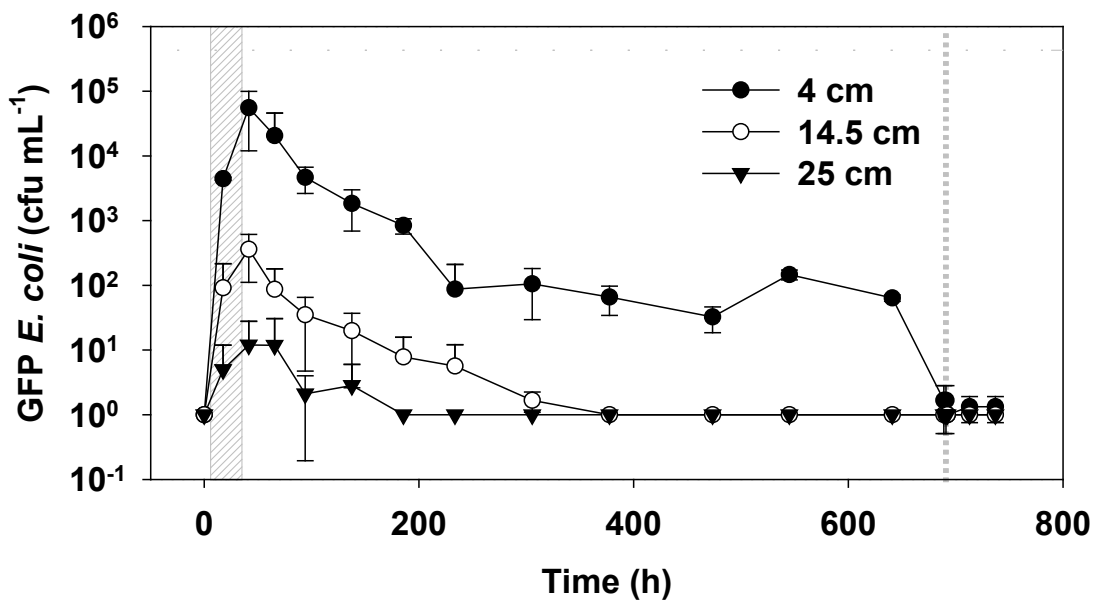


Figure D-2. Mean (n=3) Concentration of GFP *E. coli* in Drainage Water from Sandy Soil (RI) STU Mesocosms Before Biomat Formation.

Bars represent one standard deviation. Shaded area indicates period of bacteria addition. Horizontal dashed line indicates initial concentration of bacteria added. Vertical dotted line indicates addition of tap water. Values ≤ 1 were assigned a value of 1.

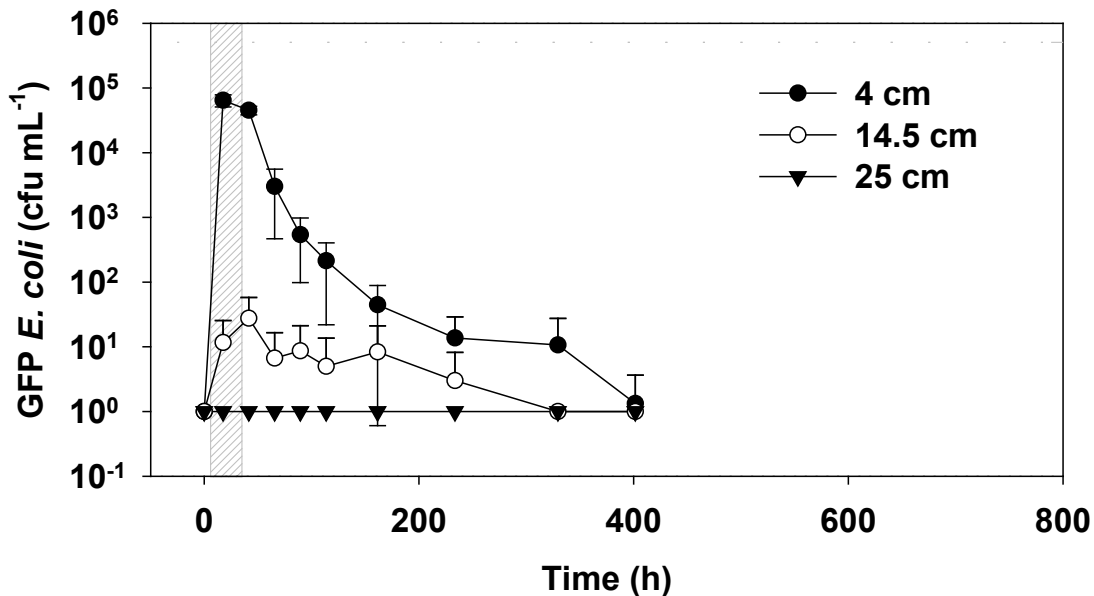


Figure D-3. Mean (n=3) Concentration of GFP *E. coli* in Drainage Water from Sandy Soil (RI) STU Mesocosms After Biomat Formation.

Bars represent one standard deviation. Shaded area indicates period of bacteria addition. Horizontal dashed line indicates initial concentration of bacteria added. Values ≤ 1 were assigned a value of 1.

Sandy Loam Soil GFP-labeled *E. coli* were added to sandy loam soil mesocosms two weeks after STE dosing began at an initial concentration of 6×10^6 cfu mL⁻¹ STE as previously

described. At 41 hr, GFP *E. coli* levels draining from the 4 cm depth peaked at 1.1×10^6 cfu mL⁻¹ and levels from the 14.5 cm depth peaked at 3.7×10^4 ; levels from the 25 cm depth peaked at 6.0×10^2 at 65 hr (Figure D-4). Detection limits were reached by 714, 498, and 402 hr, for the mesocosm depths, respectively. The simulated rainfall experiment was conducted 714 hr after the initial addition of *E. coli*. No GFP-labeled *E. coli* were observed exiting any of the mesocosms.

The addition experiment was repeated 20 weeks after STE dosing with GFP-labeled *E. coli* at an initial concentration of 4×10^5 cfu mL⁻¹ STE. GFP *E. coli* levels peaked at 41hr at 2.2×10^5 cfu mL⁻¹ in water draining from the 4 cm depth, reaching the detection limit by 402 hr, and at 7.4×10^4 cfu mL⁻¹ in water draining from the 14.5 cm depth, also reaching the detection limit by 402 hr. At 65 hr, levels peaked at 5.7×10^3 cfu mL⁻¹ in water draining from the 25 cm depth (Figure D-5), and the detection limit was reached by 114 hr.

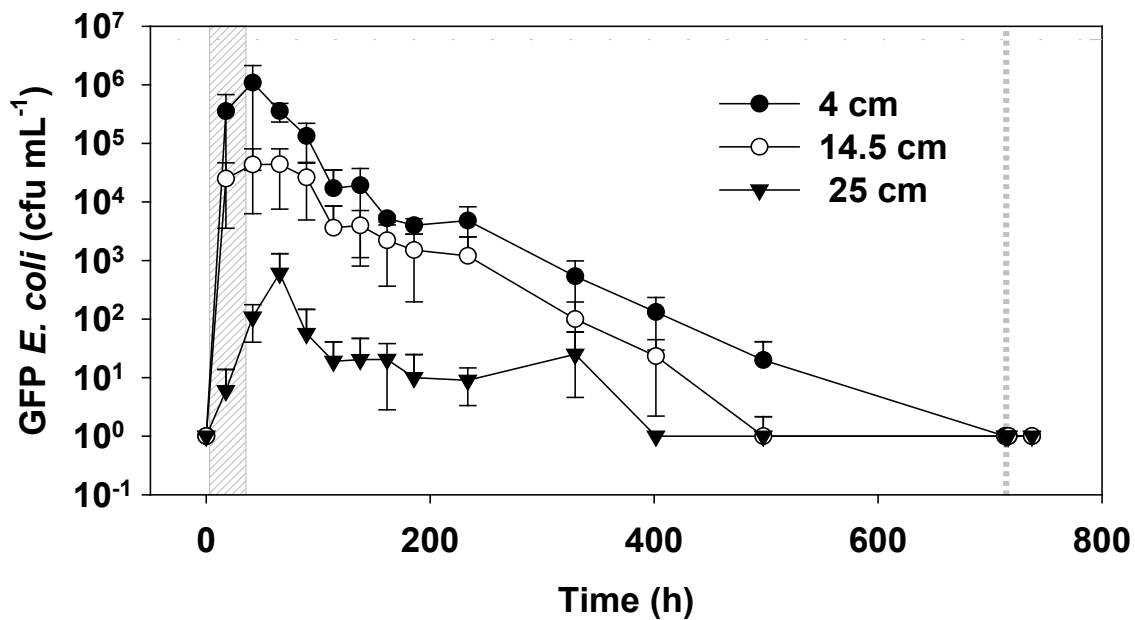


Figure D-4. Mean (n=3) Concentration of GFP *E. coli* in Drainage Water from Sandy Loam Soil (CO) STU Mesocosms Before Biomat Formation.

Bars represent one standard deviation. Shaded area indicates period of bacteria addition. Horizontal dashed line indicates initial concentration of bacteria added. Vertical dotted line indicates addition of tap water. Values ≤ 1 were assigned a value of 1.

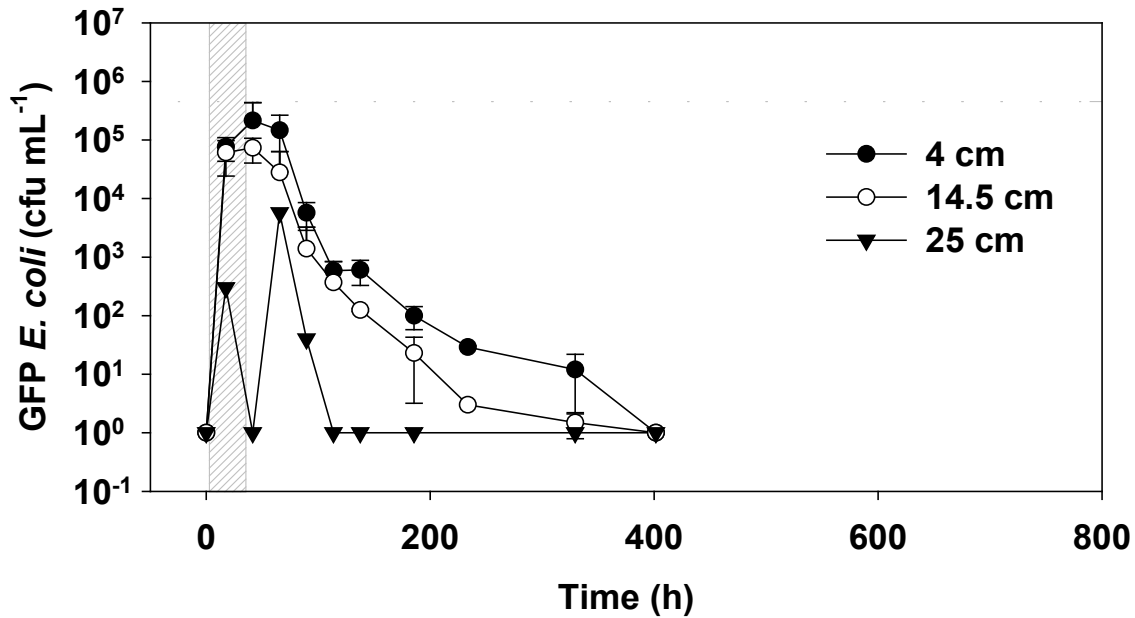


Figure D-5. Mean (n=3) Concentration of GFP *E. coli* in Drainage Water from Sandy Loam Soil (CO) STU Mesocosms After Biomat Formation.

Bars represent one standard deviation. Shaded area indicates period of bacteria addition.

Horizontal dashed line indicates initial concentration of bacteria added. Values ≤ 1 were assigned a value of 1.

Clay Loam Soil Two weeks after STE dosing began in the clay loam soil, GFP *E. coli* were added at an initial concentration of 3×10^5 cfu mL⁻¹ STE. GFP *E. coli* levels in water draining from the 4 cm depth reached a maximum of 2.0×10^5 at 37 hr, and levels in water draining from the 14.5 cm depth reached a maximum of 1.0×10^5 at 13 hr. GFP bacteria were never observed in water from the 25 cm depth (Figure D-6). The detection limits for 4 and 14.5 cm depths were reached by 469 and 349 hr, respectively. The simulated rainfall experiment was conducted 480 hr after the initial bacteria addition and, again, no GFP-labeled *E. coli* were observed exiting any of the mesocosms.

The GFP *E. coli* addition experiment was repeated 20 weeks after STE dosing began. Water draining from all depths reached maximums of 4.2×10^3 for 4 cm, 3.8×10^2 for 14.5 cm, and 5.3×10^1 for 25 cm at 37 hr (Figure D-7) and reached the detection limit by 661 hr for the 4 cm and 14.5 cm mesocosms, and 61 hr for the 25 cm mesocosm.

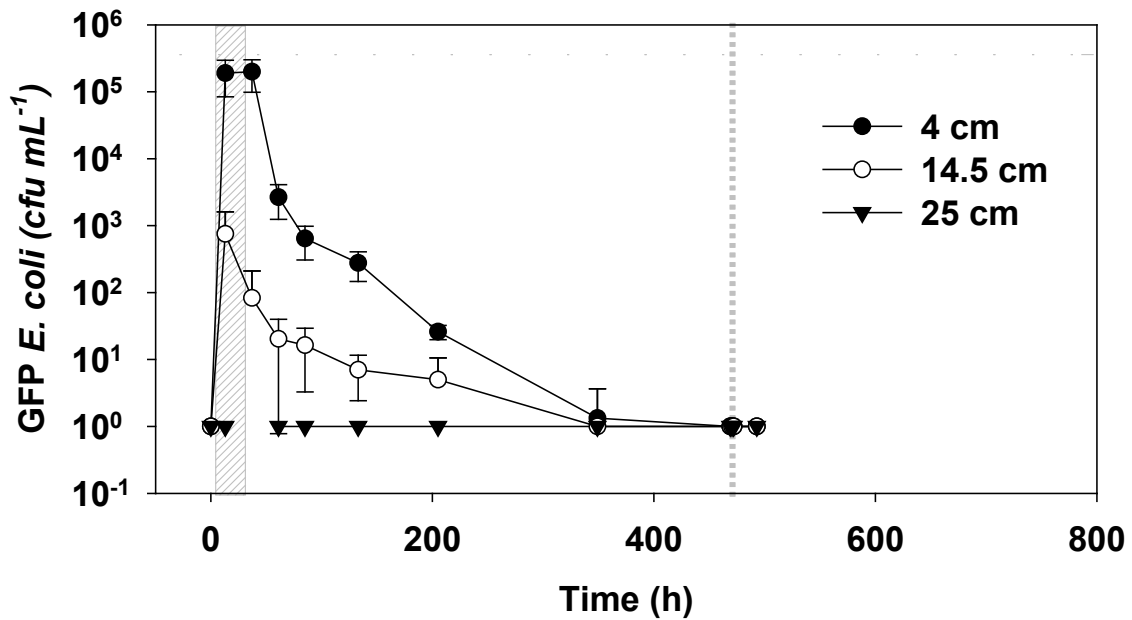


Figure D-6. Mean (n=3) Concentration of GFP *E. coli* in Drainage Water from Clay Loam Soil (GA) STU Mesocosms Before Biomat Formation.

Bars represent one standard deviation. Shaded area indicates period of bacteria addition. Horizontal dashed line indicates initial concentration of bacteria added. Vertical dotted line indicates addition of tap water. Values ≤ 1 were assigned a value of 1.

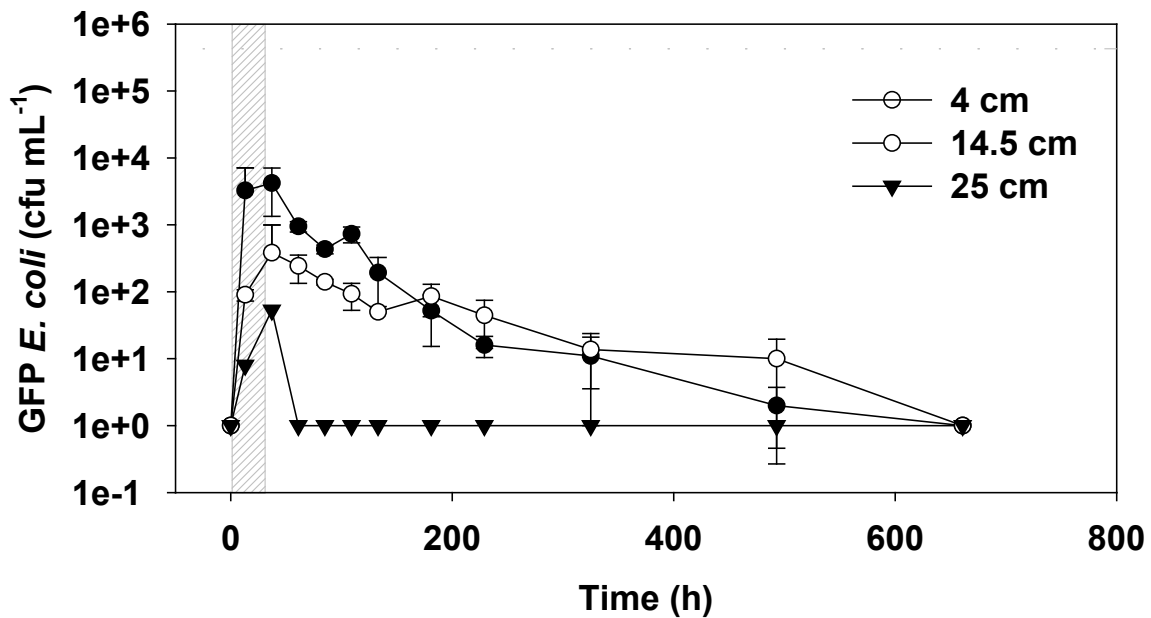


Figure D-7. Mean (n=3) Concentration of GFP *E. coli* in Drainage Water from Clay Loam Soil (GA) STU Mesocosms After Biomat Formation.

Bars represent one standard deviation. Shaded area indicates period of bacteria addition. Horizontal dashed line indicates initial concentration of bacteria added. Values ≤ 1 were assigned a value of 1.

D.1.2.2 Evaluation of the Fate of MS-2 Coliphage in STU Mesocosms

Sandy Soil MS-2 coliphage was added to the mesocosms at an initial concentration of 3×10^5 pfu mL⁻¹ STE coincident with dosing over a 37-hr period. A maximum of 1.1×10^3 pfu mL⁻¹ were observed leaving the 4 cm depth at 41 hr (Figure D-8) and declined to the detection limit by 689 hr. Four coliphage per mL⁻¹ were detected in one replicate at the 14.5 cm depth four days after the addition, and no coliphage were detected in the 25 cm drainage water at any time. Tap water was added to the mesocosms 528 hr after the initial addition of coliphage, and a slight increase in virus concentration leaving the 4 cm mesocosm was seen at 1.5 hr.

MS-2 coliphage was again added to the sandy soil mesocosms 29 weeks after STE dosing began at an initial concentration of 2×10^5 pfu mL⁻¹ STE coincident with STE dosing over a 37-hr period. Coliphage levels peaked at 5.4×10^2 at 17 hr in water draining from the 4 cm mesocosm depth, and the detection limit was reached by 306 hr. Coliphage were only detected at 41 hr at a level of 1.7×10^1 pfu mL⁻¹ in water draining from the 14.5 cm depth and were never observed exiting the 25 cm mesocosm (Figure D-9).

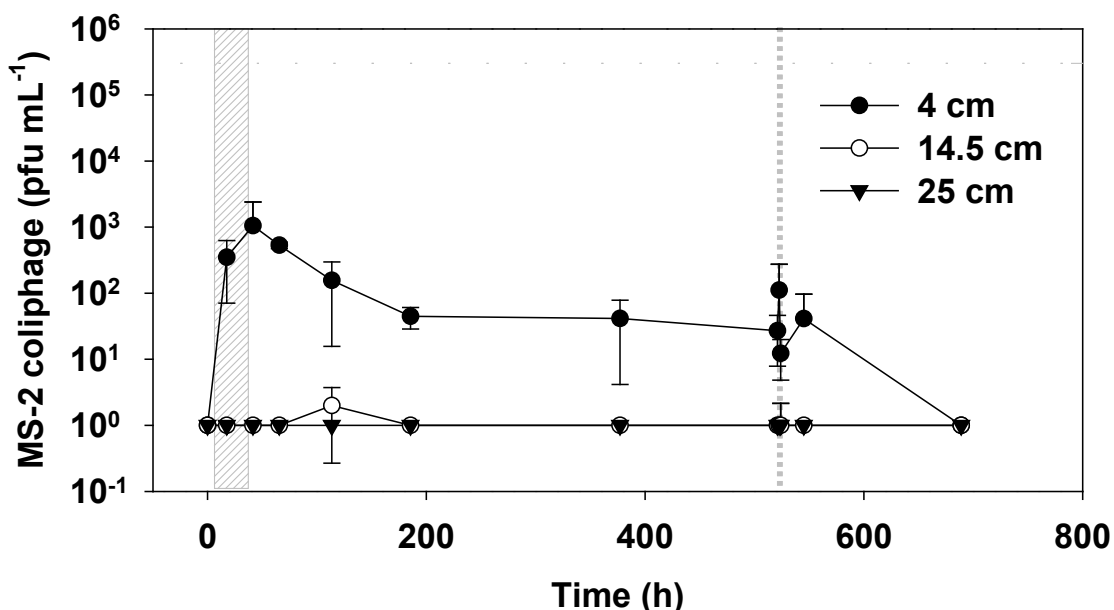


Figure D-8. Mean (n=3) Concentration of MS-2 Coliphage in Drainage Water from Sandy Soil (RI) STU Mesocosms Before Biomat Formation.

Bars represent one standard deviation. Shaded area indicates period of bacteria addition. Horizontal dashed line indicates initial concentration of bacteria added. Vertical dotted line indicates addition of tap water. Values ≤ 1 were assigned a value of 1.

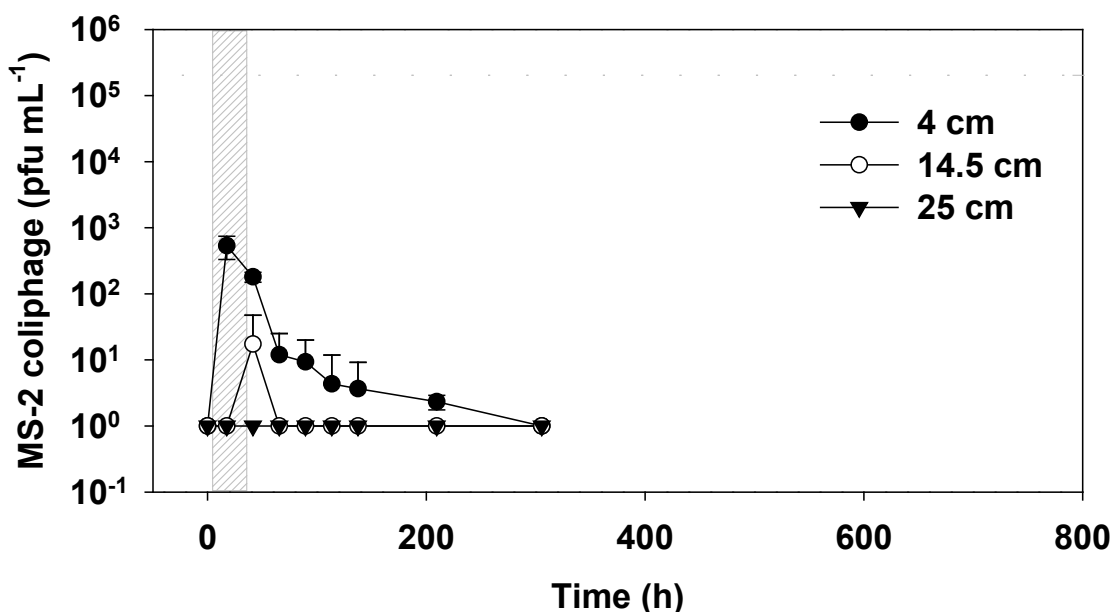


Figure D-9. Mean (n=3) Concentration of MS-2 Coliphage in Drainage Water from Sandy Soil (RI) STU Mesocosms After Biomat Formation.

Bars represent one standard deviation. Shaded area indicates period of bacteria addition. Horizontal dashed line indicates initial concentration of bacteria added. Vertical dotted line indicates addition of tap water. Values ≤ 1 were assigned a value of 1.

Sandy Loam Soil Coliphage was added to the sandy loam soil mesocosms eight weeks and 23 weeks after STE dosing began. MS-2 coliphage was added at a concentration of 2×10^5 pfu mL⁻¹ STE 192 hr after STE dosing began. At 17 hr, virus levels from the 4 cm depth peaked at 6.8×10^2 pfu mL⁻¹ drainage water declining to BDL by 426 hr. Levels from the 14.5 cm depth peaked at 7.0×10^1 pfu mL⁻¹ at 41 hr and reached the detection limit by 90 hr; virus concentrations above the detection limit were not observed in water from the 25 cm depth (Figure D-10). Tap water (3.9 cm) was added 312 hr after the addition experiment began and an increase in virus concentrations in drainage water was not observed.

After the formation of a biomat (23 weeks), coliphage was again added at a concentration of 2.9×10^5 pfu mL⁻¹ STE. Virus concentrations reached a maximum of 1.1×10^3 pfu mL⁻¹ at 13 hr in drainage water from the 4 cm depth, reaching the detection limit by 254 hr; 6.5×10^2 pfu mL⁻¹ at 37 hr in drainage water from the 14.5 cm depth, again reaching the detection limit by 254 hr; and no coliphage were observed from the 25 cm depth at any time (Figure D-11).

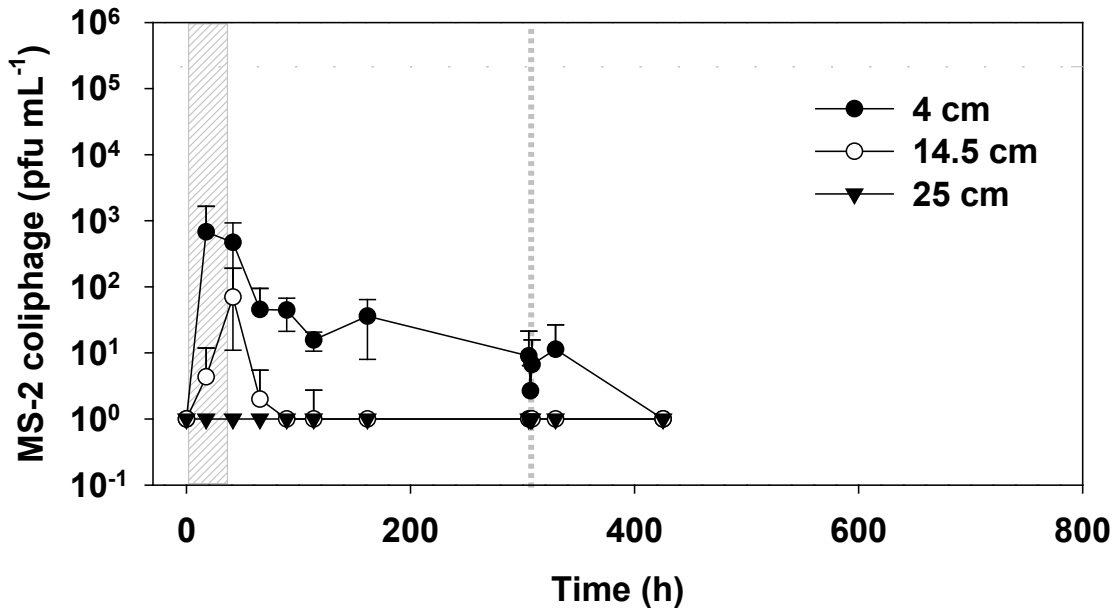


Figure D-10. Mean (n=3) Concentration of MS-2 Coliphage in Drainage Water from Sandy Loam Soil (CO) STU Mesocosms Before Biomat Formation.

Bars represent one standard deviation. Shaded area indicates period of bacteria addition. Horizontal dashed line indicates initial concentration of bacteria added. Vertical dotted line indicates addition of tap water. Values ≤ 1 were assigned a value of 1.

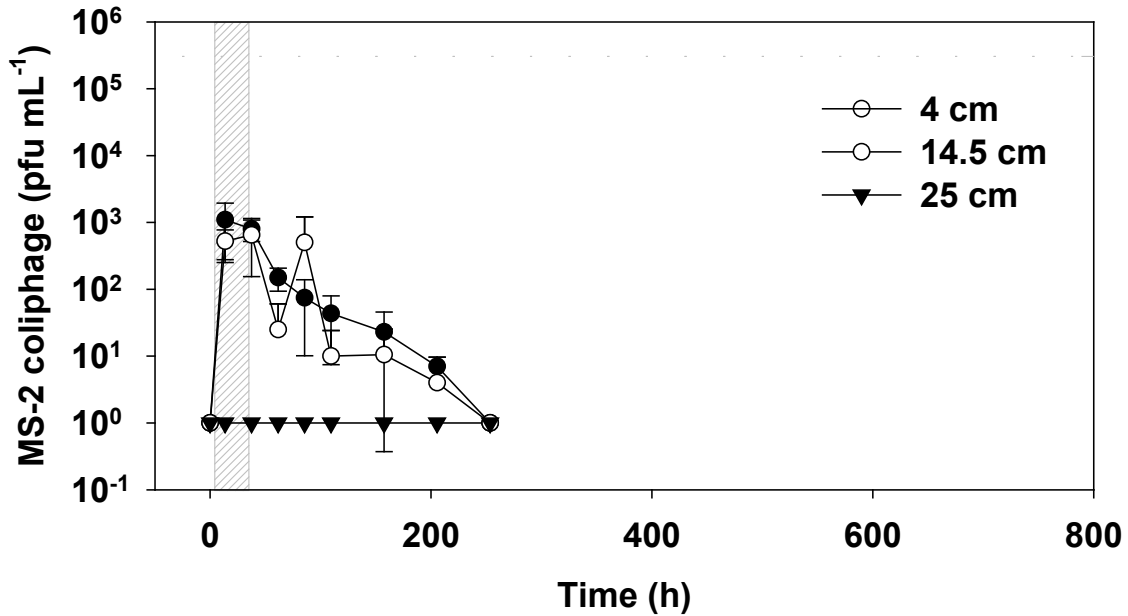


Figure D-11. Mean (n=3) Concentration of MS-2 Coliphage in Drainage Water from Sandy Loam Soil (CO) STU Mesocosms After Biomat Formation.

Bars represent one standard deviation. Shaded area indicates period of bacteria addition. Horizontal dashed line indicates initial concentration of bacteria added. Vertical dotted line indicates addition of tap water. Values ≤ 1 were assigned a value of 1.

Clay Loam Soil Coliphage was added at a concentration of 2.8×10^5 pfu mL⁻¹ STE 5 weeks after STE dosing began in the clay loam soil. A maximum level of 2.4×10^2 pfu mL⁻¹ in water

draining from the 4 cm mesocosm was reached 13 hr after dosing began, reaching the detection limit by 350 hr. An average of 2 pfu mL⁻¹ was observed at 13 hr in water draining from the 14.5 cm mesocosm. At all other times, coliphage levels remained BDL. Coliphage was not observed exiting from the 25 cm depth at any time (Figure D-12). Tap water was added 360 hr after coliphage addition, but no coliphage was observed exiting the mesocosms.

Twenty-three weeks after STE dosing began, MS-2 coliphage was again added at a concentration of 1.8 x 10⁵ pfu mL⁻¹ STE. Maximum concentrations of 1.4 x 10² and 4 pfu mL⁻¹ were reached at 37 hr in drainage water from 4 cm and 14.5 cm respectively. Coliphage was never observed exiting the 25 cm mesocosm depth, and by 61 hr concentrations exceeding the detection limit were not observed in any depth (Figure D-13).

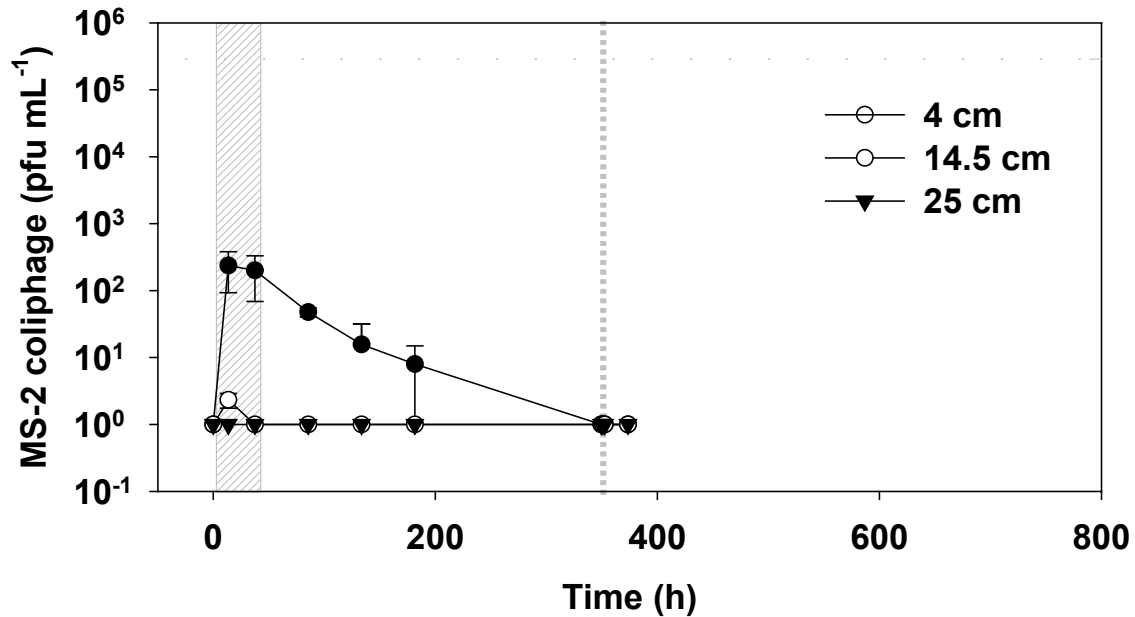


Figure D-12. Mean (n=3) Concentration of MS-2 Coliphage in Drainage Water from Clay Loam Soil (GA) STU Mesocosms Before Biomat Formation.

Bars represent one standard deviation. Shaded area indicates period of bacteria addition. Horizontal dashed line indicates initial concentration of bacteria added. Vertical dotted line indicates addition of tap water. Values ≤1 were assigned a value of 1.

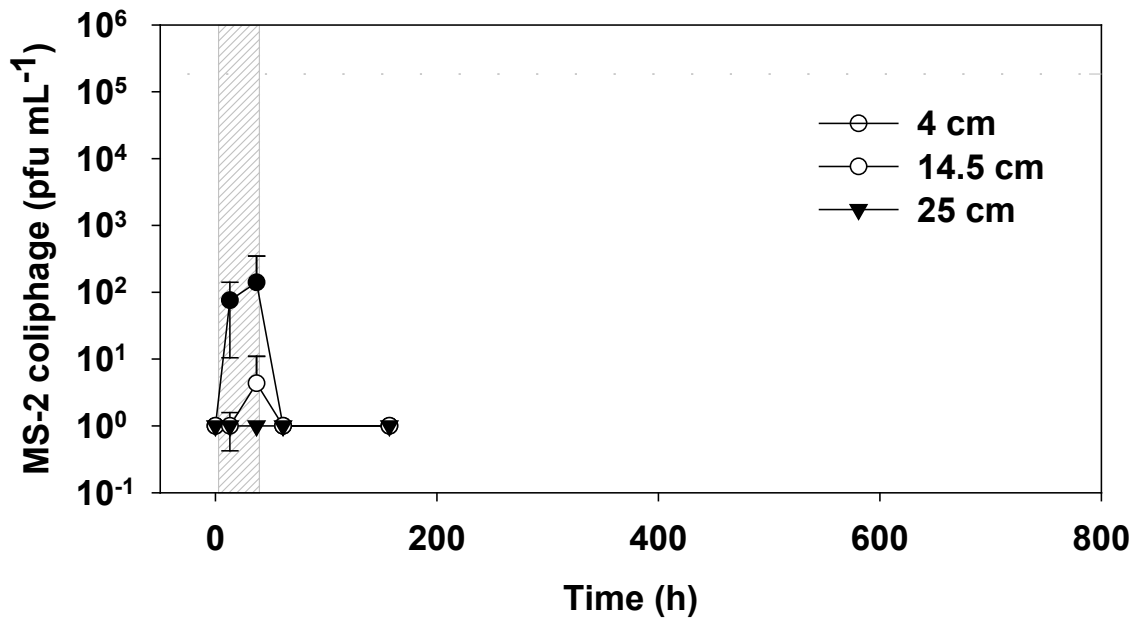


Figure D-13. Mean (n=3) Concentration of MS-2 Coliphage in Drainage Water from Clay Loam Soil (GA) STU Mesocosms After Biomat Formation.

Bars represent one standard deviation. Shaded area indicates period of bacteria addition. Horizontal dashed line indicates initial concentration of bacteria added. Vertical dotted line indicates addition of tap water. Values ≤ 1 were assigned a value of 1.

D.1.2.3 Survival of GFP *E. coli* in Soil and STE

Sandy Soil GFP *E. coli* were added to sandy soil at an initial concentration of 2.2×10^4 cfu per gram of soil. Immediate extraction and enumeration (Day=0) yielded concentrations of 6.8×10^3 cfu g⁻¹ soil in non-sterile soil and 4.2×10^3 cfu g⁻¹ soil in sterile soil (Figure D-14). Concentrations of GFP *E. coli* then declined to BDL of 10 cfu g⁻¹ soil over 16 days in non-sterile soil. In sterile soil detection limits were reached on Days 3 and 6, but on Day 9 concentrations increased to 9×10^1 cfu g⁻¹ soil, declining again to BDL by Day 16.

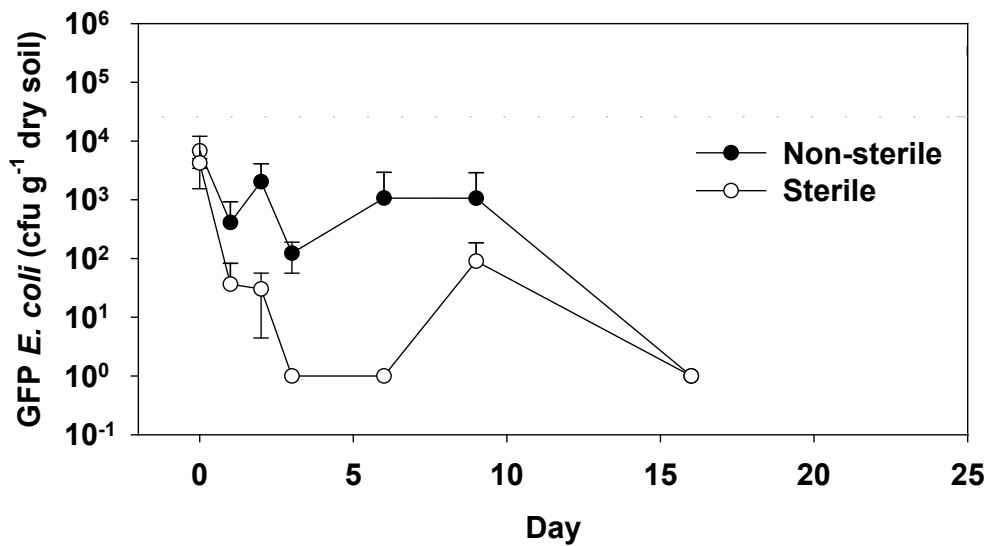


Figure D-14. Mean (n=3) Concentration of GFP *E. coli* Surviving in Sterile and Non-sterile Sandy Soil (RI). Bars represent one standard deviation. Horizontal dashed line indicates initial concentration of bacteria added. Values ≤ 10 were assigned a value of 1.

Sandy Loam Soil Sandy loam soil was amended with GFP *E. coli* at an initial concentration of 1.2×10^6 cfu g⁻¹ soil. Initial extraction on Day 0 yielded concentrations of 4.5×10^5 cfu g⁻¹ non-sterile soil and 3.7×10^5 cfu g⁻¹ sterile soil (Figure D-15). GFP *E. coli* concentrations in non-sterile soil declined steadily to 1.2×10^2 cfu g⁻¹ soil over 21 days, while concentrations in sterile soil increased to 6.8×10^7 cfu g⁻¹ soil by Day 4, remaining above 10^6 cfu g⁻¹ soil over the 21-day sampling period.

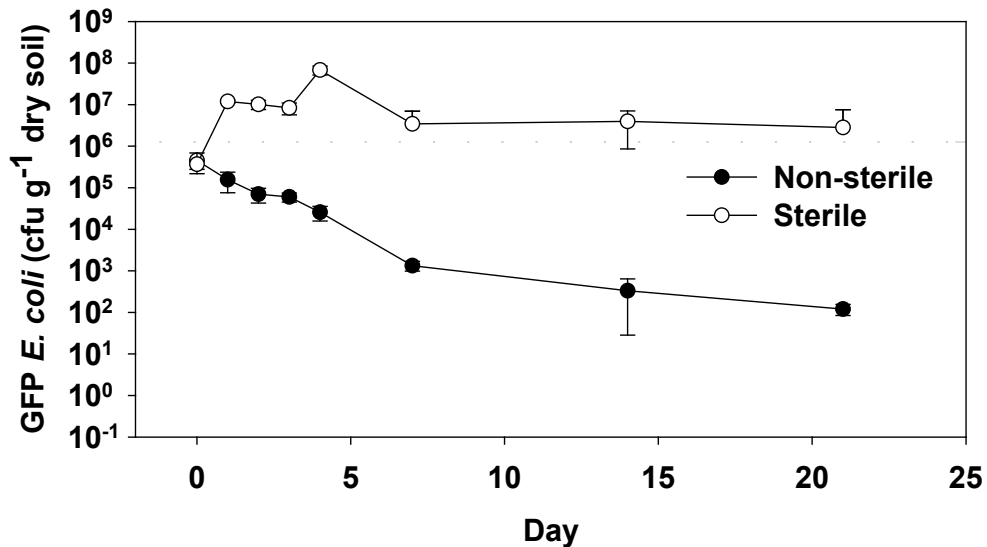


Figure D-15. Mean (n=3) Concentration of GFP *E. coli* Surviving in Sterile and Non-sterile Sandy Loam Soil (CO). Bars represent one standard deviation. Horizontal dashed line indicates initial concentration of bacteria added. Values ≤ 10 were assigned a value of 1.

Clay Loam Soil Fluorescent *E. coli* were added to clay loam soil at an initial concentration of 1.4×10^5 cfu g⁻¹ soil, with immediate extraction yielding only 5.3×10^1 cfu g⁻¹ on-sterile soil and 3.3×10^1 cfu g⁻¹ sterile soil (Figure D-16). Concentrations BDL were seen in both soils on Days 1 and 2.

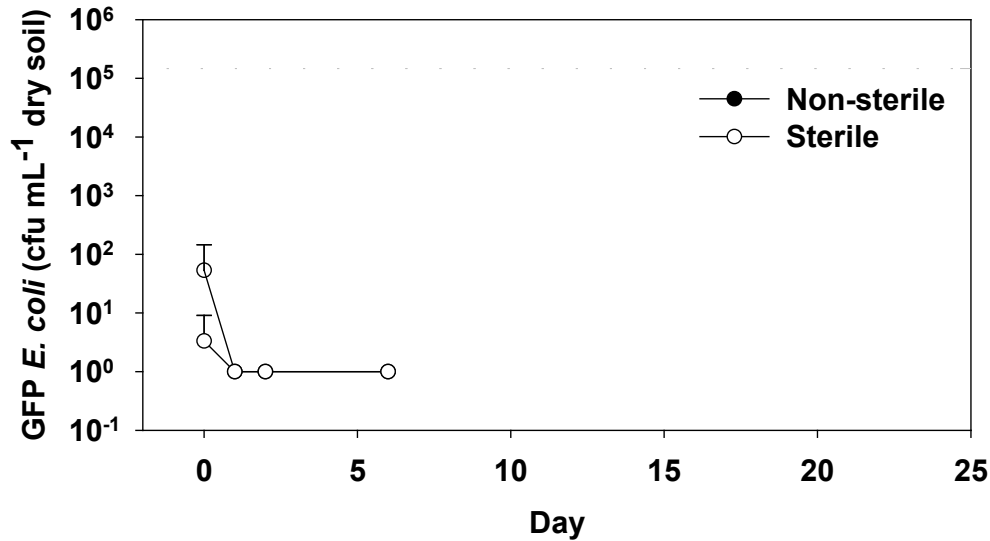


Figure D-16. Mean (n=3) Concentration of GFP *E. coli* Surviving in Sterile and Non-sterile Clay Loam Soil (GA).
 Bars represent one standard deviation.
 Horizontal dashed line indicates initial concentration of bacteria added.
 Values ≤ 10 were assigned a value of 1.

STE STE was amended with GFP *E. coli* at initial concentrations of 4.8×10^2 cfu mL⁻¹ or 5.2×10^6 cfu mL⁻¹. Immediate enumeration (Day 0) produced concentrations close to initial levels (Figure D-17). In the treatment with lower concentration, GFP *E. coli* declined to BDL by Day 3, while the higher concentration treatment declined to 1.6×10^1 cfu mL⁻¹ by Day 10.

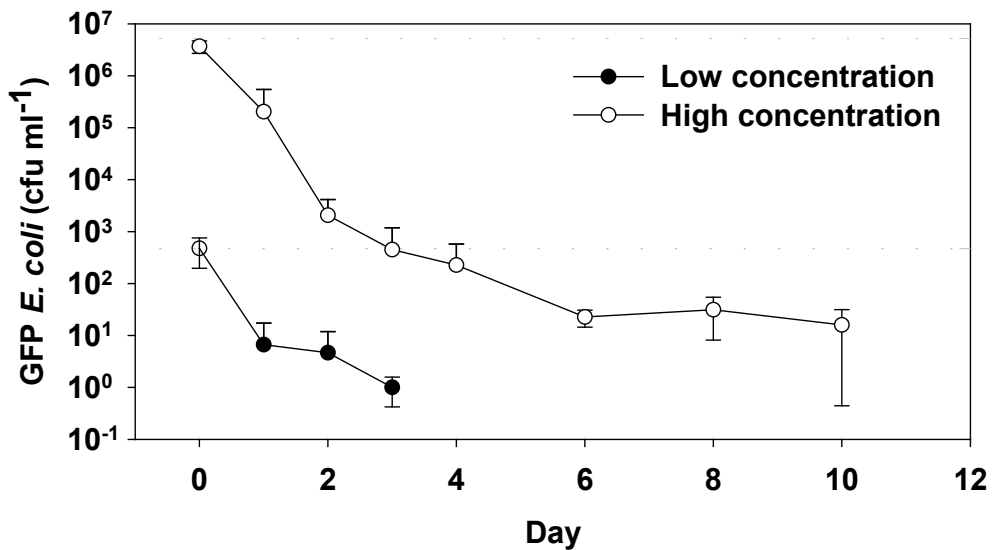


Figure D-17. Mean (n=3) Concentration of GFP *E. coli* Surviving in Wastewater When Added at Different Concentrations. Bars represent one standard deviation. Horizontal dashed lines indicate initial concentrations of bacteria added. Values ≤ 1 were assigned a value of 1.

D.1.2.4 Survival of MS-2 Coliphage in Soil and STE

Sandy Soil MS-2 coliphage were added to sandy soil at an initial concentration of 1.0×10^4 pfu g⁻¹ soil. Extraction and enumeration at Day 0 gave concentrations of 3.8×10^3 pfu g⁻¹ non-sterile soil and 2.0×10^3 pfu g⁻¹ sterile soil, declining to BDL of 10 pfu g⁻¹ soil in both treatments on Day 1 (Figure D-18). However, Days 2 and 3 had concentration of MS-2 coliphage on the order of 10² pfu g⁻¹ soil, declining again to BDL by Day 8.

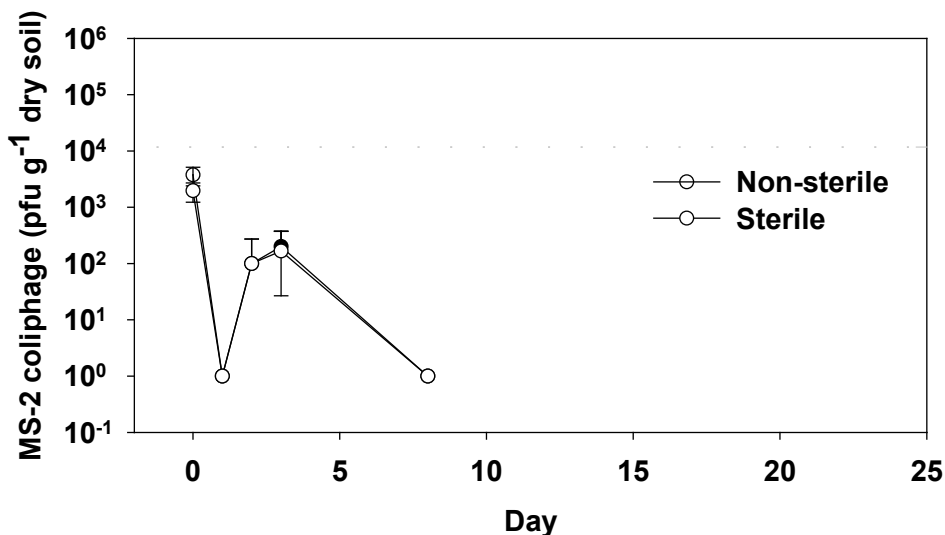


Figure D-18. Mean (n=3) Concentration of MS-2 Coliphage Surviving in Sterile and Non-sterile Sandy Soil (RI). Bars represent one standard deviation. Horizontal dashed line indicates initial concentration of bacteria added. Values ≤ 10 were assigned a value of 1.

Sandy Loam Soil Coliphage were added to sandy loam soil at an initial concentration of 2.6×10^4 pfu g⁻¹ soil. In sterile soil only 2.7×10^2 pfu g⁻¹ soil were immediately extractable, while in non-sterile soil, 5.6×10^3 pfu g⁻¹ soil were immediately extractable (Figure D-19). By Day 21, sterile soil contained 1.5×10^3 pfu g⁻¹ soil, and non-sterile soil contained 1.7×10^2 pfu g⁻¹ soil.

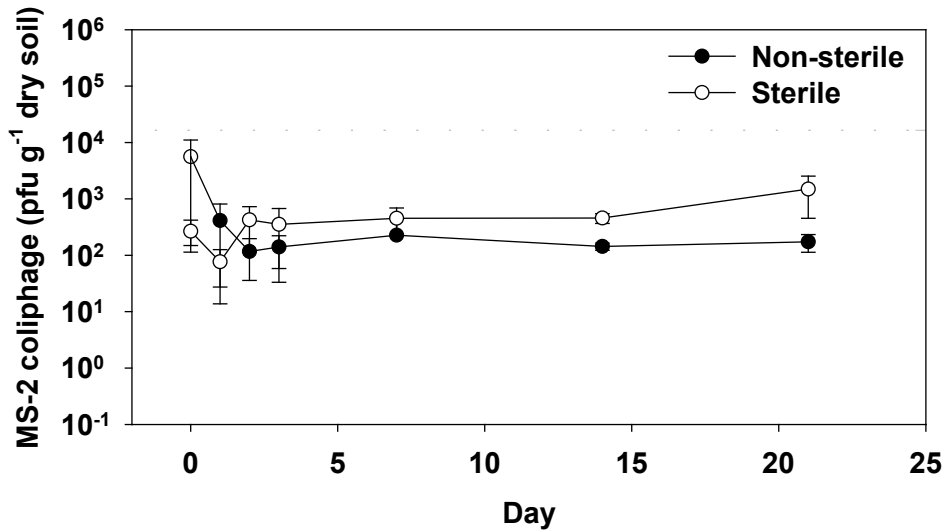


Figure D-19. Mean (n=3) Concentration of MS-2 Coliphage Surviving in Sterile and Non-sterile Sandy Loam Soil (CO). Bars represent one standard deviation. Horizontal dashed line indicates initial concentration of bacteria added. Values ≤ 10 were assigned a value of 1.

Clay Loam Soil MS-2 coliphage were added to clay loam soil at an initial concentration of 2.4×10^4 pfu g⁻¹ soil. Immediate extraction yielded concentrations of 9.7×10^2 pfu g⁻¹ non-sterile soil and 1.9×10^4 pfu g⁻¹ sterile soil (Figure D-20). Concentrations BDL were seen on all subsequent days.

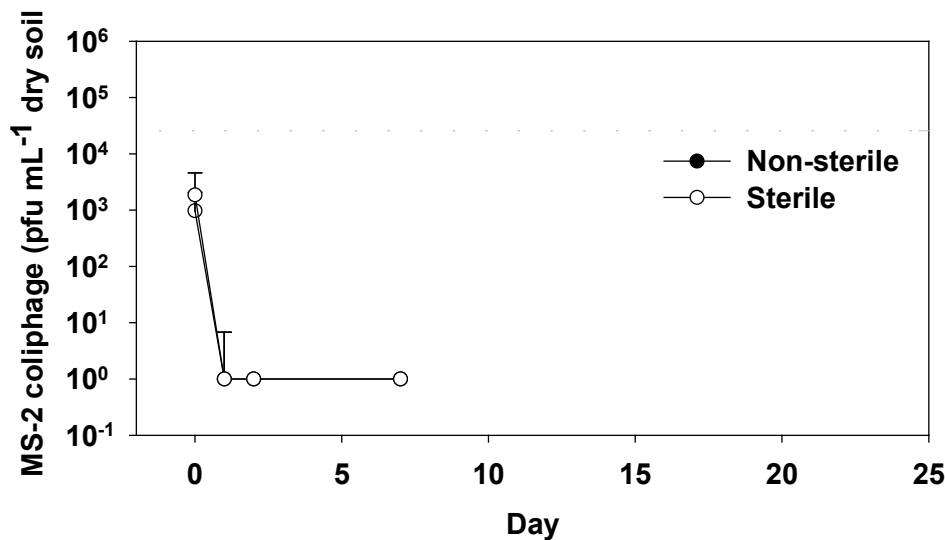


Figure D-20. Mean (n=3) Concentration of MS-2 Coliphage Surviving in Sterile and Non-sterile Clay Loam Soil (GA). Bars represent one standard deviation. Horizontal dashed line indicates initial concentration of bacteria added. Values ≤ 10 were assigned a value of 1.

STE Coliphage was added to *STE* at concentrations of 2.3×10^2 pfu mL⁻¹ and 4.4×10^6 pfu mL⁻¹. Immediate enumeration gave concentrations BDL for the low initial concentration and of 5.0×10^3 for the higher initial concentration (Figure 21). Concentrations of coliphage increased after Day 0 in the low concentration treatment but remained below 1.3×10^1 cfu mL⁻¹. In the high concentration treatment, coliphage increased by Day 2 to 3.0×10^5 , decreasing afterwards to 4.3×10^3 by Day 10.

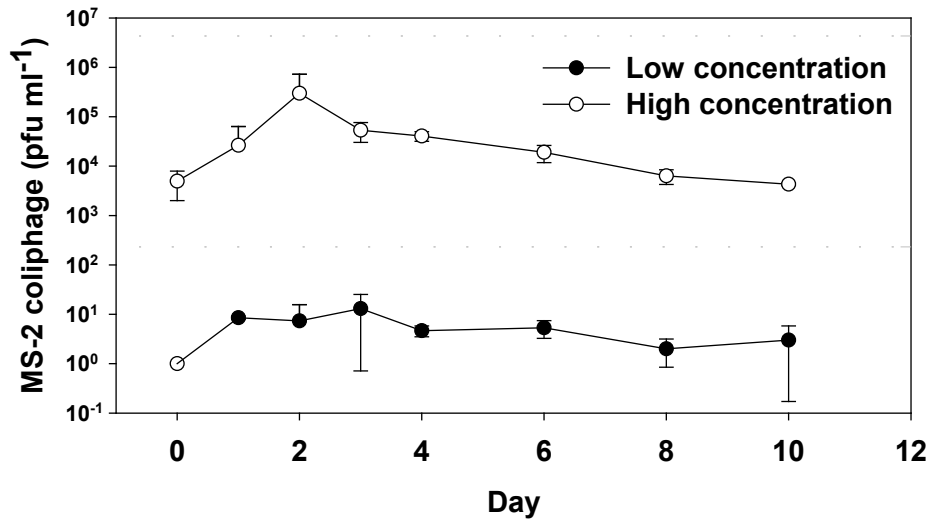


Figure D-21. Mean (n=3) Concentration of MS-2 Coliphage Surviving in Wastewater When Added at Different Concentrations.

Bars represent one standard deviation. Horizontal dashed lines indicate initial concentrations of coliphage added. Values ≤ 1 were assigned a value of 1.

D.1.3 Summary

Table D-2 shows the measured infiltration rates (cm min⁻¹) of the three soils before and after biofilm formation. These tests were conducted by applying the same volume of water at the same rate as during the dosing of the columns with microbial matter. The infiltration rate prior to the formation of a biofilm was lower for the sandy soil from RI (0.35 cm min⁻¹) than for the structured clay loam from GA (5.92 cm min⁻¹). No tests were carried out with the CO sandy loam. The measured infiltration rates for sandy soil from RI prior to the biofilm formation are similar to literature values (van Genuchten, 1980) (Table D-1). However, the structured clay loam soil from GA exhibited a measured infiltration rate three order of magnitude higher than the literature value. This difference is likely due to observed macroscopic heterogeneities in the structured clay that provide preferential pathways for the aqueous phase.

After the biofilm matured the infiltration rate decreased between 2 and 16 times in order from GA clay loam to CO sandy loam to RI sand. The largest decrease was observed in the soil that apparently had the highest initial infiltration rate (i.e., sandy soil from RI).

Table D-2. Experimentally Determined Infiltration Rates (cm min⁻¹) and Literature Values.

Reported are averages of three tests, after Van Genuchten (1980).

Infiltration Rate Tests	RI	CO	GA
Before biofilm developed	0.347	NA	5.92
After biofilm matured	0.022	0.70	2.65
Literature	0.447	0.027	0.006

The magnitude of the naturally occurring decay of the microbe concentration is expressed by the first-order die-off rate (hr⁻¹). The results of the die-off experiments are summarized in Table D-3. According to these results, *E. coli* die-off progressed fastest in the clay loam from GA and is about one order of magnitude slower in the sandy loam from CO. The die-off rate in the sandy soil from RI is about five times lower than the GA soil and similar to the die-off rate in septic tank effluent (STE) that was not in contact to any soil.

In case of MS-2 coliphage, the fastest die-off was again measured in the GA soil, followed by the soils from CO and RI. The die-off in STE was the slowest. Relative to each other, *E. coli* and MS-2 die-off rates in each soil were similar. These findings indicate that microbes, particularly viruses, must be expected to survive in greater numbers in the aqueous STE phase. However, once in contact with the soil, both virus and bacteria die-off accelerates. Overall, of all three soils tested the GA clay loam is most effective in removing microbial matter.

Table D-3. Results of the *E. coli* and MS-2 Die-off Experiments.

Experimental Condition	Rate (hr ⁻¹)	Coefficient of Determination (R ²)
<i>E. coli</i>		
RI-soil	-0.0617	0.791
CO-soil	-0.0298	0.965
GA-soil	-0.2476	0.965
STE	-0.0824	0.891
MS-2		
RI-soil	-0.0425	0.738
CO-soil	-0.0731	0.869
GA-soil	-0.2101	0.958
STE	-0.0271	0.665

Inspection of the column experimental data plotted with time reveals the following:

- ◆ *E. coli* and MS-2 concentrations decreased with depth by at least 2 to 3 orders of magnitude.
- ◆ In the presence of a mature biofilm, MS-2 concentrations at 25 cm depth were BDL in all three soils.
- ◆ In sandy soil from RI, *E. coli* concentrations declined much more rapidly after the biofilm layer matured. In the other two soils, there was little difference between experiment before and after biofilm formation.

Probably the most important observation from the column tests is that the virus (MS-2 coliphage) concentrations in all three soils were BDL at 25 cm depth level, whereas bacteria still eluted from the soils. It is evident that the design of STUs should primarily focus on bacteria removal as those appear to be transported farther downwards than viruses. Hence, the following analysis with the HYDRUS software package concentrates on the transport and fate of bacteria.

D.2 Modeling Laboratory Experiments with HYDRUS

HYDRUS versions are available for one-, two- and three-dimensional transport modeling, including simulation of microbial transport and fate processes, such as the transport of viruses, colloids, and/or bacteria by either attachment/detachment theory or filtration theory. The hydraulics of each column system were first described using the CXTFIT 2.1 model (Toride et al., 1995) to obtain the flow field dispersivity and the aqueous phase flow velocity from the breakthrough curve of a conservative tracer (potassium bromide). The results of the microbe transport and fate studies were then modeled using the HYDRUS (Ver. 1.10) software package (Šimůnek et al., 2006).

D.2.1 Model Domain

The modeling effort using HYDRUS was a step-by-step process. First, a 2D columnar hydraulic model domain was developed. This model closely resembled the experimental conditions of the *E. coli* and MS-2 coliphage column experiments described in Section D.1. That is, the model boundary on top of the flow domain was open to the atmosphere, permitting pulsed injections of microbial and conservative tracer (bromide) into an initially unsaturated columnar environment. The bottom boundary was set at a fixed negative pressure head (-70 cm) to simulate drainage into the unsaturated zone beneath. No-flux boundaries define the system everywhere else. The flow and transport through soil was modeled either with or without a 4 cm thick biofilm/gravel layer on top. The properties of the porous materials were obtained from the HYDRUS soil catalog (van Genuchten, 1980). Based on literature data, the diameter of *E. coli* was set at 1.1 μm and 0.025 μm for the MS-2 coliphage.

The model was calibrated using the conservative tracer (bromide) breakthrough curves. Figure D-22 illustrates the bromide results for sandy soil from RI for the fit obtained for each of the three soil column depth intervals sampled (0-4 cm, 4-10.5 cm, and 10.5-25 cm). The code CXTFIT 2.1 was used to determine the column system dispersivity (λ). The model was then fitted to the experimental bacteria and virus transport data using the HYDRUS attachment/detachment module.

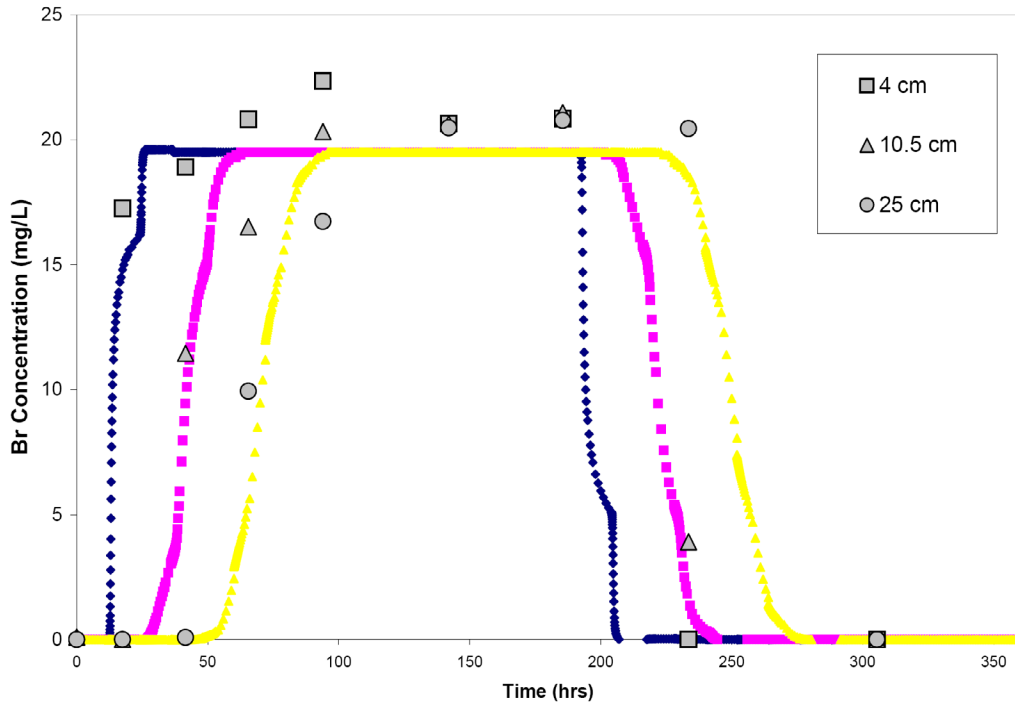


Figure D-22. Bromide Tracer Test Results for Sandy Soil (RI) and Best Fit Obtained for Each of the Three Soil Column Depth Intervals (0-4 cm, 4-10.5 cm, and 10.5-25 cm).

D.2.2 Attachment-Detachment Model

Virus and bacteria transport and fate models commonly employ a modified form of the convection-dispersion equation (Šimůnek et al., 2006). In this study the mass balance equation for these applications is:

$$\frac{\partial \theta c}{\partial t} + \rho \frac{\partial s_e}{\partial t} + \rho \frac{\partial s_l}{\partial t} = \frac{\delta}{\delta t} \left(\theta D_{ij}^w \frac{\delta c}{\delta x_j} \right) - \frac{\delta q_i c}{\delta x_i} - \mu_w \theta c - \mu_s \rho (s_e + s_l) \quad (\text{D.2.2-1})$$

where c and s are the (virus, bacteria) solution concentration [$N_c \text{ L}^{-3}$] and the solid phase (virus, bacteria) concentration [$N_c \text{ L}^{-3}$], respectively. Subscripts e and l represent equilibrium and kinetic sorption sites. N_c is a number of microbial particles, and μ_w and μ_s represent inactivation and degradation processes (die-off) in the liquid and solid phases, respectively. D_{ij}^w is the dispersion coefficient for the liquid phase [$\text{L}^2 \text{ T}^{-1}$], θ is the volumetric water content [$\text{L}^3 \text{ L}^{-3}$], and ρ is the bulk density of porous medium [ML^{-3}]. Parameters μ_w and μ_s are used as fitting variables. Mass transfer between the aqueous and both solid kinetic phases can be described as:

$$\rho \frac{\partial s}{\partial t} = \theta k_a \psi c - k_d \rho s \quad (\text{D.2.2-2})$$

where k_a is the first-order attachment coefficient [T^{-1}] and k_d the first-order detachment coefficient [T^{-1}]. The colloid retention function (ψ) was not activated, i.e., was set to unity. According to Šimůnek et al., (2006), the attachment and detachment coefficients have been found to strongly depend upon water content, with attachment significantly increasing as the

water content decreases. Linear adsorption kinetics were assumed. The chemical non-equilibrium model was used with 50% of all sorption sites assumed to sorb instantaneously and the other 50% are governed by kinetic sorption.

D.2.3 Modeling Results

The best-fit simulations of the column bacteria and virus test data are depicted in Figures D-23 to D-27. Included are the experimental data and the model fit, both as “normal-normal” and “log-normal” graphs to emphasize the two principle parts of these experiments, i.e., early “high” concentration breakthrough, followed by a tailing phase characterized by “low” microbe concentrations. The graphs are organized by showing the results from the shallowest sample port (4 cm) on top, followed by the second sample port (10.5 cm) and the third port at 25 cm on the bottom of each page.

More weight was given to fitting breakthrough curves at the deeper port because the data from greater treatment depths are assumed to be more critical for the performance characterization onsite wastewater treatment systems – either during the subsequent simulation using the trench model or in real-world systems. Further, the apparent oscillations of the simulation are not a modeling artifact, but a reflection of the 12-hr periodic dosing of the trench system which causes detachment/attachment cycles.

Note that that no MS-2 coliphage column experiments were simulated except for the sandy RI soil before biofilm formation because little to no MS-2 breakthrough was observed at the lower ports which makes fitting of the model to the data meaningless. Also, an attempt was made to simulate the *E. coli* transport in column experiments with structured clay from GA. As the simulation results for the pre-biofilm experiments show, no good fit could be obtained attributed to preferential flow conditions that prevail in this soil. The current trench model, however, cannot adequately capture preferential flow. More work is required to address the preferential flow phenomenon. Finally, the post-biofilm transport of *E. coli* was simulated for the sandy RI soil data. Based on visual observations during the column experiment, it was assumed that the differences between pre- and post-biofilm experiments (i.e., lower *E. coli* concentrations in the post-biofilm data set) were solely due to changes in the uppermost 4 cm of the column modeling domain. The fit obtained was fairly good for the middle sample port, but underestimated the effluent concentrations in the lowest port. Again, more work is needed to investigate the reasons for this.

Given these limitations, including the modeling MS-2 transport and the *E. coli* transport in structured materials, no attempt was made to further extrapolate the data to the trench model. However, the overall fit of *E. coli* data to the model prior to biofilm formation, together with the much higher effluent concentrations during these experiments, provided for a meaningful simulation of bacteria transport within the trench model domain.

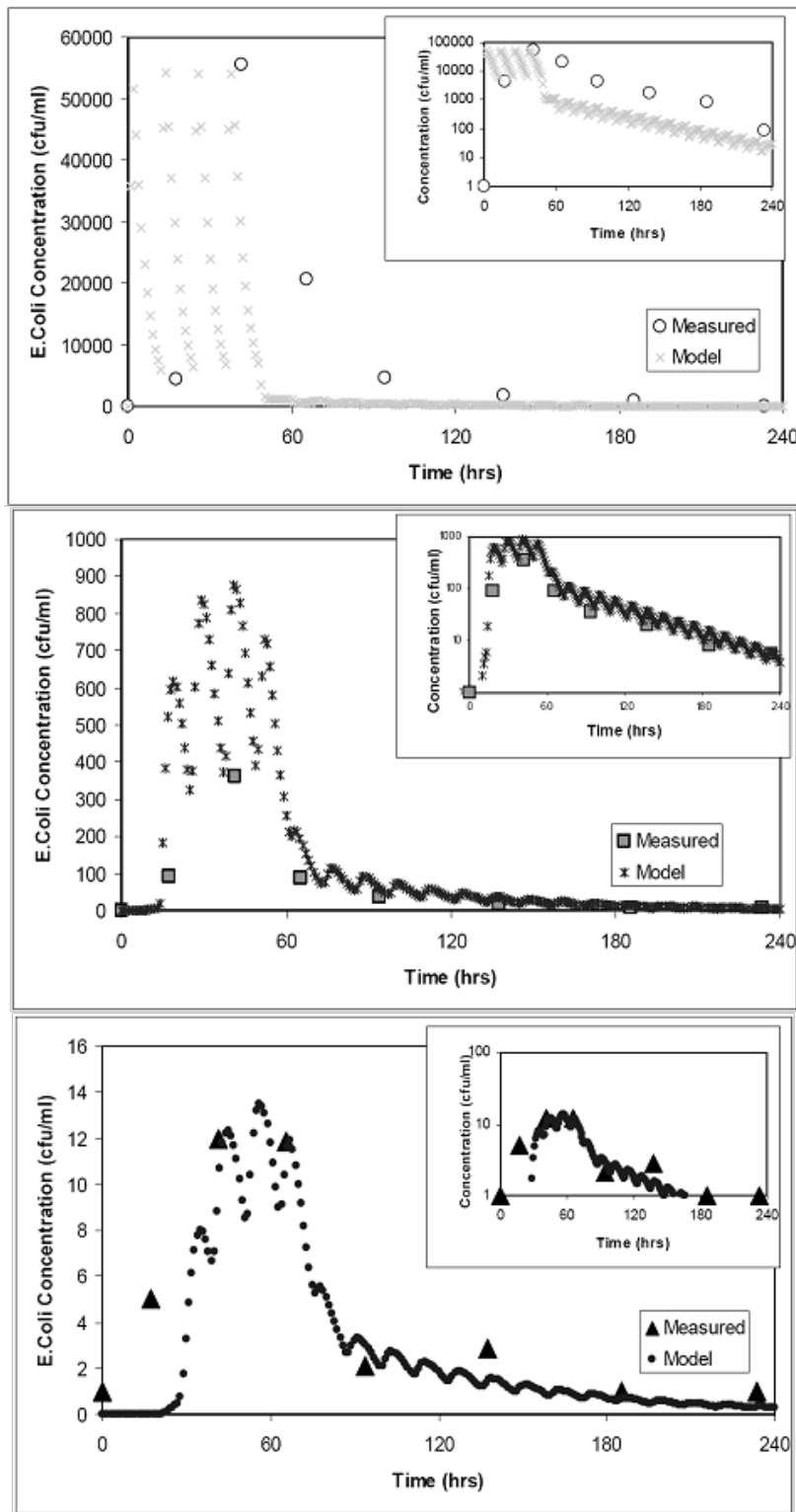


Figure D-23. Experimental *E. coli* Data and Best-Fit Using the HYDRUS Attachment/Detachment Module for Sandy Soil (RI) before Biofilm Formation.

Top graph is 4 cm depth, middle graph is 10.5 cm depth, and bottom graph is 25 cm depth. Data plotted in "log-normal" format to emphasize the tailing phase.

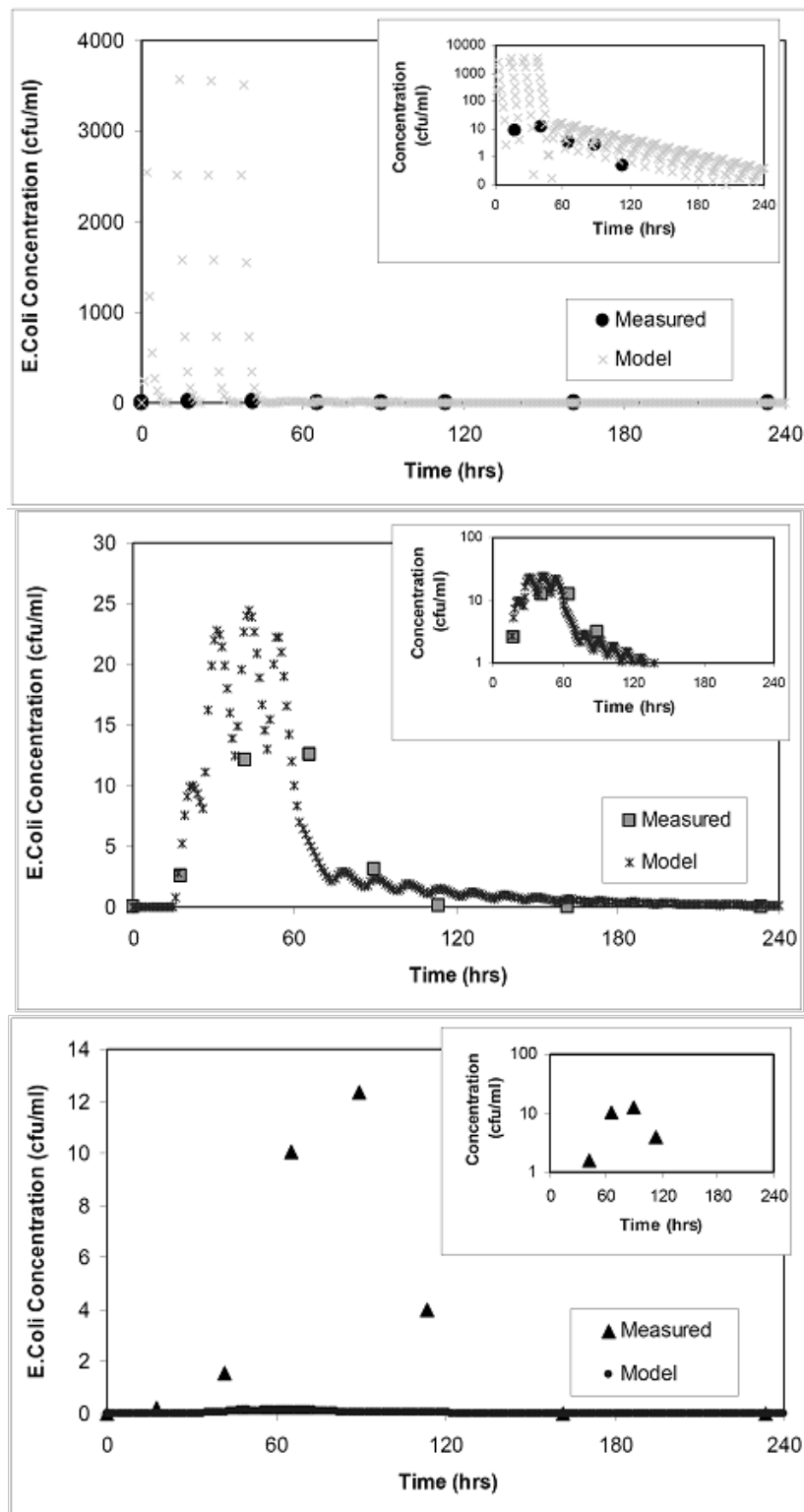


Figure D-24. Experimental *E. coli* Data and Best-Fit Using the HYDRUS Attachment/Detachment Module for the Sandy Soil from RI After Biofilm Formation.

Graph on top shows the results for the sample port at 4 cm depth, middle: sample port at 10.5 cm, bottom: sample port at 25 cm.

Insert: data plotted in "log-normal" format to emphasize the tailing phase.

Notice that in the lower graph, *E. coli* concentrations are underestimated.

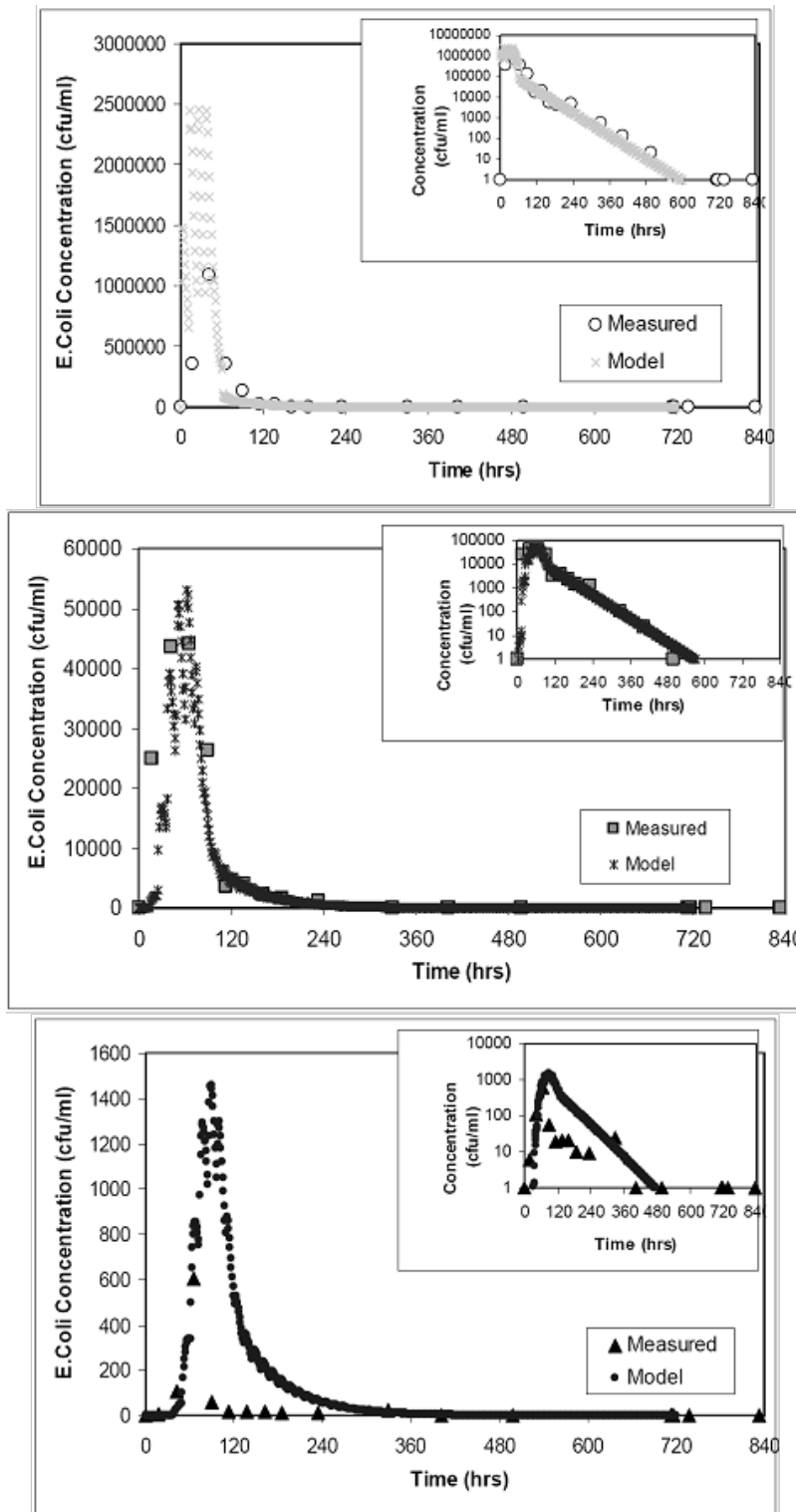


Figure D-25. Experimental *E. coli* Data and Best-Fit Using the HYDRUS Attachment/Detachment Module for the Sandy Loam Soil from CO Before Biofilm Formation.

Graph on top shows the results for the sample port at 4 cm depth, middle: sample port at 10.5 cm, bottom: sample port at 25 cm. Insert: data plotted in "log-normal" format to emphasize the tailing phase.

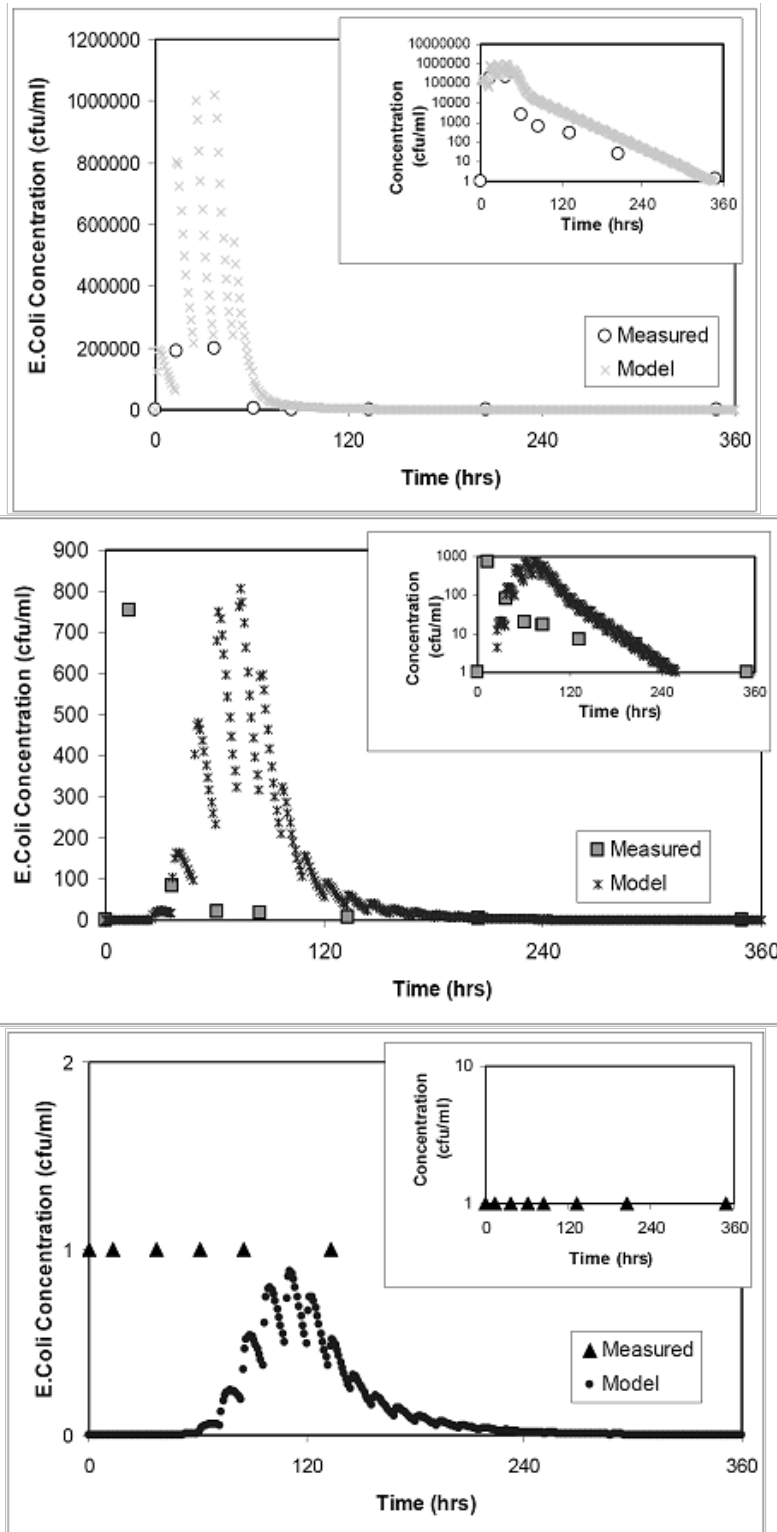


Figure D-26. Experimental *E. coli* Data and Best-Fit Using the HYDRUS Attachment/ Detachment Module for the Clay Loam Soil from GA Before Biofilm Formation.

Graph on top shows the results for the sample port at 4 cm depth, middle: sample port at 10.5 cm, bottom: sample port at 25 cm. Insert: data plotted in "log-normal" format to emphasize the tailing phase. Notice the early breakthrough due to preferential flow.

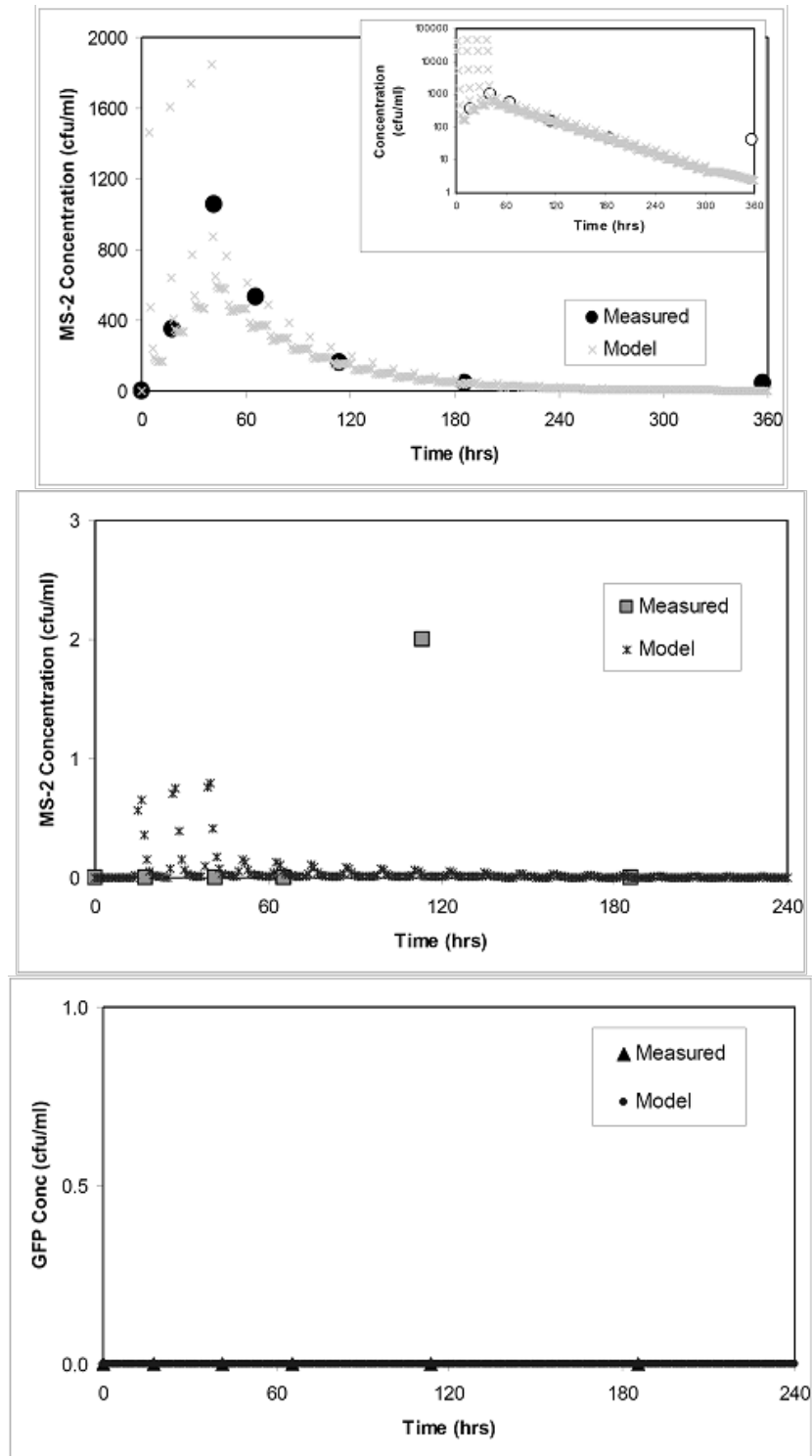


Figure D-27. Experimental MS-2 Coliphage Data and Best-Fit Using the HYDRUS Attachment/Detachment Module for the Sandy Soil from RI Before Biofilm Formation.

Graph on top shows the results for the sample port at 4 cm depth, middle: sample port at 10.5 cm, bottom: sample port at 25 cm. Insert in top graph: data plotted in "log-normal" format to emphasize the tailing phase. Note the almost complete absence of MS-2 in the deeper sample ports.

D.3 Modeling Microbial Transport with HYDRUS

The modeling with HYDRUS is described in detail in Section D.2. Briefly, the best-fit transport parameters were first determined from the column experiments. These parameters were then imported into a model that simulated a trench STU with pulsed pumping (twice daily for one hour). The trench model was run under steady state conditions, and was stressed by increasing or decreasing modeling parameters. The response of the trench model was examined at six observation points beneath the pipe (10 cm, 17 cm, 23.3 cm, 42 cm, 70 cm, and 105 cm). The following scenarios were simulated:

- ◆ Variable hydraulic conductivity (RI)
- ◆ Variable initial *E. coli* concentration (RI)
- ◆ Variable HLR (RI and CO)
- ◆ Variable precipitation or irrigation from the surface (RI)

The HYRUS modeling effort focused on simulating the microbe transport before biofilm formation. The rationale for this approach was that the once a biofilm formed, microbe removal was either similar to or more effective compared to pre-biofilm conditions. Therefore, under “real world” conditions, OWTS designers have to be most cautions in regards to microbial transport with newly installed systems that have not yet developed a mature biofilm. Hence, the results summarized herein can be interpreted as a conservative approach to the design of new treatment systems. Once these systems mature, more efficient removal can be assumed.

The sandy RI soil was examined in greater detail than the other two soils. One major reason was that the structured clay loam from GA could not be modeled because the preferential flow observed in the column experiments could not be adequately parameterized in HYDRUS. Also, the RI soil exhibited comparably slow microbe die-off characteristics (Table D-3) and for this reason was of greater interest to estimation of the response to system stresses.

D.3.1 Effect of Variable Hydraulic Conductivity

The trench model consisted of three materials (Figure D-28). Material 1 was one of the three soils. Material 2 was assumed to be gravel into which an infiltration pipe is embedded. The bottom of the pipe rests 15 cm above Material 3, which is the biofilm with a thickness of 2 cm. The bottom of the biofilm is 88 cm above the bottom of the unsaturated zone. The top of the trench model is equivalent to an unsealed surface, such as a lawn.

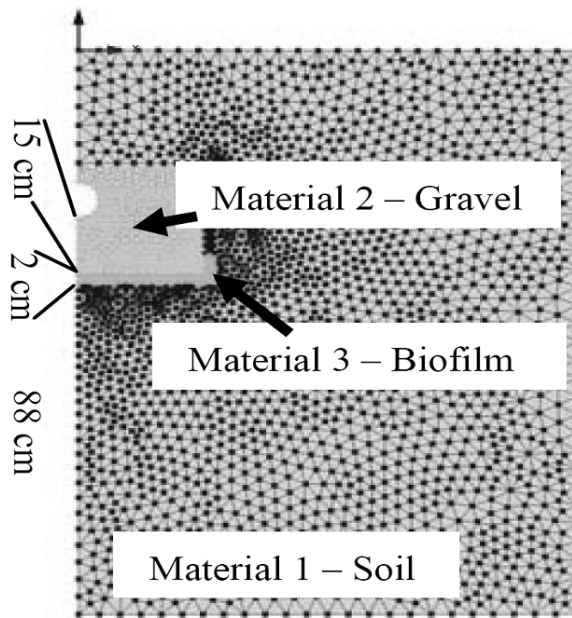


Figure D-28. Trench Model Material Distribution.

The HYDRUS model provides a library of common soil properties, including their unsaturated hydraulic conductivity. These library values were selected as the Material 1 properties and were assumed to be constant and not affected by clogging or other changes that could occur over the lifetime of the trench system. However, it is reasonable to assume that as a biofilm matures, the hydraulic conductivity of Material 2 and 3 will decrease with time. To simulate the response of decreasing hydraulic conductivity, its value was decreased from initially 83.3 cm/hr for Material 2 and 0.017 cm/hr for material 3 by factors 10 and 100, respectively. The unlikely case that the hydraulic conductivity of the material increased was also simulated, assuming a 5 time greater value than initial. Modeling results are shown in Table D-4 and Figures D-29 and D-30.

The results expectedly indicate that *E. coli* concentrations decrease with decreasing hydraulic conductivity. This is because slower infiltration provides more time for bacteria die-off to take effect. In terms of percentage reduction of *E. coli* concentration, 99.997% or greater removal was achieved at a depth of 42 cm. Higher removal percentages were associated with lower hydraulic conductivity values.

Table D-4. Reduction in *E. coli* Concentration from RI Sandy Soil Modeling as a Function of Hydraulic Conductivity and Depth.

Relative Hydraulic Conductivity	Hydraulic Conductivity		% Reduction by Depth below Infiltration Pipe			
	Material 2 (cm hr ⁻¹)	Material 3 (cm hr ⁻¹)	10 cm	17 cm	23.3 cm	42 cm
5	416.5	0.0085	89.208%	95.188%	98.642%	99.997%
1	83.3	0.0017	91.803%	95.905%	99.089%	99.998%
0.1	8.33	0.00017	92.141%	98.981%	99.851%	100.000%
0.01	0.833	0.000017	97.606%	100.000%	100.000%	100.000%

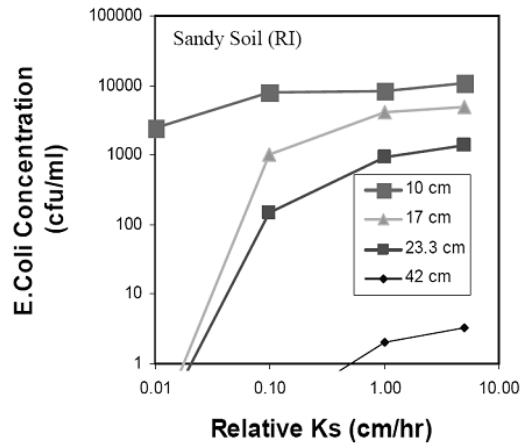


Figure D-29. *E. coli* Concentration in Sandy Soil (RI) as a Function of Variable Hydraulic Conductivities of Materials 2 and 3. The initial hydraulic conductivity of material 1 = 83.3 cm hr⁻¹ and 0.017 cm hr⁻¹ for material 3. Influent *E. coli* concentration = 10⁵ cfu mL⁻¹. Concentrations shown for four observation points at increasing depths below the influent pipe.

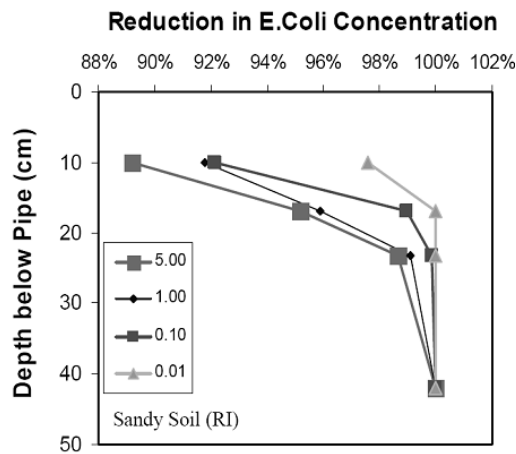


Figure D-30. Reduction of *E. coli* Concentration in Sandy Soil (RI) as a Function of Variable Hydraulic Conductivity and Depth. Legend numbers are initial hydraulic conductivity multipliers. Initial hydraulic conductivity of material 1 = 83.3. cm hr⁻¹ and 0.017 cm hr⁻¹ for material 3. Influent *E. coli* concentration = 10⁵ cfu mL⁻¹.

D.3.2 Effect of Variable Initial *E. coli* Concentration

The HYDRUS simulations were developed based on the column experiments where the initial *E. coli* concentration was 10⁵ cfu mL⁻¹. Although this is a typical *E. coli* concentration, higher concentrations may enter a treatment system if the number of infected people discharging to the system increases. Hence, the trench model was stressed with *E. coli* concentrations that were up to three orders of magnitude higher, i.e., up to 10⁸ cfu mL⁻¹. The results are summarized in Table D-5 and Figures D-31 and D-32.

The results indicate that the rate of the reduction is independent of the influent *E. coli* concentration, i.e., higher influent concentrations are decaying at the same rate as lower concentrated influent. This result was expected because bacteria die-off was simulated using a

first-order reaction constant, which is independent of initial concentration. More important, the results demonstrate that a three order of magnitude reduction in *E. coli* concentration can be expected within the first 42 cm of treatment depth. Independent on initial concentration, the *E. coli* removal was complete at 70 cm depth (results not shown).

Table D-5. Reduction in *E. coli* Concentration from RI Sandy Soil Modeling as a Function of Influent Concentration and Depth.

Influent <i>E. coli</i> Concentration (cfu mL ⁻¹)	% Reduction by Depth below Infiltration Pipe			
	10 cm	17 cm	23.3 cm	42 cm
1.E+05	91.803%	95.905%	99.089%	99.998%
1.E+06	91.803%	95.905%	99.089%	99.998%
1.E+07	91.803%	95.905%	99.089%	99.998%
1.E+08	91.803%	95.905%	99.089%	99.998%

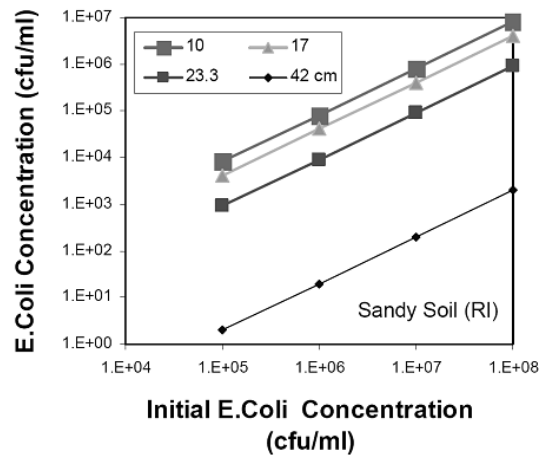


Figure D-31. *E. coli* Concentration in Sandy Soil (RI) as a Function of Variable Influent *E. coli* Concentration (cfu mL⁻¹). Model concentrations shown for four observation points at increasing depths below the influent pipe.

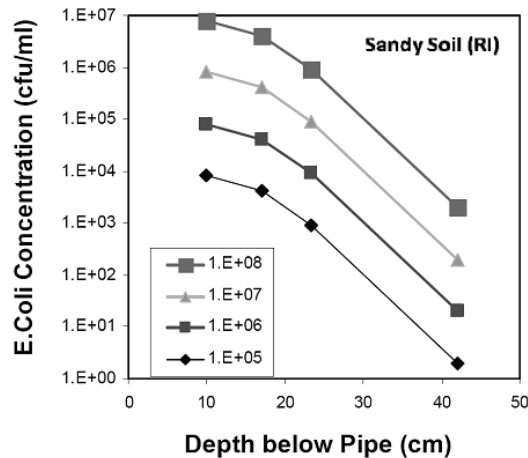


Figure D-32. Reduction of *E. coli* Concentration in Sandy Soil (RI) as a Function of Variable Influent *E. coli* concentration (cfu mL⁻¹).

Model concentrations shown for four observation points at increasing depths below the influent pipe.

D.3.3 Effect of Variable Hydraulic Loading Rate

The HLR of a treatment system is the volume of wastewater applied to the treatment system per time unit. For the trench model, an operational HLR of 0.424 cm hr⁻¹ at the trench bottom was assumed. This HLR is equivalent to about 3 cm d⁻¹ at the pipe level. Because variable HLR can be assumed to occur over the lifetime of any onsite wastewater treatment system, it was simulated how the trench model responds to increasing and decreasing HLR. A range of 50% lower to 170% higher HLRs were modeled. The results are shown in Table D-6 and Figures D-33 and D-34 for the sandy RI soil.

E. coli concentration decreased in a non-linear fashion with decreasing HLR, i.e., removal was relatively more efficient at lower HLR. Overall, removal at 42 cm depth was at least 99.979%, demonstrating that even if the design HLR is exceeded by 170%, the trench system is still removing *E. coli* quite effectively. Very similar results were obtained from simulating the sandy loam from CO (Table D-7 and Figures D-35 and D-36). Again, only minimal differences in the percentage removal efficiencies at all depth levels are indicated. Removal of 99.994% and above was achieved within 42 cm depth, indicating that higher initial influent concentrations can be tolerated by the treatment system. In terms of absolute concentrations, *E. coli* concentrations were less than 1 cfu mL⁻¹ at 70 cm or deeper.

Table D-6. Reduction in *E. coli* Concentration for Sandy Soil (RI) Modeling as a Function of the Hydraulic Loading Rate and Depth.

HLR (cm hr ⁻¹)	% Reduction by Depth below Infiltration Pipe			
	10 cm	17 cm	23.3 cm	42 cm
0.212	94.608%	98.649%	99.858%	100.000%
0.424	91.803%	95.905%	99.089%	99.998%
0.530	90.810%	94.952%	98.576%	99.994%
0.635	90.049%	94.287%	98.152%	99.987%
0.720	89.508%	93.842%	97.837%	99.979%

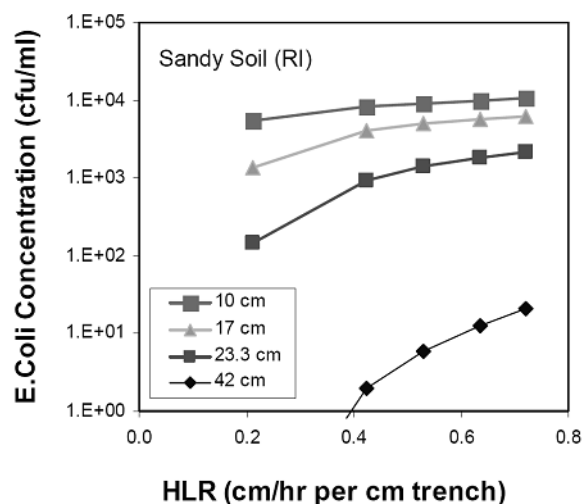


Figure D-33. *E. coli* Concentration in Sandy Soil (RI) as a Function of Variable Hydraulic Loading Rate. Model concentrations shown for four observation points at increasing depths below the influent pipe.

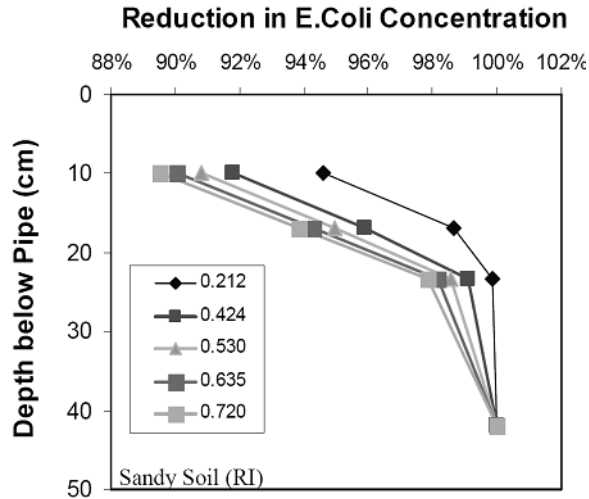


Figure D-34. Reduction of *E. coli* Concentration in Sandy Soil (RI) as a Function of Variable Hydraulic Loading Rate (cm hr⁻¹). Model concentrations shown for four observation points at increasing depths below the influent pipe.

Table D-7. Reduction in *E. coli* Concentration for Sandy Loam Soil (CO) Modeling as a Function of the Hydraulic Loading Rate and Depth.

HLR (cm hr ⁻¹)	% Reduction by Depth below Infiltration Pipe			
	10 cm	17 cm	23.3 cm	42 cm
Influent <i>E. coli</i> Concentration = 10⁵ cfu mL⁻¹				
0.212	87.052%	96.132%	99.753%	100.000%
0.424	81.743%	91.562%	98.654%	100.000%
0.530	80.013%	90.037%	97.981%	99.999%
0.635	78.581%	88.975%	97.418%	99.997%
0.720	77.846%	88.424%	97.019%	99.994%
Influent <i>E. coli</i> Concentration = 5.9×10⁶ cfu mL⁻¹				
0.212	87.047%	96.132%	99.753%	100.000%
0.424	81.745%	91.566%	98.654%	100.000%
0.530	80.027%	90.043%	97.980%	99.999%
0.635	78.581%	88.988%	97.420%	99.997%
0.720	77.851%	88.415%	97.018%	99.994%

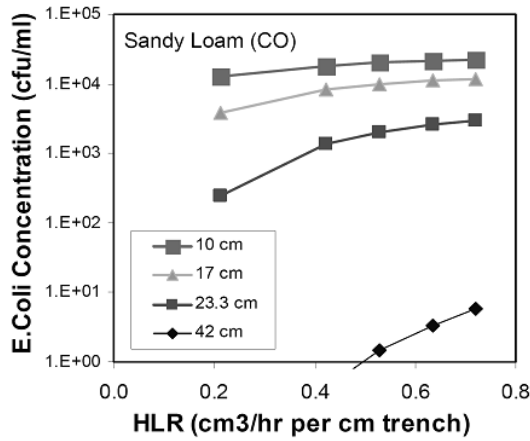


Figure D-35. *E. coli* Concentration in Sandy Loam Soil (CO) as a Function of Variable Hydraulic Loading Rate and Initial *E. coli* Influent Concentration = 1×10^5 cfu mL⁻¹. Model concentrations shown for four observation points at increasing depths below the influent pipe.

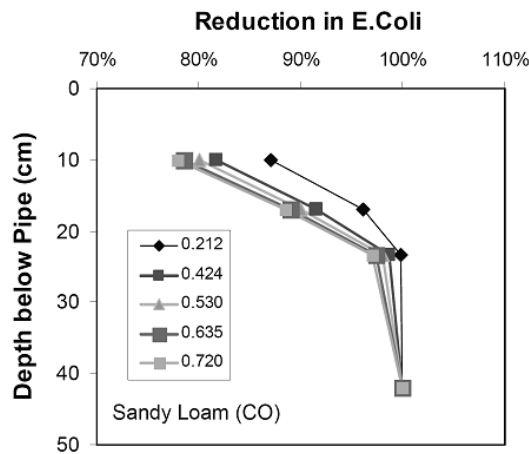


Figure D-36. Reduction of *E. coli* Concentration in Sandy Loam Soil (CO) as a Function of Variable Hydraulic Loading Rate (cm hr⁻¹) and Initial *E. coli* Influent Concentration = 1×10^5 cfu mL⁻¹. Model concentrations shown for four observation points at increasing depths below the influent pipe.

In addition, the CO sandy loam trench system was not only modeled with an influent concentration of 10^5 cfu mL⁻¹, but also with a higher concentration of 5.9×10^6 cfu mL⁻¹. These simulations were carried out to investigate the response to higher influent bacteria concentration in addition to variable HLR (Figures D-37 and D-38).

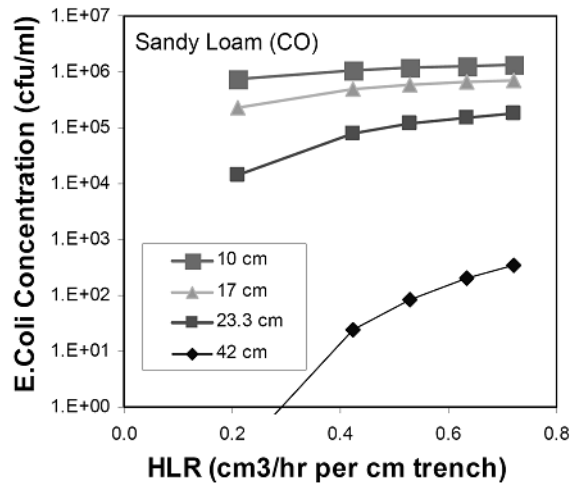


Figure D-37. *E. coli* Concentration in Sandy Loam Soil (CO) as a Function of Variable Hydraulic Loading Rate (cm hr⁻¹) and Initial *E. coli* Influent Concentration = 5.9×10⁶ cfu mL⁻¹. Model concentrations shown for four observation points at increasing depths below the influent pipe.

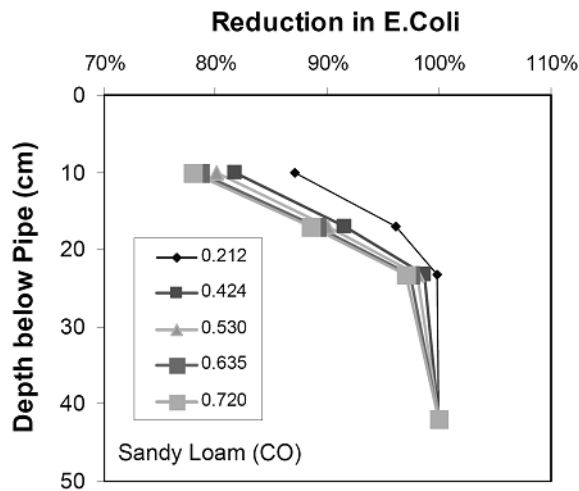


Figure D-38. Reduction of *E. coli* Concentration in Sandy Loam Soil (CO) as a Function of Variable Hydraulic Loading Rate (cm hr⁻¹) and Initial *E. coli* Influent Concentration = 5.9×10⁶ cfu mL⁻¹. Model concentrations shown for four observation points at increasing depths below the influent pipe.

D.3.4 Variable Precipitation or Irrigation

STUs are also affected by percolating water from precipitation and/or irrigation events. This additional inflow of water from the surface may influence the overall performance of the treatment system, i.e., enhanced infiltration may cause microbial matter to be transported faster and possibly deeper into the subsurface. To investigate this stress scenario on the STU, various infiltration events over a 17.5 days period were simulated (Table D-8).

Table D-8. Infiltration Patterns Used to Represent Stresses the Trench STU.

Scenario	Infiltration Pattern
5 cm	2.5 cm hr ⁻¹ for two hours on day 12.
10 cm	1 cm hr ⁻¹ for five hours on day 1 followed by 2.5 cm hr ⁻¹ for two hours on day 12.
15 cm	1 cm hr ⁻¹ for five hours on day 1 followed 0.5 cm hr ⁻¹ for ten hours on days 4 followed by 2.5 cm hr ⁻¹ for two hours on day 12.
25 cm	1 cm hr ⁻¹ for five hours on day 1 followed 0.5 cm hr ⁻¹ for ten hours on days 4 and 8 followed by 2.5 cm hr ⁻¹ for two hours on day 12.
35 cm	1 cm hr ⁻¹ for five hours on day 1 followed 0.5 cm hr ⁻¹ for ten hours on days 2, 4, 6, 8, and 10 followed by 2.5 cm hr ⁻¹ for two hours on day 12.
35 cm / HLR	As scenario "35 cm" but with HLR increased 1.7 times (from 0.424 cm hr ⁻¹)

Table D-9 summarizes the removal percentage for each scenario at constant HLR (0.424 cm/hr). Figure D-39 shows the simulated *E. coli* concentrations for Scenario "35 cm/day" at 42 cm depth. All four infiltration events clearly increased the *E. coli* concentration. However, the maximum increase was less than an order of magnitude and only lasted for a comparable short time. Similar results were observed during the column experiments when addition of water caused the microbe effluent to spike only minimally. In Figure D-40, the response of the trench system to high infiltration rates and increased HLR is shown (Scenarios "35 cm" and "35 cm/HLR"). As expected the higher HLR caused lower reduction percentages at shallow depths, but at 42 cm depth bacteria removal was almost quantitative. No *E. coli* was observed at the 70 cm or below.

Table D-9. Reduction in *E. coli* Concentration for Sandy Soil (RI) as a Function of Variable Infiltration Patterns and Depth.

Scenario	% Reduction by Depth below Infiltration Pipe			
	10 cm	17 cm	23.3 cm	42 cm
5 cm	91.780%	95.904%	99.074%	99.997%
10 cm	91.784%	95.907%	99.074%	99.996%
15 cm	91.787%	95.907%	99.072%	99.996%
25 cm	91.794%	95.928%	99.072%	99.995%
35 cm	91.793%	95.938%	99.043%	99.991%

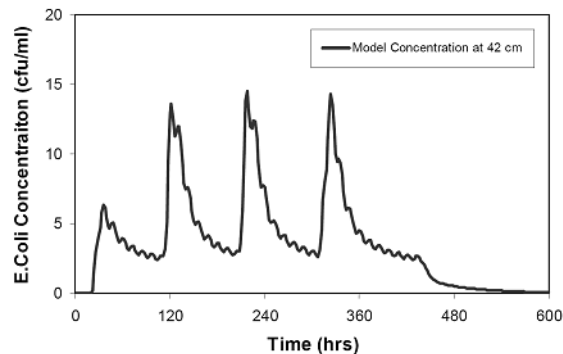


Figure D-39. Response of the *E. coli* Concentration in Sandy Soil (RI) Scenario at 42 cm to Scenario "35 cm/HLR".

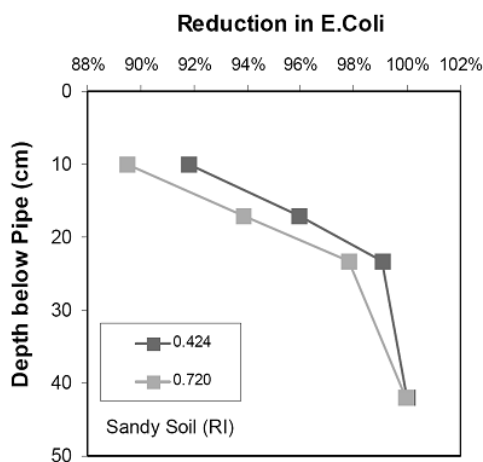


Figure D-40. Reduction of *E. coli* Concentration in Sandy Soil (RI) as a Function of Surface Water Infiltration and HLR (cm hr⁻¹). Light: Scenario “35 cm”, dark: Scenario “35 cm/HLR”.

D.4 Summary of Laboratory Experiments Coupled with HYDRUS Modeling

Results from the laboratory experiments coupled with numerical modeling using HYDRUS-2D suggest high microorganism removal could be attained in the STU. Even prior to the formation of a mature biofilm, bacteria removal is quantitative at depths exceeding 70 cm. The removal effectiveness varied only slightly under variably high stress conditions, with changes in the HLR having the greatest impact. However, specific simple tools could not be developed to address microorganism attenuation in the STU because attenuation relies on difficult to obtain field parameters. Specifically, to calibrate a numerical model requires: 1) conservative tracer test results, 2) lab column studies of microbial transport under unsaturated conditions, and 3) inactivation studies. In addition, even though laboratory experiments showed that the structured clay loam soil from GA efficiently removed bacteria from the aqueous phase, HYDRUS modeling could not be conducted due to preferential flow paths. Furthermore, structured soils with preferential flow paths requires further complexity within a numerical model to incorporate fractured flow which is not included in HYDRUS. Simulations were not conducted for the removal of MS-2 because the laboratory results indicated that the removal of MS-2 (viruses) was much more effective relative to *E. coli*. Hence, if one can model under which conditions the transport/removal of *E. coli* is efficient, then the MS-2 removal is at least as effective. Thus, the experiments and simulations clearly indicate that the design of STUs for microorganism attenuation should focus primarily on bacteria.

The clear differences in factors controlling the fate of different types of pathogenic organisms found in STE presents a challenge for optimization of removal of these organisms in conventional STUs. For example, in principle, the use of soils with a sufficient amount of appropriate clay minerals would increase the probability of optimizing removal of viruses, bacteria and protozoa. However, soils with these properties are not evenly distributed in space, either requiring the use of engineered soils using imported clays minerals, or foregoing the benefits of virus removal in areas that lack appropriate clay minerals. However, the presence of high levels of clay minerals restricts infiltration, which would alternatively require an increase in the STU infiltrative surface area. Alterations in these design parameters also affect the

biogeochemical processes involved in removal of nutrients which may be of equal importance (based on treatment goals).

Furthermore, field-scale evaluations of pathogen removal are scant, and they focus on a particular type of organism, with little or no consideration of other functions performed by the STU. To better assess overall STU performance, future research should integrate field evaluation of the role of system design and soil properties in determining removal of different types of enteropathogenic organisms within the context of other STU functions, such as infiltration and nutrient removal. These data could then be used in support of predictive mathematical models that describe the various functions of the STU in terms of design parameters and available information on soil properties.

REFERENCES

- Abdul-Talib, S., T. Hvitved-Jacobsen, J. Vollertsen, and Z. Ujang. 2002. Half saturation constants for nitrate and nitrite by in-sewer anoxic transformations of wastewater organic matter. *Water Science and Technology* 46 (9):185-192.
- Adams, M.H. 1959. *Bacteriophages*. Interscience Publishers, New York.
- Addiscott, T.M. 1983. Kinetics and temperature relationships of mineralization and nitrification in Rothamsted soils with differing histories. *European Journal of Soil Science* 34 (2):343-353.
- Anderson, D.L. 1998. Natural denitrification in groundwater impacted by onsite wastewater treatment systems. Proceedings of the Eighth National Symposium on Individual and Small Community Sewage Systems, in Orlando, FL. American Society of Agricultural Engineers (ASAE).
- Anderson, D.L. and R.L. Siegrist. 1989. The performance of ultra low-volume flush toilets in Phoenix. *Journal of American Water Works* 81 (3):52-57.
- Anderson, D.L., D.M. Mulville-Friel, and W L. Nero. 1993. The impact of water conserving plumbing fixtures on residential water use characteristics in Tampa, Florida. Proceedings of the Conserv93 Conference. American Water Works Association. p 611-628.
- Andreoli A., N. Bartilucci, R. Forgione, R. Reynolds. 1979. Nitrogen removal in a subsurface disposal system. *Journal of the American Water Pollution Control Federation* 51(4):841-854.
- APHA. 2005. *Standard Methods for the Examination of Water and Wastewater*. 21st ed. Prepared for American Public Health Association by American Water Works Association, and Water Pollution Control Federation, Washington, D.C.
- Arah, J.R.M. 1990. Diffusion-reaction models of denitrification in soil microsites. *Denitrification in Soil and Sediment*:245-258.
- Aulakh, M.S., J.W. Doran, D.T. Walters, and J.F. Power. 1991a. Legume residue and soil water effects on denitrification in soils of different textures. *Soil Biology and Biochemistry* 23 (12):1161-1167.
- Aulakh, M.S., J.W. Doran, and A.R. Mosier. 1991b. Field evaluation of four methods for measuring denitrification. *Soil Science Society of America Journal* 55:1332-1338.
- Aulakh, M.S., T.S. Khera, and J.W. Doran. 2000a. Mineralization and denitrification in upland, nearly saturated and flooded subtropical soil. I. Effect of nitrate and ammoniacal nitrogen. *Biology and Fertility of Soils* 31 (2):162-167.
- Aulakh, M.S., T.S. Khera, and J.W. Doran. 2000b. Mineralization and denitrification in upland, nearly saturated and flooded subtropical soil. II. Effect of organic manures varying in N content and C:N ratio. *Biology and Fertility of Soils* 31 (2):168-174.
- Avalakki, U.K., W.M. Strong, and P.G. Saffigna. 1995a. Measurement of gaseous emissions from denitrification of applied Nitrogen-15. II. Effects of temperature and added straw. *Australian Journal of Soil Research* 33:89-99.

- Avalakki, U.K., W.M. Strong, and P.G. Saffigna. 1995b. Measurement of gaseous emissions from denitrification of applied Nitrogen-15. III. Field measurements. *Australian Journal of Soil Research* 33:101-111.
- Avrahami, S., W. Liesack, and R. Conrad. 2003. Effects of temperature and fertilizer on activity and community structure of soil ammonia oxidizers. *Environmental Microbiology* 5 (8):691-705.
- Bandibas, J., A. Vermosen, C. De Groot, and O. Van Cleemput. 1994. The effect of different moisture regimes and soil characteristics on nitrous oxide emission and consumption by different soils. *Soil Science* 158 (2):106-114.
- Barton, L., C. McLay, L. Schipper, and C. Smith. 1998. Procedures for characterizing denitrification rates in a wastewater-irrigated forest soil. *Australian Journal of Soil Research* 36:997-1008.
- Bastug, R. and D. Buyuktas. 2003. The effects of different irrigation levels applied in golf courses on some quality characteristics of turfgrass. *Irrigation Science* 22 (2):87-93.
- Bateman, E.J. and E.M. Baggs. 2005. Contributions of nitrification and denitrification to N₂O emissions from soils at different water-filled pore space. *Biology and Fertility of Soils* 41:379-388.
- Beach, D.N. 2001. *The Use of One-dimensional Columns and Unsaturated Flow Modeling to Assess the Hydraulic Processes in Soil-based Wastewater Treatment Systems*. MS Thesis, Geological Engineering, Colorado School of Mines (CSM), Golden, CO.
- Beach, D.N. and J.E. McCray. 2003. Numerical modeling of unsaturated flow in wastewater soil absorption systems. *Ground Water Monitoring Remediation* 23 (2):64-72.
- Beach, D.N., J.E. McCray, K.S. Lowe, and R.L. Siegrist. 2005. Temporal changes in hydraulic conductivity of sand porous media biofilters during wastewater infiltration due to biomat formation. *Journal of Hydrology* 311:230-243.
- Beal, C.D., E.A. Gardner, and N.W. Menzies. 2005. Process, performance and pollution potential: A review of septic tank-soil absorption systems. *Australian Journal of Soil Research* 43:781-802.
- Beal, C.D., D.W. Rassam, E.A. Gardner, G. Kirchhof, and N.W. Menzies. 2008. Influence of Hydraulic Loading and Effluent Flux on Surface Surcharging in Soil Absorption Systems. *Journal of Hydrologic Engineering* 13 (8):681:692.
- Beard, J.B. 1994. The water-use rate of turfgrasses. *TurfCraft Australia* 39:79-81.
- Beard, J.B. and R.L. Green. 1994. The role of turfgrasses in environmental protection and their benefits to humans. *Journal of Environmental Quality* 23 (3):452-460.
- Beauchamp, E., C. Gale, and J. Yeomans. 1980. Organic matter availability for denitrification in soils of different textures and drainage class. *Soil Science and Plant Analysis* 11(12):1221-1233.
- Bergstrom, D.W. and E.G. Beauchamp. 1993. Relationships between denitrification rate and determinant soil properties under barley. *Canadian Journal of Soil Science* 73:567-578.
- Bollman, A. and R. Conrad. 1997. Acetylene blockage technique leads to underestimation of denitrification rates in oxic soils due to scavenging of intermediate nitric oxide. *Soil Biology & Biochemistry* 29(7):1067-1077.

- Bollman, A. and R. Conrad. 1998. Influence of O₂ availability on NO and N₂O release by nitrification and denitrification in soils. *Global Change Biology* 4(4):387-396.
- Bouma, J. 1975. Unsaturated flow during soil treatment of septic tank effluent. *J. Environ. Eng.* 101(6):967-983.
- Boyd, P.M., J.L. Baker, S.K. Mickelson, and S.I. Ahmed. 2003. Pesticide transport with surface runoff and subsurface drainage through a vegetative filter strip. *Transactions of the ASAE* 46:675-684.
- Bradley, P.M., M. Fernandez Jr., and F.H. Chapelle. 1992. Carbon limitation of denitrification rates in an anaerobic groundwater system. *Environmental Science and Technology* 26(12):2377-2381.
- Brady, N.C. and R.R. Weil. 2002. *The Nature and Properties of Soil*. 13th ed. Prentice Hall, Upper Saddle River, NJ.
- Bremner, J.M. and K. Shaw. 1958. Denitrification in soil. II. Factors affecting denitrification. *Journal of Agricultural Science* 51:40-52.
- Brettar, I. and M. Höfle. 2002. Close correlation between the nitrate elimination rate by denitrification and the organic matter content in hardwood forest soils of the Upper Rhine floodplain (France). *Wetlands* 22(2):214-224.
- Brown, R. B. 2003. *Soils and Septic Systems. SL-118, A series of the Soil and Water Science Department*. Prepared by Florida Cooperative Extension Service, Institute of Food and Agricultural Sciences, University of Florida.
- Brown and Caldwell. 1984. *Residential Water Conservation Projects*. Research Report 903. Prepared by U.S. Department of Housing and Urban Development, Office of Policy Development, Washington, D.C.
- Brye, K.R., J.M. Norman, L.G. Bundy, and S.T. Gower. 2000. Nitrogen and carbon leaching in agroecosystems and their role in denitrification potential. *Journal of Environmental Quality* 30:58-70.
- Brown, A., A. Riddle, N. Cunningham, T. Kedwards, N. Shillabeer, and T. Hutchinson. 2003. Predicting the effects of endocrine disrupting chemicals on fish populations. *Human and Ecological Risk Assessment* 9(3):761-788.
- Bumgarner, J.R. and J.E. McCray. 2007. Estimating biozone hydraulic conductivity in wastewater soil-infiltration systems using inverse numerical modeling. *Water Research* 41(11):2349-2360.
- Burford, J.R. and J.M. Bremner. 1975. Relationship between the denitrification capacities of soils and total water-soluble and readily decomposable soil organic matter. *Soil Biology & Biochemistry* 7:389-394.
- Buss, S., A. Herbert, P. Morgan, S. Thornton, and J. Smith. 2004. A review of ammonium attenuation in soil and groundwater. *Quarterly Journal of Engineering Geology and Hydrogeology* 37(4):347-359.
- Buss, S.R., M.O. Rivett, P. Morgan, and C.D. Bemment. 2005. *Attenuation of Nitrate in the Sub-surface Environment*. SC030155/SR2. Prepared for Environmental Agency. Bristol, England by ESI Ltd, Shrewsbury, England.

- Campbell, C.A., Y.W. Jame, and G.E. Winkleman. 1984. Mineralization rate constants and their use for estimating nitrogen mineralization in some Canadian prairie soils. *Canadian Journal of Soil Science* 64(3):333-343.
- Cannavo, P., A. Richaume, and F. Lafolie. 2004. Fate of nitrogen and carbon in the vadose zone: in situ and laboratory measurements of seasonal variations in aerobic respiratory and denitrifying activities. *Soil Biology & Biochemistry* 36:463-478.
- Carsel, R.F. and R.S. Parrish. 1988. Developing joint probability distributions of soil water retention characteristics. *Water Resources Research* 24:755-769.
- Cavigelli, M.A. and G.P. Robertson. 2000. The functional significance of denitrifier community composition in a terrestrial ecosystem. *Ecology* 81(5):1402-1414.
- Choubert, J., Y. Racault, A. Grasmick, C. Beck, and A. Heduit. 2005. Maximum nitrification rate in activated sludge processes at low temperature: key parameters, optimal value. In *E-Water*: European Water Association (EWA).
- Christensen, M.J. 1977. Biological denitrification of sewage: A literature review. *Progress in Water Technol.* 8(4/5):509-555.
- Christensen, S. 1980. Percolation studies on denitrification. *Acta Agriculture Scandinavia* 30:225-236.
- Christensen, S. and J. Tiedje. 1988. Sub-parts-per-billion nitrate method: Use of an N₂O-producing denitrifier to convert NO₃⁻ or 15NO₃⁻ to N₂O. *Applied and Environmental Microbiology* 54(6):1409-1413.
- Clough, T.J., S.F. Ledgard, M.S. Sprosen, and M.J. Kear. 1998. Fate of 15N labeled urine on four soil types. *Plant and Soil* 199:195-203.
- Cogger, C.G. and B.L. Carlile. 1984. Field performance of conventional and alternative septic systems in wet soils. *J. Environmental Quality* 13(1):137-142.
- Cogger, C.G., L.M. Hajjar, C.L. Moe and M.D. Sobsey. 1988. Septic system performances on a coastal barrier island. *J. Environmental Quality* 17(3):401-407.
- Conn, K.E., R.L. Siegrist, L.B. Barber, and M.T. Myers. 2009. Fate of Trace Organic compounds during vadose zone soil treatment in an onsite wastewater system. *Env. Tox. and Chemistry*, 29(2):285-293.
- Cosandey, A.C., V. Maitre, and C. Guenat. 2003. Temporal denitrification patterns in different horizons of two riparian soils. *European Journal of Soil Science* 54:25-37.
- Craswell, E.T. 1974. Effect of moisture content on denitrification in a clay soil. *Soil Biology & Biochemistry* 6:127-129.
- Crites, R.C. and G. Tchobanoglous. 1998. *Small and Decentralized Wastewater Management Systems*. McGraw-Hill Publishing Co., Boston, MA.
- Das, B.S., L S. Lee, P S C. Rao, and R P. Hultgren. 2004. Sorption and degradation of steroid hormones in soils during transport: Column studies and model evaluation. *Environmental Science and Technology* 38(5):1460-1470.
- Daughton, C.G. and T.A. Ternes. 1999. Pharmaceuticals and personal care products in the environment: Agents of subtle change? *Environmental Health Perspectives* 907-938.

- Del Grosso, S., W. Parton, A. Mosier, D. Ojima, A. Kulmala, and S. Phongpan. 2000. General model for N₂O and N₂ gas emissions from soils due to denitrification. *Global Biogeochemical Cycles* 14:1045-1060.
- Davidson, T.E. and M. Ståhl. 2000. The influence of organic carbon on nitrogen transformations in five wetland soils. *Soil Science Society of America Journal* 64(3):1129-1136.
- de Klein, C.A.M. and R.S.P. van Logtestijn. 1994. Denitrification in the top soil of managed grasslands in The Netherlands in relation to soil type and fertilizer level. *Plant and Soil* 163:33-44.
- de Klein, C.A.M. and R.S.P. van Logtestijn. 1996. Denitrification in grassland soils in the Netherlands in relation to irrigation, N-application rate, soil water content and soil temperature. *Soil Biology & Biochemistry* 28(2):231-237.
- DeSimone, L.A. and B.L. Howes. 1998. Nitrogen transport and transformations in a shallow aquifer receiving wastewater discharge: a mass balance approach. *Water Resources Research* 34:271-285.
- Devito, K.J., D. Fitzgerald, A.R. Hill, and R. Aravena. 2000. Nitrate dynamics in relation to lithology and hydrologic flow path in a river riparian zone. *Journal of Environmental Quality* 29:1075-1084.
- Dimick, C.A. 2005. *Field Evaluation of Vadose Zone Purification and the Effects of Applied Wastewater Quality and Hydraulic Loading Rate*. M.S. Thesis, Environmental Science & Engineering Division, CSM, Golden, CO.
- Doane, T.A. and W.R. Horváth. 2003. Spectrophotometric determination of nitrate with a single reagent. *Analytical Letters*. 36(12):2713-2722.
- Dontsova, K.M., L.D. Norton, and C.T. Johnston. 2005. Calcium and magnesium effects on ammonia adsorption by soil clays. *Soil Science Society of America Journal* 69:1225-1232.
- Downing, A.L., H.A. Painter, and G. Knowles. 1964. Nitrification in the activated sludge. *Journal of Proc. Inst. Sew. Purif.* 64(2):130-158.
- Driscoll, F.G. 1987. *Groundwater and Wells, Second Edition*. U.S. Filter / Johnson Screens Publisher, St. Paul, MN.
- Drtil, M., P. Nemeth, and I. Bodik. 1993. Kinetic constants of nitrification. *Water Resources Research* 27(1):35-39.
- Drury, C.F., D.J. McKenney, and W.I. Findlay. 1991. Relationships between denitrification, microbial biomass and indigenous soil properties. *Soil Biology & Biochemistry* 23(8):751-755.
- Ekpete, D.M. and A.H. Cornfield. 1964. Losses, through denitrification, from soil of applied inorganic nitrogen even at low moisture contents. *Nature* 201:322.
- Ekpete, D.M. and A.H. Cornfield. 1965. Effect of pH and addition of organic materials on denitrification losses from soil. *Nature* 208:1200.
- Engberg, D.J. and E.D. Schroeder. 1975. Kinetics and stoichiometry of bacterial denitrification as a function of cell residence time. *Water Research* 9:1051-1054.

- Erickson, J. and E. Tyler. 2001. A model for soil oxygen delivery to wastewater infiltration surfaces. Proceedings of the On-Site Wastewater Treatment - Ninth National Symposium on Individual and Small Community Sewage Systems, in Fort Worth, TX. ASAE.
- Fang, C. and J B. Moncrieff. 2005. The variation of soil microbial respiration with depth in relation to soil carbon composition. *Plant and Soil* 268:243-253.
- Feachem, R G., D J. Bradley, H. Garelick, and D.D. Mara. 1983. *Sanitation and Disease Health Aspects of Excreta and Wastewater Management*. Washington, D.C., The World Bank.
- Feddes, R.A., P.J. Kowalik, and H. Zaradny. 1978. *Simulation of Field Water Use and Crop Yield*. Prepared by Centre for Agricultural Publishing and Documentation Wageningen.
- Fedler, C.B., C.J. Green, B. Mueller, and P.R. Pearson. 2003. *Denitrification for Land Applied Treated Wastewater*. Prepared by Departments of Civil Engineering and Plant and Soil Science, Texas Tech University.
- Fernando, W., K. Xia, and C. Rice. 2005. Sorption and desorption of ammonium from liquid swine waste in soils. *Soil Sci Soc Am J* 69(4):1057-1065.
- Finch, S.D., D.E. Radcliffe, and L.T. West. 2008. Modeling trench sidewall and bottom flow in on-site wastewater systems. *Journal of Hydrologic Engineering* 13(8):693-701.
- Flowers, T.H. and J.R. O'Callaghan. 1983. Nitrification in soils incubated with pig slurry or ammonum sulphate. *Soil Biology & Biochemistry* 15(3):337-342.
- Garrido, F., C. Henault, H. Gaillard, and J. Germon. 2000. Inhibitory capacities of acetylene on nitrification in two agricultural soils. *Soil Biology & Biochemistry* 32:1799-1802.
- Gee, C.S., M.T. Suidan, and J.T. Pfeffer. 1990. Modeling of nitrification under substrate-inhibiting conditions. *Journal of Environmental Engineering* 116(1):18-31.
- Glaser, A. 2004. The ubiquitous triclosan: A common antibacterial agent exposed. Beyond Pesticides Fact Sheet. <http://www.beyondpesticides.org/pesticides/factsheets/Triclosan%20cited.pdf>.
- Goel, K.C. and A.F. Gaudy. 1969. Studies on the relationship between specific growth rate and concentration of nitrogen source for heterogeneous microbial population of sewage origin. *Biotech and Bioeng.* 11:67-78.
- Grant, R.F. 1995. Mathematical modelling of nitrous oxide evolution during nitrification. *Soil Biology and Biochemistry* 27(9):1117-1125.
- Groffman, P.M. 1984. Nitrification and denitrification in conventional and no-tillage soils. *Soil Science Society of America Journal* 49:329-334.
- Groffman, P.M. and J.M. Tiedje. 1988. Denitrification hysteresis during wetting and drying cycles in soil. *Soil Science Society of America Journal* 52(6):1626-1629.
- Groffman, P.M. and J.M. Tiedje. 1989. Denitrification in north temperate forest soils: Relationships between denitrification and environmental factors at the landscape scale. *Soil Biology & Biochemistry* 21(6):621-626.
- Groffman, P.M. and J.M. Tiedje. 1989a. Denitrification in north temperate forest soils: Spatial and temporal patterns at the landscape and seasonal scales. *Soil Biology & Biochemistry* 21(6):613-620.

- Grundmann, G.L. and D.E. Rolston. 1987. A water function approximation to degree of anaerobiosis associated with denitrification. *Soil Science* 144(6):437-441.
- Grundmann, G.L., P. Renault, L. Rosso, and R. Bardin. 1995. Differential effects of soil water content and temperature on nitrification and aeration. *Soil Science Society of America Journal* 59(5):1342-1349.
- Gujer, W. 1977. Design of nitrifying activated sludge process with the aid of dynamic simulation. *Prog. Water Technol.* 9:323-336.
- Günkör, K. and K. Ünlö. 2005. Nitrite and nitrate removal efficiencies of soil aquifer treatment columns. *Turkish Journal of Engineering and Environmental Sciences* 29:159-170.
- Hall, J.M., E. Paterson, and K. Killham. 1998. The effect of elevated CO₂ concentration and soil pH on the relationship between plant growth and rhizosphere denitrification potential. *Global Change Biology* 4(2):209-216.
- Harden, H. and J. Chanton. 2010. *Interim Report on Performance Based Treatment Systems*. FDEP Agreement No: WM926. Prepared for Florida Department of Environmental Health by Florida State University Department of Oceanography, Tallahassee, FL.
- Hari, A.C., R.A. Paruchuri, D.A. Sabatini, and T. C. Kibbey. 2005. Effects of pH and cationic and nonionic surfactants on the adsorption of pharmaceuticals to a natural aquifer material. *Environmental Science and Technology* 39(8):2592-2598.
- Heberer, T. 2002. Occurrence, fate, and removal of pharmaceutical residues in the aquatic environment: a review of recent research data. *Toxicology Letters* 131 (1-2):5-17.
- Hemond, H.F. and E.J. Fechner-Levy. 2000. *Chemical Fate and Transport in the Environment*. 2nd ed. Academic Press.
- Henault, C., D. Cheneby, K. Heurlier, F. Garrido, S. Perez, and J. Germon. 2001. Laboratory kinetics of soil denitrification are useful to discriminate soils with potentially high levels of N₂O emission on the field scale. *Agronomie* 21:713-723.
- Henrich, M. and K. Haselwandter. 1997. Denitrification and gaseous losses from an acid spruce forest soil. *Soil Biology & Biochemistry* 29 (9/10):1529-1537.
- Henze, M., J. Grady, W. Gujer, G. Marais, and T. Matsue. 1987. *Activated Sludge Model*. IAWPRC Scientific and Technical Reports, No. 1.
- Henze, M., P. Harremoës, and J. Jansen. 2002. *Wastewater Treatment: Biological and Chemical Processes*. 3rd ed. Springer.
- Higgins, C., J. Sharp, J. Sepulvado, B. Littrell, G. O'Connor, E. Snyder, and D. McAvoy. 2010. *State-of-the-Science Review of Occurrence and Physical, Chemical and Biological Processes Affecting Biosolids-borne Trace Organic Chemicals in Soils*. Project No. SRSK5T09. Prepared for Water Environment Research Foundation (WERF), Alexandria, VA by CSM, Golden CO.
- Hill, C.G. 1977. *Chemical Engineering Kinetics & Reactor Design*. John Wiley & Sons.
- Hoffmann, C., S. Rysgaard, and P. Berg. 2000. Denitrification rates predicted by nitrogen-15 labeled nitrate microcosm studies, in situ measurements, and modeling. *Journal of Environmental Quality* 29(6):2020-2028.

- Huang, B. and J. D. Fry. 1999. Turfgrass evapotranspiration. In: *Water Use In Crop Production*. Edited by Kirkham, M. B. Food Products Press, Binghamton, NY.
- Jardine, P.M., J.F. McCarthy, and N.L. Weber. 1989. Mechanisms of dissolved organic carbon adsorption on soil. *Soil Science Society of America Journal* 53(5):1378-1385.
- Jarvis, S.C. and D.J. Hatch. 1994. Potential for denitrification at depth below long-term grass swards. *Soil Biology & Biochemistry* 26:1629-1636.
- Jenkins, M.C. and W.M. Kemp. 1984. The coupling of nitrification and denitrification in two estuarine sediments. *Limnology Oceanography* 29(3):609-619.
- Jenssen, P.D. and R.L. Siegrist. 1990. Technology assessment of wastewater treatment by soil infiltration systems. *Water Science & Technology* 22(34):83-92.
- Johns, D., H. Williams, K. Farrish, and S. Wagner. 2004. Denitrification and soil characteristics of wetlands created on two mine soils in east Texas, U.S.A. *Wetlands* 24(1):57-67.
- Jorgensen, T.C. and L.R. Weatherley. 2003. Ammonia removal from wastewater by ion exchange in the presence of organic contaminants. *Water Research* 37:1723-1728.
- Joss, A., S. Zabczynski, A. Göbel, B. Hoffmann, D. Löffler, C. McArde, T. Ternes, A. Thomsen, and H. Siegrist. 2006. Biological degradation of pharmaceuticals in municipal wastewater treatment: Proposing a classification scheme. *Water Research* 40(8):1686-1696.
- Jury, W.A. and R. Horton. 2004. *Soil Physics*. 6th ed. Wiley.
- Kapagiannidis, A.G., E. Vaiopoulou, and A. Aivasidis. 2006. Determination of kinetic parameters in a pilot scale BNR system treating municipal wastewater. *Global NEST Journal* 8(1):68-74.
- Keeney, D.R., I.R. Fillery, and G.P. Marx. 1979. Effect of temperature on the gaseous nitrogen products of denitrification in a silt loam soil. *Soil Science Society of America Journal* 43(5):1124-1129.
- Klemedtsson, L., S. Simkins, B. Svensson, H. Johnsson, and T. Rosswall. 1991. Soil denitrification in three cropping systems characterized by differences in nitrogen and carbon supply: II. Water and NO₃ effects on the denitrification process. *Plant and Soil* 138:273-286.
- Klemedtsson, L., Å. Klemedtsson, F. Moldan, and P. Weslien. 1997. Nitrous oxide emission from Swedish forest soils in relation to liming and simulated increased N-deposition. *Biology and Fertility of Soils* 25(3):290-295.
- Kneebone, W.R., D.M. Kopec, and C.F. Mancino. 1992. Water requirement and irrigation In: *Turfgrass* (Agronomy No 32) Edited by D. Waddington, R. Carrow, and R. Shearman. Madison, WI.
- Knowles, G., A.L. Downing, and M.J. Barrett. 1965. Determination of kinetic constants for nitrifying bacteria in mixed culture, with the aid of an electronic computer. *Journal of General Microbiology* 38:263-278.
- Kohl, D., F. Vithayathil, P. Whitlow, G. Shearer, and S.H. Chien. 1976. Denitrification kinetics in soil systems: The significance of good fits of data to mathematical forms. *Soil Science Society of America Journal* 40(2):249-253.

- Korom, S.F. 1992. Natural denitrification in the saturated zone: A review. *Water Resources Research* 28(6):1657-1668.
- Kowal, N.E. 1982. *Health Effects of Land Treatment: Microbiological*. Cincinnati, OH, U.S. Environmental Protection Agency.
- Kristiansen, R. 1981. Sand filter trenches for purification of septic tank effluent. *J. Environmental Quality* 10(3):358-360.
- Kunjikutty, S.P., S.O. Prasher, R.M. Patel, S.F. Barrington, and S.H. Kim. 2007. Simulation of nitrogen transport in soil under municipal wastewater application using LEACHN. *Journal of American Water Resources Association* 43(5):1097-1107.
- Laima, M., M. Girard, F. Vouve, G. Blanchard, D. Gouleau, R. Galois, and P. Richard. 1999. Distribution of adsorbed ammonium pools in two intertidal sedimentary structures, Marennes-Oleron Bay, France. *Marine Ecology Progress Series* 182:29-35.
- Lance, J.C. 1972. Nitrogen removal by soil mechanisms. *Journal of Water Pollution Control Federation* 44(7):1352-1361.
- Langergraber, G. 2007. Simulation of the treatment performance of outdoor subsurface flow constructed wetlands in temperate climates. *Science of The Total Environment* 380(1-3):210-219.
- Langergraber, G. and J. Šimůnek. 2005. Modeling variably saturated water flow and multicomponent reactive transport in constructed wetlands. *Vadose Zone Journal* 4(4):924-938.
- Laudelout, H., R. Lambert, and M. L. Pham. 1976. The effect of pH and partial pressure of oxygen on nitrification. *Collect. Ann. Inst. Pasteur* 127A(3):367-382.
- Lee, L.S., T.J. Strock, A.K. Sarmah, and P.S.C. Rao. 2003. Sorption and dissipation of testosterone, estrogens, and their primary transformation products in soils and sediment. *Environmental Science and Technology* 37(18):4098-4105.
- Lepore, B.J. and P. Barak. 2009. A colorimetric microwell method for determining bromide concentrations. *Soil Sci. Soc. Am. J.* 73:1130-1136.
- Lijklema, L. 1973. Model for nitrification in the activated sludge process. *Environmental Science & Technology* 7(5):428.
- Linn, D.M. and J.W. Doran. 1984. Effect of water-filled pore space on carbon dioxide and nitrous oxide production in tilled and non-tilled soils. *Soil Science Society of America Journal* 48:1264-1272.
- Long, T. 1995. Methodolgy to predict nitrogen loading from on-site sewage treatment systems. In: Proceedings: 8th Northwest On-Site Wastewater Treatment Short Course, ed: R.W. Seabloom. University of Washington, Department of Civil Engineering, Seattle, WA.
- Lotse, E.G., J.D. Jabro, K.E. Simmons, and D. Baker. 1992. Simulation of nitrogen dynamics and leaching from arable soils. *Journal of Contaminant Hydrology* 10:183-196.
- Lowe, K., N. Rothe, J. Tomaras, K. DeJong, M. Tucholke, J. Drewes, J. McCray, and J. Munakata-Marr. 2007. Influent Constituent Characteristics of the Modern Waste Stream from Single Sources: Literature Review. Project No. 04-DEC-1. Prepared for WERF, Alexandria, VA by CSM, Golden CO.

- Lowe, K.S., S.M. Van Cuyk, and R.L. Siegrist. 2007b. Soil treatment unit performance as affected by hydraulic loading rate and applied effluent quality. Proceedings of the Eleventh National Symposium on Individual and Small Community Sewage System, in Warwick, RI. American Society of Agricultural and Biological Engineers (ASABE), St. Joseph, MI.
- Lowe, K.S., S.M. Van Cuyk, R.L. Siegrist, and J.E. Drewes. 2008. Field evaluation of the performance of engineered on-site wastewater treatment units. *Journal of Hydrologic Engineering* 13(8):735-743.
- Lowe, K., M. Tucholke, J. Tomaras, K. Conn, C. Hoppe, J. Drewes, J. McCray, and J. Munakata-Marr. 2009. *Influent Constituent Characteristics of the Modern Waste Stream from Single Sources: Final Report*. Project No. 04-DEC-1. Prepared for WERF, Alexandria, VA by CSM, Golden CO.
- Lowrance, R. and R K. Hubbard. 2001. Denitrification from swine lagoon overland flow treatment system at a pasture-riparian zone interface. *Journal of Environmental Quality* 30:617-624.
- Lucas, S.D. and D.L. Jones. 2006. Biodegradation of estrone and 17 β -estradiol in grassland soils amended with animal wastes. *Soil Biology & Biochemistry* 38:2803-2815.
- Lundquist, E.J., L.E. Jackson, and K.M. Scow. 1999. Wet-dry cycles affect dissolved organic carbon in two California agricultural soils. *Soil Biology & Biochemistry* 31:1031-1038.
- Maag, M. and F.P. Vinther. 1996. Nitrous oxide emission by nitrification and denitrification in different soil types and at different soil moisture contents and temperatures. *Applied Soil Ecology* 4(1):5-14.
- Maag, M., M. Malinovsky, and S. Nielsen. 1997. Kinetics and temperature dependence of potential denitrification in riparian soils. *Journal of Environmental Quality* 26:215-223.
- Machefert, S.E. and N.B. Dise. 2004. Hydrological controls on denitrification in riparian ecosystems. *Hydrology and Earth System Sciences* 8(4):686-694.
- MacQuarrie, K.T.B., E.A. Sudicky, and W.D. Robertson. 2001. Multicomponent simulation of wastewater-derived nitrogen and carbon in shallow unconfined aquifers: II. Model application to a field site. *Journal of Contaminant Hydrology* 47:85-104.
- Malhi, S.S. and W.B. McGill. 1982. Nitrification in three Alberta soils: Effect of temperature, moisture, and substrate concentration on the rate of nitrification. *Soil Biology & Biochemistry* 14(4):393-399.
- Malhi, S.S., W.B. McGill, and M. Nyborg. 1990. Nitrate losses in soils: Effect of temperature, moisture and substrate concentration. *Soil Biology and Biochemistry* 22(6):733-737.
- Mayer, P., W. DeOreo, E. Opitz, J. Kiefer, W. Davis, B. Dziegielewski, and J. Nelson. 1999. *Residential End Uses of Water*. Prepared for American Water Works Research Foundation, Denver, CO.
- McCarty, G.W. and J.M. Bremner. 1992. Availability of organic carbon for denitrification of nitrate in subsoils. *Biology and Fertility of Soils* 14:219-222.
- McCarty, G.W. and J.M. Bremner. 1995. Factors affecting the availability of organic carbon for denitrification of nitrate in subsoils. *Biology and Fertility of Soils* 15:132-136.

- McCray, J.E., S.L. Kirkland, R.L. Siegrist, and G.D. Thyne. 2005. Model parameters for simulating fate and transport of on-site wastewater nutrients. *Ground Water* 43(4):628-639.
- McCray, J., K. Lowe, M. Geza, J. Drewes, S. Roberts, A. Wunsch, D. Radcliffe, J. Amador, J. Atoyan, T. Boving, D. Kalen, and G. Loomis. 2008. *Development of Quantitative Tools to Determine the Expected Performance of Wastewater Soil Treatment Units: Literature Review*. Report No. DEC1R06. Prepared for WERF by CSM, Golden CO.
- McGarity, J.W. 1961. Denitrification studies on some South Australian soils. *Plant and Soil* 14(1):1-21.
- McKinley, J. 2008. *Occurrence and Environmental Behavior of Humic Substances and Polysaccharides Accumulating in Soil Wastewater Treatment Units*. Ph.D. Dissertation, Environmental Science & Engineering Division, CSM, Golden, CO.
- McLaren, A.D. 1970. Temporal and vectoral reactions of nitrogen in soil: A review. *Canadian Journal of Fisheries and Aquatic Science* 50(2):97-109.
- Messer, J. and P. Brezonik. 1983. Laboratory evaluation of kinetic parameters for lake sediment denitrification models. *Ecological Modelling* 21:277-286.
- Millington, R.J. and J.P. Quirk. 1960. Transport in porous media. *Trans. 7th Int. Congr. Soil Sci* 1(97):106.
- Morris, J.T., G.J. Whiting, and F.H. Chapelle. 1988. Potential denitrification rates in deep sediments from the southeastern coastal plain. *Environmental Science and Technology* 22:832-836.
- Mortland, M.M. and K.V. Raman. 1968. Surface acidities of smectites in relation to hydration, exchangeable cation and structure. *Clay Miner* 16:393-398.
- Müller, C., R.J. Stevens, and R.J. Laughlin. 2003. Evidence of carbon stimulated N transformations in grassland soil after slurry application. *Soil Biology and Biochemistry* 35(2):285-293.
- Myrold, D.D. and J. M. Tiedje. 1986. Simultaneous estimation of several nitrogen cycle rates using ¹⁵N: Theory and application. *Soil Biology & Biochemistry* 18:559-568.
- Oaks, J., M. Gilbert, M. Virani, R. Watson, C. Meteyer, B. Rideout, H. Shivaprasad, S. Ahmed, M. Chaudhry, and M. Arshad. 2002. Diclofenac residues as the cause of vulture population decline in Pakistan. *Nature* 40:65-81.
- Otis, R.J. 1985. Soil clogging mechanisms and control. Proceedings of the On-Site Wastewater Treatment - Fourth National Symposium on Individual and Small Community Sewage Systems. ASAE, St. Joseph, MI. p 238-250.
- Otis, R.J. 2007. *Estimates of Nitrogen Loadings to Groundwater from Onsite Wastewater Systems in the Wekiva Study Area*. Task 2 Report, Prepared for Florida Department of Health Bureau of Onsite Sewage Programs, Tallahassee, FL.
- Pabich, W.J., I. Valiela, and H.F. Hemond. 2001. Relationship between DOC concentration and vadose zone thickness and depth below water table in groundwater of Cape Cod, U.S.A. *Biogeochemistry* 55:247-268.

- Parkin, T.B. 1987. Soil microsites as a source of denitrification variability. *Soil Science Society of America Journal* 51(5):1194-1199.
- Parton, W., A. Mosier, D. Ojima, D. Valentine, D. Schimel, K. Weier, and A. Kulmala. 1996. Generalized model for N₂ and N₂O production from nitrification and denitrification. *Global Biogeochemical Cycles* 10(3):401-412.
- Perez, C.A., M.R. Carmona, and J.J. Armesto. 2003. Non-symbiotic nitrogen fixation, net nitrogen mineralization and denitrification in evergreen forests of Chiloe Island, Chile: A comparison with other temperate forests *Gayana Botanica* 60(1):25-33.
- Philip, J.R. 1969. Theory of infiltration. *Advances in Hydroscience* 5:215-296.
- Pinay, G., L. Roques, and A. Fabre. 1993. Spatial and temporal patterns of denitrification in riparian forest. *Journal of Applied Ecology* 30:581-591.
- Poduska, R.A. and J.F. Andrews. 1974. *Dynamics of Nitrification in the Activated Sludge process*. Prepared by Dept. of Environ. Systems Eng., Clemson Univ., Clemson, SC.
- Potts, D.A., J.H. Görres, E.L. Nicosia, and J.A. Amador. 2004. Effects of aeration on water quality from septic system leachfields. *J. Environ. Qual.* 33:1828-1838.
- Powelson, D.K., Simpson, J.R. and C.P. Gerba. 1990. Virus transport and survival in saturated and unsaturated flow through soil columns. *J. Environ. Qual.* 19(3): 396-401.
- Powlson, D.S., P.G. Saffigna, and M. Kragt-Cottaar. 1988. Denitrification at sub-optimal temperatures in soils from different climatic zones. *Soil Biology & Biochemistry* 20(5):719-723.
- Quinlan, A.V. 1984. Prediction of the optimum pH for ammonia-N oxidation by *Nitrosomonas europaea* in well-aerated natural and domestic -waste water. *Water Research* 18:561-566.
- Radcliffe, D. 2009. Unpublished experimental data on removal rates on a clayey soils from UGA Test Site.
- Radcliffe, D.E. and L.T. West. 2007. Modeling long term acceptance rates for OWMSs. Proceedings of the Eleventh National Symposium on Individual and Small Community Sewage Systems, in Warwick, RI. ASABE, St. Joseph, MI.
- Radcliffe, D.E., and L.T. West. 2009. Design hydraulic loading rates for onsite wastewater systems. *Vadose Zone Journal* 8(1):1-11.
- Rauch, T. 2004. *The Removal of Effluent-derived Organic Matter Components during Infiltration into Porous Media*. Ph.D. Dissertation, Environmental Science & Engineering Division, CSM, Golden, CO.
- Reddy, K.R., W.H. Patrick, and R.E. Phillips. 1978. The role of nitrate diffusion in determining the order and rate of denitrification in flooded soil: I. Experimental results. *Soil Science Society of America Journal* 42(1):268-272.
- Rittmann, B.E. and V.L. Snoeyink. 1984. Achieving biologically stable drinking water. *Journal of the American Water Works Association* 76(10):106-114.
- Rivett, M., S. Buss, P. Morgan, J. Smith, and C. Bemment. 2008. Nitrate attenuation in groundwater: A review of biogeochemical controlling processes. *Water Research* 42(16):4215-4232.

- Robertson, W.D. 1994. Chemical fate and transport in a domestic septic system: site description and attenuation of dichlorobenzene. *Environmental Toxicology and Chemistry* 13(2):183-191.
- Robertson, L.A. and J.G. Kuenen. 1984. Aerobic denitrification: a controversy revived. *Archives of Microbiology* 139(4):351-354.
- Robertson, W.D., J.A. Cherry, and E.A. Sudicky. 1991. Ground-water contamination from two small septic systems on sand aquifers. *Ground Water* 29(1):82-92.
- Rodriguez, S.B., A. Alonso-Gaite, and J. Alvarez-Benedi. 2005. Characterization of nitrogen transformations, sorption and volatilization processes in urea fertilized soils. *Vadose Zone J* 4(2):329-336.
- Rothe, N. 2006. *Comparison of Raw Wastewater and Septic Tank Effluent Composition through Literature and Field Investigations*. M.S. Thesis. Environmental Science & Engineering Division, CSM, Golden, CO.
- Ryan, M. 1998. *Relative Denitrification Rates in Surface and Subsurface Mineral Soil Layers*. Prepared by Johnstown Castle Research Centre, Wexford, Ireland.
- Ryden, J.C., J.H. Skinner, and D.J. Nixon. 1987. Soil core incubation system for the field measurement of denitrification using acetylene-inhibition. *Soil Biology & Biochemistry* 19(6):753-757.
- Saad, O. and R. Conrad. 1993. Temperature dependence of nitrification, denitrification, and turnover of nitric oxide in different soils. *Biology and Fertility of Soils* 15:21-27.
- Schaap, M.G., F.J. Leij, and M.T. van Genuchten. 2001. Rosetta: a computer program for estimating soil hydraulic parameters with hierarchical pedotransfer functions. *Journal of Hydrology* 251:163-176.
- Schjonning, P., I. Thomsen, P. Moldrup, and B. Christensen. 2003. Linking soil microbial activity to water- and air-phase contents and diffusivities. *Soil Science Society of America Journal* 67:156-165.
- Schoenau, J.J. and R.E. Karamanos. 1993. *Soil Sampling and Methods of Analysis*. M.R. Carter, ed. Lewis Publishers, Boca Raton, FL.
- Sears, C L. 2005. A dynamic partnership: Celebrating our gut flora. *Anaerobe* 11(5): 247-251.
- Shah, V., R. Ordonez, K. Jahan, and R. P. Ramachandran. 2001. Nonlinear parameter estimation of nonylphenol biodegradation. Proceedings of the IEEE International Conference, in Mexico City, Mexico. Control Applications.919-924.
- Sheibley, R.W., A.P. Jackman, J.H. Duff, and F.J. Triska. 2003. Numerical modeling of coupled nitrification-denitrification in sediment perfusion cores from the hyporheic zone of Shingobee River, MN. *Advances in Water Resources* 26:977-987.
- Siegrist, H. and W. Gujer. 1987. Demonstration of mass transfer and pH effects in a nitrifying biofilm. *Water Research* 21:1481-1487.
- Siegrist, R.L. 1987. Soil clogging during subsurface wastewater infiltration as affected by effluent composition and loading rate. *Journal of Environmental Quality* 1 (3):181-187.
- Siegrist, R.L. 2001. Perspectives on advancing the science and engineering of onsite wastewater systems. *Small Flows Quarterly* (4):8-13.

- Siegrist, R.L. 2006. Evolving a rational design approach for sizing soil treatment units: Design for wastewater effluent infiltration. *Small Flows Quarterly* (5):16-24.
- Siegrist, R.L., E.J. Tyler, and P.D. Jenssen. 2001. *Design and Performance of Onsite Wastewater Soil Absorption Systems*. EPRI Report No 1001446. Prepared for Electric Power Research Institute, Palo Alto, CA.
- Siegrist, R.L., J.E. McCray, and K.S. Lowe. 2004. Wastewater infiltration into soil and the effects of infiltrative surface architecture. *Small Flows Journal* 5(1):29-39.
- Šimek, M. and J.E. Cooper. 2002. The influence of soil pH on denitrification: progress towards the understanding of this understanding over the last 50 years. *European Journal of Soil Science* 53(3):345-354.
- Šimůnek, J., M. Sejna, and M.T. van Genuchten. 1999. *The HYDRUS-2D Software Package for Simulating Two-dimensional Movement of Water, Heat, and Multiple Solutes in Variably Saturated Media*. Version 2.0. Agricultural Research Service, U.S. Department of Agriculture, Riverside, CA.
- Šimůnek, J., M.T. van Genuchten, and M. Senja. 2006. *The HYDRUS-2D Software Package for Simulating Two-dimensional Movement of Water, Heat, and Multiple Solutes in Variably Saturated Media*. Version 1.0. Technical Manual. PC Progress, Prague.
- Singh, L. 2007. An experiment to identify levels of triclosan that are harmful to bacteria in Puget Sound. Prepared for Triclosan Effects on Marine Bacteria by University of Washington.
- Skaggs, R.W. 1978. *A Water Management Model for Shallow Water Table Soils*. Report #134. Prepared by Water Resources Research Institute of the University of North Carolina.
- Smith, R.L. and J.H. Duff. 1988. Denitrification in a sand and gravel aquifer. *Applied and Environmental Microbiology* 54(5):1071-1078.
- Spalding, R.F., M.E. Exner, G.E. Martin, and D.D. Snow. 1993. Effects of sludge disposal on groundwater nitrate concentrations. *Journal of Hydrology* 142:213-228.
- Stanford, G., R.A. Vander Pol, and S. Dzienia. 1975. Effect of temperature on denitrification rate in soils. *Soil Science Society of America Journal* 39:867-870.
- Stanford, G., R.A. Vander Pol, and S. Dzienia. 1975a. Denitrification rates in relation to total extractable soil carbon. *Soil Science Society of America Journal* 39:284-289.
- Stark, J.M. 1996. Modeling the temperature response of nitrification. *Biogeochemistry* 35(3):433-445.
- Stark, J.M. and M.K. Firestone. 1995. Mechanisms for soil moisture effects on activity of nitrifying bacteria. *Applied and Environmental Microbiology* 61:218-221.
- Stark, J.M. and M.K. Firestone. 1996. Kinetic characteristics of ammonium-oxidizer communities in a California oak woodland-annual grassland. *Soil Biology & Biochemistry* 28(10/11):1307-1317.
- Starr, R.C. and R.W. Gillham. 1993. Denitrification and organic carbon availability in two aquifers. *Ground Water* 31(6):934-947.

- Suarez, S., M. Dodd, F. Omil, and U. von Gunten. 2007. Kinetics of triclosan oxidation by aqueous ozone and consequent loss of antibacterial activity: Relevance to municipal wastewater ozonation. *Water Research* 41:2481-2490.
- Suzuki, I., U. Dular, and S. Kwok. 1974. Ammonia or ammonium ion as substrate for oxidation by *Nitrosomonas europaea* cells and extracts. *Journal of Bacteriology* 120(1):556-558.
- Tackett, K.N. 2004. *Vadose Zone Treatment During Effluent Reclamation as Effected by Infiltrative Surface Architecture and Hydraulic Loading Rate*. M.S. Thesis. Environmental Science & Engineering Division, CSM, Golden, CO.
- Tackett, K.N., K.S. Lowe, R.L. Siegrist, and S.M. Van Cuyk. 2004. Vadose zone treatment during effluent reclamation as affected by infiltrative surface architecture and hydraulic loading rate. Proceedings of the Proceedings of the Tenth National Symposium on Individual and Small Community Sewage Systems, in Sacramento, CA. 701P0104:655–667. ASAE.
- Tillotson, B.E. 2009. *The Longer Term Removal of Organic Matter and Nutrients from within the Vadose Zone of Onsite Wastewater Treatment Systems as Affected by Key System Design Parameters*. M.S. Thesis, Environmental Science & Engineering Division, CSM, Golden, CO.
- Toride, N., F.J. Leij and M.T. van Genuchten .1995. *The CXTFIT Code for Estimating Transport Parameters from Laboratory or Field Tracer Experiments, Version 2.1*. Research Report from the U.S. Salinity Laboratory 137.
- Tucholke, M.B. 2007. *Statistical Assessment of Relationships Between Denitrification and Easily Measurable Soil Properties: A simple Predictive Tool for Watershed-scale Modeling*. MS Thesis, Environmental Science & Engineering, CSM, Golden, CO.
- Tucholke, M.B., J.E. McCray, G.D. Thyne, and R.M. Waskom. 2007. Variability in denitrification rates: Literature review and analysis. Proceedings of the National Onsite Wastewater Recycling Association 16th Annual Technical Education & Exposition Conference, in Baltimore, MD. NOWRA, Santa Cruz, CA.
- Turco, R.F. 1994. *Methods of Soil Analysis: Part 2 – Microbiological and Biochemical Properties*. R. Weaver, J. Angle, and P. Bottomley, eds. Soil Science Society of America, Madison, WI.
- USDA. 1999. *Soil Taxonomy*. [cited 2009]. Available from: ftp://ftp-nc.sc.egov.usda.gov/NSSC/Soil_Taxonomy/tax.pdf.
- U.S. EPA. 1993. *Manual: Nitrogen Control* EPA/625/R/-93/010. U.S. EPA, Office of Research and Development and Office of Water. Washington, D.C.
- U.S. EPA. 2002. *Onsite Wastewater Treatment Systems Manual*. Report No. 625/R-00/008. U.S. EPA, Office of Water. Cincinnati, OH.
- U.S. EPA. 2004. Enhanced nutrient removal – Nitrogen. Onsite wastewater treatment systems technology - Fact Sheet 9. U.S. EPA.
- U.S. EPA. 2008, February 15, 2008). Drinking Water Contaminants. Retrieved April 7, 2008, <http://www.epa.gov/safewater/contaminants/index.html>.
- Van Cuyk, S., R. Siegrist, A. Logan, S. Masson, E. Fischer, and L. Figueroa. 2001. Hydraulic and purification behaviors and their interactions during wastewater treatment in soil infiltration systems. *Water Research* 35(4):953-964.

- Van Cuyk, S., R. Siegrist, K. Lowe, J. Drewes, J. Munakata-Marr, and L. Figueroa. 2005. *Performance of Engineered Treatment Units and Their Effects on Biozone Formation in Soil and System Purification Efficiency*. Project No. WU-HT-03-36. Prepared for National Decentralized Water Resources Capacity Development Project (NDWRCDP). Washington University, St. Louis, MO by CSM, Golden, CO.
- van Genuchten, M.T. 1980. A closed-form equation for predicting the hydraulic conductivity of unsaturated soils. *Soil Science Society of America Journal* 44(5):892-898.
- van Genuchten, M.T. 1985. Convective-dispersive transport of solutes involved in sequential first-order decay reactions. *Computers & Geosciences* 11(2):129-147.
- van Raaphorst, W. and J.F.P. Malschaert. 1996. Ammonium adsorption in superficial North Sea sediments. *Continental Shelf Research* 16(11):1415-1435.
- Vinther, F.P. 1992. Measured and simulated denitrification activity in a cropped sandy and loamy soil. *Biology and Fertility of Soils* 14:43-48.
- Vrugt, J., J. Hopmans, and J. Simunek. 2001. Calibration of a two-dimensional root water uptake model. *Soil Science Society of America Journal* 65(4):1027-1037.
- Walker, W.G., J. Bouma, D.R. Keeney and F.R. Magdoff. 1973. Nitrogen transformations during subsurface disposal of septic tank effluent in sands: II. Groundwater Quality. *J. Environmental Quality* 2:521-525.
- Walsh, D.R. 2006. *Infiltration Rate Behavior in Sand Porous Media as Affected by Effluent Quality, Infiltrative Surface Architecture, and Hydraulic Loading Rate*. MS Thesis, Environmental Science & Engineering, CSM, Golden, CO.
- Wang, X., M.A. Youssef, R.W. Skaggs, J.D. Atwood, and J.R. Frankenberger. 2005. Sensitivity analyses of the nitrogen simulation model, DRAINMOD-N II. *Transactions of the American Society of Agricultural Engineers* 48(6):2205-2212.
- Weier, K.L., J.W. Doran, J.F. Power, and D.T. Walters. 1993. Denitrification and the dinitrogen/nitrous oxide ratio as affected by soil water, available carbon, and nitrate. *Soil Science Society of America Journal* 57(1):66-72.
- Well, R. and D.D. Myrold. 2002. A proposed method for measuring subsoil denitrification in situ. *Soil Science Society of America Journal* 66:507-518.
- Whelan, B.R. 1988. Disposal of septic tank effluent in calcareous sands. *J. Environmental Quality* 17(2):272-277.
- Wren, A., R. Siegrist, K. Lowe, and R. Laws. 2004. Field performance evaluation of textile filter units employed in onsite wastewater treatment systems. Proceedings of the Tenth National Symposium on Individual and Small Community Sewage Systems, in Sacramento, CA. ASAE. 10:514-525.
- Wu, L. 1985. Matching irrigation to turfgrass root depth. *California Turfgrass Culture*, 1-2.
- Yamaguchi, T., P. Moldrop, S. Teranishi, and D. Rolston. 1990. Denitrification in porous media during rapid, continuous leaching of synthetic wastewater at saturated water flow. *Journal of Environmental Quality* 19:676-683.

- Yamaguchi, T., P. Moldrop, D. Rolston, S. Ito, and S. Teranishi. 1996. Nitrification in porous media during rapid unsaturated water flow. *Water Research* 30(3):531-540.
- Ying, G.G. and R.S. Kookana. 2007. Triclosan in wastewaters and biosolids from Australian wastewater treatment plants. *Environmental International* 33(2):199-205.
- Youssef, M.A., R.W. Skaggs, G.M. Chescheir, and J.W. Gilliam. 2005. The nitrogen simulation model, DRAINMOD-N II. *Transactions of the American Society of Agricultural Engineers* 48(2):611-626.
- Yu, Z., B. Xiao, W. Huang, and P. Peng. 2004. Sorption of steroid estrogens to soils and sediments. *Environmental Toxicology and Chemistry* 23(3):531-539.
- Zwiener, C. and F.H. Frimmel. 2003. Short-term tests with a pilot sewage plant and biofilm reactors for the biological degradation of the pharmaceutical compounds clofibrac acid, ibuprofen, and diclofenac. *Science of the Total Environment* 309(1-3):201-211.



Water Environment Research Foundation

635 Slaters Lane, Suite G-110 ■ Alexandria, VA 22314-1177

Phone: 571-384-2100 ■ Fax: 703-299-0742 ■ Email: werf@werf.org

www.werf.org

WERF Stock No. DEC1R06b

Co-published by

IWA Publishing

Alliance House, 12 Caxton Street

London SW1H 0QS

United Kingdom

Phone: +44 (0)20 7654 5500

Fax: +44 (0)20 7654 5555

Email: publications@iwap.co.uk

Web: www.iwapublishing.co

IWAP ISBN: 978-1-84339-537-9/1-84339-537-1



Nov 2010



Water Environment Research Foundation
Collaboration. Innovation. Results.

Decentralized Systems

A collage of four images: top-left shows water cascading over a brown, porous filter medium; top-center shows a person in a white lab coat looking through a microscope; top-right shows a hand holding a glass slide with a circular pattern of cells; bottom-left shows a close-up of a blue, porous filter medium.

**FINAL
REPORT**

Quantitative Tools to Determine the Expected Performance of Wastewater Soil Treatment Units

VISUAL-GRAPHIC TOOLS

Co-published by



DEC1R06c

QUANTITATIVE TOOLS TO DETERMINE
THE EXPECTED PERFORMANCE OF
WASTEWATER SOIL TREATMENT UNITS

VISUAL-GRAPHIC TOOLS

2010



The Water Environment Research Foundation, a not-for-profit organization, funds and manages water quality research for its subscribers through a diverse public-private partnership between municipal utilities, corporations, academia, industry, and the federal government. WERF subscribers include municipal and regional water and wastewater utilities, industrial corporations, environmental engineering firms, and others that share a commitment to cost-effective water quality solutions. WERF is dedicated to advancing science and technology addressing water quality issues as they impact water resources, the atmosphere, the lands, and quality of life.

For more information, contact:

Water Environment Research Foundation
635 Slaters Lane, Suite G-110
Alexandria, VA 22314-1177
Tel: (571) 384-2100
Fax: (703) 299-0742
www.werf.org
werf@werf.org

This report was co-published by the following organization.

IWA Publishing
Alliance House, 12 Caxton Street
London SW1H 0QS, United Kingdom
Tel: +44 (0) 20 7654 5500
Fax: +44 (0) 20 7654 5555
www.iwapublishing.com
publications@iwap.co.uk

© Copyright 2010 by the Water Environment Research Foundation. All rights reserved. Permission to copy must be obtained from the Water Environment Research Foundation.

Library of Congress Catalog Card Number: 2010937540

Printed in the United States of America

IWAP ISBN: 978-1-84339-536-2/1-84339-536-3

This report was prepared by the organization(s) named below as an account of work sponsored by the Water Environment Research Foundation (WERF). Neither WERF, members of WERF, the organization(s) named below, nor any person acting on their behalf: (a) makes any warranty, express or implied, with respect to the use of any information, apparatus, method, or process disclosed in this report or that such use may not infringe on privately owned rights; or (b) assumes any liabilities with respect to the use of, or for damages resulting from the use of, any information, apparatus, method, or process disclosed in this report.

Colorado School of Mines

The research on which this report is based was developed, in part, by the United States Environmental Protection Agency (EPA) through Cooperative Agreement No. X-83085101-0 with the Water Environment Research Foundation (WERF). However, the views expressed in this document are not necessarily those of the EPA and EPA does not endorse any products or commercial services mentioned in this publication. This report is a publication of WERF, not EPA. Funds awarded under the Cooperative Agreement cited above were not used for editorial services, reproduction, printing, or distribution.

This document was reviewed by a panel of independent experts selected by WERF. Mention of trade names or commercial products or services does not constitute endorsement or recommendations for use. Similarly, omission of products or trade names indicates nothing concerning WERF's or EPA's positions regarding product effectiveness or applicability.

ACKNOWLEDGMENTS

This research was funded by the Water Environment Research Foundation.

Project Team

Principal Investigator:

John McCray, Ph.D.
Colorado School of Mines

Co-Principal Investigators:

Jörg Drewes, Ph.D.
Mengistu Geza, Ph.D.
Kathryn Lowe
Colorado School of Mines

Project Team:

Sarah Roberts
Maria Tucholke
Assaf Wunsch
Colorado School of Mines

David Radcliffe, Ph.D.
Ken Bradshaw
University of Georgia

Thomas Boving, Ph.D.
Jose Amador, Ph.D.
Janet Atoyan, Ph.D.
David Kalen
George Loomis
University of Rhode Island

Issue Area Team

Steven Berkowitz
North Carolina Department of Environment & Natural Resources

Matt Byers, Ph.D.
Zoeller Company

Bob Freeman, P.E.
U.S. Environmental Protection Agency

Anish Jantrania, Ph.D., P.E.
NCS Wastewater Solutions

Charles McEntyre, P.E., CHMM
Tennessee Valley Authority

Eberhard Roeder, Ph.D.
Florida Department of Health

Robert Rubin, Ed.D.
McKim Creed

Edwin Swanson, P.E.
Arizona Dept. of Environmental Quality

George Tchobanoglous, Ph.D.
Tchobanoglous Consulting

Water Environment Research Foundation Staff

Director of Research:	Daniel M. Woltering, Ph.D.
Senior Program Manager:	Amit Pramanik, Ph.D., BCEEM

INTRODUCTION

This file includes the visual-graphic tools: nomographs, cumulative probability graphs, and scenario illustrations. Chapter 1.0 includes nomographs illustrating the fraction of total-nitrogen remaining with depth. Chapter 2.0 includes cumulative probability graphs that illustrate the likely range of treatment outcomes. Chapter 3.0 includes HYDRUS simulation outputs that illustrate various operational scenarios. Finally, a list of visual-graphic tools is provided to aid in locating the visual-graphic tool of interest.

This is a separate document that must be used in conjunction with the Guidance Manual and User's Guide. The companion Guidance Manual is organized into four chapters describing the toolkit and providing guidance for tool selection and use. The fundamental assumptions that were incorporated and a detailed description of the tool development for these visual-graphic tools are provided in the companion User's Guide. Additional tools provided as separate files include STUMOD and N-CALC as Microsoft™ Excel files.

In both the nomograph and the cumulative probability graphs, treatment information provided by these tools is based on data generated by numerical models that can incorporate complex and robust treatment and operating conditions. The parameters used for nomograph development are summarized in Table VG-1. Table VG-2 provides a definition for each parameter. Because the choices for representative OWTS conditions are limited, the user must decide how their OWTS system fits within the limited treatment estimations displayed by the graphics. Nomographs and cumulative probability graphs were developed for the following fixed operating conditions:

- ◆ Effluent Quality
 - Standard Effluent = representative of septic tank effluent (STE) as 60 mg-N L⁻¹ as ammonium-nitrogen plus 1 mg-N L⁻¹ as nitrate-nitrogen
 - Nitrified Effluent = representative of aerobically treated STE to achieve nitrogen reduction and transformation as 15 mg-N L⁻¹ as nitrate-nitrogen
- ◆ Hydraulic Loading Rate (HLR)
 - 2 cm d⁻¹
 - 5% K_{sat}
- ◆ Regional Temperature Range
 - Frigid/Cryic = Average Range 0 to 8°C, Annual Mean 4.5°C
 - Mesic = Average Range 8 to 15°C, Annual Mean 11.5°C
 - Thermic = Average Range 15 to 22°C, Annual Mean 18.5°C
 - Hyperthermic = Average Range 22 to 29°C, Annual Mean 25.5°C

Table VG-1. STUMOD Input Parameters for Nomograph Development.

Parameter	Basis*	Clay	Clay loam	Loam	Loamy sand	Sand	Sandy clay	Sandy clay loam	Sandy loam	Silt	Silty clay	Silty clay loam	Silty loam
Kb	LV	0.4	0.4	0.4	0.4	0.4	0.4	0.4	0.4	0.4	0.4	0.4	0.4
BT	LV	2.0	2.0	2.0	2.0	2.0	2.0	2.0	2.0	2.0	2.0	2.0	2.0
α	PDM	0.00	0.00	0.00	0.00	0.00	0.00	0.00	0.00	0.00	0.00	0.00	0.00
HLR	FI	-	-	-	-	-	-	-	-	-	-	-	-
α_1	LV	0.02	0.03	0.02	0.08	0.09	0.05	0.04	0.05	0.01	0.03	0.02	0.01
α_2	M-R	0.02	0.02	0.01	0.03	0.04	0.03	0.02	0.03	0.01	0.02	0.01	0.01
Ks	M-R	14.75	8.18	12.04	105.12	642.98	11.35	13.19	38.25	43.74	9.61	11.11	18.26
θ_1	M-R	0.10	0.08	0.06	0.05	0.05	0.12	0.06	0.04	0.05	0.11	0.09	0.06
θ_2	M-R	0.46	0.44	0.40	0.39	0.37	0.39	0.38	0.39	0.49	0.48	0.48	0.44
n	M-R	1.26	1.41	1.47	1.75	3.18	1.21	1.33	1.45	1.68	1.32	1.52	1.66
m	M-R	0.21	0.29	0.32	0.43	0.69	0.17	0.25	0.31	0.40	0.24	0.34	0.40
l	LV	0.50	0.50	0.50	0.50	0.50	0.50	0.50	0.50	0.50	0.50	0.50	0.50
ho	LV	5.06	2.62	-6.46	-0.38	-9.95	4.76	4.76	2.35	-60.15	4.67	-5.11	-50.25
cf	CP	1.000	1.000	1.000	1.000	1.000	1.000	1.000	1.000	1.000	1.000	1.000	1.000
Co NH4	FI	-	-	-	-	-	-	-	-	-	-	-	-
Co NO3	FI	-	-	-	-	-	-	-	-	-	-	-	-
Kr-max	M-LV	56.00	56.00	56.00	56.00	56.00	56.00	56.00	56.00	56.00	56.00	56.00	56.00
Km-nit	LV	5.00	5.00	5.00	5.00	5.00	5.00	5.00	5.00	5.00	5.00	5.00	5.00
e2	PDM	2.27	2.27	2.27	2.27	2.27	2.27	2.27	2.27	2.27	2.27	2.27	2.27
e3	PDM	1.10	1.10	1.10	1.10	1.10	1.10	1.10	1.10	1.10	1.10	1.10	1.10
β_1	PDM	0.35	0.35	0.35	0.35	0.35	0.35	0.35	0.35	0.35	0.35	0.35	0.35
fs	PDM	0.0000	0.0000	0.0000	0.0000	0.0000	0.0000	0.0000	0.0000	0.0000	0.0000	0.0000	0.0000
fwp	PDM	0.0000	0.0000	0.0000	0.0000	0.0000	0.0000	0.0000	0.0000	0.0000	0.0000	0.0000	0.0000
swp	PDM	0.1537	0.1537	0.1537	0.1537	0.1537	0.1537	0.1537	0.1537	0.1537	0.1537	0.1537	0.1537
sl	PDM	0.6649	0.6649	0.6649	0.6649	0.6649	0.6649	0.6649	0.6649	0.6649	0.6649	0.6649	0.6649
sh	PDM	0.8087	0.8087	0.8087	0.8087	0.8087	0.8087	0.8087	0.8087	0.8087	0.8087	0.8087	0.8087
T	FI												
Topt1	LV	25.00	25.00	25.00	25.00	25.00	25.00	25.00	25.00	25.00	25.00	25.00	25.00
Topt2	LV	26.00	26.00	26.00	26.00	26.00	26.00	26.00	26.00	26.00	26.00	26.00	26.00

* Basis for Parameter Value Selected:

FI= Fixed Input

M-R= Mean value based on Schaap et al 2001. Rosetta program.

LV= Literature value (Philip, J.R. 1969)

CP= Calibration parameter

M-LV=Median value based on literature

PDM= Based on parameterization of Drainmod function using observed data

Table VG-1. STUMOD Input Parameters for Nomograph Development (continued).

Parameter	Basis*	Clay	Clay loam	Loam	Loamy Sand	Sand	Sandy clay	Sandy clay loam	Sandy loam	Silt	Silty clay	Silty clay loam	Silty loam
Vmax	M-LV	2.56	2.56	2.56	2.58	2.58	2.58	2.58	2.58	3.32	3.32	3.32	3.32
Km-dnt	LV	5.00	5.00	5.00	5.00	5.00	5.00	5.00	5.00	5.00	5.00	5.00	5.00
ednt	PDM	3.77	3.77	3.77	2.87	2.87	2.87	2.87	2.87	3.87	3.87	3.87	3.87
β_2	PDM	0.35	0.35	0.35	0.35	0.35	0.35	0.35	0.35	0.35	0.35	0.35	0.35
sdn	PDM	0.00	0.00	0.00	0.00	0.00	0.00	0.00	0.00	0.00	0.00	0.00	0.00
kd	LV	1.46	1.46	0.35	0.35	0.35	1.46	1.46	0.35	0.35	1.46	1.46	0.35
fr	CP	0.00	0.00	0.00	0.00	0.00	0.00	0.00	0.00	0.00	0.00	0.00	0.00
ρ	LV	1.5	1.5	1.5	1.5	1.5	1.5	1.5	1.5	1.5	1.5	1.5	1.5
D	FI	-	-	-	-	-	-	-	-	-	-	-	-

* Basis for Parameter Value Selected:

FI= Fixed Input

M-R= Mean value based on Schaap et al 2001. Rosetta program.

LV= Literature value (Philip, J.R. 1969)

CP= Calibration parameter

M-LV=Median value based on literature

PDM= Based on parameterization of Drainmod function using observed data

Table VG-2. STUMOD Input Parameters.

Parameter	Units	Definition
Biomat Parameters		
Kb	cm d ⁻¹	Biomat hydraulic conductivity
BT	cm	Biomat thickness
Carbon Parameters		
α	-	An empirical exponent for carbon content adjustment (also referred to as α_C)
Hydraulic Parameters		
HLR	cm d ⁻¹	Hydraulic loading rate
α_1	-	Parameter α in Gradner's analytical equation for pressure distribution (also referred to as α_G)
α_2	-	Parameter α in the soil water retention function (also referred to as α_{VG})
K_s	cm d ⁻¹	Saturated hydraulic conductivity (also referred to as K_{sat})
θ_1	-	Residual soil moisture (also referred to as θ_r)
θ_2	-	Saturated soil moisture (also referred to as θ_s)
n	-	Parameter n in the soil water retention function
m	-	Parameter m in the soil water retention function
l	-	Tortusity parameter
ho	cm	Pressure head at the infiltrative surface
cf	-	Calibration coefficient for pressure distribution (a multiplier from 0 to 1.5)
Effluent Quality Parameters		
Co-NH4	mg-N L ⁻¹	Effluent ammonium-nitrogen concentration
Co-NO3	mg-N L ⁻¹	Effluent nitrate-nitrogen concentration
Nitrification Parameters		
Kr-max	mg-N L ⁻¹ d ⁻¹	Maximum nitrification rate
Km-nit	mg-N L ⁻¹	Half-saturation constant for ammonium-nitrogen
e2	-	Empirical exponent for nitrification
e3	-	Empirical exponent for nitrification
β_1	-	Empirical coefficient for temperature function for nitrification (also referred to as β_{nit})
fs	-	Value of the soil water response function at saturation
fwp	-	Value of the soil water response function at wilting point
swp	-	Relative saturation at wilting point
sl	-	Relative saturation for biological process (lower limit)
sh	-	Relative saturation for biological process (upper limit)
Temperature Parameters		
T	°C	Soil temperature
Topt1	°C	Optimum soil temperature for nitrification (also referred to as Topt-nit(oC))
Topt2	°C	Optimum soil temperature for denitrification (also referred to as Topt-dnt(oC))
Denitrification Parameters		
Vmax	mg-N L ⁻¹ d ⁻¹	Maximum denitrification rate
Km-dnt	mg-N L ⁻¹	Half-saturation constant for nitrate-nitrogen
e-dnt	-	Empirical exponent for denitrification
β_2	-	An empirical coefficient for temperature function (also referred to as β_{dnt})
sdn	-	A threshold relative saturation (dimensionless)
Ammonium Sorption Parameters		
kd	L kg ⁻¹	Adsorption Isotherm
fr	-	Fraction of ammonium-nitrogen that remains sorbed on soil, calibration parameter (0 to 1)
ρ	kg L ⁻¹	Soil bulk density
Target Depth for Output Displays		
D	cm	Soil depth
Output Values at Target Depth		
C/Co NH4	mg-N L ⁻¹	Fraction of ammonium-nitrogen remaining at soil depth D
C/Co TotN	mg-N L ⁻¹	Fraction of total nitrogen remaining at soil depth D

These nomographs are organized by soil texture then HLR and effluent quality. Each nomograph includes each of the four regional temperature regions. This enables the user to visually compare the effect of temperature, HLR and effluent quality on two adjoining pages (like an open book). To further illustrate the effect of effluent concentration, one series of nomographs was prepared for standard effluent at a HLR of 2 cm d⁻¹. These nomographs show

the fraction of total nitrogen removed at 60 cm for all four different soil temperature regions based on different initial ammonium-nitrogen concentrations.

Because there is uncertainty in each of the parameters listed in Table VG-1, Chapter 2.0 includes cumulative probability graphs prepared as a result of the Monte Carlo simulations (User's Guide, Section 2.2.2.1). Similar to the nomographs in Chapter 1.0, these cumulative probability graphs are sorted by soil texture, HLR and effluent quality. These graphs illustrate the associated uncertainty within estimated nitrogen removal illustrated in the nomographs. The information can be used to evaluate the probability associated with any particular treatment effectiveness, or provide an understanding of the variability based on key parameters (i.e., effluent quality, HLR, temperature). In this way, the cumulative probability graphs can help users make decisions based on their willingness to accept an agreed-upon level of quantified risk. Cumulative probability graphs include three different depths (30 cm, 60 cm and 120 cm) for a given soil texture, effluent type (standard or nitrified), and average annual soil temperature.

Finally, a flexible tool capable of simulating complex conditions is necessarily quite complex. The tools developed and presented in this toolkit required general assumptions and simplifications (User's Guide, Chapters 1.0, and 2.0). These assumptions and simplifications preclude the assessment of pollutant removal under certain design and environmental conditions including, subsurface heterogeneity, trench geometry, large multiple-trench systems, drip systems, or water table position. For toolkit users who do not wish to implement a complex model to assess the impacts of these conditions on STU performance, a series of different "scenarios" were simulated using HYDRUS-2D with model outputs generated for subsurface nitrogen concentrations, spatial treatment distributions, and mass-flux below a specified boundary illustrated.

These qualitative scenario illustrations show the power of a numerical model, as well as provide some end-member treatment evaluations for the selected scenarios. Finally, all possible design and environmental conditions could not be realistically covered by numerical simulations. However, select scenarios were chosen because they represent typical systems under a range of conditions providing insight into different outcomes that might result. Table VG-3 summarizes the HYDRUS scenario simulations. Complete description of scenario development conditions can be found in the User's Guide, Section 2.4. More importantly, the simulation outputs show the difference in nitrogen removal between two systems that have some common features, yet differ by a certain parameter, such as soil texture, effluent quality, HLR, or depth to groundwater. In this manner, comparison of the scenario outputs provides a qualitative assessment of the expected STU performance.

The scenario output data sheets for trench simulations is similar to the drip simulations data sheet, with a slight difference; the calculation of nitrogen mass flux at the bottom of the domain refers to flux from a linear meter of trench, whereas the drip output refers to a mass flux resulting from one emitter. Mass flux in both cases is per day and provides understanding of the footprint from an STU rather than just an expected nitrogen concentration below the infiltrative surface. The total mass load to the environment may be of more concern than a specific concentration in environmentally sensitive locations, when setting TMDLs for a watershed, or for assessing the total nitrogen-contamination impact of cluster units. Such information can then be used to back calculate how many trenches could be utilized at a site without exceeding the desired treatment goal.

Table VG-3. Illustrated Scenario Simulations.

Scenario Figure	Soil Texture	Effluent Quality	HLR	Groundwater Depth	Illustrated Effect
Trench System Scenarios					
VG-253	sand	STE	2 cm/d	deep (>90 cm)	base case for comparison
VG-254	sand	STE	10% K_{sat}	deep (>90 cm)	high loading rate
VG-255	sandy loam	STE	2 cm/d	deep (>90 cm)	soil type
VG-256	sandy loam	STE	2 cm/d	shallow (60 cm)	soil type and high water table
VG-257	sandy loam	STE	2 cm/d	deep (>90 cm)	soil type and closely spaced trenches
VG-258	sandy loam	STE	10% K_{sat}	deep (>90 cm)	soil type and high loading rate
VG-259	silty clay	STE	2 cm/d	deep (>90 cm)	soil type
VG-260	silty clay	STE	10% K_{sat}	deep (>90 cm)	soil type and high loading rate
Drip System Scenarios					
VG-261	sand	STE	7 min, 5x/d*	shallow (60 cm)	base case for comparison
VG-262	sand	STE	19 min, 5x/d	shallow (60 cm)	high loading rate
VG-263	sand	NE	7 min, 5x/d	shallow (60 cm)	effluent quality
VG-264	sand	NE	19 min, 5x/d	shallow (60 cm)	effluent quality and high loading rate
VG-265	sandy loam	STE	7 min, 5x/d	shallow (60 cm)	soil type
VG-266	sandy loam	STE	19 min, 5x/d	shallow (60 cm)	soil type and high loading rate
VG-267	sandy loam	NE	7 min, 5x/d	shallow (60 cm)	soil type and effluent quality
VG-268	sandy loam	NE	19 min, 5x/d	shallow (60 cm)	soil type, effluent quality, and high loading rate
VG-269	silty clay	STE	7 min, 5x/d	shallow (60 cm)	soil type
VG-270	silty clay	STE	7 min, 10x/d	shallow (60 cm)	soil type and high loading rate
VG-271	silty clay	NE	7 min, 5x/d	shallow (60 cm)	soil type and effluent quality
VG-272	silty clay	NE	7 min, 10x/d	shallow (60 cm)	soil type, effluent quality, and high loading rate

* All drip simulations at 0.65 gal/emitter/hr, dose time changed to increase HLR to soil. Additional drip scenarios provided because STUMOD is limited to assessing trench systems only.

STE = septic tank effluent: 60 mg-N L⁻¹ as ammonium-nitrogen

NE = nitrified effluent: 15 mg-N L⁻¹ as nitrate-nitrogen

LIST OF VISUAL-GRAPHIC TOOLS

1.0 **Nomographs: STUMOD Output for Fraction of Nitrogen Remaining in the Soil for Deep Water Tables**

VG-1	Clay Soil, Standard Effluent, HLR = 2 cm d ⁻¹	VG-22
VG-2	Clay Soil, Standard Effluent, HLR = 5% of K _{sat}	VG-22
VG-3	Clay Soil, Nitrified Effluent, HLR = 2 cm d ⁻¹	VG-23
VG-4	Clay Soil, Nitrified Effluent, HLR = 5% of K _{sat}	VG-23
VG-5	Clay Loam Soil, Standard Effluent, HLR = 2 cm d ⁻¹	VG-24
VG-6	Clay Loam Soil, Standard Effluent, HLR = 5% of K _{sat}	VG-24
VG-7	Clay Loam Soil, Nitrified Effluent, HLR = 2 cm d ⁻¹	VG-25
VG-8	Clay Loam Soil, Nitrified Effluent, HLR = 5% of K _{sat}	VG-25
VG-9	Loam Soil, Standard Effluent, HLR = 2 cm d ⁻¹	VG-26
VG-10	Loam Soil, Standard Effluent, HLR = 5% of K _{sat}	VG-26
VG-11	Loam Soil, Nitrified Effluent, HLR = 2 cm d ⁻¹	VG-27
VG-12	Loam Soil, Nitrified Effluent, HLR = 5% of K _{sat}	VG-27
VG-13	Loamy Sand Soil, Standard Effluent, HLR = 2 cm d ⁻¹	VG-28
VG-14	Loamy Sand Soil, Standard Effluent, HLR = 5% of K _{sat}	VG-28
VG-15	Loamy Sand Soil, Nitrified Effluent, HLR = 2 cm d ⁻¹	VG-29
VG-16	Loamy Sand Soil, Nitrified Effluent, HLR = 5% of K _{sat}	VG-29
VG-17	Sandy Soil, Standard Effluent, HLR = 2 cm d ⁻¹	VG-30
VG-18	Sandy Soil, Standard Effluent, HLR = 5% of K _{sat}	VG-30
VG-19	Sandy Soil, Nitrified Effluent, HLR = 2 cm d ⁻¹	VG-31
VG-20	Sandy Soil, Nitrified Effluent, HLR = 5% of K _{sat}	VG-31
VG-21	Sandy Clay Soil, Standard Effluent, HLR = 2 cm d ⁻¹	VG-32
VG-22	Sandy Clay Soil, Standard Effluent, HLR = 5% of K _{sat}	VG-32
VG-23	Sandy Clay Soil, Nitrified Effluent, HLR = 2 cm d ⁻¹	VG-33
VG-24	Sandy Clay Soil, Nitrified Effluent, HLR = 5% of K _{sat}	VG-33
VG-25	Sandy Clay Loam Soil, Standard Effluent, HLR = 2 cm d ⁻¹	VG-34
VG-26	Sandy Clay Loam Soil, Standard Effluent, HLR = 5% of K _{sat}	VG-34
VG-27	Sandy Clay Loam Soil, Nitrified Effluent, HLR = 2 cm d ⁻¹	VG-35
VG-28	Sandy Clay Loam Soil, Nitrified Effluent, HLR = 5% of K _{sat}	VG-35
VG-29	Sandy Loam Soil, Standard Effluent, HLR = 2 cm d ⁻¹	VG-36
VG-30	Sandy Loam Soil, Standard Effluent, HLR = 5% of K _{sat}	VG-36
VG-31	Sandy Loam Soil, Nitrified Effluent, HLR = 2 cm d ⁻¹	VG-37
VG-32	Sandy Loam Soil, Nitrified Effluent, HLR = 5% of K _{sat}	VG-37
VG-33	Silty Soil, Standard Effluent, HLR = 2 cm d ⁻¹	VG-38
VG-34	Silty Soil, Standard Effluent, HLR = 5% of K _{sat}	VG-38
VG-35	Silty Soil, Nitrified Effluent, HLR = 2 cm d ⁻¹	VG-39
VG-36	Silty Soil, Nitrified Effluent, HLR = 5% of K _{sat}	VG-39
VG-37	Silty Clay Soil, Standard Effluent, HLR = 2 cm d ⁻¹	VG-40
VG-38	Silty Clay Soil, Standard Effluent, HLR = 5% of K _{sat}	VG-40
VG-39	Silty Clay Soil, Nitrified Effluent, HLR = 2 cm d ⁻¹	VG-41
VG-40	Silty Clay Soil, Nitrified Effluent, HLR = 5% of K _{sat}	VG-41
VG-41	Silty Clay Loam Soil, Standard Effluent, HLR = 2 cm d ⁻¹	VG-42
VG-42	Silty Clay Loam Soil, Standard Effluent, HLR = 5% of K _{sat}	VG-42

VG-43	Silty Clay Loam Soil, Nitrified Effluent, HLR = 2 cm d ⁻¹	VG-43
VG-44	Silty Clay Loam Soil, Nitrified Effluent, HLR = 5% of K _{sat}	VG-43
VG-45	Silty Loam Soil, Standard Effluent, HLR = 2 cm d ⁻¹	VG-44
VG-46	Silty Loam Soil, Standard Effluent, HLR = 5% of K _{sat}	VG-44
VG-47	Silty Loam Soil, Nitrified Effluent, HLR = 2 cm d ⁻¹	VG-45
VG-48	Silty Loam Soil, Nitrified Effluent, HLR = 5% of K _{sat}	VG-45
VG-49	Total Nitrogen Removal at 60 cm, Clay Soil, Standard Effluent, HLR = 2 cm d ⁻¹	VG-46
VG-50	Total Nitrogen Removal at 60 cm, Clay Loam Soil, Standard Effluent, HLR = 2 cm d ⁻¹	VG-46
VG-51	Total Nitrogen Removal at 60 cm, Loam Soil, Standard Effluent, HLR = 2 cm d ⁻¹	VG-47
VG-52	Total Nitrogen Removal at 60 cm, Loamy Sand Soil, Standard Effluent, HLR = 2 cm d ⁻¹	VG-47
VG-53	Total Nitrogen Removal at 60 cm, Sandy Soil, Standard Effluent, HLR = 2 cm d ⁻¹	VG-48
VG-54	Total Nitrogen Removal at 60 cm, Sandy Clay Soil, Standard Effluent, HLR = 2 cm d ⁻¹	VG-48
VG-55	Total Nitrogen Removal at 60 cm, Sandy Clay Loam Soil, Standard Effluent, HLR = 2 cm d ⁻¹	VG-49
VG-56	Total Nitrogen Removal at 60 cm, Sandy Loam Soil, Standard Effluent, HLR = 2 cm d ⁻¹	VG-49
VG-57	Total Nitrogen Removal at 60 cm, Silty Soil, Standard Effluent, HLR = 2 cm d ⁻¹	VG-50
VG-58	Total Nitrogen Removal at 60 cm, Silty Clay Soil, Standard Effluent, HLR = 2 cm d ⁻¹	VG-50
VG-59	Total Nitrogen Removal at 60 cm, Silty Clay Loam Soil, Standard Effluent, HLR = 2 cm d ⁻¹	VG-51
VG-60	Total Nitrogen Removal at 60 cm, Silty Loam Soil, Standard Effluent, HLR = 2 cm d ⁻¹	VG-51

2.0 Cumulative Probability Graphs: STUMOD Monte Carlo Simulation Results for Deep Water Tables

VG-61	Clay Soil, Frigid/Cryic Temperature Region, Standard Effluent, HLR = 2 cm d ⁻¹	VG-54
VG-62	Clay Soil, Frigid/Cryic Temperature Region, Standard Effluent, HLR = 5% of K _{sat}	VG-54
VG-63	Clay Soil, Mesic Temperature Region, Standard Effluent, HLR = 2 cm d ⁻¹	VG-55
VG-64	Clay Soil, Mesic Temperature Region, Standard Effluent, HLR = 5% of K _{sat}	VG-55
VG-65	Clay Soil, Thermic Temperature Region, Standard Effluent, HLR = 2 cm d ⁻¹	VG-56
VG-66	Clay Soil, Thermic Temperature Region, Standard Effluent, HLR = 5% of K _{sat}	VG-56
VG-67	Clay Soil, Hyperthermic Temperature Region, Standard Effluent, HLR = 2 cm d ⁻¹	VG-57
VG-68	Clay Soil, Hyperthermic Temperature Region, Standard Effluent, HLR = 5% of K _{sat}	VG-57
VG-69	Clay Soil, Frigid/Cryic Temperature Region, Nitrified Effluent, HLR = 2 cm d ⁻¹	VG-58

VG-70	Clay Soil, Frigid/Cryic Temperature Region, Nitrified Effluent, HLR = 5% of K_{sat}	VG-58
VG-71	Clay Soil, Mesic Temperature Region, Nitrified Effluent, HLR = 2 cm d ⁻¹	VG-59
VG-72	Clay Soil, Mesic Temperature Region, Nitrified Effluent, HLR = 5% of K_{sat}	VG-59
VG-73	Clay Soil, Thermic Temperature Region, Nitrified Effluent, HLR = 2 cm d ⁻¹	VG-60
VG-74	Clay Soil, Thermic Temperature Region, Nitrified Effluent, HLR = 5% of K_{sat} ...	VG-60
VG-75	Clay Soil, Hyperthermic Temperature Region, Nitrified Effluent, HLR = 2 cm d ⁻¹	VG-61
VG-76	Clay Soil, Hyperthermic Temperature Region, Nitrified Effluent, HLR = 5% of K_{sat}	VG-61
VG-77	Clay Loam Soil, Frigid/Cryic Temperature Region, Standard Effluent, HLR = 2 cm d ⁻¹	VG-62
VG-78	Clay Loam Soil, Frigid/Cryic Temperature Region, Standard Effluent, HLR = 5% of K_{sat}	VG-62
VG-79	Clay Loam Soil, Mesic Temperature Region, Standard Effluent, HLR = 2 cm d ⁻¹	VG-63
VG-80	Clay Loam Soil, Mesic Temperature Region, Standard Effluent, HLR = 5% of K_{sat}	VG-63
VG-81	Clay Loam Soil, Thermic Temperature Region, Standard Effluent, HLR = 2 cm d ⁻¹	VG-64
VG-82	Clay Loam Soil, Thermic Temperature Region, Standard Effluent, HLR = 5% of K_{sat}	VG-64
VG-83	Clay Loam Soil, Hyperthermic Temperature Region, Standard Effluent, HLR = 2 cm d ⁻¹	VG-65
VG-84	Clay Loam Soil, Hyperthermic Temperature Region, Standard Effluent, HLR = 5% of K_{sat}	VG-65
VG-85	Clay Loam Soil, Frigid/Cryic Temperature Region, Nitrified Effluent, HLR = 2 cm d ⁻¹	VG-66
VG-86	Clay Loam Soil, Frigid/Cryic Temperature Region, Nitrified Effluent, HLR = 5% of K_{sat}	VG-66
VG-87	Clay Loam Soil, Mesic Temperature Region, Nitrified Effluent, HLR = 2 cm d ⁻¹	VG-67
VG-88	Clay Loam Soil, Mesic Temperature Region, Nitrified Effluent, HLR = 5% of K_{sat}	VG-67
VG-89	Clay Loam Soil, Thermic Temperature Region, Nitrified Effluent, HLR = 2 cm d ⁻¹	VG-68
VG-90	Clay Loam Soil, Thermic Temperature Region, Nitrified Effluent, HLR = 5% of K_{sat}	VG-68
VG-91	Clay Loam Soil, Hyperthermic Temperature Region, Nitrified Effluent, HLR = 2 cm d ⁻¹	VG-69
VG-92	Clay Loam Soil, Hyperthermic Temperature Region, Nitrified Effluent, HLR = 5% of K_{sat}	VG-69
VG-93	Loam Soil, Frigid/Cryic Temperature Region, Standard Effluent, HLR = 2 cm d ⁻¹	VG-70
VG-94	Loam Soil, Frigid/Cryic Temperature Region, Standard Effluent, HLR = 5% of K_{sat}	VG-70
VG-95	Loam Soil, Mesic Temperature Region, Standard Effluent, HLR = 2 cm d ⁻¹	VG-71
VG-96	Loam Soil, Mesic Temperature Region, Standard Effluent, HLR = 5% of K_{sat}	VG-71

VG-97	Loam Soil, Thermic Temperature Region, Standard Effluent, HLR = 2 cm d ⁻¹	VG-72
VG-98	Loam Soil, Thermic Temperature Region, Standard Effluent, HLR = 5% of K _{sat}	VG-72
VG-99	Loam Soil, Hyperthermic Temperature Region, Standard Effluent, HLR = 2 cm d ⁻¹	VG-73
VG-100	Loam Soil, Hyperthermic Temperature Region, Standard Effluent, HLR = 5% of K _{sat}	VG-73
VG-101	Loam Soil, Frigid/Cryic Temperature Region, Nitrified Effluent, HLR = 2 cm d ⁻¹	VG-74
VG-102	Loam Soil, Frigid/Cryic Temperature Region, Nitrified Effluent, HLR = 5% of K _{sat}	VG-74
VG-103	Loam Soil, Mesic Temperature Region, Nitrified Effluent, HLR = 2 cm d ⁻¹	VG-75
VG-104	Loam Soil, Mesic Temperature Region, Nitrified Effluent, HLR = 5% of K _{sat}	VG-75
VG-105	Loam Soil, Thermic Temperature Region, Nitrified Effluent, HLR = 2 cm d ⁻¹	VG-76
VG-106	Loam Soil, Thermic Temperature Region, Nitrified Effluent, HLR = 5% of K _{sat}	VG-76
VG-107	Loam Soil, Hyperthermic Temperature Region, Nitrified Effluent, HLR = 2 cm d ⁻¹	VG-77
VG-108	Loam Soil, Hyperthermic Temperature Region, Nitrified Effluent, HLR = 5% of K _{sat}	VG-77
VG-109	Loamy Sand Soil, Frigid/Cryic Temperature Region, Standard Effluent, HLR = 2 cm d ⁻¹	VG-78
VG-110	Loamy Sand Soil, Frigid/Cryic Temperature Region, Standard Effluent, HLR = 5% of K _{sat}	VG-78
VG-111	Loamy Sand Soil, Mesic Temperature Region, Standard Effluent, HLR = 2 cm d ⁻¹	VG-79
VG-112	Loamy Sand Soil, Mesic Temperature Region, Standard Effluent, HLR = 5% of K _{sat}	VG-79
VG-113	Loamy Sand Soil, Thermic Temperature Region, Standard Effluent, HLR = 2 cm d ⁻¹	VG-80
VG-114	Loamy Sand Soil, Thermic Temperature Region, Standard Effluent, HLR = 5% of K _{sat}	VG-80
VG-115	Loamy Sand Soil, Hyperthermic Temperature Region, Standard Effluent, HLR = 2 cm d ⁻¹	VG-81
VG-116	Loamy Sand Soil, Hyperthermic Temperature Region, Standard Effluent, HLR = 5% of K _{sat}	VG-81
VG-117	Loamy Sand Soil, Frigid/Cryic Temperature Region, Nitrified Effluent, HLR = 2 cm d ⁻¹	VG-82
VG-118	Loamy Sand Soil, Frigid/Cryic Temperature Region, Nitrified Effluent, HLR = 5% of K _{sat}	VG-82
VG-119	Loamy Sand Soil, Mesic Temperature Region, Nitrified Effluent, HLR = 2 cm d ⁻¹	VG-83
VG-120	Loamy Sand Soil, Mesic Temperature Region, Nitrified Effluent, HLR = 5% of K _{sat}	VG-83
VG-121	Loamy Sand Soil, Thermic Temperature Region, Nitrified Effluent, HLR = 2 cm d ⁻¹	VG-84
VG-122	Loamy Sand Soil, Thermic Temperature Region, Nitrified Effluent, HLR = 5% of K _{sat}	VG-84
VG-123	Loamy Sand Soil, Hyperthermic Temperature Region, Nitrified Effluent, HLR = 2 cm d ⁻¹	VG-85

VG-124	Loamy Sand Soil, Hyperthermic Temperature Region, Nitrified Effluent, HLR = 5% of K_{sat}	VG-85
VG-125	Sandy Soil, Frigid/Cryic Temperature Region, Standard Effluent, HLR = 2 cm d ⁻¹	VG-86
VG-126	Sandy Soil, Frigid/Cryic Temperature Region, Standard Effluent, HLR = 5% of K_{sat}	VG-86
VG-127	Sandy Soil, Mesic Temperature Region, Standard Effluent, HLR = 2 cm d ⁻¹	VG-87
VG-128	Sandy Soil, Mesic Temperature Region, Standard Effluent, HLR = 5% of K_{sat}	VG-87
VG-129	Sandy Soil, Thermic Temperature Region, Standard Effluent, HLR = 2 cm d ⁻¹	VG-88
VG-130	Sandy Soil, Thermic Temperature Region, Standard Effluent, HLR = 5% of K_{sat}	VG-88
VG-131	Sandy Soil, Hyperthermic Temperature Region, Standard Effluent, HLR = 2 cm d ⁻¹	VG-89
VG-132	Sandy Soil, Hyperthermic Temperature Region, Standard Effluent, HLR = 5% of K_{sat}	VG-89
VG-133	Sandy Soil, Frigid/Cryic Temperature Region, Nitrified Effluent, HLR = 2 cm d ⁻¹	VG-90
VG-134	Sandy Soil, Frigid/Cryic Temperature Region, Nitrified Effluent, HLR = 5% of K_{sat}	VG-90
VG-135	Sandy Soil, Mesic Temperature Region, Nitrified Effluent, HLR = 2 cm d ⁻¹	VG-91
VG-136	Sandy Soil, Mesic Temperature Region, Nitrified Effluent, HLR = 5% of K_{sat}	VG-91
VG-137	Sandy Soil, Thermic Temperature Region, Nitrified Effluent, HLR = 2 cm d ⁻¹	VG-92
VG-138	Sandy Soil, Thermic Temperature Region, Nitrified Effluent, HLR = 5% of K_{sat} .	VG-92
VG-139	Sandy Soil, Hyperthermic Temperature Region, Nitrified Effluent, HLR = 2 cm d ⁻¹	VG-93
VG-140	Sandy Soil, Hyperthermic Temperature Region, Nitrified Effluent, HLR = 5% of K_{sat}	VG-93
VG-141	Sandy Clay Soil, Frigid/Cryic Temperature Region, Standard Effluent, HLR = 2 cm d ⁻¹	VG-94
VG-142	Sandy Clay Soil, Frigid/Cryic Temperature Region, Standard Effluent, HLR = 5% of K_{sat}	VG-94
VG-143	Sandy Clay Soil, Mesic Temperature Region, Standard Effluent, HLR = 2 cm d ⁻¹	VG-95
VG-144	Sandy Clay Soil, Mesic Temperature Region, Standard Effluent, HLR = 5% of K_{sat}	VG-95
VG-145	Sandy Clay Soil, Thermic Temperature Region, Standard Effluent, HLR = 2 cm d ⁻¹	VG-96
VG-146	Sandy Clay Soil, Thermic Temperature Region, Standard Effluent, HLR = 5% of K_{sat}	VG-96
VG-147	Sandy Clay Soil, Hyperthermic Temperature Region, Standard Effluent, HLR = 2 cm d ⁻¹	VG-97
VG-148	Sandy Clay Soil, Hyperthermic Temperature Region, Standard Effluent, HLR = 5% of K_{sat}	VG-97
VG-149	Sandy Clay Soil, Frigid/Cryic Temperature Region, Nitrified Effluent, HLR = 2 cm d ⁻¹	VG-98
VG-150	Sandy Clay Soil, Frigid/Cryic Temperature Region, Nitrified Effluent, HLR = 5% of K_{sat}	VG-98
VG-151	Sandy Clay Soil, Mesic Temperature Region, Nitrified Effluent, HLR = 2 cm d ⁻¹	VG-99

VG-152	Sandy Clay Soil, Mesic Temperature Region, Nitrified Effluent, HLR = 5% of K_{sat}	VG-99
VG-153	Sandy Clay Soil, Thermic Temperature Region, Nitrified Effluent, HLR = 2 cm d ⁻¹	VG-100
VG-154	Sandy Clay Soil, Thermic Temperature Region, Nitrified Effluent, HLR = 5% of K_{sat}	VG-100
VG-155	Sandy Clay Soil, Hyperthermic Temperature Region, Nitrified Effluent, HLR = 2 cm d ⁻¹	VG-101
VG-156	Sandy Clay Soil, Hyperthermic Temperature Region, Nitrified Effluent, HLR = 5% of K_{sat}	VG-101
VG-157	Sandy Clay Loam Soil, Frigid/Cryic Temperature Region, Standard Effluent, HLR = 2 cm d ⁻¹	VG-102
VG-158	Sandy Clay Loam Soil, Frigid/Cryic Temperature Region, Standard Effluent, HLR = 5% of K_{sat}	VG-102
VG-159	Sandy Clay Loam Soil, Mesic Temperature Region, Standard Effluent, HLR = 2 cm d ⁻¹	VG-103
VG-160	Sandy Clay Loam Soil, Mesic Temperature Region, Standard Effluent, HLR = 5% of K_{sat}	VG-103
VG-161	Sandy Clay Loam Soil, Thermic Temperature Region, Standard Effluent, HLR = 2 cm d ⁻¹	VG-104
VG-162	Sandy Clay Loam Soil, Thermic Temperature Region, Standard Effluent, HLR = 5% of K_{sat}	VG-104
VG-163	Sandy Clay Loam Soil, Hyperthermic Temperature Region, Standard Effluent, HLR = 2 cm d ⁻¹	VG-105
VG-164	Sandy Clay Loam Soil, Hyperthermic Temperature Region, Standard Effluent, HLR = 5% of K_{sat}	VG-105
VG-165	Sandy Clay Loam Soil, Frigid/Cryic Temperature Region, Nitrified Effluent, HLR = 2 cm d ⁻¹	VG-106
VG-166	Sandy Clay Loam Soil, Frigid/Cryic Temperature Region, Nitrified Effluent, HLR = 5% of K_{sat}	VG-106
VG-167	Sandy Clay Loam Soil, Mesic Temperature Region, Nitrified Effluent, HLR = 2 cm d ⁻¹	VG-107
VG-168	Sandy Clay Loam Soil, Mesic Temperature Region, Nitrified Effluent, HLR = 5% of K_{sat}	VG-107
VG-169	Sandy Clay Loam Soil, Thermic Temperature Region, Nitrified Effluent, HLR = 2 cm d ⁻¹	VG-108
VG-170	Sandy Clay Loam Soil, Thermic Temperature Region, Nitrified Effluent, HLR = 5% of K_{sat}	VG-108
VG-171	Sandy Clay Loam Soil, Hyperthermic Temperature Region, Nitrified Effluent, HLR = 2 cm d ⁻¹	VG-109
VG-172	Sandy Clay Loam Soil, Hyperthermic Temperature Region, Nitrified Effluent, HLR = 5% of K_{sat}	VG-109
VG-173	Sandy Loam Soil, Frigid/Cryic Temperature Region, Standard Effluent, HLR = 2 cm d ⁻¹	VG-110
VG-174	Sandy Loam Soil, Frigid/Cryic Temperature Region, Standard Effluent, HLR = 5% of K_{sat}	VG-110
VG-175	Sandy Loam Soil, Mesic Temperature Region, Standard Effluent, HLR = 2 cm d ⁻¹	VG-111

VG-176	Sandy Loam Soil, Mesic Temperature Region, Standard Effluent, HLR = 5% of K_{sat}	VG-111
VG-177	Sandy Loam Soil, Thermic Temperature Region, Standard Effluent, HLR = 2 cm d ⁻¹	VG-112
VG-178	Sandy Loam Soil, Thermic Temperature Region, Standard Effluent, HLR = 5% of K_{sat}	VG-112
VG-179	Sandy Loam Soil, Hyperthermic Temperature Region, Standard Effluent, HLR = 2 cm d ⁻¹	VG-113
VG-180	Sandy Loam Soil, Hyperthermic Temperature Region, Standard Effluent, HLR = 5% of K_{sat}	VG-113
VG-181	Sandy Loam Soil, Frigid/Cryic Temperature Region, Nitrified Effluent, HLR = 2 cm d ⁻¹	VG-114
VG-182	Sandy Loam Soil, Frigid/Cryic Temperature Region, Nitrified Effluent, HLR = 5% of K_{sat}	VG-114
VG-183	Sandy Loam Soil, Mesic Temperature Region, Nitrified Effluent, HLR = 2 cm d ⁻¹	VG-115
VG-184	Sandy Loam Soil, Mesic Temperature Region, Nitrified Effluent, HLR = 5% of K_{sat}	VG-115
VG-185	Sandy Loam Soil, Thermic Temperature Region, Nitrified Effluent, HLR = 2 cm d ⁻¹	VG-116
VG-186	Sandy Loam Soil, Thermic Temperature Region, Nitrified Effluent, HLR = 5% of K_{sat}	VG-116
VG-187	Sandy Loam Soil, Hyperthermic Temperature Region, Nitrified Effluent, HLR = 2 cm d ⁻¹	VG-117
VG-188	Sandy Loam Soil, Hyperthermic Temperature Region, Nitrified Effluent, HLR = 5% of K_{sat}	VG-117
VG-189	Silty Soil, Frigid/Cryic Temperature Region, Standard Effluent, HLR = 2 cm d ⁻¹	VG-118
VG-190	Silty Soil, Frigid/Cryic Temperature Region, Standard Effluent, HLR = 5% of K_{sat}	VG-118
VG-191	Silty Soil, Mesic Temperature Region, Standard Effluent, HLR = 2 cm d ⁻¹	VG-119
VG-192	Silty Soil, Mesic Temperature Region, Standard Effluent, HLR = 5% of K_{sat}	VG-119
VG-193	Silty Soil, Thermic Temperature Region, Standard Effluent, HLR = 2 cm d ⁻¹	VG-120
VG-194	Silty Soil, Thermic Temperature Region, Standard Effluent, HLR = 5% of K_{sat}	VG-120
VG-195	Silty Soil, Hyperthermic Temperature Region, Standard Effluent, HLR = 2 cm d ⁻¹	VG-121
VG-196	Silty Soil, Hyperthermic Temperature Region, Standard Effluent, HLR = 5% of K_{sat}	VG-121
VG-197	Silty Soil, Frigid/Cryic Temperature Region, Nitrified Effluent, HLR = 2 cm d ⁻¹	VG-122
VG-198	Silty Soil, Frigid/Cryic Temperature Region, Nitrified Effluent, HLR = 5% of K_{sat}	VG-122
VG-199	Silty Soil, Mesic Temperature Region, Nitrified Effluent, HLR = 2 cm d ⁻¹	VG-123
VG-200	Silty Soil, Mesic Temperature Region, Nitrified Effluent, HLR = 5% of K_{sat}	VG-123
VG-201	Silty Soil, Thermic Temperature Region, Nitrified Effluent, HLR = 2 cm d ⁻¹	VG-124
VG-202	Silty Soil, Thermic Temperature Region, Nitrified Effluent, HLR = 5% of K_{sat}	VG-124
VG-203	Silty Soil, Hyperthermic Temperature Region, Nitrified Effluent, HLR = 2 cm d ⁻¹	VG-125

VG-204 Silty Soil, Hyperthermic Temperature Region, Nitrified Effluent, HLR = 5% of K_{sat}	VG-125
VG-205 Silty Clay Soil, Frigid/Cryic Temperature Region, Standard Effluent, HLR = 2 cm d ⁻¹	VG-126
VG-206 Silty Clay Soil, Frigid/Cryic Temperature Region, Standard Effluent, HLR = 5% of K_{sat}	VG-126
VG-207 Silty Clay Soil, Mesic Temperature Region, Standard Effluent, HLR = 2 cm d ⁻¹	VG-127
VG-208 Silty Clay Soil, Mesic Temperature Region, Standard Effluent, HLR = 5% of K_{sat}	VG-127
VG-209 Silty Clay Soil, Thermic Temperature Region, Standard Effluent, HLR = 2 cm d ⁻¹	VG-128
VG-210 Silty Clay Soil, Thermic Temperature Region, Standard Effluent, HLR = 5% of K_{sat}	VG-128
VG-211 Silty Clay Soil, Hyperthermic Temperature Region, Standard Effluent, HLR = 2 cm d ⁻¹	VG-129
VG-212 Silty Clay Soil, Hyperthermic Temperature Region, Standard Effluent, HLR = 5% of K_{sat}	VG-129
VG-213 Silty Clay Soil, Frigid/Cryic Temperature Region, Nitrified Effluent, HLR = 2 cm d ⁻¹	VG-130
VG-214 Silty Clay Soil, Frigid/Cryic Temperature Region, Nitrified Effluent, HLR = 5% of K_{sat}	VG-130
VG-215 Silty Clay Soil, Mesic Temperature Region, Nitrified Effluent, HLR = 2 cm d ⁻¹	VG-131
VG-216 Silty Clay Soil, Mesic Temperature Region, Nitrified Effluent, HLR = 5% of K_{sat}	VG-131
VG-217 Silty Clay Soil, Thermic Temperature Region, Nitrified Effluent, HLR = 2 cm d ⁻¹	VG-132
VG-218 Silty Clay Soil, Thermic Temperature Region, Nitrified Effluent, HLR = 5% of K_{sat}	VG-132
VG-219 Silty Clay Soil, Hyperthermic Temperature Region, Nitrified Effluent, HLR = 2 cm d ⁻¹	VG-133
VG-220 Silty Clay Soil, Hyperthermic Temperature Region, Nitrified Effluent, HLR = 5% of K_{sat}	VG-133
VG-221 Silty Clay Loam Soil, Frigid/Cryic Temperature Region, Standard Effluent, HLR = 2 cm d ⁻¹	VG-134
VG-222 Silty Clay Loam Soil, Frigid/Cryic Temperature Region, Standard Effluent, HLR = 5% of K_{sat}	VG-134
VG-223 Silty Clay Loam Soil, Mesic Temperature Region, Standard Effluent, HLR = 2 cm d ⁻¹	VG-135
VG-224 Silty Clay Loam Soil, Mesic Temperature Region, Standard Effluent, HLR = 5% of K_{sat}	VG-135
VG-225 Silty Clay Loam Soil, Thermic Temperature Region, Standard Effluent, HLR = 2 cm d ⁻¹	VG-136
VG-226 Silty Clay Loam Soil, Thermic Temperature Region, Standard Effluent, HLR = 5% of K_{sat}	VG-136
VG-227 Silty Clay Loam Soil, Hyperthermic Temperature Region, Standard Effluent, HLR = 2 cm d ⁻¹	VG-137

VG-228	Silty Clay Loam Soil, Hyperthermic Temperature Region, Standard Effluent, HLR = 5% of K_{sat}	VG-137
VG-229	Silty Clay Loam Soil, Frigid/Cryic Temperature Region, Nitrified Effluent, HLR = 2 cm d ⁻¹	VG-138
VG-230	Silty Clay Loam Soil, Frigid/Cryic Temperature Region, Nitrified Effluent, HLR = 5% of K_{sat}	VG-138
VG-231	Silty Clay Loam Soil, Mesic Temperature Region, Nitrified Effluent, HLR = 2 cm d ⁻¹	VG-139
VG-232	Silty Clay Loam Soil, Mesic Temperature Region, Nitrified Effluent, HLR = 5% of K_{sat}	VG-139
VG-233	Silty Clay Loam Soil, Thermic Temperature Region, Nitrified Effluent, HLR = 2 cm d ⁻¹	VG-140
VG-234	Silty Clay Loam Soil, Thermic Temperature Region, Nitrified Effluent, HLR = 5% of K_{sat}	VG-140
VG-235	Silty Clay Loam Soil, Hyperthermic Temperature Region, Nitrified Effluent, HLR = 2 cm d ⁻¹	VG-141
VG-236	Silty Clay Loam Soil, Hyperthermic Temperature Region, Nitrified Effluent, HLR = 5% of K_{sat}	VG-141
VG-237	Silty Loam Soil, Frigid/Cryic Temperature Region, Standard Effluent, HLR = 2 cm d ⁻¹	VG-142
VG-238	Silty Loam Soil, Frigid/Cryic Temperature Region, Standard Effluent, HLR = 5% of K_{sat}	VG-142
VG-239	Silty Loam Soil, Mesic Temperature Region, Standard Effluent, HLR = 2 cm d ⁻¹	VG-143
VG-240	Silty Loam Soil, Mesic Temperature Region, Standard Effluent, HLR = 5% of K_{sat}	VG-143
VG-241	Silty Loam Soil, Thermic Temperature Region, Standard Effluent, HLR = 2 cm d ⁻¹	VG-144
VG-242	Silty Loam Soil, Thermic Temperature Region, Standard Effluent, HLR = 5% of K_{sat}	VG-144
VG-243	Silty Loam Soil, Hyperthermic Temperature Region, Standard Effluent, HLR = 2 cm d ⁻¹	VG-145
VG-244	Silty Loam Soil, Hyperthermic Temperature Region, Standard Effluent, HLR = 5% of K_{sat}	VG-145
VG-245	Silty Loam Soil, Frigid/Cryic Temperature Region, Nitrified Effluent, HLR = 2 cm d ⁻¹	VG-146
VG-246	Silty Loam Soil, Frigid/Cryic Temperature Region, Nitrified Effluent, HLR = 5% of K_{sat}	VG-146
VG-247	Silty Loam Soil, Mesic Temperature Region, Nitrified Effluent, HLR = 2 cm d ⁻¹	VG-147
VG-248	Silty Loam Soil, Mesic Temperature Region, Nitrified Effluent, HLR = 5% of K_{sat}	VG-147
VG-249	Silty Loam Soil, Thermic Temperature Region, Nitrified Effluent, HLR = 2 cm d ⁻¹	VG-148
VG-250	Silty Loam Soil, Thermic Temperature Region, Nitrified Effluent, HLR = 5% of K_{sat}	VG-148
VG-251	Silty Loam Soil, Hyperthermic Temperature Region, Nitrified Effluent, HLR = 2 cm d ⁻¹	VG-149

VG-252	Silty Loam Soil, Hyperthermic Temperature Region, Nitrified Effluent, HLR = 5% of K_{sat}	VG-149
--------	--	--------

3.0 Scenario Illustrations: HYDRUS Simulation Output of STU Operating Conditions

VG-253	Scenario Output: Trench, Sandy Soil, Standard Effluent, HLR = 2cm d ⁻¹	VG-152
VG-254	Scenario Output: Trench, Sandy Soil, Standard Effluent, HLR = 10% of K_{sat}	VG-153
VG-255	Scenario Output: Trench, Sandy Loam Soil, Standard Effluent, HLR = 2cm d ⁻¹	VG-154
VG-256	Scenario Output: Trench, Sandy Loam Soil, Standard Effluent, HLR = 2cm d ⁻¹ , “High Water Table”	VG-155
VG-257	Scenario Output: Trench, Sandy Loam Soil, Standard Effluent, HLR = 2cm d ⁻¹ , “Closely Spaced Trenches”	VG-156
VG-258	Scenario Output: Trench, Sandy Loam Soil, Standard Effluent, HLR = 10% of K_{sat}	VG-157
VG-259	Scenario Output: Trench, Silty Clay Soil, Standard Effluent, HLR = 2cm d ⁻¹	VG-158
VG-260	Scenario Output: Trench, Silty Clay Soil, Standard Effluent, HLR = 10% of K_{sat}	VG-159
VG-261	Scenario Output: Drip Dispersal, Sandy Soil, Standard Effluent, HLR = “Low”	VG-160
VG-262	Scenario Output: Drip Dispersal, Sandy Soil, Standard Effluent, HLR = “High”	VG-161
VG-263	Scenario Output: Drip Dispersal, Sandy Soil, Nitrified Effluent, HLR = “Low”	VG-162
VG-264	Scenario Output: Drip Dispersal, Sandy Soil, Nitrified Effluent, HLR = “High”	VG-163
VG-265	Scenario Output: Drip Dispersal, Sandy Loam Soil, Standard Effluent, HLR = “Low”	VG-164
VG-266	Scenario Output: Drip Dispersal, Sandy Loam Soil, Standard Effluent, HLR = “High”	VG-165
VG-267	Scenario Output: Drip Dispersal, Sandy Loam Soil, Nitrified Effluent, HLR = “Low”	VG-166
VG-268	Scenario Output: Drip Dispersal, Sandy Loam Soil, Nitrified Effluent, HLR = “High”	VG-167
VG-269	Scenario Output: Drip Dispersal, Silty Clay Soil, Standard Effluent, HLR = “Low”	VG-168
VG-270	Scenario Output: Drip Dispersal, Silty Clay Soil, Standard Effluent, HLR = “High”	VG-169
VG-271	Scenario Output: Drip Dispersal, Silty Clay Soil, Nitrified Effluent, HLR = “Low”	VG-170
VG-272	Scenario Output: Drip Dispersal, Silty Clay Soil, Nitrified Effluent, HLR = “High”	VG-171

CHAPTER 1.0

NOMOGRAPHS: STUMOD OUTPUT FOR FRACTION OF NITROGEN REMAINING IN SOIL FOR DEEP WATER TABLES

1.1 Clay

1.1.1 Standard Effluent

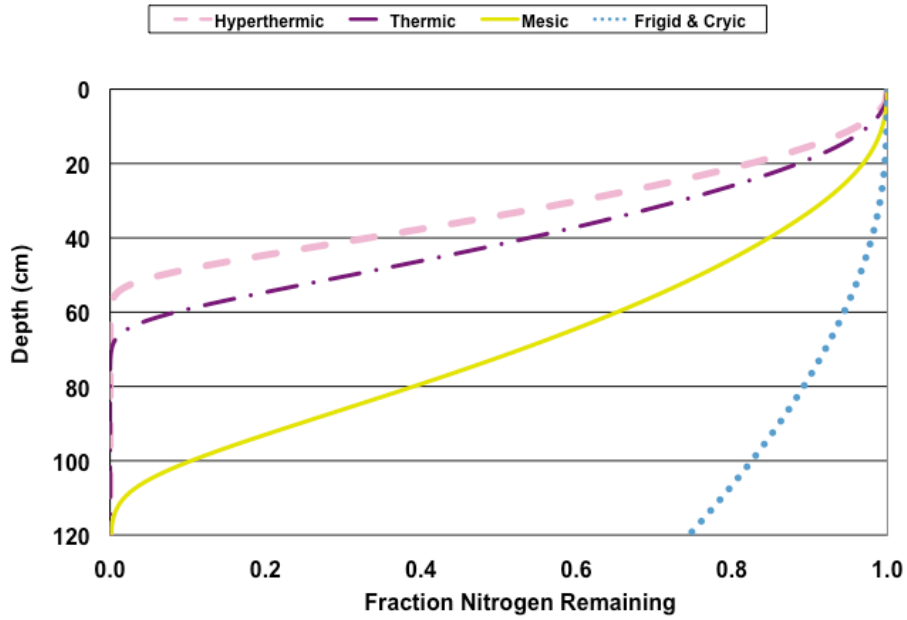


Figure VG-1. Nomograph: Clay Soil, Standard Effluent, HLR = 2 cm d⁻¹.

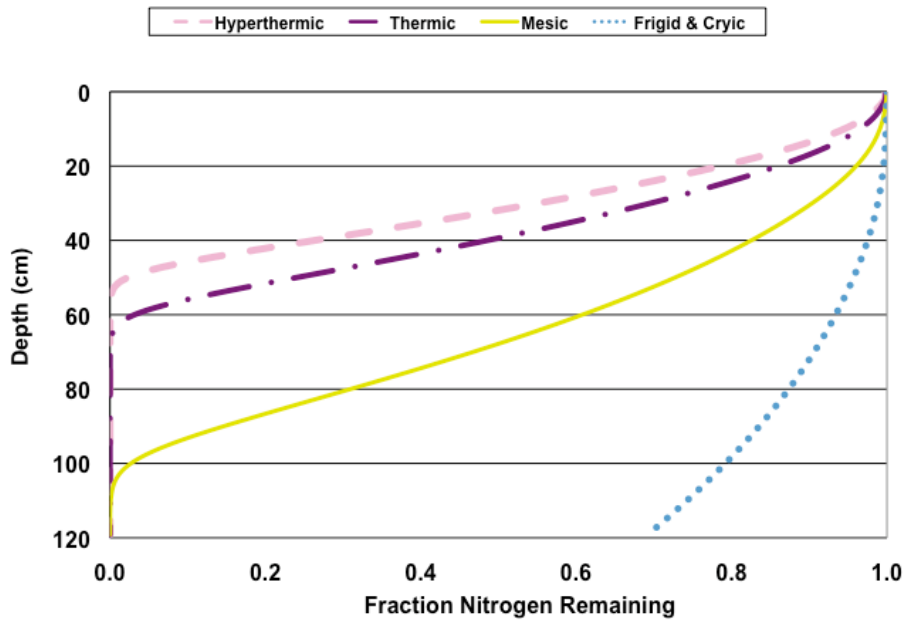


Figure VG-2. Nomograph: Clay Soil, Standard Effluent, HLR = 5 % of K_{sat}.

1.1.2 Nitrified Effluent

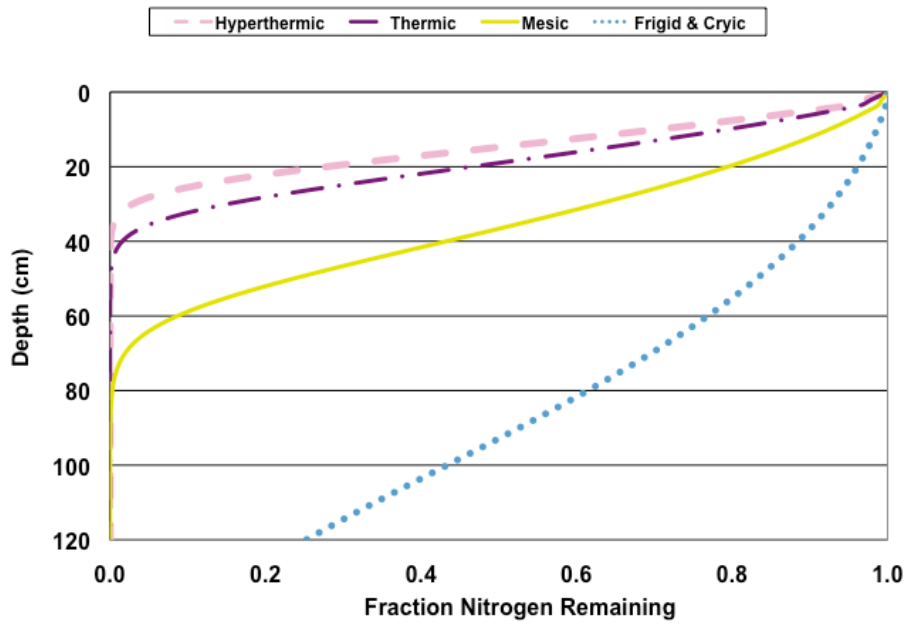


Figure VG-3. Nomograph: Clay Soil, Nitrified Effluent, HLR = 2 cm d⁻¹.

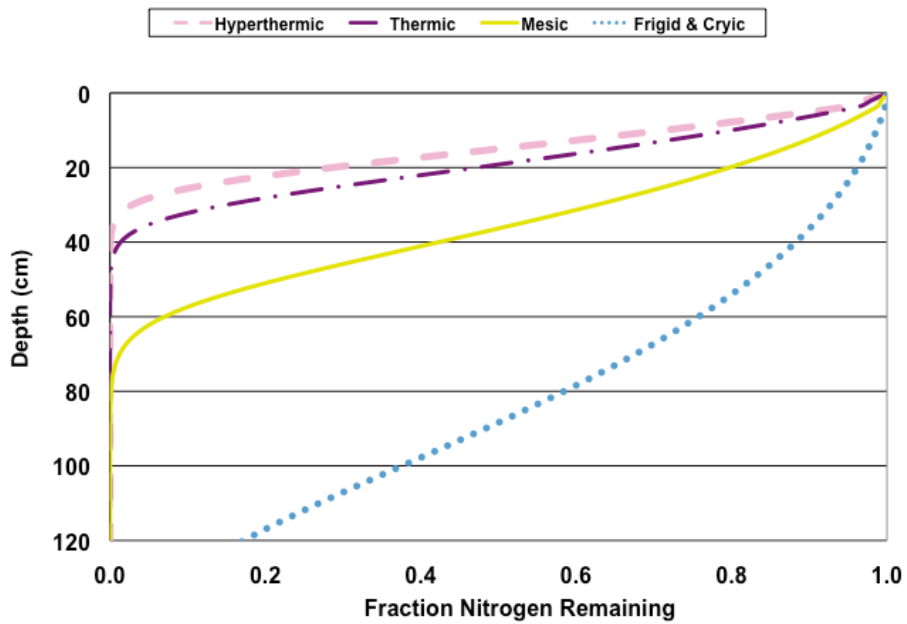


Figure VG-4. Nomograph: Clay Soil, Nitrified Effluent, HLR = 5 % of K_{sat} .

1.2 Clay Loam

1.2.1 Standard Effluent

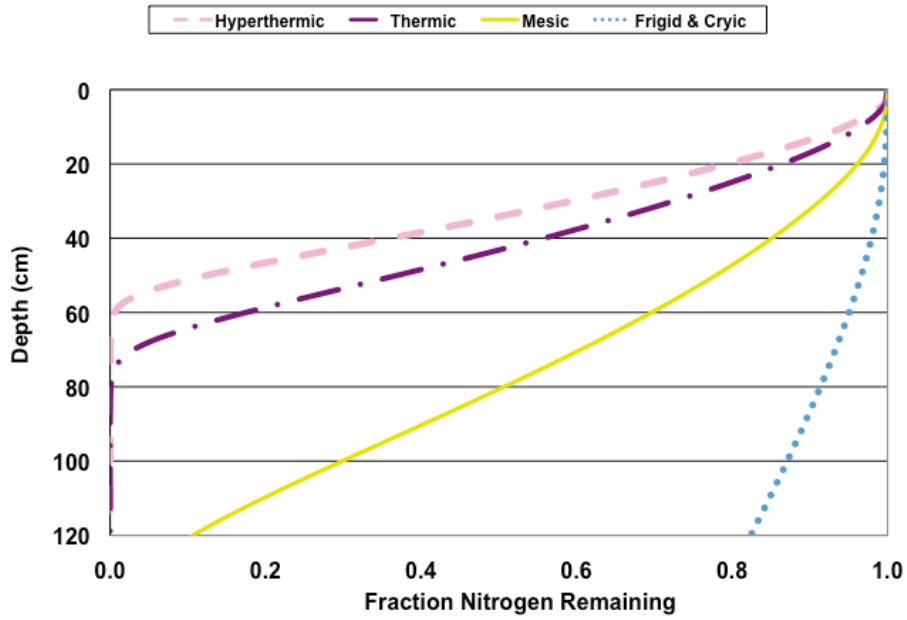


Figure VG-5. Nomograph: Clay Loam Soil, Standard Effluent, HLR = 2 cm d⁻¹.

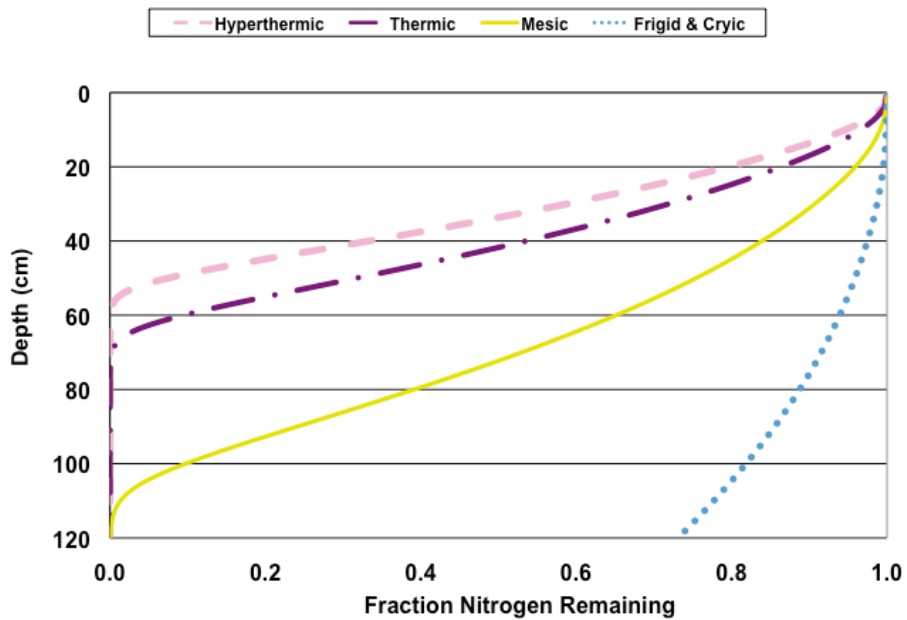


Figure VG-6. Nomograph: Clay Loam Soil, Standard Effluent, HLR = 5% of K_{sat}.

1.2.2 Nitrified Effluent

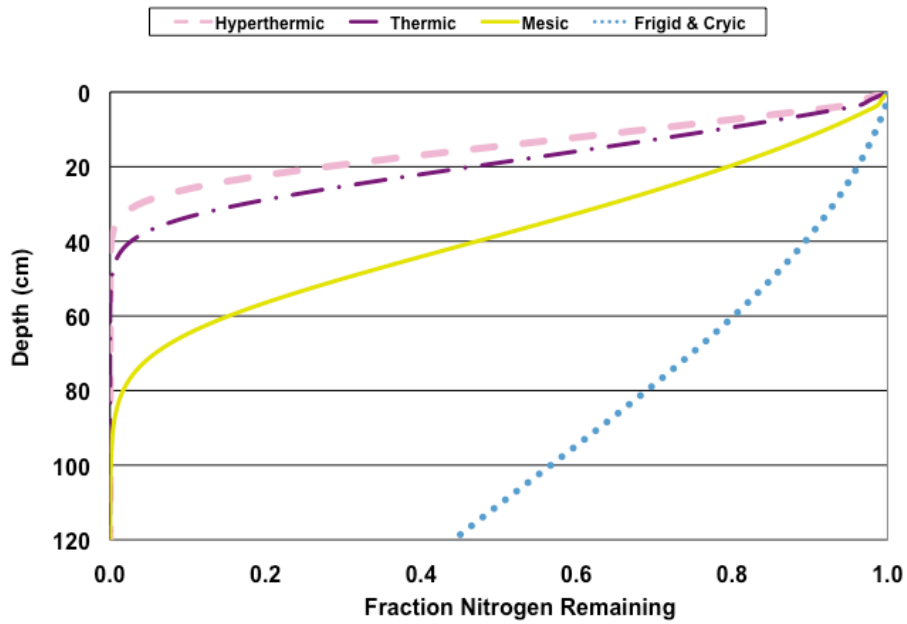


Figure VG-7. Nomograph: Clay Loam Soil, Nitrified Effluent, HLR = 2 cm d⁻¹.

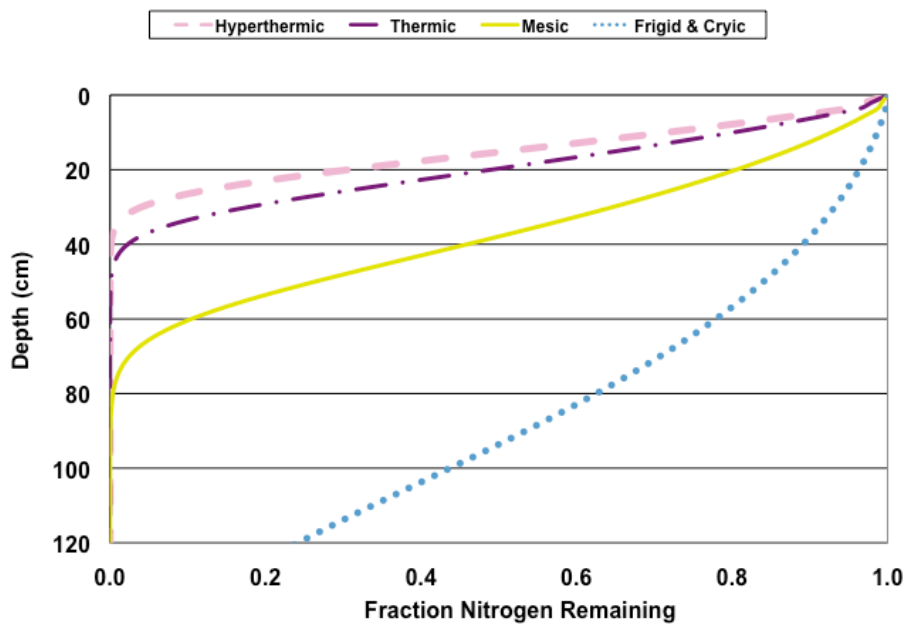


Figure VG-8. Nomograph: Clay Loam Soil, Nitrified Effluent, HLR = 5 % of K_{sat} .

1.3 Loam

1.3.1 Standard Effluent

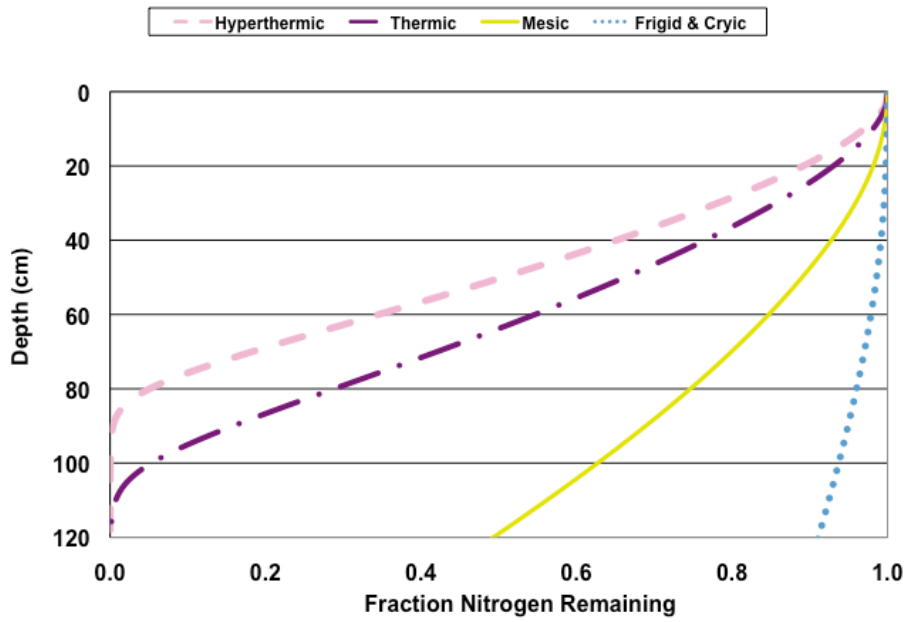


Figure VG-9. Nomograph: Loam Soil, Standard Effluent, HLR = 2 cm d⁻¹.

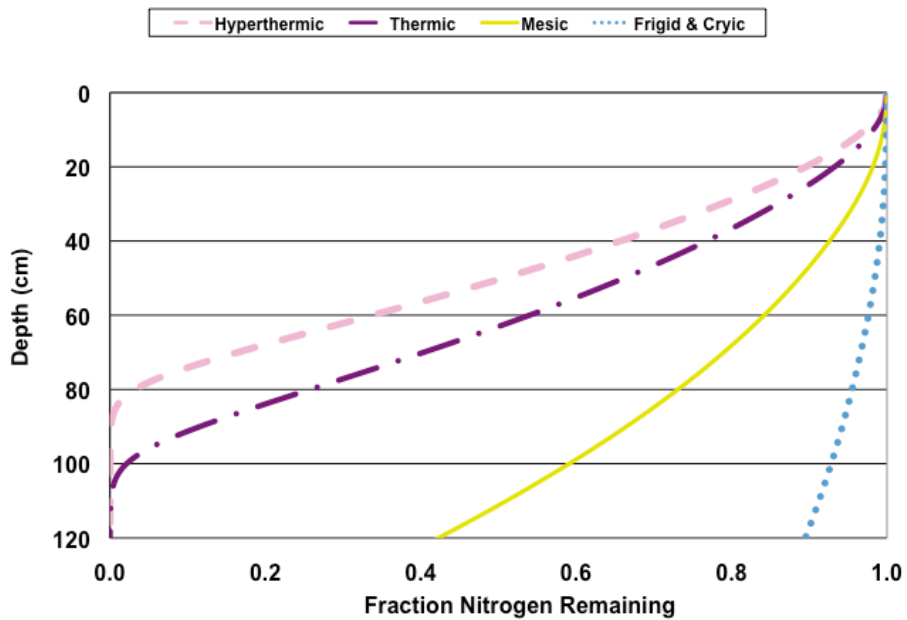


Figure VG-10. Nomograph: Loam Soil, Standard Effluent, HLR = 5 % of K_{sat} .

1.3.2 Nitrified Effluent

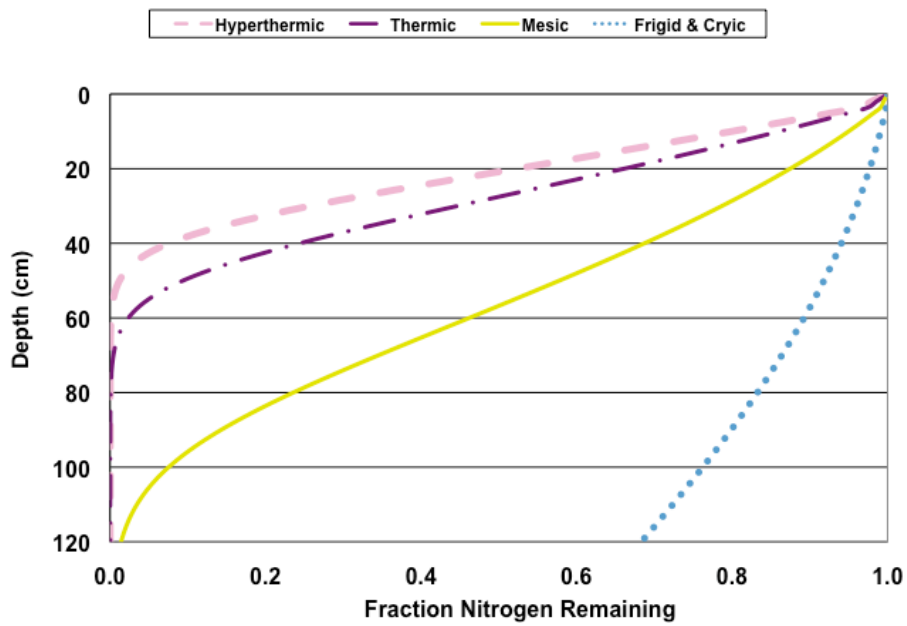


Figure VG-11. Nomograph: Loam Soil, Nitrified Effluent, HLR = 2 cm d⁻¹.

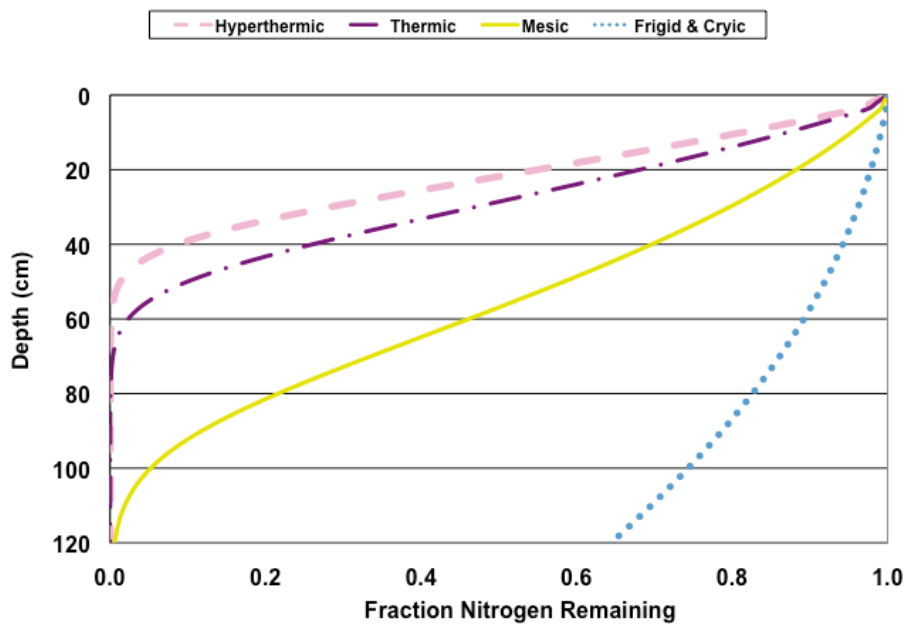


Figure VG-12. Nomograph: Loam Soil, Nitrified Effluent, HLR = 5% of K_{sat}.

1.4 Loamy Sand

1.4.1 Standard Effluent

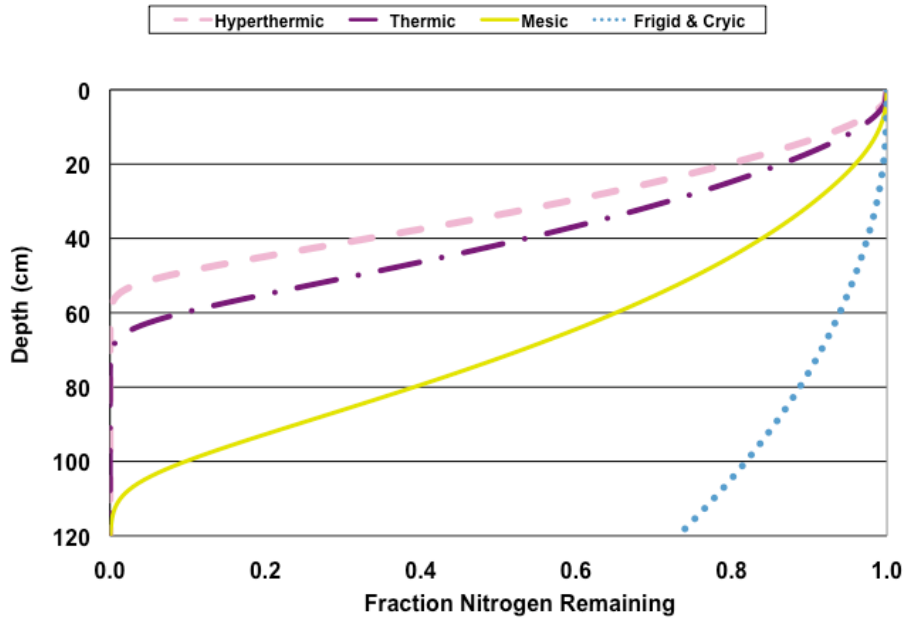


Figure VG-13. Nomograph: Loamy Sand Soil, Standard Effluent, HLR = 2 cm d⁻¹.

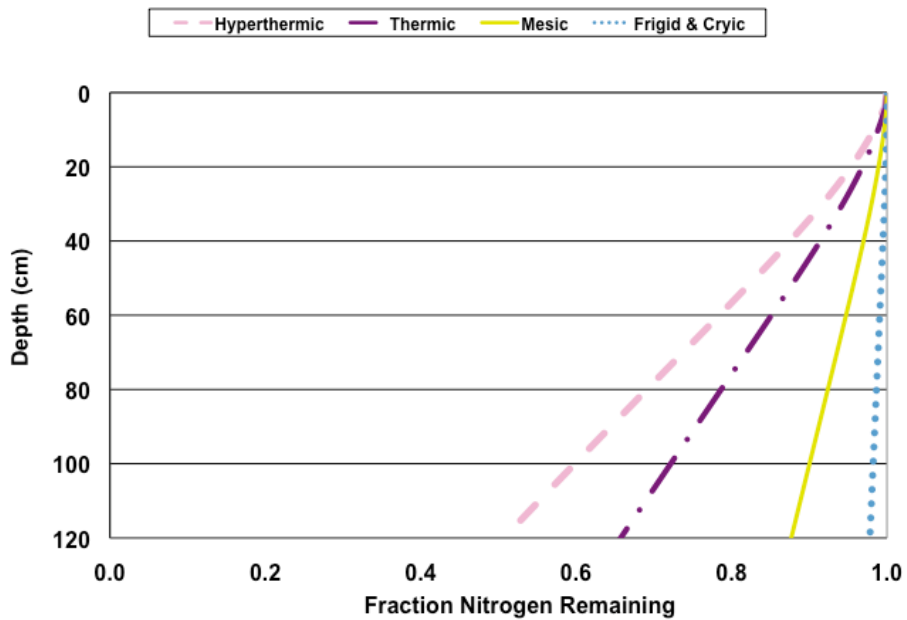


Figure VG-14. Nomograph: Loamy Sand Soil, Standard Effluent, HLR = 5% K_{sat}.

1.4.2 Nitrified Effluent

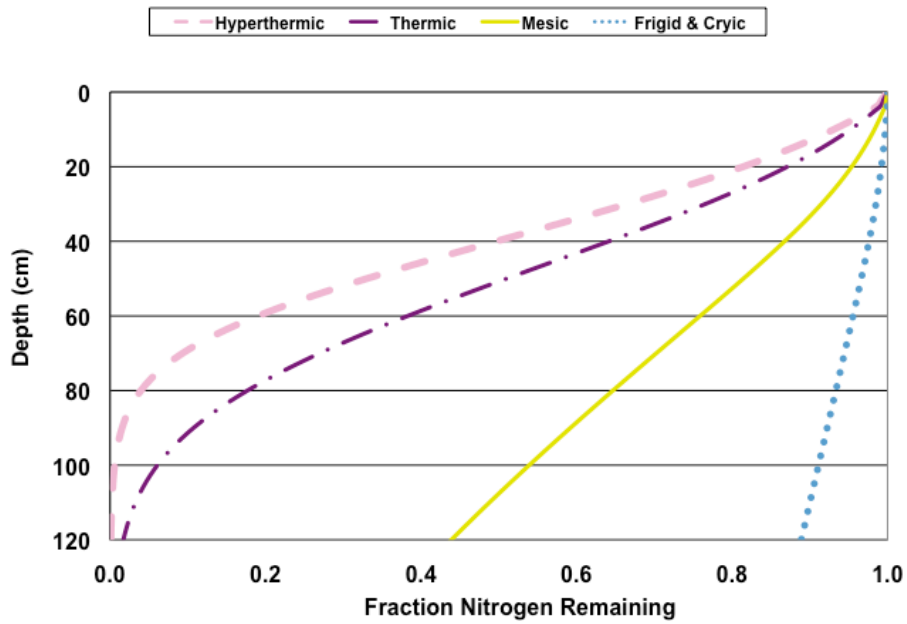


Figure VG-15. Nomograph: Loamy Sand Soil, Nitrified Effluent, HLR = 2 cm d⁻¹.

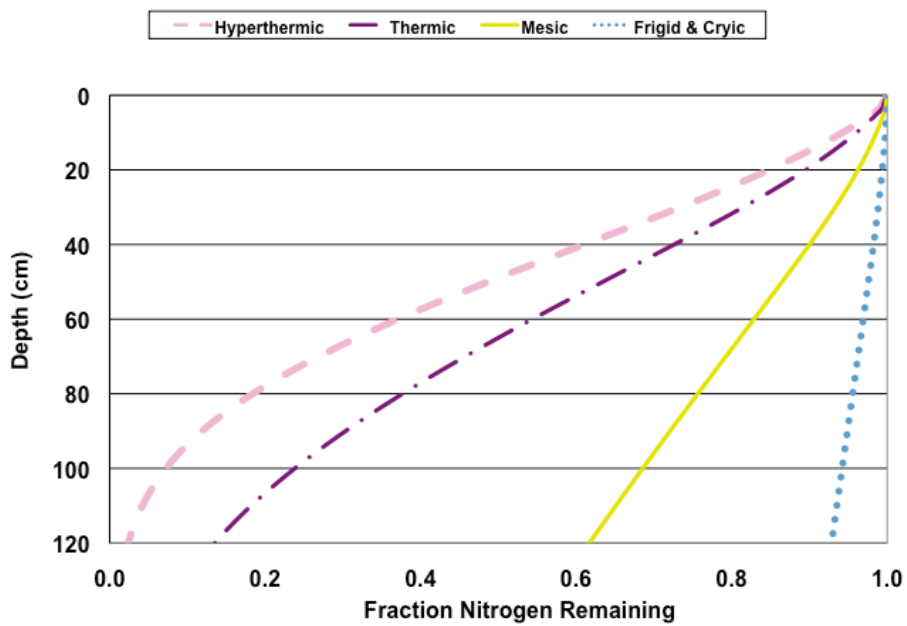


Figure VG-16 . Nomograph: Loamy Sand Soil, Nitrified Effluent, HLR = 5 % of K_{sat}.

1.5 Sand

1.5.1 Standard Effluent

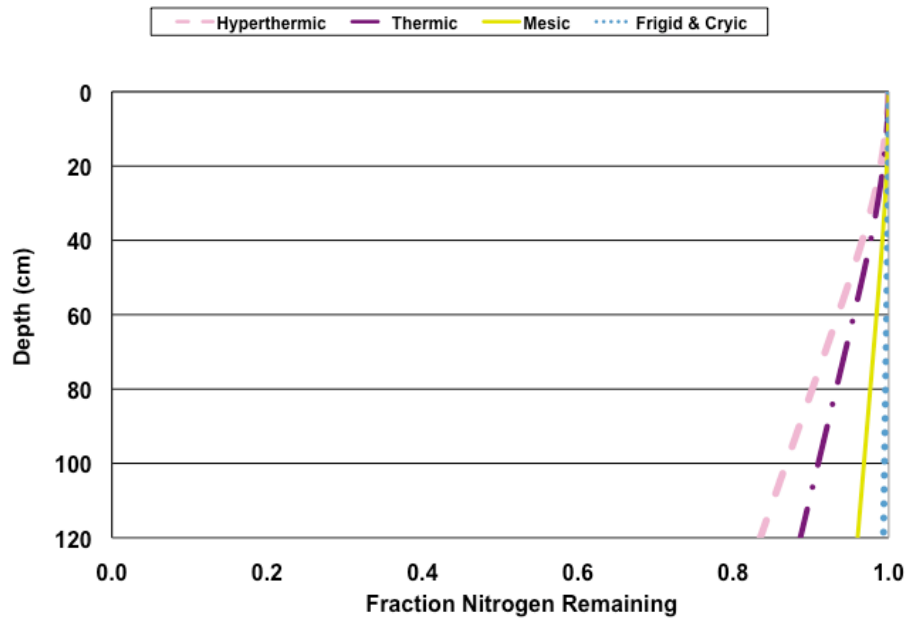


Figure VG-17. Nomograph: Sandy Soil, Standard Effluent, HLR = 2 cm d⁻¹.

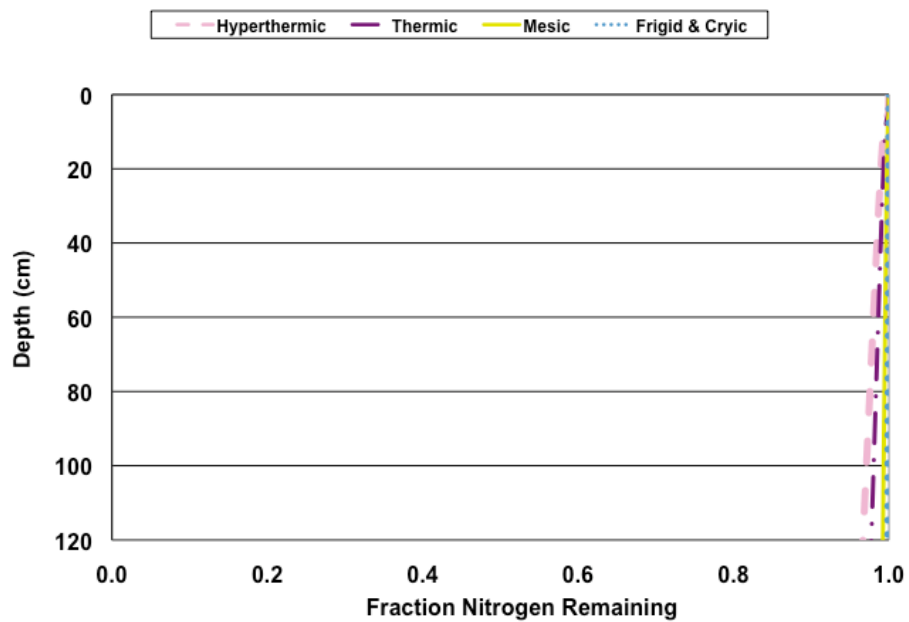


Figure VG-18. Nomograph: Sandy Soil, Standard Effluent, HLR = 5 % of K_{sat} .

1.5.2 Nitrified Effluent

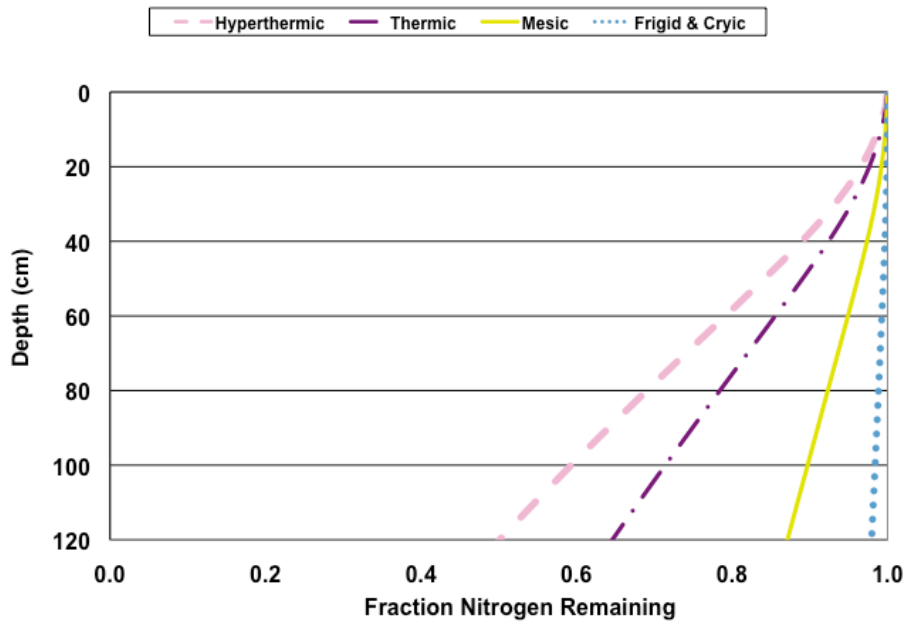


Figure VG-19. Nomograph: Sandy Soil, Nitrified Effluent, HLR = 2 cm d⁻¹.

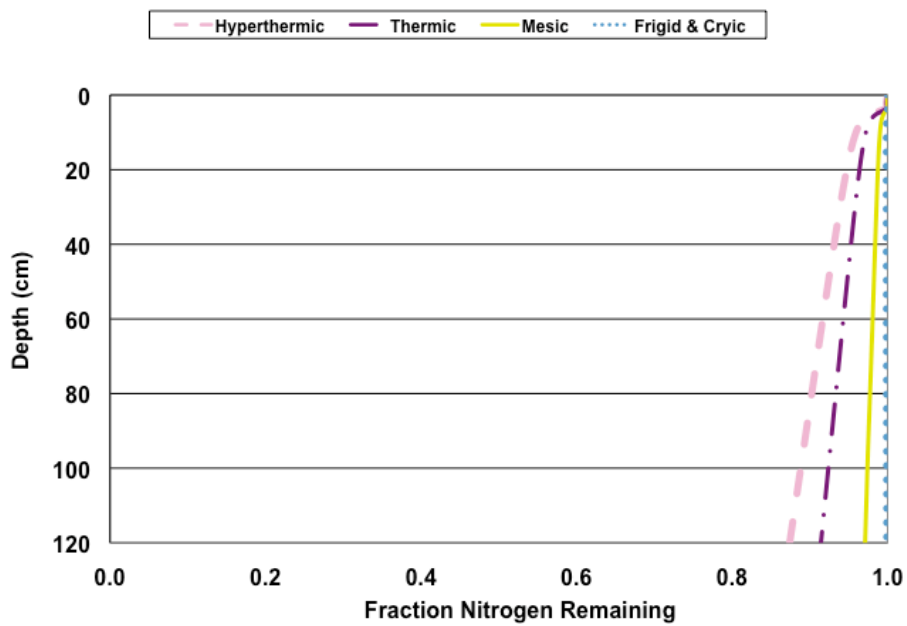


Figure VG-20. Nomograph: Sandy Soil, Nitrified Effluent, HLR = 5 % of K_{sat}.

1.6 Sandy Clay

1.6.1 Standard Effluent

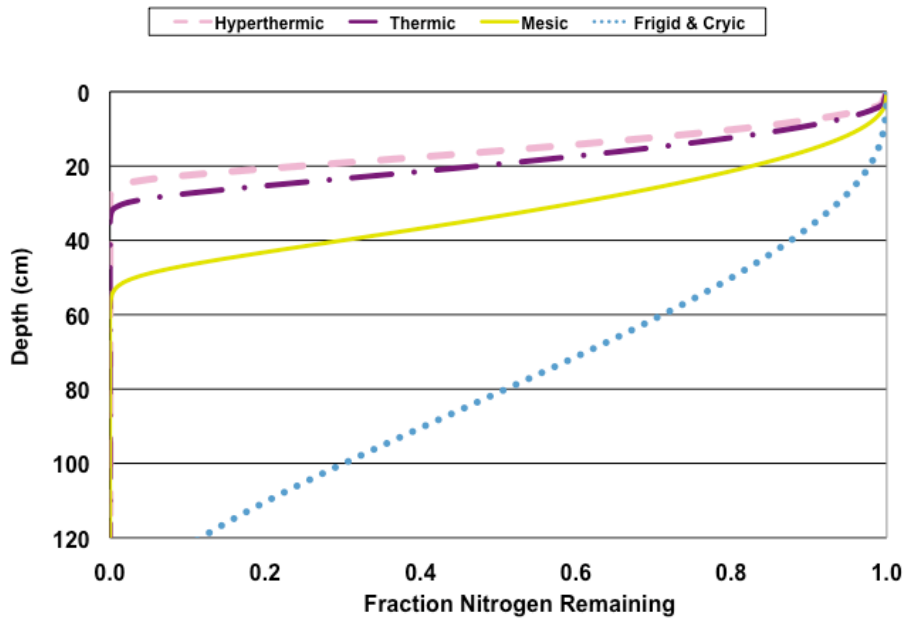


Figure VG-21. Nomograph: Sandy Clay Soil, Standard Effluent, HLR = 2 cm d⁻¹.

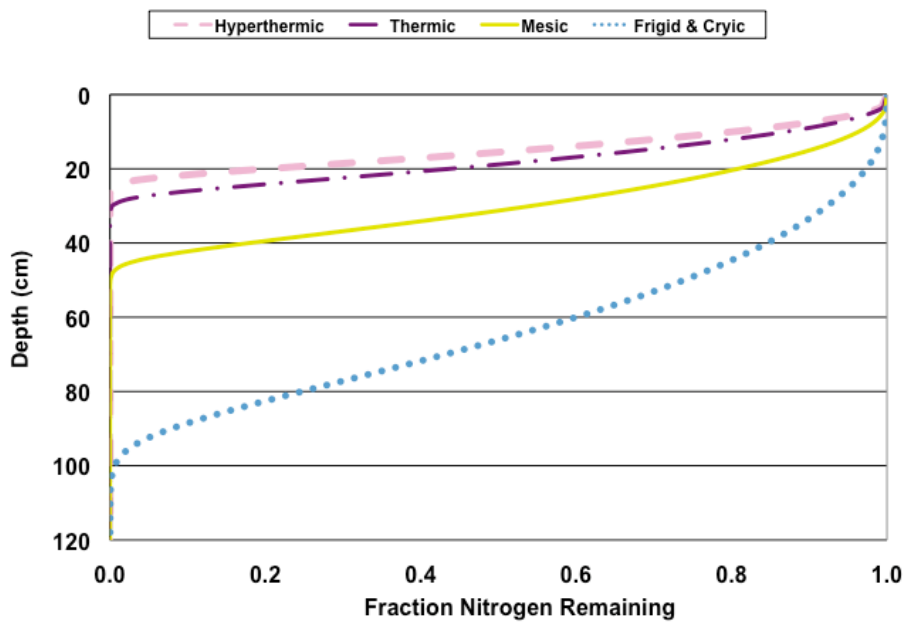


Figure VG-22. Nomograph: Sandy Clay Soil, Standard Effluent, HLR = 5 % of K_{sat} .

1.6.2 Nitrified Effluent

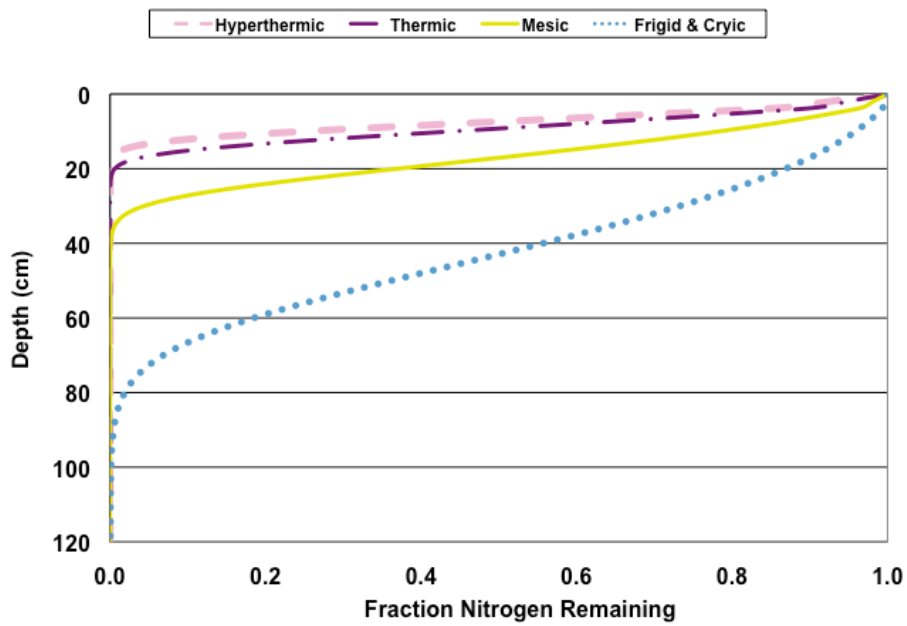


Figure VG-23. Nomograph: Sandy Clay Soil, Nitrified Effluent, HLR = 2 cm d⁻¹.

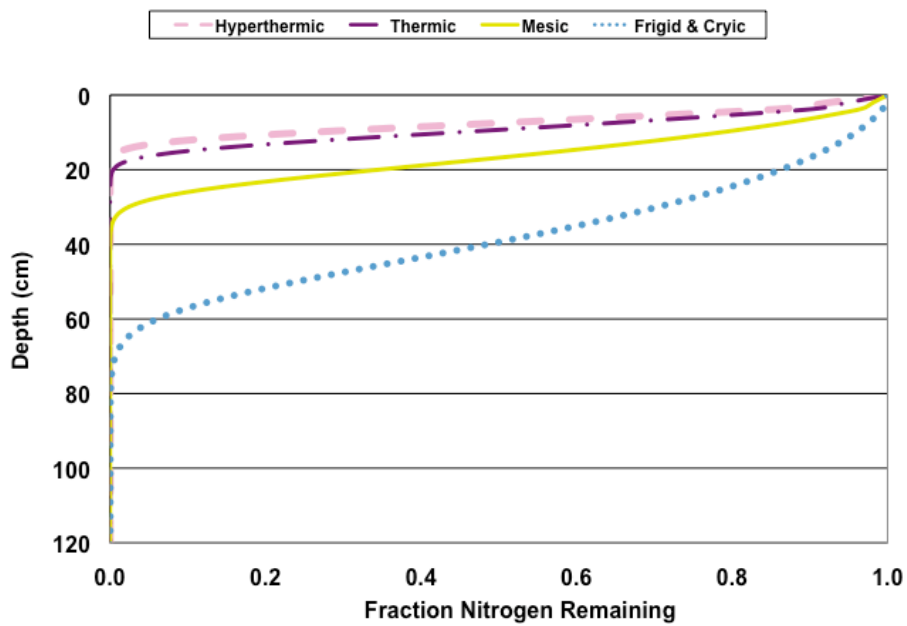


Figure VG-24. Nomograph: Sandy Clay Soil, Nitrified Effluent, HLR = 5 % of K_{sat} .

1.7 Sandy Clay Loam

1.7.1 Standard Effluent

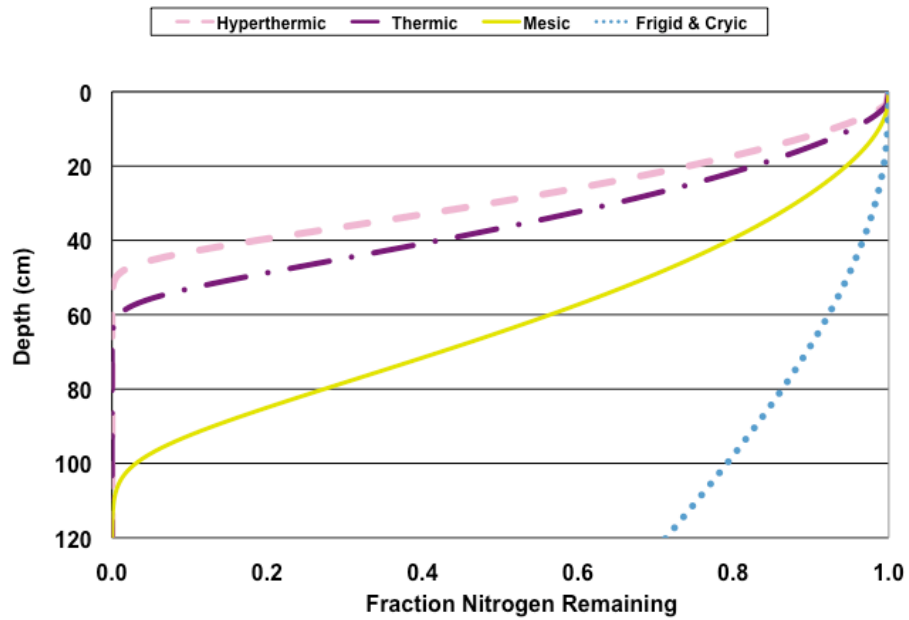


Figure VG-25. Nomograph: Sandy Clay Loam Soil, Standard Effluent, HLR = 2 cm d⁻¹.

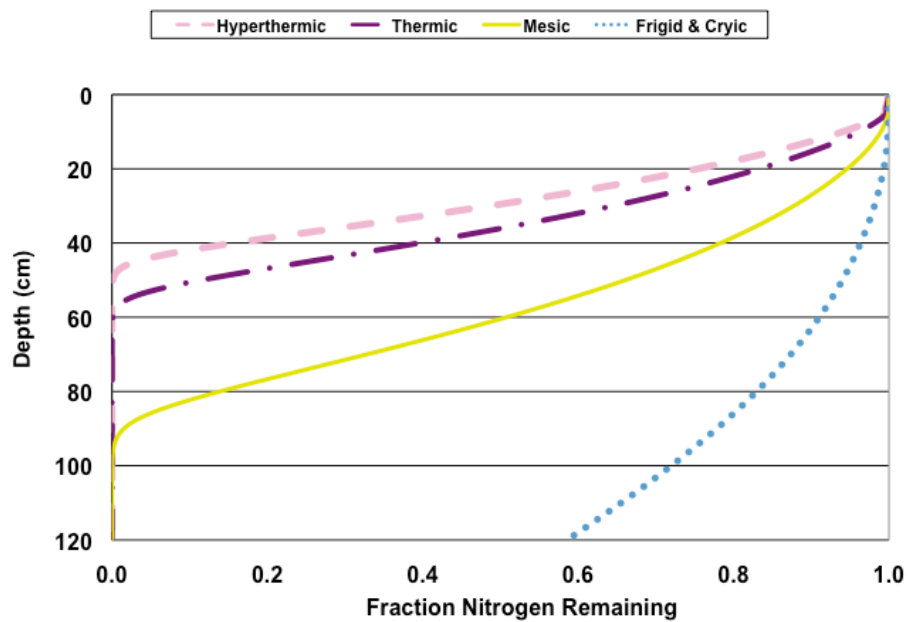


Figure VG-26. Nomograph: Sandy Clay Loam Soil, Standard Effluent, HLR = 5 % of K_{sat}.

1.7.2 Nitrified Effluent

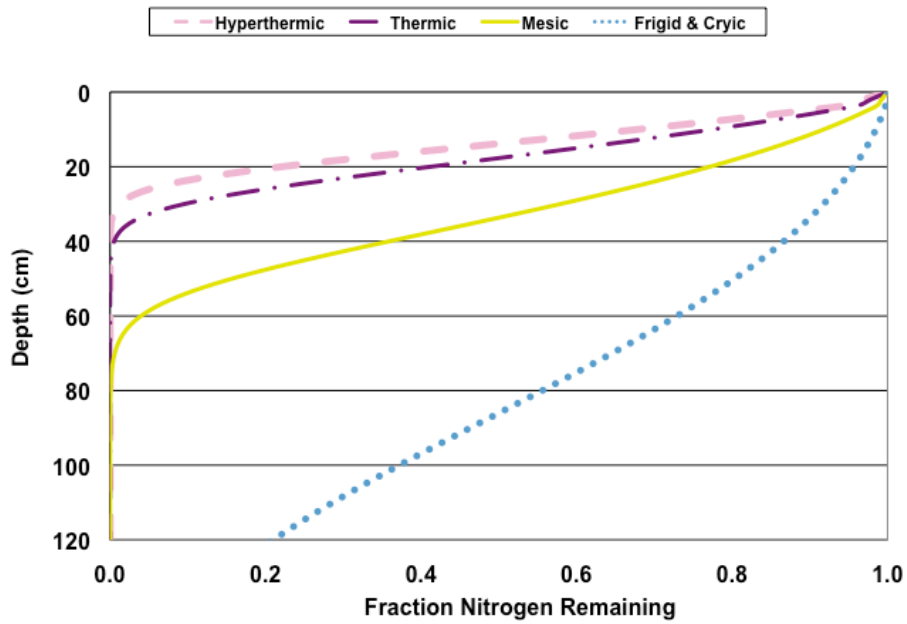


Figure VG-27. Nomograph: Sandy Clay Loam Soil, Nitrified Effluent, HLR = 2 cm d⁻¹.

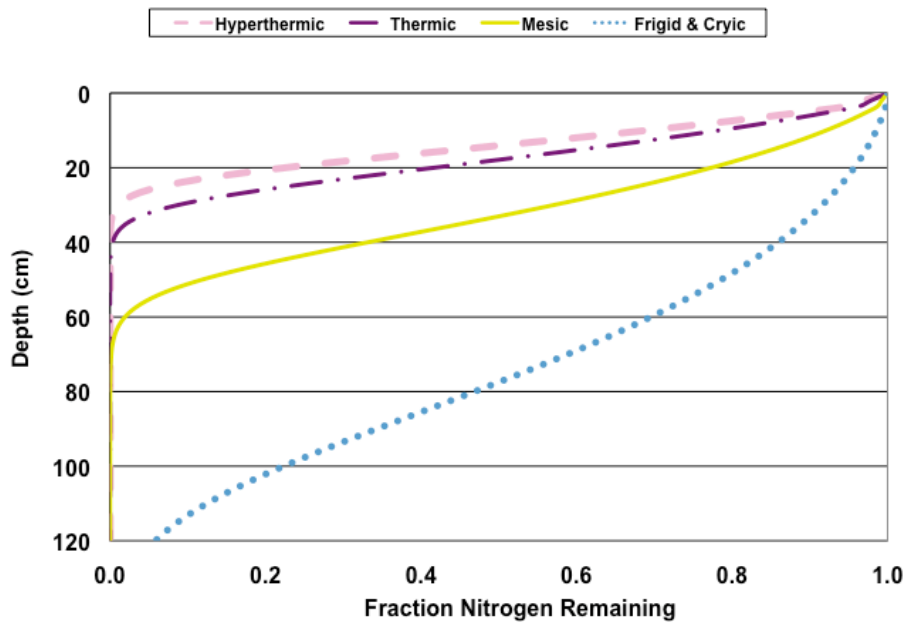


Figure VG-28. Nomograph: Sandy Clay Loam Soil, Nitrified Effluent, HLR = 5 % of K_{sat}.

1.8 Sandy Loam

1.8.1 Standard Effluent

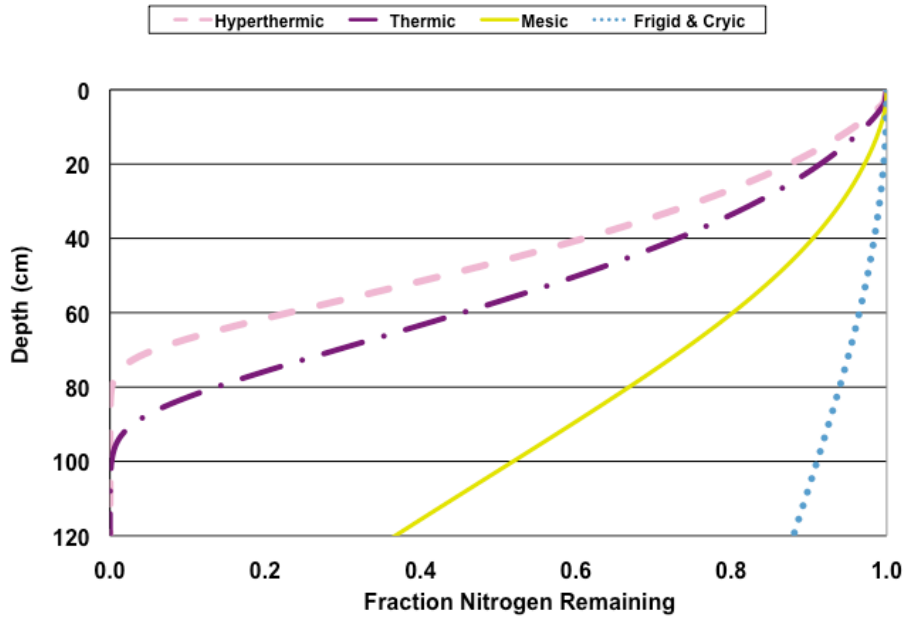


Figure VG-29. Nomograph: Sandy Loam Soil, Standard Effluent, HLR = 2 cm d⁻¹.

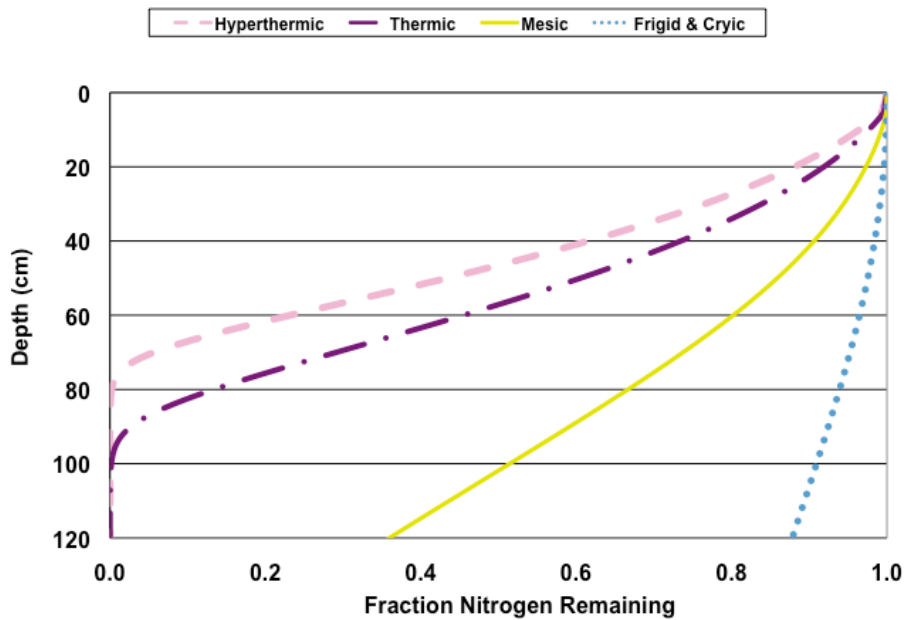


Figure VG-30. Nomograph: Sandy Loam Soil, Standard Effluent, HLR = 5 % of K_{sat} .

1.8.2 Nitrified Effluent

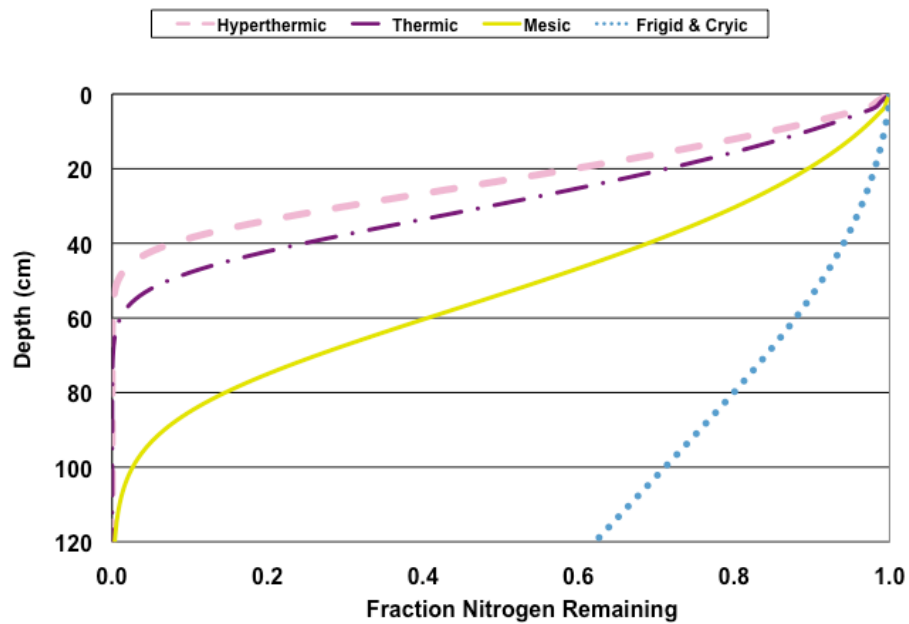


Figure VG-31. Nomograph: Sandy Loam Soil, Nitrified Effluent, HLR = 2 cm d⁻¹.

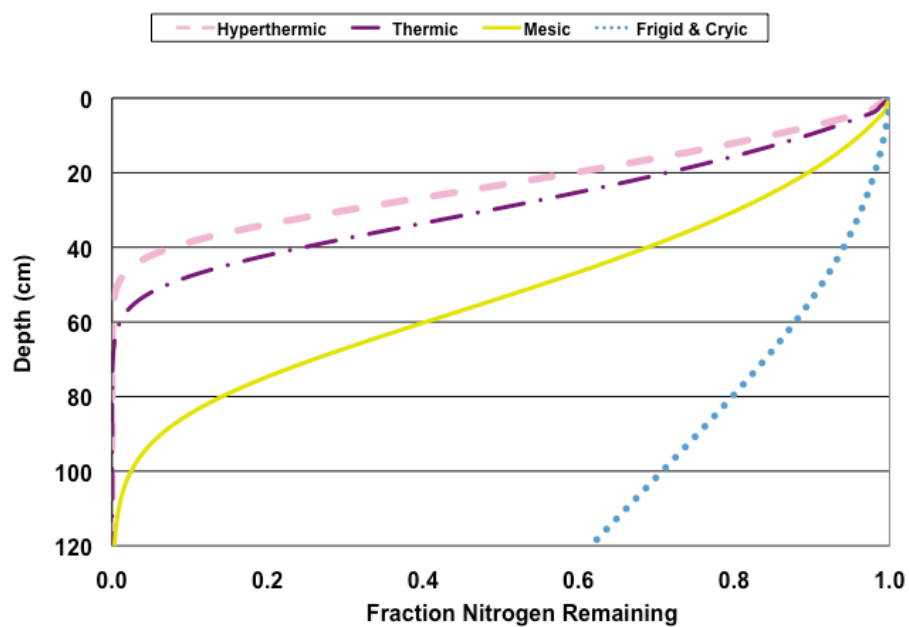


Figure VG-32. Nomograph: Sandy Loam Soil, Nitrified Effluent, HLR = 5% of K_{sat}.

1.9 Silt

1.9.1 Standard Effluent

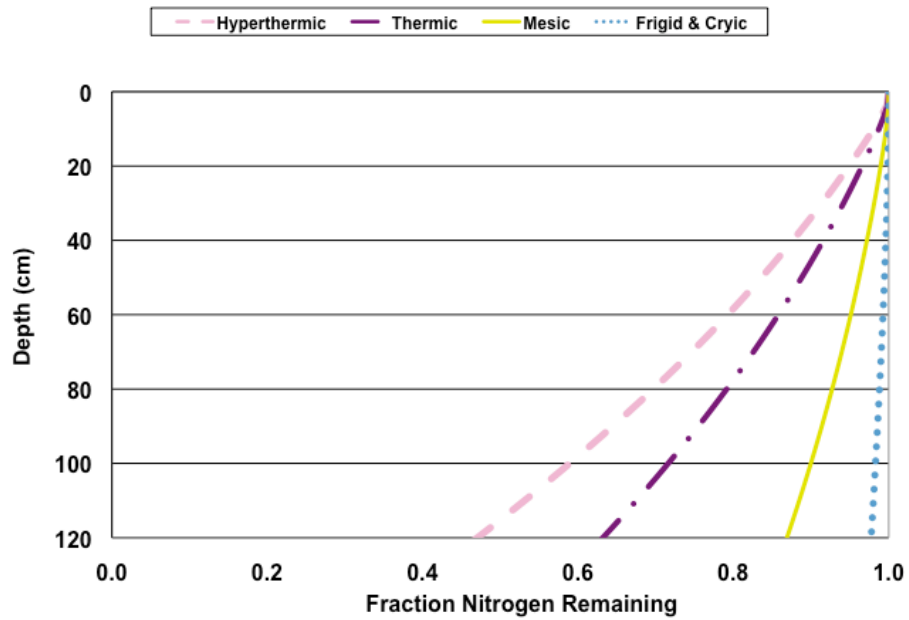


Figure VG-33. Nomograph: Silty Soil, Standard Effluent, HLR = 2 cm d⁻¹.

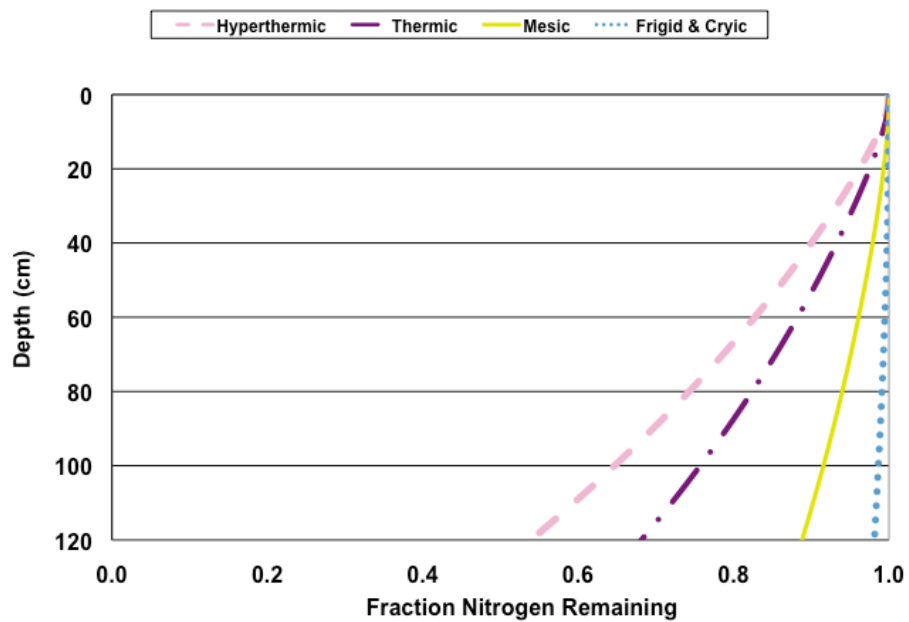


Figure VG-34. Nomograph: Silty Soil, Standard Effluent, HLR = 5 % of K_{sat}.

1.9.2 Nitrified Effluent

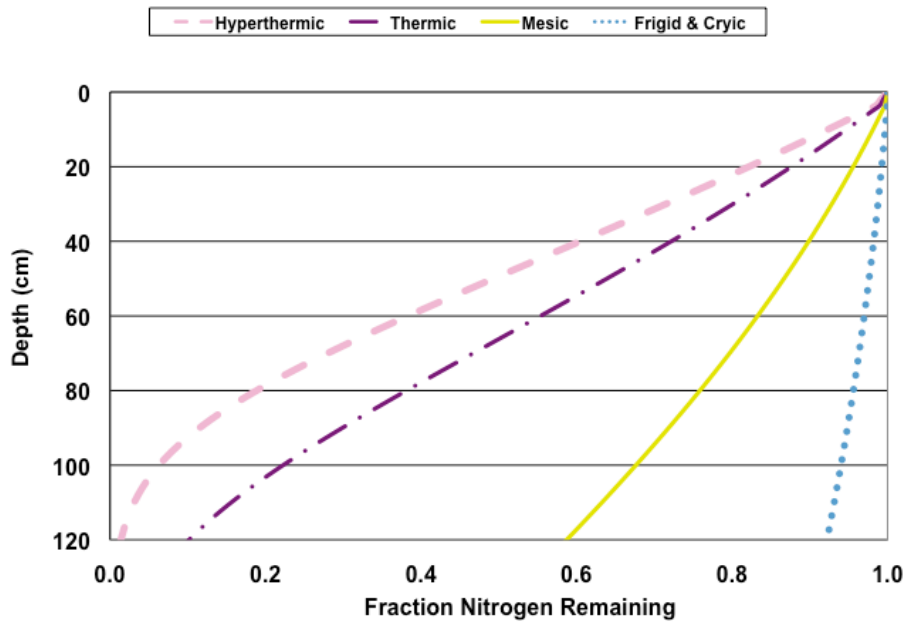


Figure VG-35. Nomograph: Silty Soil, Nitrified Effluent, HLR = 2 cm d⁻¹.

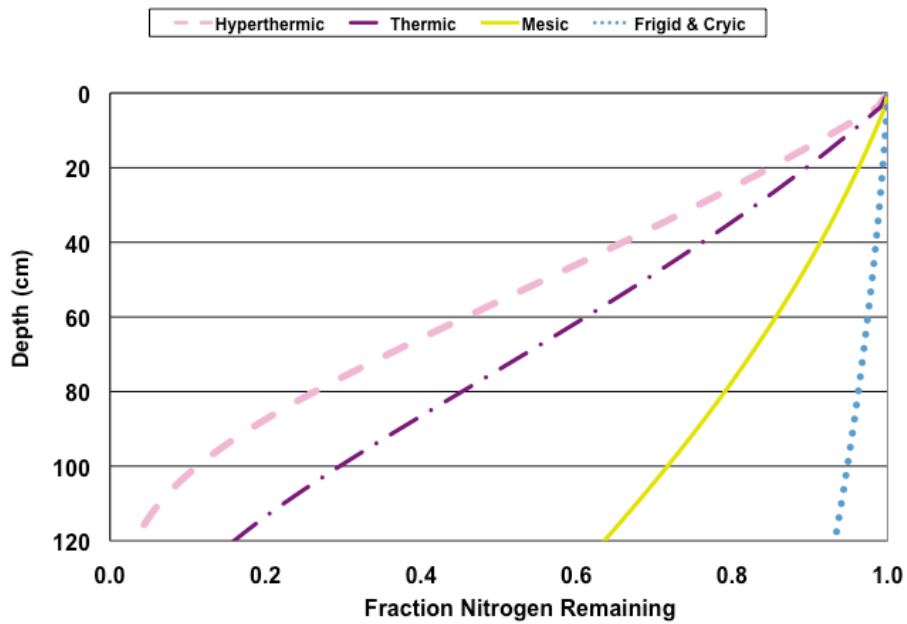


Figure VG-36. Nomograph: Silty Soil, Nitrified Effluent, HLR = 5 % of K_{sat}.

1.10 Silty Clay

1.10.1 Standard Effluent

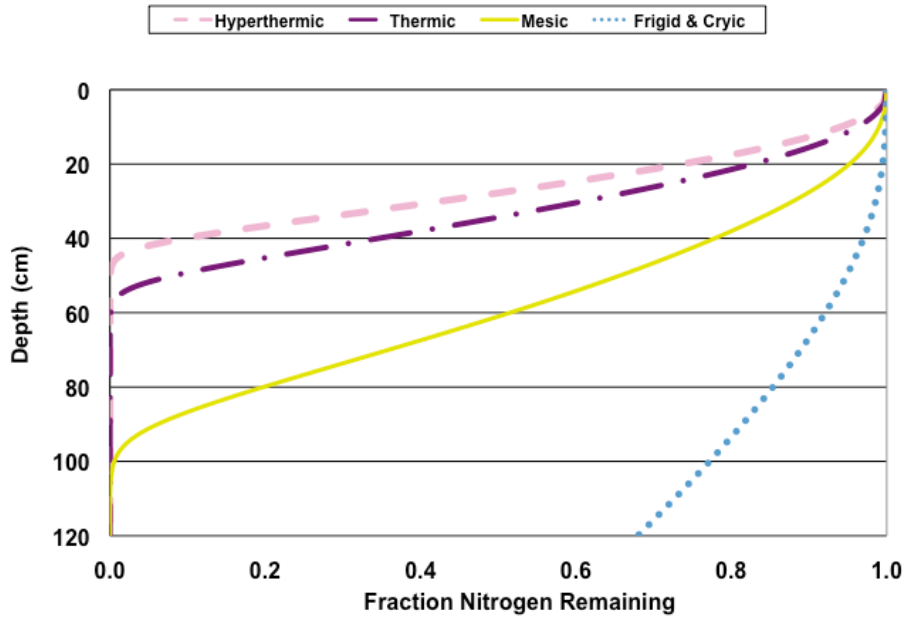


Figure VG-37. Nomograph: Silty Clay Soil, Standard Effluent, HLR = 2 cm d⁻¹.

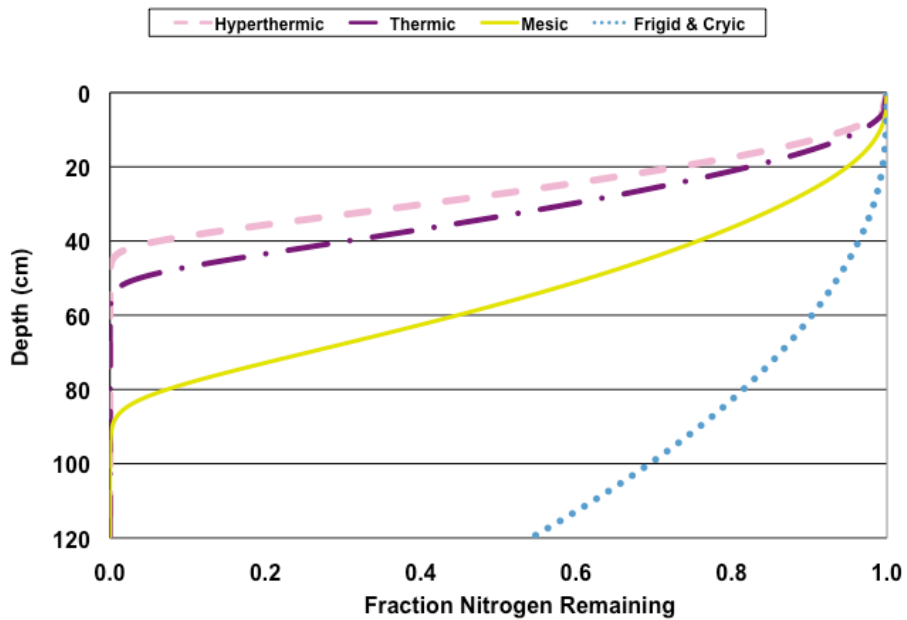


Figure VG-38. Nomograph: Silty Clay Soil, Standard Effluent, HLR = 5 % of K_{sat}.

1.10.2 Nitrified Effluent

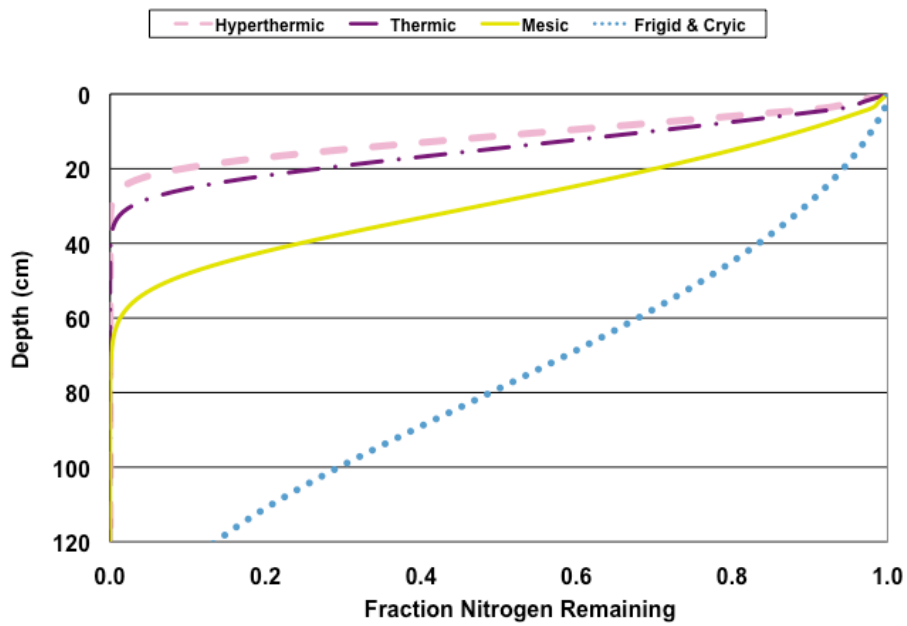


Figure VG-39. Nomograph: Silty Clay Soil, Nitrified Effluent, HLR = 2 cm d⁻¹.

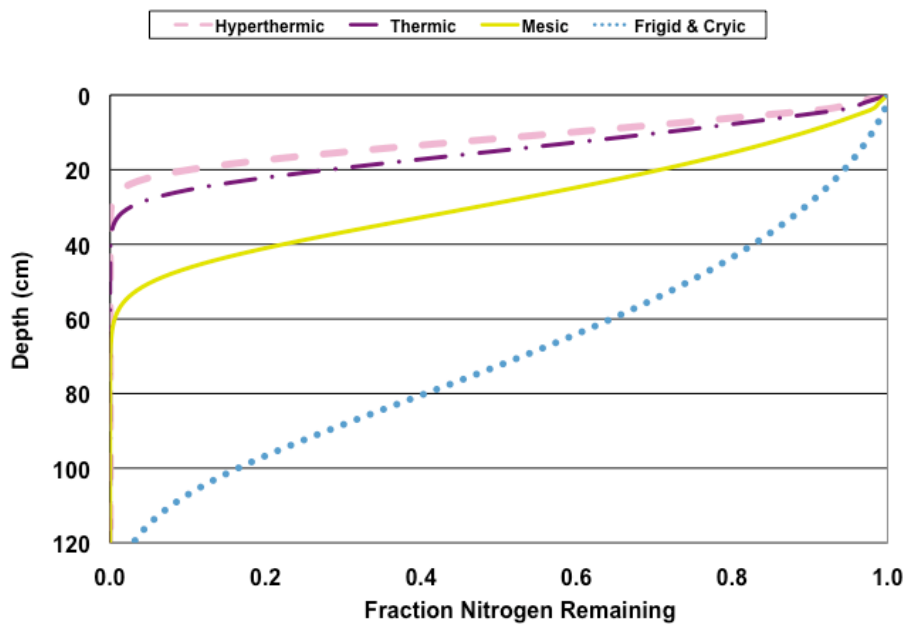


Figure VG-40. Nomograph: Silty Clay Soil, Nitrified Effluent, HLR = 5 % of K_{sat} .

1.11 Silty Clay Loam

1.11.1 Standard Effluent

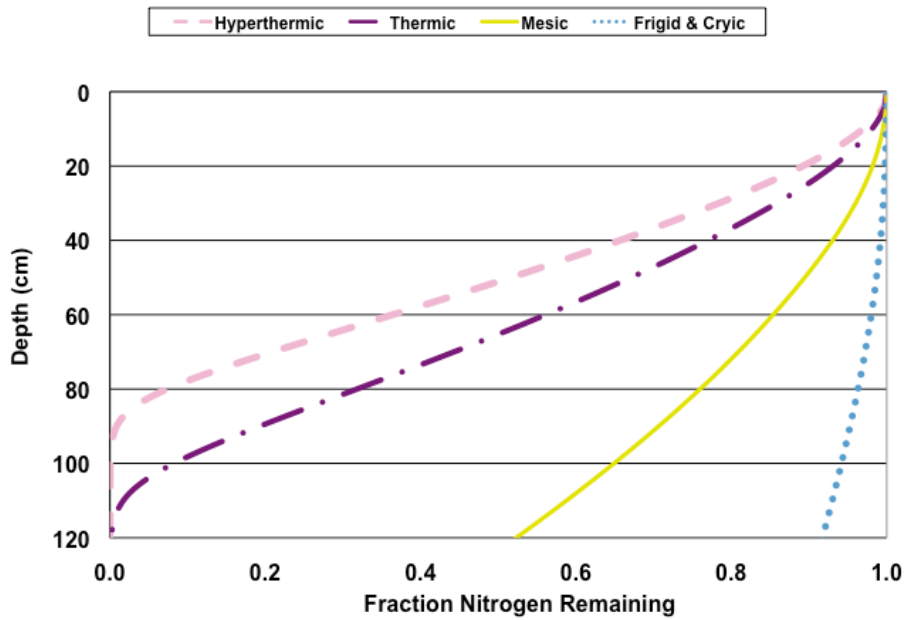


Figure VG-41. Nomograph: Silty Clay Loam Soil, Standard Effluent, HLR = 2 cm d⁻¹.

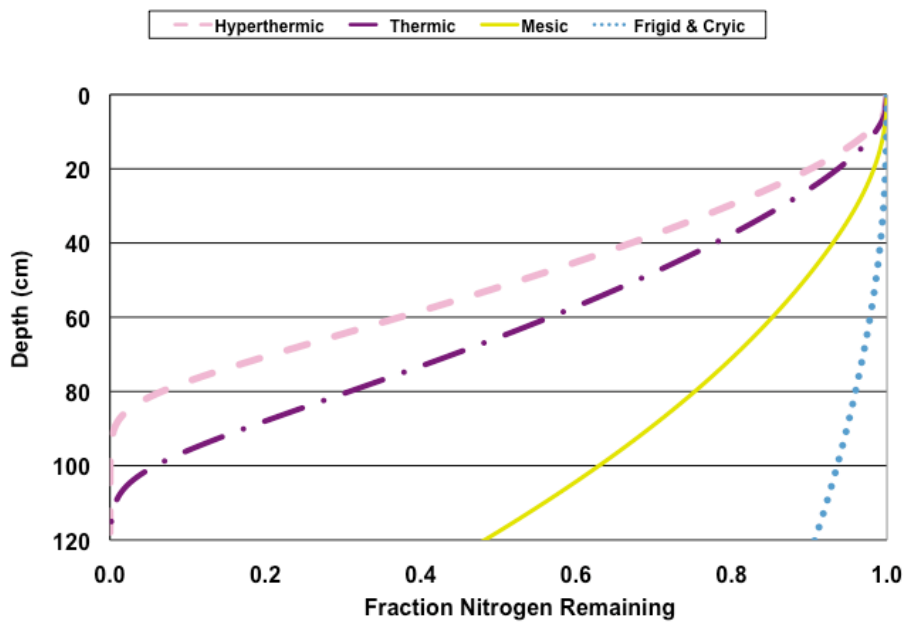


Figure VG-42. Nomograph: Silty Clay Loam Soil, Standard Effluent, HLR = 5 % of K_{sat}.

1.11.2 Nitrified Effluent

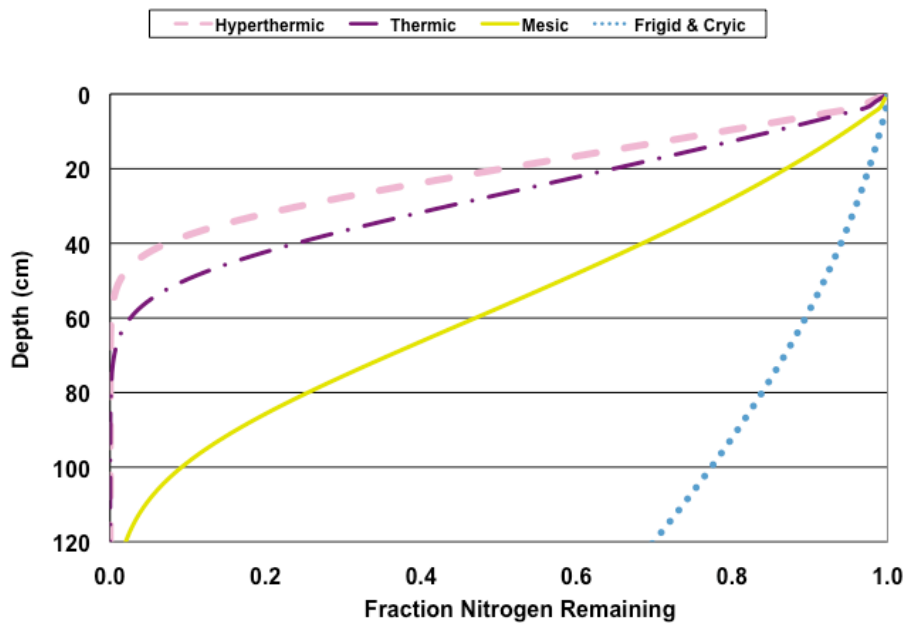


Figure VG-43. Nomograph: Silty Clay Loam Soil, Nitrified Effluent, HLR = 2 cm d⁻¹.

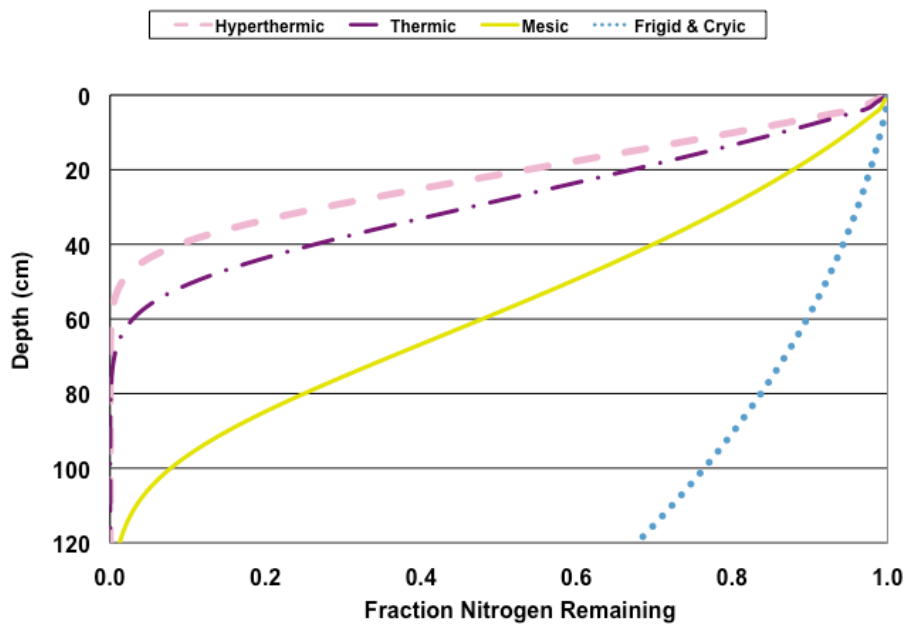


Figure VG-44. Nomograph: Silty Clay Loam Soil, Nitrified Effluent, HLR = 5 % of K_{sat}.

112 Silty Loam

1.12.1 Standard Effluent

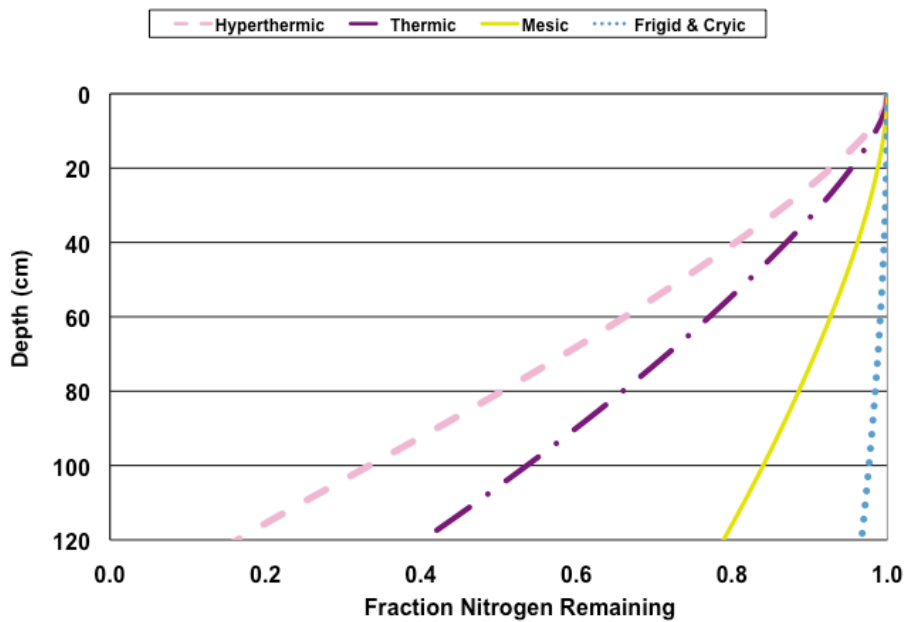


Figure VG-45. Nomograph: Silty Loam Soil, Standard Effluent, HLR = 2 cm d⁻¹.

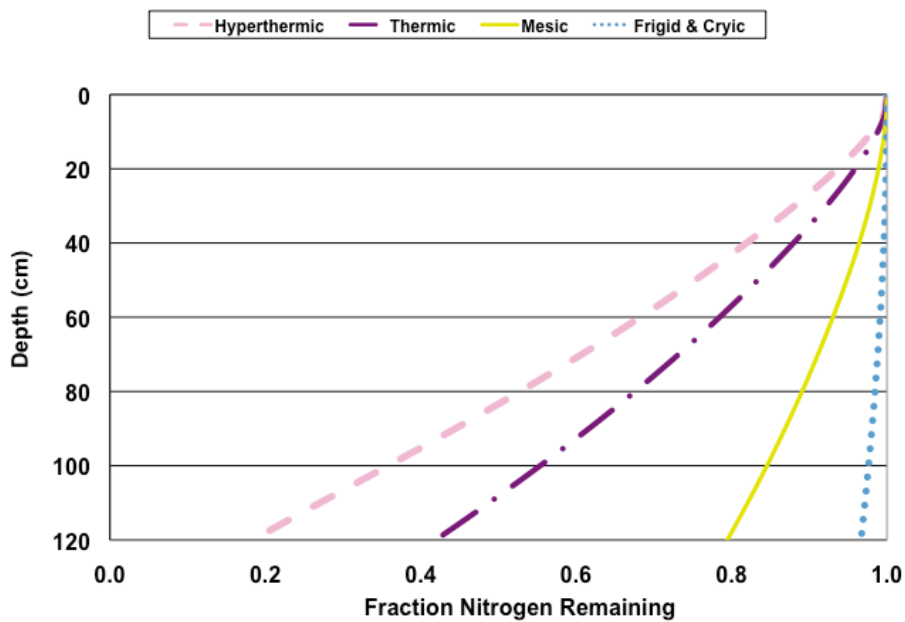


Figure VG-46. Nomograph: Silty Loam Soil, Standard Effluent, HLR = 5 % of K_{sat} .

1.12.2 Nitrified Effluent

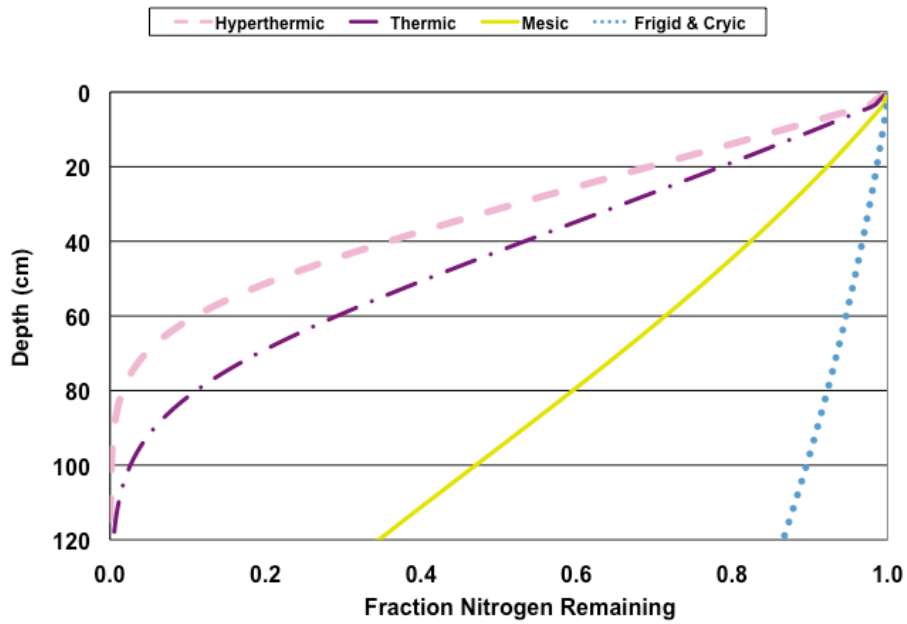


Figure VG-47. Nomograph: Silty Loam Soil, Nitrified Effluent, HLR = 2 cm d⁻¹.

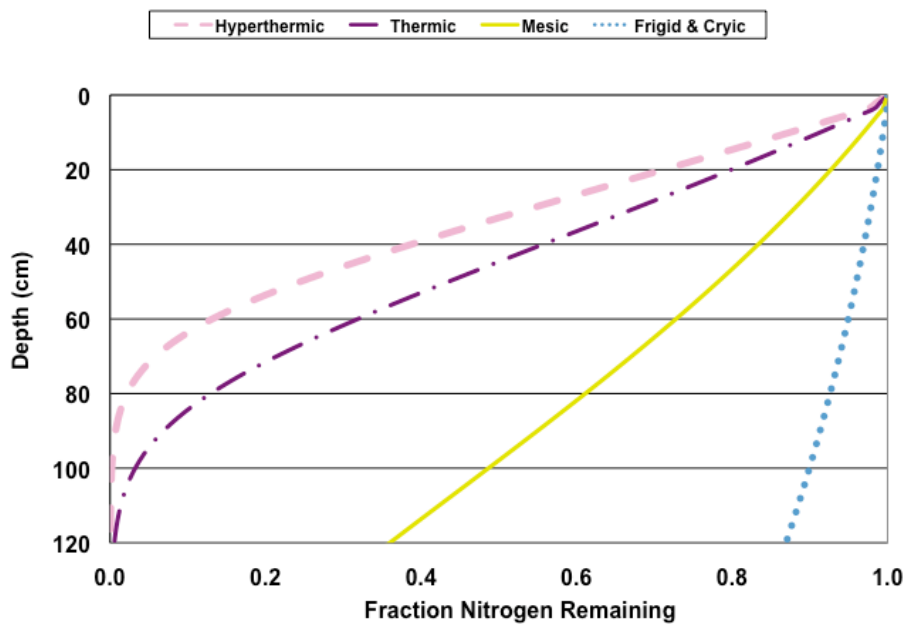


Figure VG-48. Nomograph: Silty Loam Soil, Nitrified Effluent, HLR = 5 % of K_{sat} .

1.13 Fraction of Nitrogen Removed at 60cm with Varied Ammonium-Nitrogen Input Concentrations

1.13.1 Clay

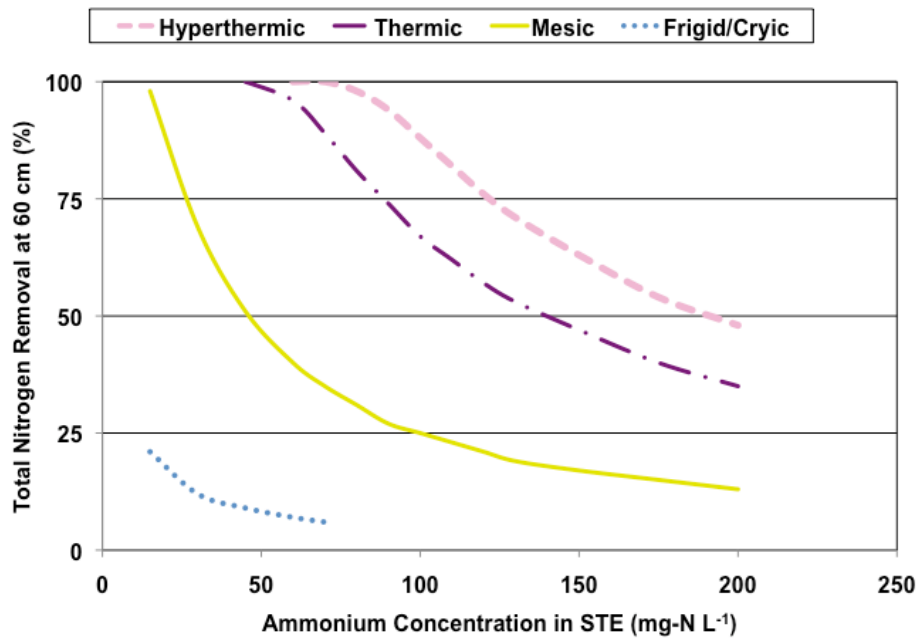


Figure VG-49. Nomograph: Total Nitrogen Removed at 60 cm, Clay Soil, HLR = 2 cm d⁻¹.

1.13.2 Clay Loam

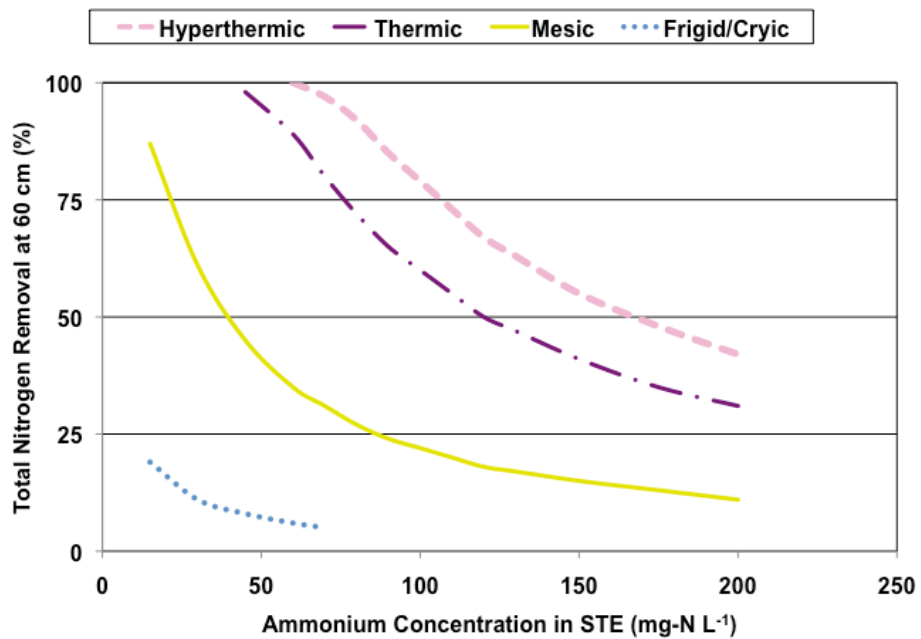


Figure VG-50. Nomograph: Total Nitrogen Removed at 60 cm, Clay Loam Soil, HLR = 2 cm d⁻¹.

1.13.3 Loam

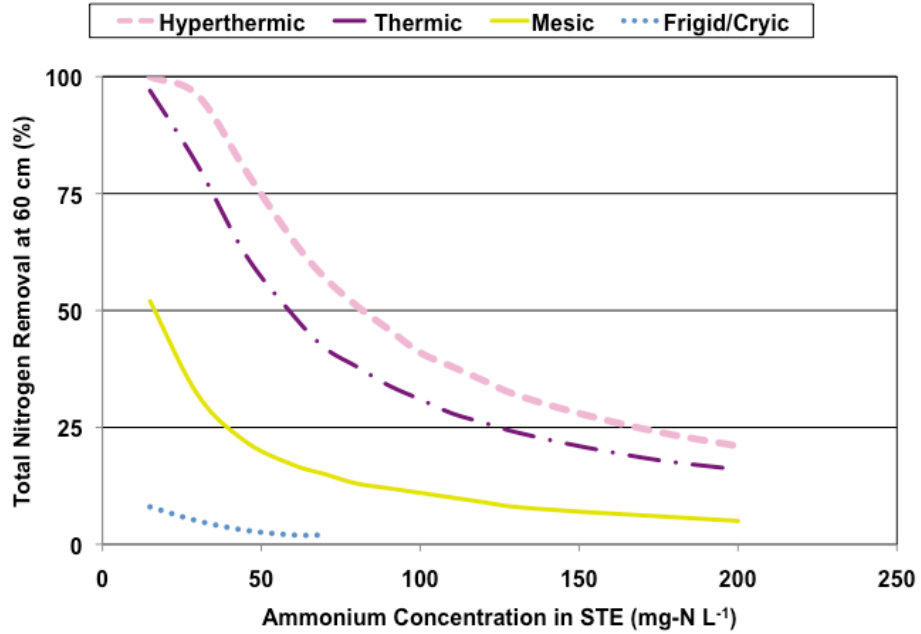


Figure VG-51. Nomograph: Total Nitrogen Removed at 60 cm, Loam Soil, HLR = 2 cm d⁻¹.

1.13.4 Loamy Sand

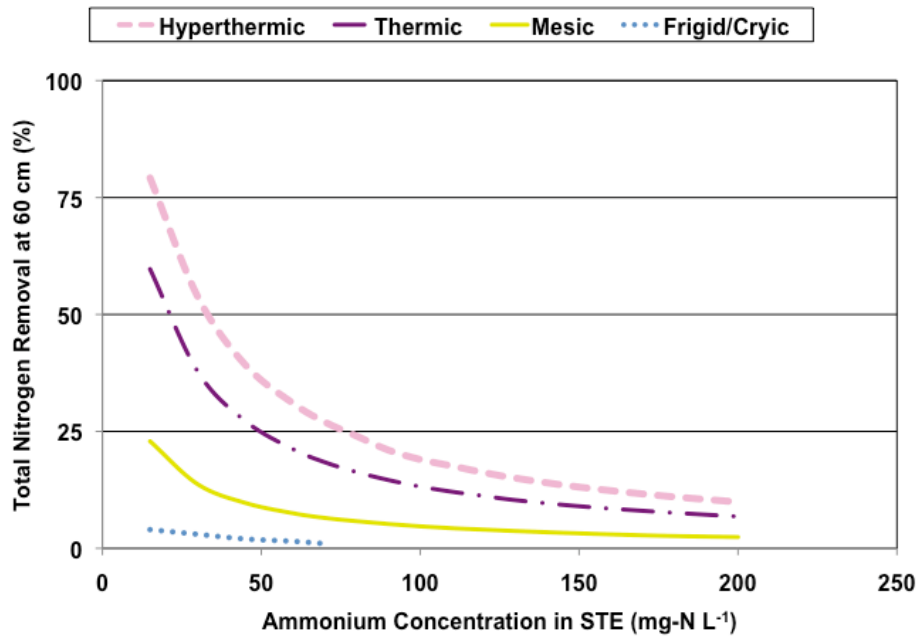


Figure VG-52. Nomograph: Total Nitrogen Removed at 60 cm, Loamy Sand Soil, HLR = 2 cm d⁻¹.

1.13.5 Sand

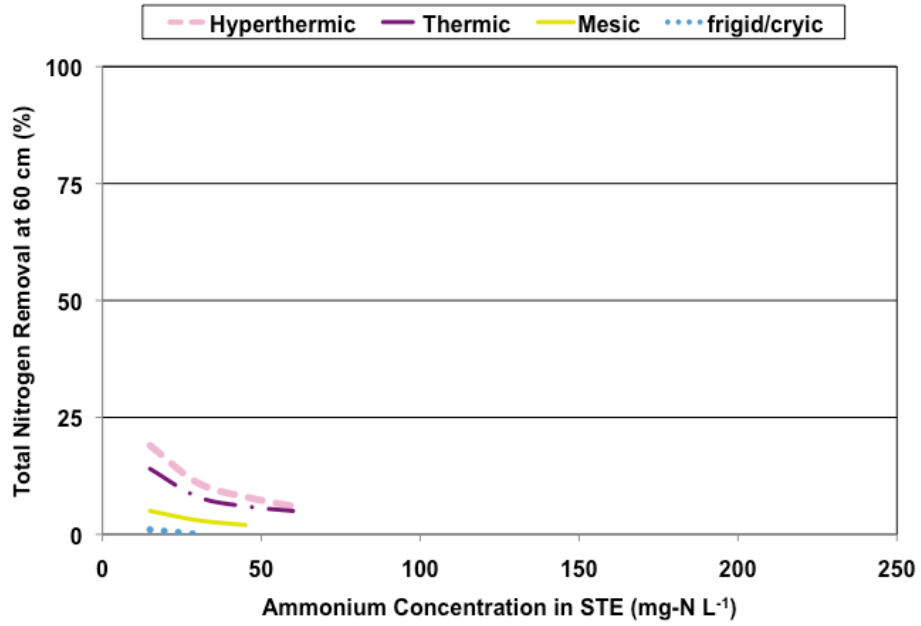


Figure VG-53. Nomograph: Total Nitrogen Removed at 60 cm, Sandy Soil, HLR = 2 cm d⁻¹.

1.13.6 Sandy Clay

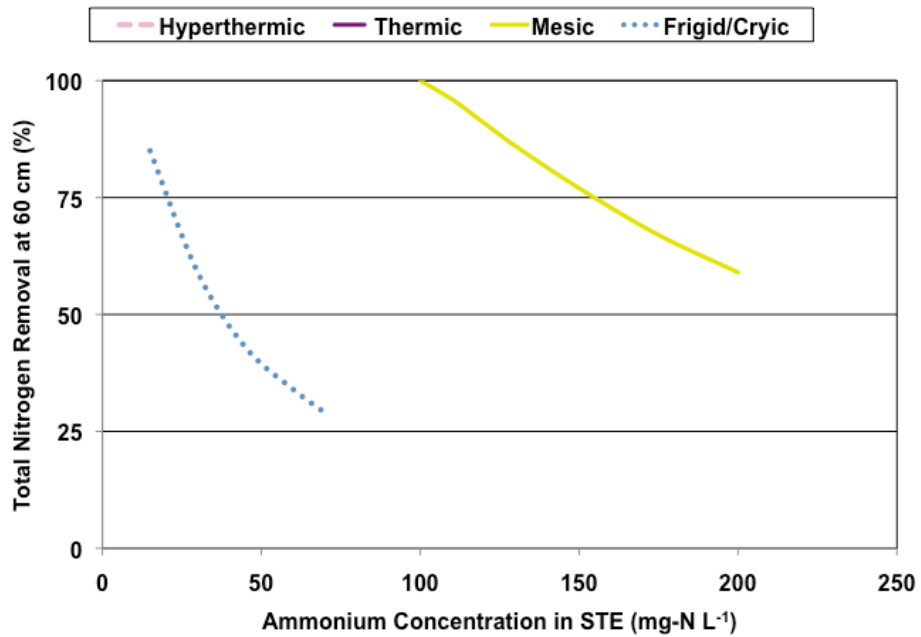


Figure VG-54. Nomograph: Total Nitrogen Removed at 60 cm, Sandy Clay Soil, HLR = 2 cm d⁻¹.

1.13.7 Sandy Clay Loam

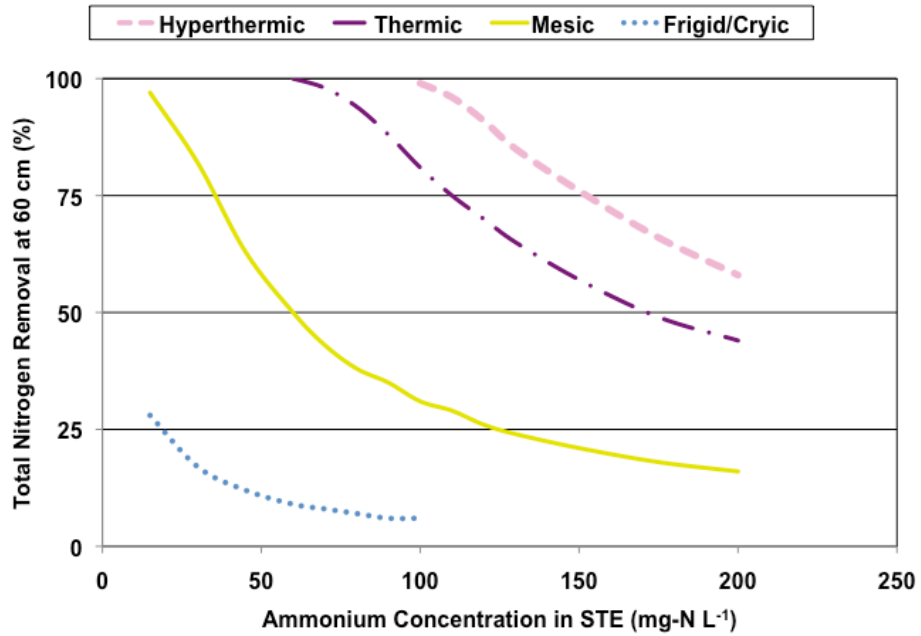


Figure VG-55. Nomograph: Total Nitrogen Removed at 60 cm, Sandy Clay Loam Soil, HLR = 2 cm d⁻¹.

1.13.8 Sandy Loam

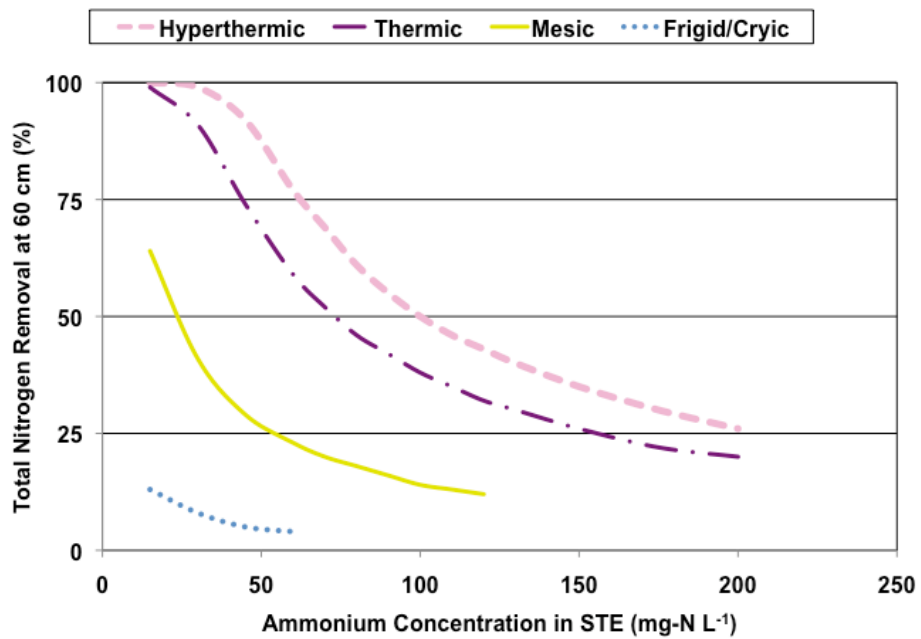


Figure VG-56. Nomograph: Total Nitrogen Removed at 60 cm, Sandy Loam Soil, HLR = 2 cm d⁻¹.

1.13.9 Silt

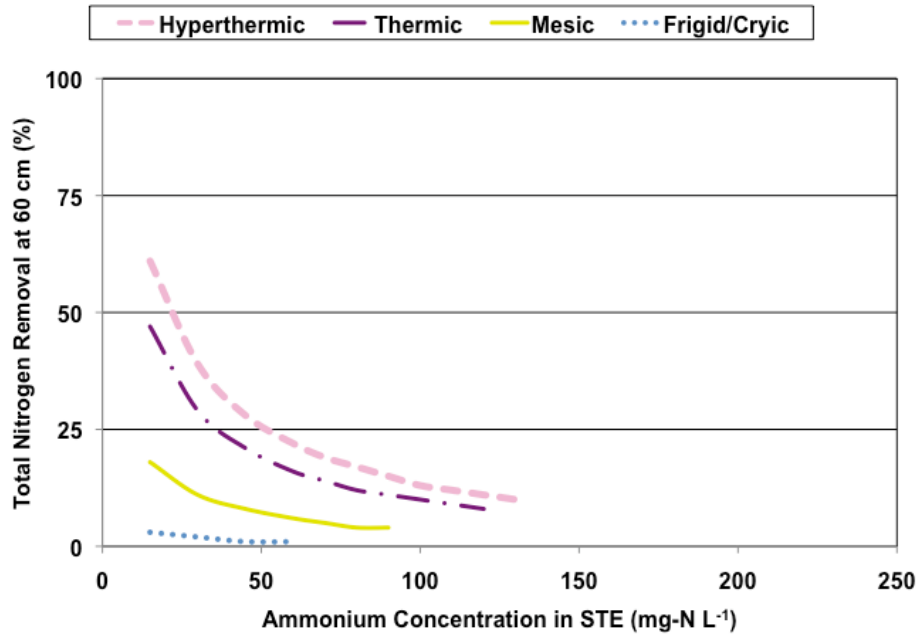


Figure VG-57. Nomograph: Total Nitrogen Removed at 60 cm, Silty Soil, HLR = 2 cm d⁻¹.

1.13.10 Silty Clay

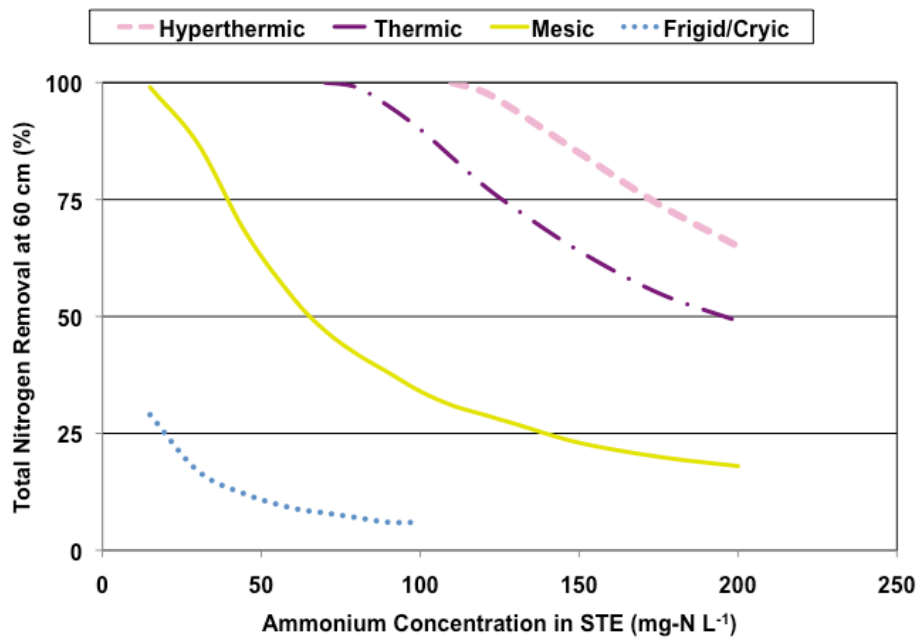


Figure VG-58. Nomograph: Total Nitrogen Removed at 60 cm, Silty Clay Soil, HLR = 2 cm d⁻¹.

1.13.11 Silty Clay Loam

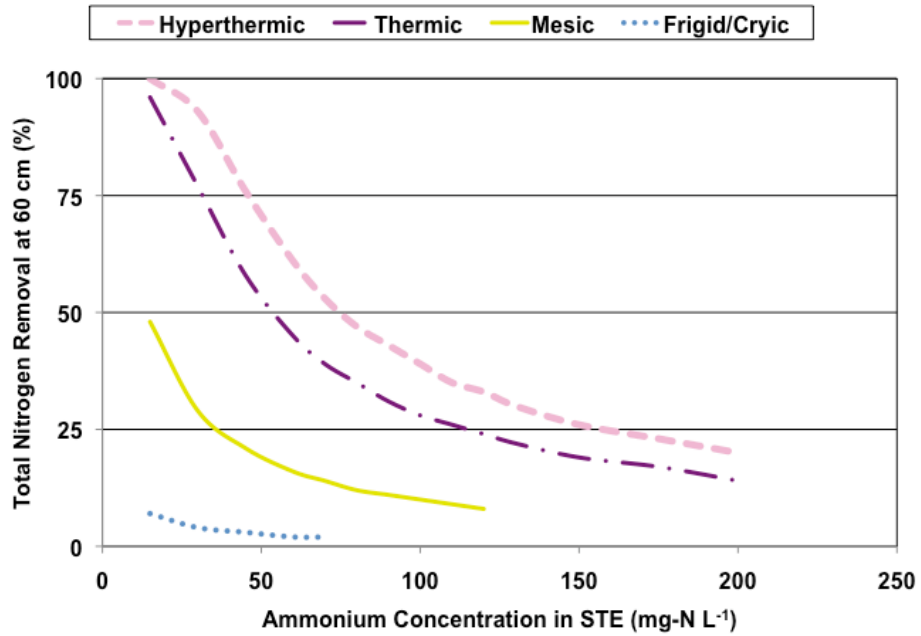


Figure VG-59. Nomograph: Total Nitrogen Removed at 60 cm, Silty Clay Loam Soil, HLR = 2 cm d⁻¹.

1.13.12 Silty Loam

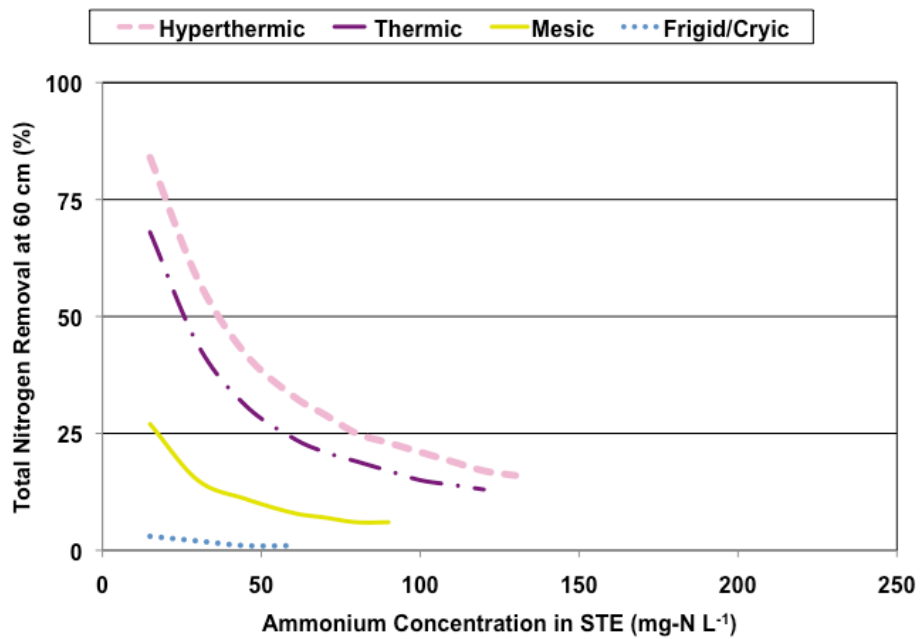


Figure VG-60. Nomograph: Total Nitrogen Removed at 60 cm, Silty Loam Soil, HLR = 2 cm d⁻¹.

CHAPTER 2.0

CUMULATIVE PROBABILITY GRAPHS: STUMOD MONTE CARLO SIMULATION RESULTS FOR DEEP WATER TABLES

2.1 Clay

2.1.1 Standard Effluent

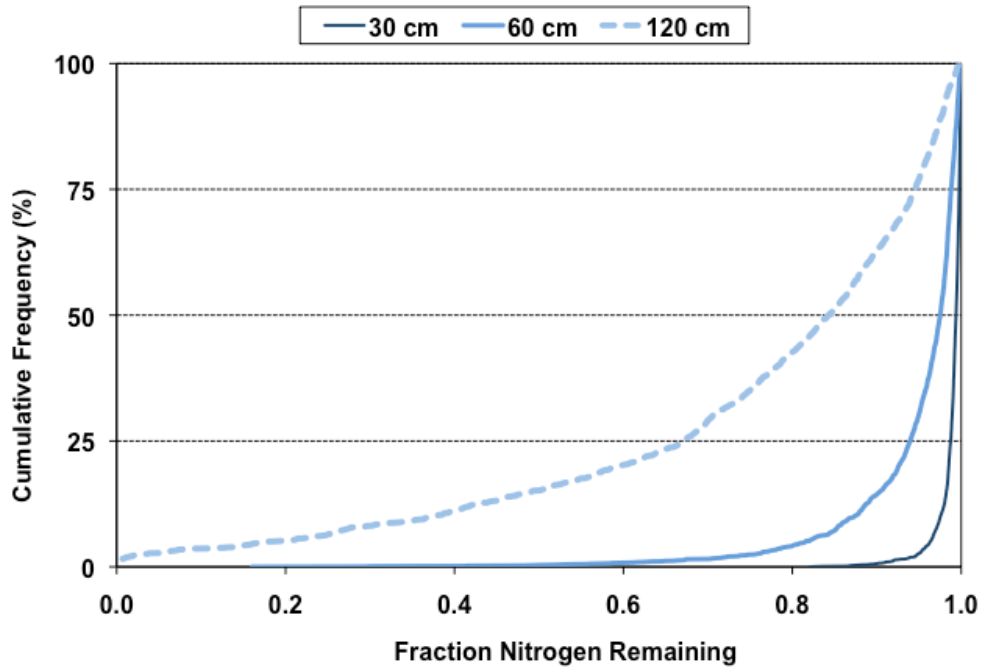


Figure VG-61. Cumulative Probability Graph: Clay Soil, Frigid/Cryic Temperature Region, Standard Effluent, HLR = 2 cm d⁻¹.

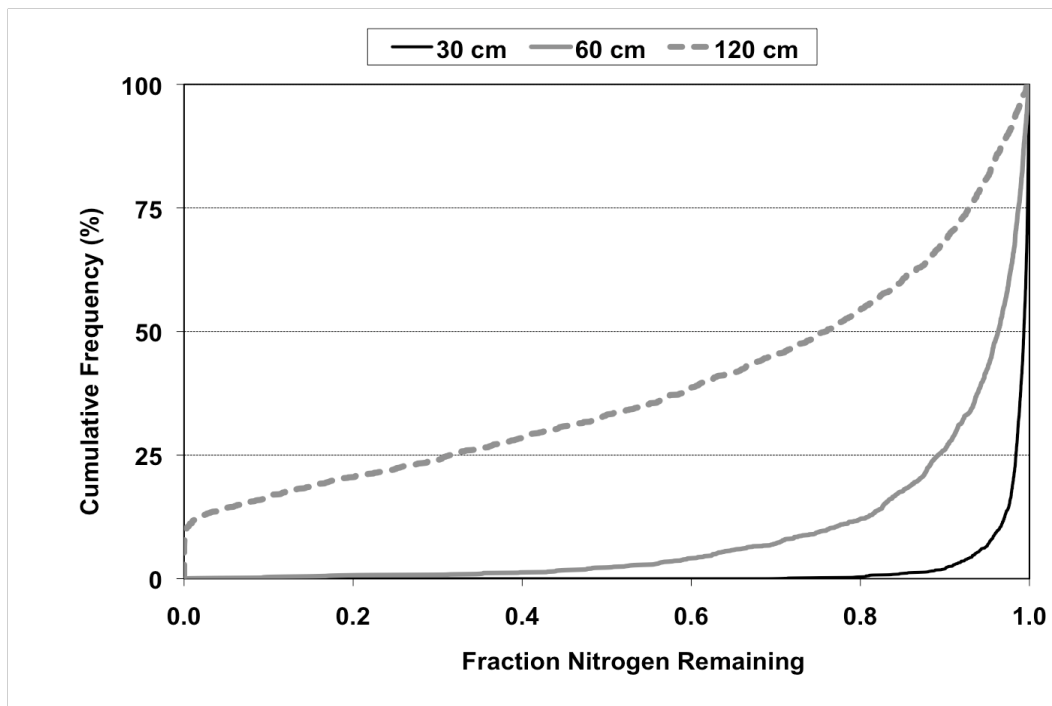


Figure VG-62. Cumulative Probability Graph: Clay Soil, Frigid/Cryic Temperature Region, Standard Effluent, HLR = 5% of K_{sat}.

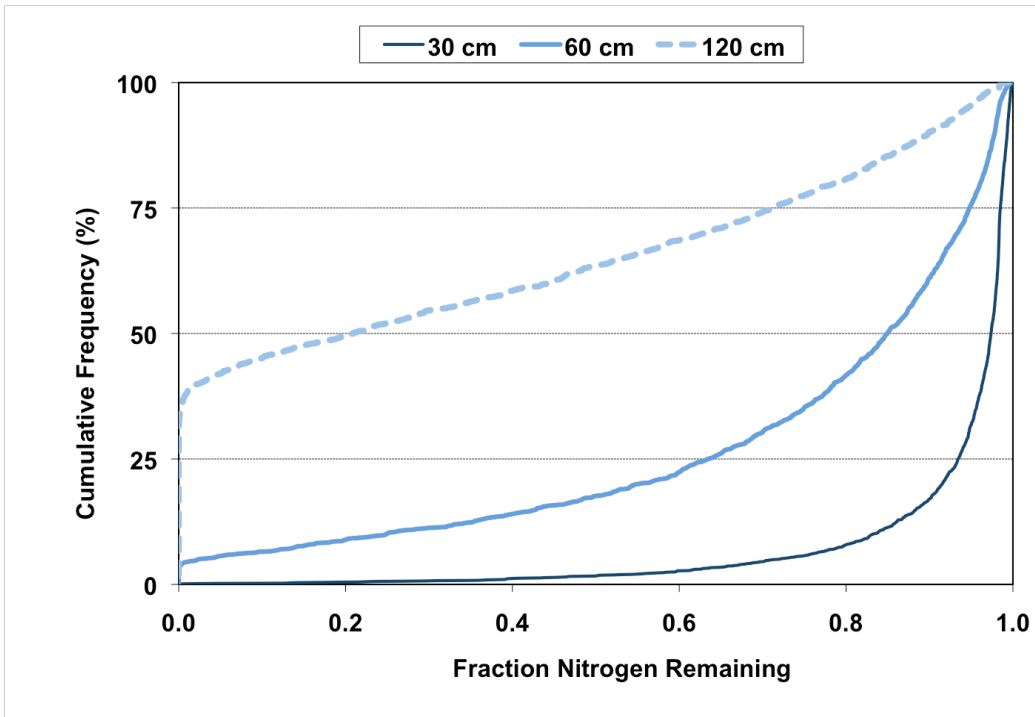


Figure VG-63. Cumulative Probability Graph: Clay Soil, Mesic Temperature Region, Standard Effluent, HLR = 2 cm d⁻¹.

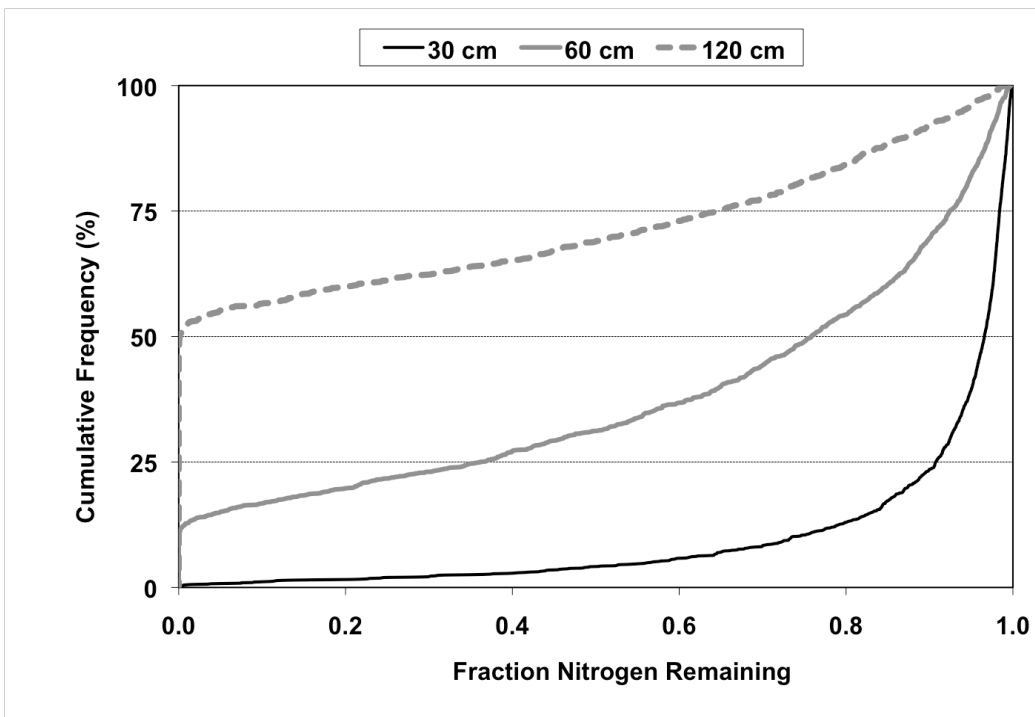


Figure VG-64. Cumulative Probability Graph: Clay Soil, Mesic Temperature Region, Standard Effluent, HLR = 5% of K_{sat} .

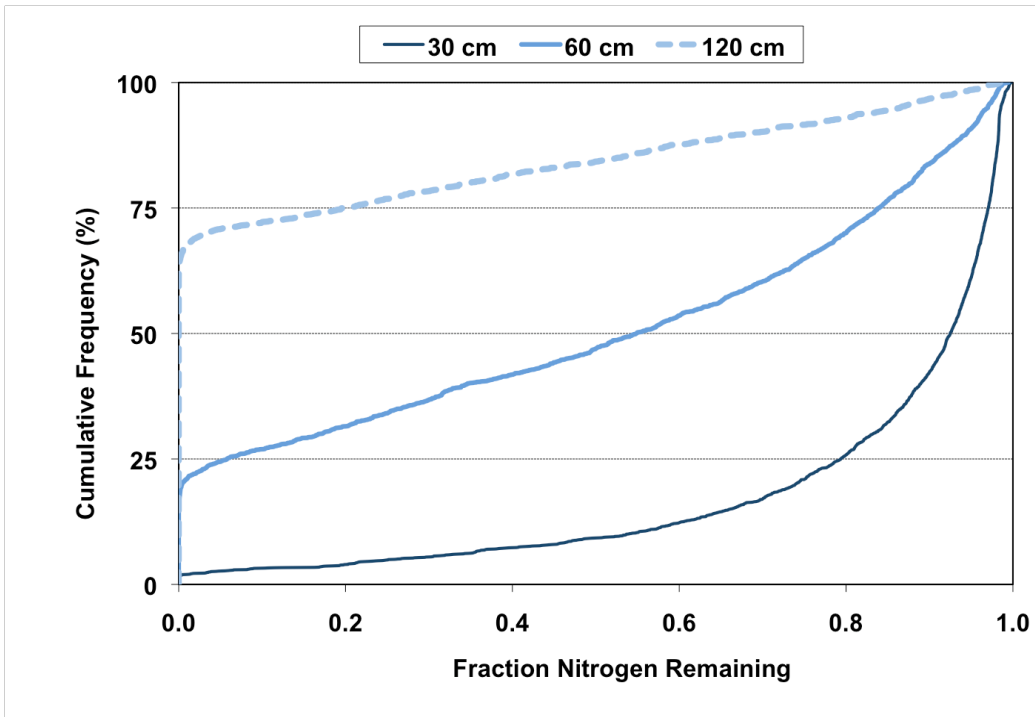


Figure VG-65. Cumulative Probability Graph: Clay Soil, Thermic Temperature Region, Standard Effluent, HLR = 2 cm d⁻¹.

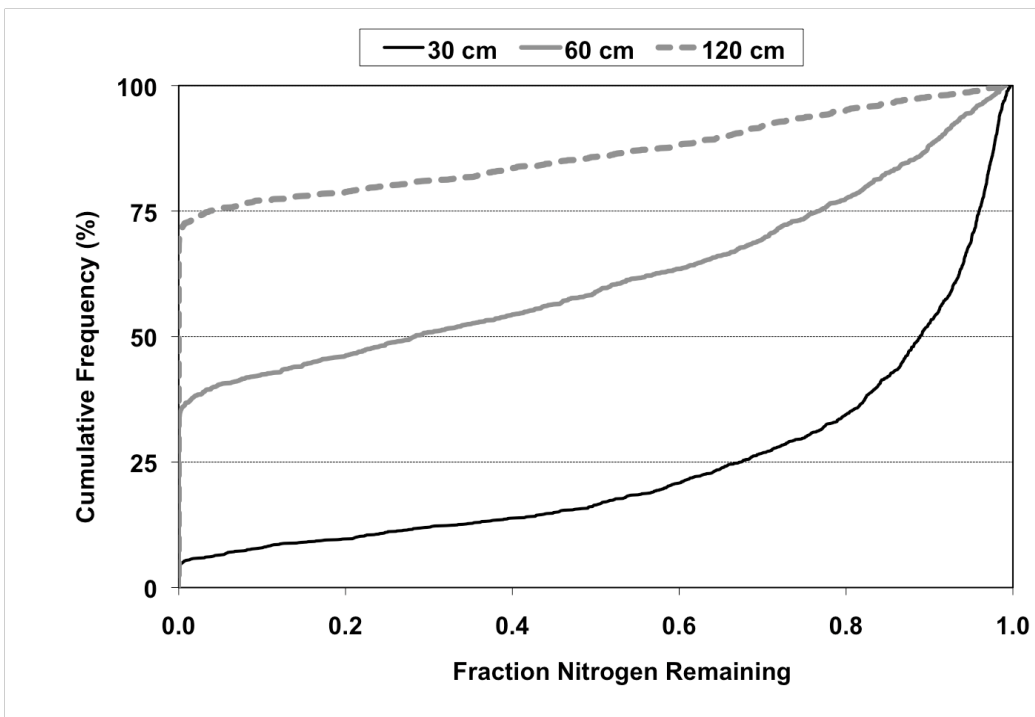


Figure VG-66. Cumulative Probability Graph: Clay Soil, Thermic Temperature Region, Standard Effluent, HLR = 5% of K_{sat} .

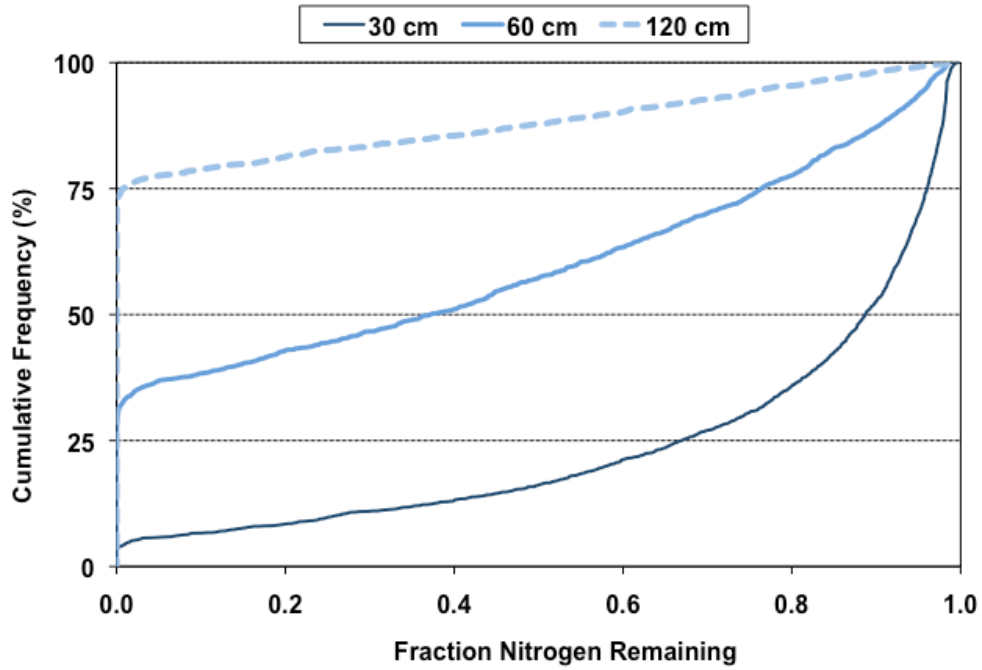


Figure VG-67. Cumulative Probability Graph: Clay Soil, Hyperthermic Temperature Region, Standard Effluent, HLR = 2 cm d⁻¹.

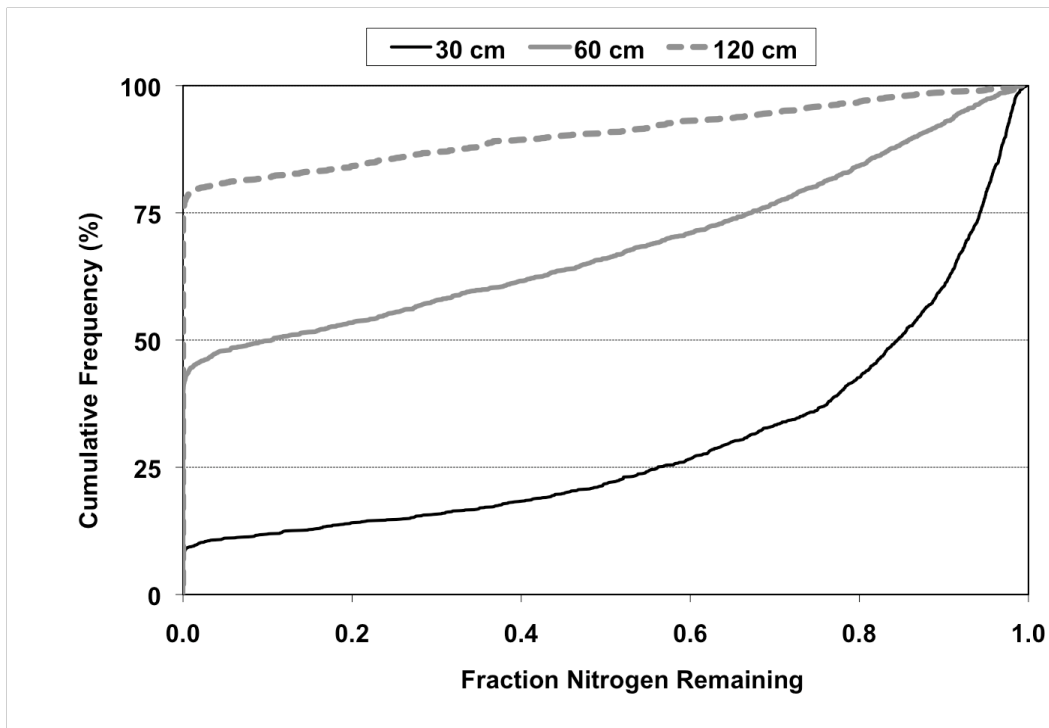


Figure VG-68. Cumulative Probability Graph: Clay Soil, Hyperthermic Temperature Region, Standard Effluent, HLR = 5% of K_{sat} .

2.1.2 Nitrified Effluent

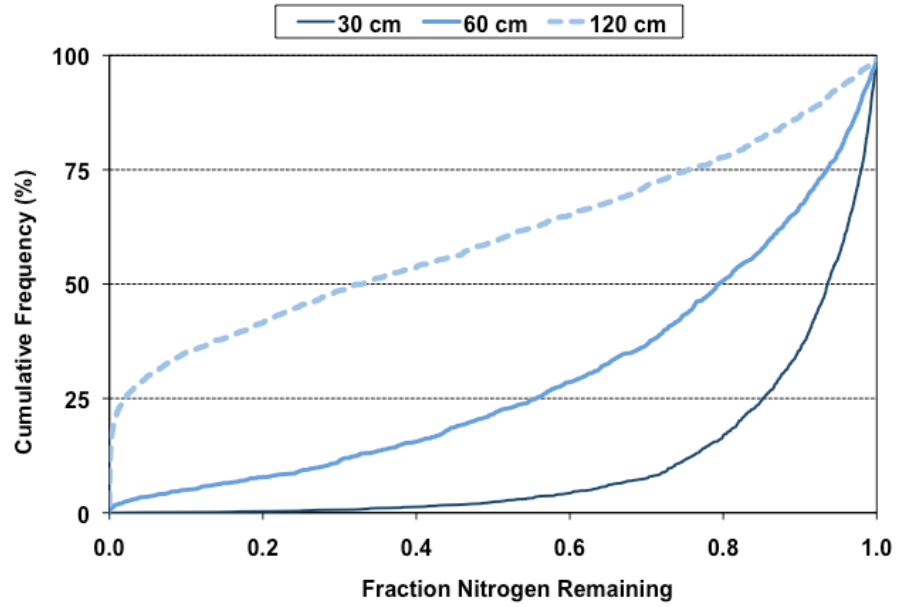


Figure VG-69. Cumulative Probability Graph: Clay Soil, Frigid/Cryic Temperature Region, Nitrified Effluent, HLR = 2 cm d⁻¹.

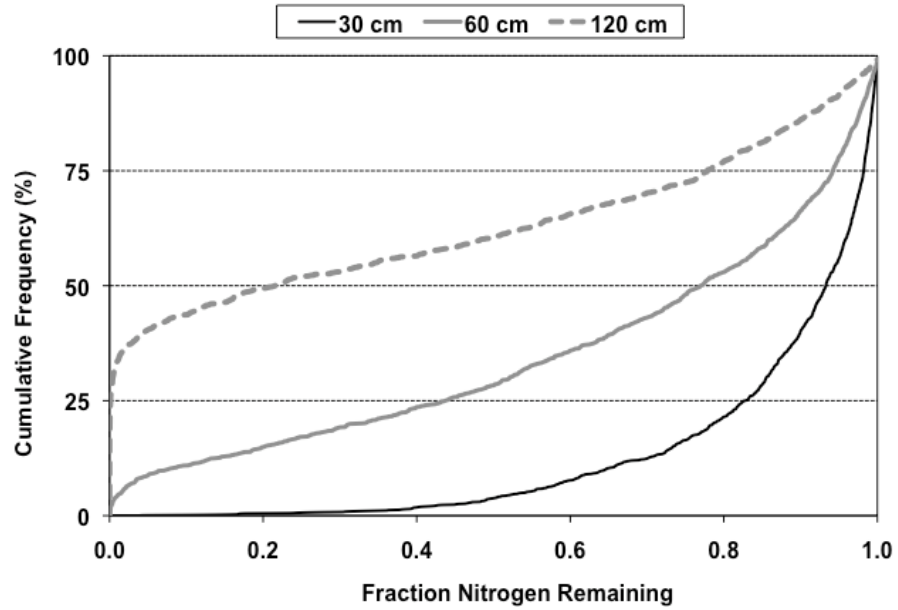


Figure VG-70. Cumulative Probability Graph: Clay Soil, Frigid/Cryic Temperature Region, Nitrified Effluent, HLR = 5% of K_{sat} .

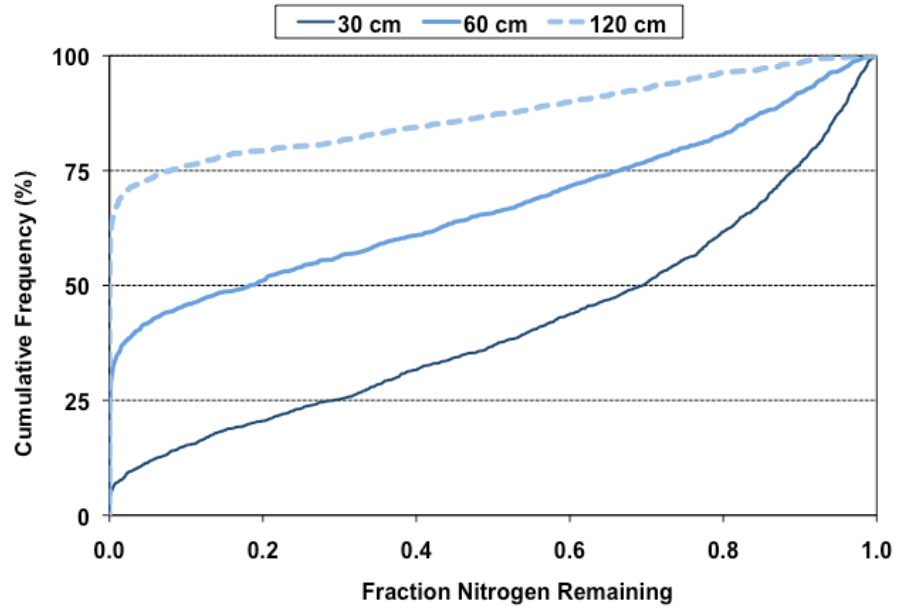


Figure VG-71. Cumulative Probability Graph: Clay Soil, Mesic Temperature Region, Nitrified Effluent, HLR = 2 cm d⁻¹.

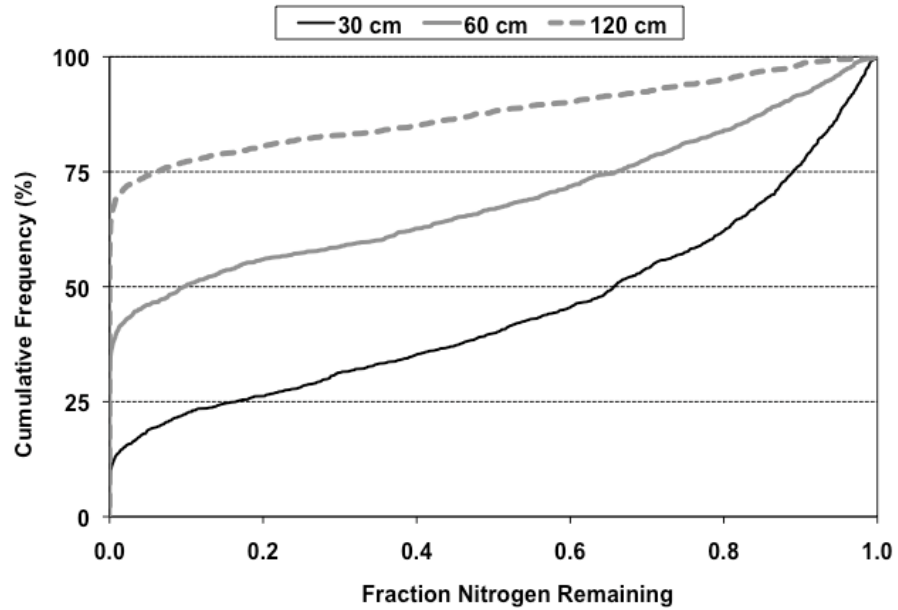


Figure VG-72. Cumulative Probability Graph: Clay Soil, Mesic Temperature Region, Nitrified Effluent, HLR = 5% of K_{sat}.

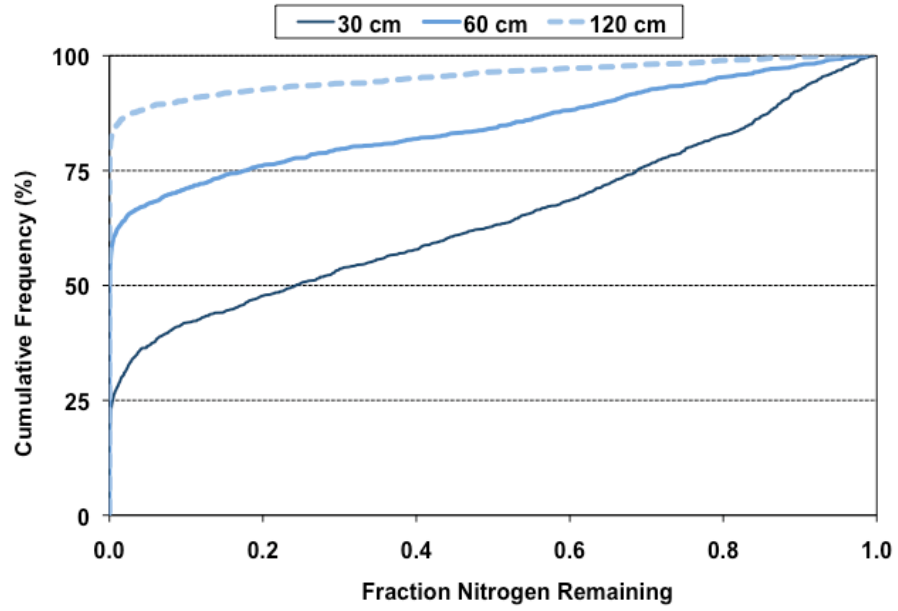


Figure VG-73. Cumulative Probability Graph: Clay Soil, Thermic Temperature Region, Nitrified Effluent, HLR = 2 cm d⁻¹.

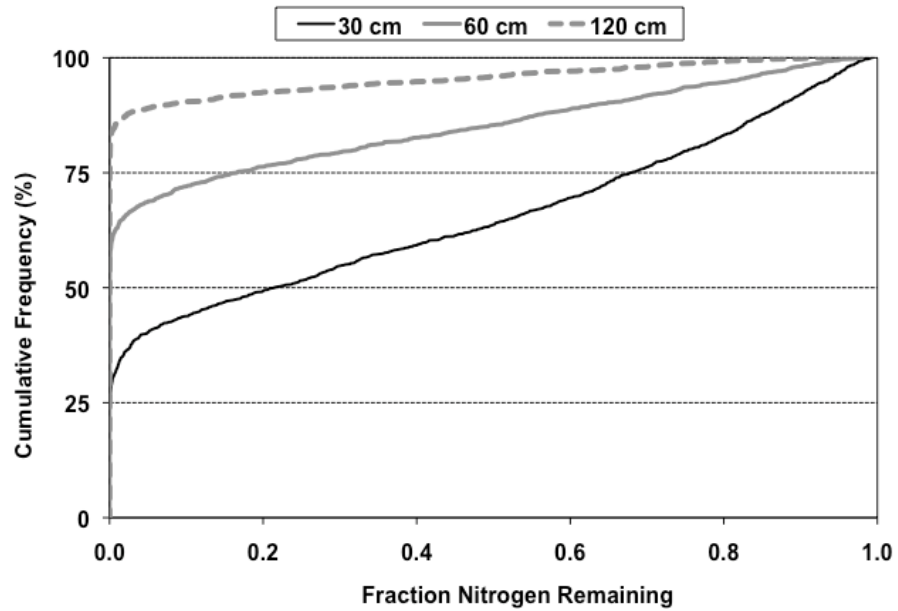


Figure VG-74. Cumulative Probability Graph: Clay Soil, Thermic Temperature Region, Nitrified Effluent, HLR = 5% of K_{sat} .

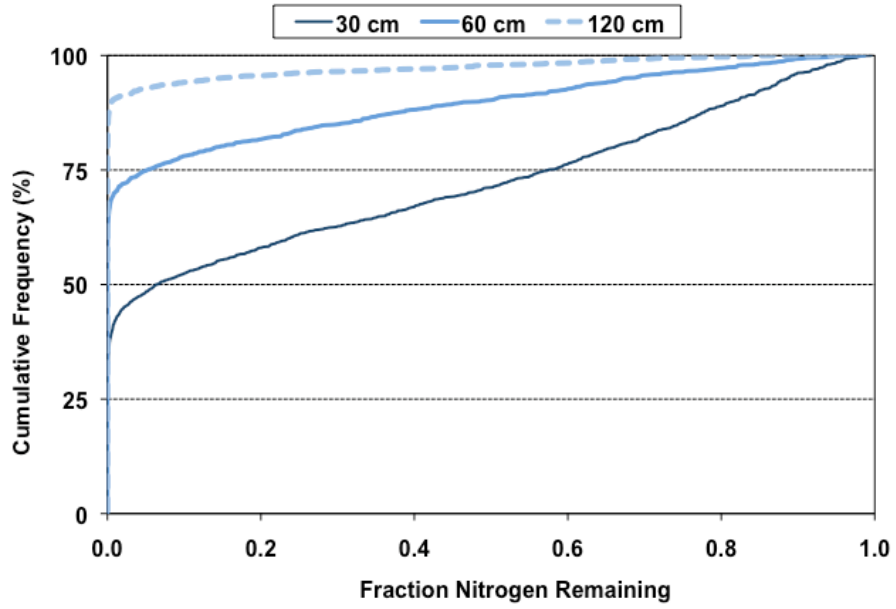


Figure VG-75. Cumulative Probability Graph: Clay Soil, Hyperthermic Temperature Region, Nitrified Effluent, HLR = 2 cm d⁻¹.

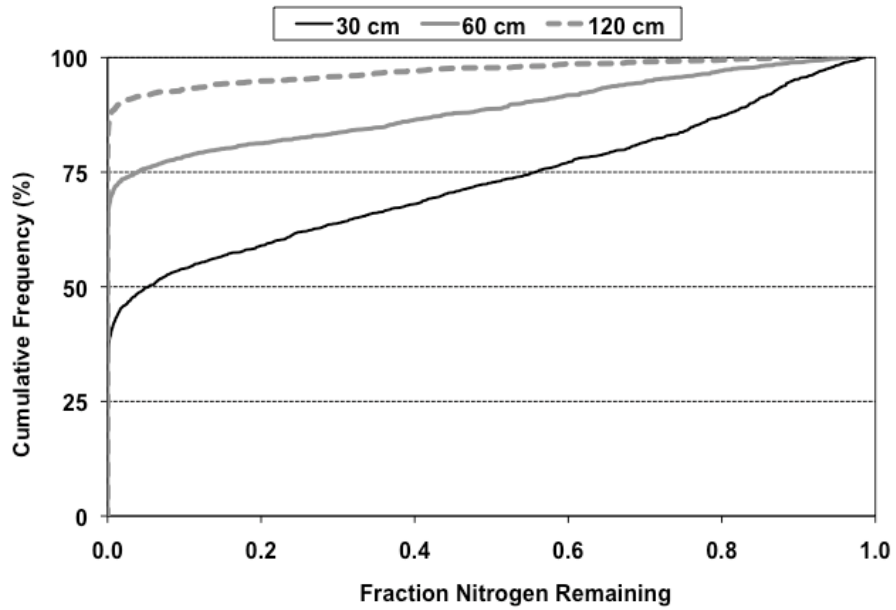


Figure VG-76. Cumulative Probability Graph: Clay Soil, Hyperthermic Temperature Region, Nitrified Effluent, HLR = 5% of K_{sat}.

2.2 Clay Loam

2.2.1 Standard Effluent

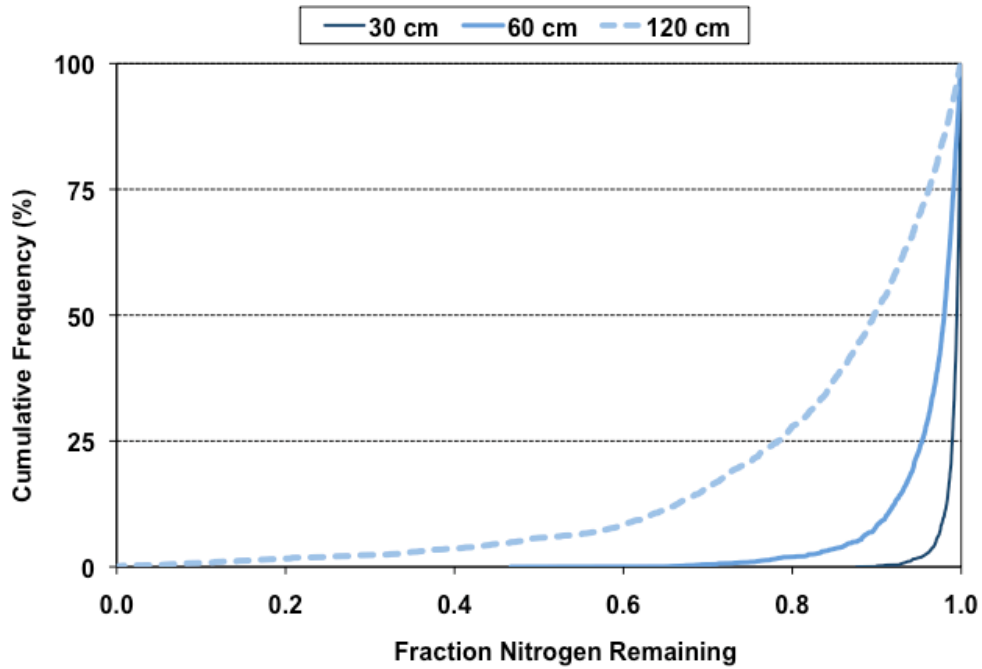


Figure VG-77. Cumulative Probability Graph: Clay Loam Soil, Frigid/Cryic Temperature Region, Standard Effluent, HLR = 2 cm d⁻¹.

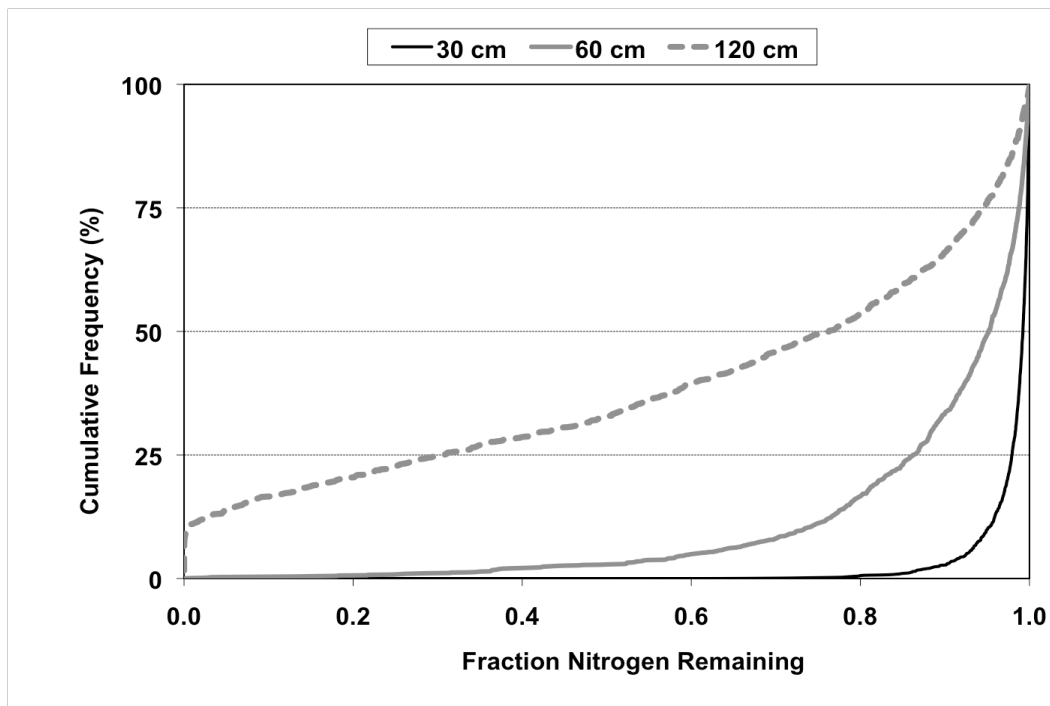


Figure VG-78. Cumulative Probability Graph: Clay Loam Soil, Frigid/Cryic Temperature Region, Standard Effluent, HLR = 5% of K_{sat}.

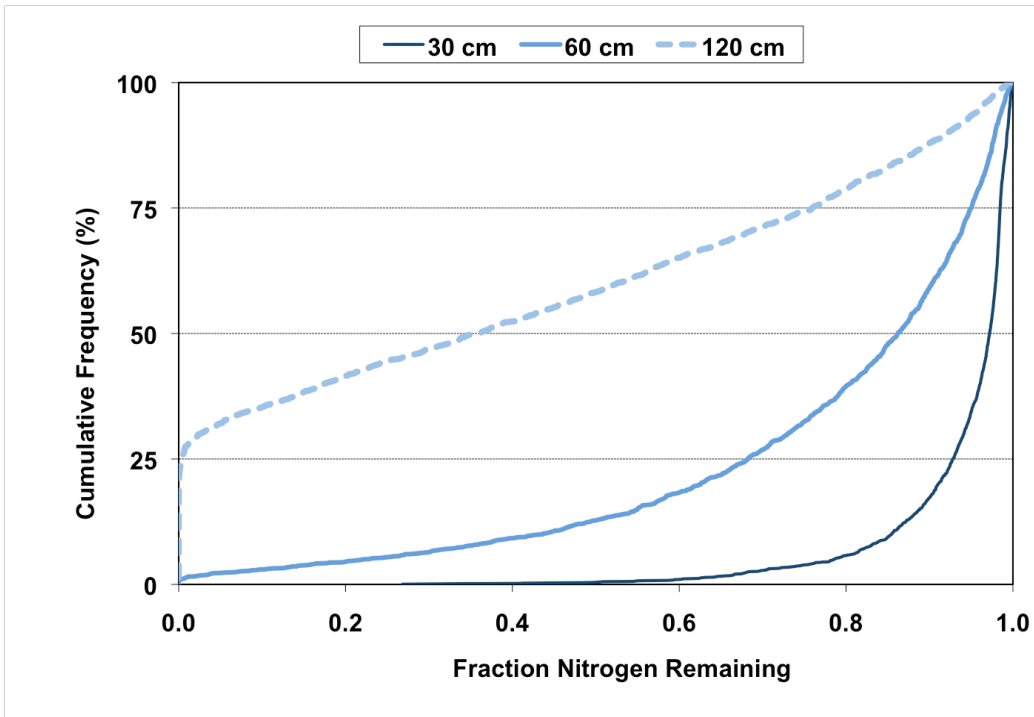


Figure VG-79. Cumulative Probability Graph: Clay Loam Soil, Mesic Temperature Region, Standard Effluent, HLR = 2 cm d⁻¹.

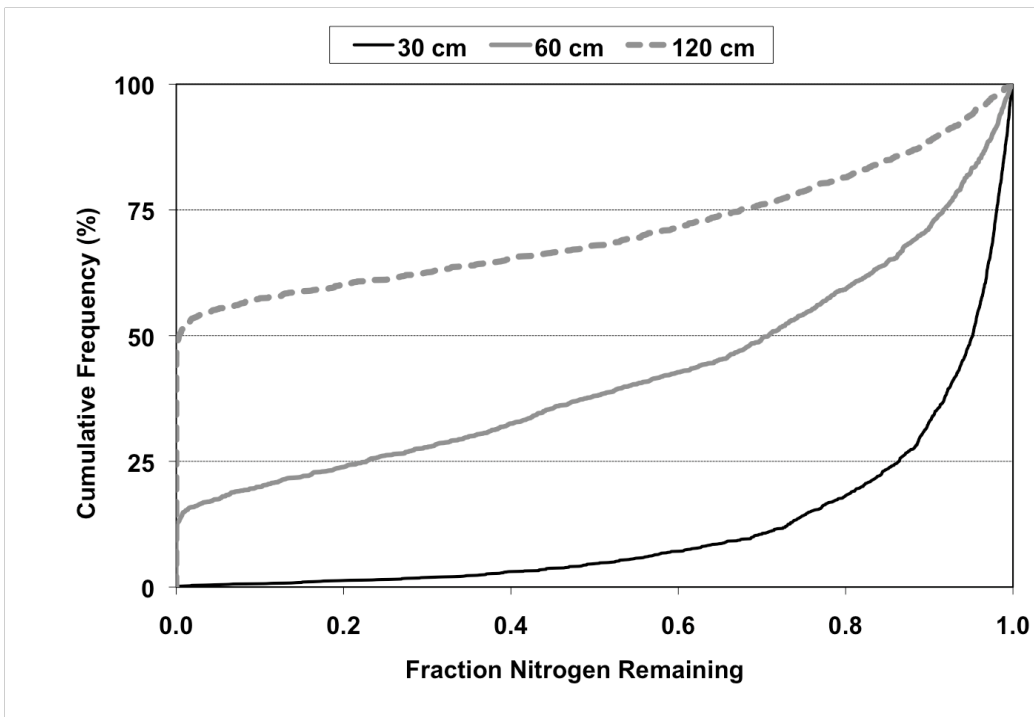


Figure VG-80. Cumulative Probability Graph: Clay Loam Soil, Mesic Temperature Region, Standard Effluent, HLR = 5% of K_{sat}.

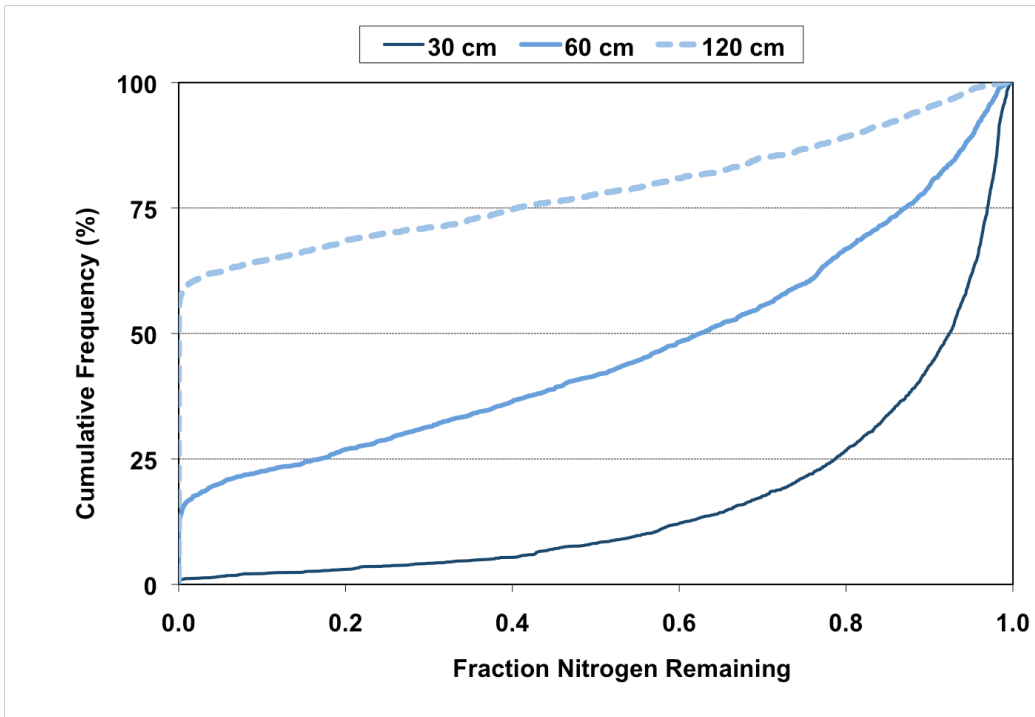


Figure VG-81. Cumulative Probability Graph: Clay Loam Soil, Thermic Temperature Region, Standard Effluent, HLR = 2 cm d⁻¹.

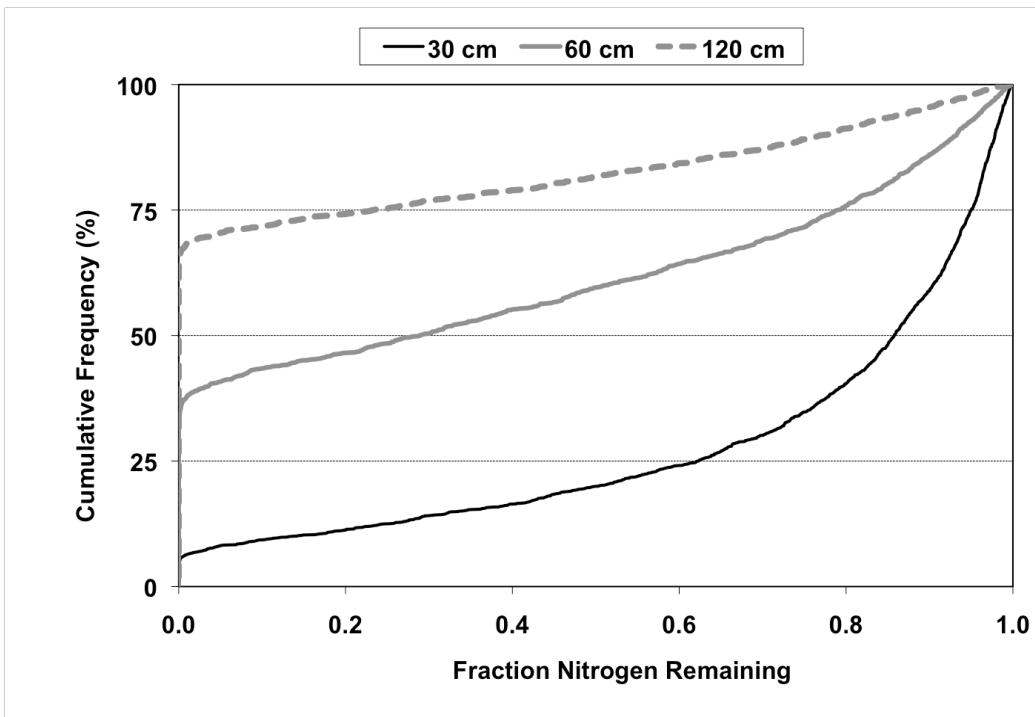


Figure VG-82. Cumulative Probability Graph: Clay Loam Soil, Thermic Temperature Region, Standard Effluent, HLR = 5% of K_{sat}.

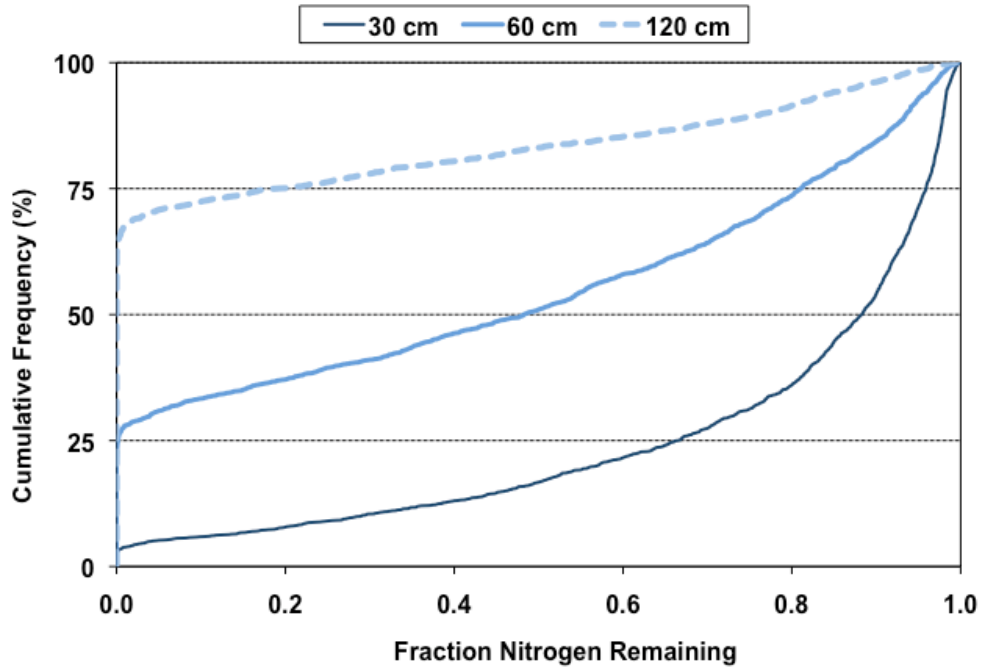


Figure VG-83. Cumulative Probability Graph: Clay Loam Soil, Hyperthermic Temperature Region, Standard Effluent, HLR = 2 cm d⁻¹.

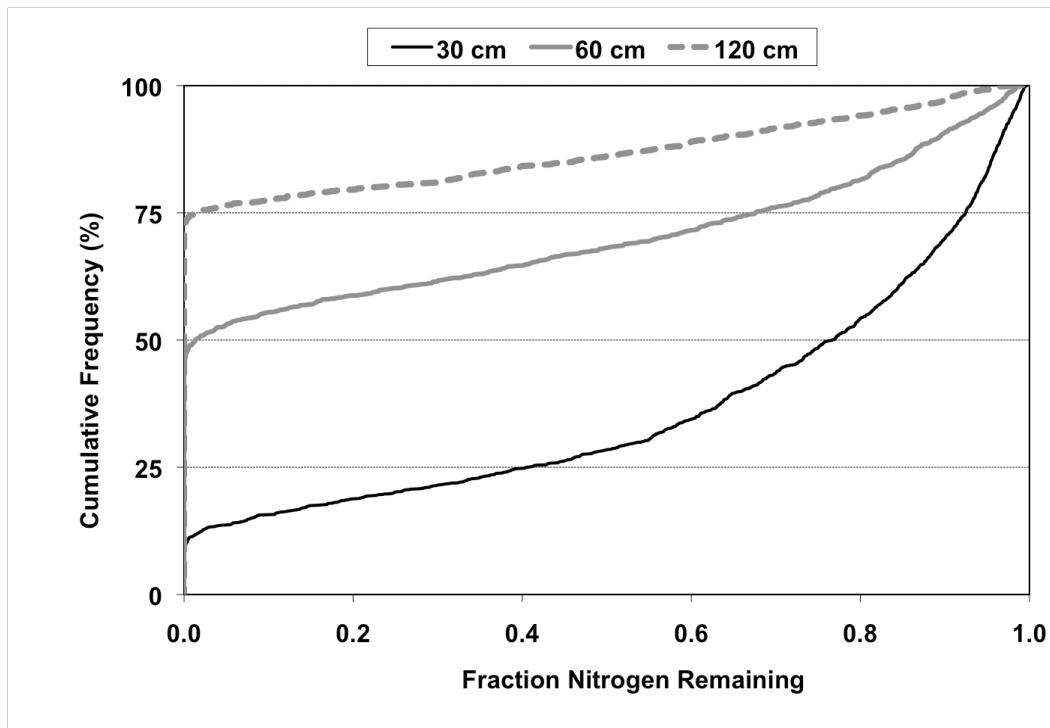


Figure VG-84. Cumulative Probability Graph: Clay Loam Soil, Hyperthermic Temperature Region, Standard Effluent, HLR = 5% of K_{sat} .

2.2.2 Nitrified Effluent

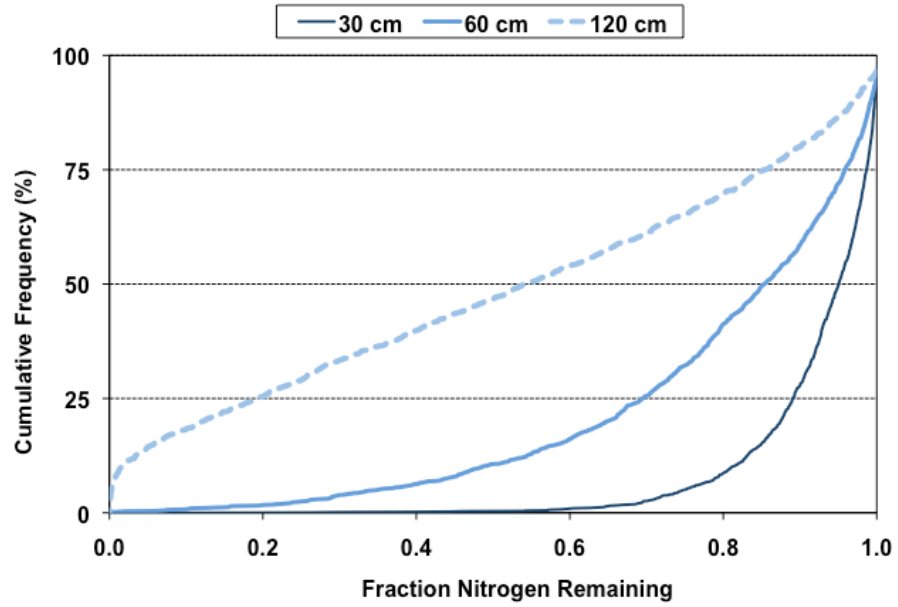


Figure VG-85. Cumulative Probability Graph: Clay Loam Soil, Frigid/Cryic Temperature Region, Nitrified Effluent, HLR = 2 cm d⁻¹.

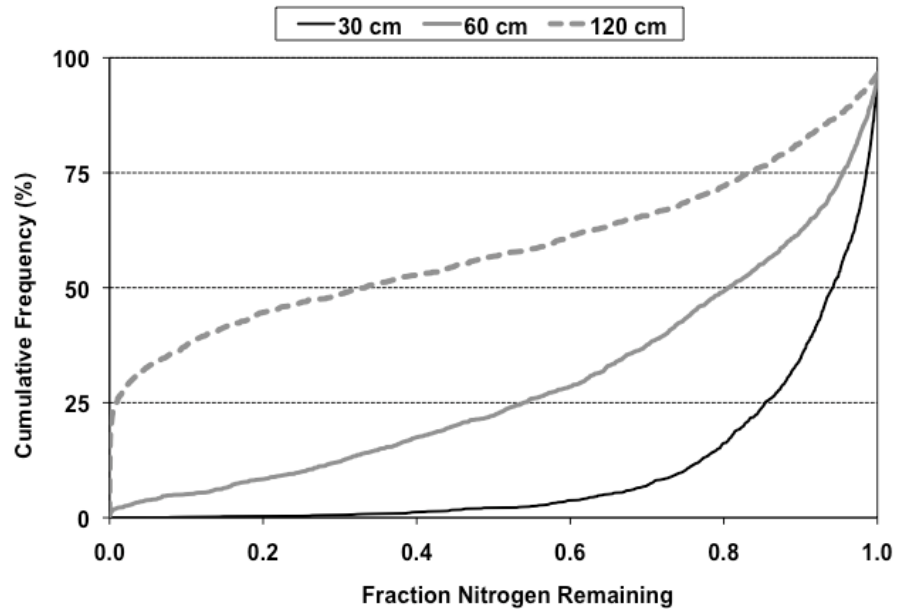


Figure VG-86. Cumulative Probability Graph: Clay Loam Soil, Frigid/Cryic Temperature Region, Nitrified Effluent, HLR = 5% of K_{sat}.

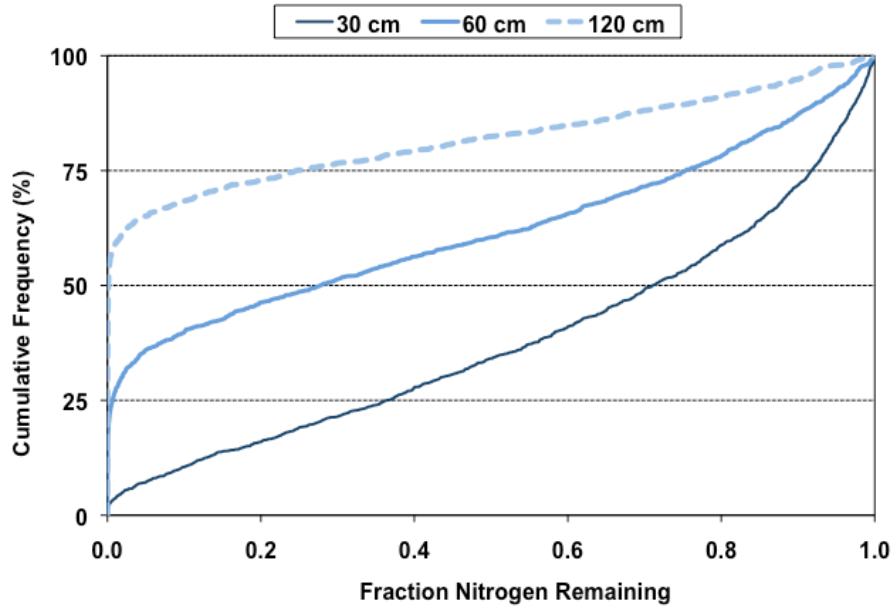


Figure VG-87. Cumulative Probability Graph: Clay Loam Soil, Mesic Temperature Region, Nitrified Effluent, HLR = 2 cm d⁻¹.

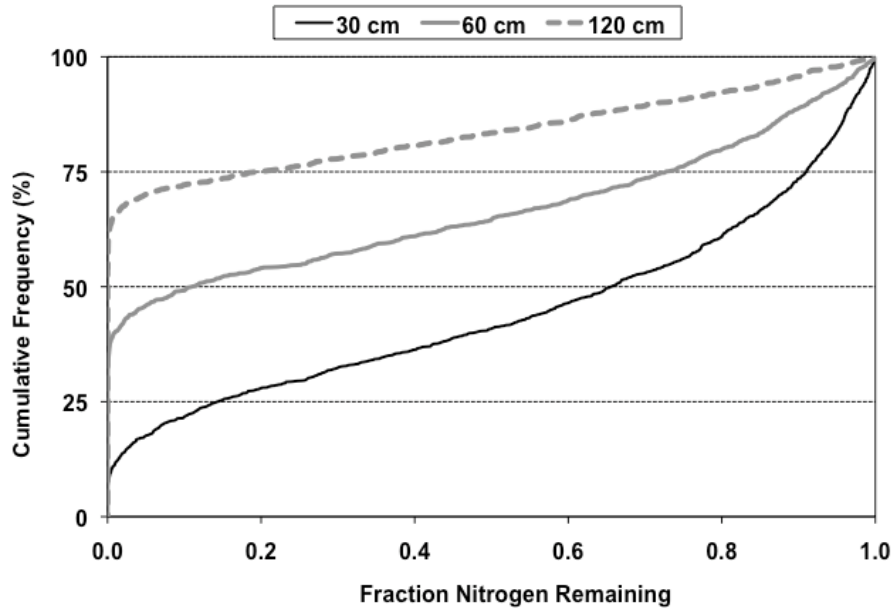


Figure VG-88. Cumulative Probability Graph: Clay Loam Soil, Mesic Temperature Region, Nitrified Effluent, HLR = 5% of K_{sat}.

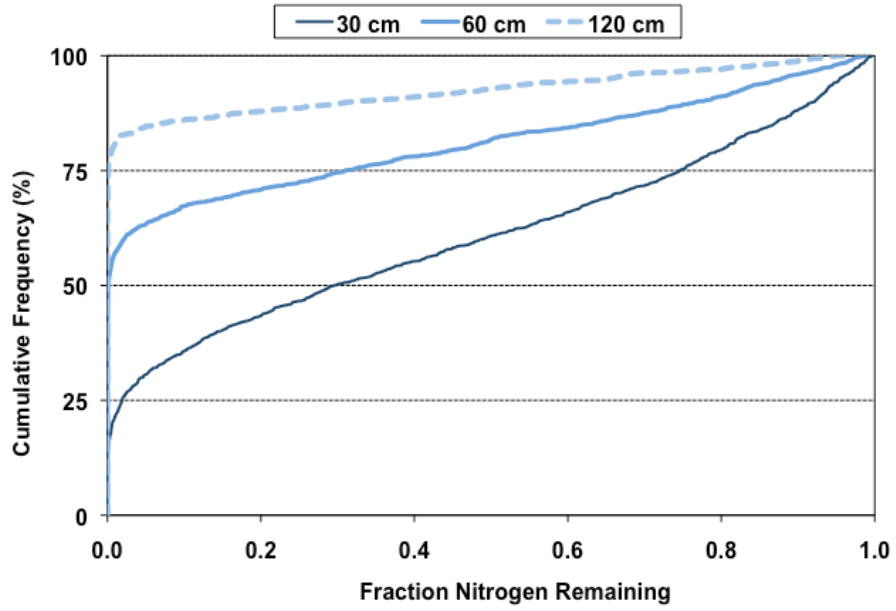


Figure VG-89. Cumulative Probability Graph: Clay Loam Soil, Thermic Temperature Region, Nitrified Effluent, HLR = 2 cm d⁻¹.

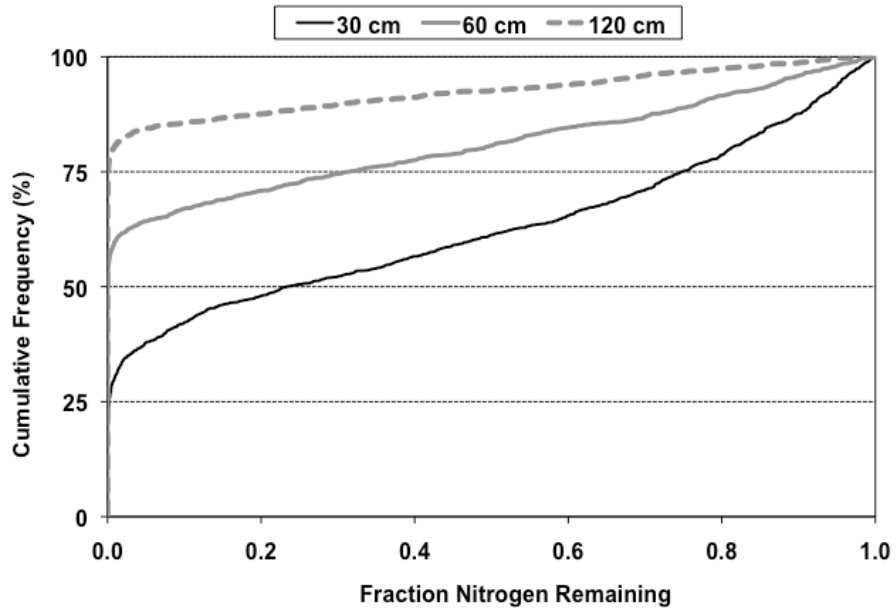


Figure VG-90. Cumulative Probability Graph: Clay Loam Soil, Thermic Temperature Region, Nitrified Effluent, HLR = 5% of K_{sat} .

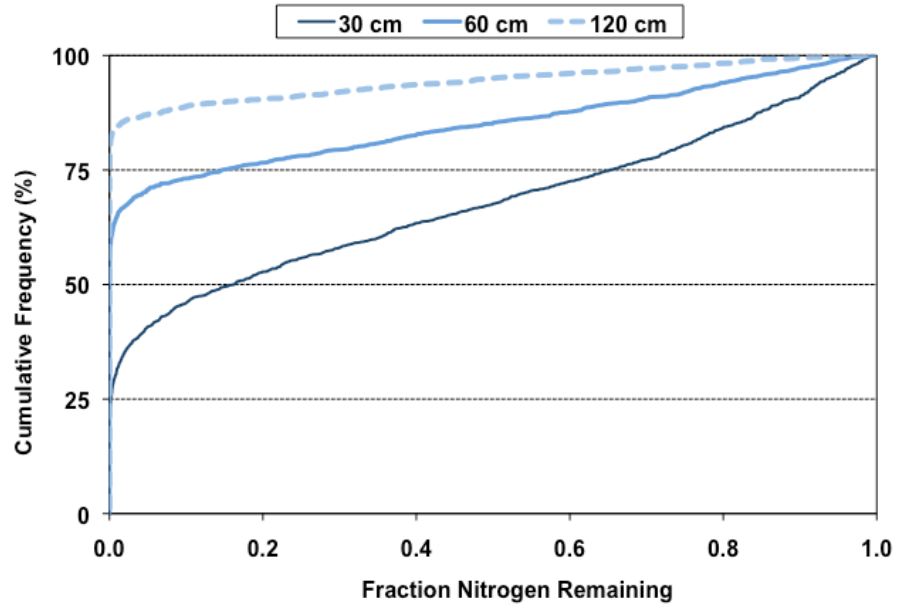


Figure VG-91. Cumulative Probability Graph: Clay Loam Soil, Hyperthermic Temperature Region, Nitrified Effluent, HLR = 2 cm d⁻¹.

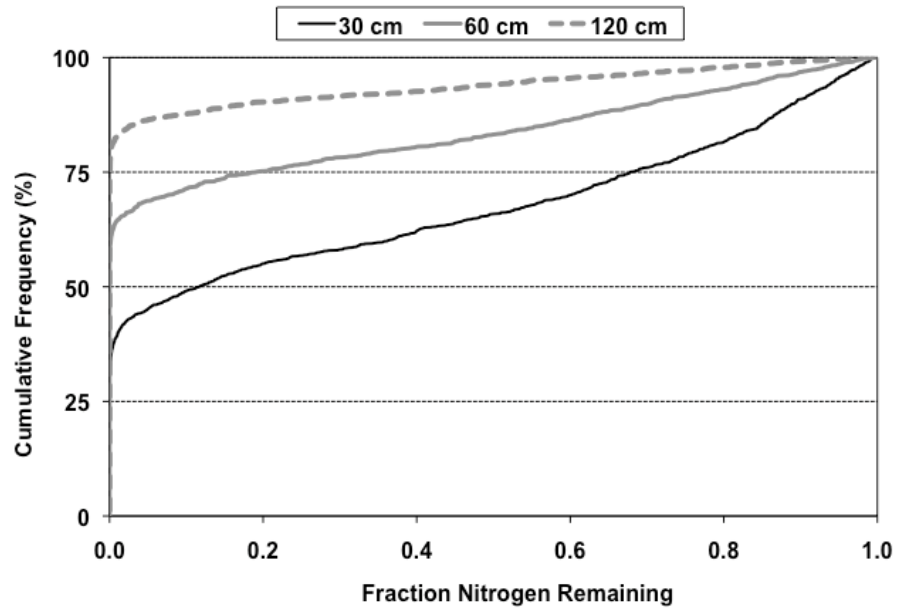


Figure VG-92. Cumulative Probability Graph: Clay Loam Soil, Hyperthermic Temperature Region, Nitrified Effluent, HLR = 5% of K_{sat} .

2.3 Loam

2.3.1 Standard Effluent

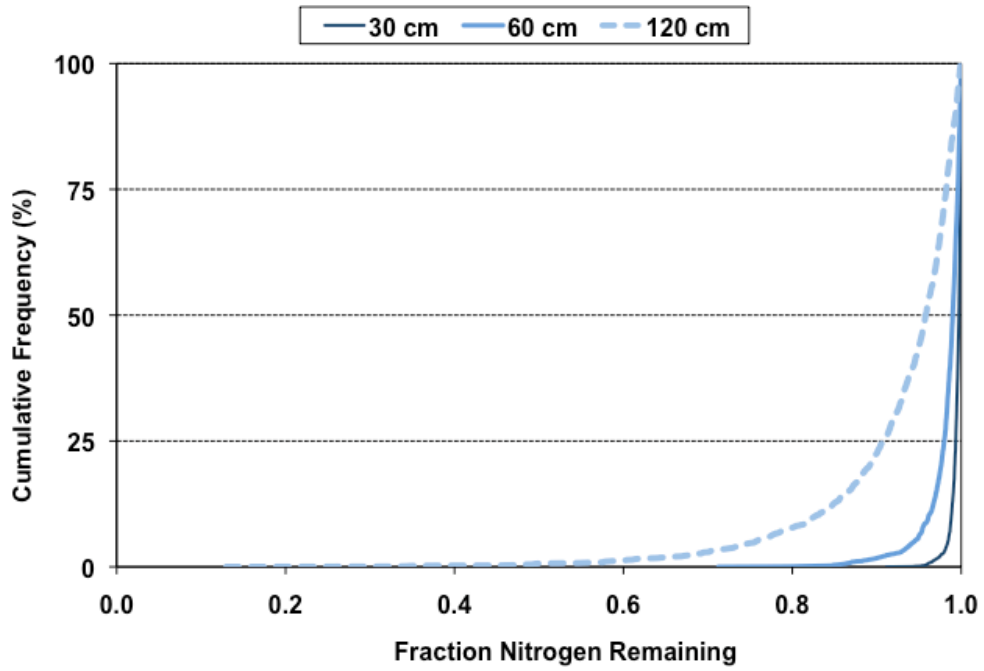


Figure VG-93. Cumulative Probability Graph: Loam Soil, Frigid/Cryic Temperature Region, Standard Effluent, HLR = 2 cm d⁻¹.

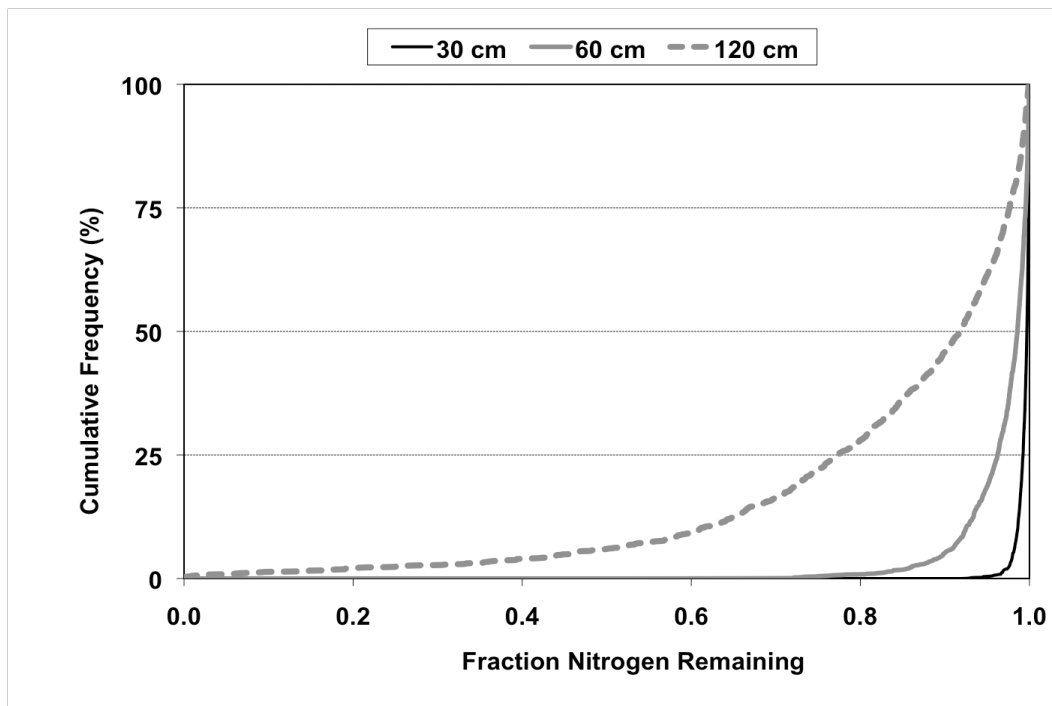


Figure VG-94. Cumulative Probability Graph: Loam Soil, Frigid/Cryic Temperature Region, Standard Effluent, HLR = 5% of K_{sat}.

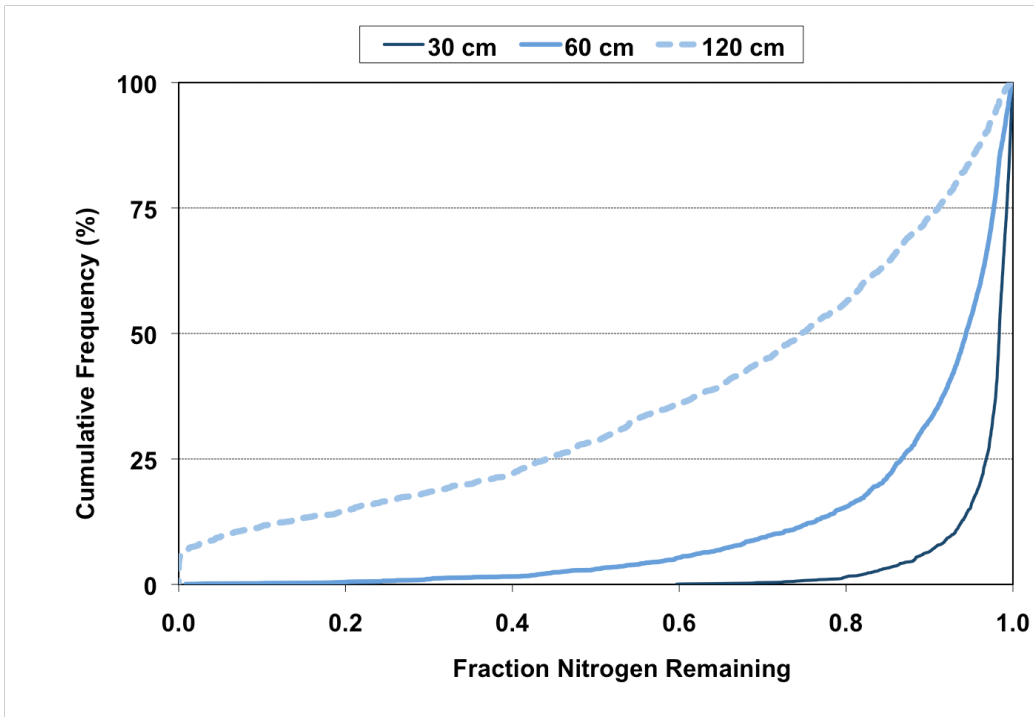


Figure VG-95. Cumulative Probability Graph: Loam Soil, Mesic Temperature Region, Standard Effluent, HLR = 2 cm d⁻¹.

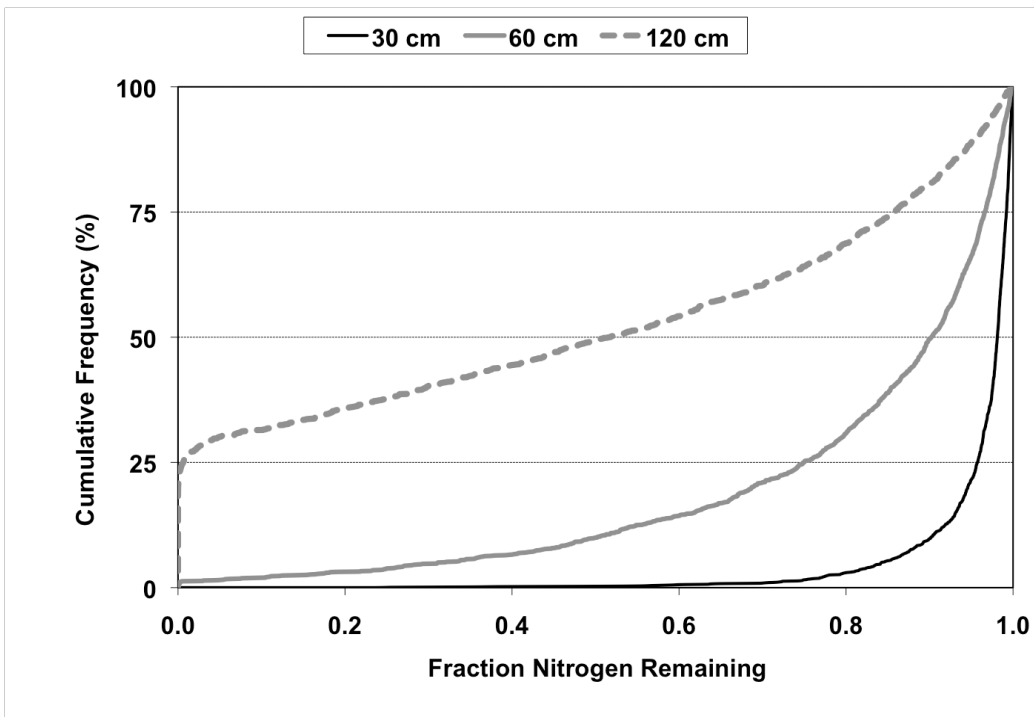


Figure VG-96. Cumulative Probability Graph: Loam Soil, Mesic Temperature Region, Standard Effluent, HLR = 5% of K_{sat} .

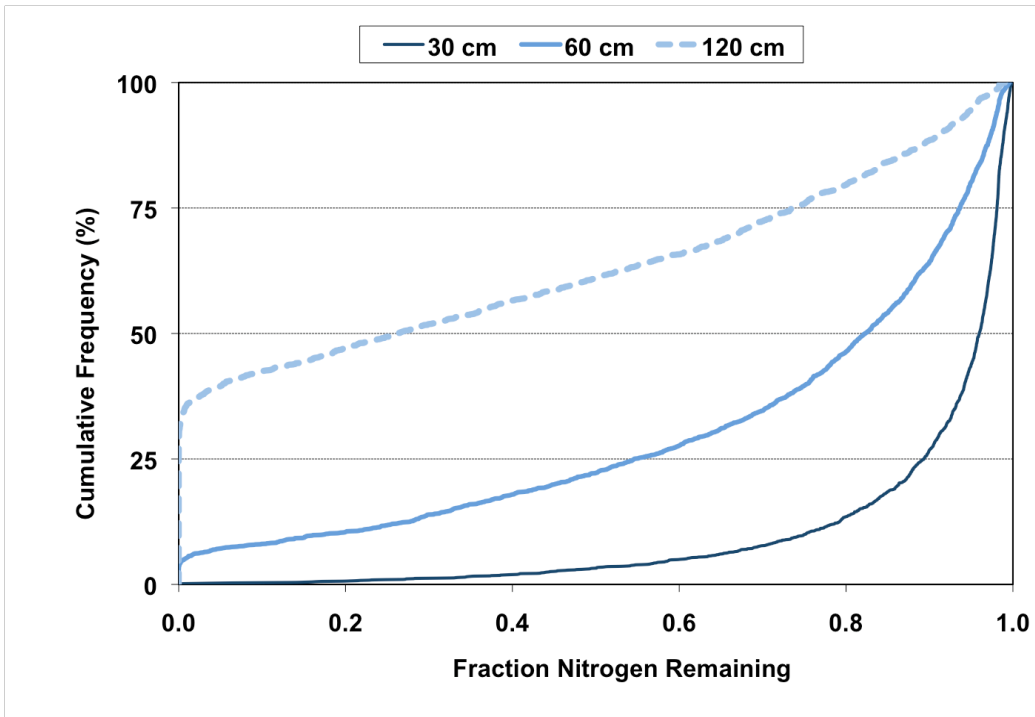


Figure VG-97. Cumulative Probability Graph: Loam Soil, Thermic Temperature Region, Standard Effluent, HLR = 2 cm d⁻¹.

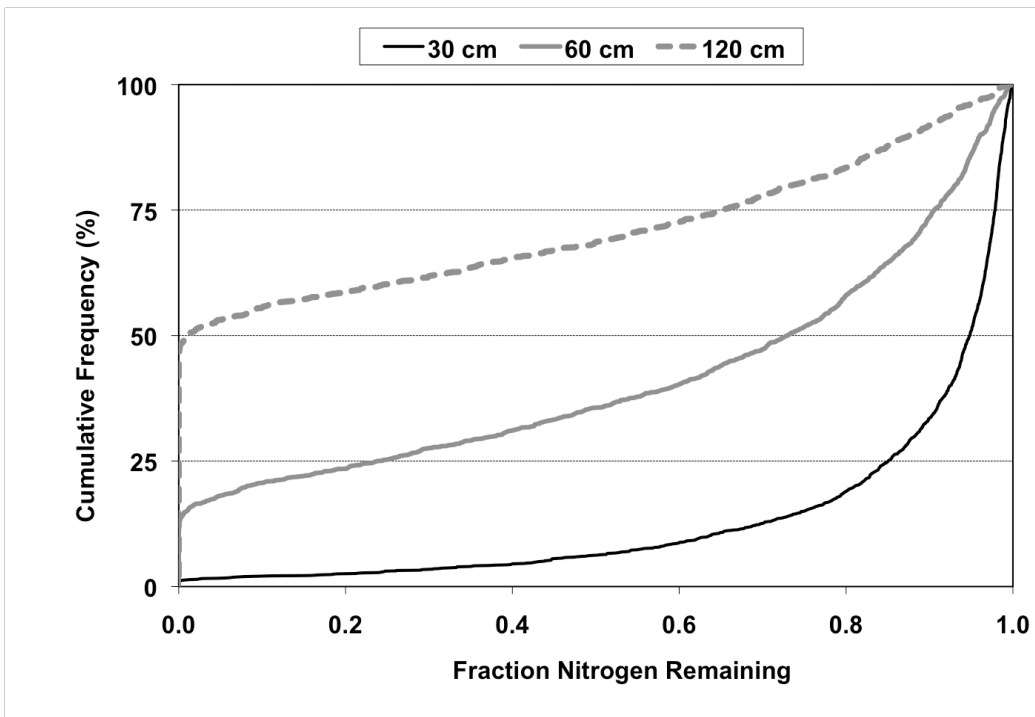


Figure VG-98. Cumulative Probability Graph: Loam Soil, Thermic Temperature Region, Standard Effluent, HLR = 5% of K_{sat}.

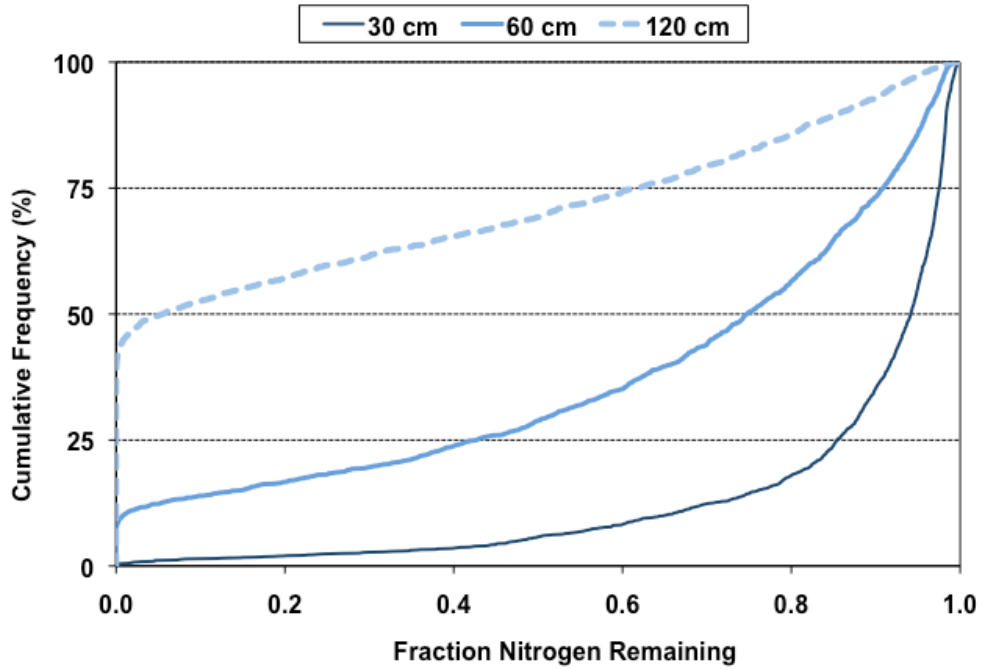


Figure VG-99. Cumulative Probability Graph: Loam Soil, Hyperthermic Temperature Region, Standard Effluent, HLR = 2 cm d⁻¹.

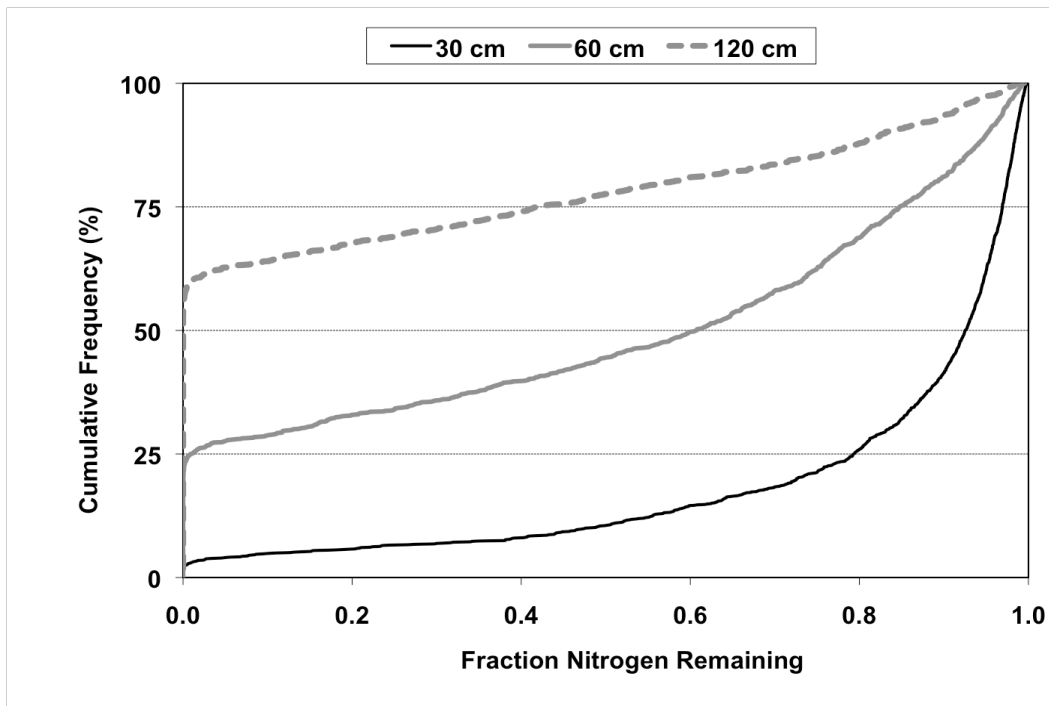


Figure VG-100. Cumulative Probability Graph: Loam Soil, Hyperthermic Temperature Region, Standard Effluent, HLR = 5% of K_{sat}.

2.3.2 Nitrified Effluent

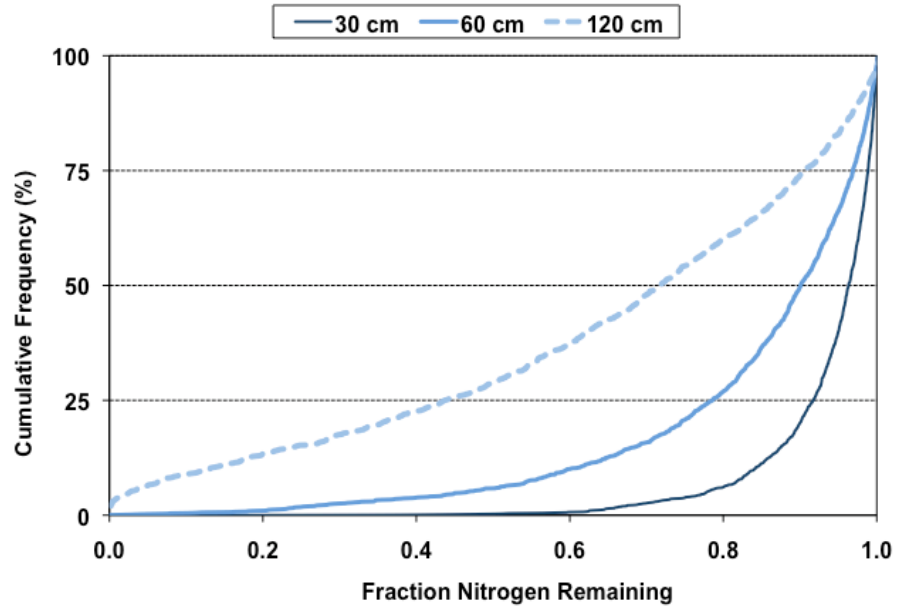


Figure VG-101. Cumulative Probability Graph: Loam Soil, Frigid/Cryic Temperature Region, Nitrified Effluent, HLR = 2 cm d⁻¹.

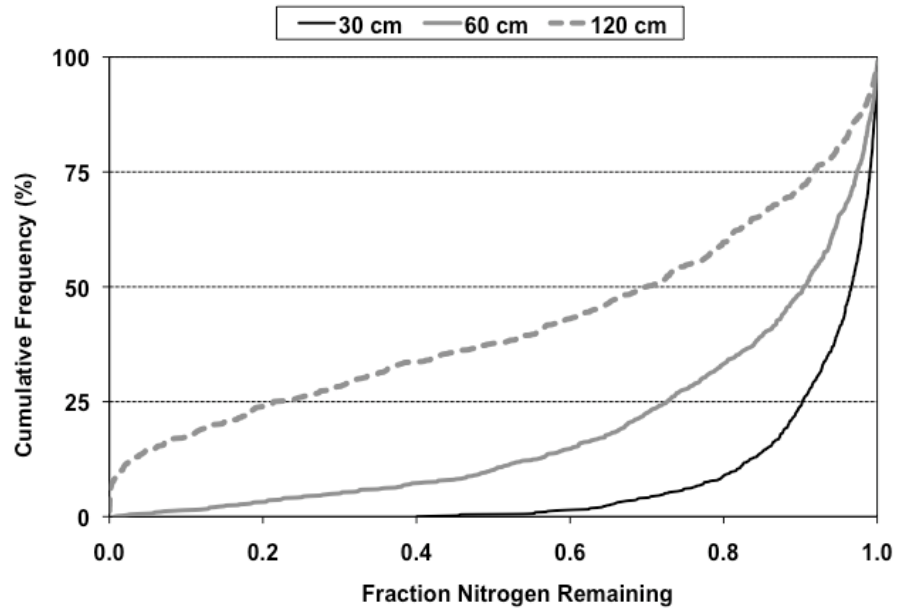


Figure VG-102. Cumulative Probability Graph: Loam Soil, Frigid/Cryic Temperature Region, Nitrified Effluent, HLR = 5% of K_{sat}.

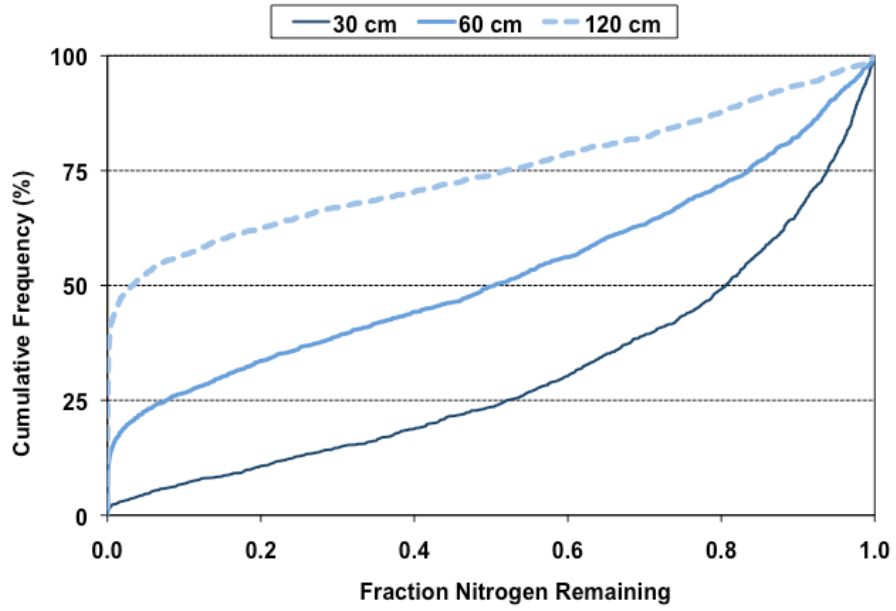


Figure VG-103. Cumulative Probability Graph: Loam Soil, Mesic Temperature Region, Nitrified Effluent, HLR = 2 cm d⁻¹.

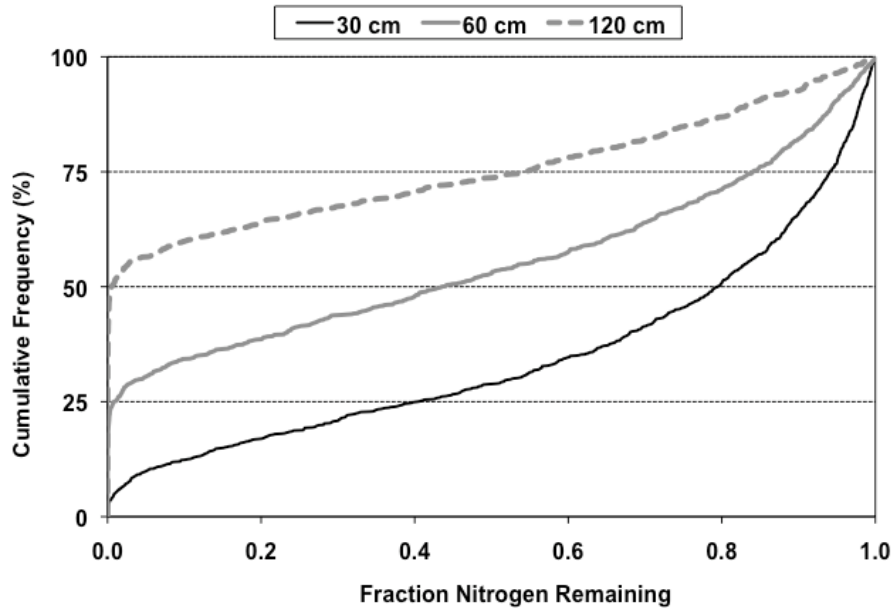


Figure VG-104. Cumulative Probability Graph: Loam Soil, Mesic Temperature Region, Nitrified Effluent, HLR = 5% of K_{sat} .

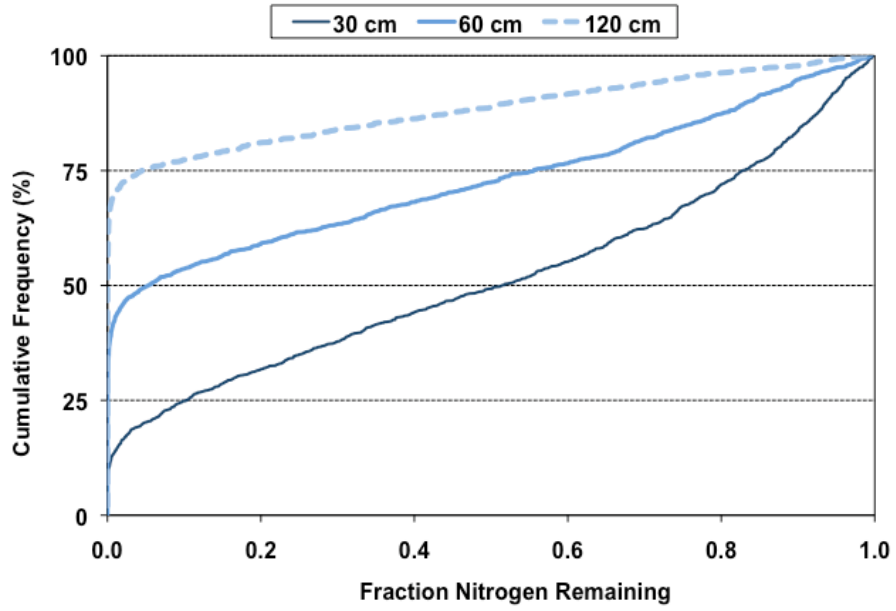


Figure VG-105. Cumulative Probability Graph: Loam Soil, Thermic Temperature Region, Nitrified Effluent, HLR = 2 cm d⁻¹.

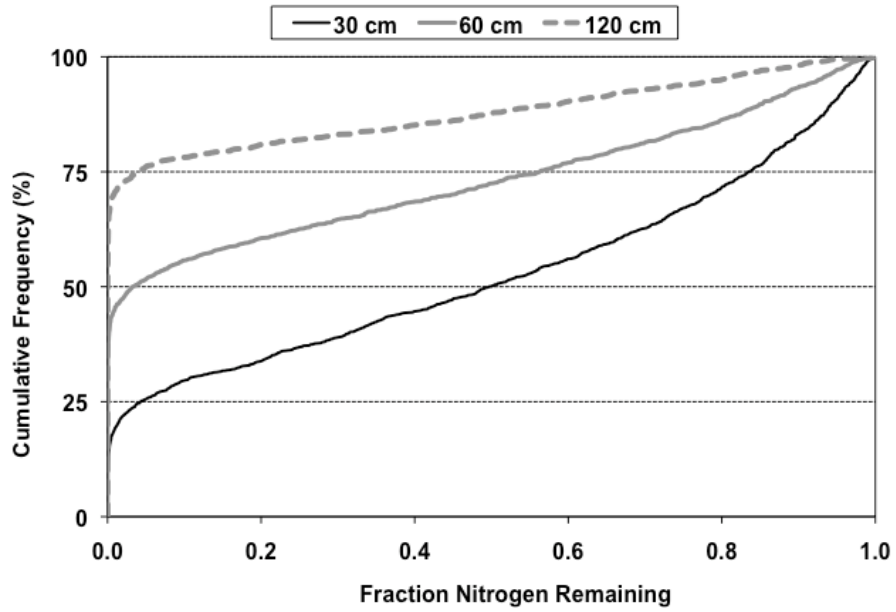


Figure VG-106. Cumulative Probability Graph: Loam Soil, Thermic Temperature Region, Nitrified Effluent, HLR = 5% of K_{sat} .

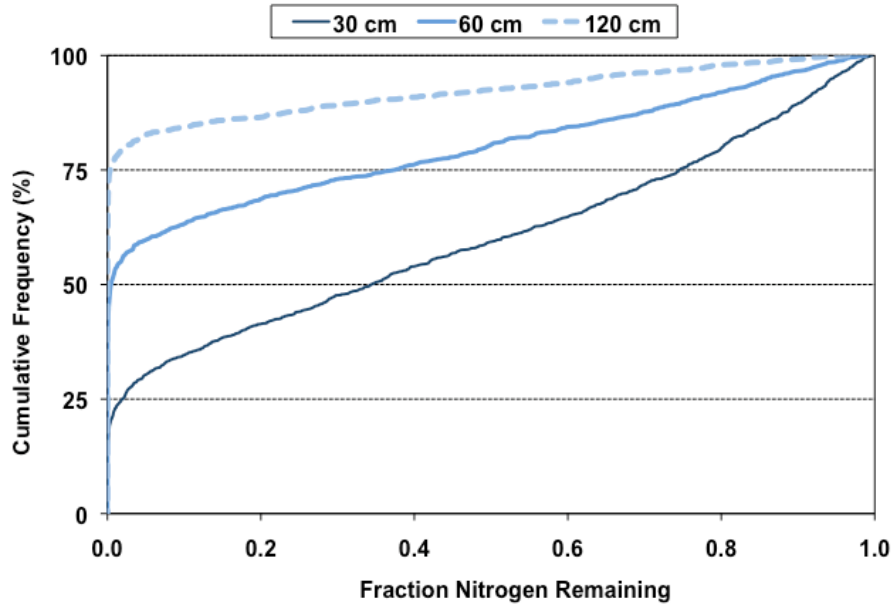


Figure VG-107. Cumulative Probability Graph: Loam Soil, Hyperthermic Temperature Region, Nitrified Effluent, HLR = 2 cm d⁻¹.

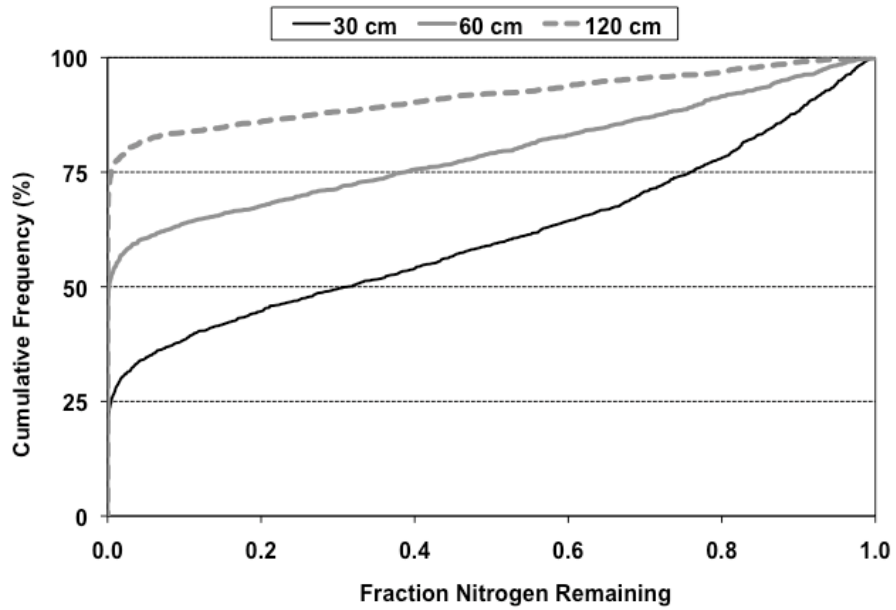


Figure VG-108. Cumulative Probability Graph: Loam Soil, Hyperthermic Temperature Region, Nitrified Effluent, HLR = 5% of K_{sat} .

2.4 Loamy Sand

2.4.1 Standard Effluent

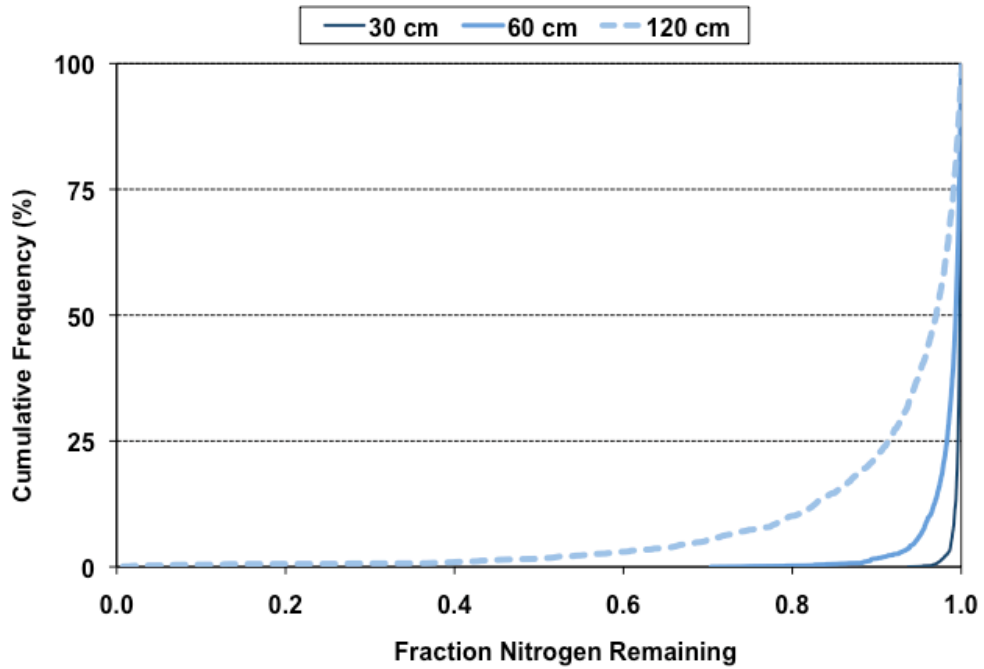


Figure VG-109. Cumulative Probability Graph: Loamy Sand Soil, Frigid/Cryic Temperature Region, Standard Effluent, HLR = 2 cm d⁻¹.

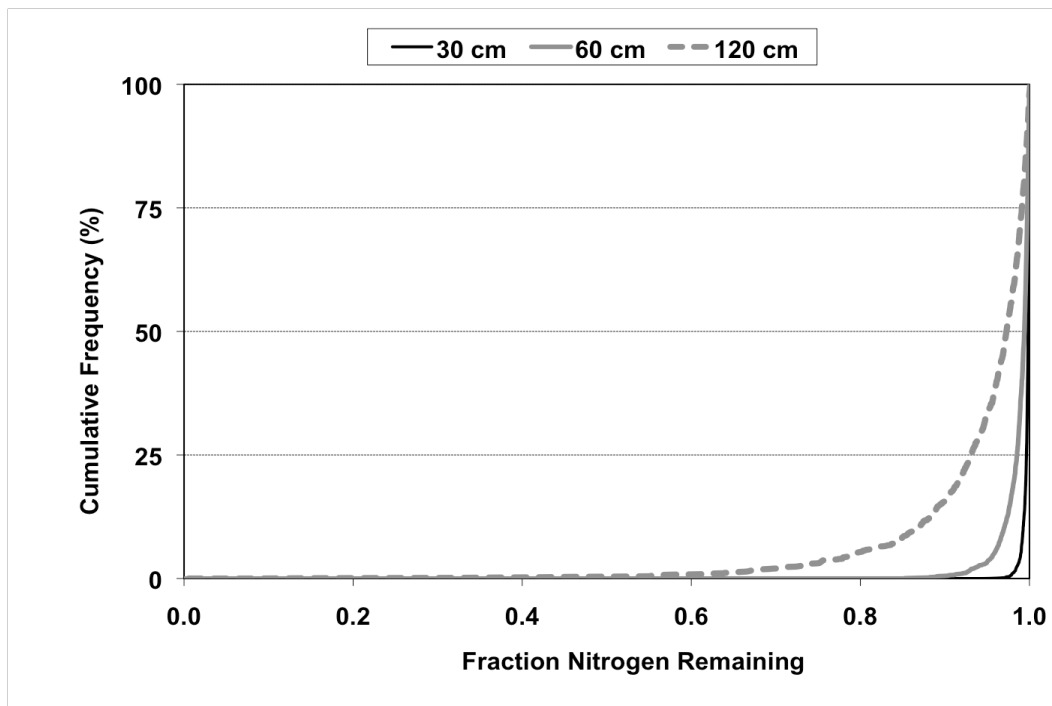


Figure VG-110. Cumulative Probability Graph: Loamy Sand Soil, Frigid/Cryic Temperature Region, Standard Effluent, HLR = 5% of K_{sat}.

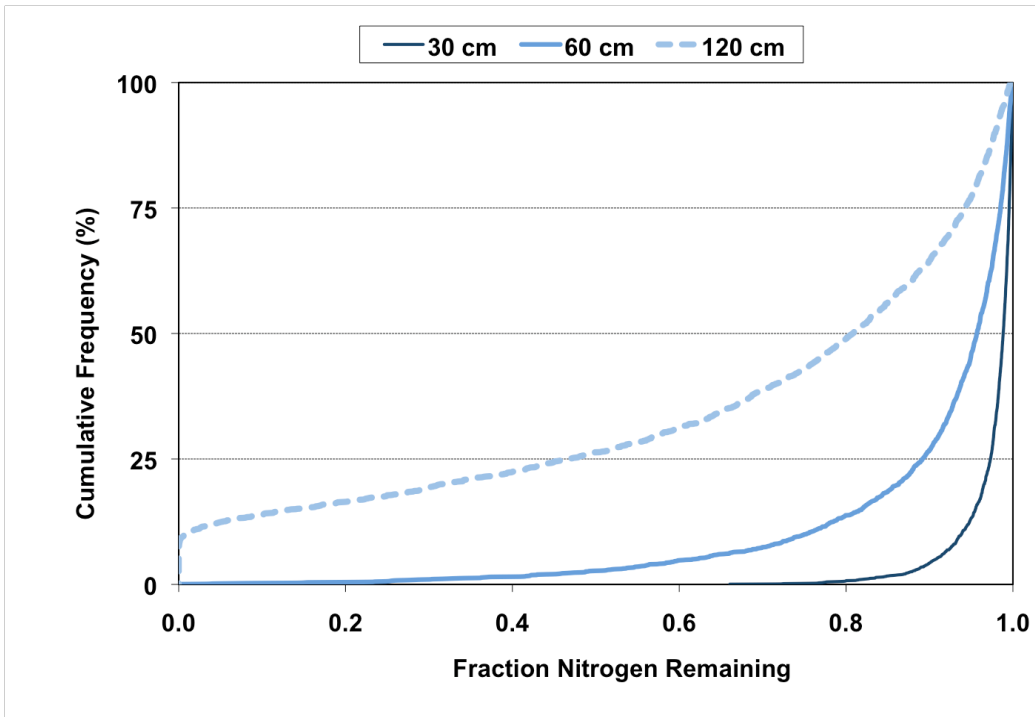


Figure VG-111. Cumulative Probability Graph: Loamy Sand Soil, Mesic Temperature Region, Standard Effluent, HLR = 2 cm d⁻¹.

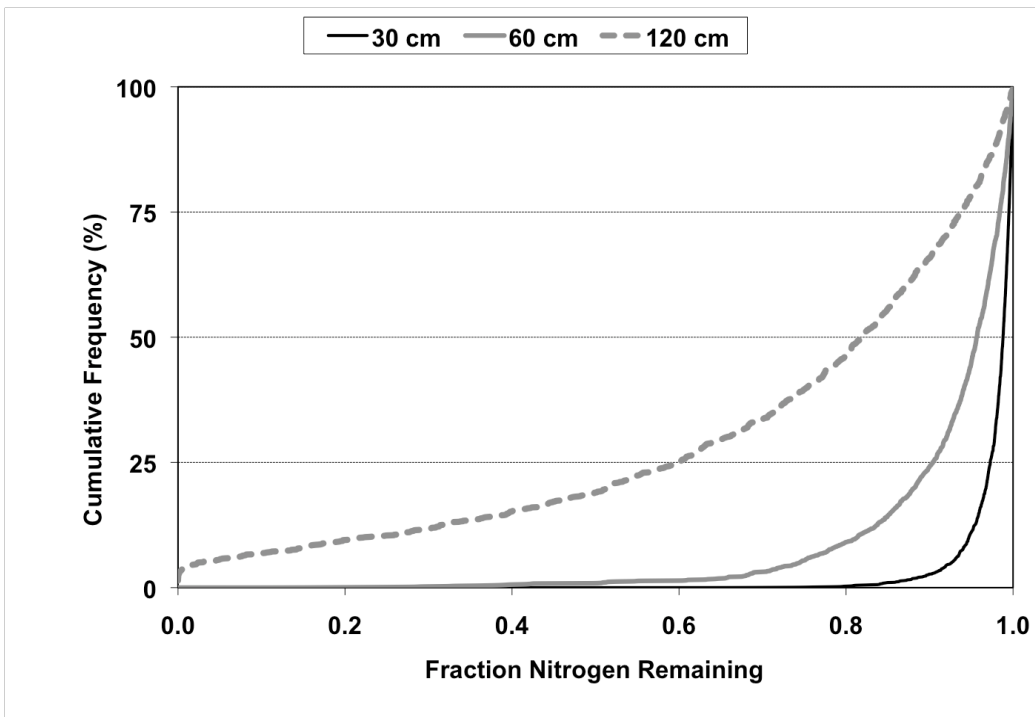


Figure VG-112. Cumulative Probability Graph: Loamy Sand Soil, Mesic Temperature Region, Standard Effluent, HLR = 5% of K_{sat} .

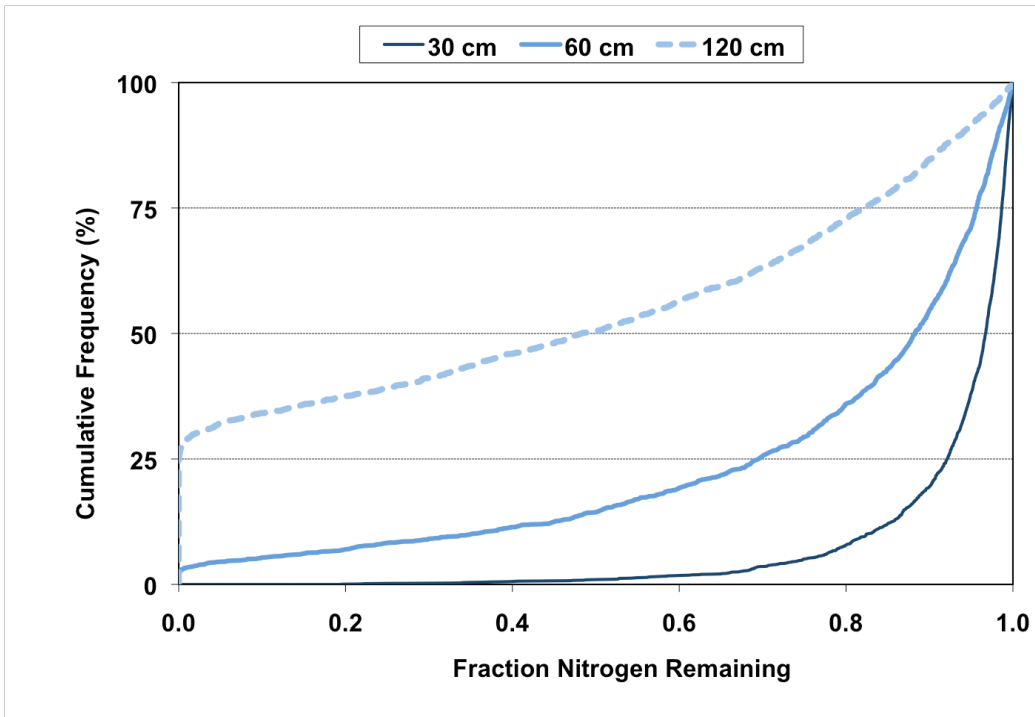


Figure VG-113. Cumulative Probability Graph: Loamy Sand Soil, Thermic Temperature Region, Standard Effluent, HLR = 2 cm d⁻¹.

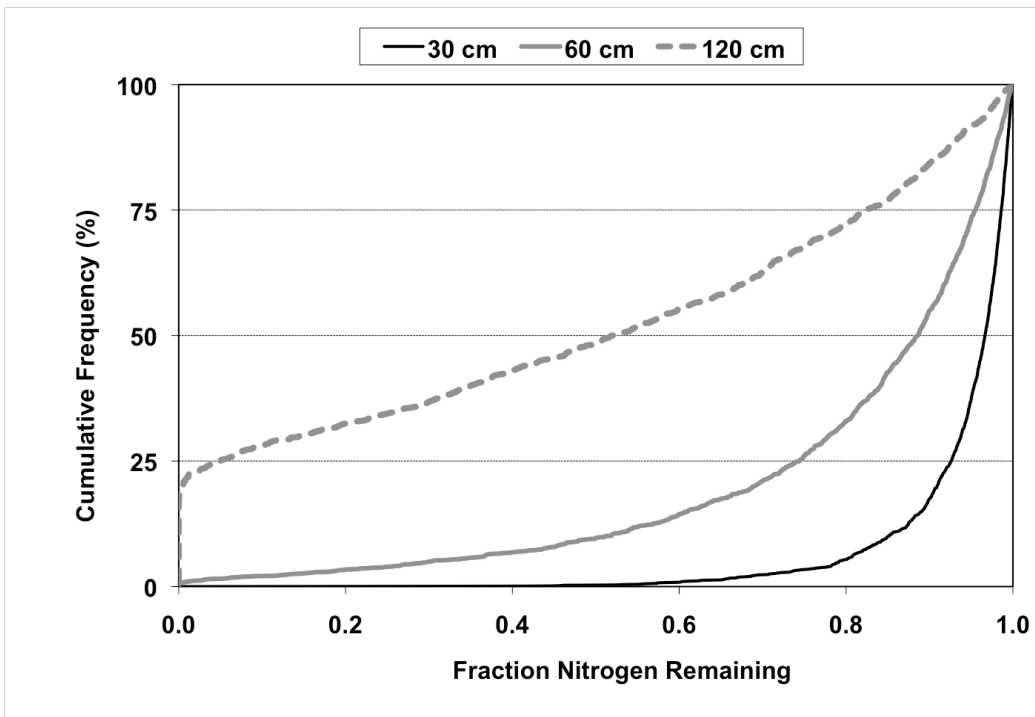


Figure VG-114. Cumulative Probability Graph: Loamy Sand Soil, Thermic Temperature Region, Standard Effluent, HLR = 5% of K_{sat}.

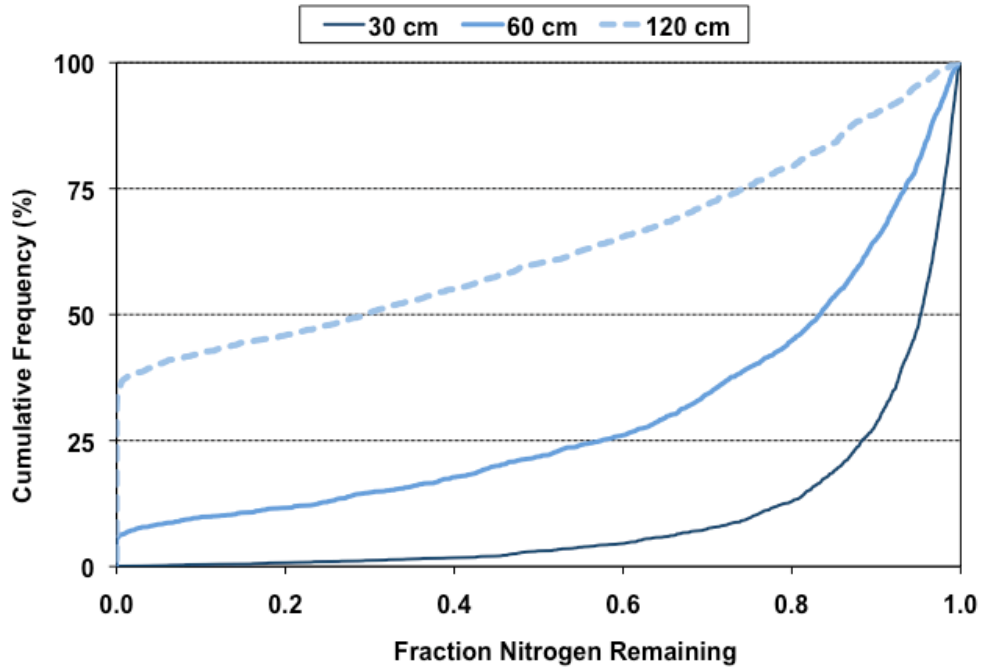


Figure VG-115. Cumulative Probability Graph: Loamy Sand Soil, Hyperthermic Temperature Region, Standard Effluent, HLR = 2 cm d⁻¹.

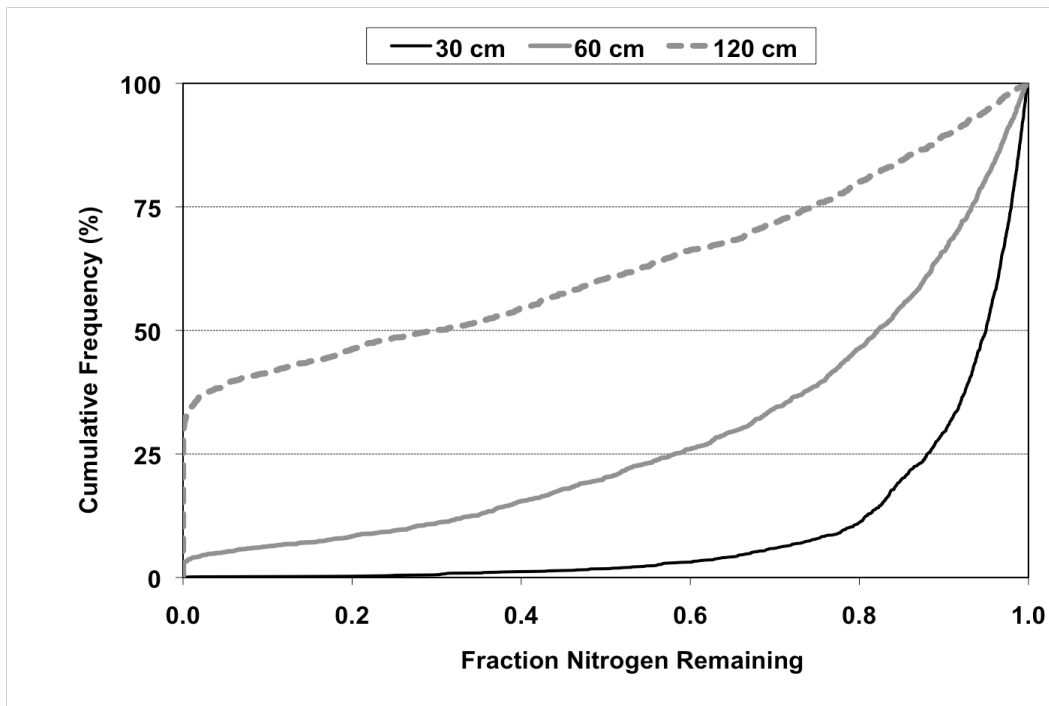


Figure VG-116. Cumulative Probability Graph: Loamy Sand Soil, Hyperthermic Temperature Region, Standard Effluent, HLR = 5% of K_{sat} .

2.4.2 Nitrified Effluent

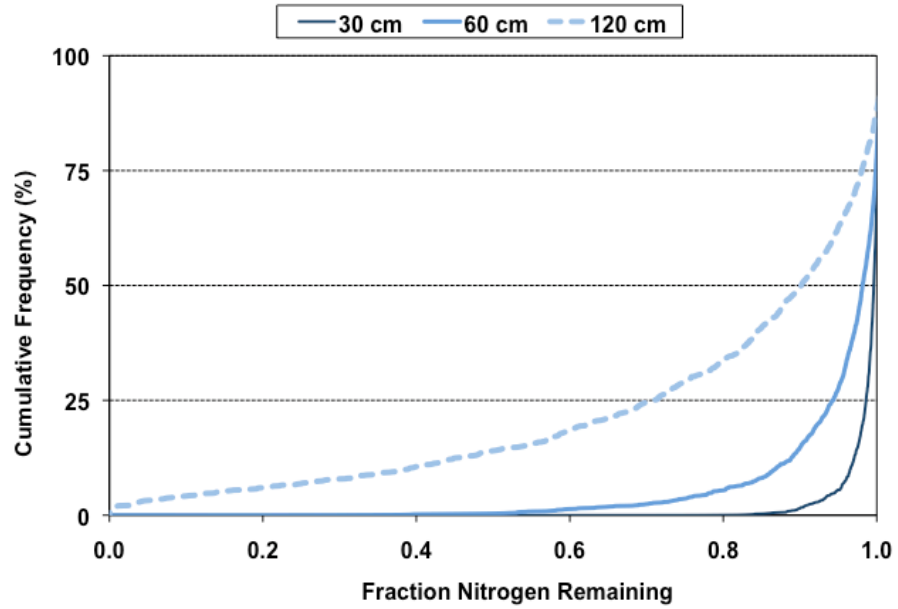


Figure VG-117. Cumulative Probability Graph: Loamy Sand Soil, Frigid/Cryic Temperature Region, Nitrified Effluent, HLR = 2 cm d⁻¹.

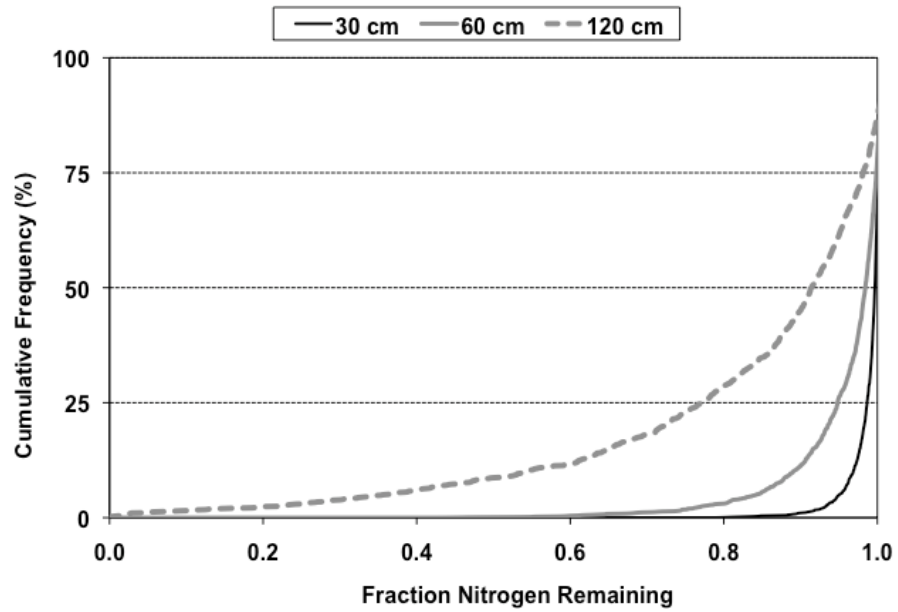


Figure VG-118. Cumulative Probability Graph: Loamy Sand Soil, Frigid/Cryic Temperature Region, Nitrified Effluent, HLR = 5% of K_{sat}.

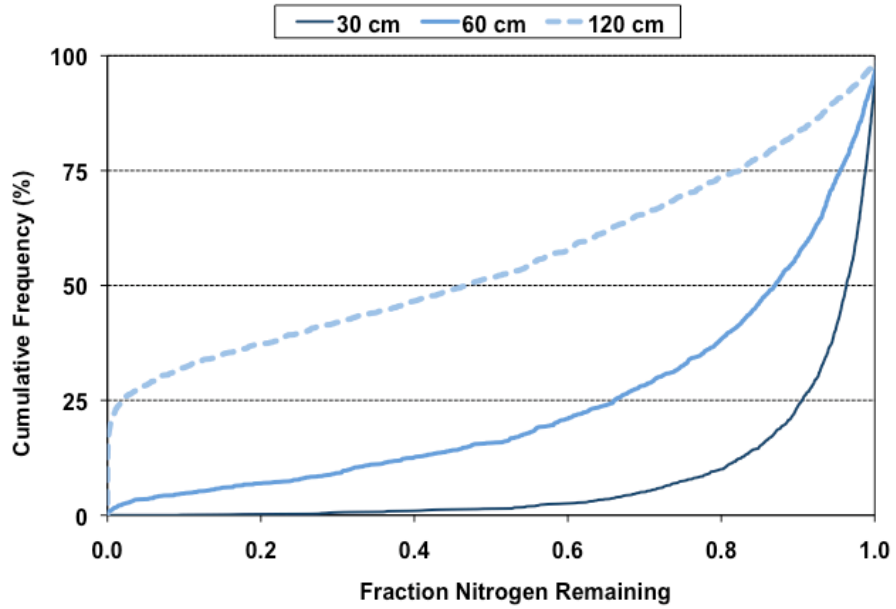


Figure VG-119. Cumulative Probability Graph: Loamy Sand Soil, Mesic Temperature Region, Nitrified Effluent, HLR = 2 cm d⁻¹.

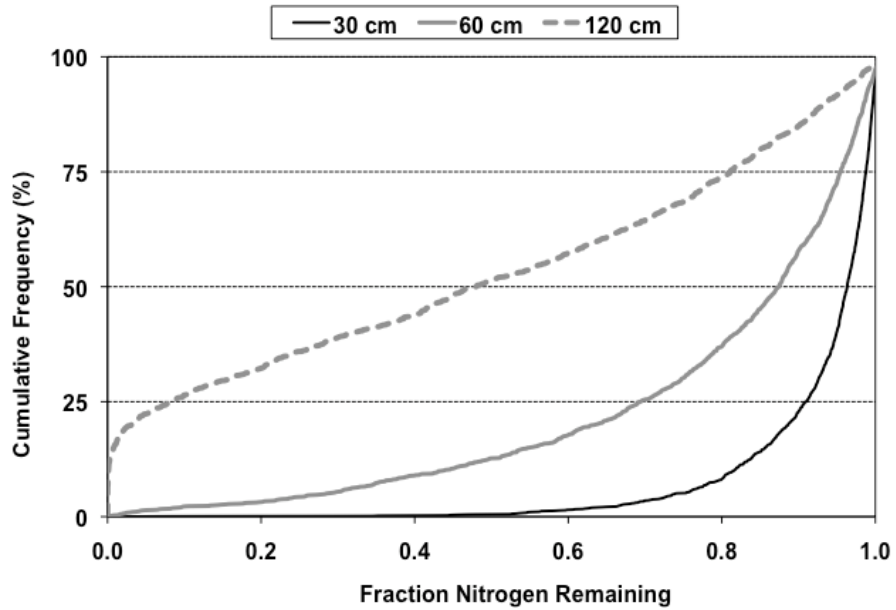


Figure VG-120. Cumulative Probability Graph: Loamy Sand Soil, Mesic Temperature Region, Nitrified Effluent, HLR = 5% of K_{sat}.

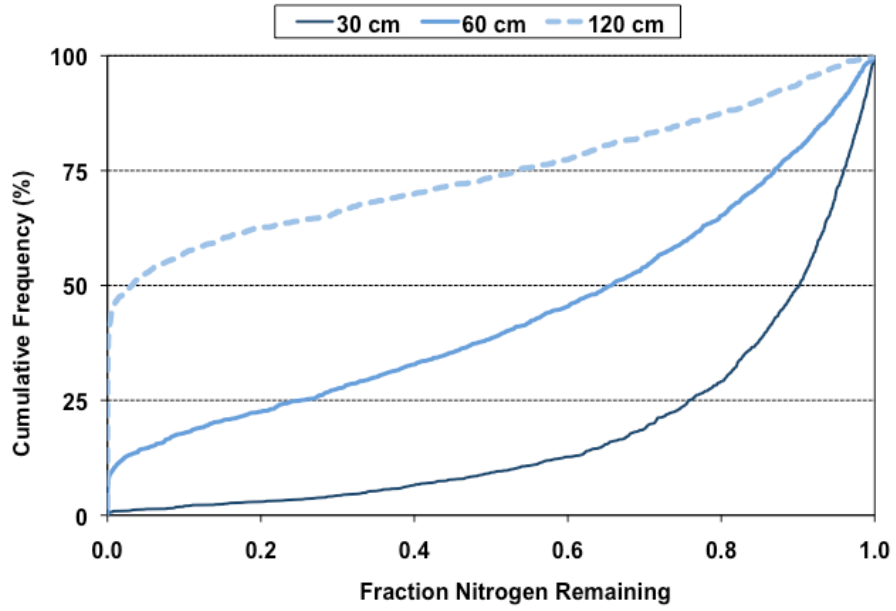


Figure VG-121. Cumulative Probability Graph: Loamy Sand Soil, Thermic Temperature Region, Nitrified Effluent, HLR = 2 cm d⁻¹.

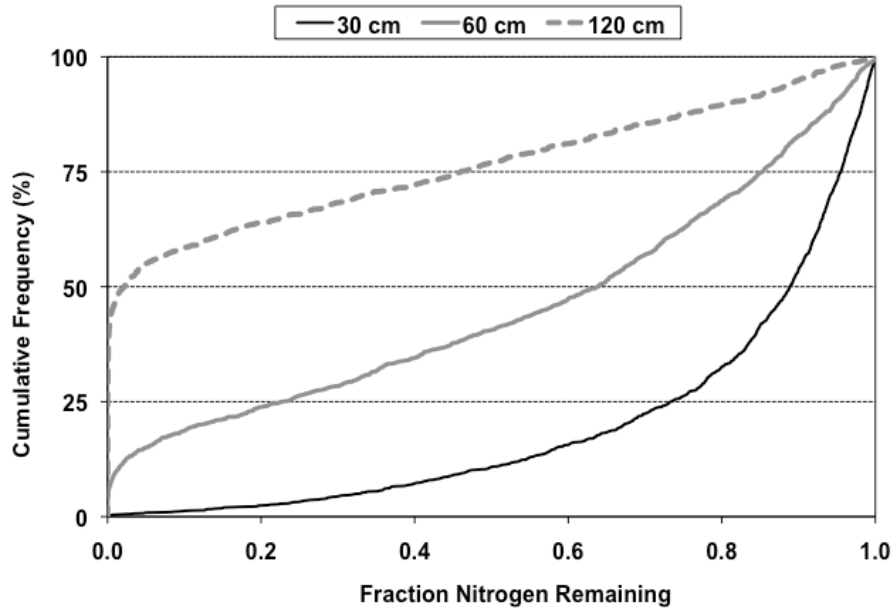


Figure VG-122. Cumulative Probability Graph: Loamy Sand Soil, Thermic Temperature Region, Nitrified Effluent, HLR = 5% of K_{sat} .

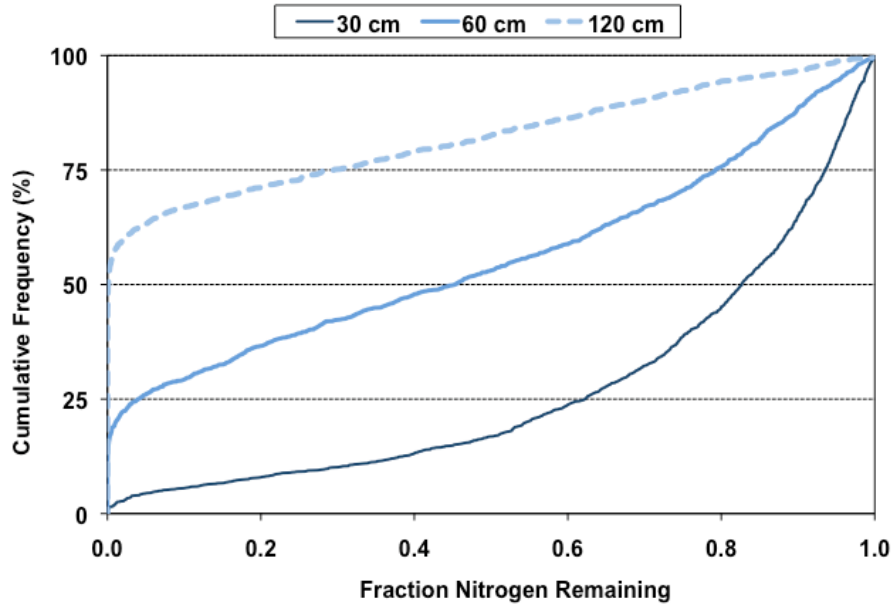


Figure VG-123. Cumulative Probability Graph: Loamy Sand Soil, Hyperthermic Temperature Region, Nitrified Effluent, HLR = 2 cm d⁻¹.

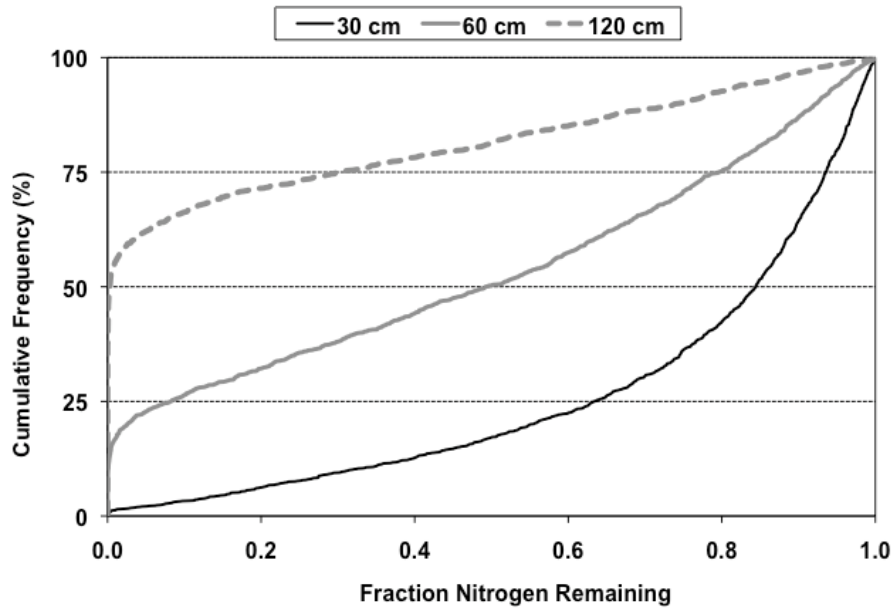


Figure VG-124. Cumulative Probability Graph: Loamy Sand Soil, Hyperthermic Temperature Region, Nitrified Effluent, HLR = 5% of K_{sat} .

2.5 Sand

2.5.1 Standard Effluent

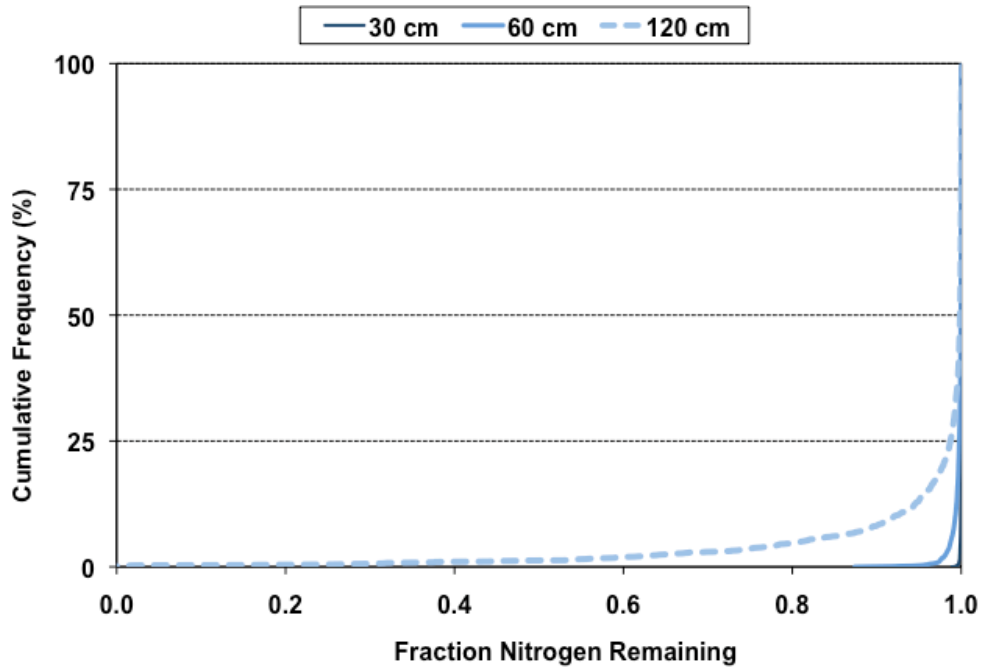


Figure VG-125. Cumulative Probability Graph: Sandy Soil, Frigid/Cryic Temperature Region, Standard Effluent, HLR = 2 cm d⁻¹.

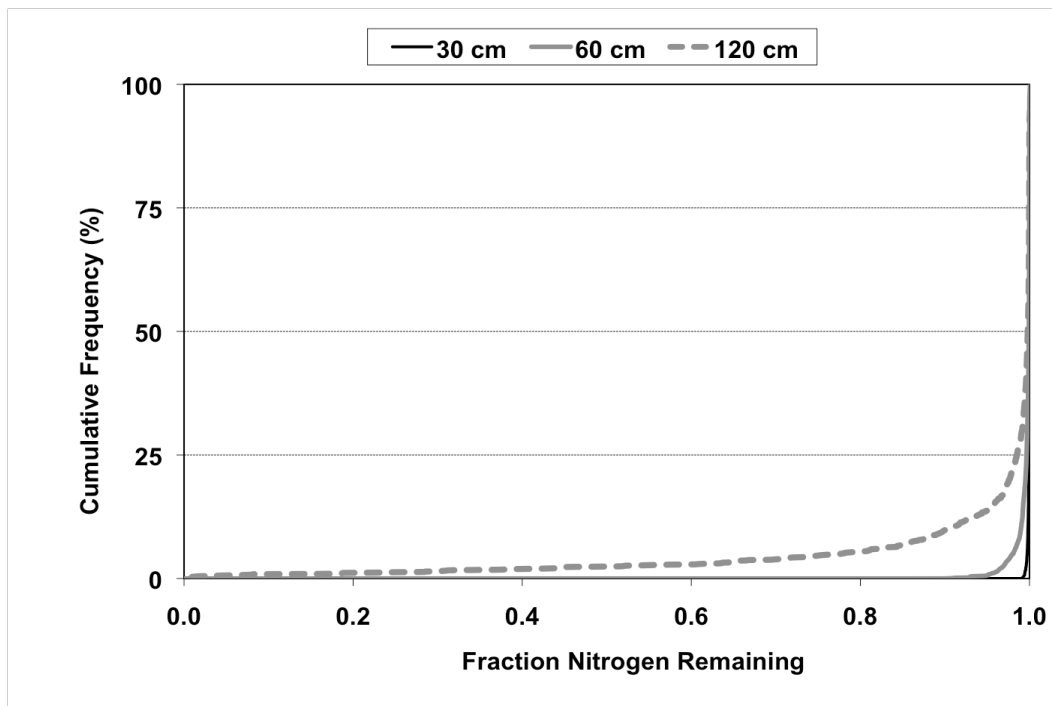


Figure VG-126. Cumulative Probability Graph: Sandy Soil, Frigid/Cryic Temperature Region, Standard Effluent, HLR = 5% of K_{sat}.

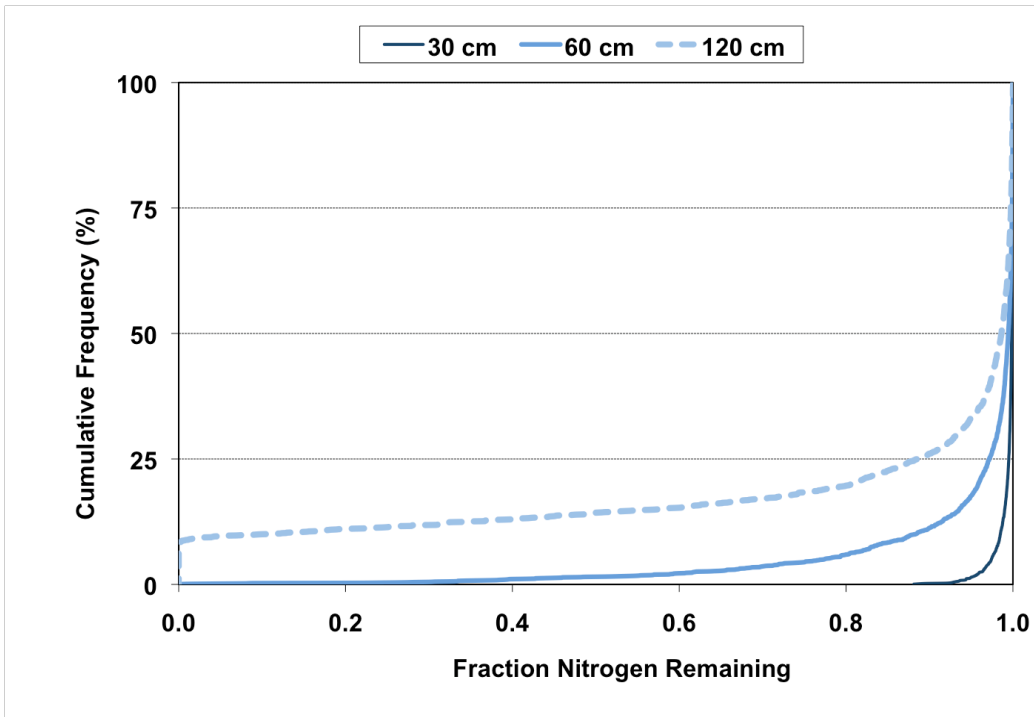


Figure VG-127. Cumulative Probability Graph: Sandy Soil, Mesic Temperature Region, Standard Effluent, HLR = 2 cm d⁻¹.

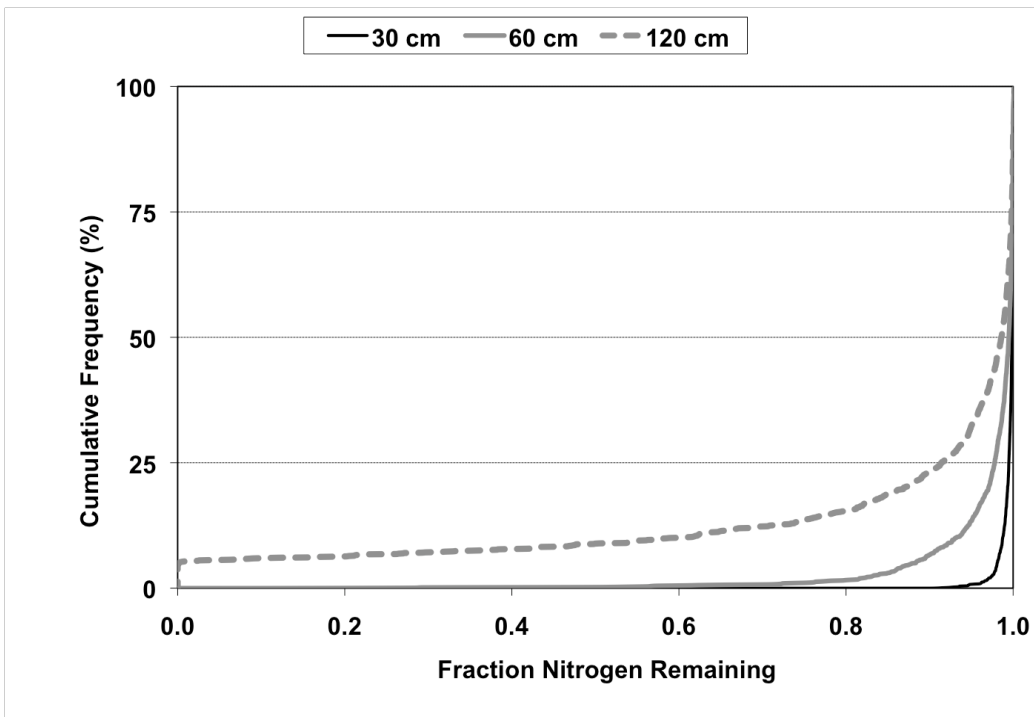


Figure VG-128. Cumulative Probability Graph: Sandy Soil, Mesic Temperature Region, Standard Effluent, HLR = 5% of K_{sat} .

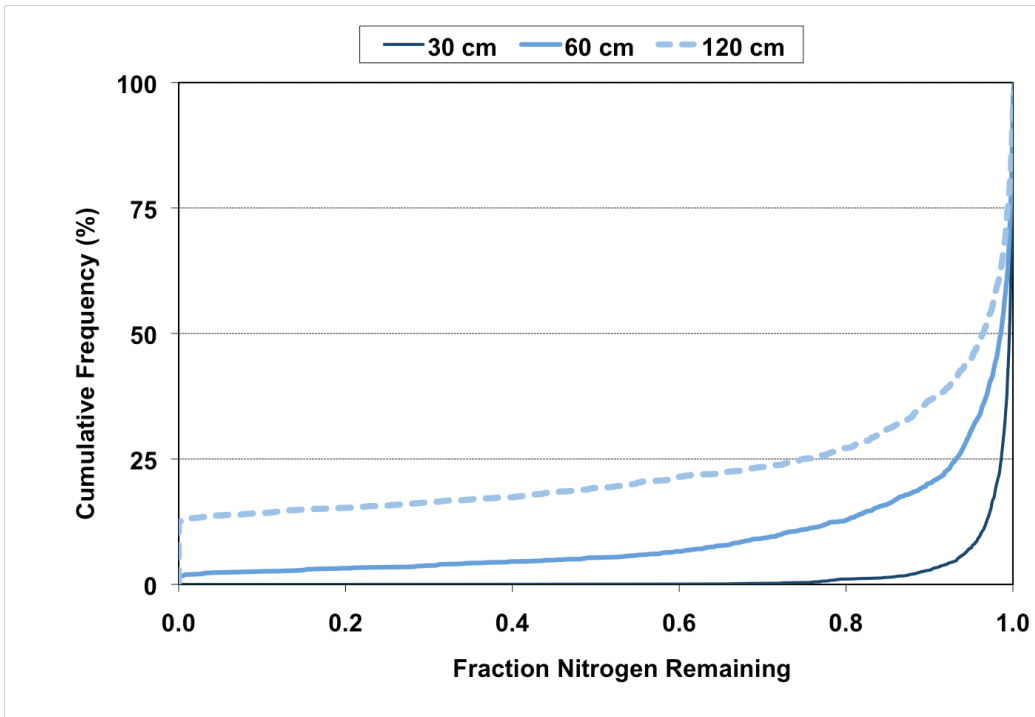


Figure VG-129. Cumulative Probability Graph: Sandy Soil, Thermic Temperature Region, Standard Effluent, HLR = 2 cm d⁻¹.

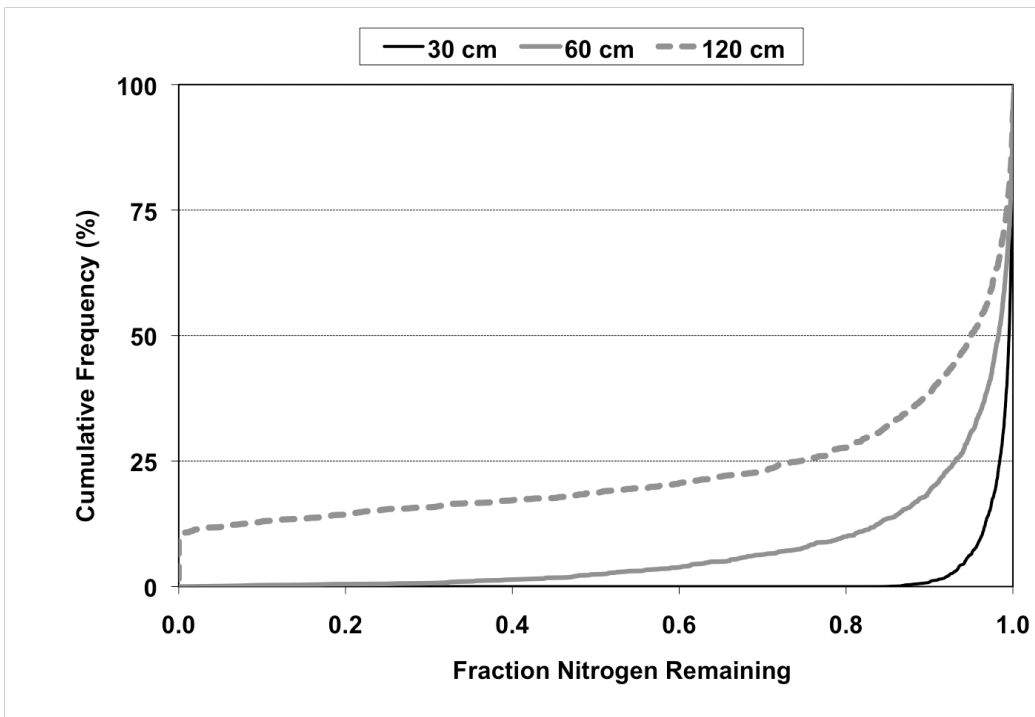


Figure VG-130. Cumulative Probability Graph: Sandy Soil, Thermic Temperature Region, Standard Effluent, HLR = 5% of K_{sat} .

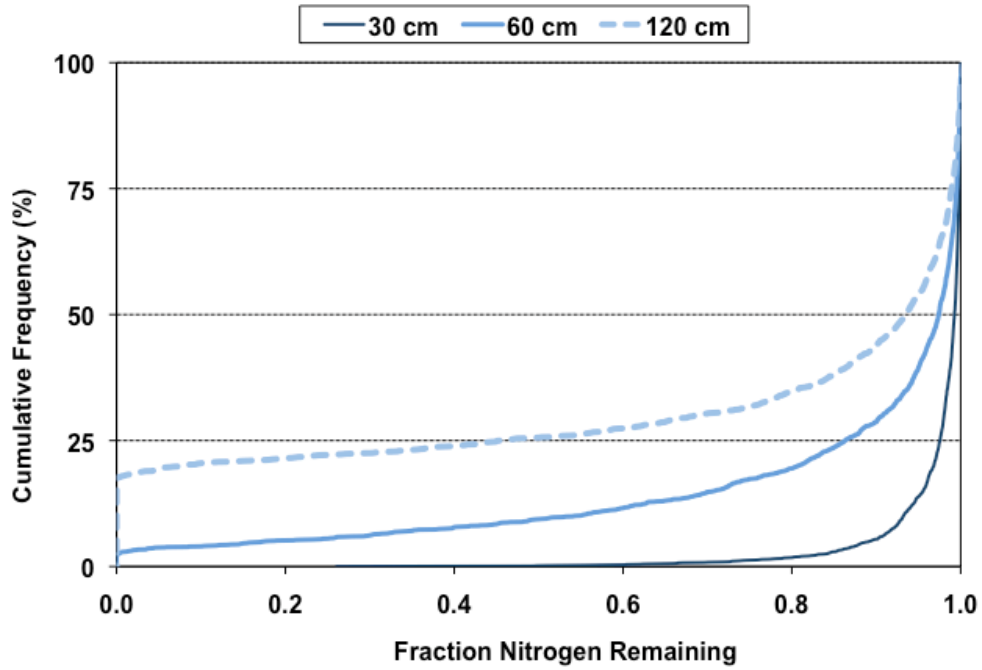


Figure VG-131. Cumulative Probability Graph: Sandy Soil, Hyperthermic Temperature Region, Standard Effluent, HLR = 2 cm d⁻¹.

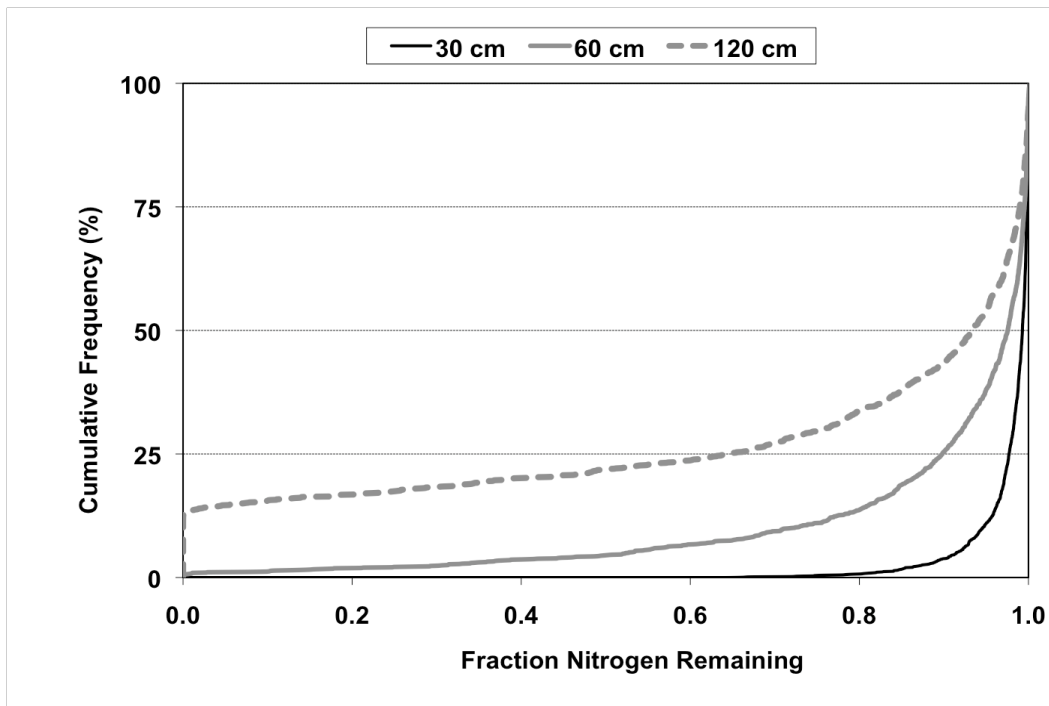


Figure VG-132. Cumulative Probability Graph: Sandy Soil, Hyperthermic Temperature Region, Standard Effluent, HLR = 5% of K_{sat} .

2.5.2 Nitrified Effluent

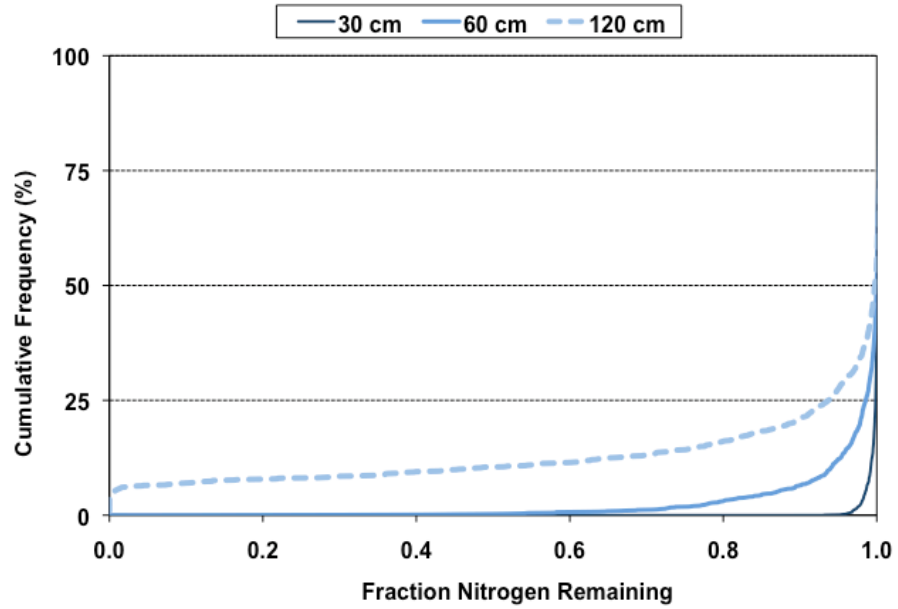


Figure VG-133. Cumulative Probability Graph: Sandy Soil, Frigid/Cryic Temperature Region, Nitrified Effluent, HLR = 2 cm d⁻¹.

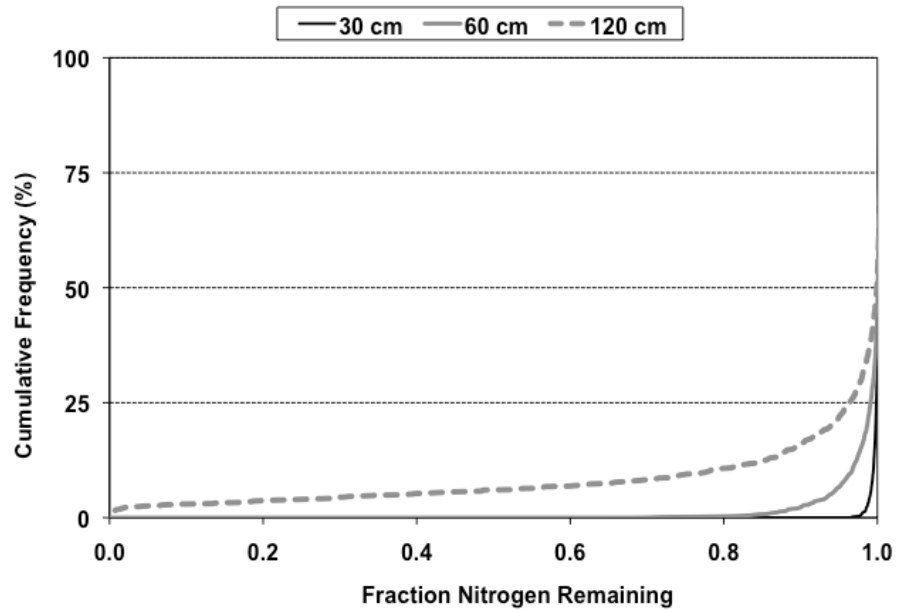


Figure VG-134. Cumulative Probability Graph: Sandy Soil, Frigid/Cryic Temperature Region, Nitrified Effluent, HLR = 5% of K_{sat}.

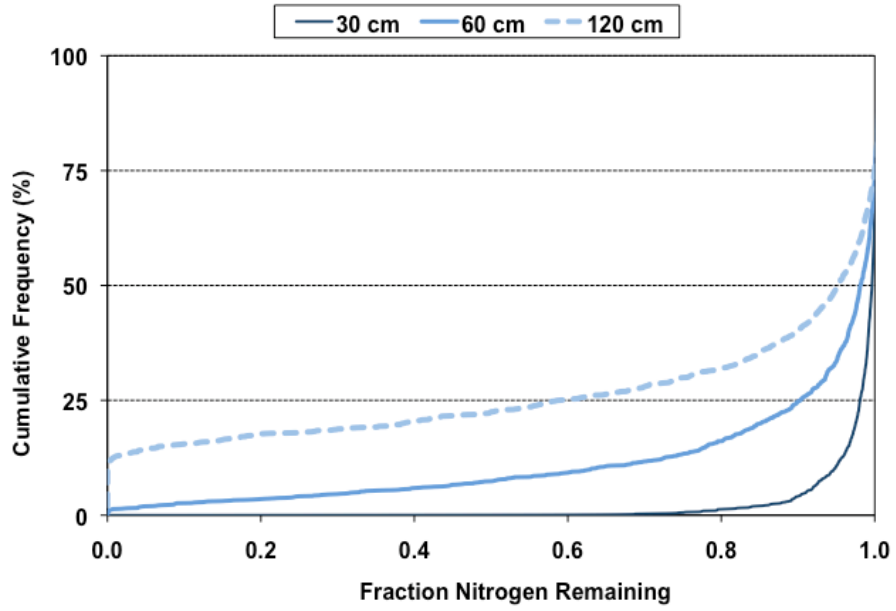


Figure VG-135. Cumulative Probability Graph: Sandy Soil, Mesic Temperature Region, Nitrified Effluent, HLR = 2 cm d⁻¹.

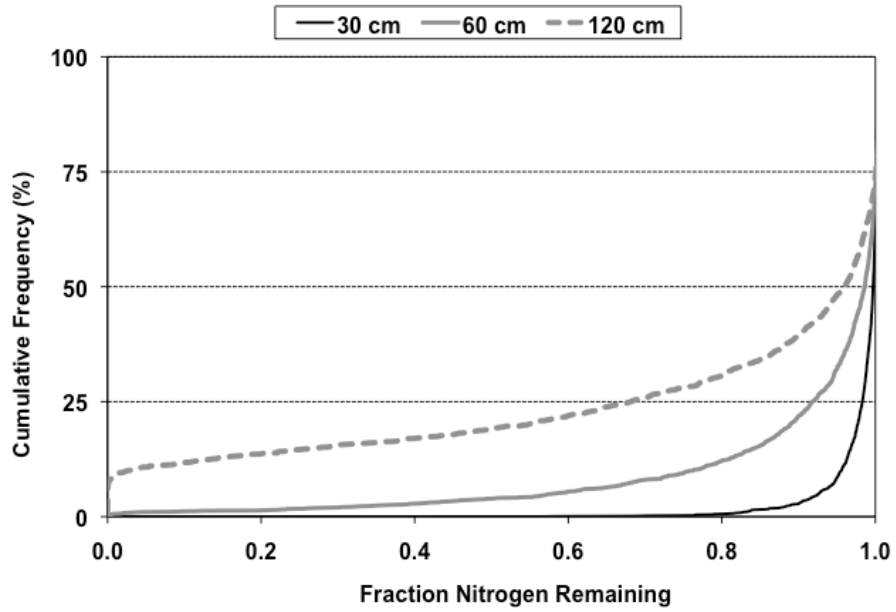


Figure VG-136. Cumulative Probability Graph: Sandy Soil, Mesic Temperature Region, Nitrified Effluent, HLR = 5% of K_{sat} .

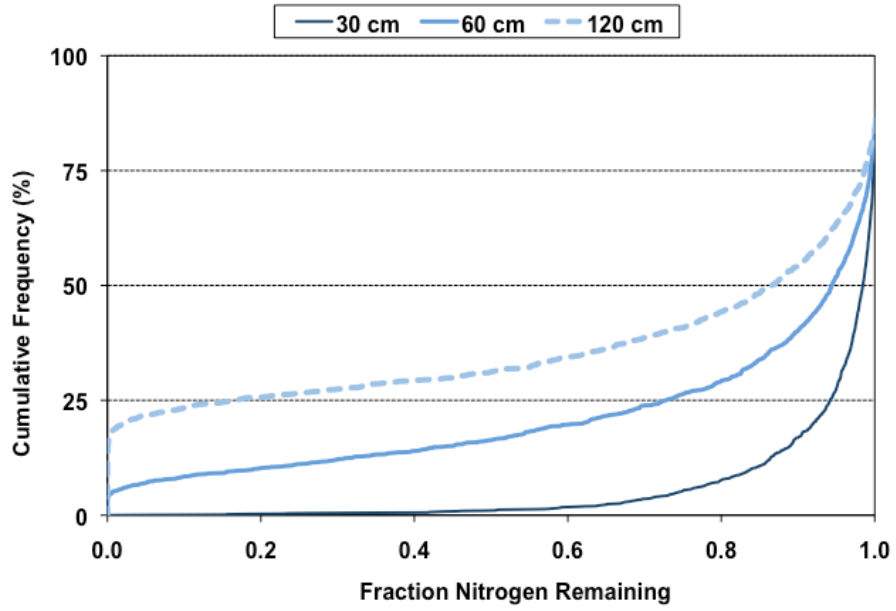


Figure VG-137. Cumulative Probability Graph: Sandy Soil, Thermic Temperature Region, Nitrified Effluent, HLR = 2 cm d⁻¹.

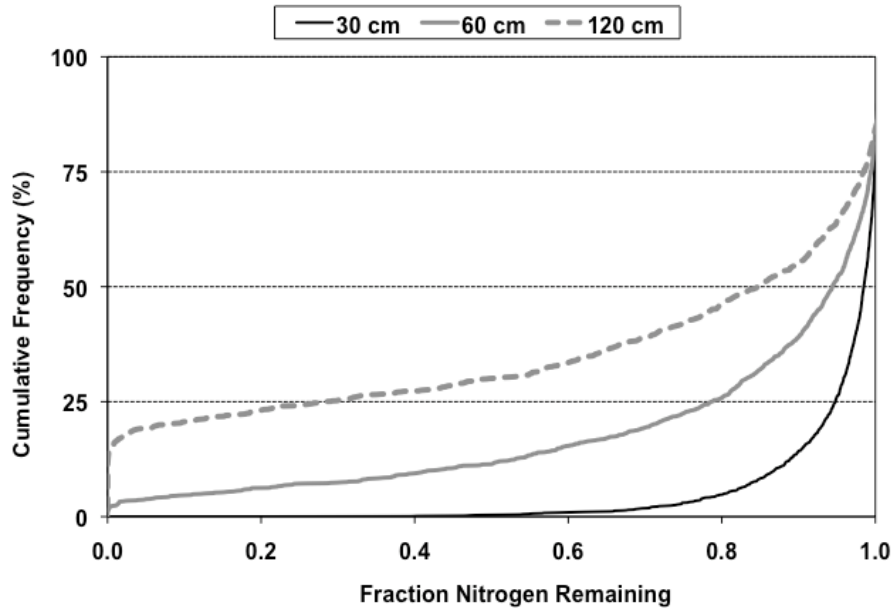


Figure VG-138. Cumulative Probability Graph: Sandy Soil, Thermic Temperature Region, Nitrified Effluent, HLR = 5% of K_{sat} .

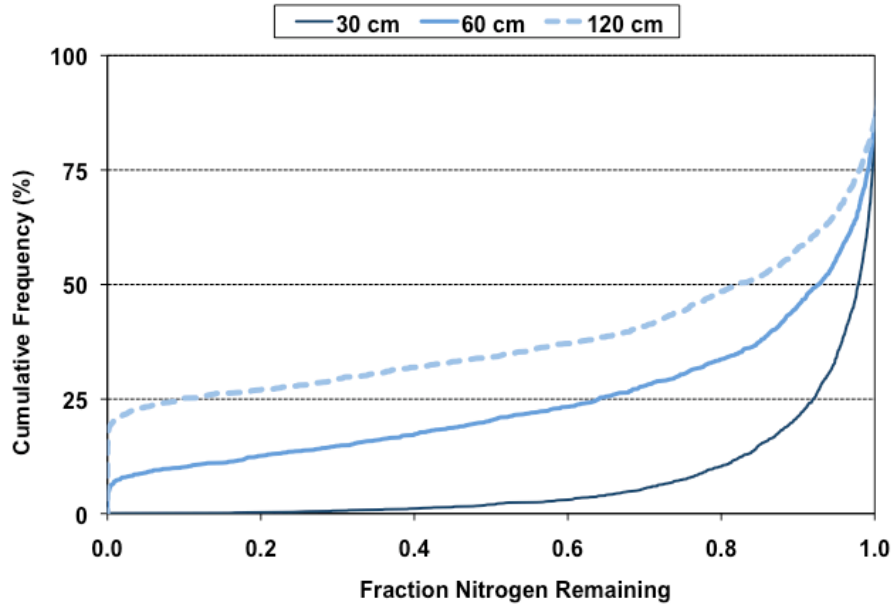


Figure VG-139. Cumulative Probability Graph: Sandy Soil, Hyperthermic Temperature Region, Nitrified Effluent, HLR = 2 cm d⁻¹.

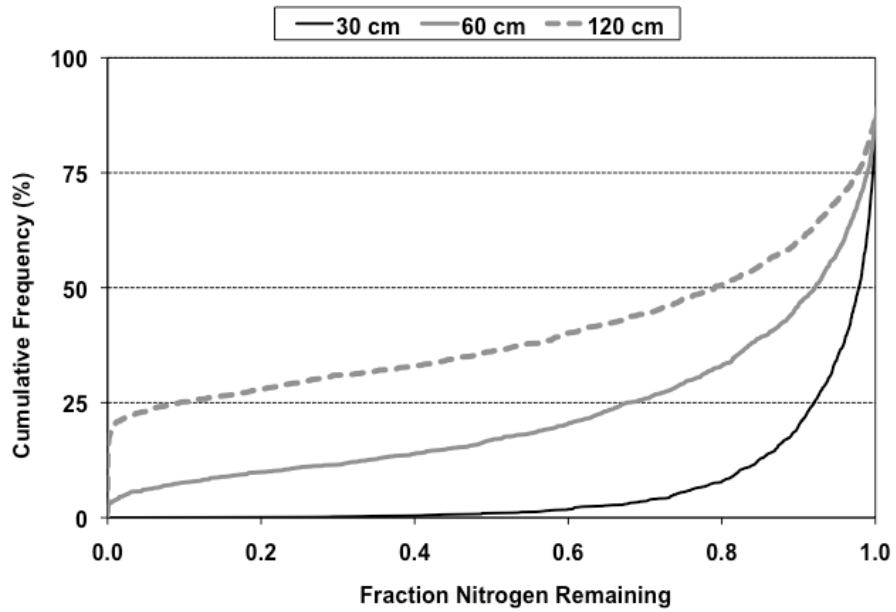


Figure VG-140. Cumulative Probability Graph: Sandy Soil, Hyperthermic Temperature Region, Nitrified Effluent, HLR = 5% of K_{sat} .

2.6 Sandy Clay

2.6.1 Standard Effluent

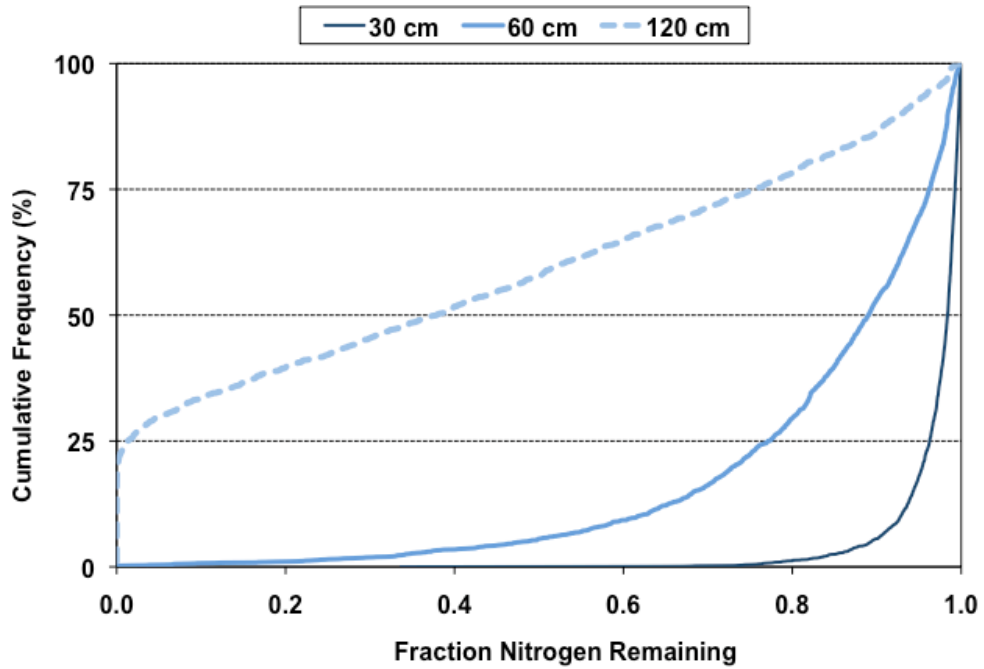


Figure VG-141. Cumulative Probability Graph: Sandy Clay Soil, Frigid/Cryic Temperature Region, Standard Effluent, HLR = 2 cm d⁻¹.

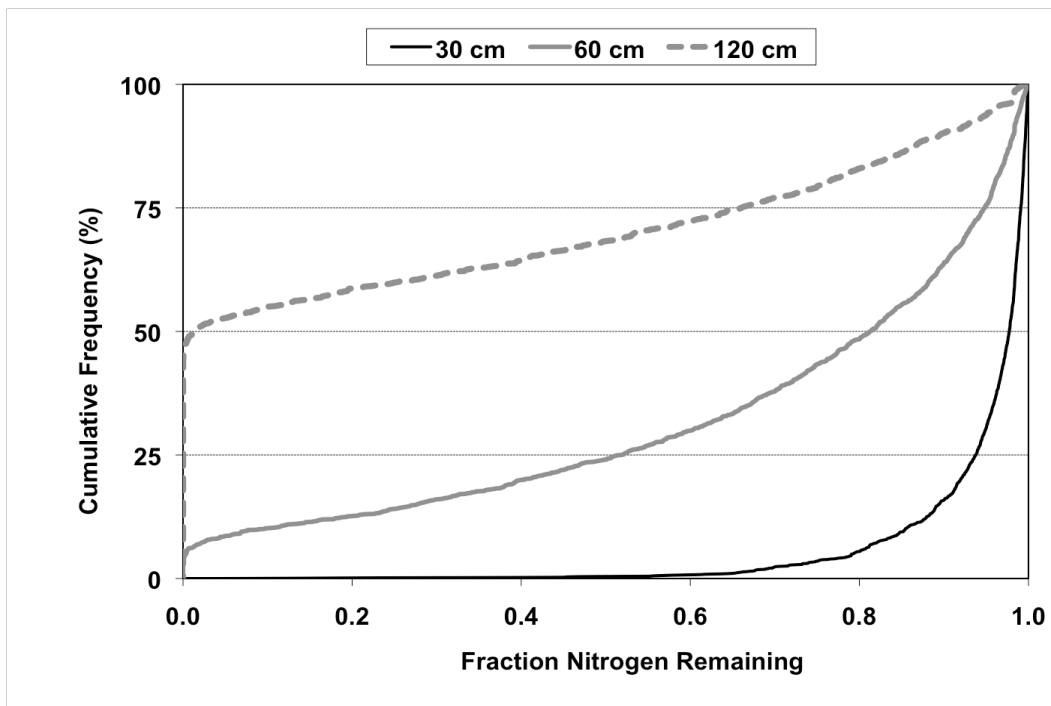


Figure VG-142. Cumulative Probability Graph: Sandy Clay Soil, Frigid/Cryic Temperature Region, Standard Effluent, HLR = 5% of K_{sat}.

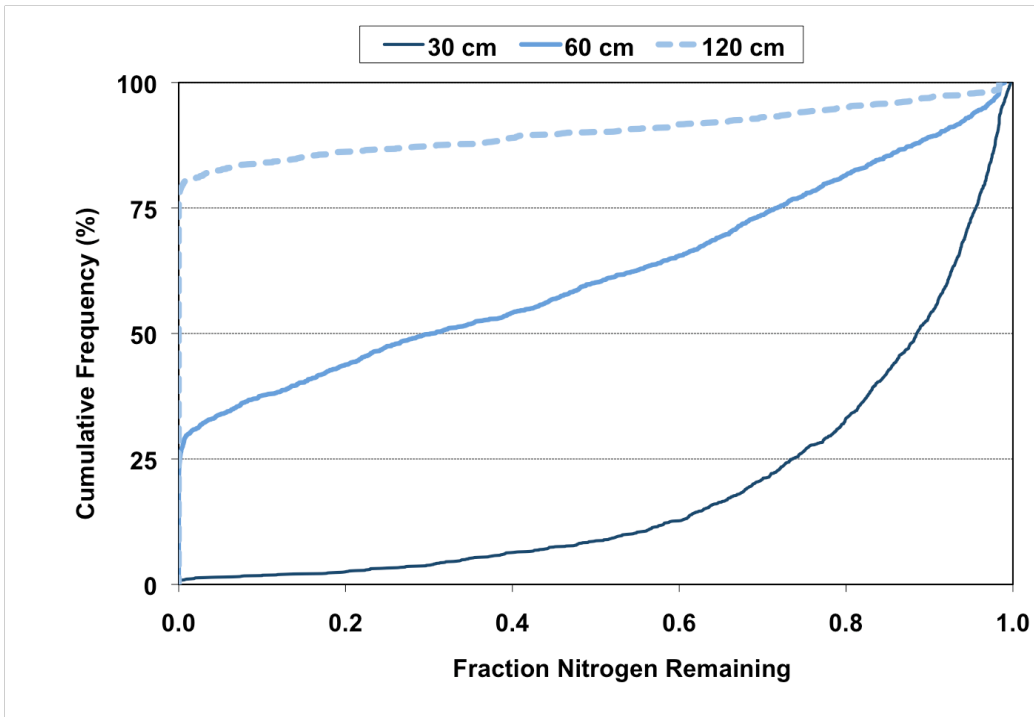


Figure VG-143. Cumulative Probability Graph: Sandy Clay Soil, Mesic Temperature Region, Standard Effluent, HLR = 2 cm d⁻¹.

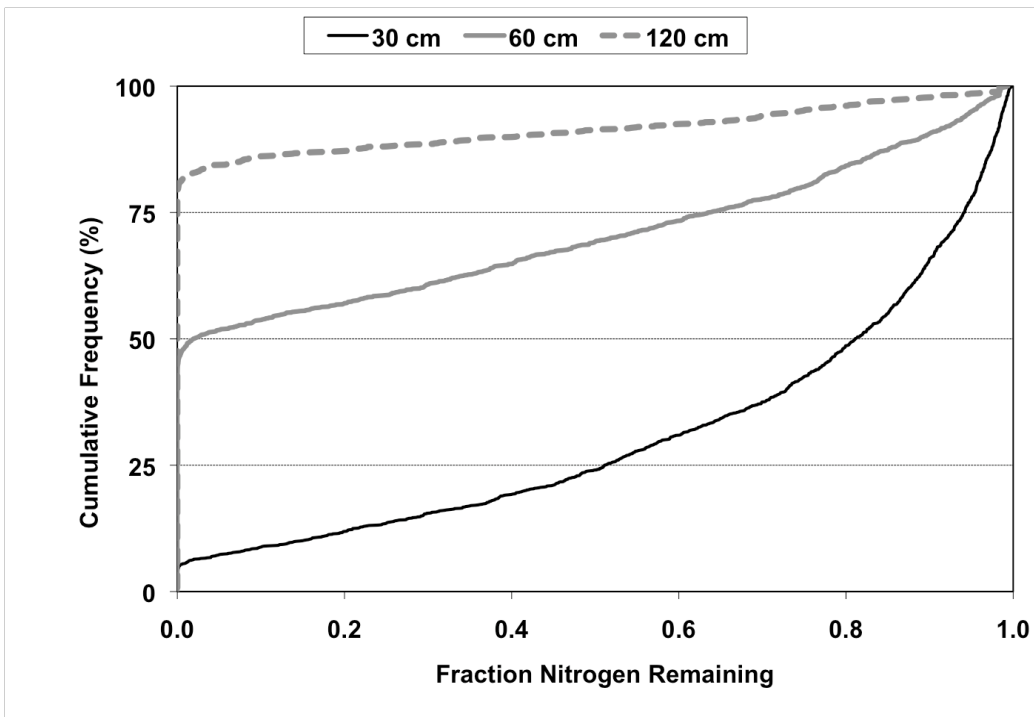


Figure VG-144. Cumulative Probability Graph: Sandy Clay Soil, Mesic Temperature Region, Standard Effluent, HLR = 5% of K_{sat}.

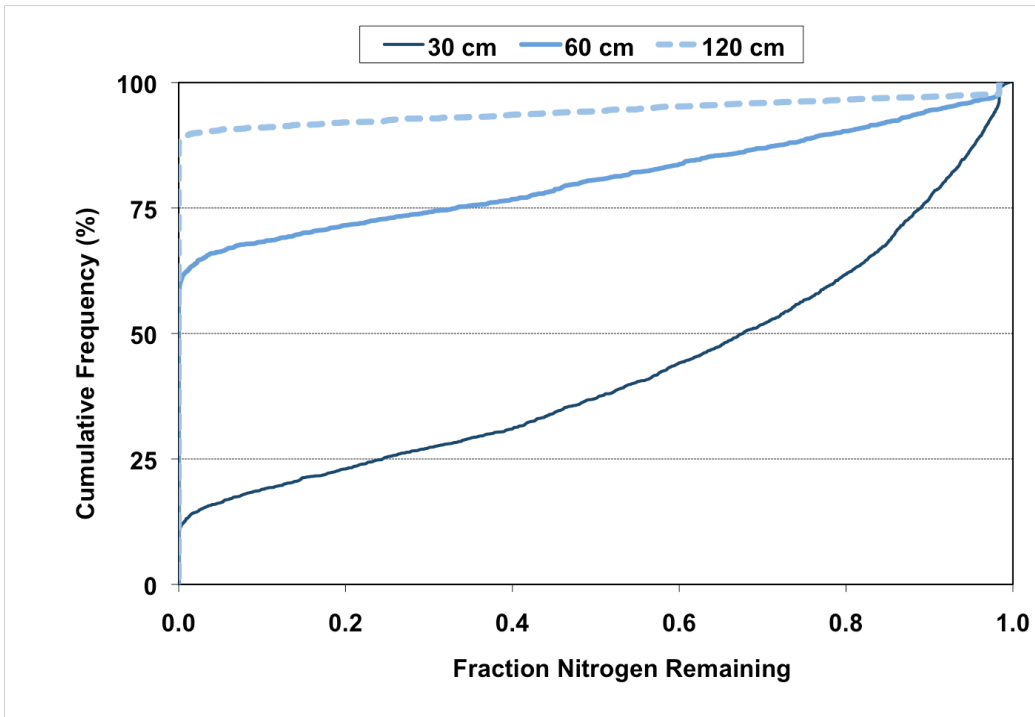


Figure VG-145. Cumulative Probability Graph: Sandy Clay Soil, Thermic Temperature Region, Standard Effluent, HLR = 2 cm d⁻¹.

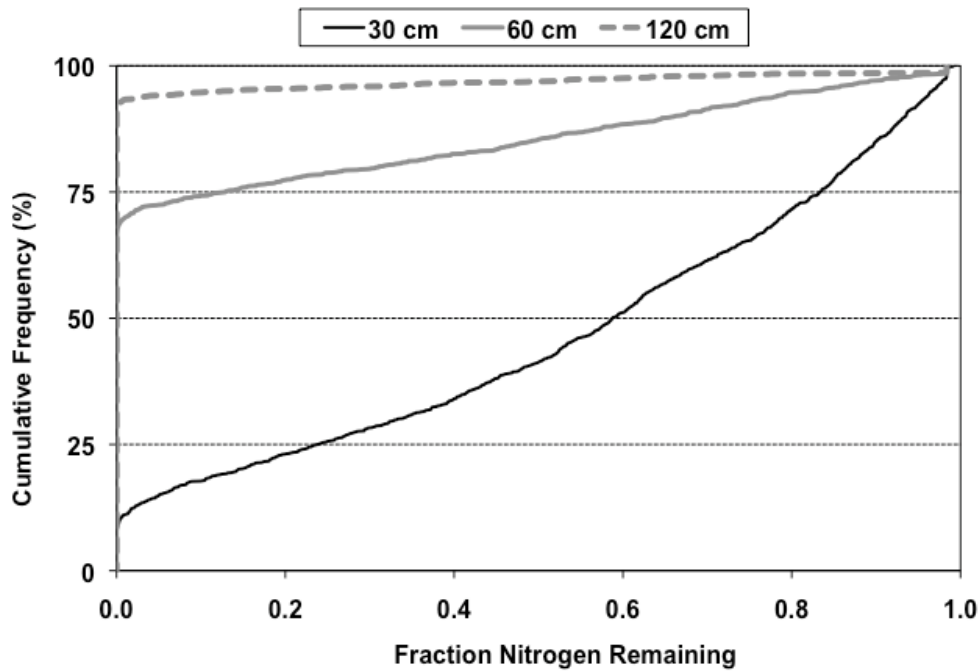


Figure VG-146. Cumulative Probability Graph: Sandy Clay Soil, Thermic Temperature Region, Standard Effluent, HLR = 5% of K_{sat}.

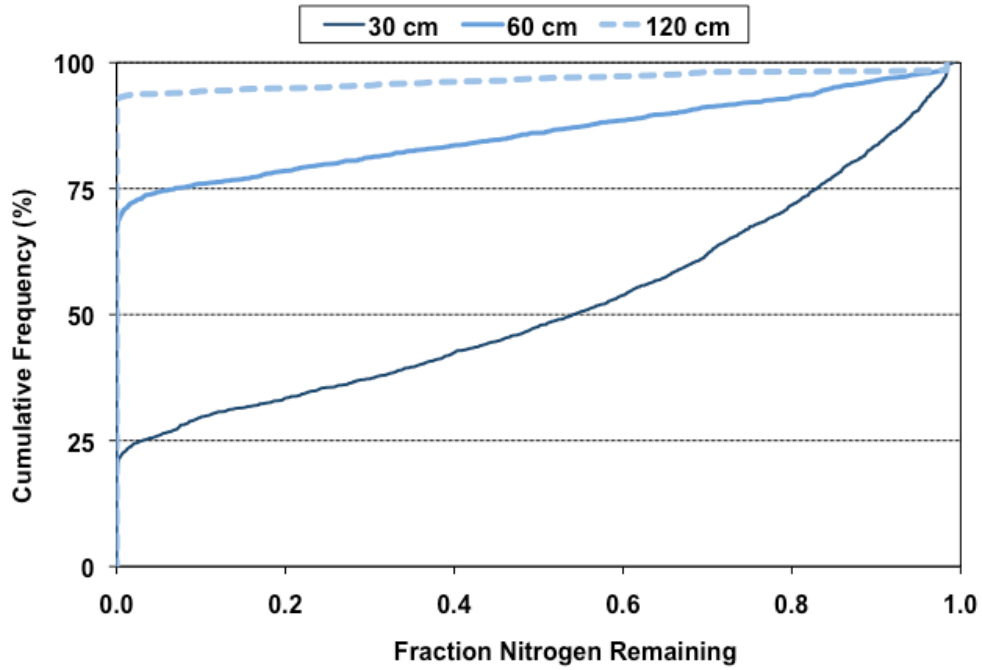


Figure VG-147. Cumulative Probability Graph: Sandy Clay Soil, Hyperthermic Temperature Region, Standard Effluent, HLR = 2 cm d⁻¹.

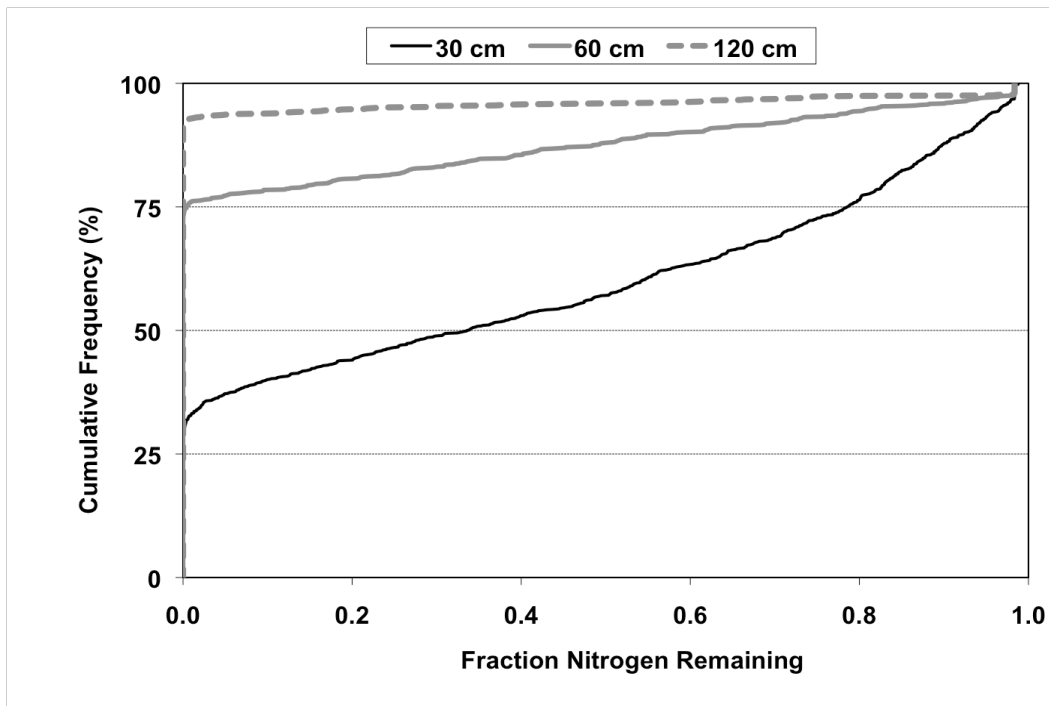


Figure VG-148. Cumulative Probability Graph: Sandy Clay Soil, Hyperthermic Temperature Region, Standard Effluent, HLR = 5% of K_{sat} .

2.6.2 Nitrified Effluent

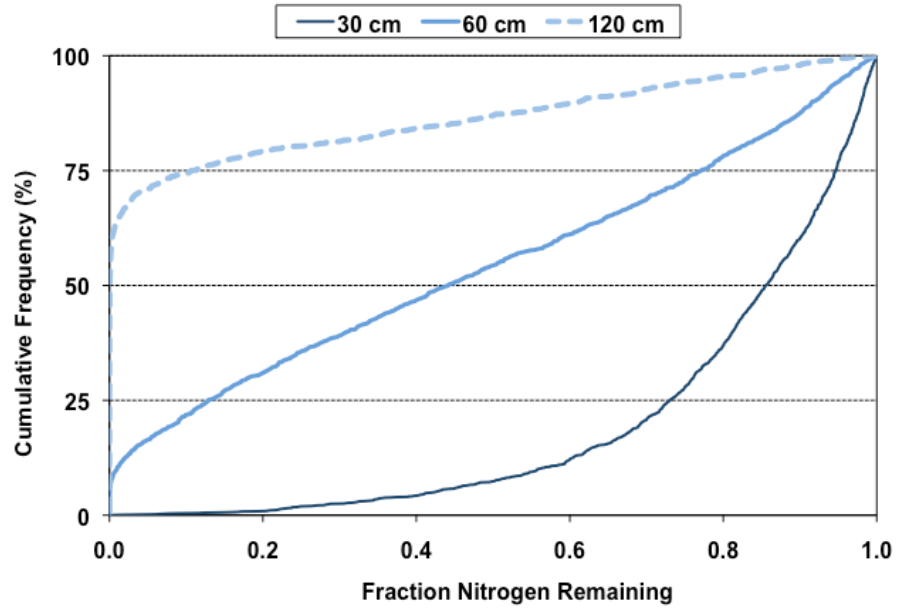


Figure VG-149. Cumulative Probability Graph: Sandy Clay Soil, Frigid/Cryic Temperature Region, Nitrified Effluent, HLR = 2 cm d⁻¹.

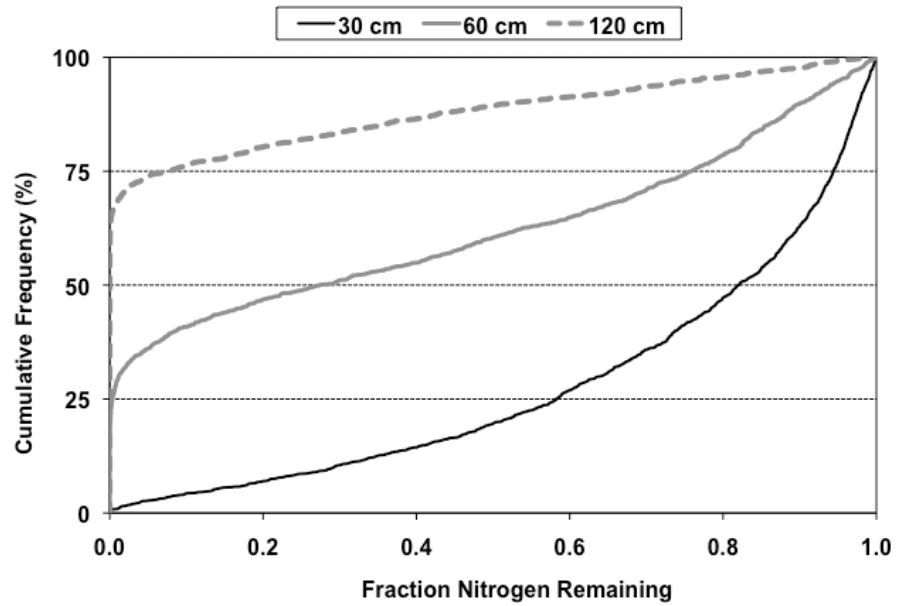


Figure VG-150. Cumulative Probability Graph: Sandy Clay Soil, Frigid/Cryic Temperature Region, Nitrified Effluent, HLR = 5% of K_{sat}.

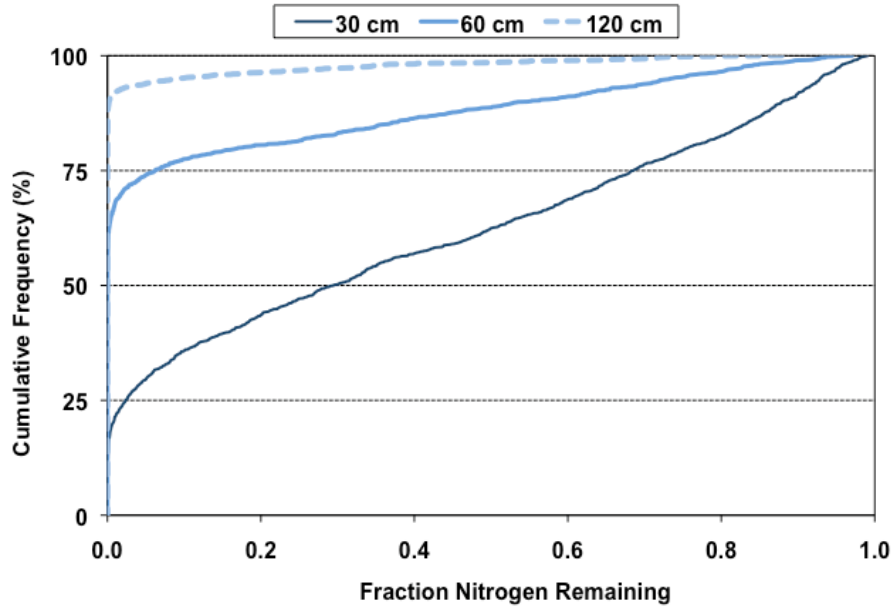


Figure VG-151. Cumulative Probability Graph: Sandy Clay Soil, Mesic Temperature Region, Nitrified Effluent, HLR = 2 cm d⁻¹.

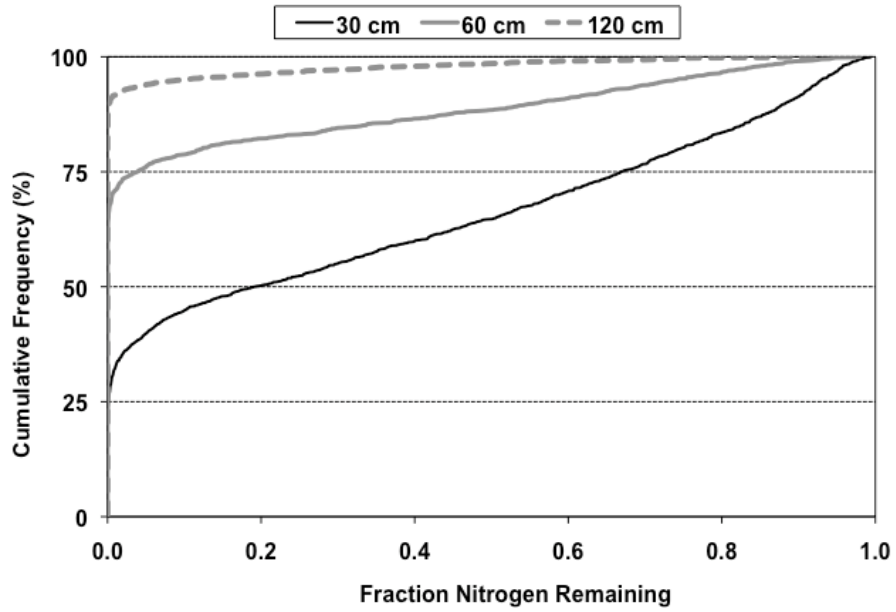


Figure VG-152. Cumulative Probability Graph: Sandy Clay Soil, Mesic Temperature Region, Nitrified Effluent, HLR = 5% of K_{sat}.

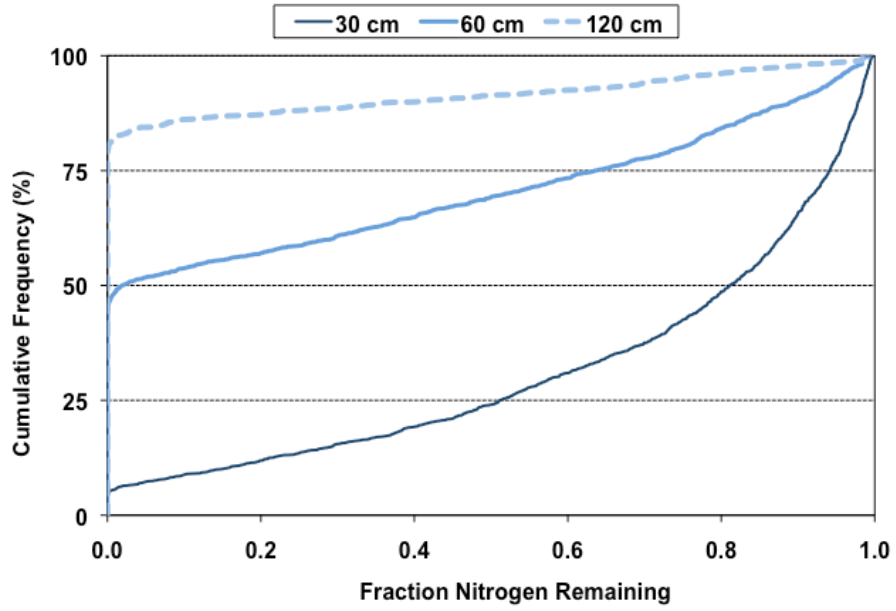


Figure VG-153. Cumulative Probability Graph: Sandy Clay Soil, Thermic Temperature Region, Nitrified Effluent, HLR = 2 cm d⁻¹.

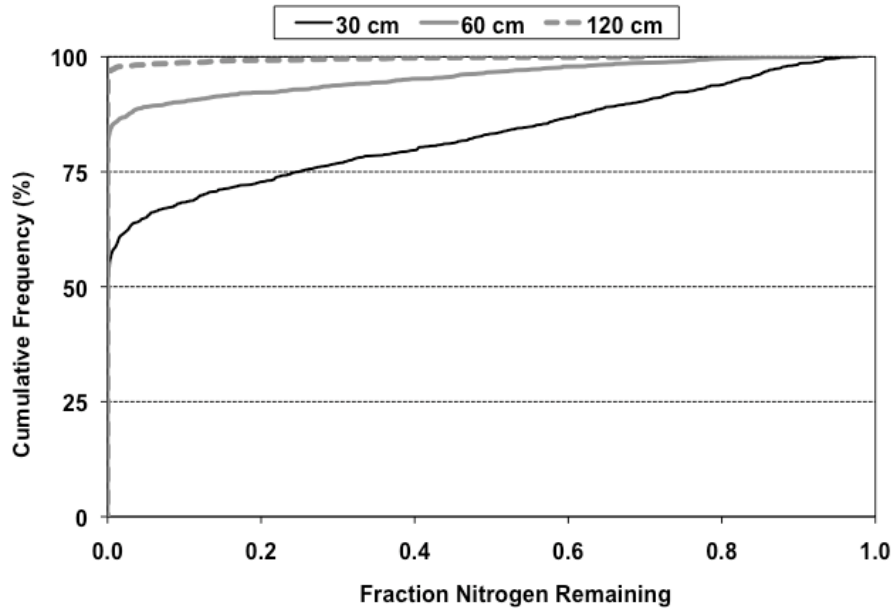


Figure VG-154. Cumulative Probability Graph: Sandy Clay Soil, Thermic Temperature Region, Nitrified Effluent, HLR = 5% of K_{sat} .

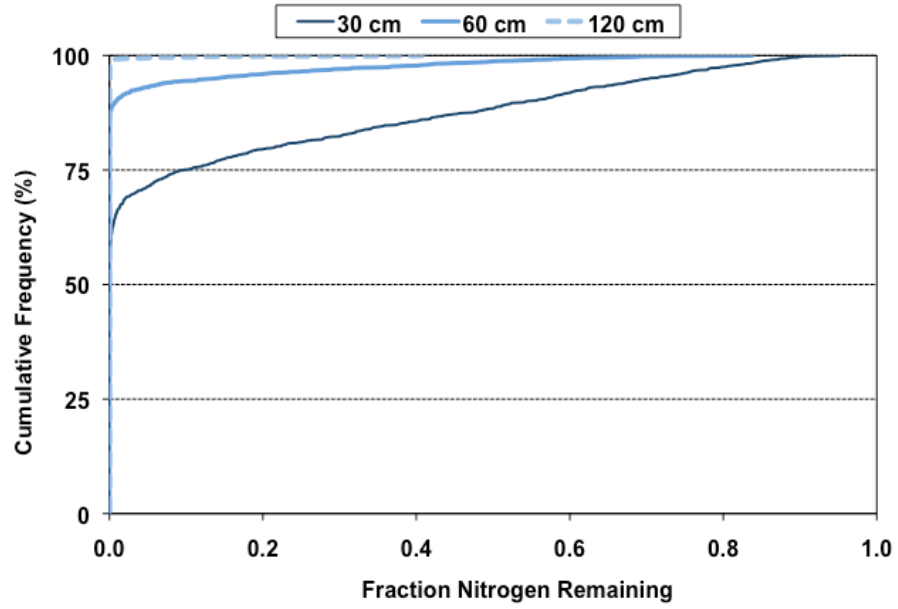


Figure VG-155. Cumulative Probability Graph: Sandy Clay Soil, Hyperthermic Temperature Region, Nitrified Effluent, HLR = 2 cm d⁻¹.

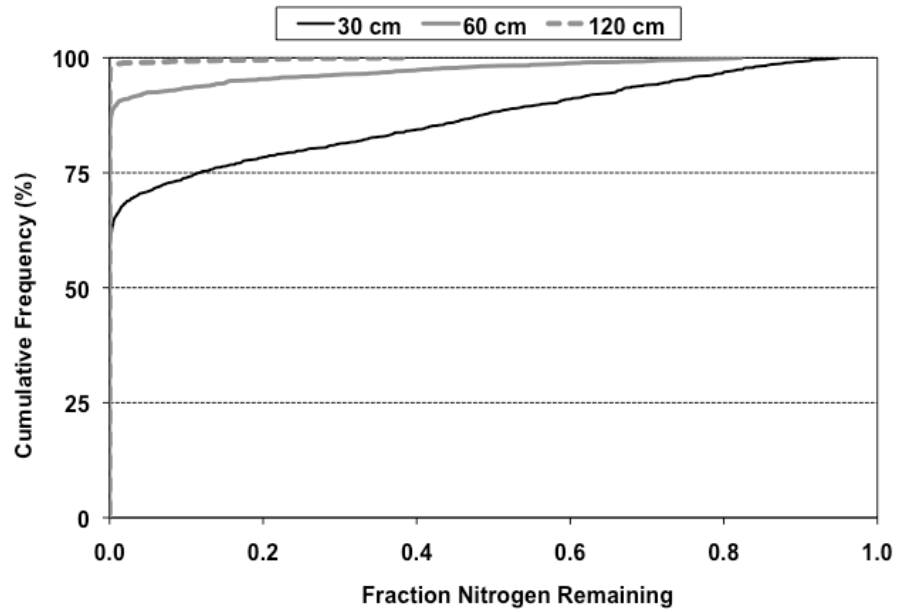


Figure VG-156. Cumulative Probability Graph: Sandy Clay Soil, Hyperthermic Temperature Region, Nitrified Effluent, HLR = 5% of K_{sat} .

2.7 Sandy Clay Loam

2.7.1 Standard Effluent

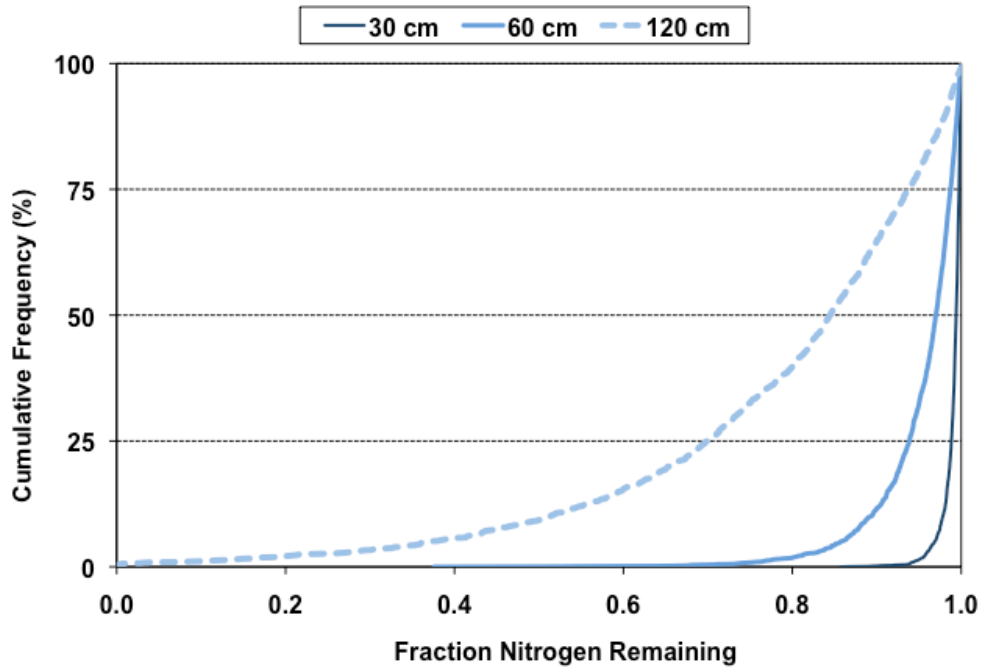


Figure VG-157. Cumulative Probability Graph: Sandy Clay Loam Soil, Frigid/Cryic Temperature Region, Standard Effluent, HLR = 2 cm d⁻¹.

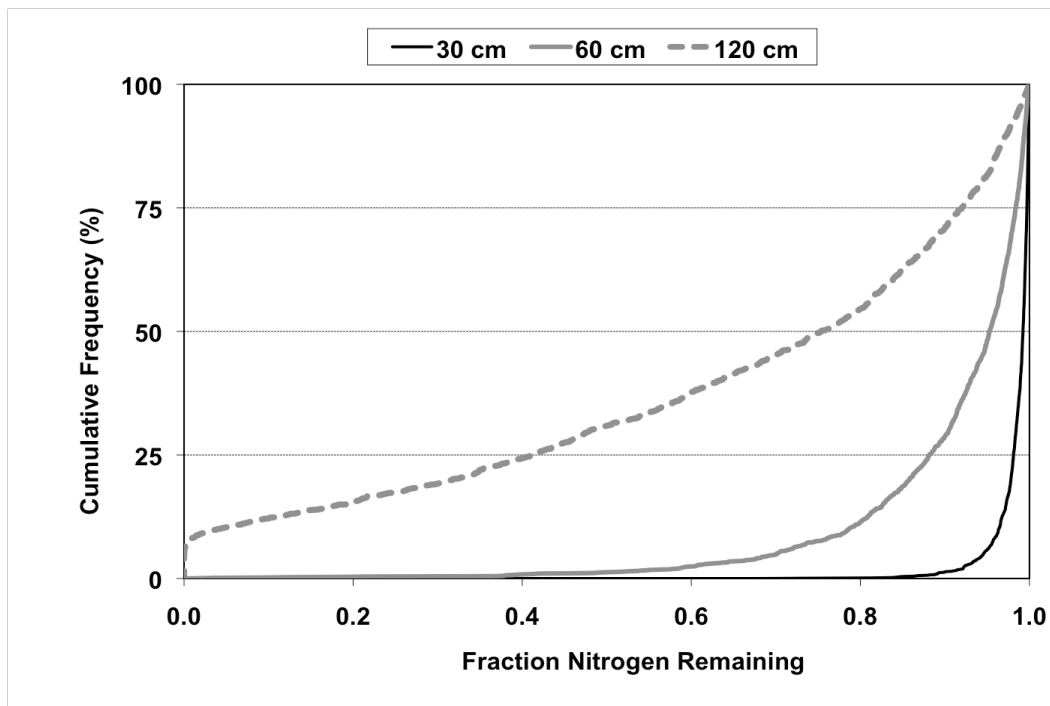


Figure VG-158. Cumulative Probability Graph: Sandy Clay Loam Soil, Frigid/Cryic Temperature Region, Standard Effluent, HLR = 5% of K_{sat} .

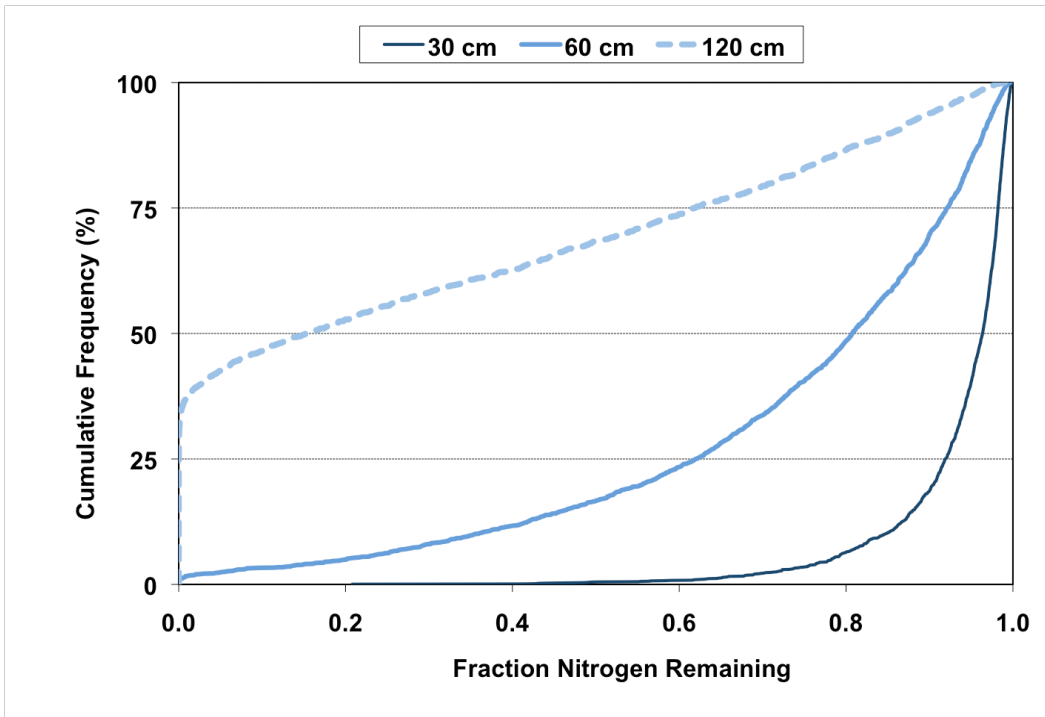


Figure VG-159. Cumulative Probability Graph: Sandy Clay Loam Soil, Mesic Temperature Region, Standard Effluent, HLR = 2 cm d⁻¹.

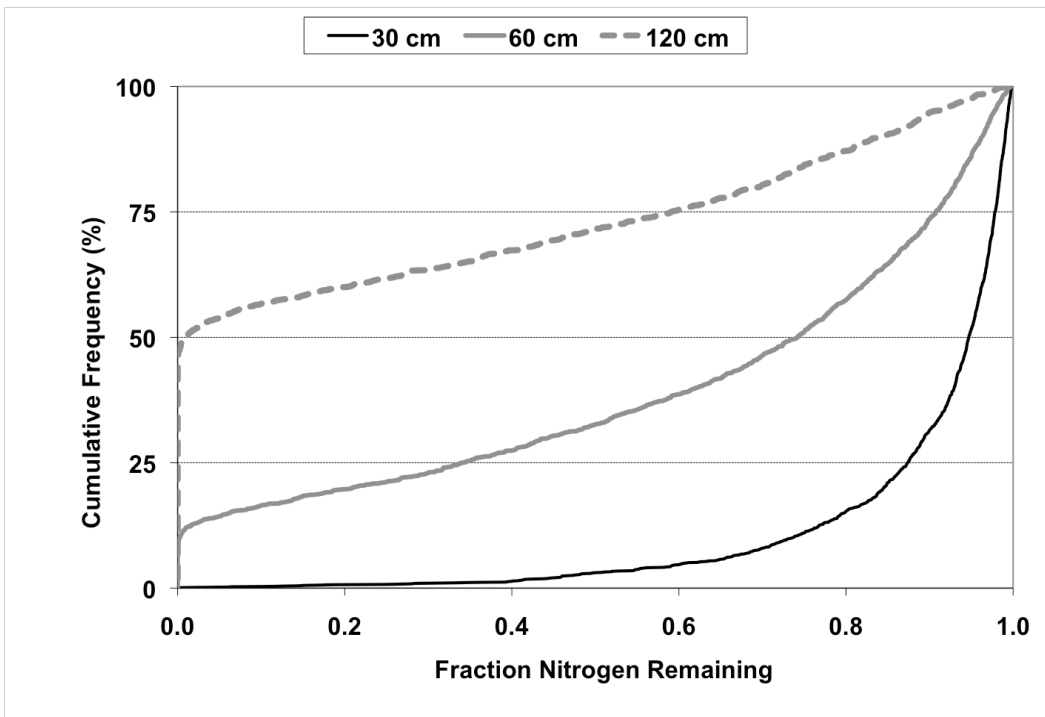


Figure VG-160. Cumulative Probability Graph: Sandy Clay Loam Soil, Mesic Temperature Region, Standard Effluent, HLR = 5% of K_{sat} .

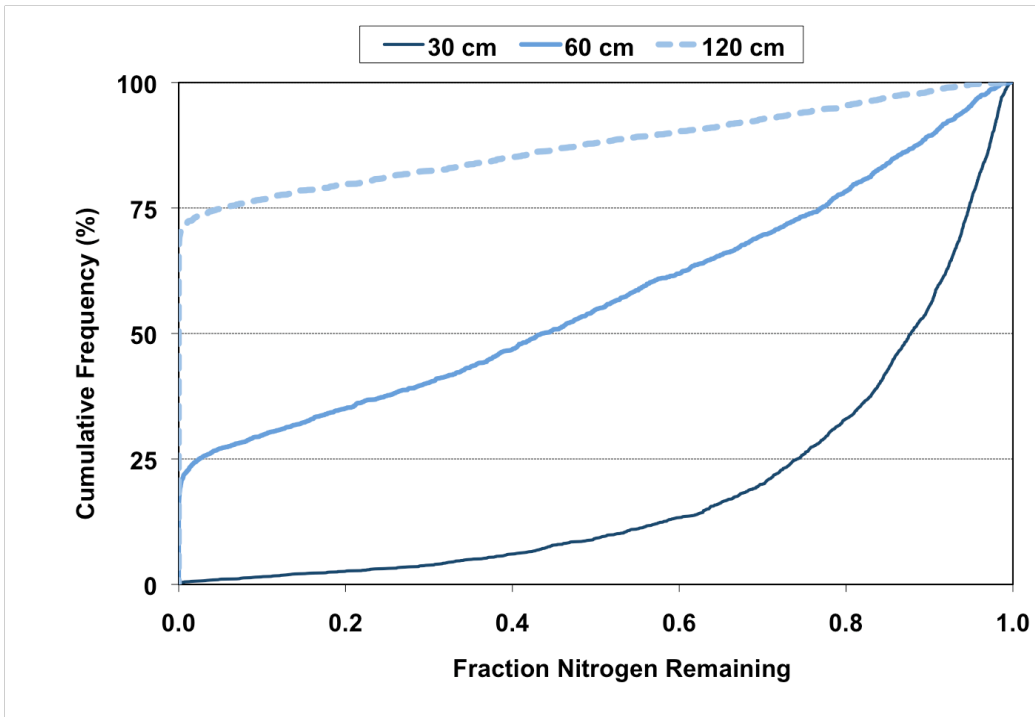


Figure VG-161. Cumulative Probability Graph: Sandy Clay Loam Soil, Thermic Temperature Region, Standard Effluent, HLR = 2 cm d⁻¹.

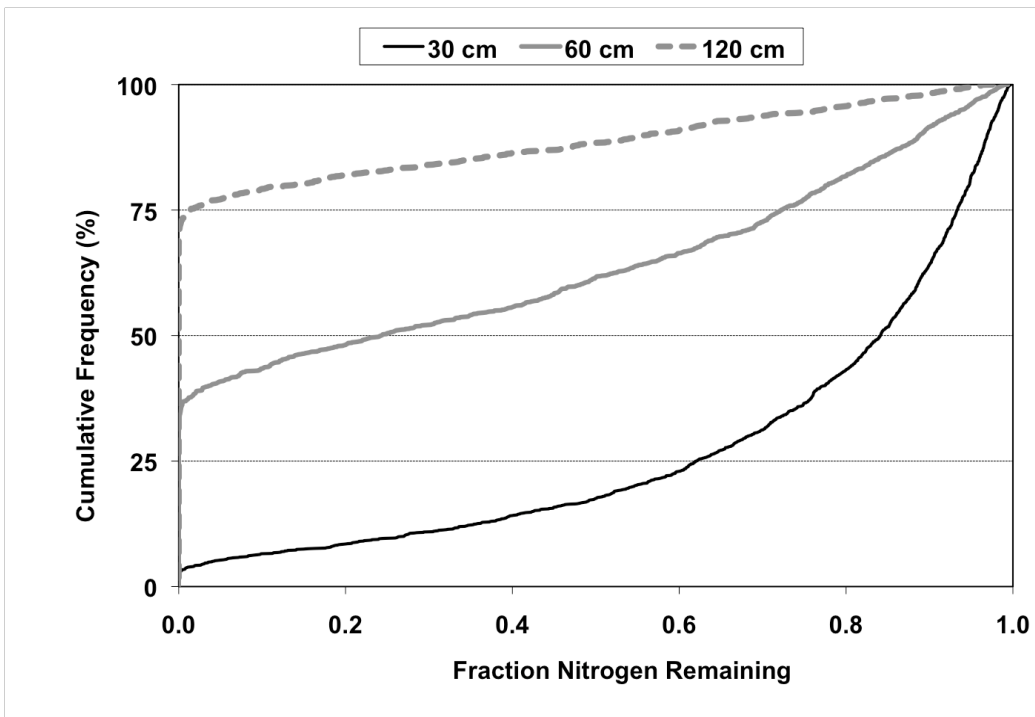


Figure VG-162. Cumulative Probability Graph: Sandy Clay Loam Soil, Thermic Temperature Region, Standard Effluent, HLR = 5% of K_{sat}.

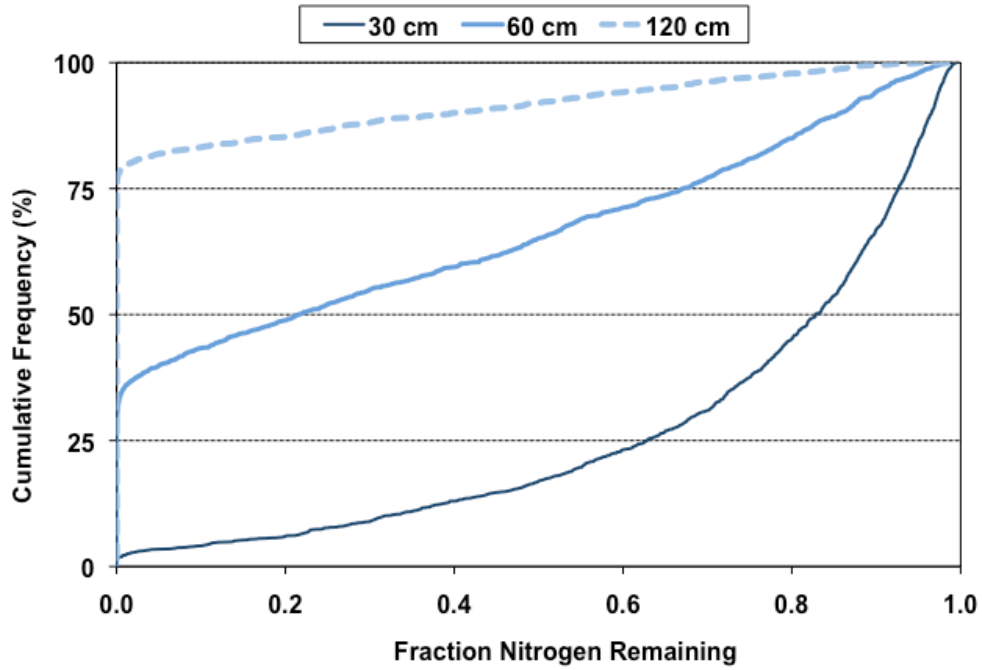


Figure VG-163. Cumulative Probability Graph: Sandy Clay Loam Soil, Hyperthermic Temperature Region, Standard Effluent, HLR = 2 cm d⁻¹.

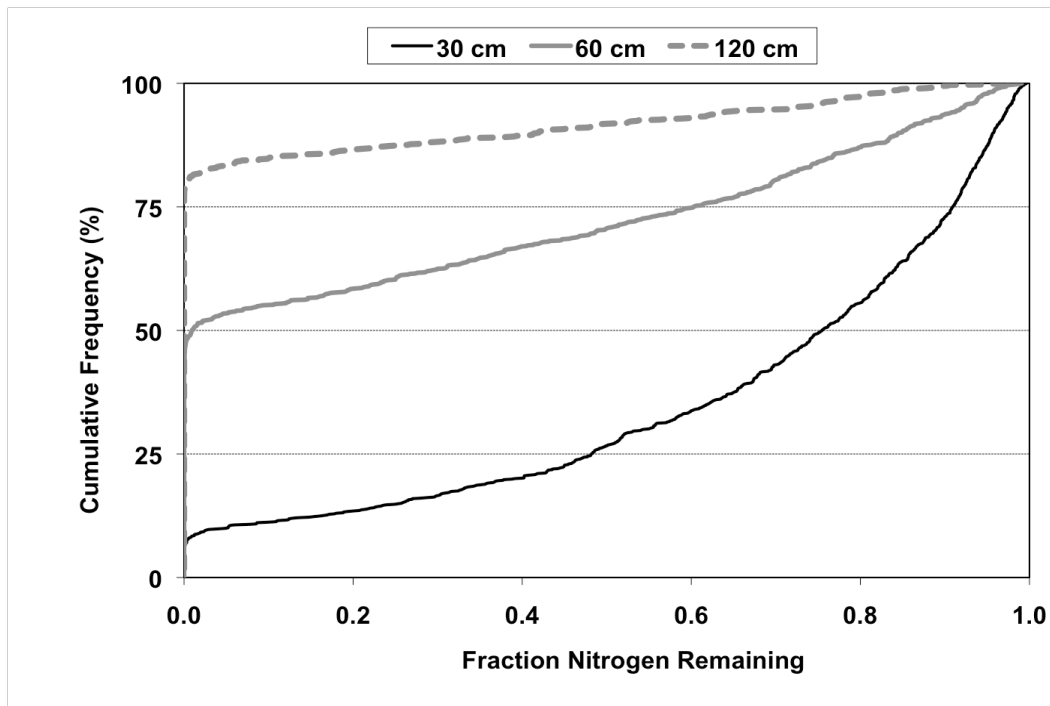


Figure VG-164. Cumulative Probability Graph: Sandy Clay Loam Soil, Hyperthermic Temperature Region, Standard Effluent, HLR = 5% of K_{sat} .

2.7.2 Nitrified Effluent

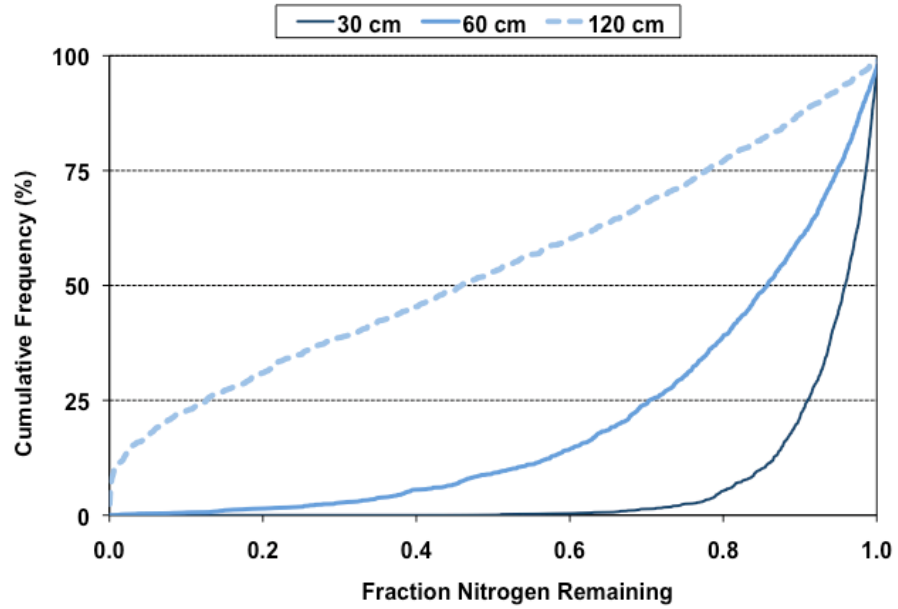


Figure VG-165. Cumulative Probability Graph: Sandy Clay Loam Soil, Frigid/Cryic Temperature Region, Nitrified Effluent, HLR = 2 cm d⁻¹.

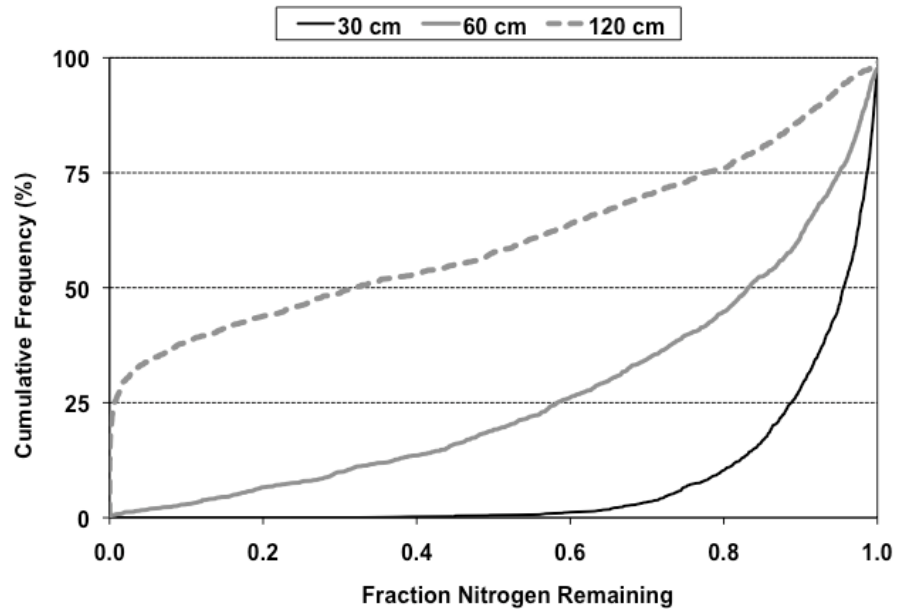


Figure VG-166. Cumulative Probability Graph: Sandy Clay Loam Soil, Frigid/Cryic Temperature Region, Nitrified Effluent, HLR = 5% of K_{sat} .

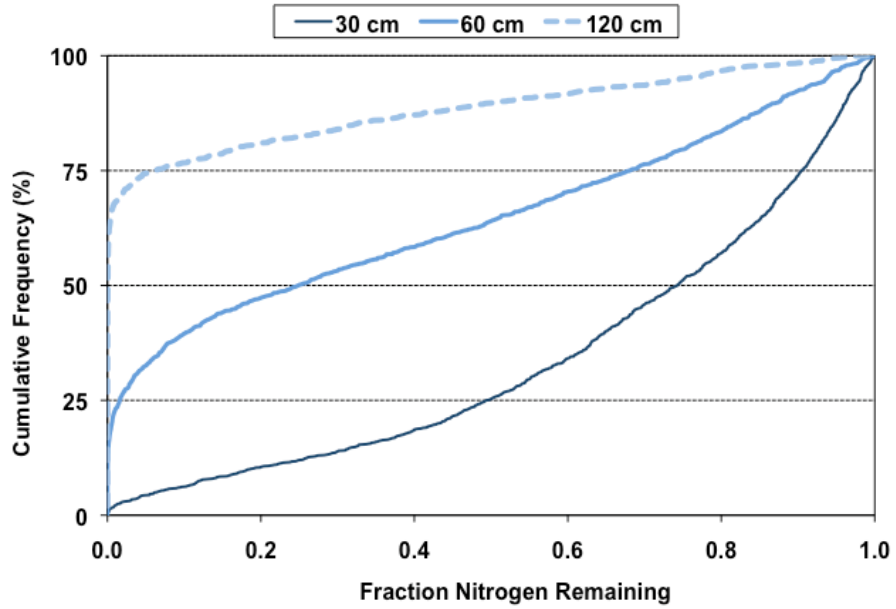


Figure VG-167. Cumulative Probability Graph: Sandy Clay Loam Soil, Mesic Temperature Region, Nitrified Effluent, HLR = 2 cm d⁻¹.

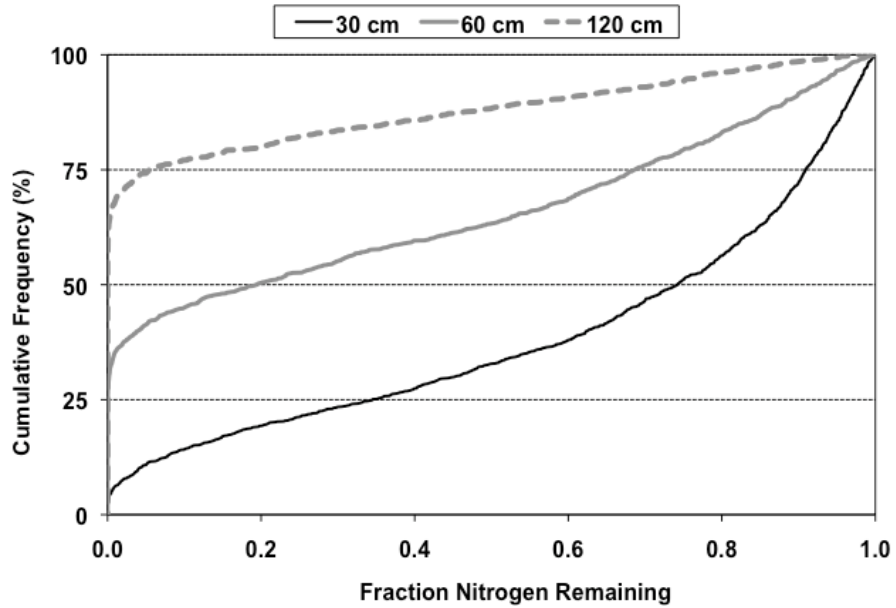


Figure VG-168. Cumulative Probability Graph: Sandy Clay Loam Soil, Mesic Temperature Region, Nitrified Effluent, HLR = 5% of K_{sat} .

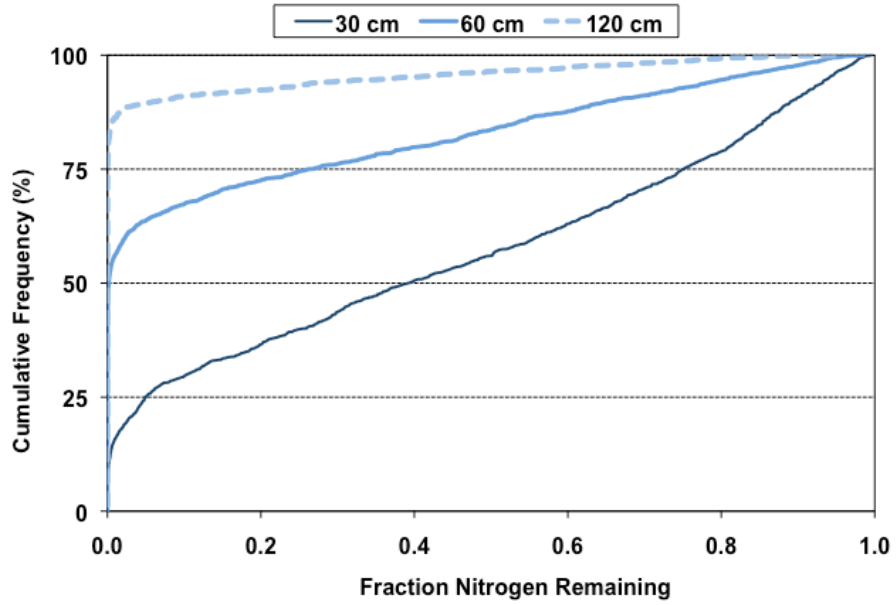


Figure VG-169. Cumulative Probability Graph: Sandy Clay Loam Soil, Thermic Temperature Region, Nitrified Effluent, HLR = 2 cm d⁻¹.

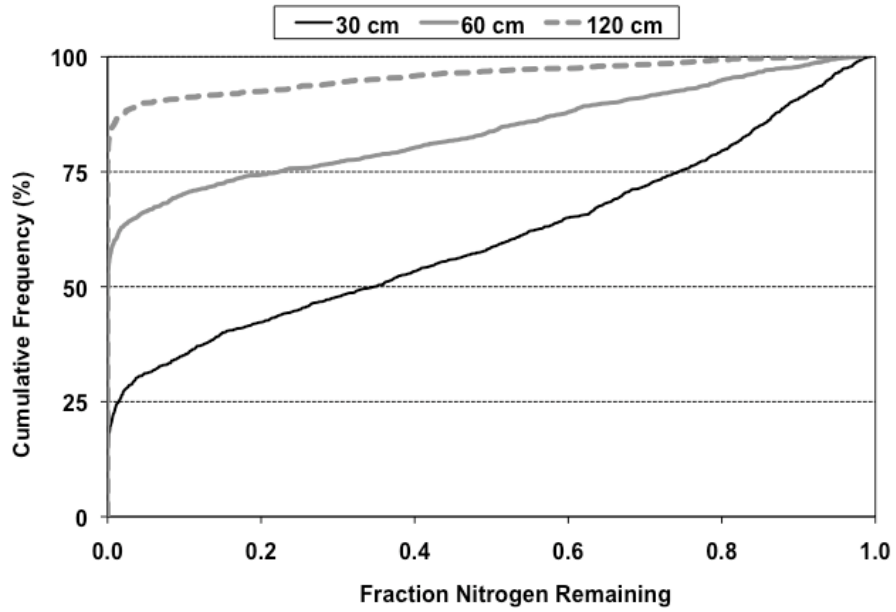


Figure VG-170. Cumulative Probability Graph: Sandy Clay Loam Soil, Thermic Temperature Region, Nitrified Effluent, HLR = 5% of K_{sat} .

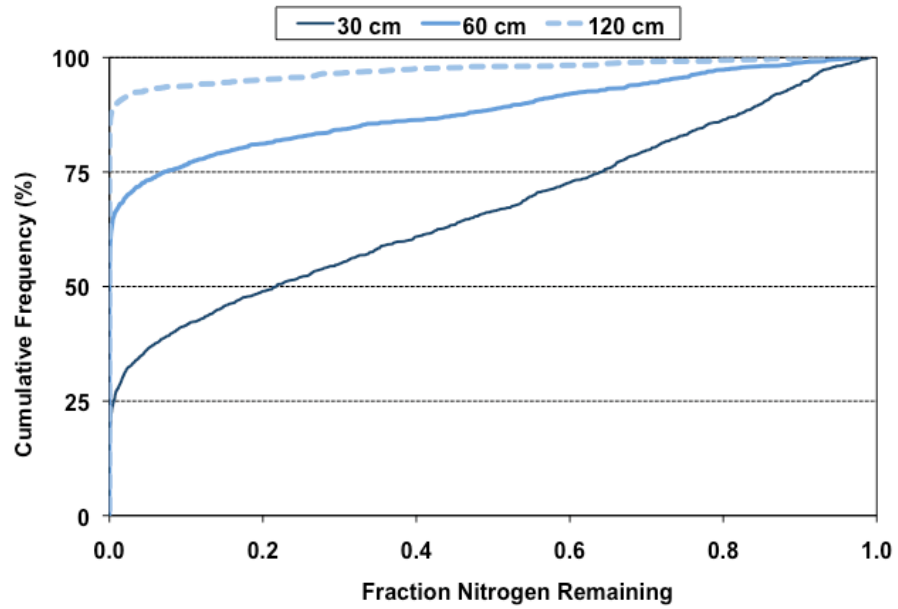


Figure VG-171. Cumulative Probability Graph: Sandy Clay Loam Soil, Hyperthermic Temperature Region, Nitrified Effluent, HLR = 2 cm d⁻¹.

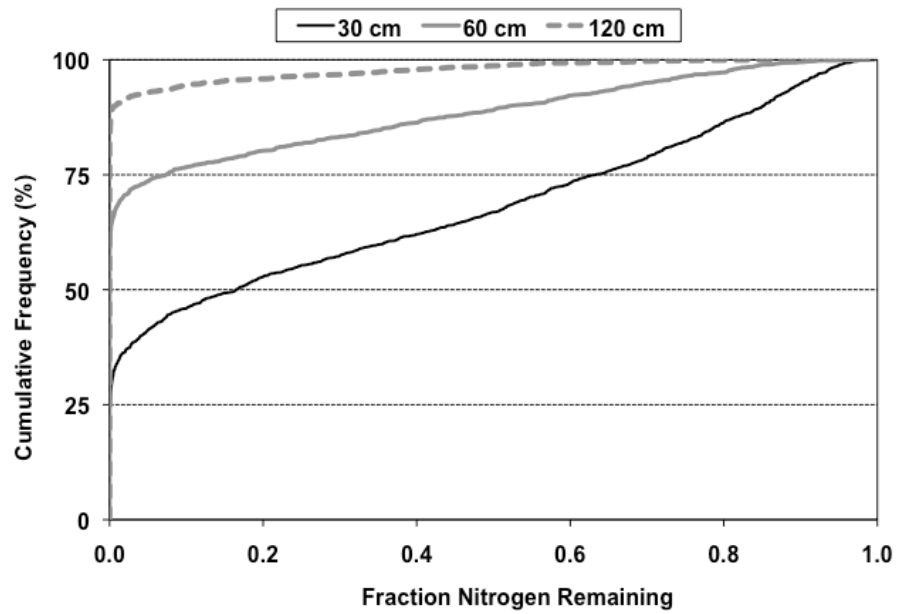


Figure VG-172. Cumulative Probability Graph: Sandy Clay Loam Soil, Hyperthermic Temperature Region, Nitrified Effluent, HLR = 5% of K_{sat} .

2.8 Sandy Loam

2.8.1 Standard Effluent

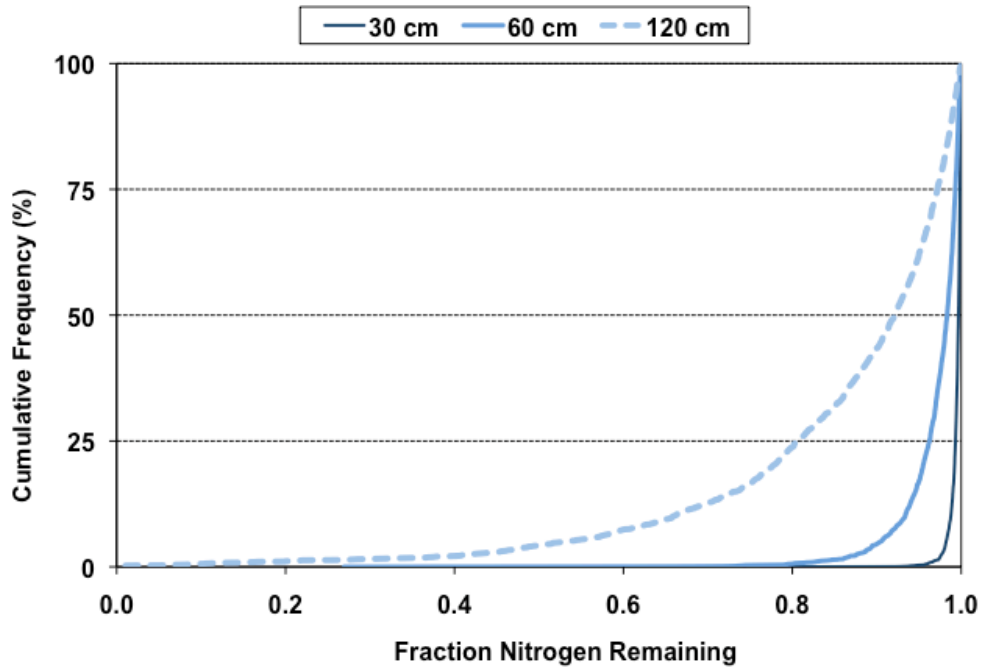


Figure VG-173. Cumulative Probability Graph: Sandy Loam Soil, Frigid/Cryic Temperature Region, Standard Effluent, HLR = 2 cm d⁻¹.

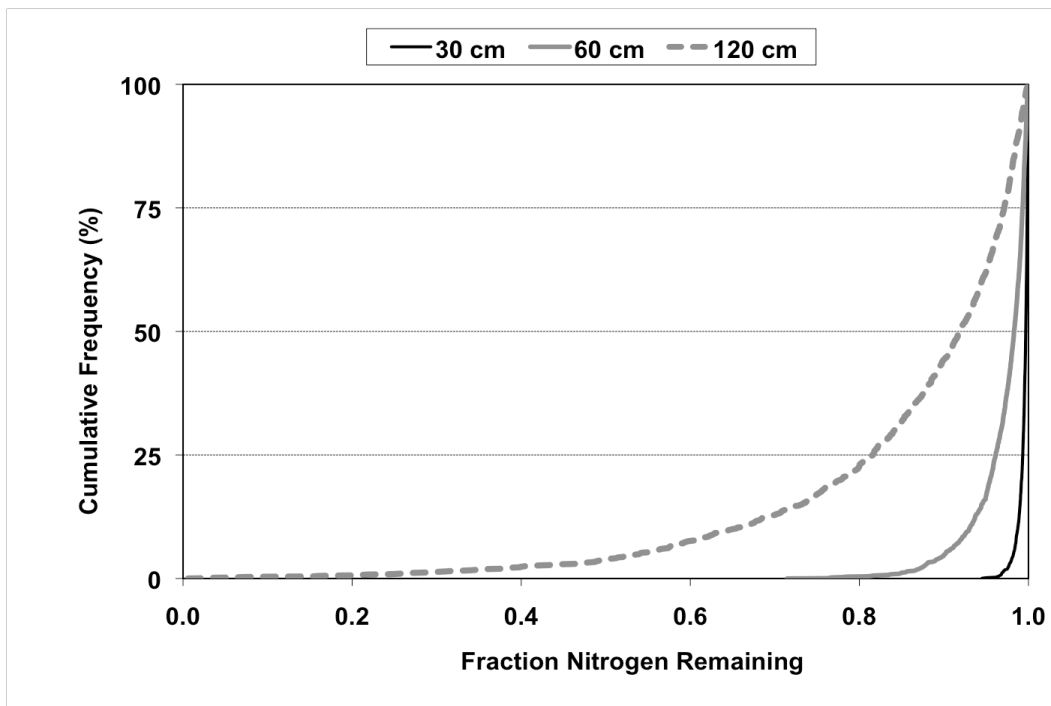


Figure VG-174. Cumulative Probability Graph: Sandy Loam Soil, Frigid/Cryic Temperature Region, Standard Effluent, HLR = 5% of K_{sat}.

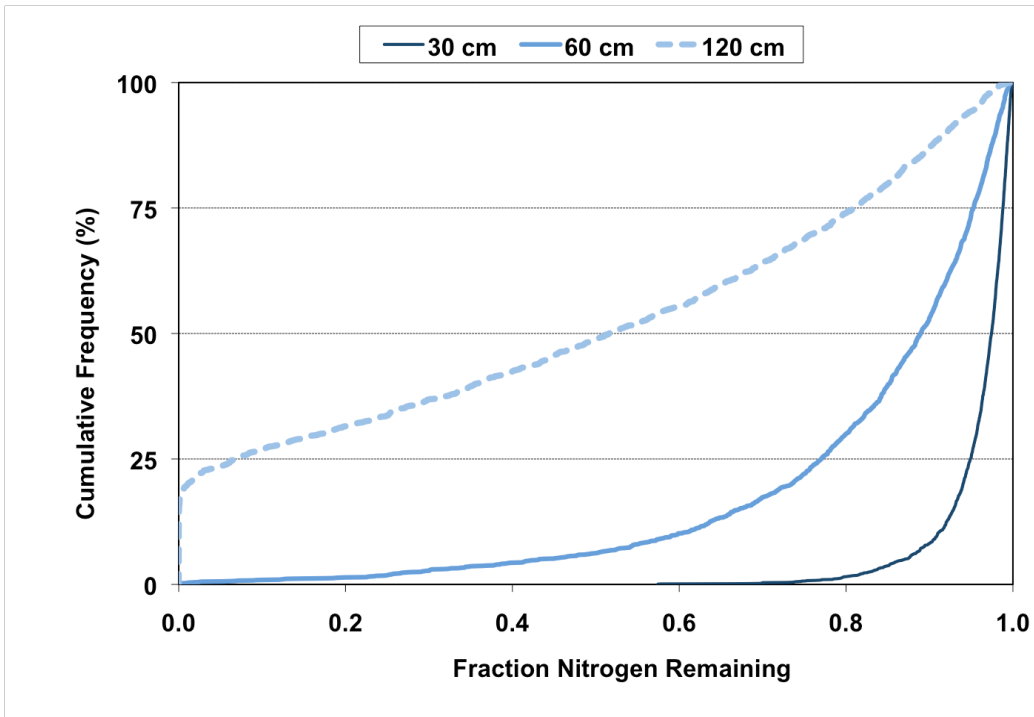


Figure VG-175. Cumulative Probability Graph: Sandy Loam Soil, Mesic Temperature Region, Standard Effluent, HLR = 2 cm d⁻¹.

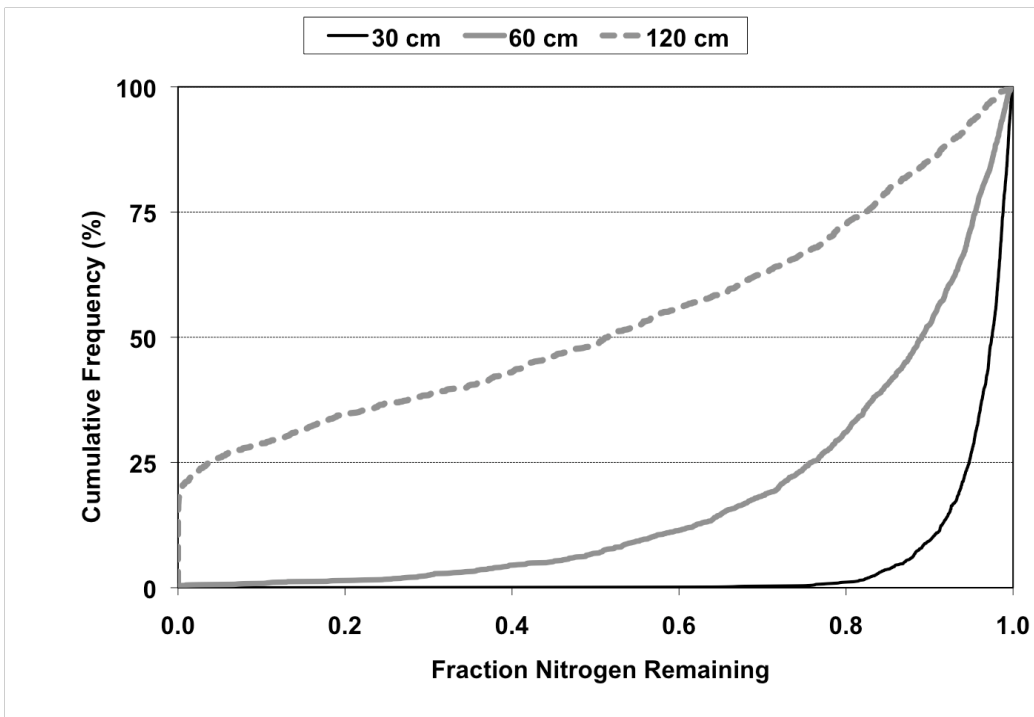


Figure VG-176. Cumulative Probability Graph: Sandy Loam Soil, Mesic Temperature Region, Standard Effluent, HLR = 5% of K_{sat}.

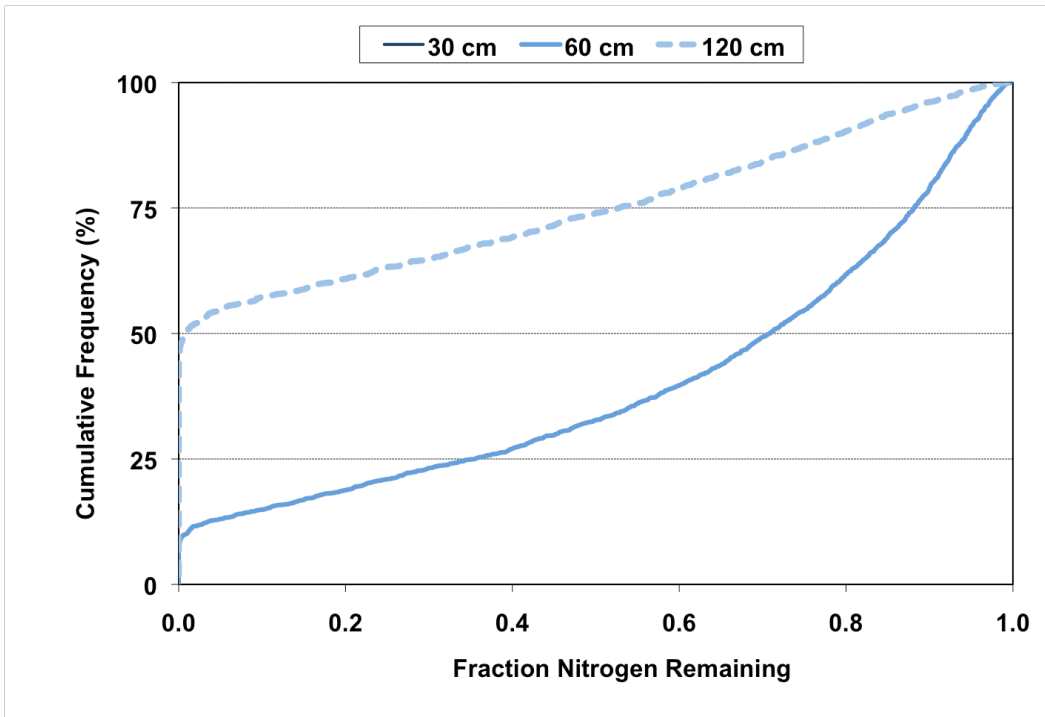


Figure VG-177. Cumulative Probability Graph: Sandy Loam Soil, Thermic Temperature Region, Standard Effluent, HLR = 2 cm d⁻¹.

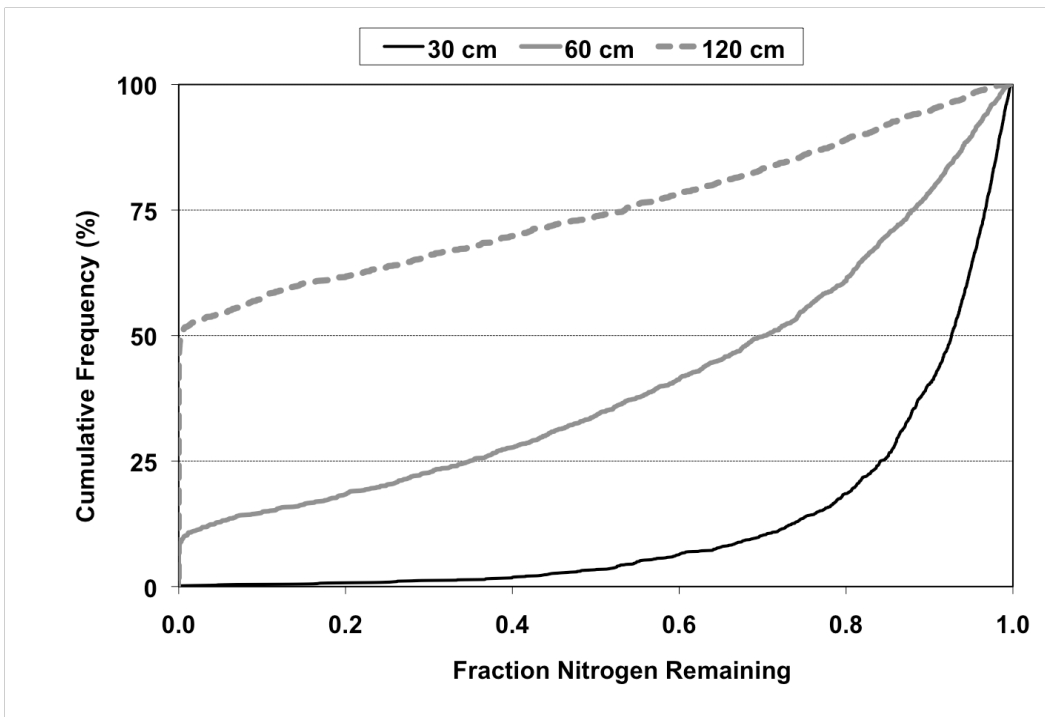


Figure VG-178. Cumulative Probability Graph: Sandy Loam Soil, Thermic Temperature Region, Standard Effluent, HLR = 5% of K_{sat}.

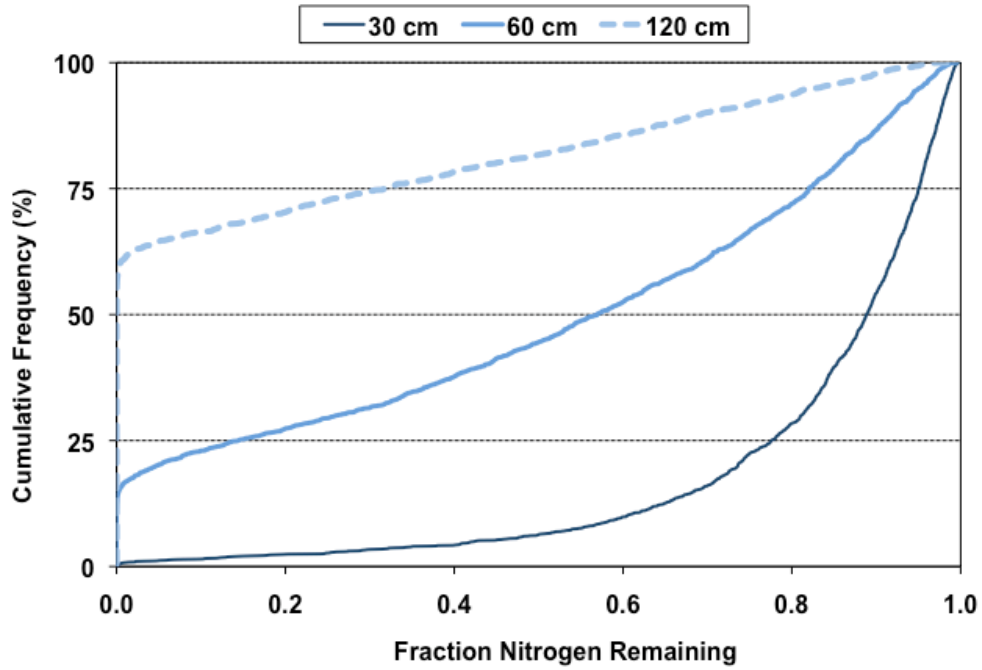


Figure VG-179. Cumulative Probability Graph: Sandy Loam Soil, Hyperthermic Temperature Region, Standard Effluent, HLR = 2 cm d⁻¹.

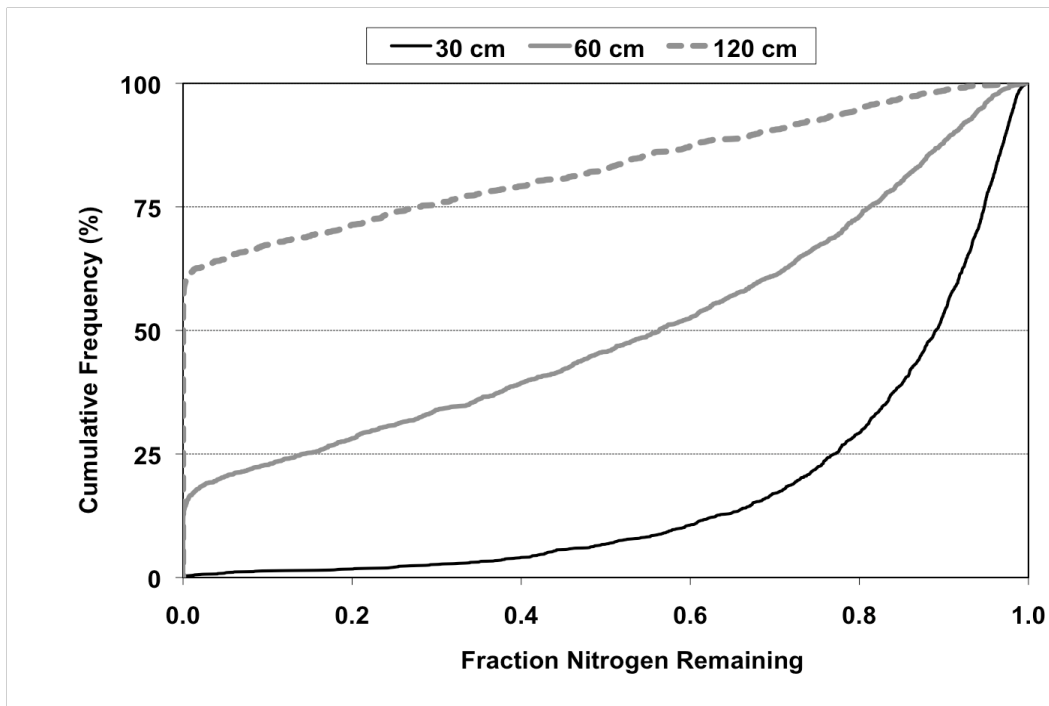


Figure VG-180. Cumulative Probability Graph: Sandy Loam Soil, Hyperthermic Temperature Region, Standard Effluent, HLR = 5% of K_{sat}.

2.8.2 Nitrified Effluent

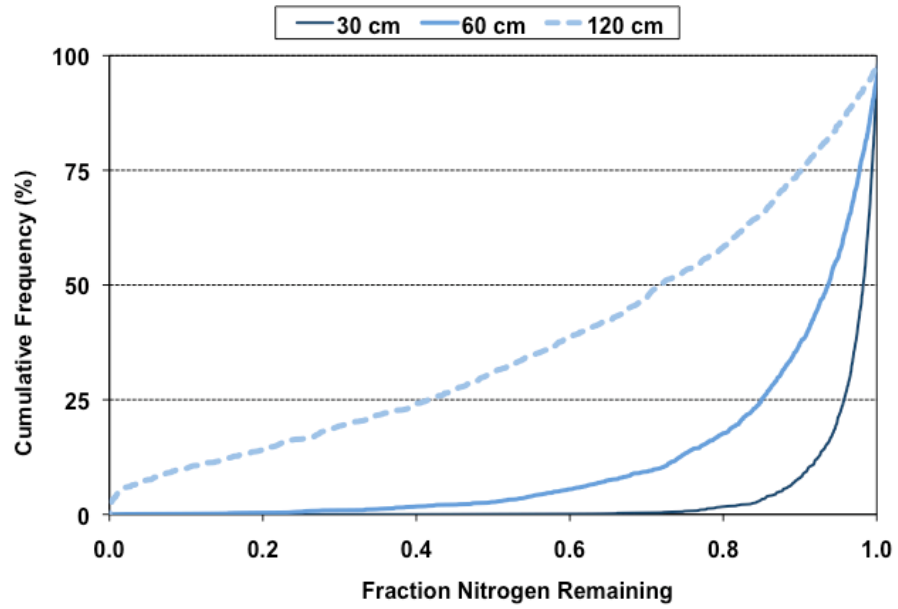


Figure VG-181. Cumulative Probability Graph: Sandy Loam Soil, Frigid/Cryic Temperature Region, Nitrified Effluent, HLR = 2 cm d⁻¹.

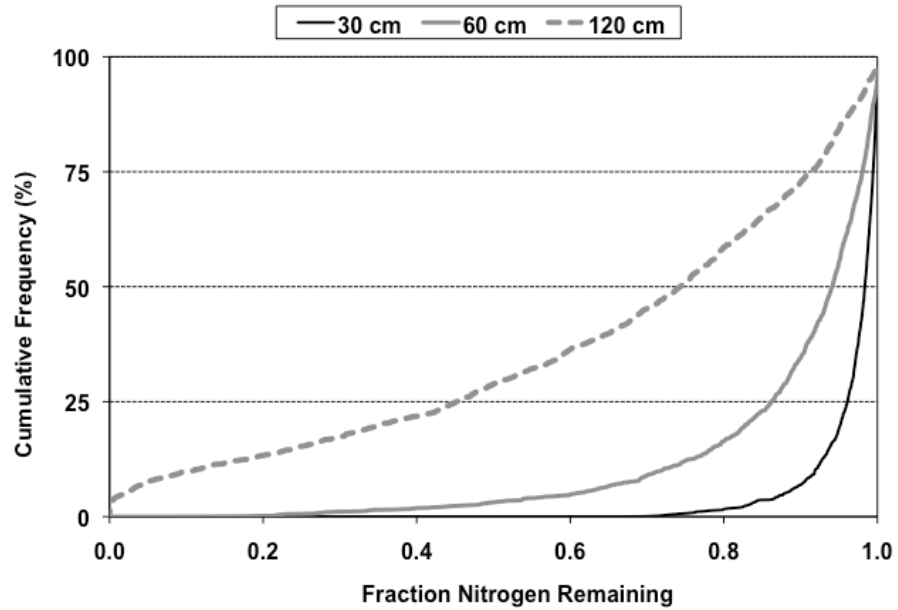


Figure VG-182. Cumulative Probability Graph: Sandy Loam Soil, Frigid/Cryic Temperature Region, Nitrified Effluent, HLR = 5% of K_{sat} .

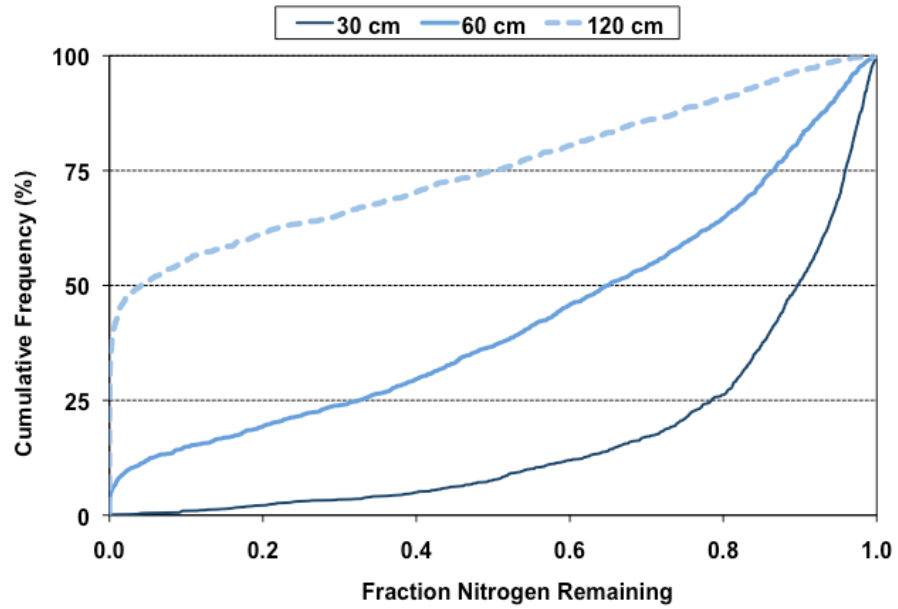


Figure VG-183. Cumulative Probability Graph: Sandy Loam Soil, Mesic Temperature Region, Nitrified Effluent, HLR = 2 cm d⁻¹.

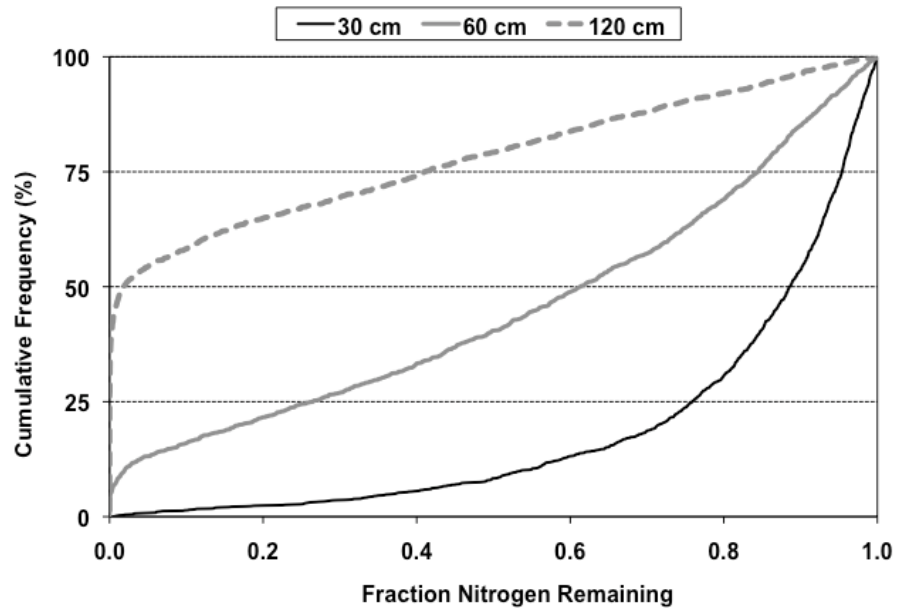


Figure VG-184. Cumulative Probability Graph: Sandy Loam Soil, Mesic Temperature Region, Nitrified Effluent, HLR = 5% of K_{sat} .

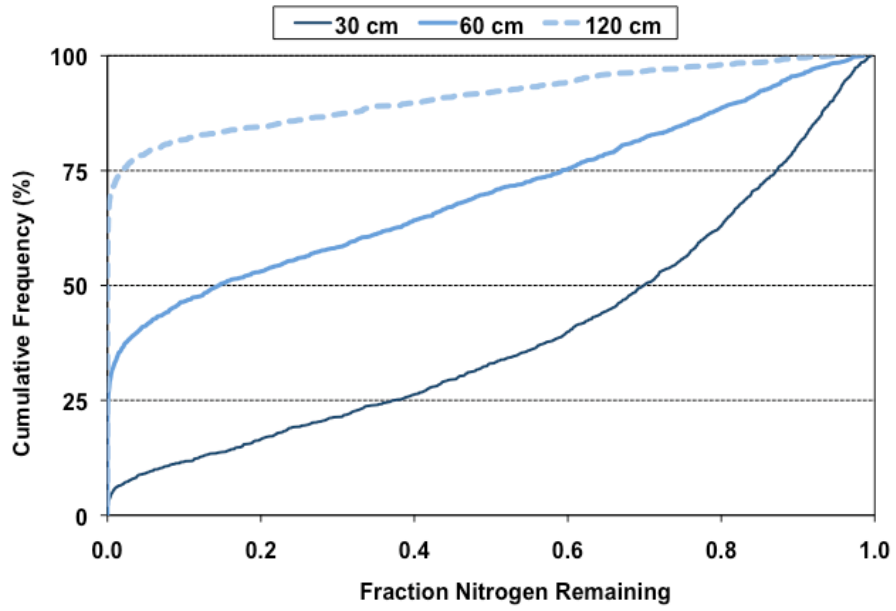


Figure VG-185. Cumulative Probability Graph: Sandy Loam Soil, Thermic Temperature Region, Nitrified Effluent, HLR = 2 cm d⁻¹.

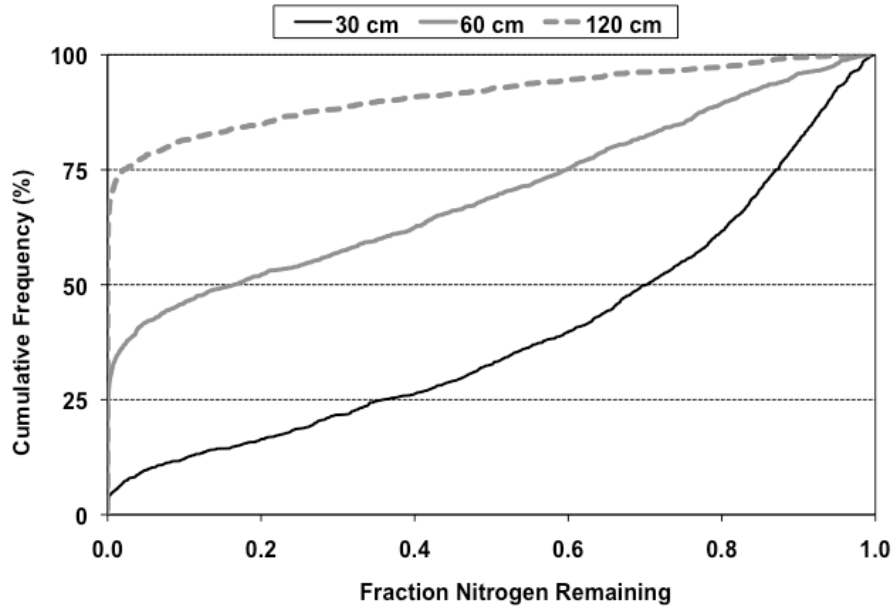


Figure VG-186. Cumulative Probability Graph: Sandy Loam Soil, Thermic Temperature Region, Nitrified Effluent, HLR = 5% of K_{sat} .

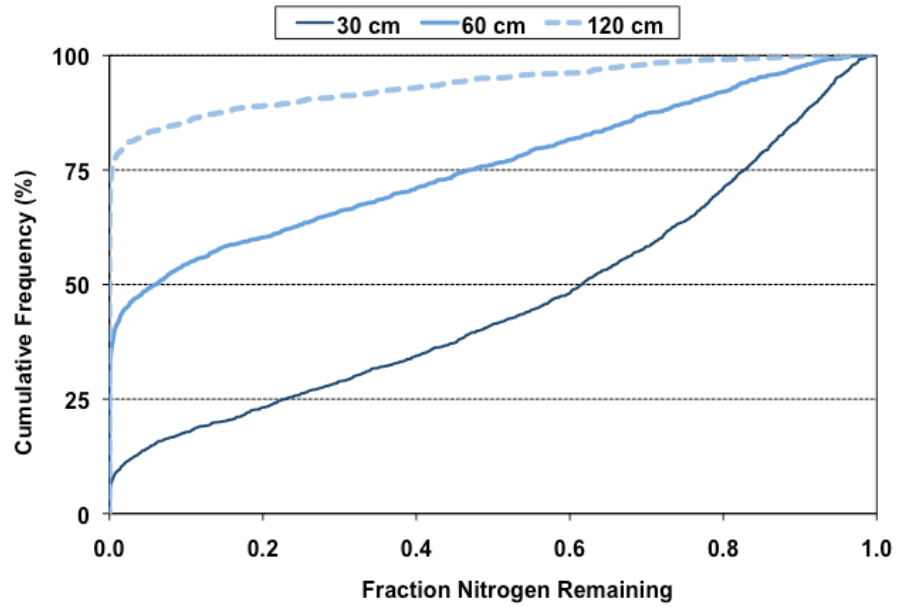


Figure VG-187. Cumulative Probability Graph: Sandy Loam Soil, Hyperthermic Temperature Region, Nitrified Effluent, HLR = 2 cm d⁻¹.

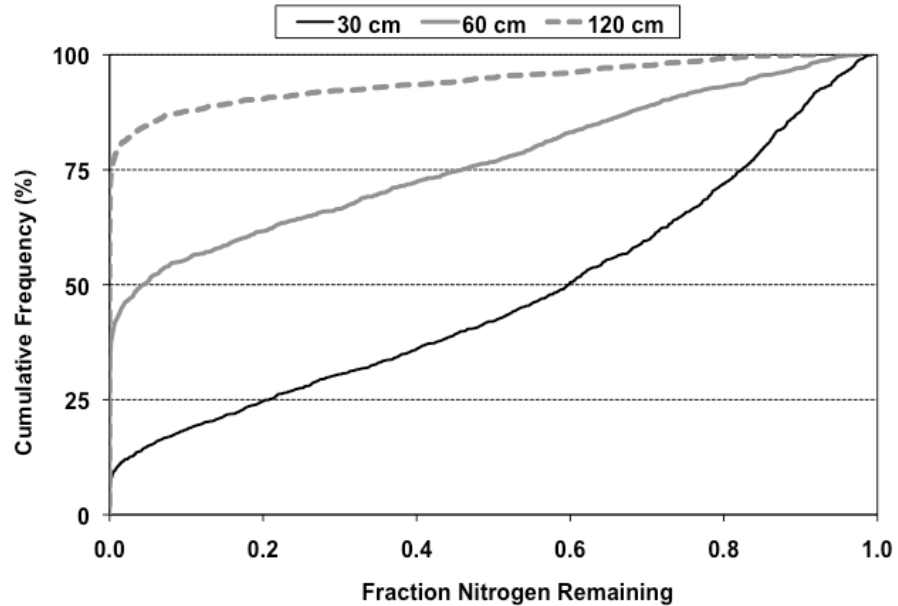


Figure VG-188. Cumulative Probability Graph: Sandy Loam Soil, Hyperthermic Temperature Region, Nitrified Effluent, HLR = 5% of K_{sat} .

2.9 Silt

2.9.1 Standard Effluent

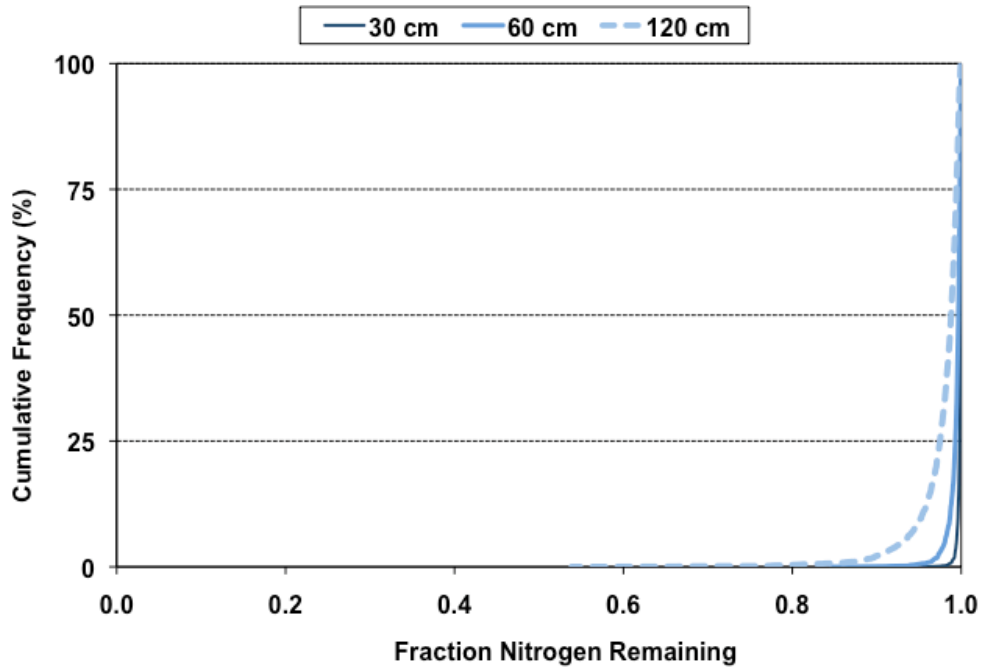


Figure VG-189. Cumulative Probability Graph: Silty Soil, Frigid/Cryic Temperature Region, Standard Effluent, HLR = 2 cm d⁻¹.

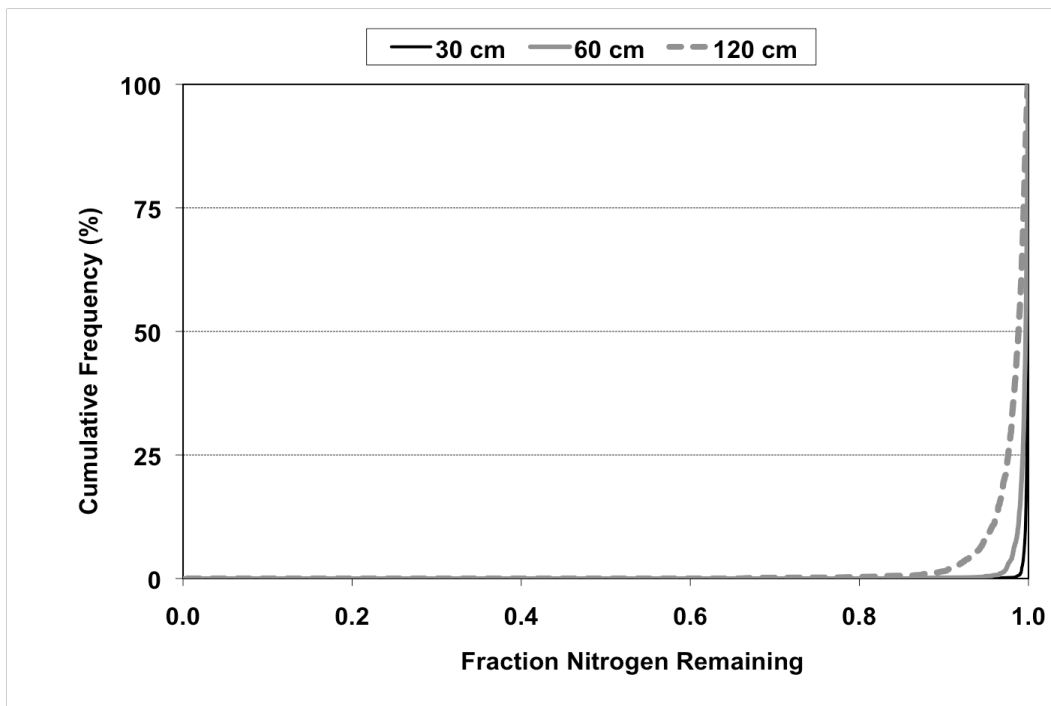


Figure VG-190. Cumulative Probability Graph: Silty Soil, Frigid/Cryic Temperature Region, Standard Effluent, HLR = 5% of K_{sat} .

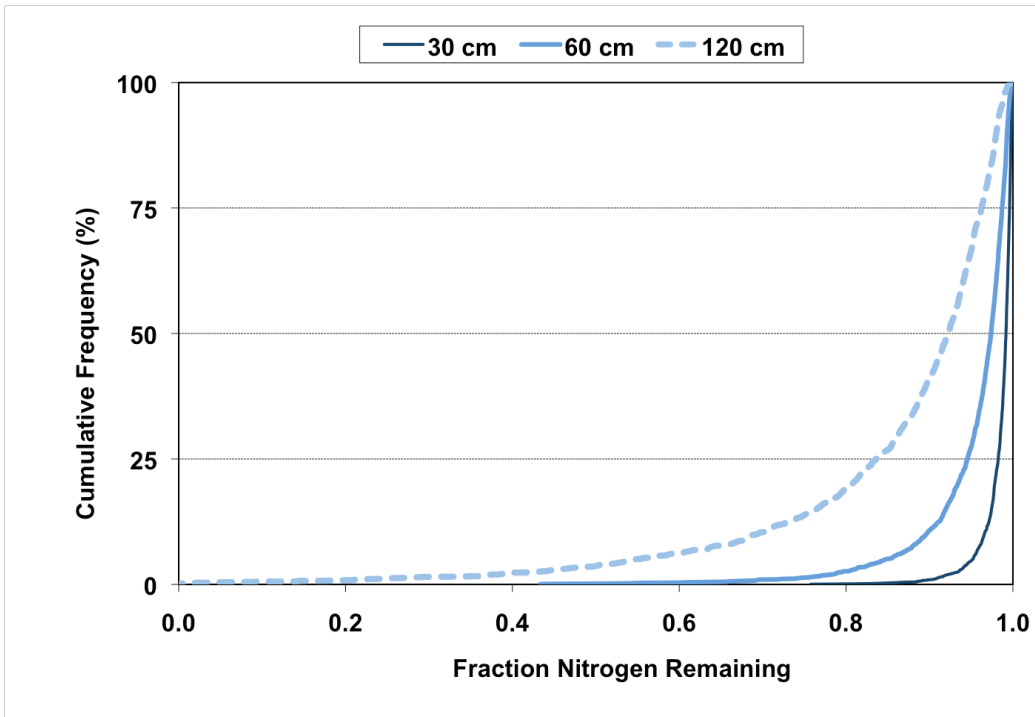


Figure VG-191. Cumulative Probability Graph: Silty Soil, Mesic Temperature Region, Standard Effluent, HLR = 2 cm d⁻¹.

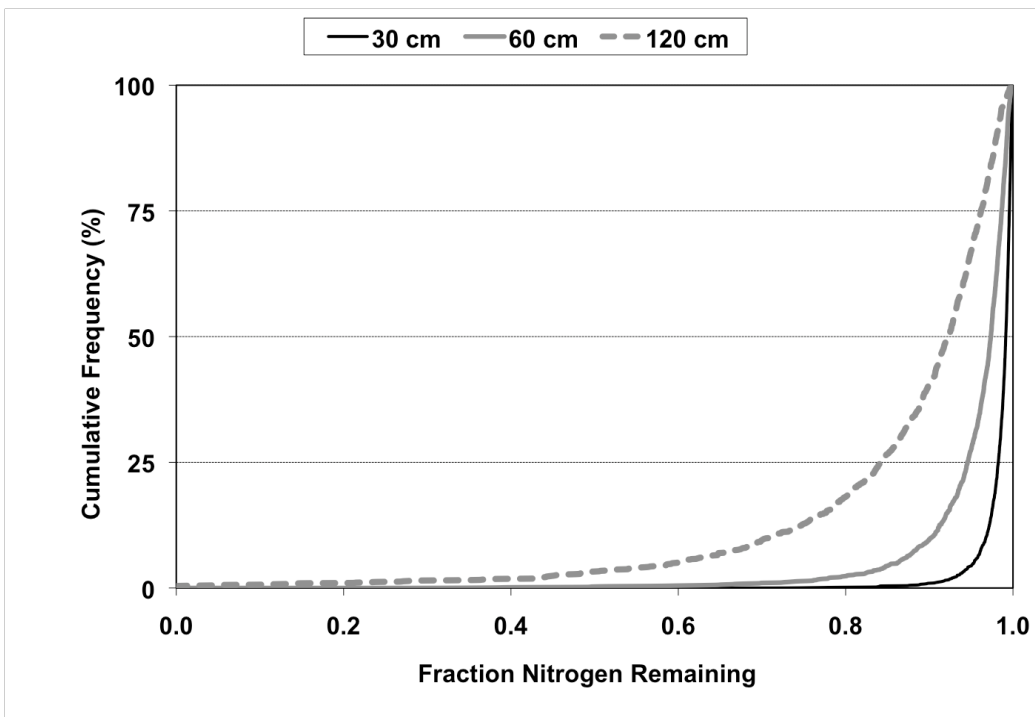


Figure VG-192. Cumulative Probability Graph: Silty Soil, Mesic Temperature Region, Standard Effluent, HLR = 5% of K_{sat} .

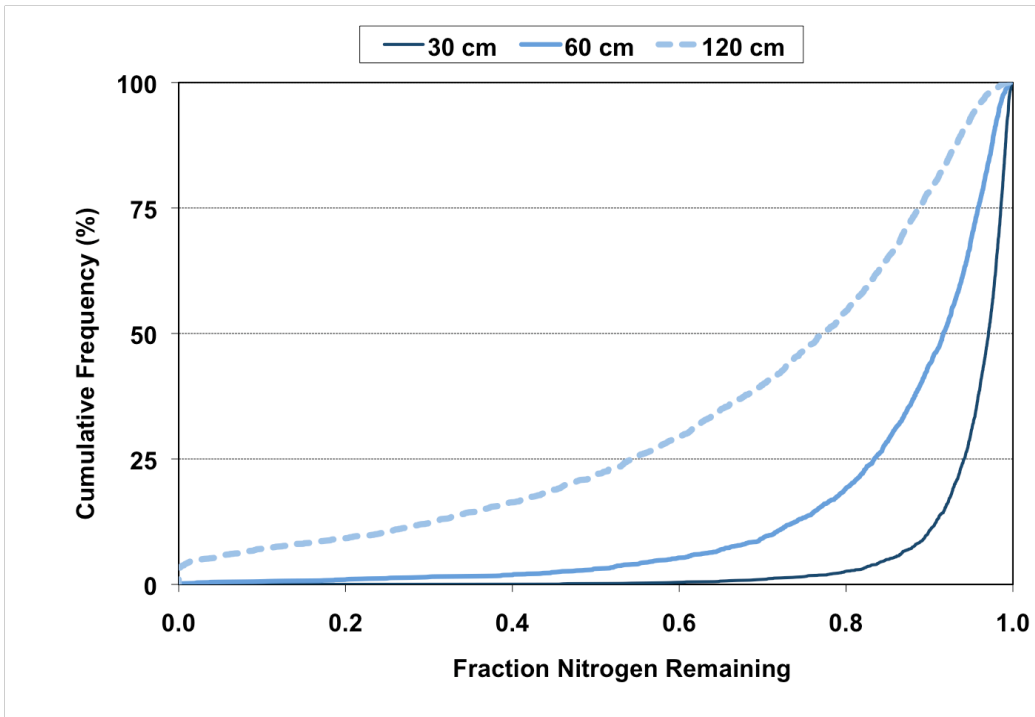


Figure VG-193. Cumulative Probability Graph: Silty Soil, Thermic Temperature Region, Standard Effluent, HLR = 2 cm d⁻¹.

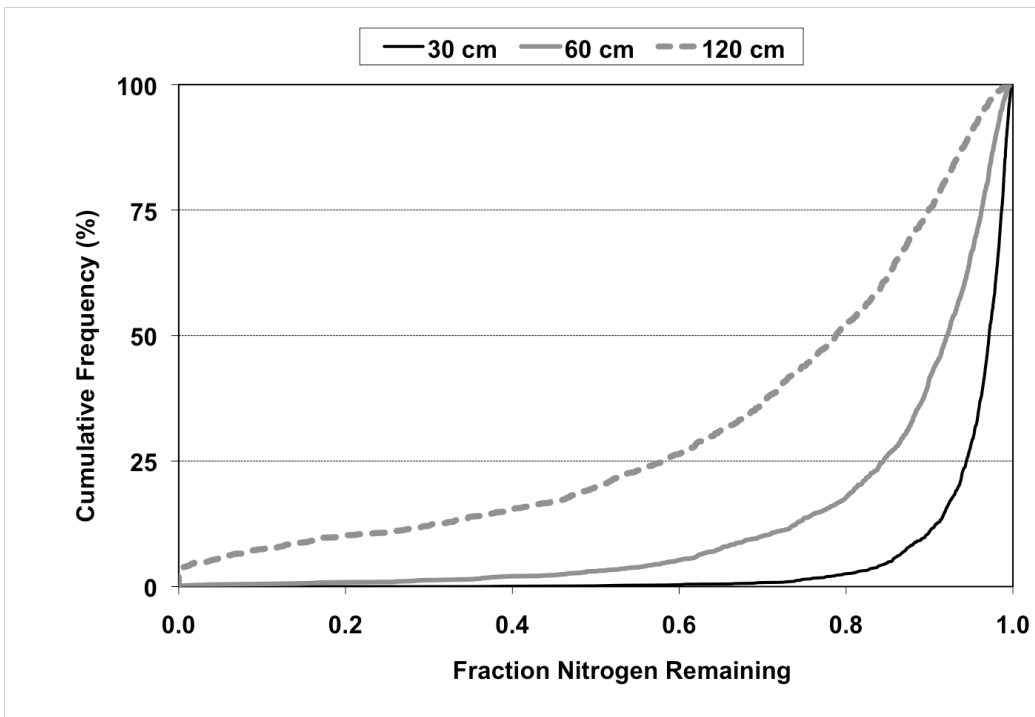


Figure VG-194. Cumulative Probability Graph: Silty Soil, Thermic Temperature Region, Standard Effluent, HLR = 5% of K_{sat}.

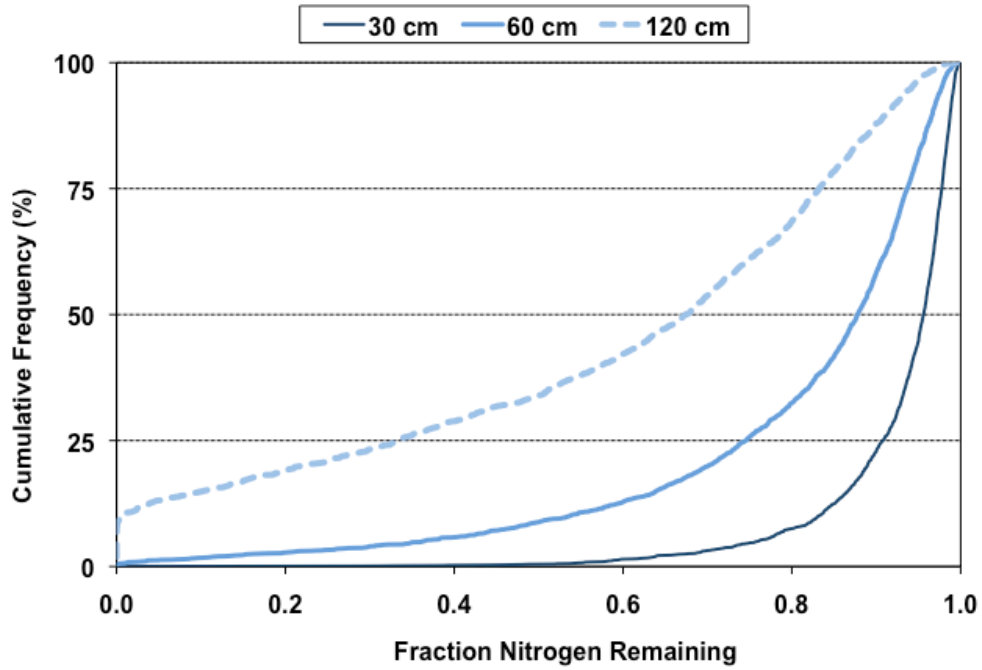


Figure VG-195. Cumulative Probability Graph: Silty Soil, Hyperthermic Temperature Region, Standard Effluent, HLR = 2 cm d⁻¹.

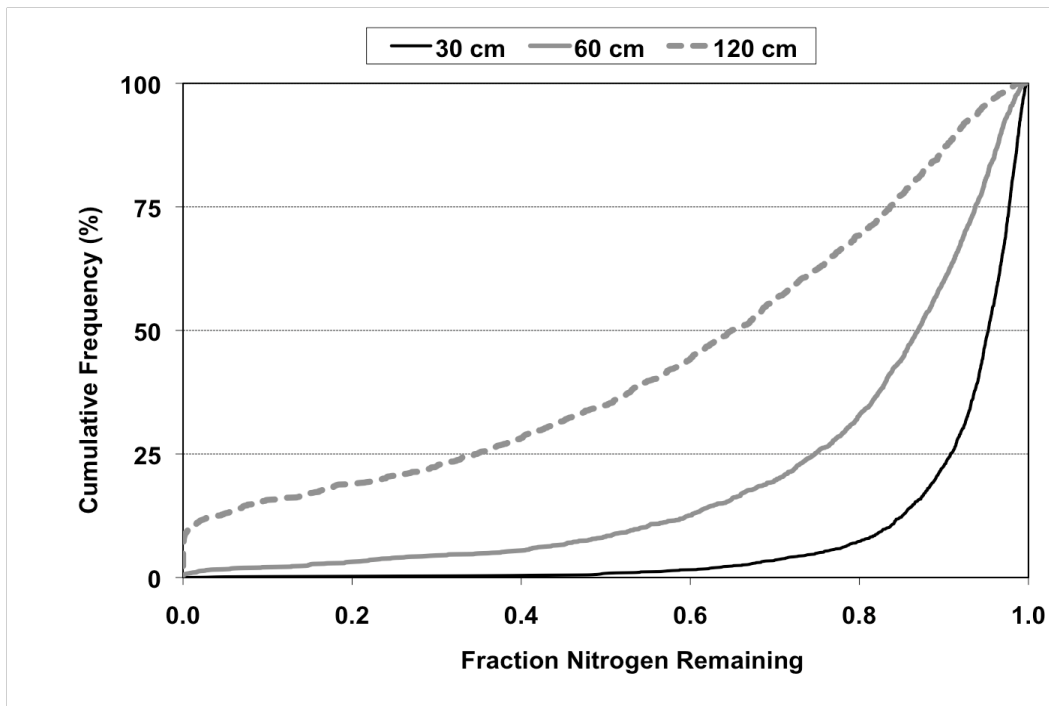


Figure VG-196. Cumulative Probability Graph: Silty Soil, Hyperthermic Temperature Region, Standard Effluent, HLR = 5% of K_{sat}.

2.9.2 Nitrified Effluent

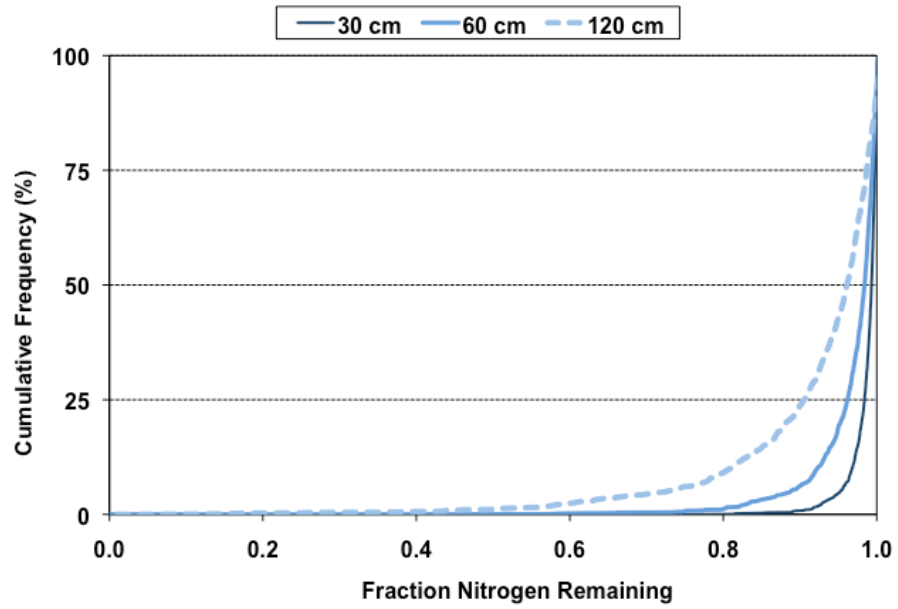


Figure VG-197. Cumulative Probability Graph: Silty Soil, Frigid/Cryic Temperature Region, Nitrified Effluent, HLR = 2 cm d⁻¹.

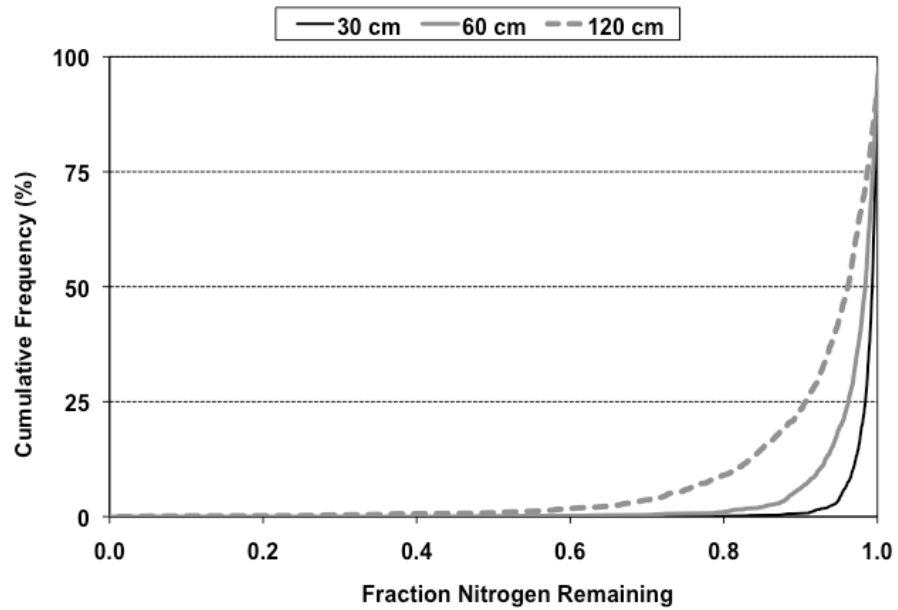


Figure VG-198. Cumulative Probability Graph: Silty Soil, Frigid/Cryic Temperature Region, Nitrified Effluent, HLR = 5% of K_{sat}.

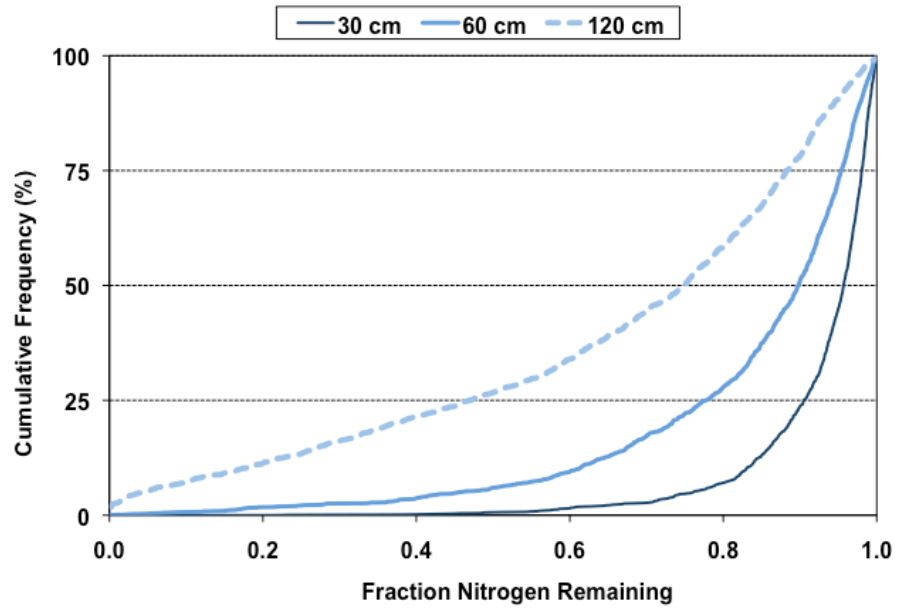


Figure VG-199. Cumulative Probability Graph: Silt Soil, Mesic Temperature Region, Nitrified Effluent, HLR = 2 cm d⁻¹.

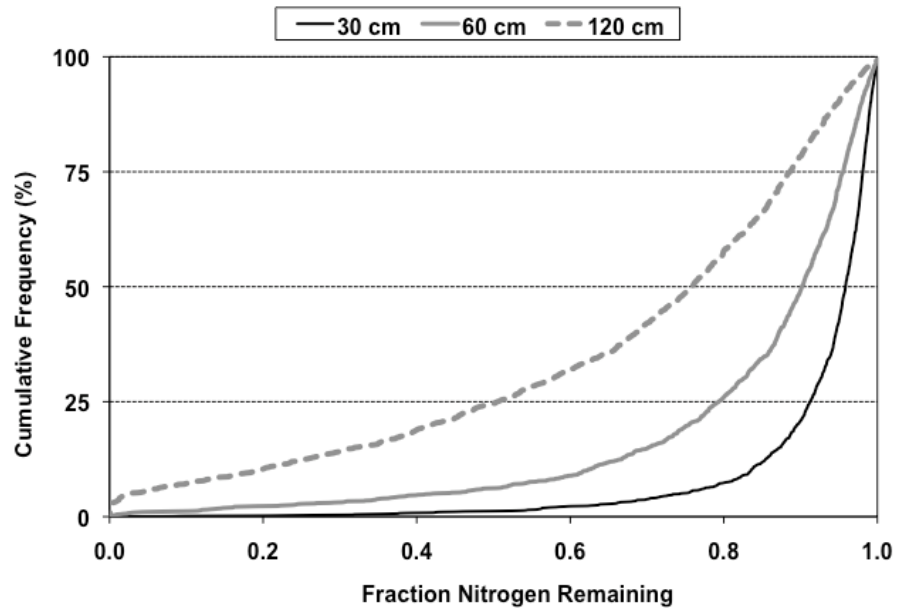


Figure VG-200. Cumulative Probability Graph: Silty Soil, Mesic Temperature Region, Nitrified Effluent, HLR = 5% of K_{sat}.

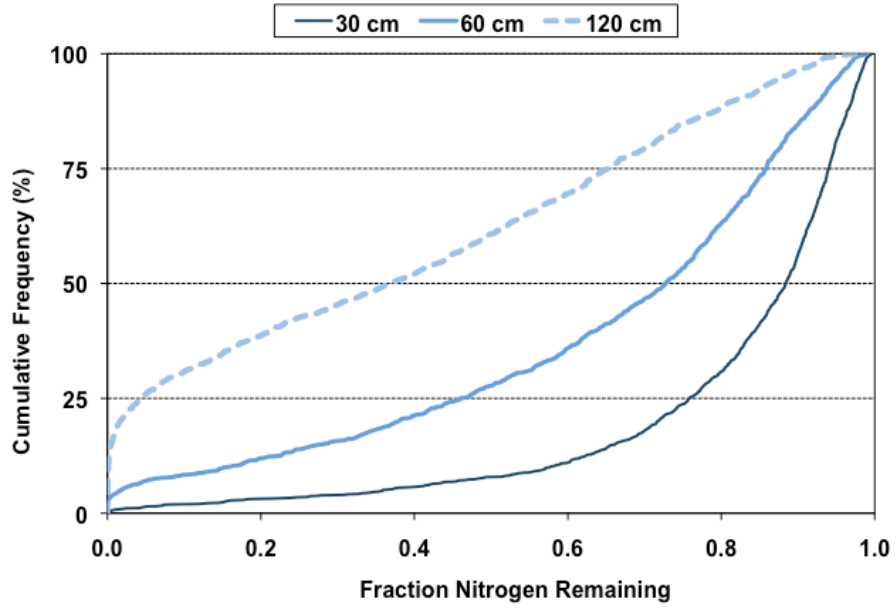


Figure VG-201. Cumulative Probability Graph: Silty Soil, Thermic Temperature Region, Nitrified Effluent, HLR = 2 cm d⁻¹.

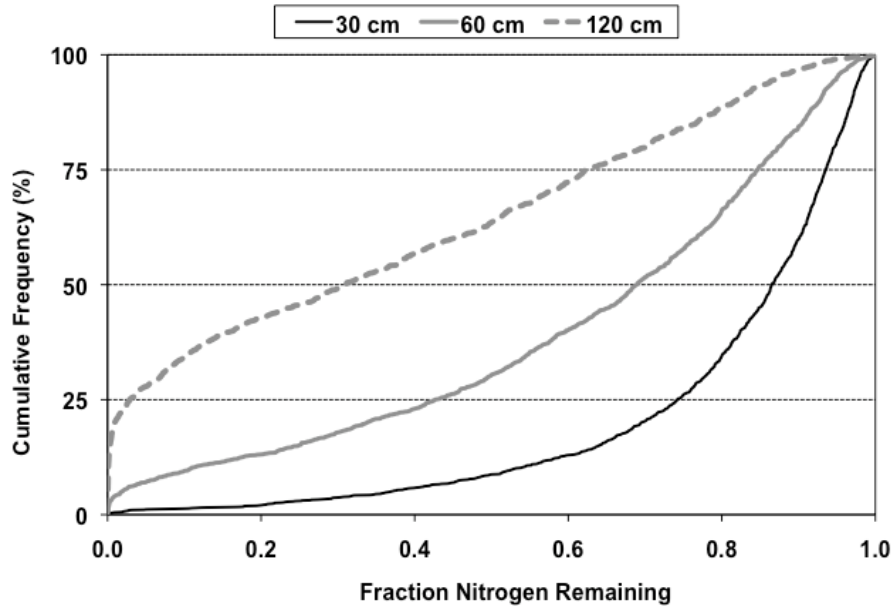


Figure VG-202. Cumulative Probability Graph: Silty Soil, Thermic Temperature Region, Nitrified Effluent, HLR = 5% of K_{sat}.

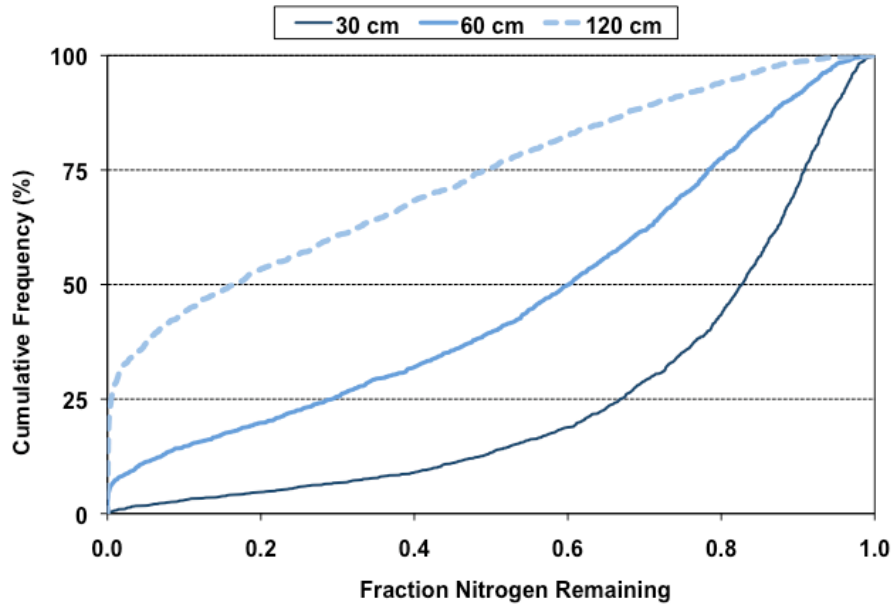


Figure VG-203. Cumulative Probability Graph: Silty Soil, Hyperthermic Temperature Region, Nitrified Effluent, HLR = 2 cm d⁻¹.

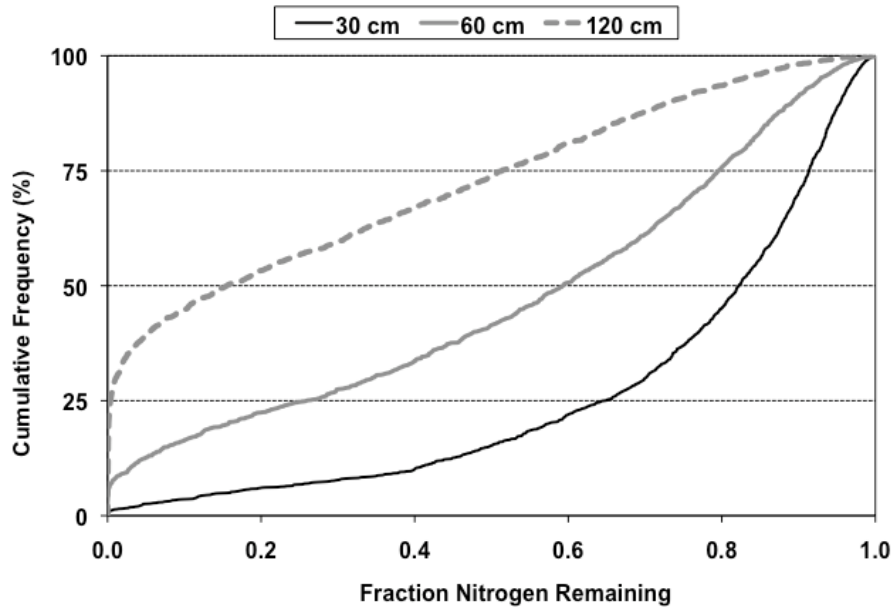


Figure VG-204. Cumulative Probability Graph: Silty Soil, Hyperthermic Temperature Region, Nitrified Effluent, HLR = 5% of K_{sat}.

2.10 Silty Clay

2.10.1 Standard Effluent

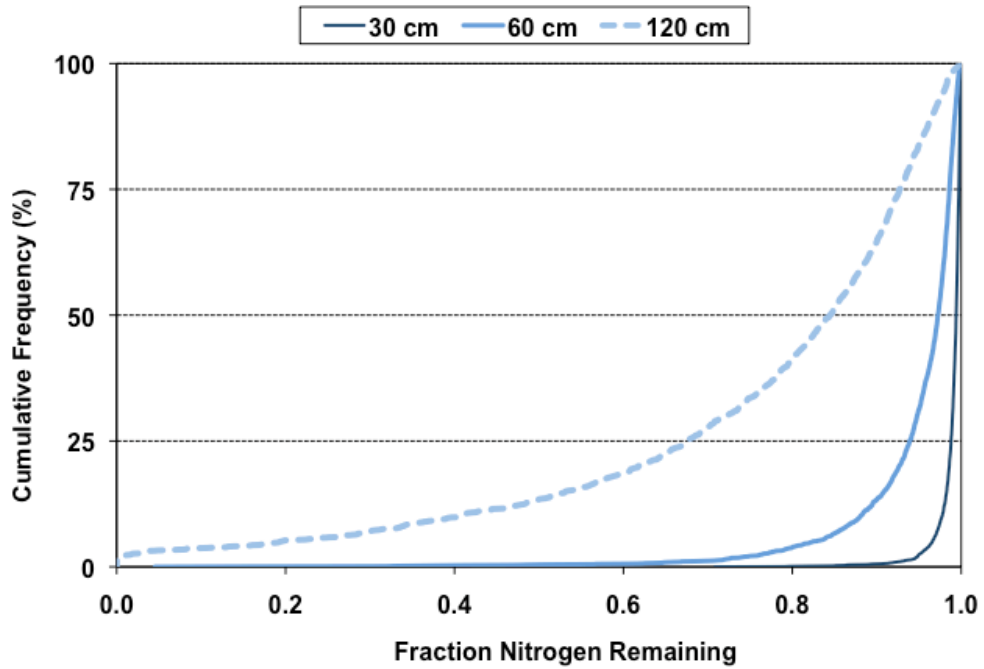


Figure VG-205. Cumulative Probability Graph: Silty Clay Soil, Frigid/Cryic Temperature Region, Standard Effluent, HLR = 2 cm d⁻¹.

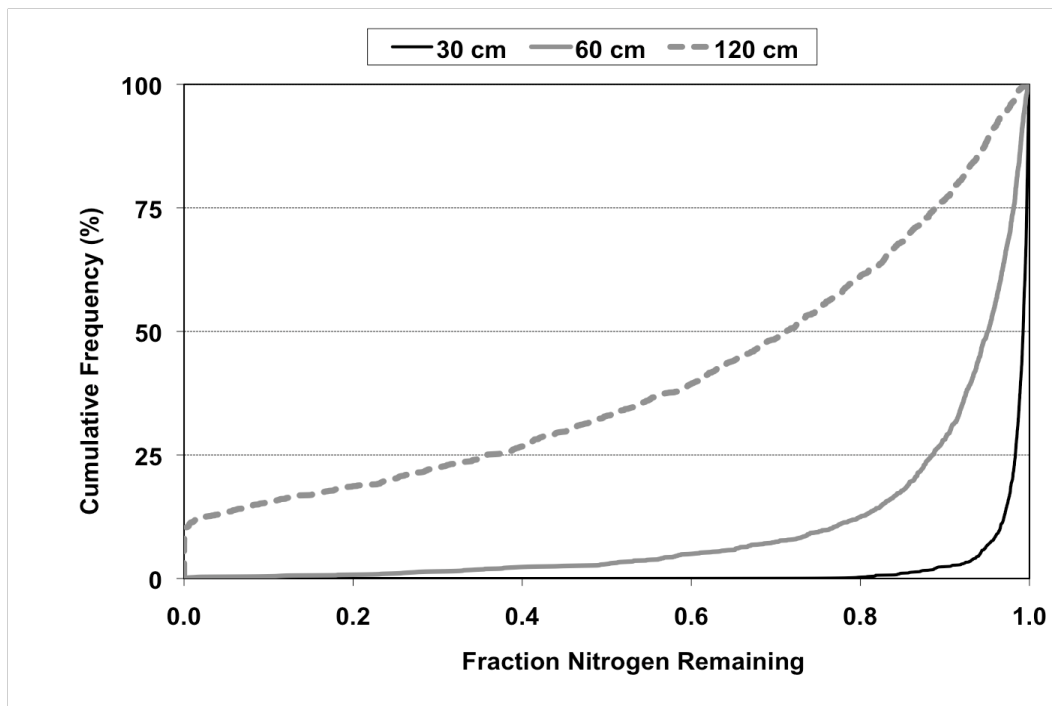


Figure VG-206. Cumulative Probability Graph: Silty Clay Soil, Frigid/Cryic Temperature Region, Standard Effluent, HLR = 5% of K_{sat}.

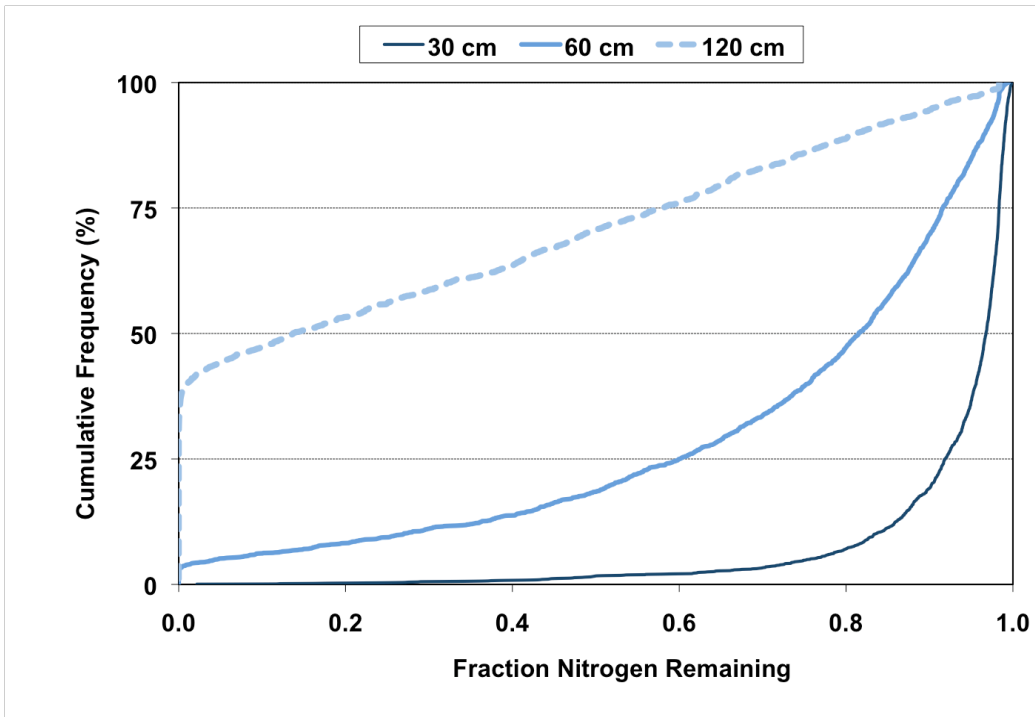


Figure VG-207. Cumulative Probability Graph: Silty Clay Soil, Mesic Temperature Region, Standard Effluent, HLR = 2 cm d⁻¹.

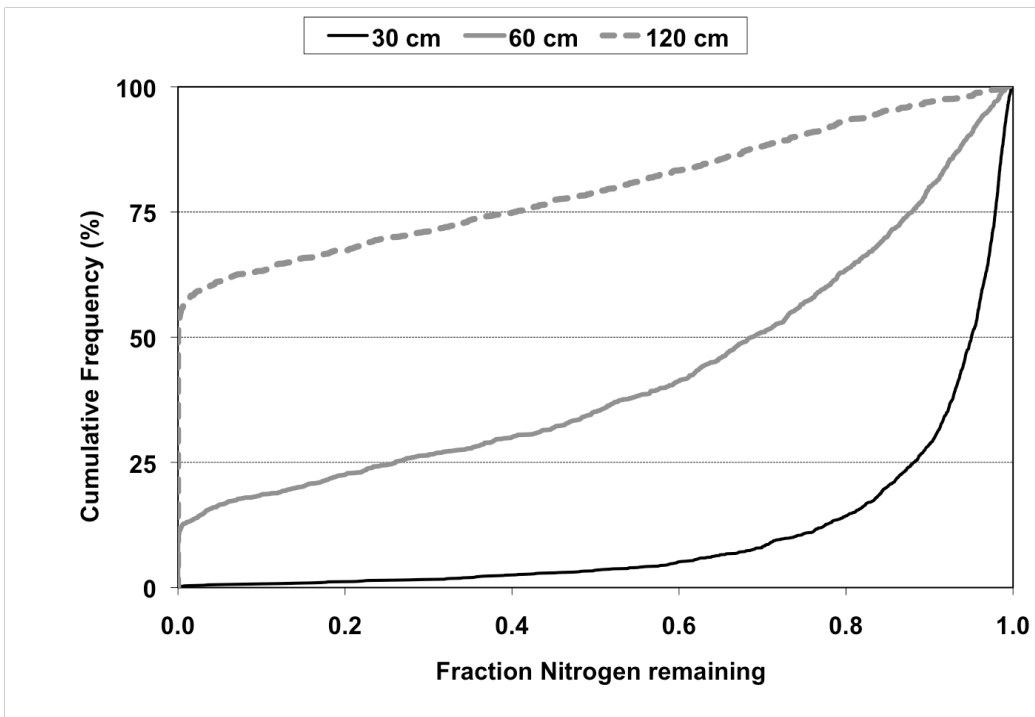


Figure VG-208. Cumulative Probability Graph: Silty Clay Soil, Mesic Temperature Region, Standard Effluent, HLR = 5% of K_{sat} .

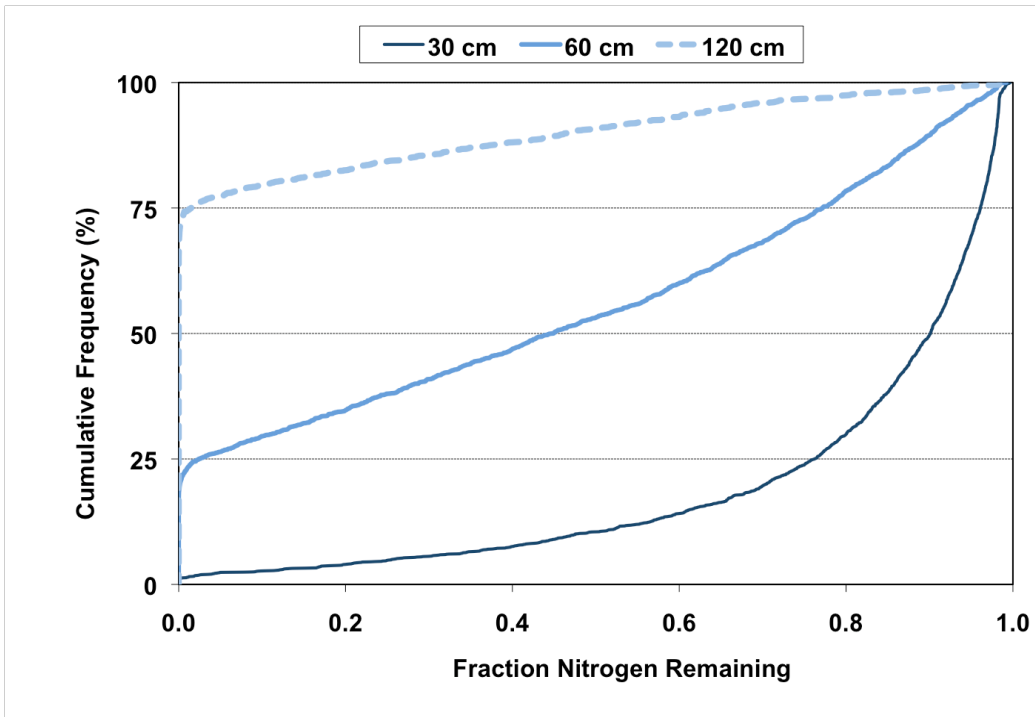


Figure VG-209. Cumulative Probability Graph: Silty Clay Soil, Thermic Temperature Region, Standard Effluent, HLR = 2 cm d⁻¹.

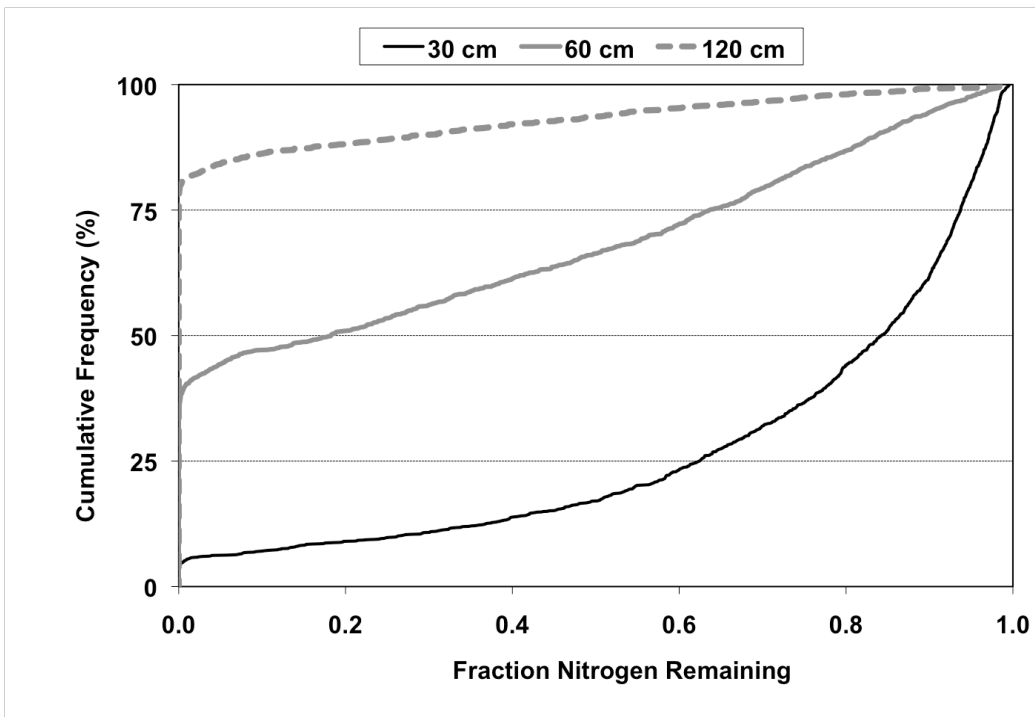


Figure VG-210. Cumulative Probability Graph: Silty Clay Soil, Thermic Temperature Region, Standard Effluent, HLR = 5% of K_{sat}.

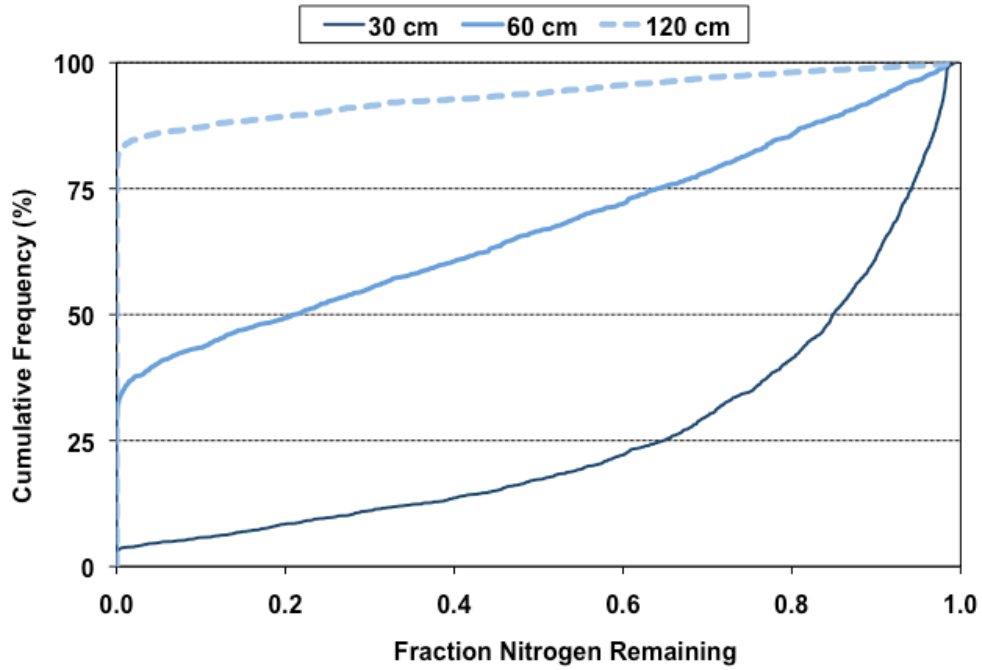


Figure VG-211. Cumulative Probability Graph: Silty Clay Soil, Hyperthermic Temperature Region, Standard Effluent, HLR = 2 cm d⁻¹.

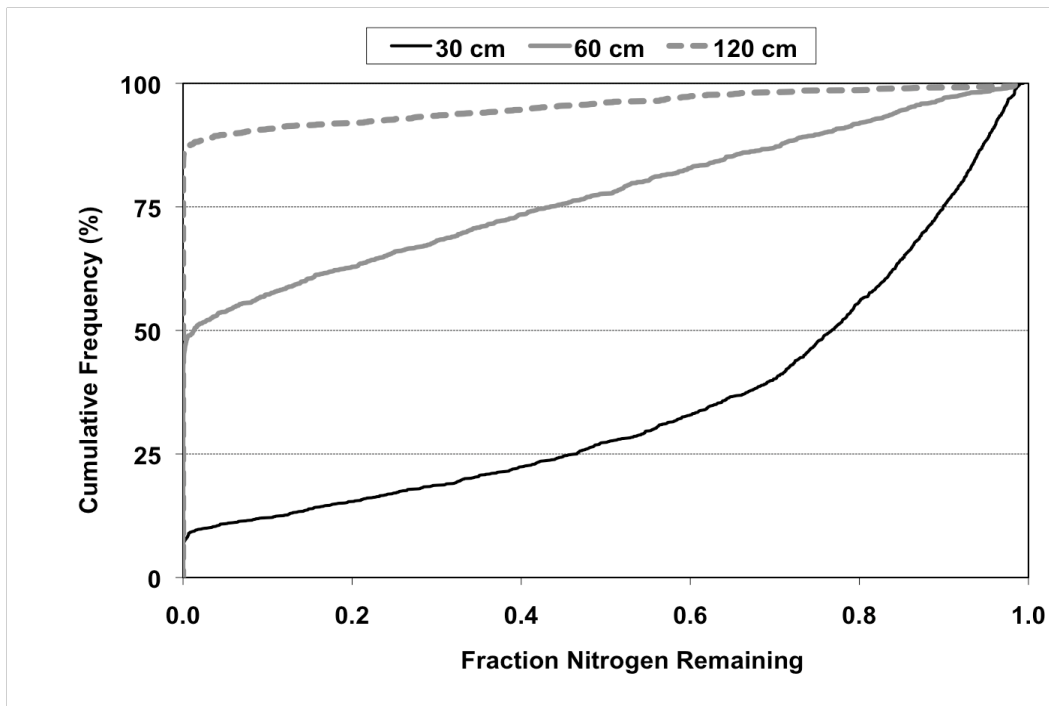


Figure VG-212. Cumulative Probability Graph: Silty Clay Soil, Hyperthermic Temperature Region, Standard Effluent, HLR = 5% of K_{sat} .

2.10.2 Nitrified Effluent

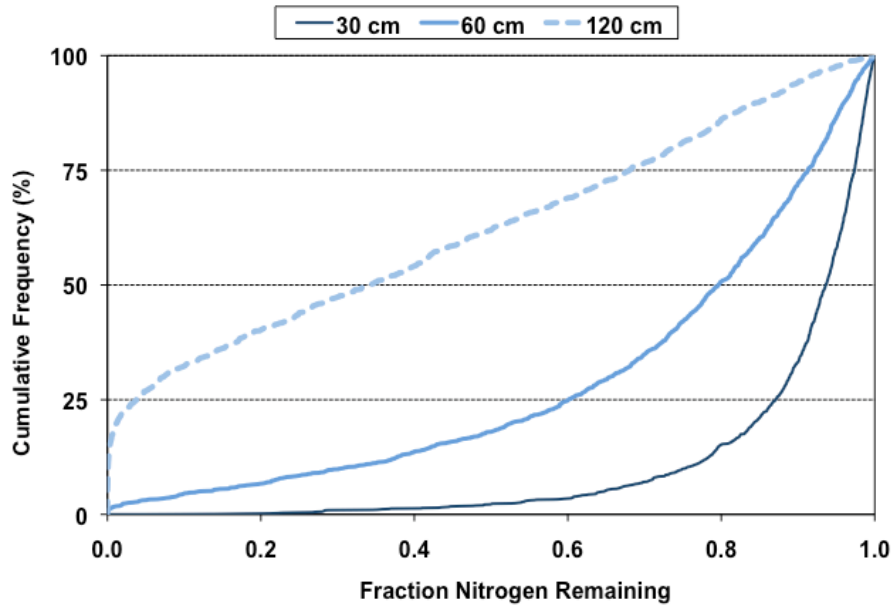


Figure VG-213. Cumulative Probability Graph: Silty Clay Soil, Frigid/Cryic Temperature Region, Nitrified Effluent, HLR = 2 cm d⁻¹.

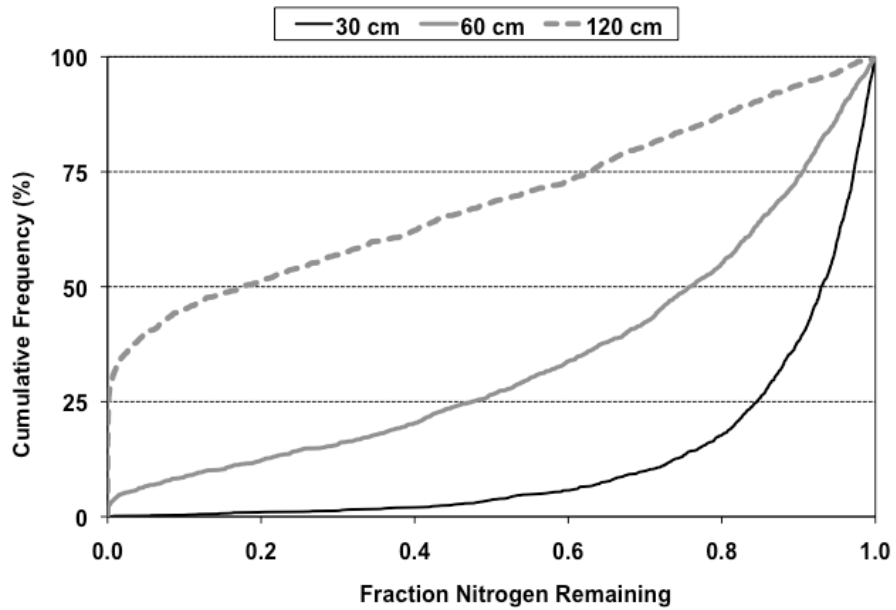


Figure VG-214. Cumulative Probability Graph: Silty Clay Soil, Frigid/Cryic Temperature Region, Nitrified Effluent, HLR = 5% of K_{sat}.

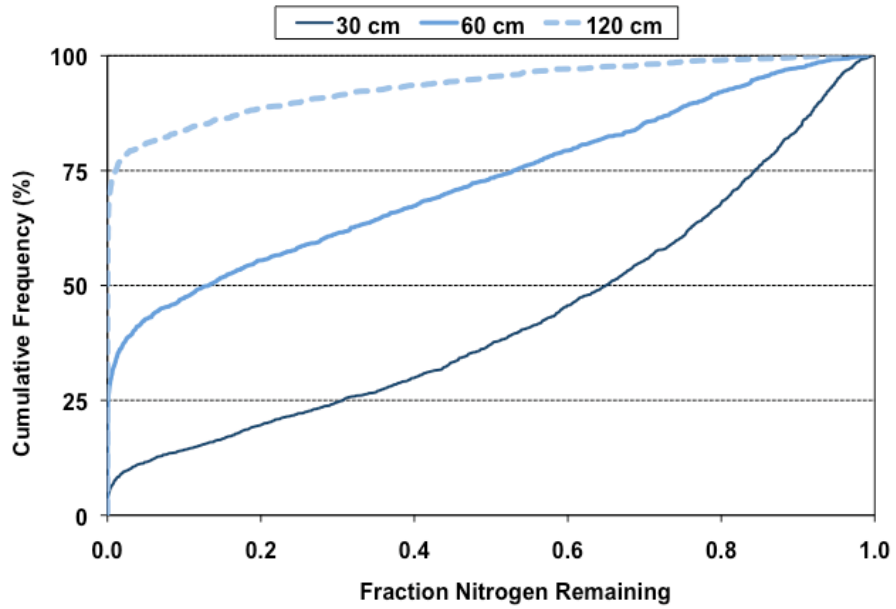


Figure VG-215. Cumulative Probability Graph: Silty Clay Soil, Mesic Temperature Region, Nitrified Effluent, HLR = 2 cm d⁻¹.

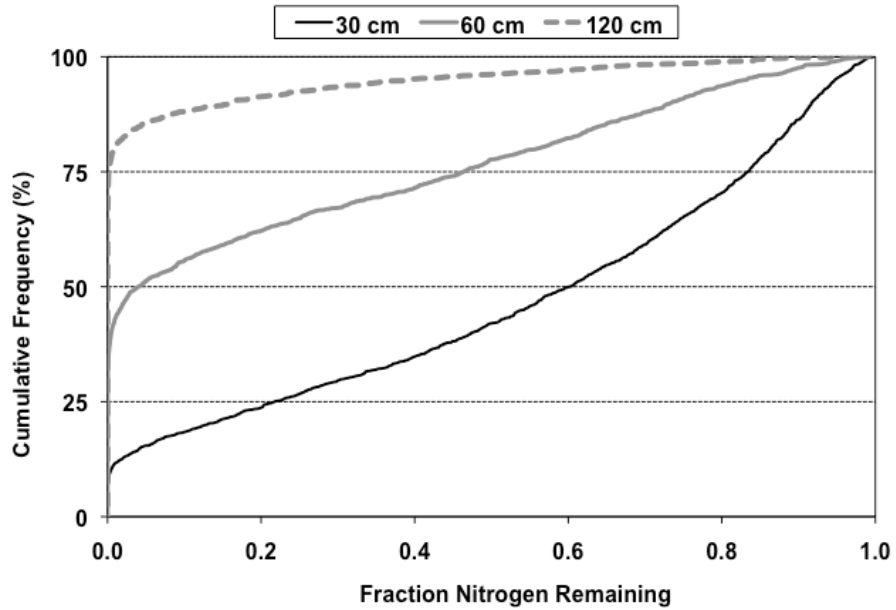


Figure VG-216. Cumulative Probability Graph: Silty Clay Soil, Mesic Temperature Region, Nitrified Effluent, HLR = 5% of K_{sat}.

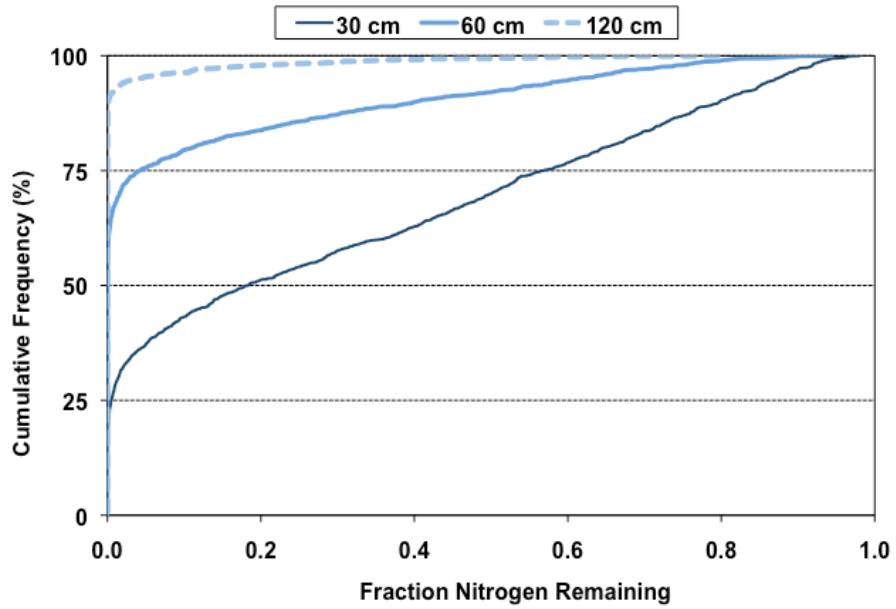


Figure VG-217. Cumulative Probability Graph: Silty Clay Soil, Thermic Temperature Region, Nitrified Effluent, HLR = 2 cm d⁻¹.

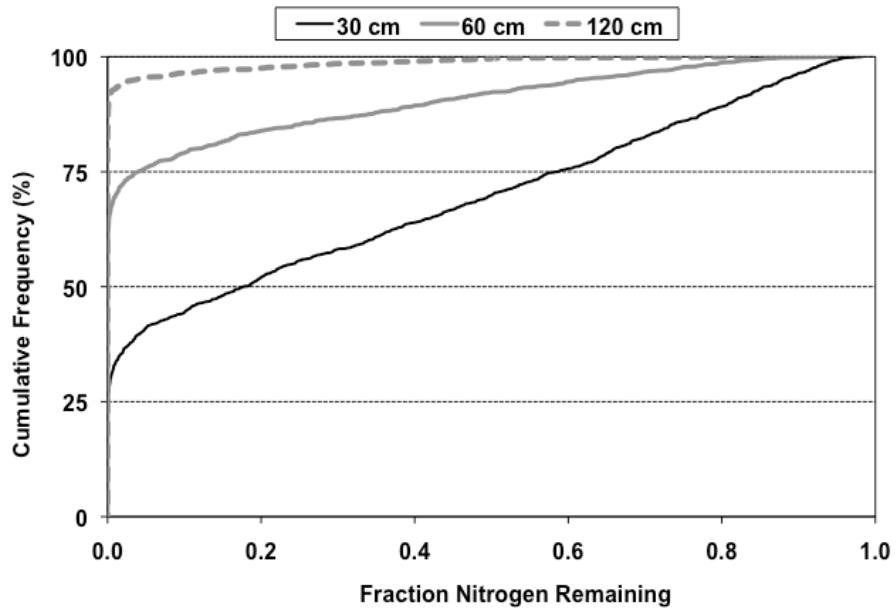


Figure VG-218. Cumulative Probability Graph: Silty Clay Soil, Thermic Temperature Region, Nitrified Effluent, HLR = 5% of K_{sat}.

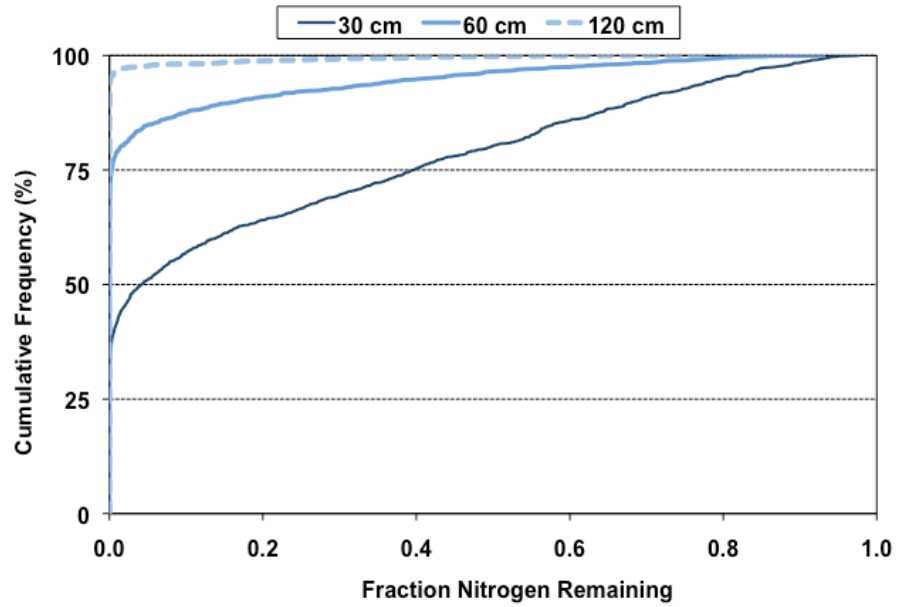


Figure VG-219. Cumulative Probability Graph: Silty Clay Soil, Hyperthermic Temperature Region, Nitrified Effluent, HLR = 2 cm d⁻¹.

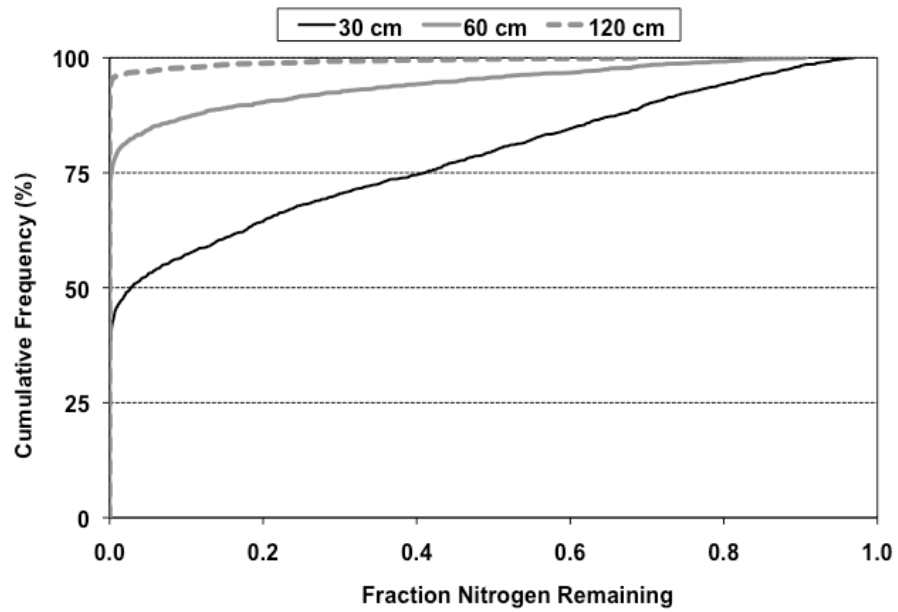


Figure VG-220. Cumulative Probability Graph: Silty Clay Soil, Hyperthermic Temperature Region, Nitrified Effluent, HLR = 5% of K_{sat} .

2.11 Silty Clay Loam

2.11.1 Standard Effluent

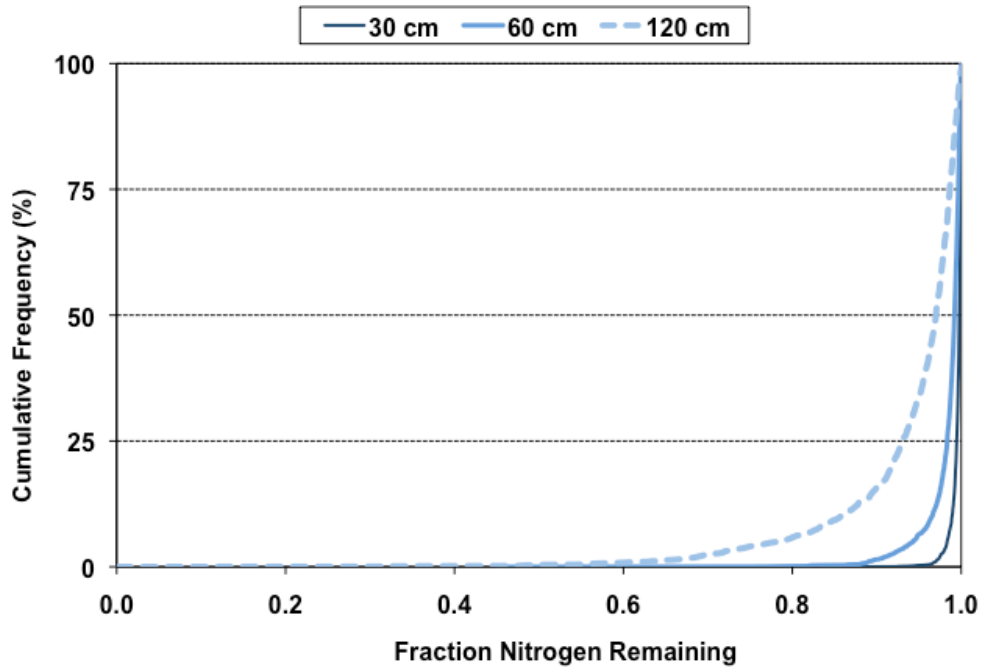


Figure VG-221. Cumulative Probability Graph: Silty Clay Loam Soil, Frigid/Cryic Temperature Region, Standard Effluent, HLR = 2 cm d⁻¹.

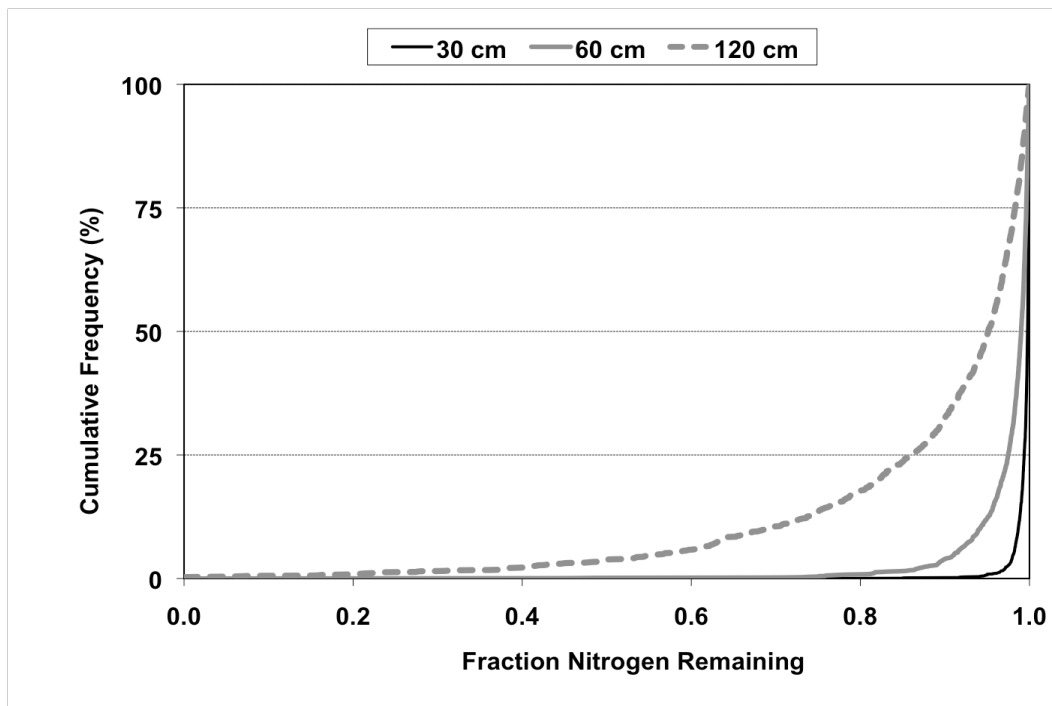


Figure VG-222. Cumulative Probability Graph: Silty Clay Loam Soil, Frigid/Cryic Temperature Region, Standard Effluent, HLR = 5% of K_{sat}.

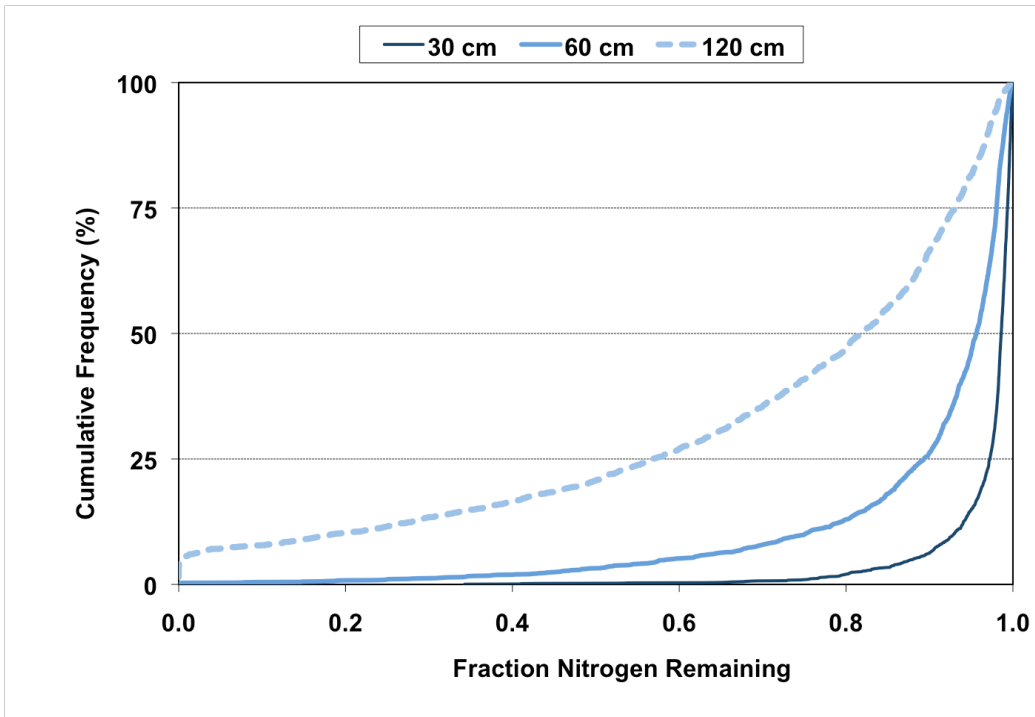


Figure VG-223. Cumulative Probability Graph: Silty Clay Loam Soil, Mesic Temperature Region, Standard Effluent, HLR = 2 cm d⁻¹.

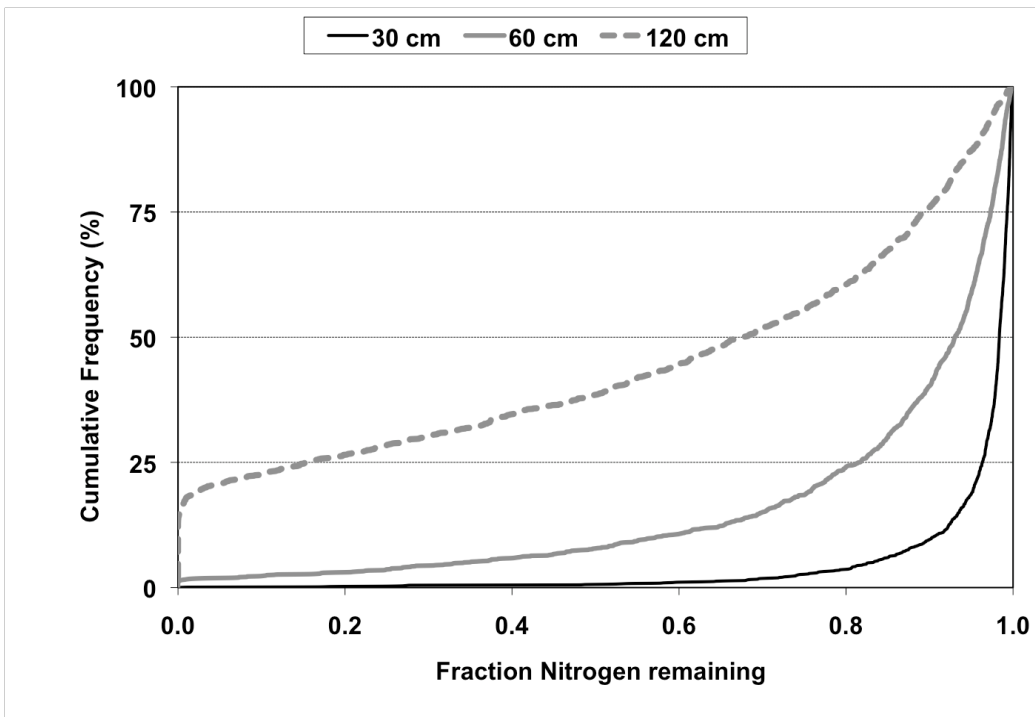


Figure VG-224. Cumulative Probability Graph: Silty Clay Loam Soil, Mesic Temperature Region, Standard Effluent, HLR = 5% of K_{sat} .

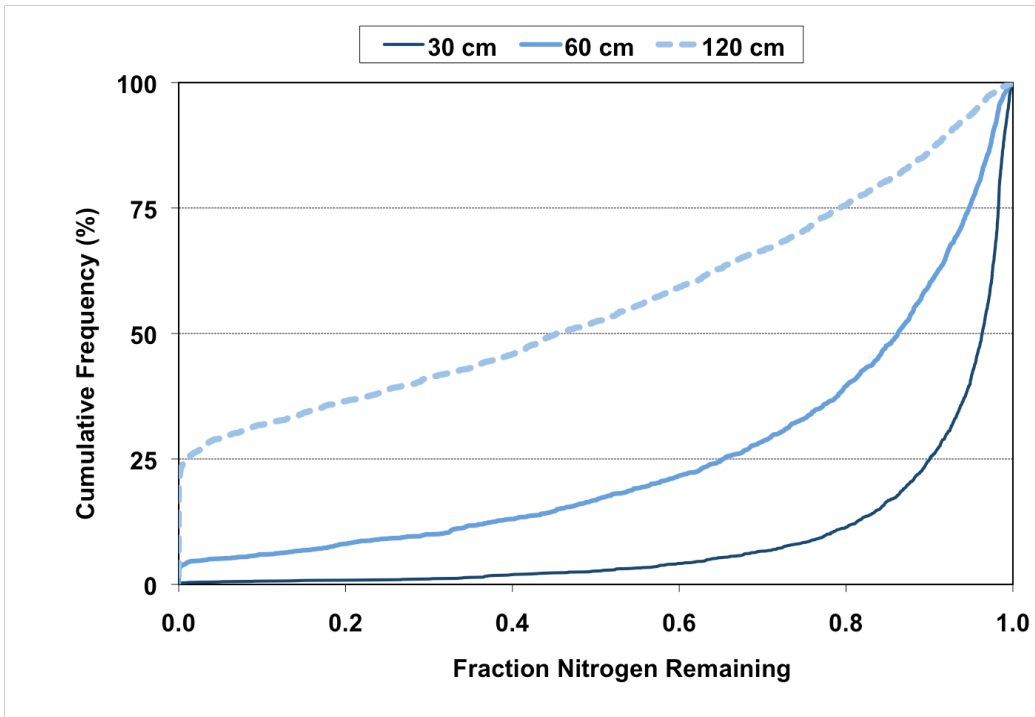


Figure VG-225. Cumulative Probability Graph: Silty Clay Loam Soil, Thermic Temperature Region, Standard Effluent, HLR = 2 cm d⁻¹.

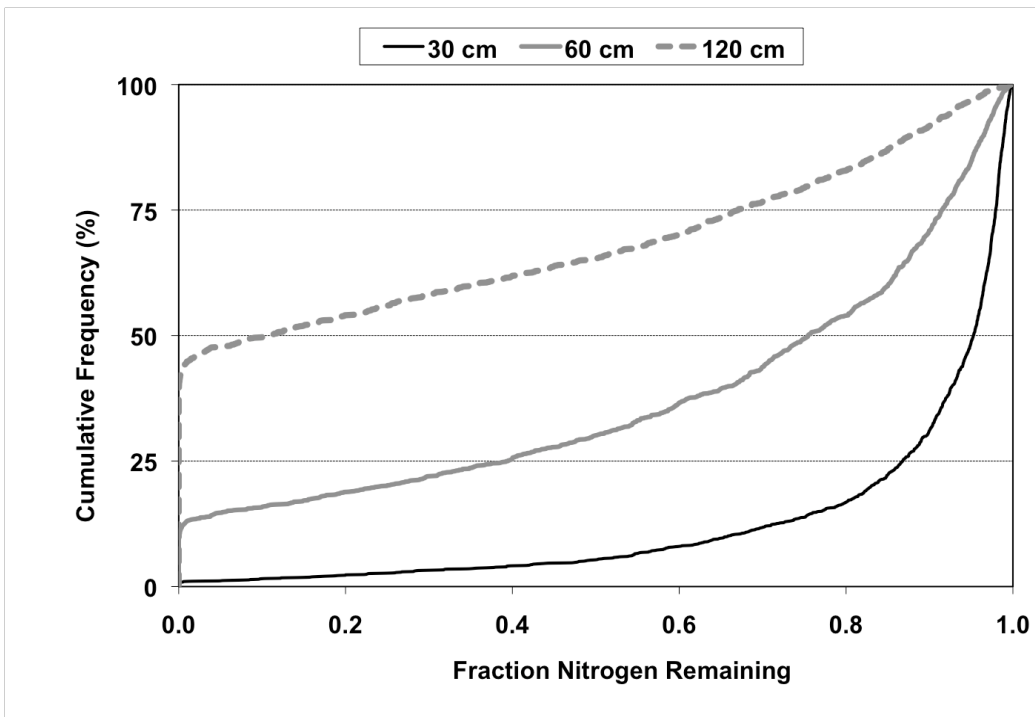


Figure VG-226. Cumulative Probability Graph: Silty Clay Loam Soil, Thermic Temperature Region, Standard Effluent, HLR = 5% of K_{sat}.

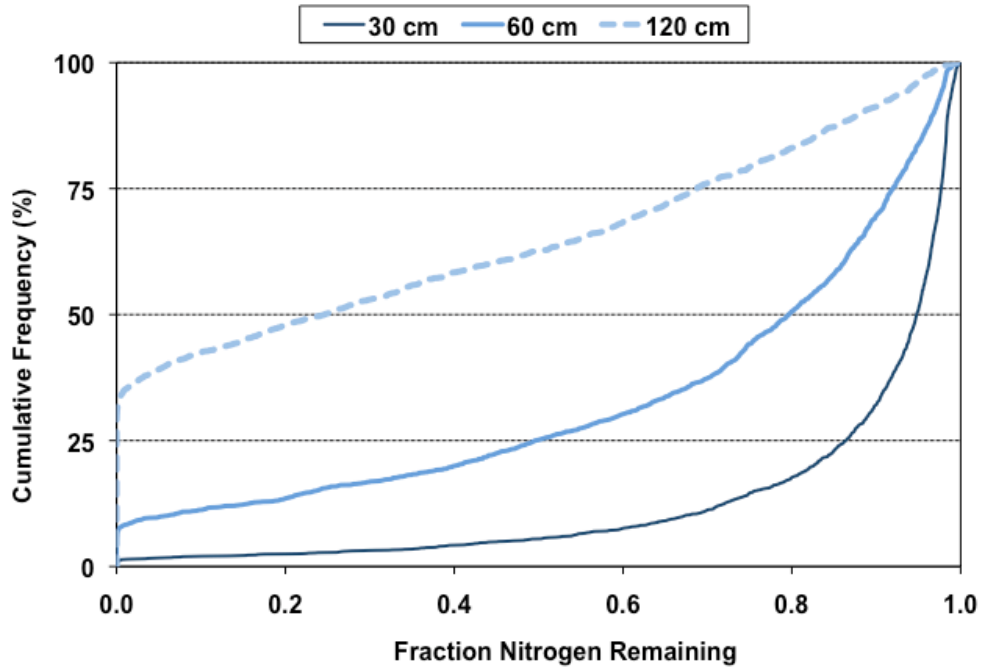


Figure VG-227. Cumulative Probability Graph: Silty Clay Loam Soil, Hyperthermic Temperature Region, Standard Effluent, HLR = 2 cm d⁻¹.

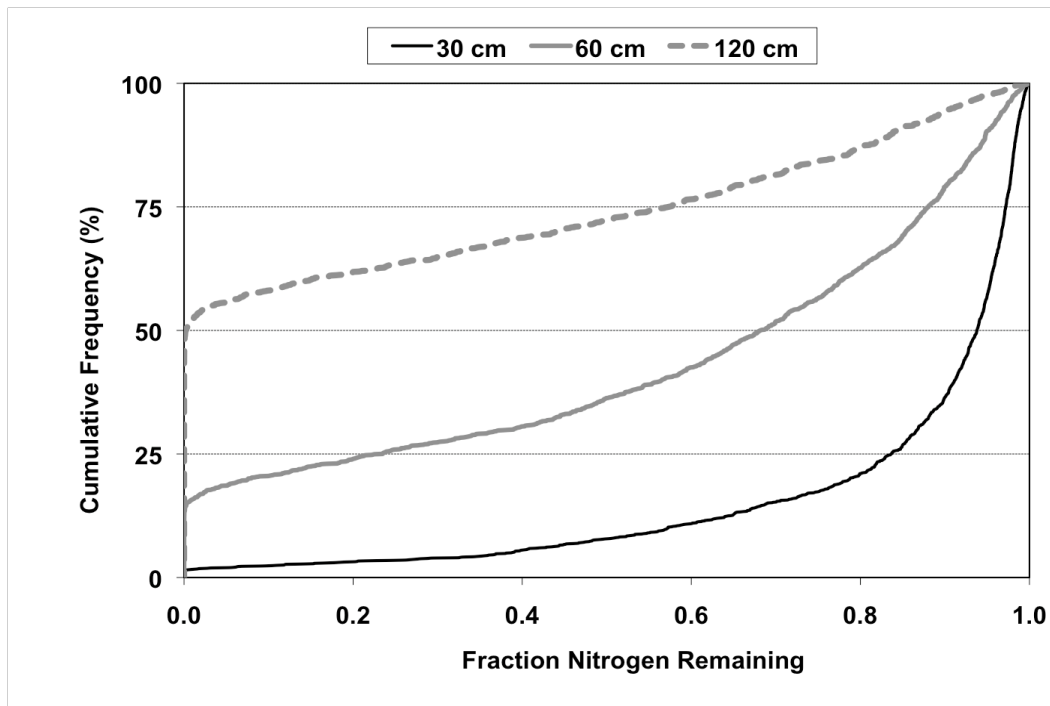


Figure VG-228. Cumulative Probability Graph: Silty Clay Loam Soil, Hyperthermic Temperature Region, Standard Effluent, HLR = 5% of K_{sat}.

2.11.2 Nitrified Effluent

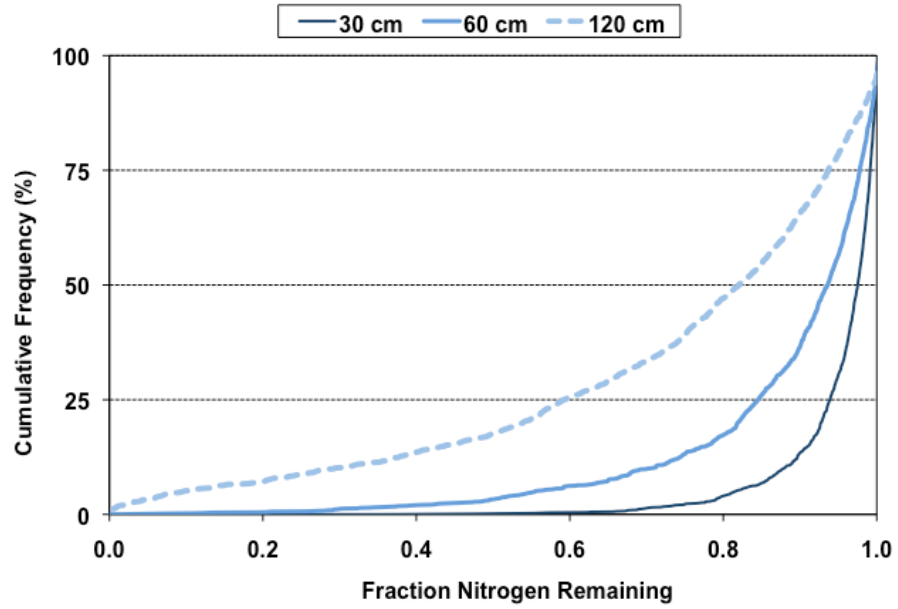


Figure VG-229. Cumulative Probability Graph: Silty Clay Loam Soil, Frigid/Cryic Temperature Region, Nitrified Effluent, HLR = 2 cm d⁻¹.

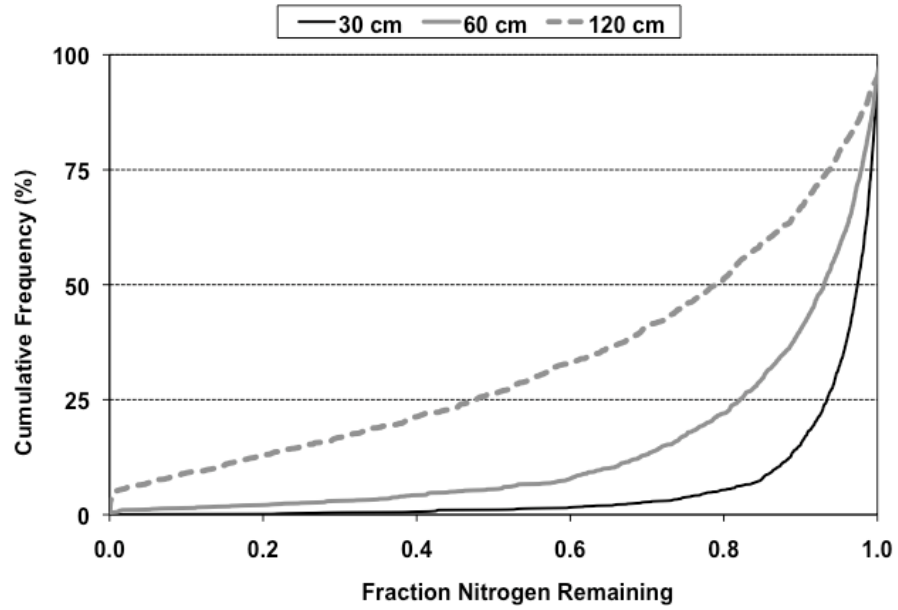


Figure VG-230. Cumulative Probability Graph: Silty Clay Loam Soil, Frigid/Cryic Temperature Region, Nitrified Effluent, HLR = 5% of K_{sat}.

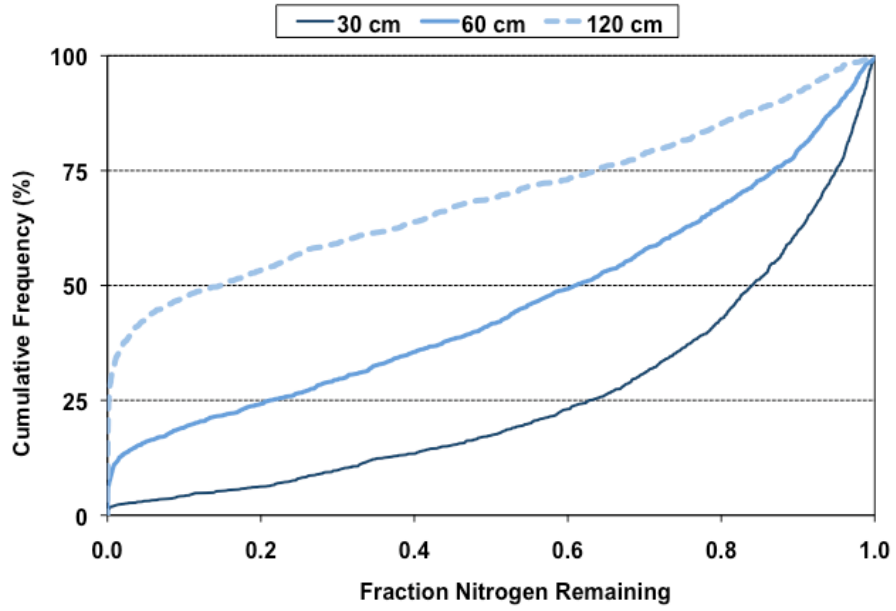


Figure VG-231. Cumulative Probability Graph: Silty Clay Loam Soil, Mesic Temperature Region, Nitrified Effluent, HLR = 2 cm d⁻¹.

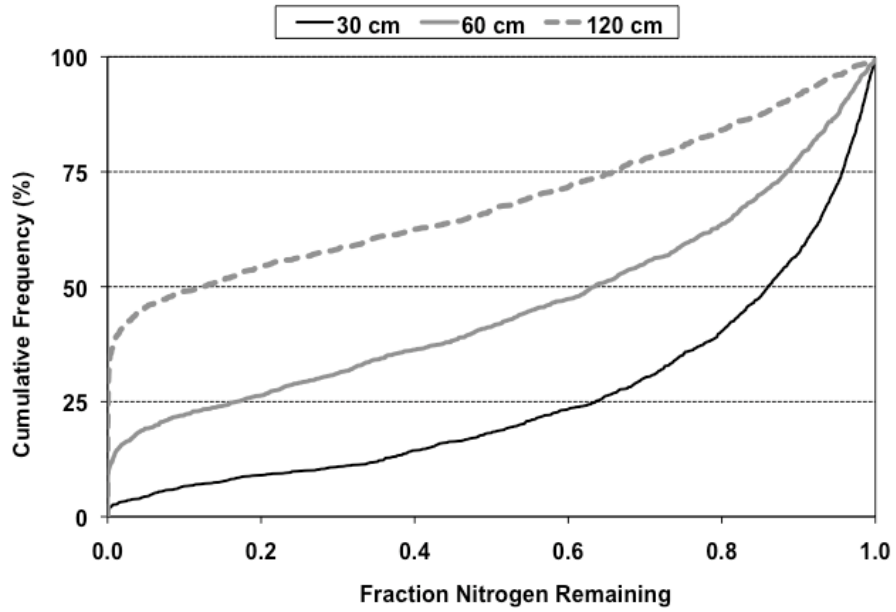


Figure VG-232. Cumulative Probability Graph: Silty Clay Loam Soil, Mesic Temperature Region, Nitrified Effluent, HLR = 5% of K_{sat}.

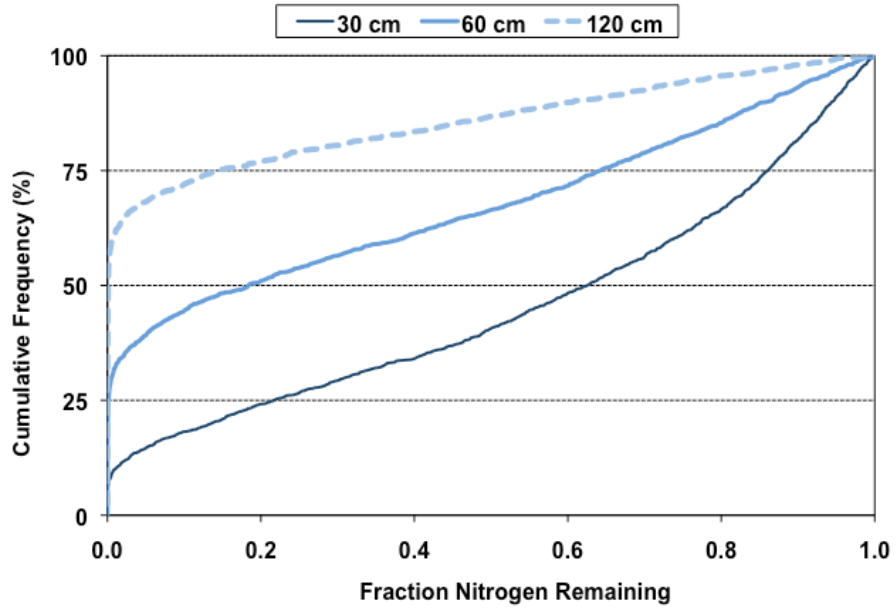


Figure VG-233. Cumulative Probability Graph: Silty Clay Loam Soil, Thermic Temperature Region, Nitrified Effluent, HLR = 2 cm d⁻¹.

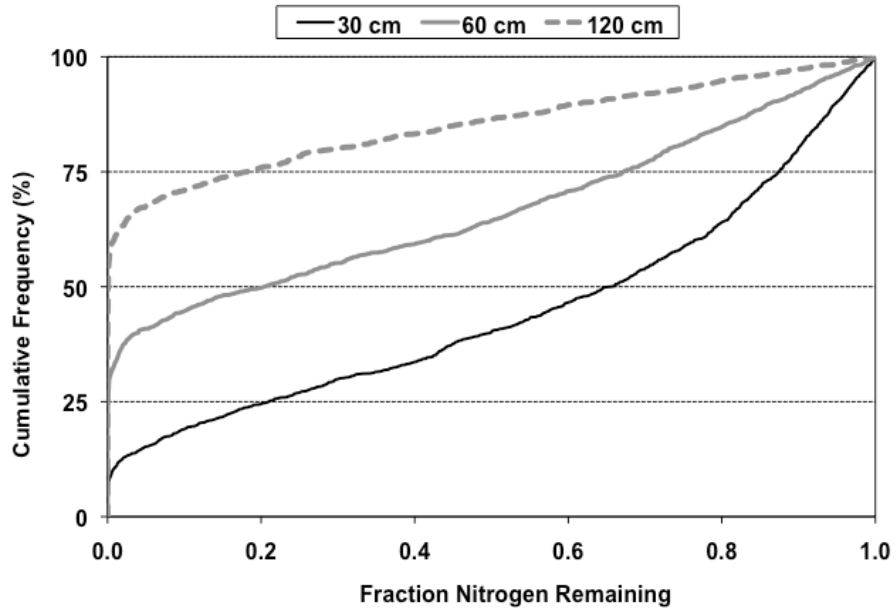


Figure VG-234. Cumulative Probability Graph: Silty Clay Loam Soil, Thermic Temperature Region, Nitrified Effluent, HLR = 5% of K_{sat}.

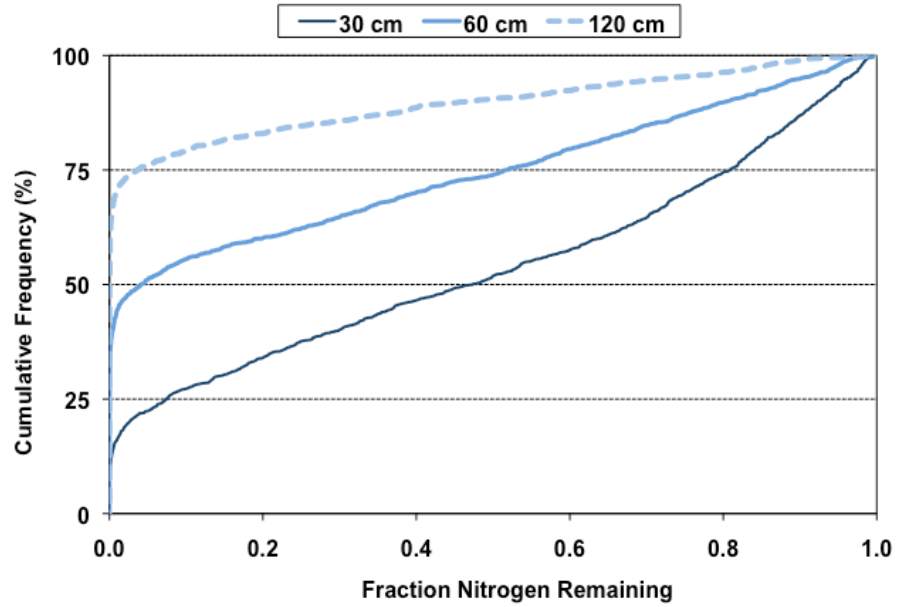


Figure VG-235. Cumulative Probability Graph: Silty Clay Loam Soil, Hyperthermic Temperature Region, Nitrified Effluent, HLR = 2 cm d⁻¹.

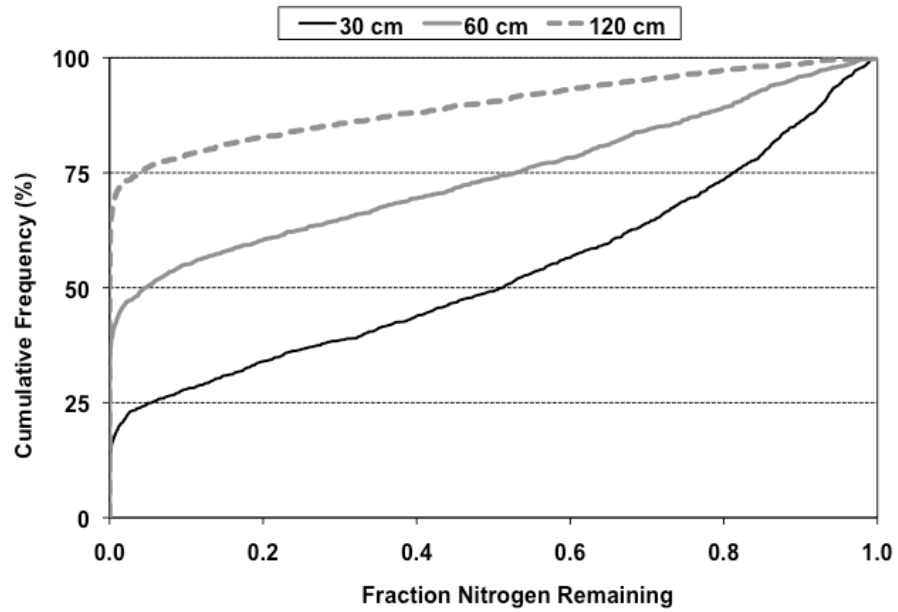


Figure VG-236. Cumulative Probability Graph: Silty Clay Loam Soil, Hyperthermic Temperature Region, Nitrified Effluent, HLR = 5% of K_{sat}.

2.12 Silty Loam

2.12.1 Standard Effluent

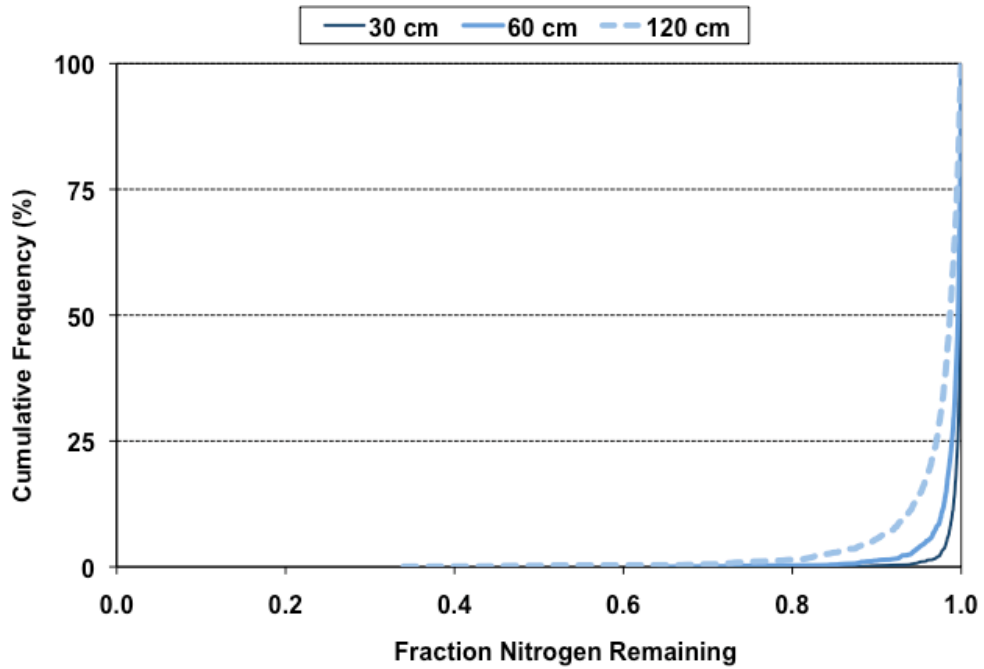


Figure VG-237. Cumulative Probability Graph: Silty Loam Soil, Frigid/Cryic Temperature Region, Standard Effluent, HLR = 2 cm d⁻¹.

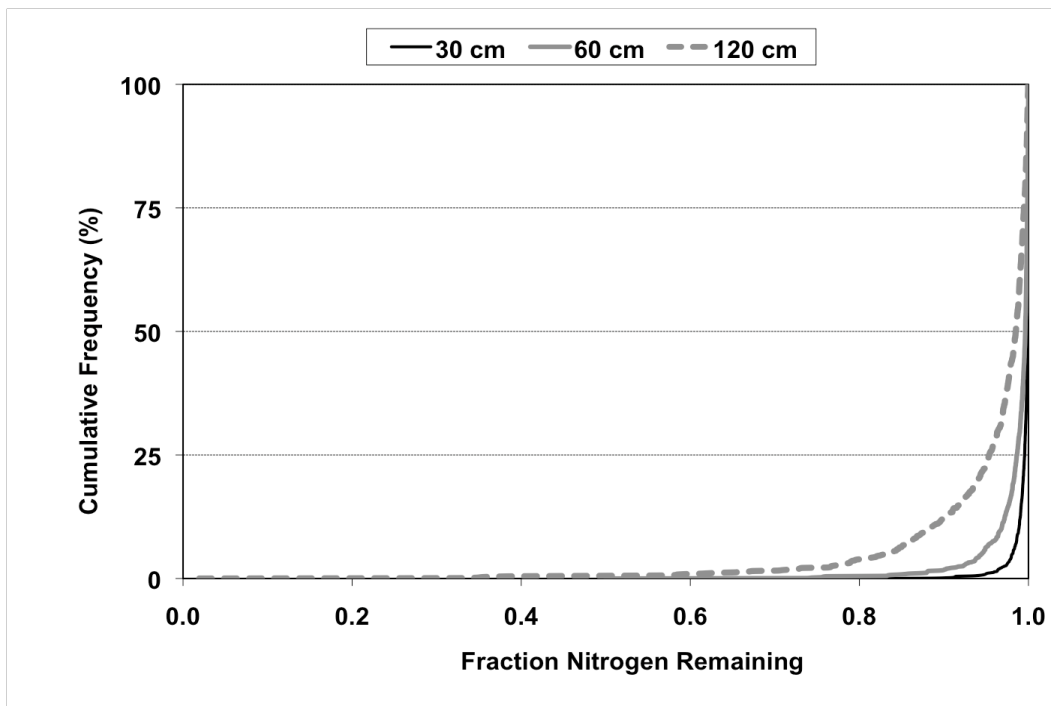


Figure VG-238. Cumulative Probability Graph: Silty Loam Soil, Frigid/Cryic Temperature Region, Standard Effluent, HLR = 5% of K_{sat}.

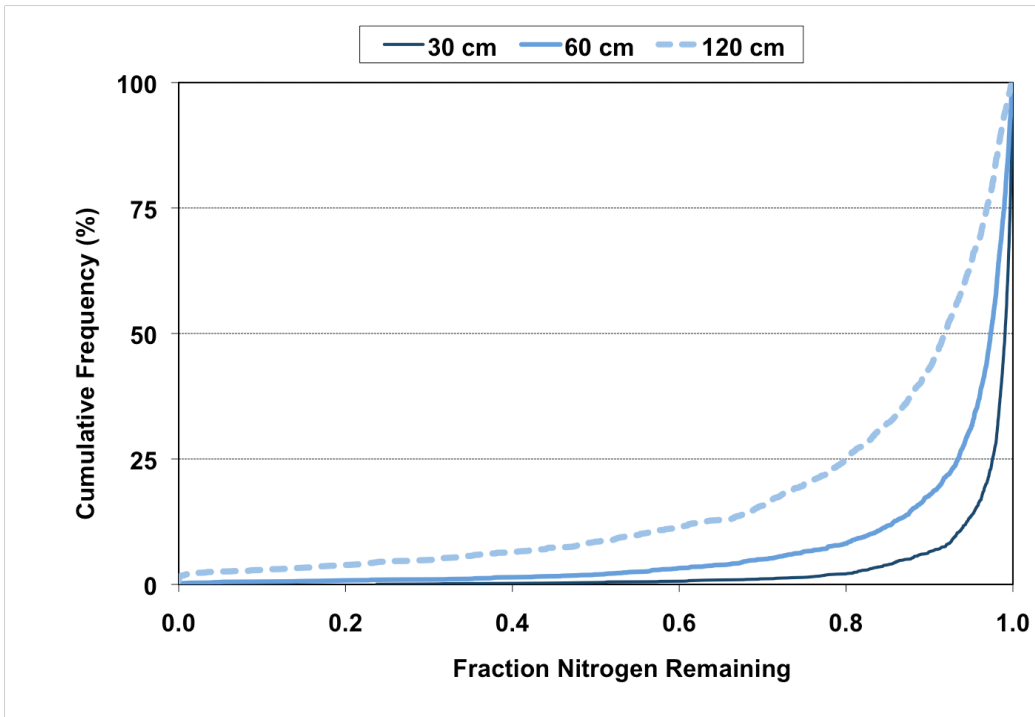


Figure VG-239. Cumulative Probability Graph: Silty Loam Soil, Mesic Temperature Region, Standard Effluent, HLR = 2 cm d⁻¹.

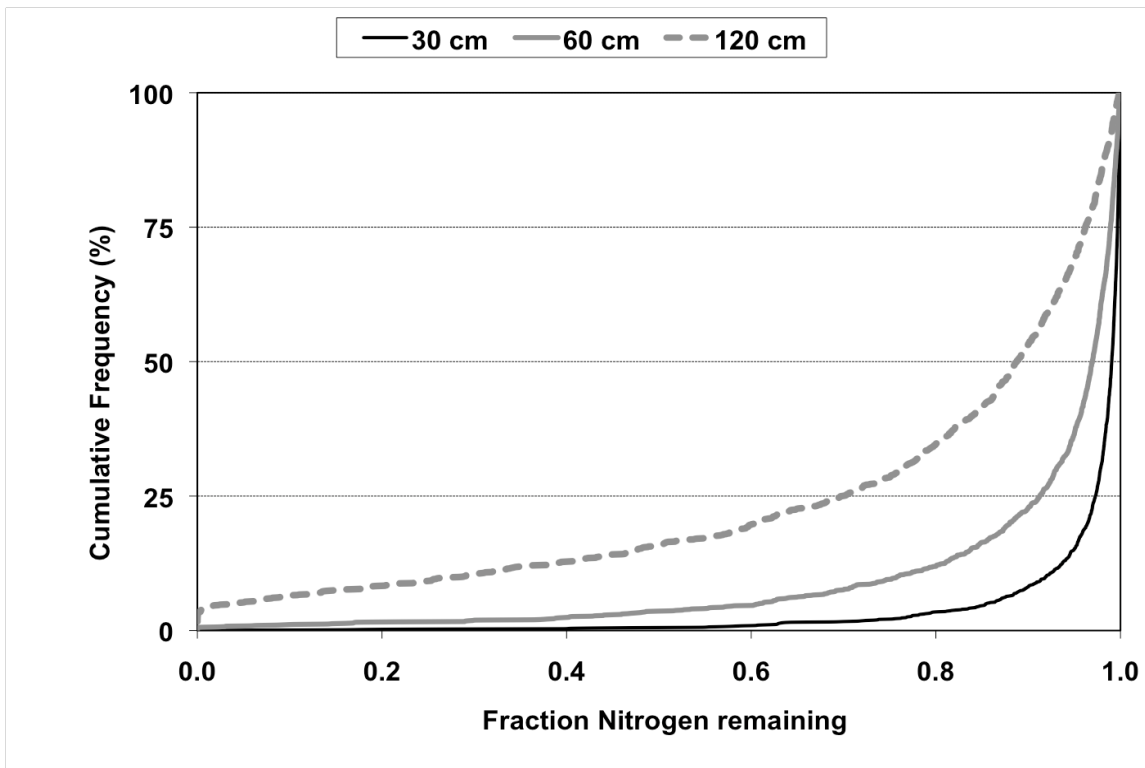


Figure VG-240. Cumulative Probability Graph: Silty Loam Soil, Mesic Temperature Region, Standard Effluent, HLR = 5% of K_{sat} .

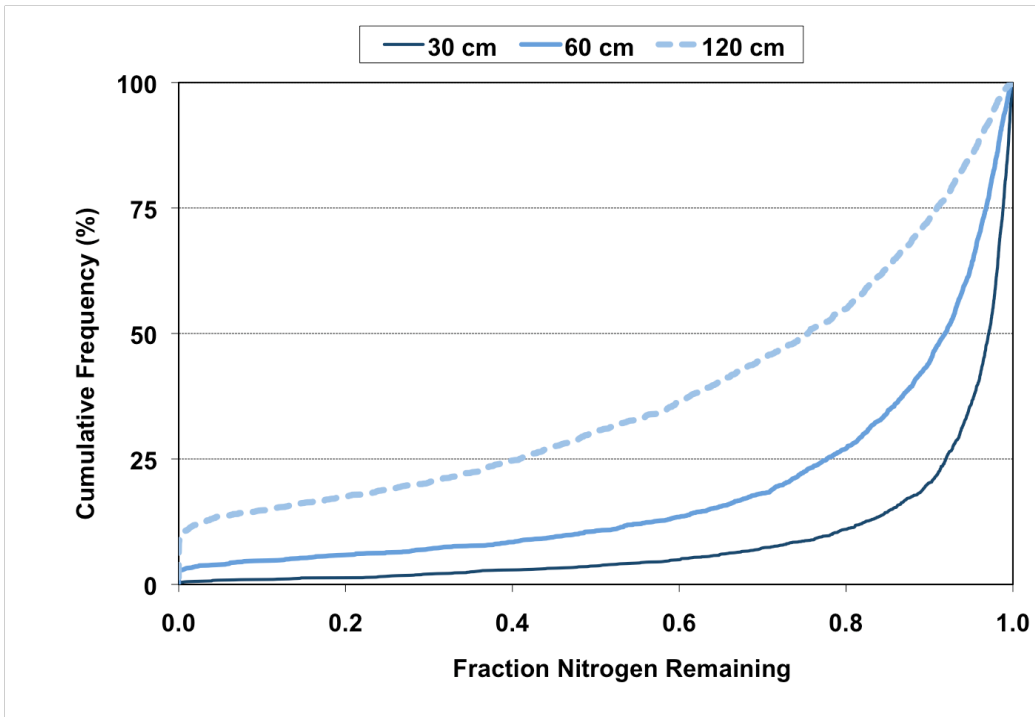


Figure VG-241. Cumulative Probability Graph: Silty Loam Soil, Thermic Temperature Region, Standard Effluent, HLR = 2 cm d⁻¹.

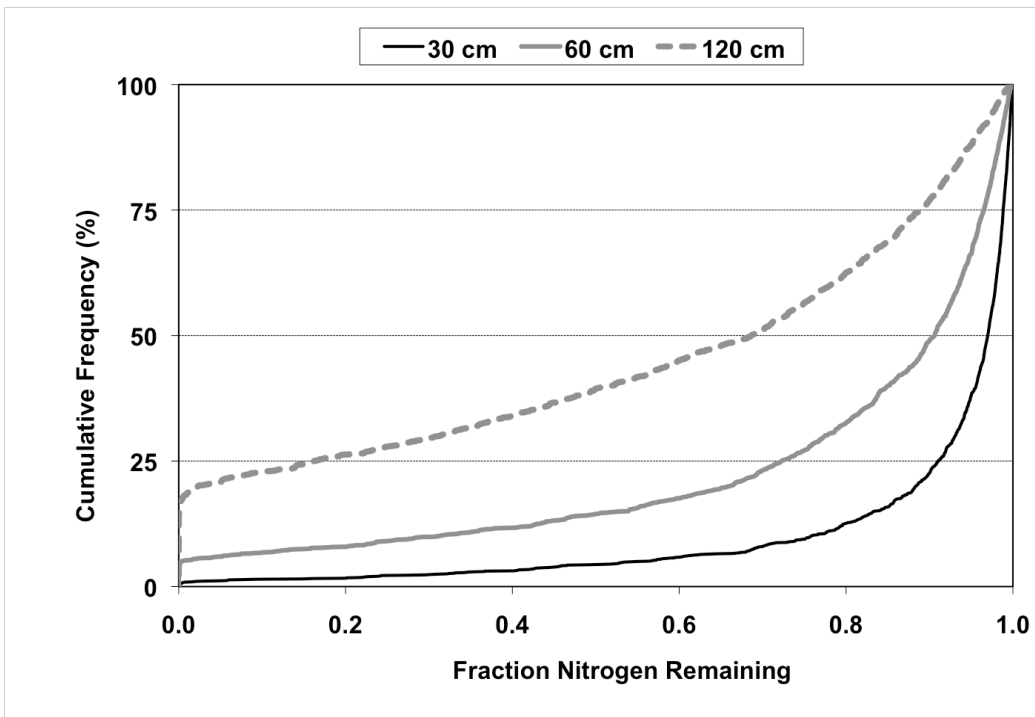


Figure VG-242. Cumulative Probability Graph: Silty Loam Soil, Thermic Temperature Region, Standard Effluent, HLR = 5% of K_{sat} .

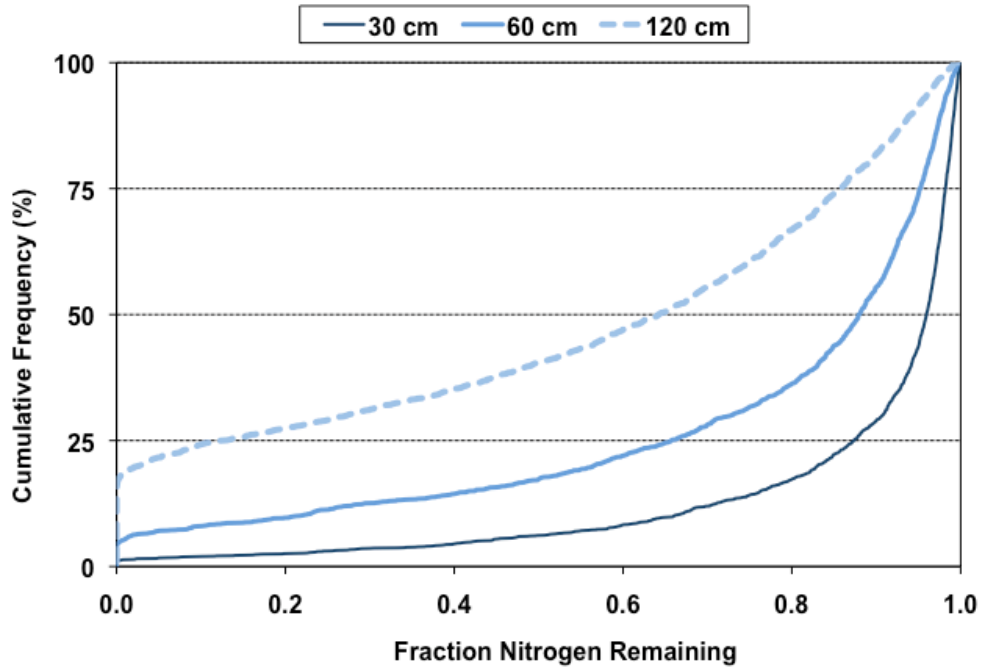


Figure VG-243. Cumulative Probability Graph: Silty Loam Soil, Hyperthermic Temperature Region, Standard Effluent, HLR = 2 cm d⁻¹.

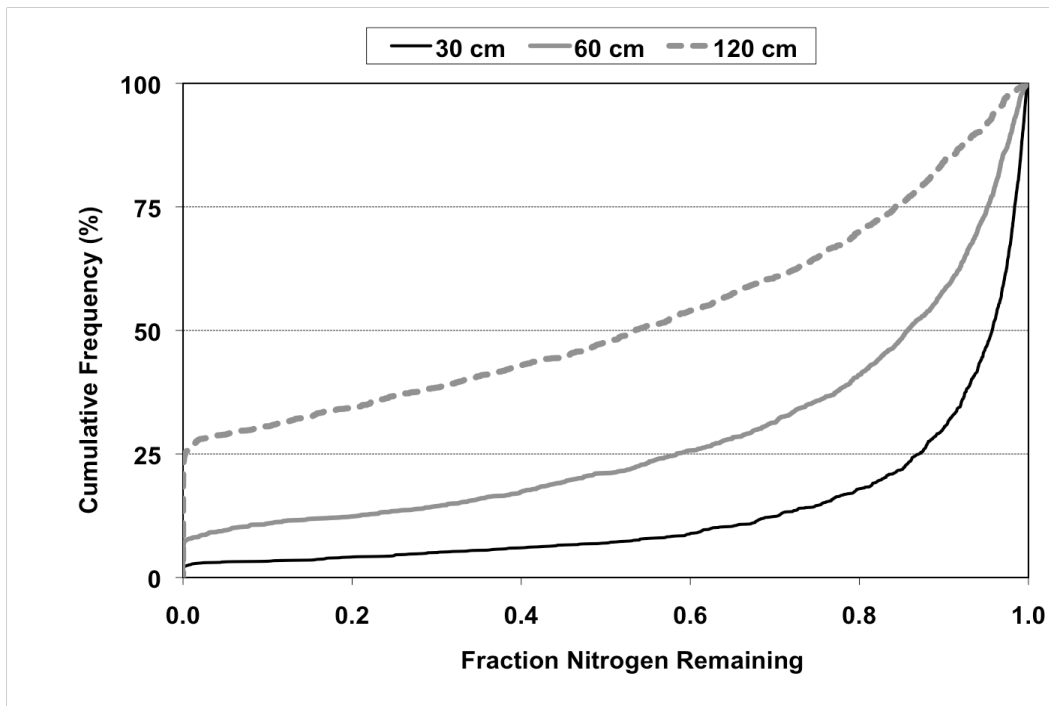


Figure VG-244. Cumulative Probability Graph: Silty Loam Soil, Hyperthermic Temperature Region, Standard Effluent, HLR = 5% of K_{sat}.

2.12.2 Nitrified Effluent

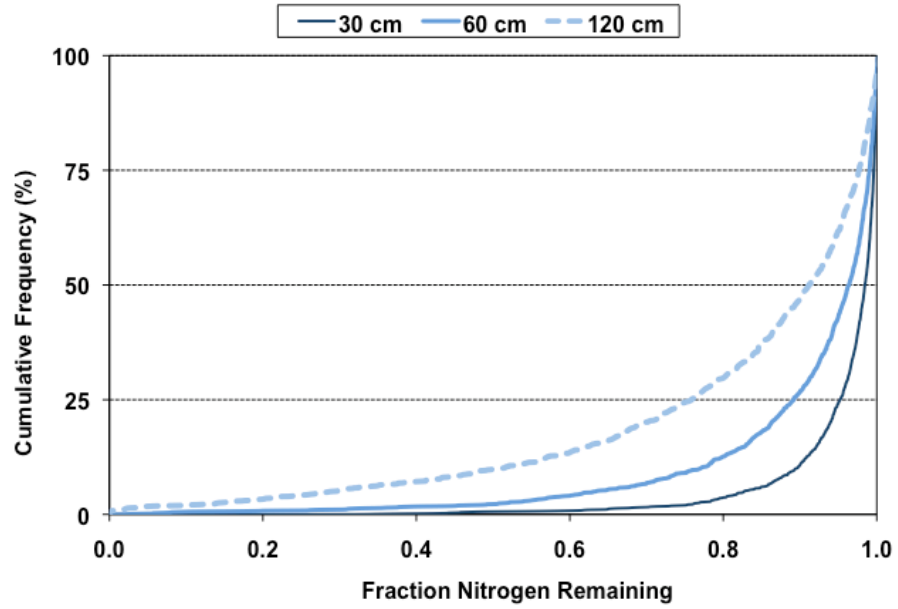


Figure VG-245. Cumulative Probability Graph: Silty Loam Soil, Frigid/Cryic Temperature Region, Nitrified Effluent, HLR = 2 cm d⁻¹.

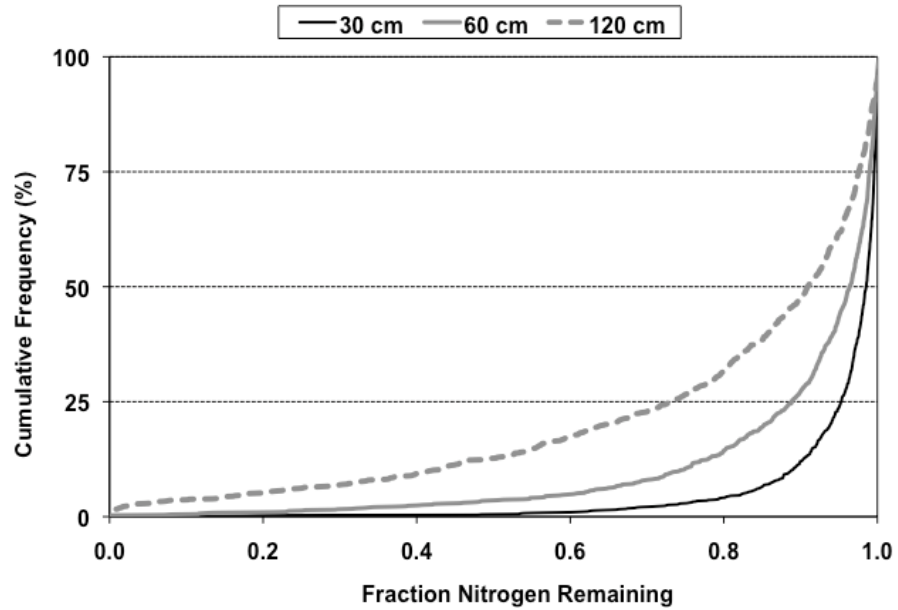


Figure VG-246. Cumulative Probability Graph: Silty Loam Soil, Frigid/Cryic Temperature Region, Nitrified Effluent, HLR = 5% of K_{sat}.

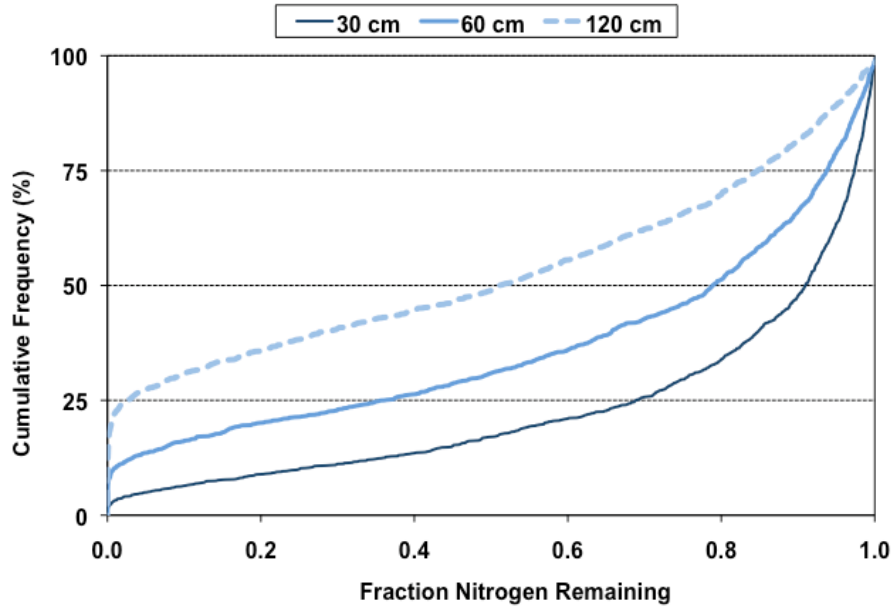


Figure VG-247. Cumulative Probability Graph: Silty Loam Soil, Mesic Temperature Region, Nitrified Effluent, HLR = 2 cm d⁻¹.

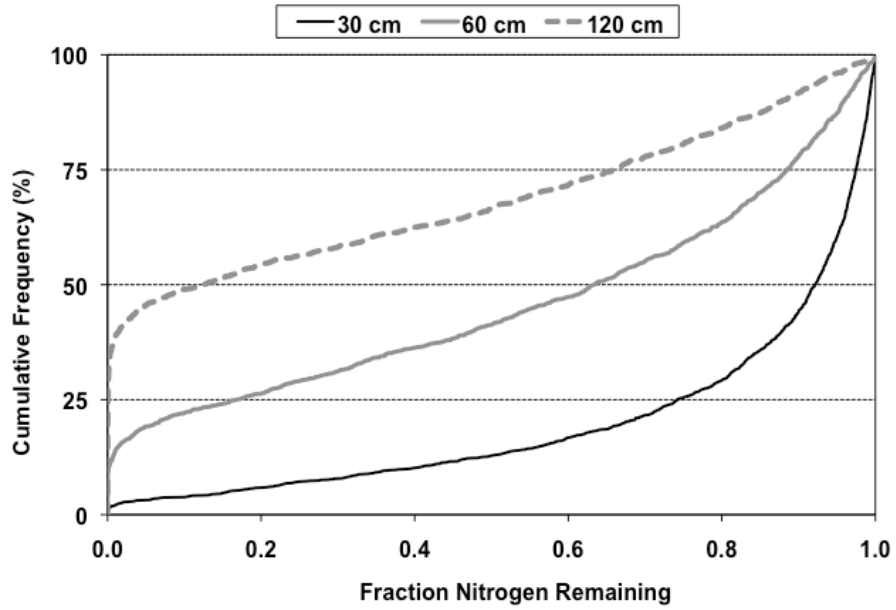


Figure VG-248. Cumulative Probability Graph: Silty Loam Soil, Mesic Temperature Region, Nitrified Effluent, HLR = 5% of K_{sat}.

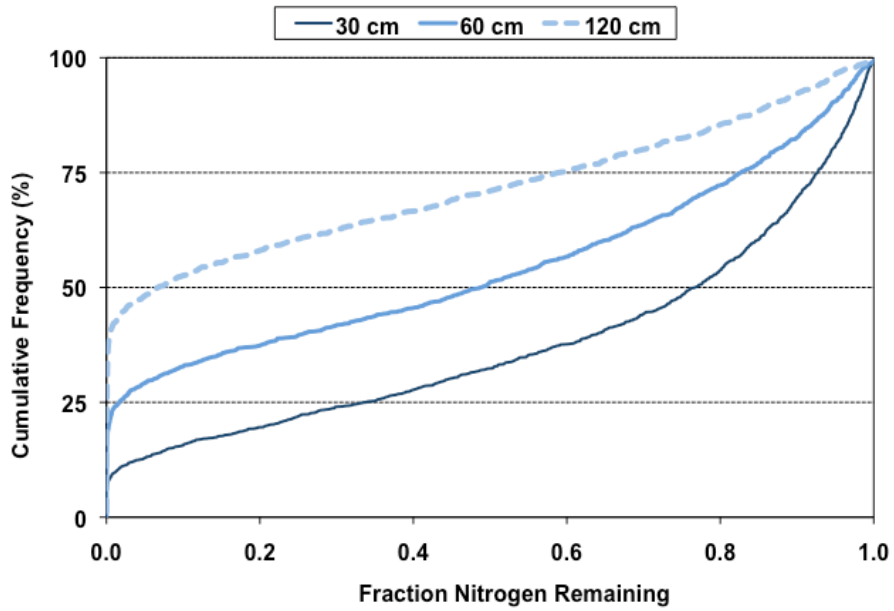


Figure VG-249. Cumulative Probability Graph: Silty Loam Soil, Thermic Temperature Region, Nitrified Effluent, HLR = 2 cm d⁻¹.

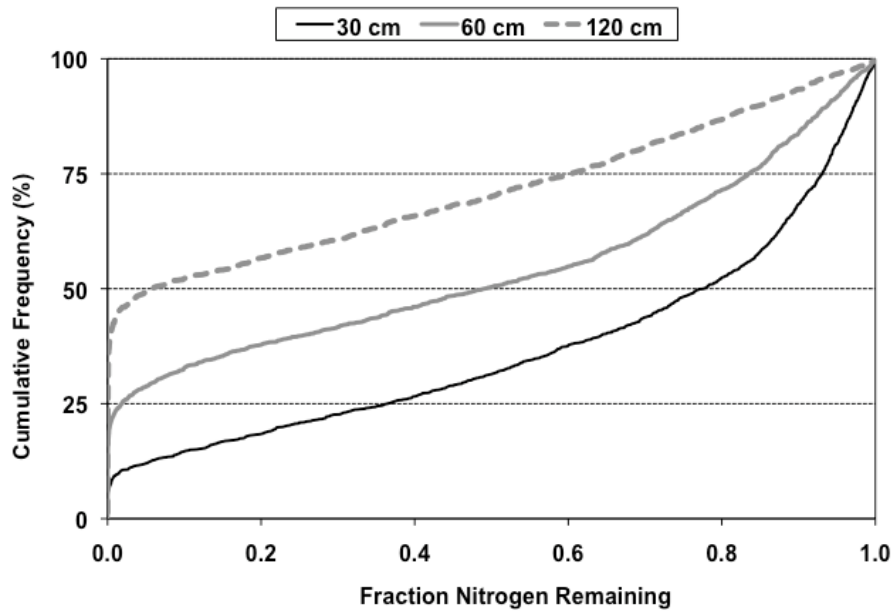


Figure VG-250. Cumulative Probability Graph: Silty Loam Soil, Thermic Temperature Region, Nitrified Effluent, HLR = 5% of K_{sat} .

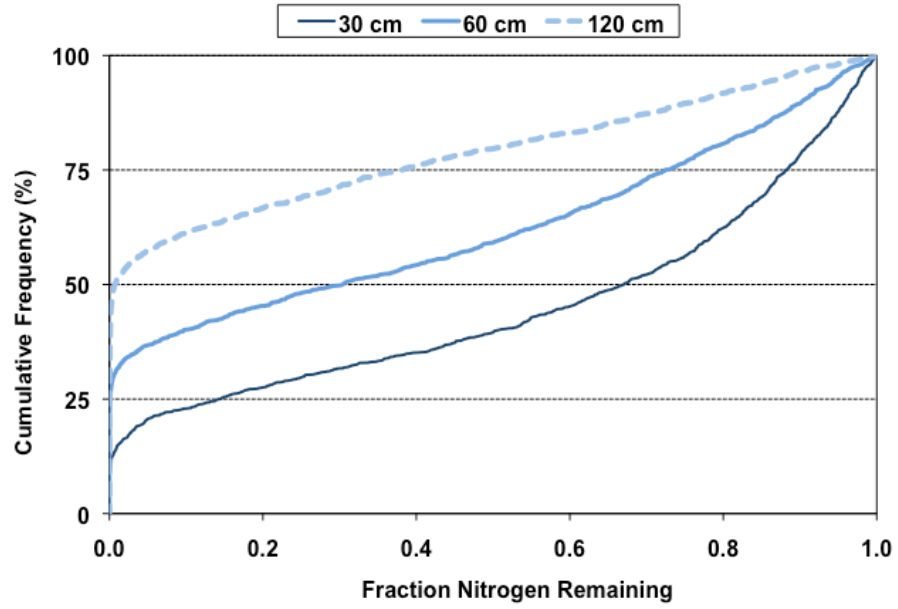


Figure VG-251. Cumulative Probability Graph: Silty Loam Soil, Hyperthermic Temperature Region, Nitrified Effluent, HLR = 2 cm d⁻¹.

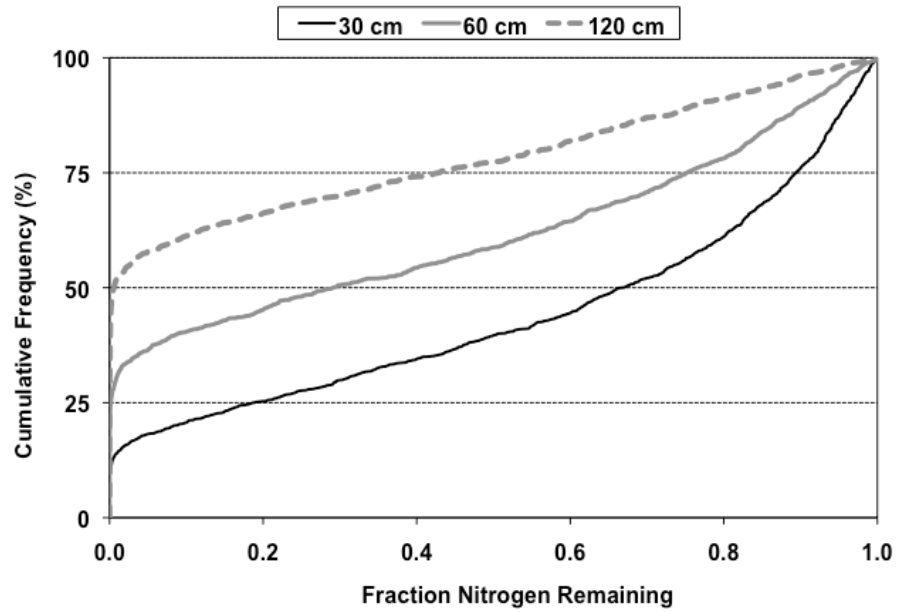


Figure VG-252. Cumulative Probability Graph: Silty Loam Soil, Hyperthermic Temperature Region, Nitrified Effluent, HLR = 5% of K_{sat}.

CHAPTER 3.0

SCENARIO ILLUSTRATIONS: HYDRUS SIMULATION OUTPUTS FOR TYPICAL STU OPERATING CONDITIONS

Soil type:	Sand
Effluent Quality:	STE
Daily Loading Rate:	2 cm/day

	NH ₄	NO ₃	Total N
% Removal at 30cm	22.2%	---	1.6%
% Removal at 90cm	45.3%	1.5%	1.4%

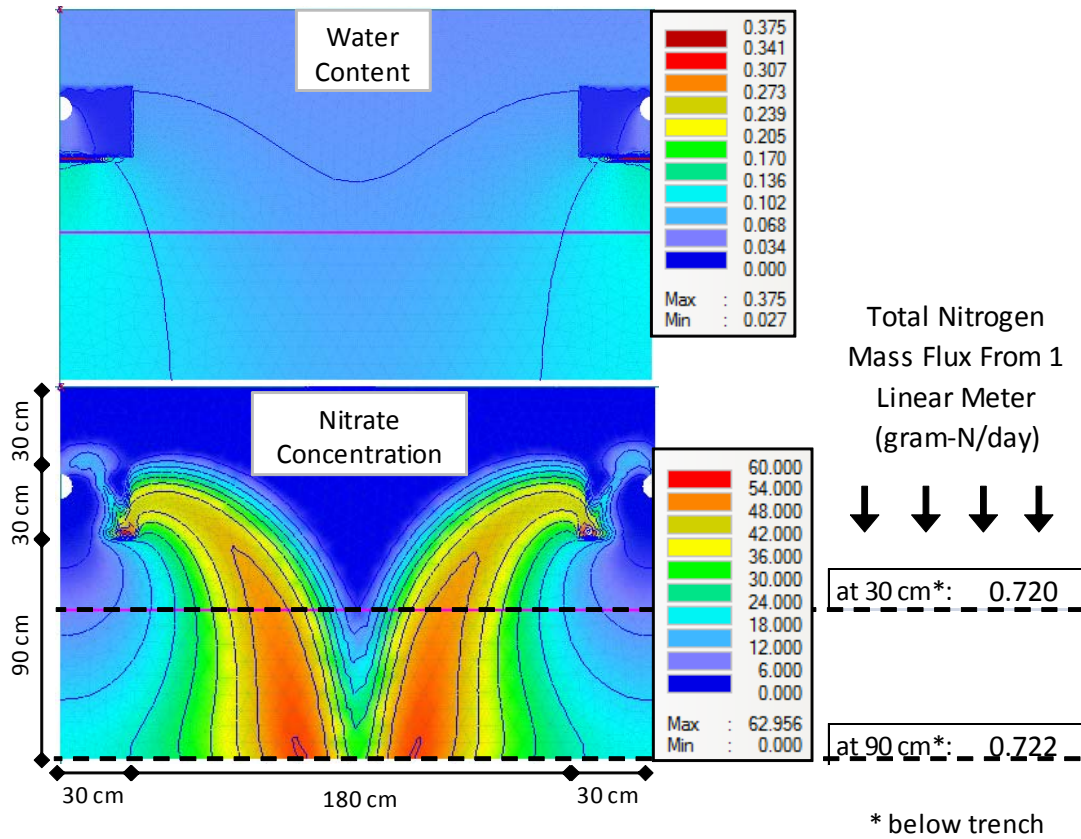
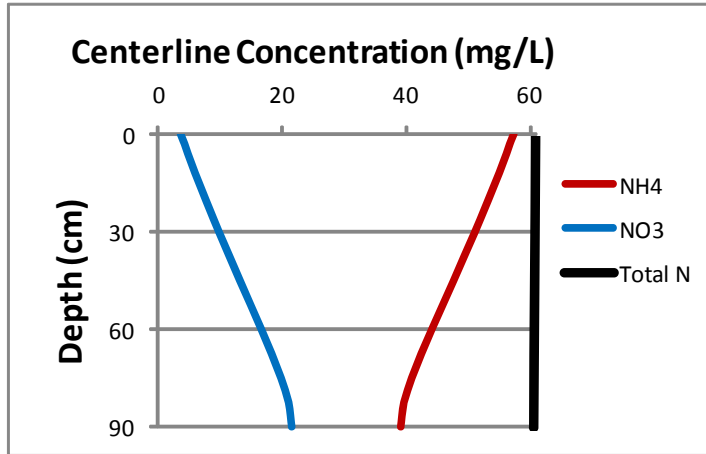


Figure VG-253. Scenario Output: Trench, Sandy Soil, Standard Effluent, HLR = 2cm d⁻¹.

Soil type:	Sand
Effluent Quality:	STE
Daily Loading Rate:	10% of K _{sat} (64.3 cm/day)

	NH ₄	NO ₃	Total N
% Removal at 30cm	15.0%	---	4.0%
% Removal at 90cm	25.0%	6.4%	3.6%

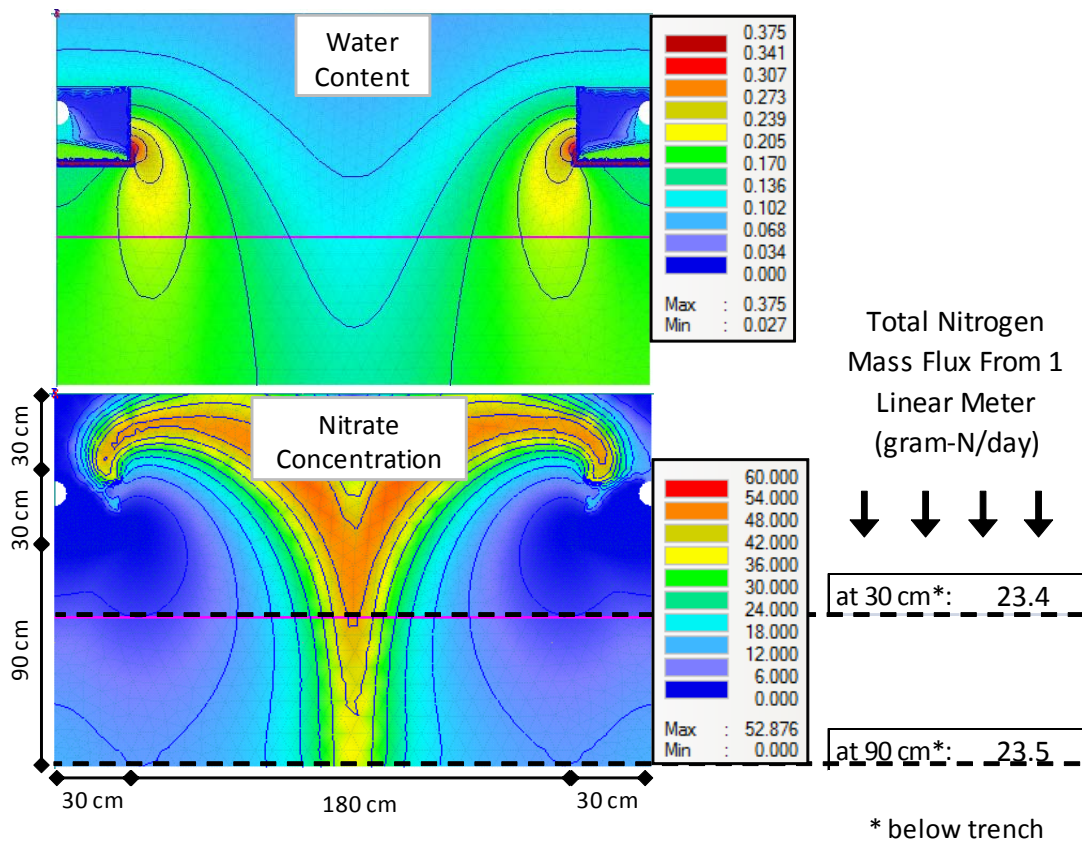
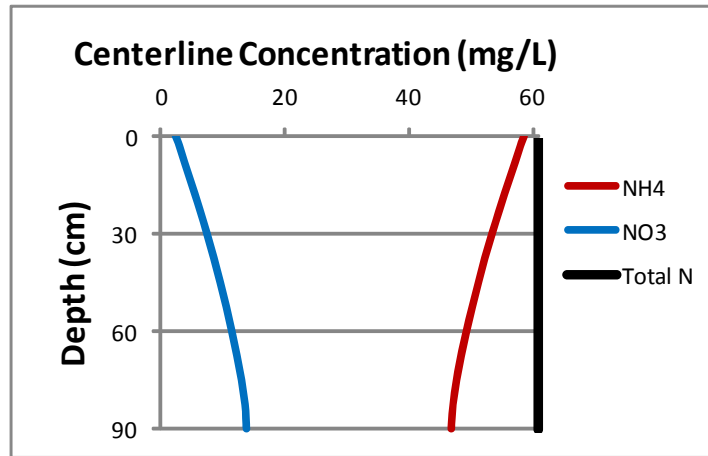


Figure VG-254. Scenario Output: Trench, Sandy Soil, Standard Effluent, HLR = 10% of K_{sat}.

Soil type:	Sandy Loam
Effluent Qaulity:	STE
Daily Loading Rate:	2 cm/day

	NH ₄	NO ₃	Total N
% Removal at 30cm	100.0%	21.1%	24.8%
% Removal at 90cm	100.0%	44.0%	46.7%

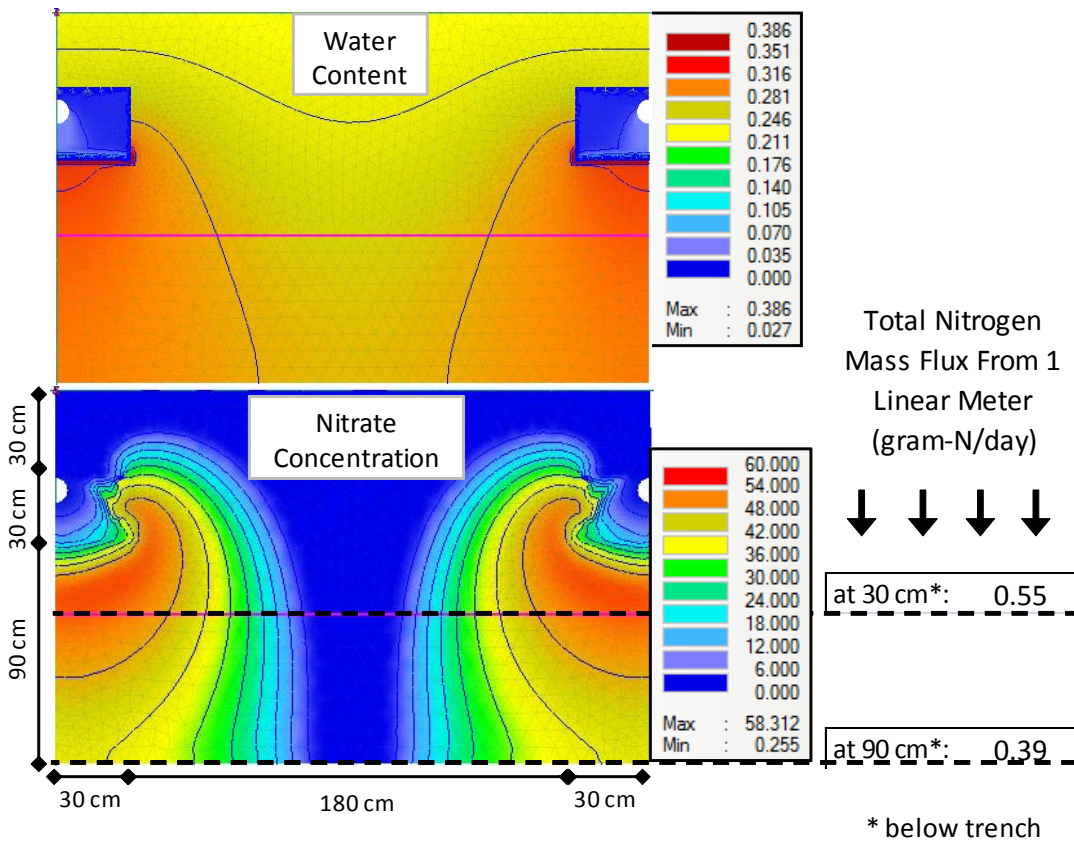
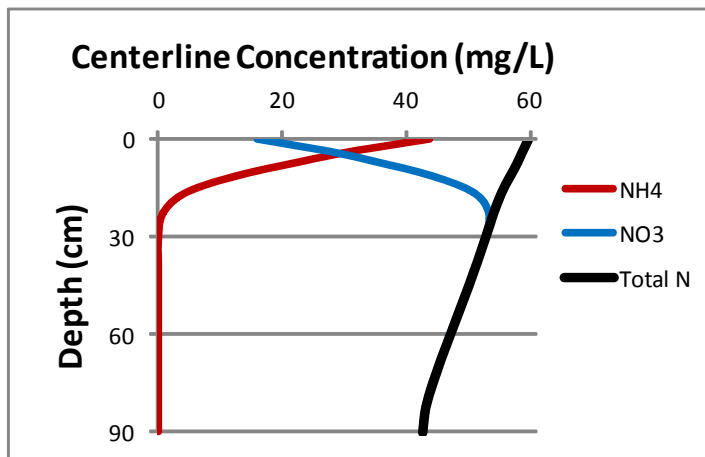


Figure VG-255. Scenario Output: Trench, Sandy Loam Soil, Standard Effluent, HLR = 2cm d⁻¹.

Soil type:	Sandy Loam
Effluent Quality:	STE
Daily Loading Rate:	2 cm/day - High Water Table

	NH ₄	NO ₃	Total N
% Removal at 60cm	99.8%	48.6%	50.7%

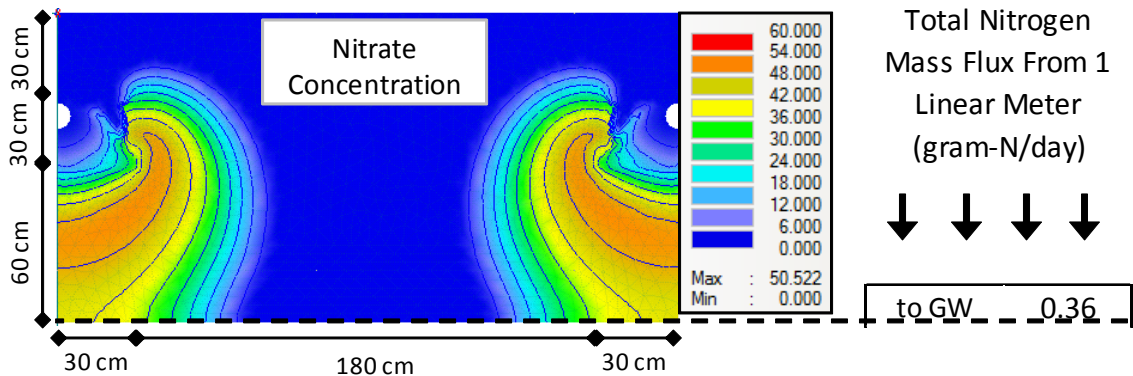
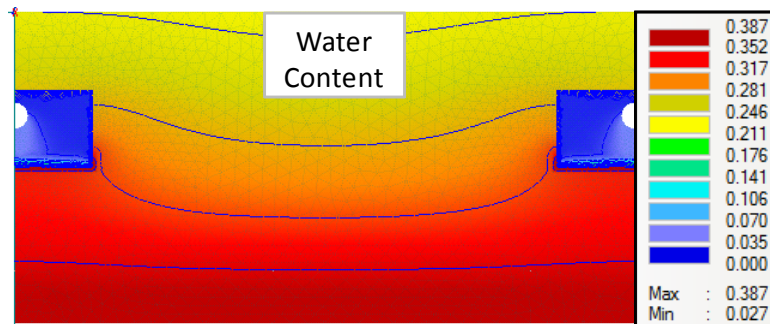
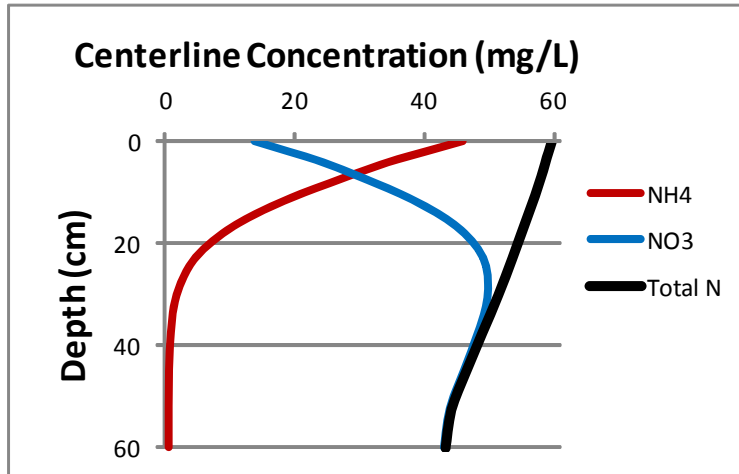


Figure VG-256. Scenario Output: Trench, Sandy Loam Soil, Standard Effluent, HLR = 2cm d⁻¹, “High Water Table”.

Soil type:	Sandy Loam
Effluent Quality:	STE
Daily Loading Rate:	2 cm/day - Closely Spaced Trenches

	NH ₄	NO ₃	Total N
% Removal at 30cm	100.0%	21.8%	24.9%
% Removal at 90cm	100.0%	37.3%	39.8%

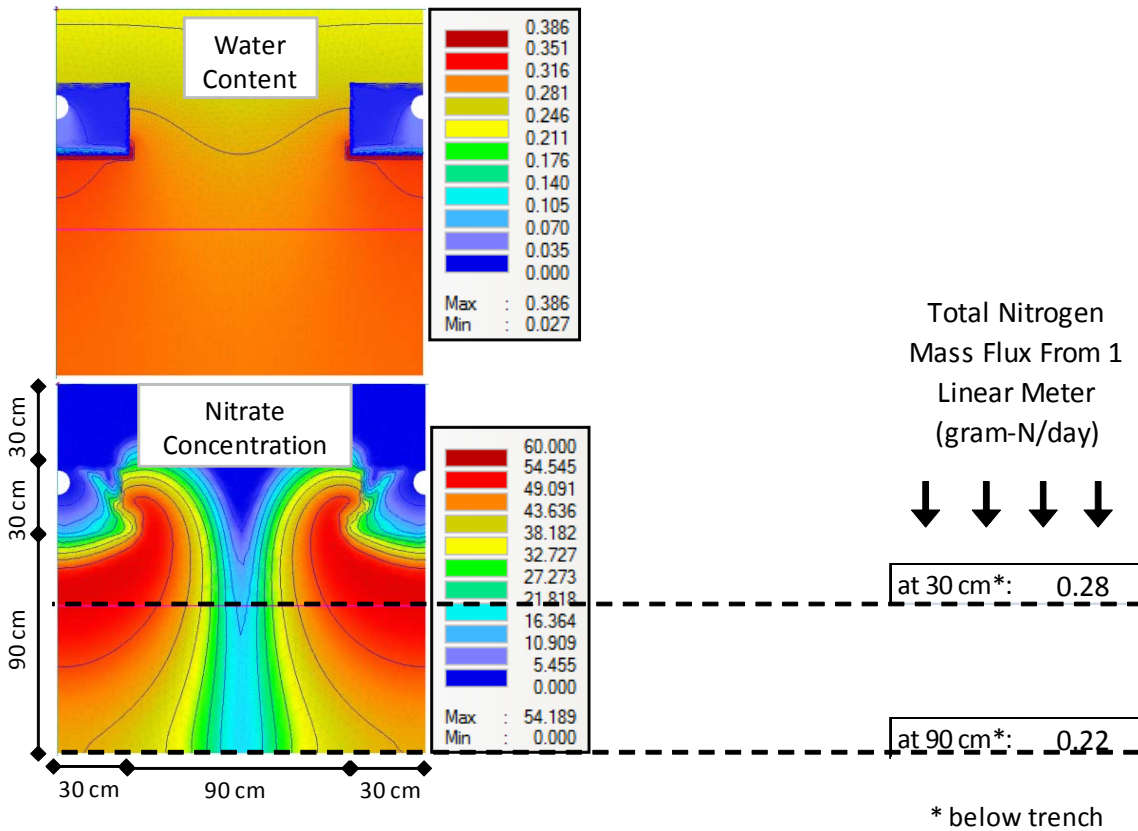
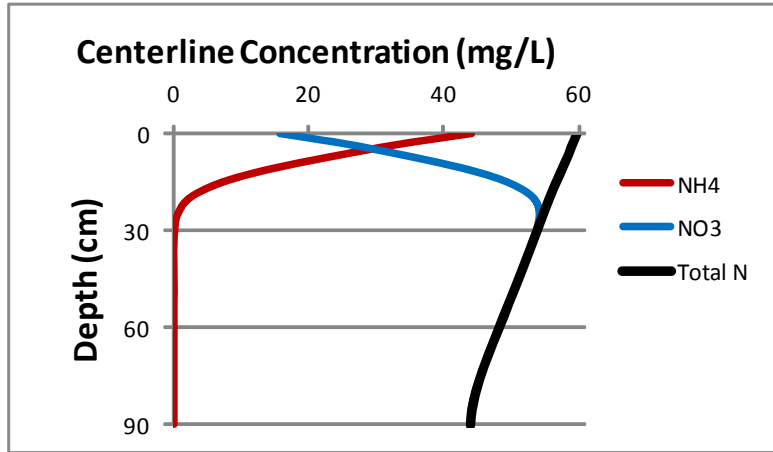


Figure VG-257. Scenario Output: Trench, Sandy Loam Soil, Standard Effluent, HLR = 2cm d⁻¹, "Closely Spaced Trenches".

Soil type:	Sandy Loam
Effluent Qaulity:	STE
Daily Loading Rate:	10% of Ksat (3.825 cm/day)

	NH ₄	NO ₃	Total N
% Removal at 30cm	97.5%	25.0%	26.2%
% Removal at 90cm	100.0%	33.2%	36.6%

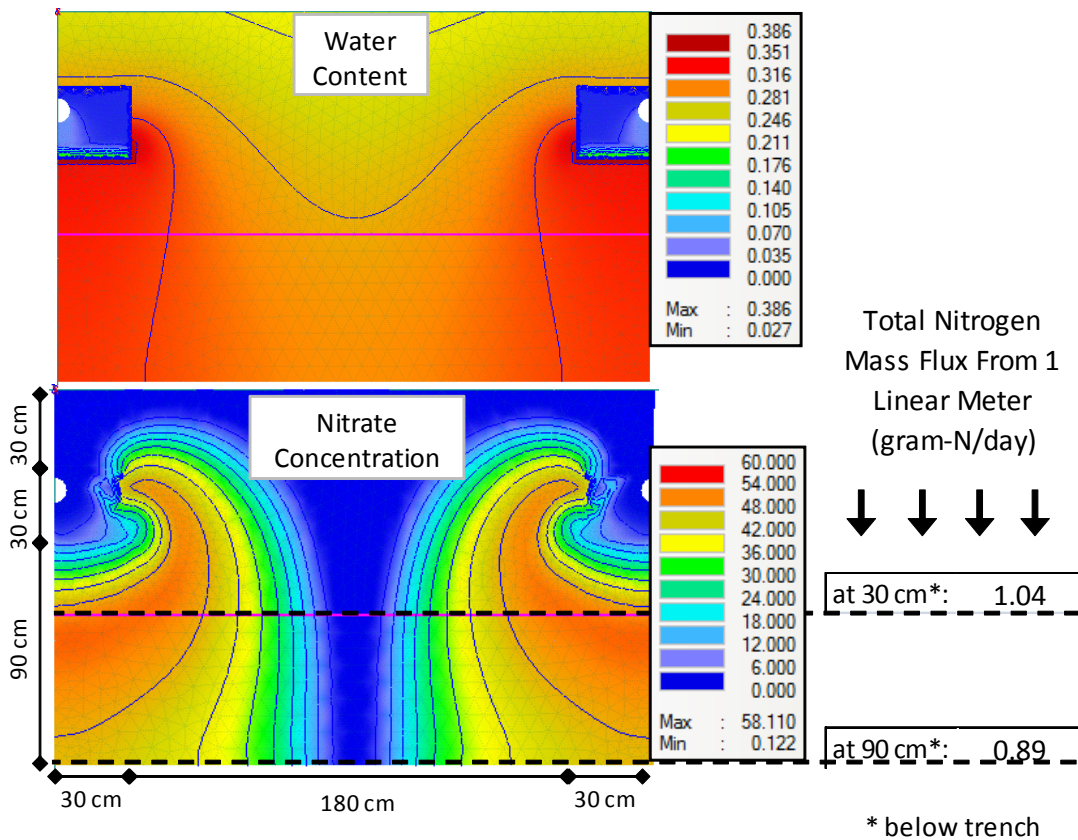
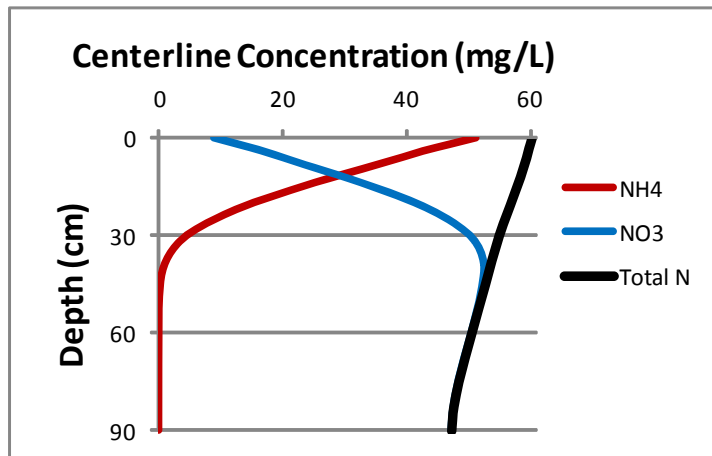


Figure VG-258. Scenario Output: Trench, Sandy Loam Soil, Standard Effluent, HLR =10% of K_{sat}.

Soil type:	Silty Clay
Effluent Quality:	STE
Daily Loading Rate:	2 cm/day

	NH ₄	NO ₃	Total N
% Removal at 30cm	58.3%	90.1%	50.1%
% Removal at 90cm	93.2%	92.8%	86.9%

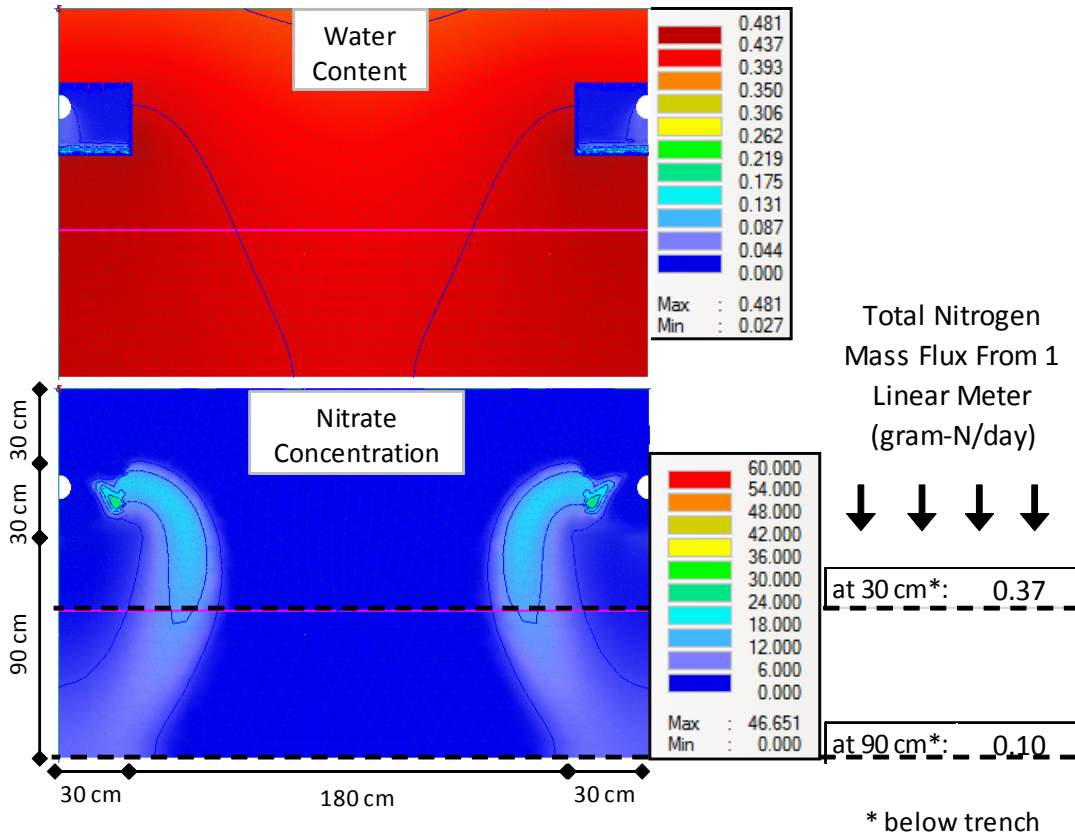
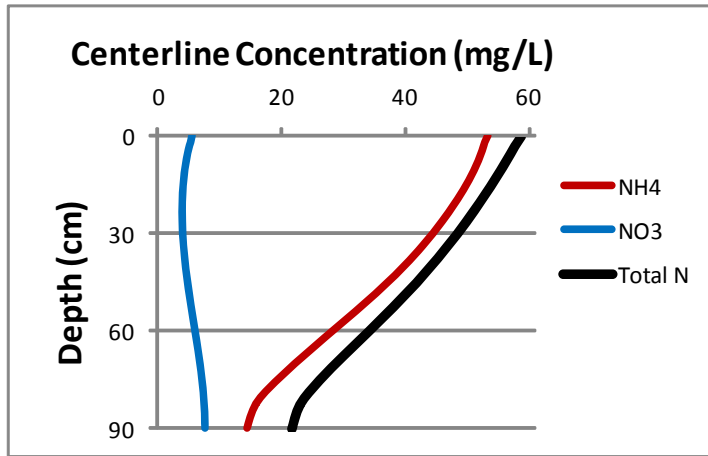


Figure VG-259. Scenario Output: Trench, Silty Clay Soil, Standard Effluent, HLR = 2cm d⁻¹.

Soil type:	Silty Clay
Effluent Quality:	STE
Daily Loading Rate:	10% of Ksat (0.961 cm/day)

	NH ₄	NO ₃	Total N
% Removal at 30cm	88.2%	79.2%	68.2%
% Removal at 90cm	100.0%	99.9%	99.9%

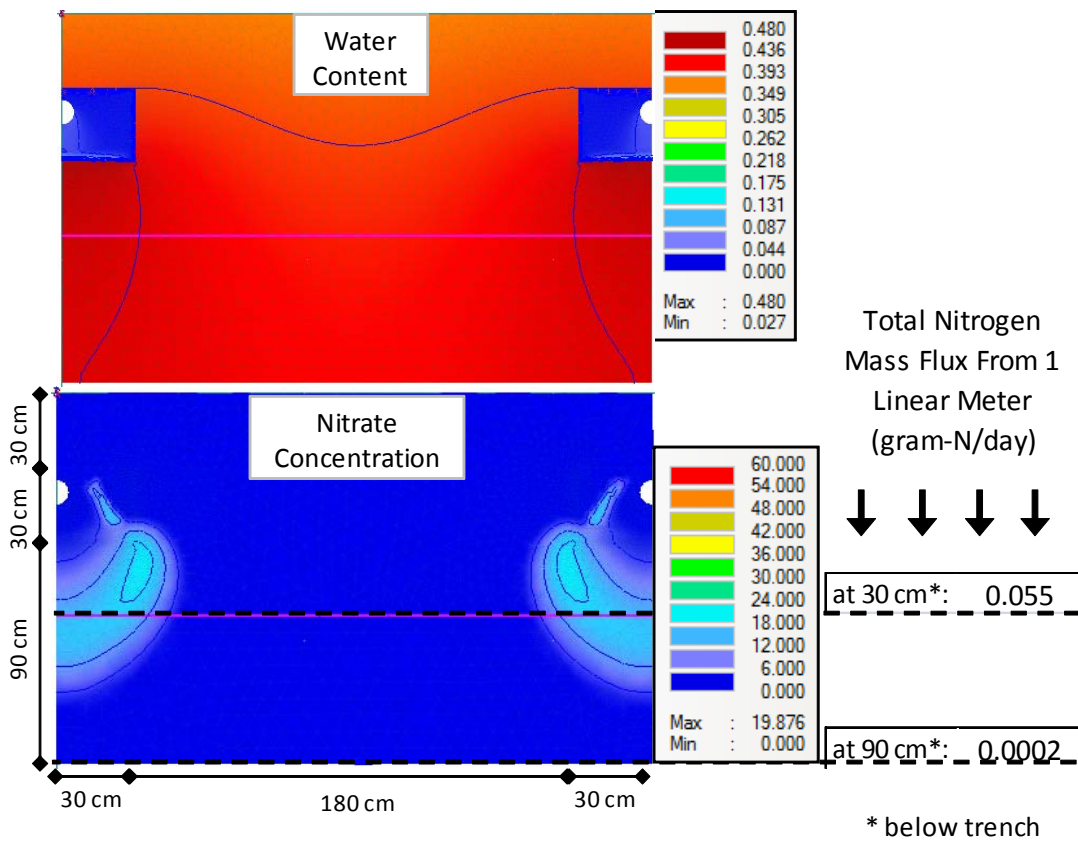
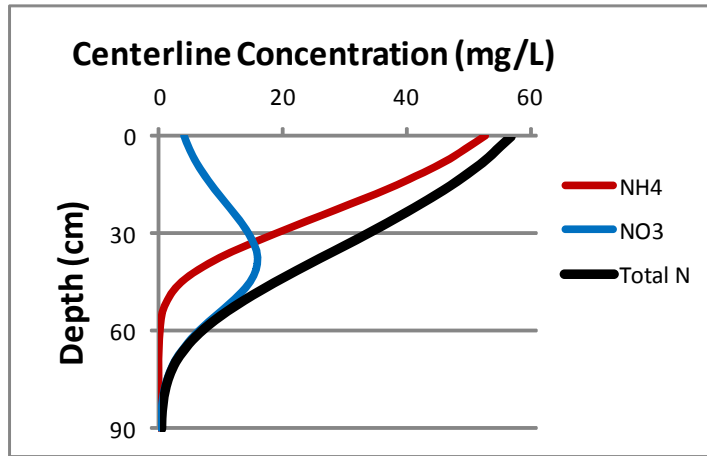


Figure VG-260. Scenario Output: Trench, Silty Clay Soil, Standard Effluent, HLR = 10% of K_{sat}.

Soil type:	Sand
Effluent Quality:	STE
Dosing Duration:	7 minutes
Dosings Per Day:	5

	NH ₄	NO ₃	Total N
% Removal at 30cm	100.0%	94.8%	97.3%
% Removal at 60cm	100.0%	100.0%	
% Uptake by plant	54.3%	80.7%	95.9%

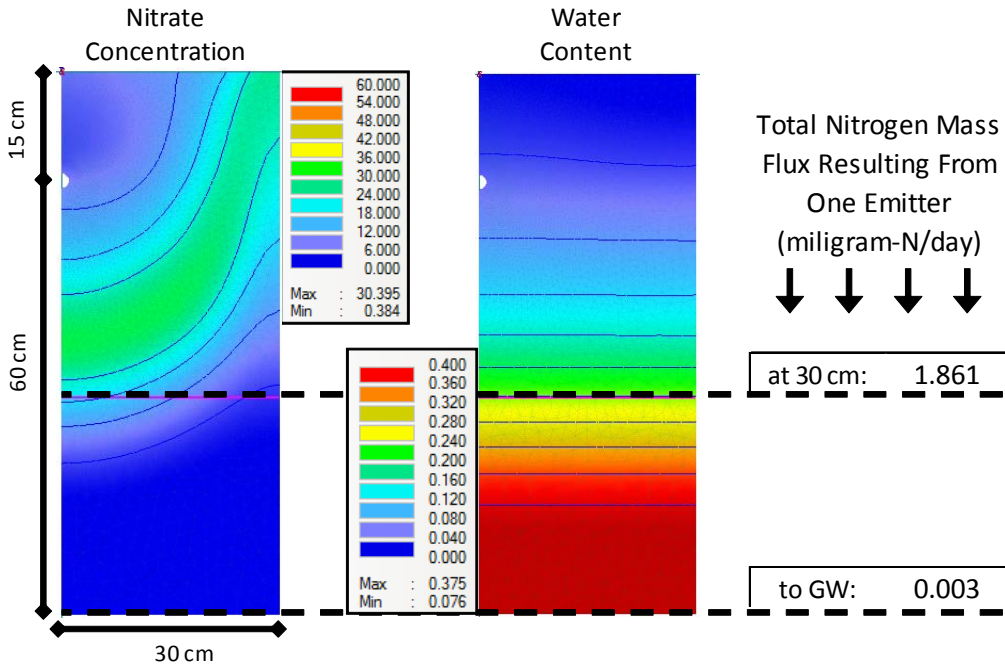
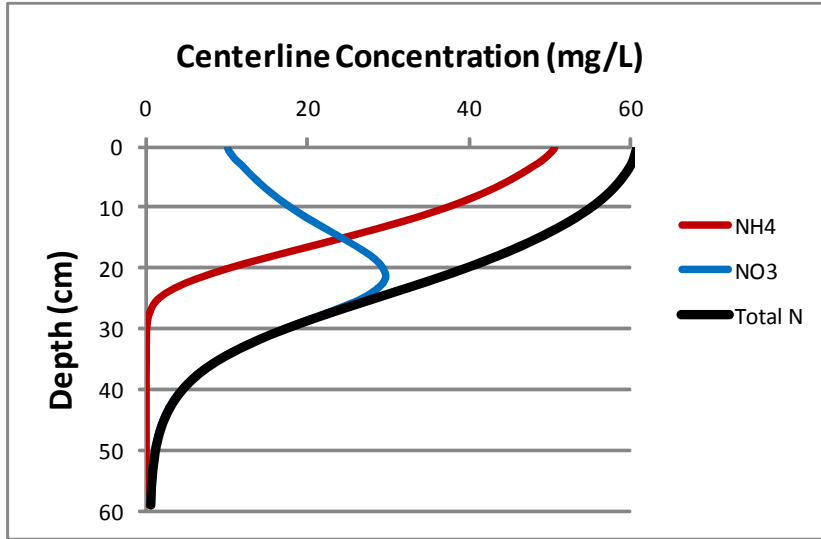


Figure VG-261. Scenario Output: Drip Dispersal, Sandy Soil, Standard Effluent, HLR = "Low".

Soil type:	Sand
Effluent Qaulity:	STE
Dosing Duration:	19 minutes
Dosings Per Day:	5

	NH₄	NO₃	Total N
% Removal at 30cm	97.4%	32.7%	52.7%
% Removal at 60cm	100.0%	43.0%	62.1%
% Uptake by plant	29.2%	19.5%	41.7%

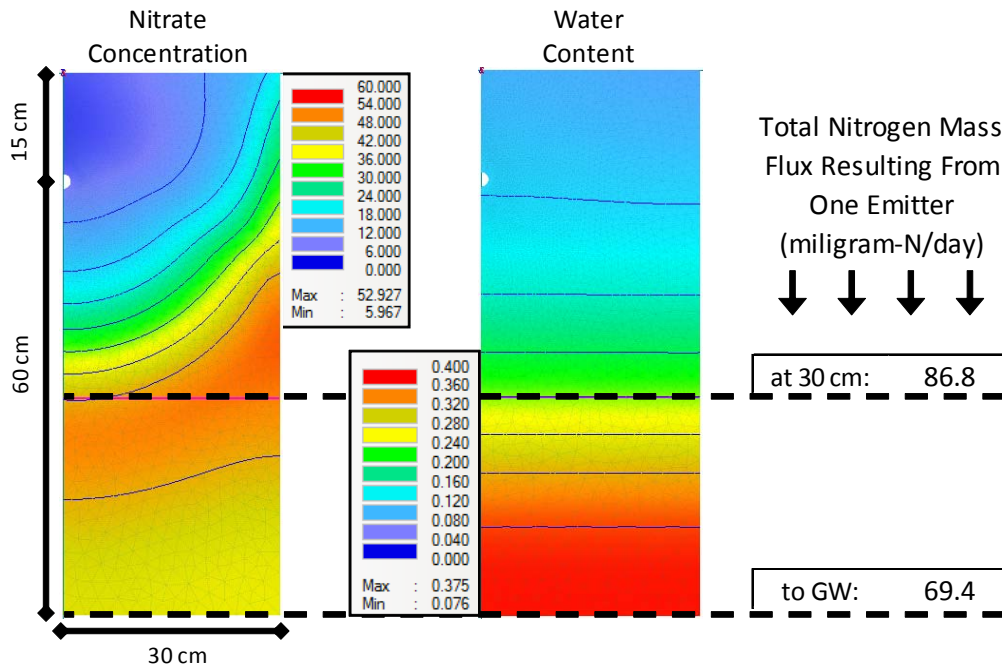
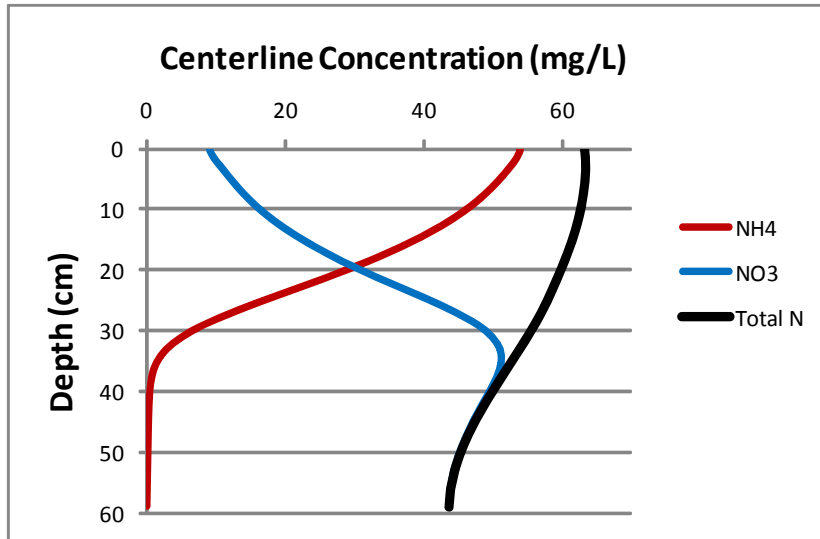


Figure VG-262. Scenario Output: Drip Dispersal, Sandy Soil, Standard Effluent, HLR = "High".

Soil type:	Sand
Effluent Quality:	NE
Dosing Duration:	7 minutes
Dosings Per Day:	5

	NH ₄	NO ₃	Total N
% Removal at 30cm	-	98.1%	98.1%
% Removal at 60cm	-	100.0%	100.0%
% Uptake by plant	-	87.2%	87.2%

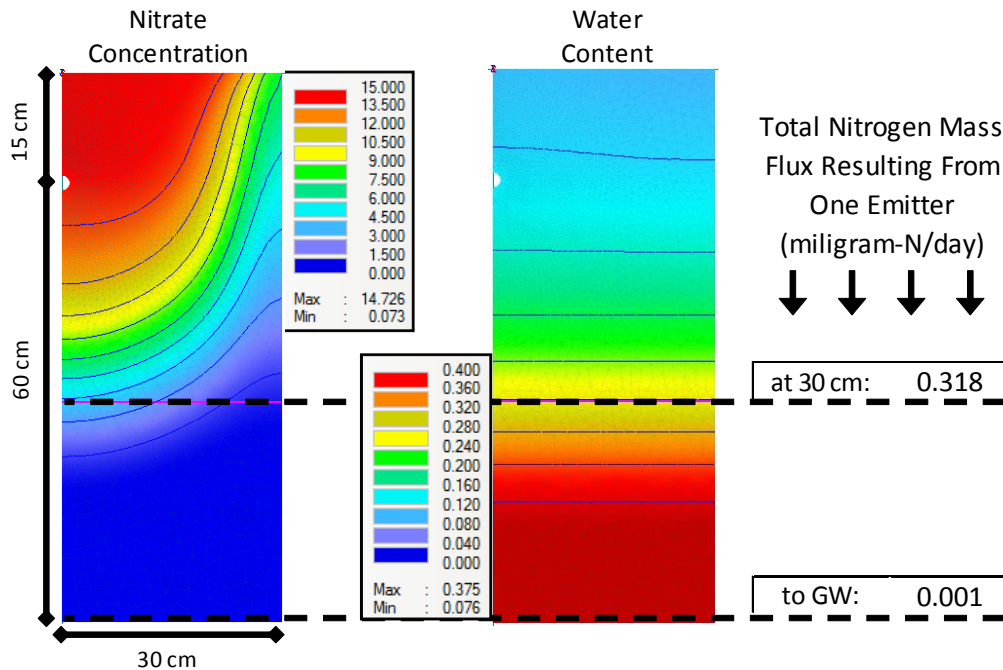
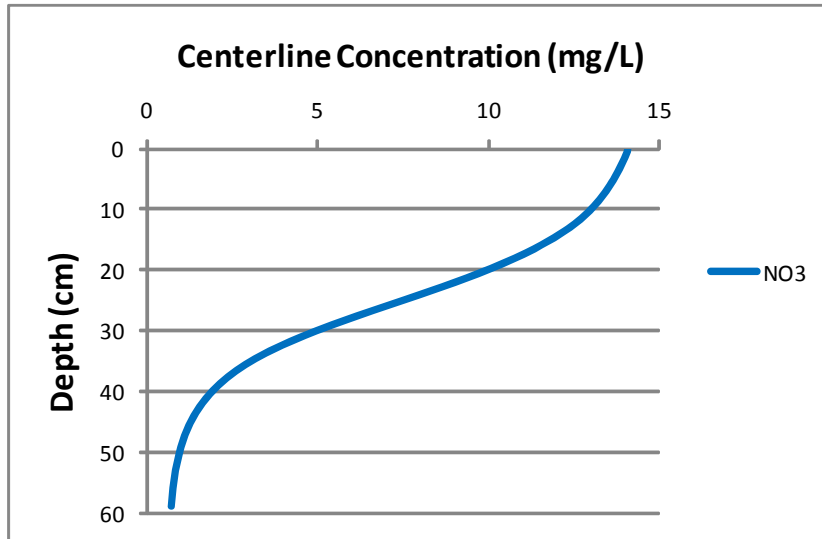


Figure VG-263. Scenario Output: Drip Dispersal, Sandy Soil, Nitrified Effluent, HLR = "Low".

Soil type:	Sand
Effluent Quality:	NE
Dosing Duration:	19 minutes
Dosings Per Day:	5

	NH ₄	NO ₃	Total N
% Removal at 30cm	-	58.3%	58.3%
% Removal at 60cm	-	78.8%	78.8%
% Uptake by plant	-	44.3%	44.3%

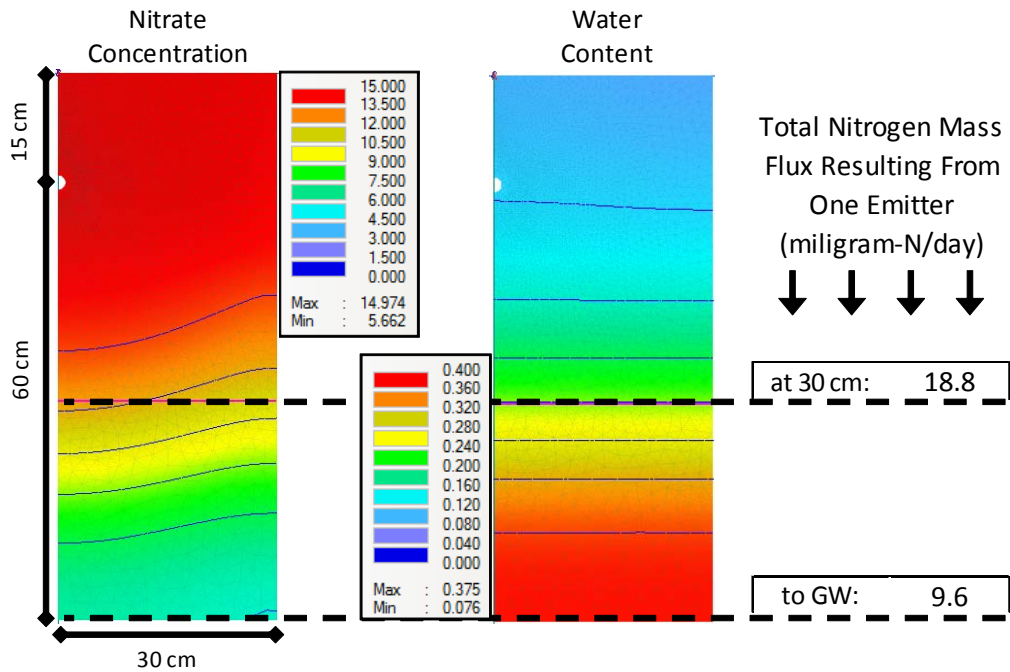
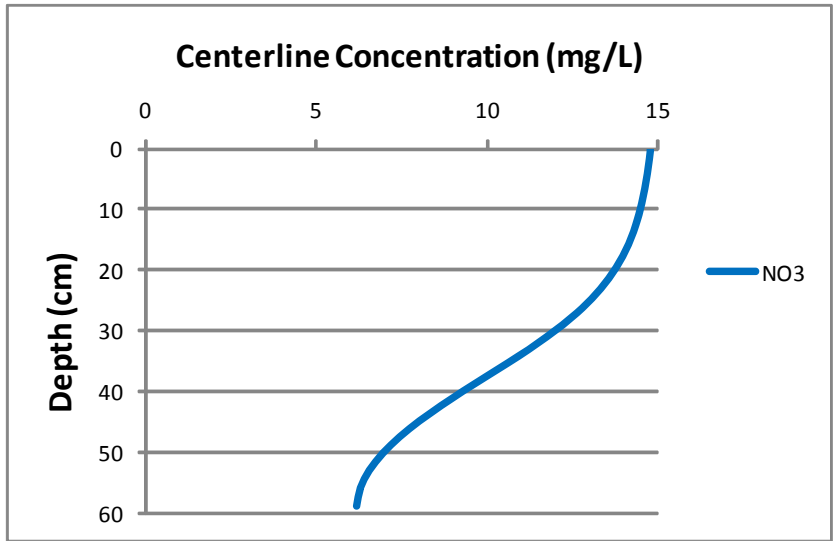


Figure VG-264. Scenario Output: Drip Dispersal, Sandy Soil, Nitrified Effluent, HLR = "High".

Soil type:	Sandy Loam
Effluent Quality:	STE
Dosing Duration:	7 minutes
Dosings Per Day:	5

	NH ₄	NO ₃	Total N
% Removal at 30cm	100.0%	99.3%	99.4%
% Removal at 60cm	100.0%	99.9%	
% Uptake by plant	3.6%	81.6%	82.4%

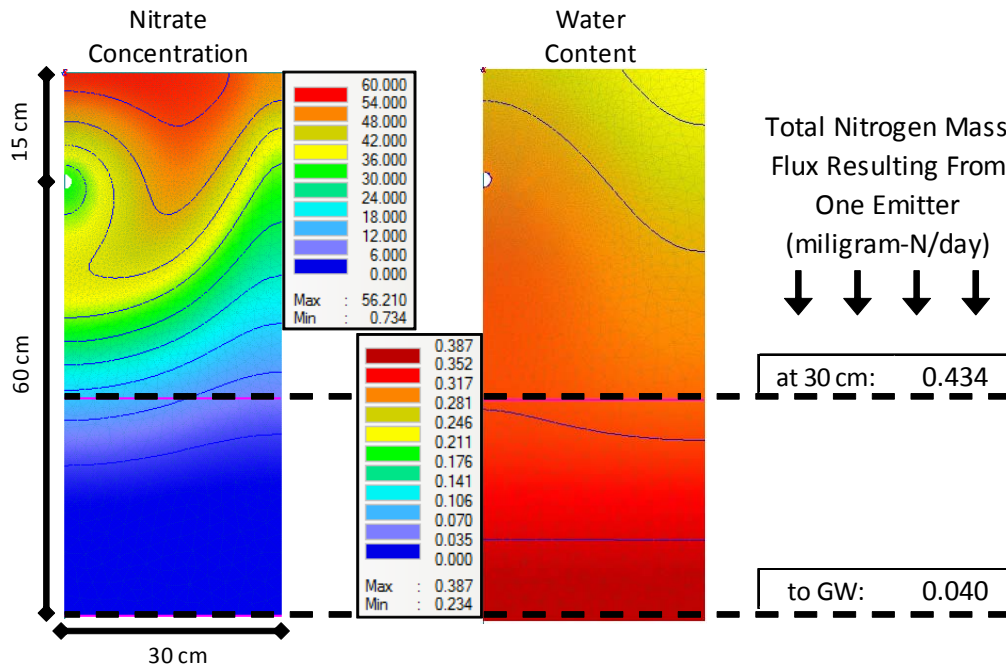
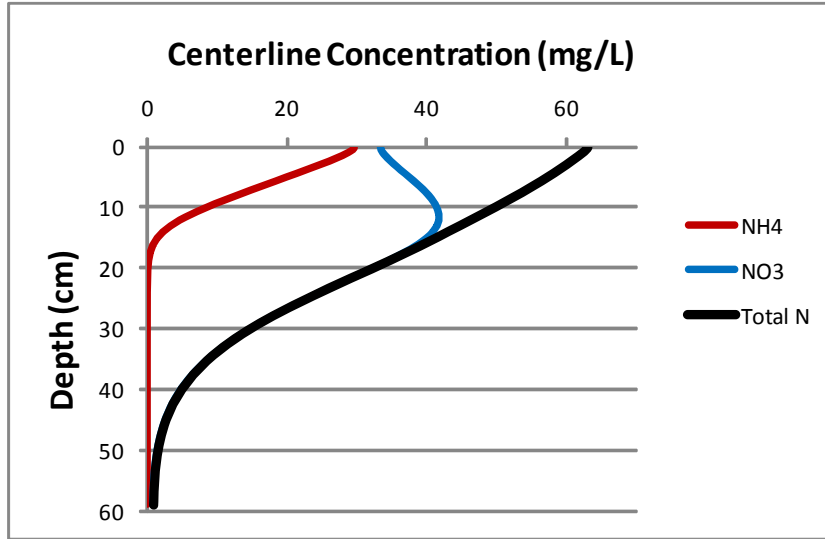


Figure VG-265. Scenario Output: Drip Dispersal, Sandy Loam Soil, Standard Effluent, HLR = "Low".

Soil type:	Sandy Loam
Effluent Quality:	STE
Dosing Duration:	19 minutes
Dosings Per Day:	5

	NH ₄	NO ₃	Total N
% Removal at 30cm	99.9%	53.6%	54.6%
% Removal at 60cm	100.0%	61.8%	62.7%
% Uptake by plant	2.3%	38.2%	39.5%

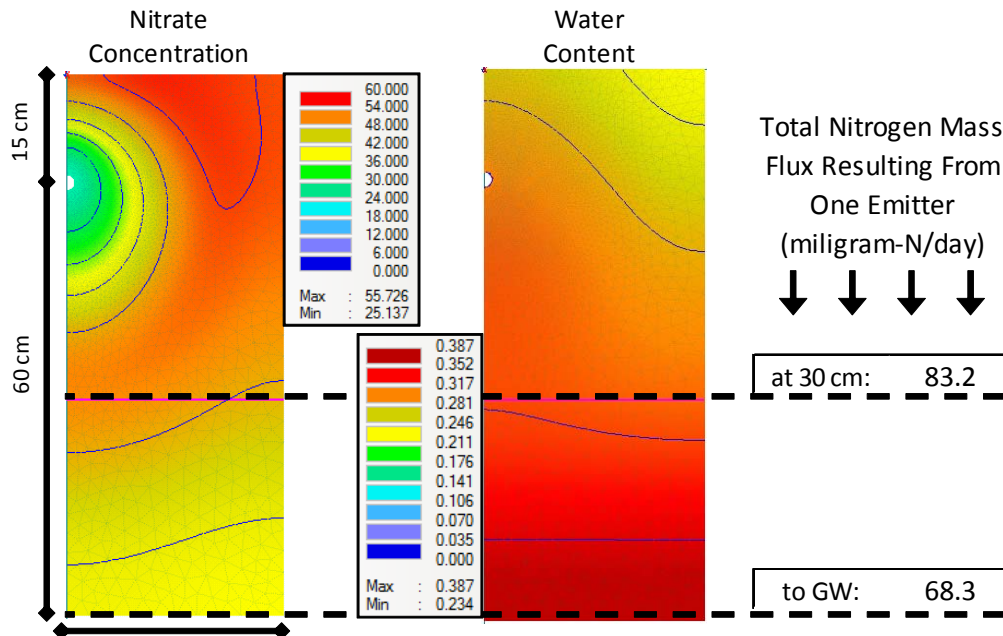
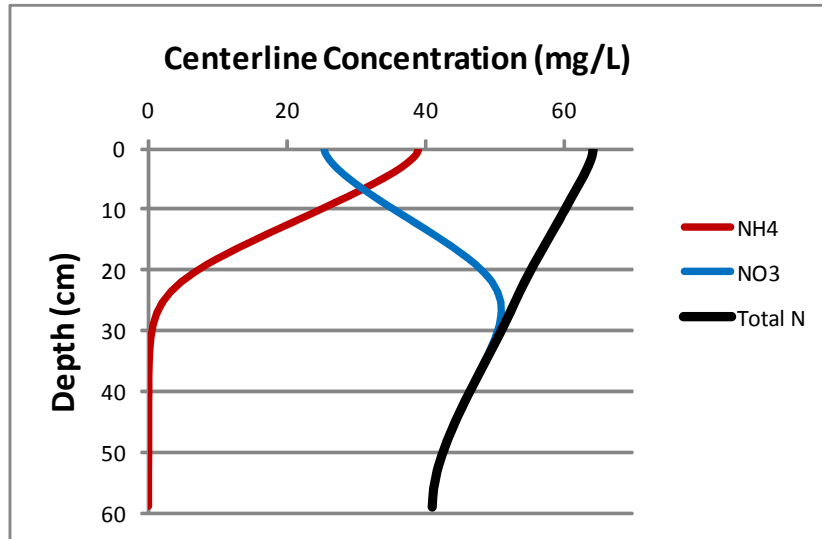


Figure VG-266. Scenario Output: Drip Dispersal, Sandy Loam Soil, Standard Effluent, HLR = "High".

Soil type:	Sandy Loam
Effluent Quality:	NE
Dosing Duration:	7 minutes
Dosings Per Day:	5

	NH ₄	NO ₃	Total N
% Removal at 30cm	-	99.8%	99.8%
% Removal at 60cm	-	100.0%	100.0%
% Uptake by plant	-	69.0%	69.0%

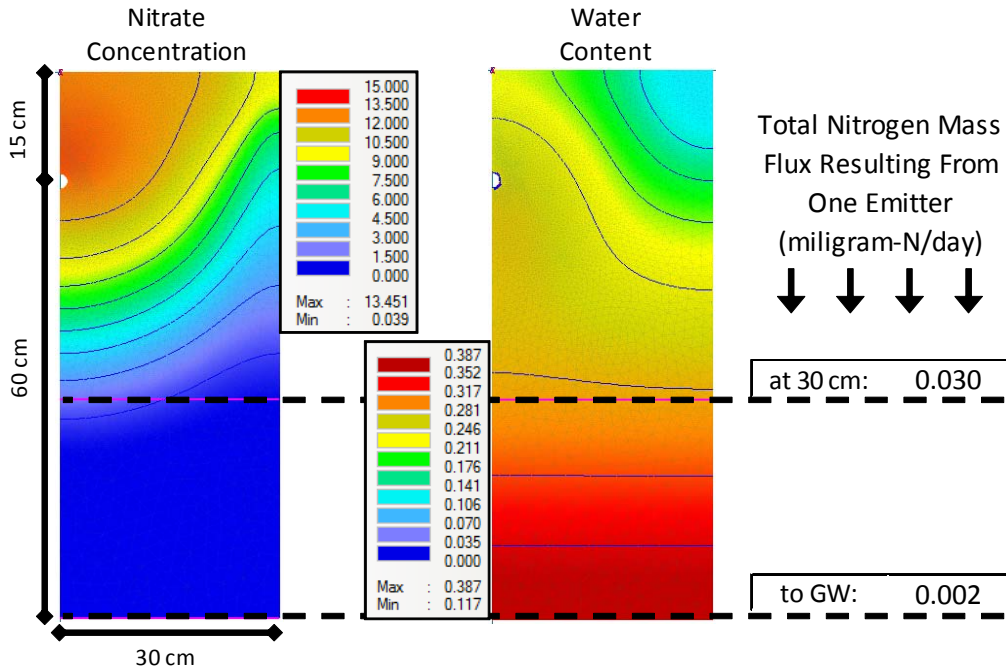
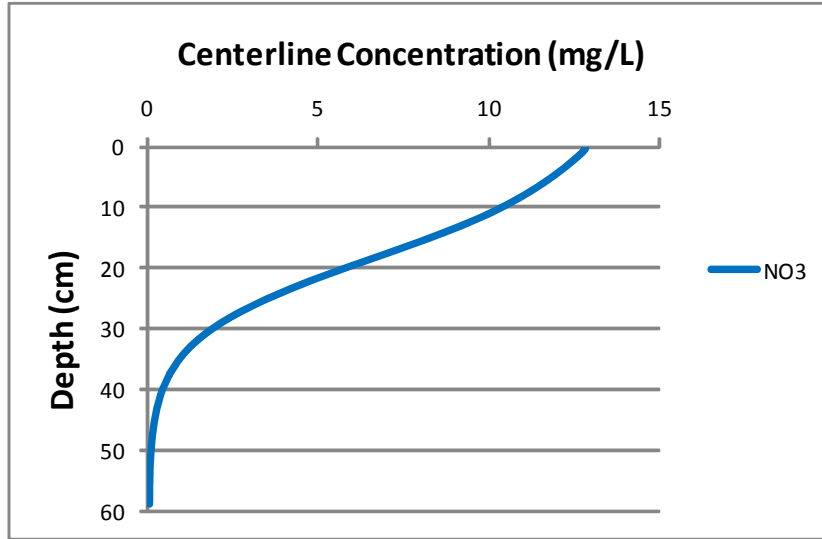


Figure VG-267. Scenario Output: Drip Dispersal, Sandy Loam Soil, Nitrified Effluent, HLR = "Low".

Soil type:	Sandy Loam
Effluent Quality:	NE
Dosing Duration:	19 minutes
Dosings Per Day:	5

	NH₄	NO₃	Total N
% Removal at 30cm	-	49.5%	49.5%
% Removal at 60cm	-	54.9%	54.9%
% Uptake by plant	-	44.9%	44.9%

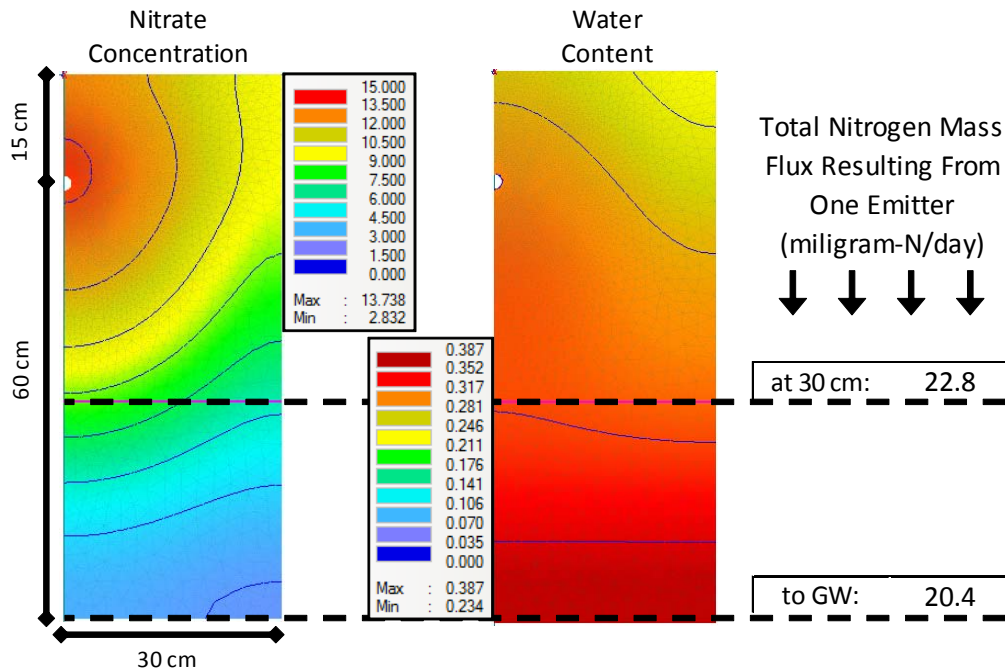
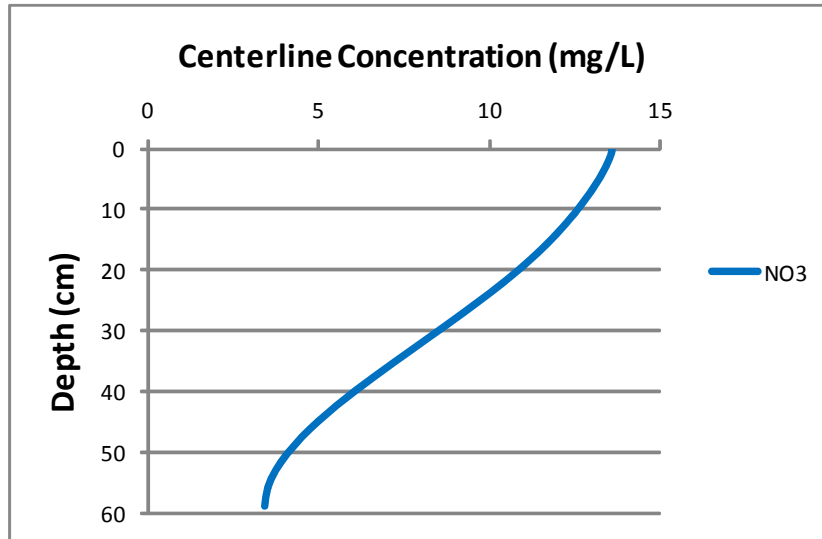


Figure VG-268. Scenario Output: Drip Dispersal, Sandy Loam Soil, Nitrified Effluent, HLR = "High".

Soil type:	Silty Clay
Effluent Qaulity:	STE
Dosing Duration:	7 minutes
Dosings Per Day:	5

	NH ₄	NO ₃	Total N
% Removal at 30cm	100.0%	99.9%	99.9%
% Removal at 60cm	100.0%	100.0%	100.0%
% Uptake by plant	3.6%	49.9%	51.2%

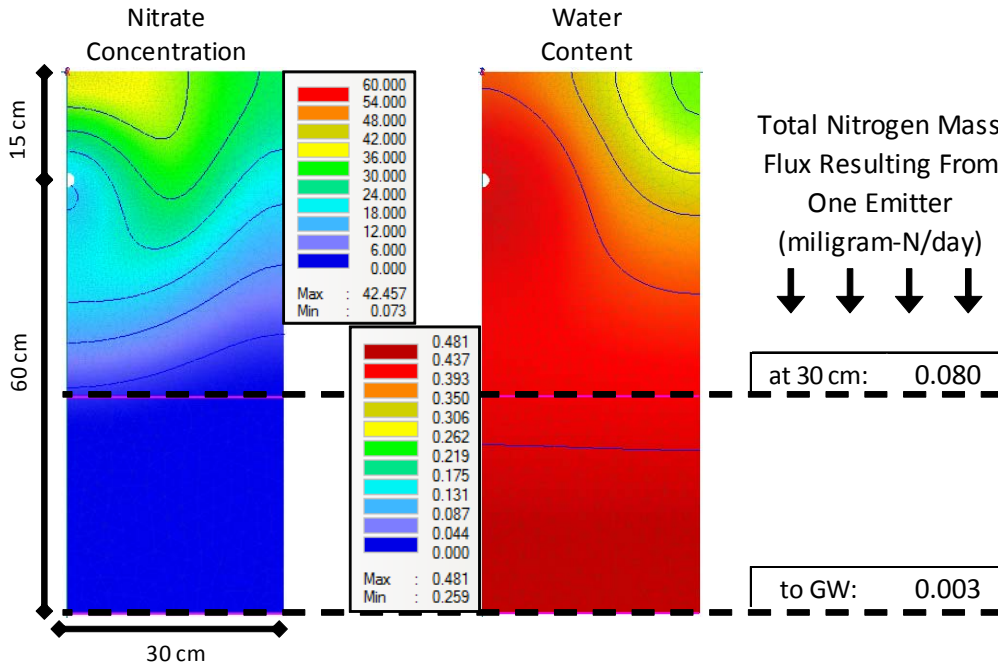
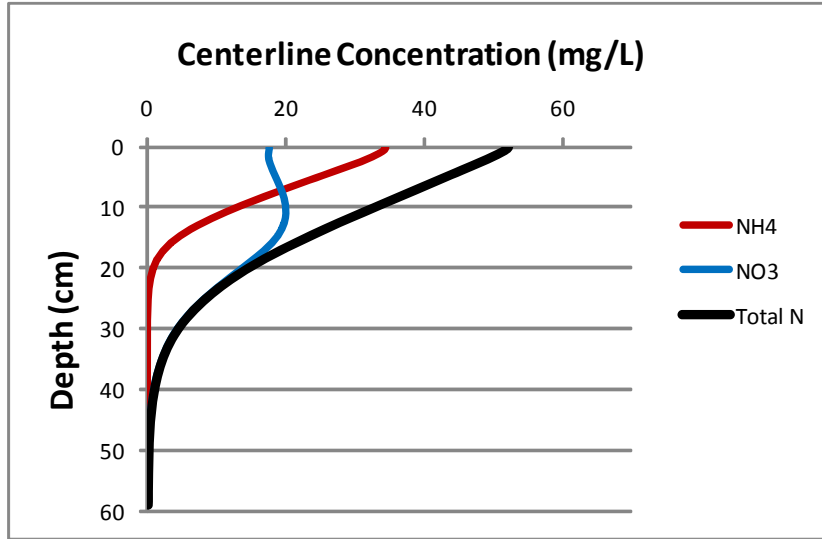


Figure VG-269. Scenario Output: Drip Dispersal, Silty Clay Soil, Standard Effluent, HLR = "Low".

Soil type:	Silty Clay
Effluent Quality:	STE
Dosing Duration:	7 minutes
Dosings Per Day:	10

	NH ₄	NO ₃	Total N
% Removal at 30cm	95.4%	95.2%	91.5%
% Removal at 60cm	99.4%	98.3%	98.0%
% Uptake by plant	11.2%	23.7%	30.8%

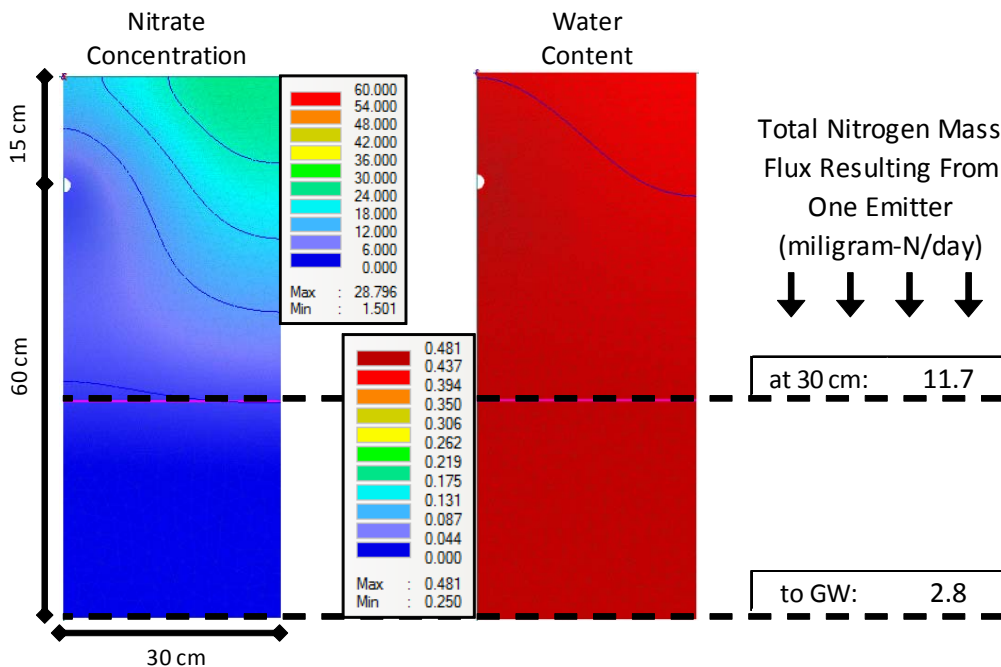
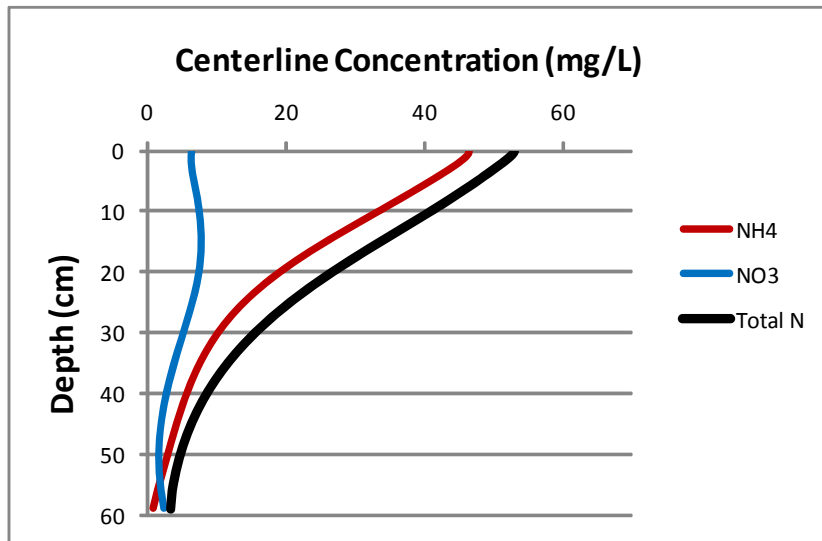


Figure VG-270. Scenario Output: Drip Dispersal, Silty Clay Soil, Standard Effluent, HLR = "High".

Soil type:	Silty Clay
Effluent Quality:	NE
Dosing Duration:	7 minutes
Dosings Per Day:	5

	NH ₄	NO ₃	Total N
% Removal at 30cm	-	99.98%	99.98%
% Removal at 60cm	-	100.0%	100.0%
% Uptake by plant	-	31.0%	31.0%

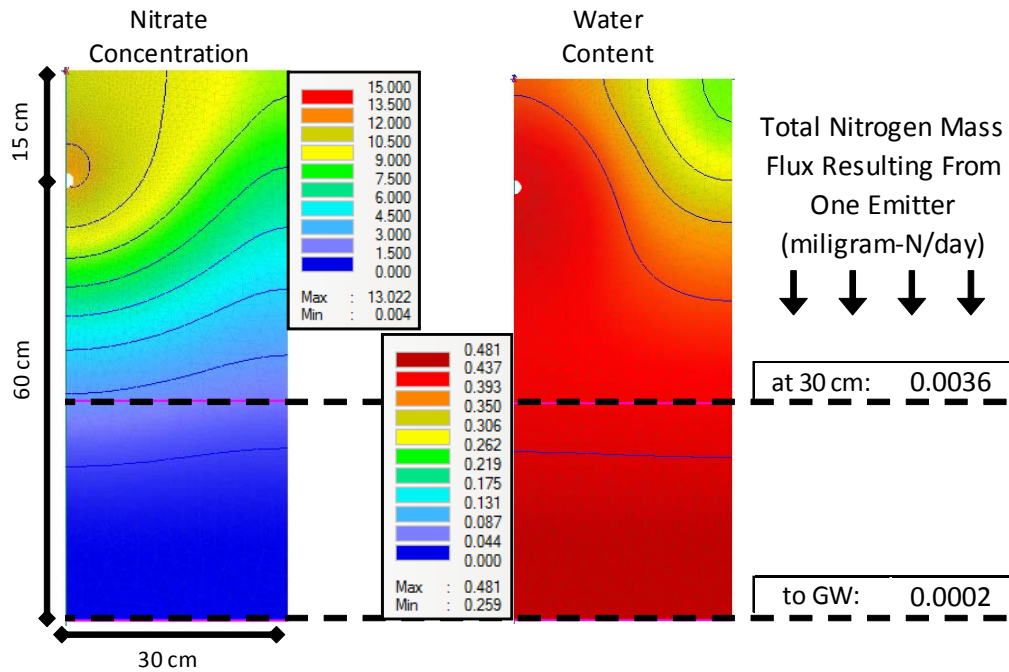
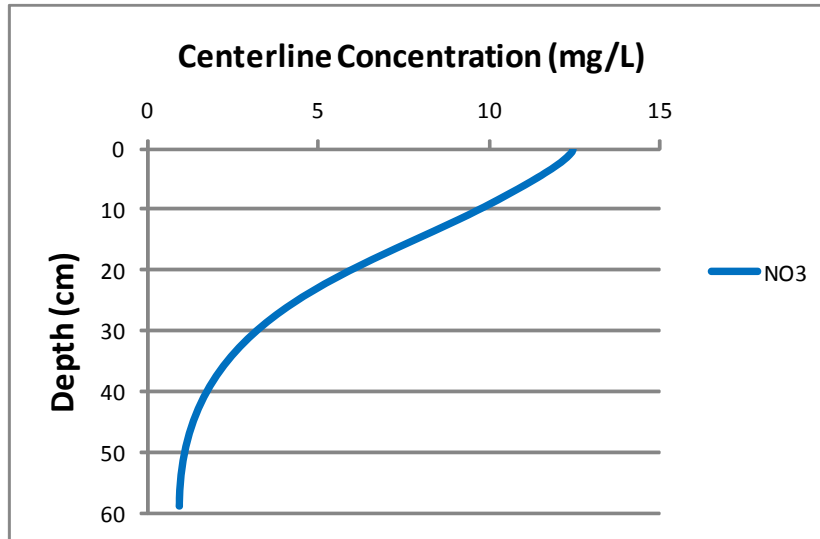


Figure VG-271. Scenario Output: Drip Dispersal, Silty Clay Soil, Nitrified Effluent, HLR = "Low".

Soil type:	Silty Clay
Effluent Quality:	NE
Dosing Duration:	7 minutes
Dosings Per Day:	10

	NH₄	NO₃	Total N
% Removal at 30cm	-	98.5%	98.5%
% Removal at 60cm	-	99.9%	99.9%
% Uptake by plant	-	13.7%	13.7%

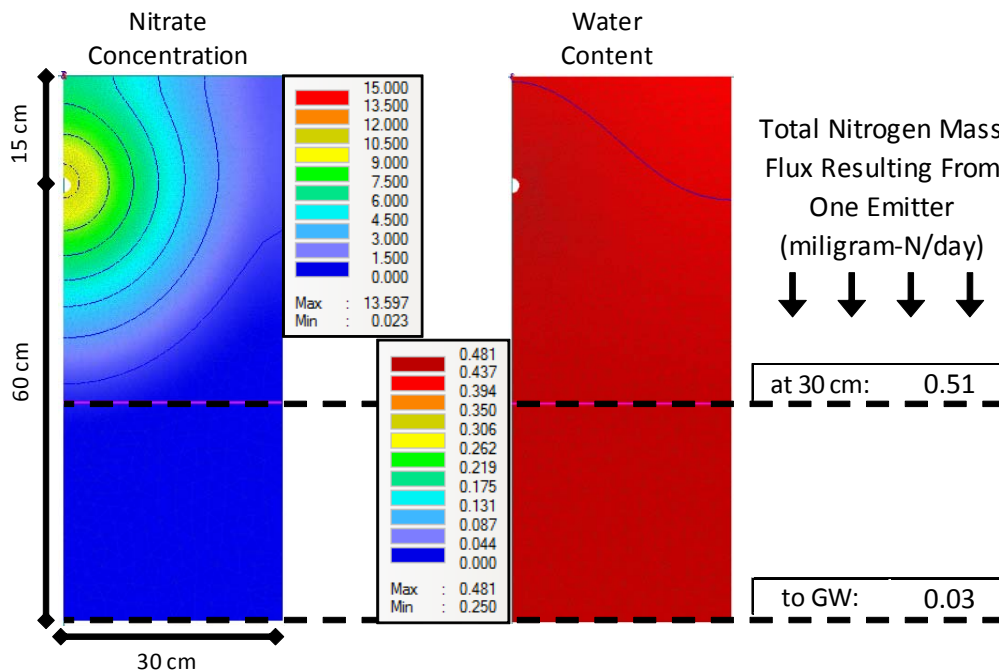
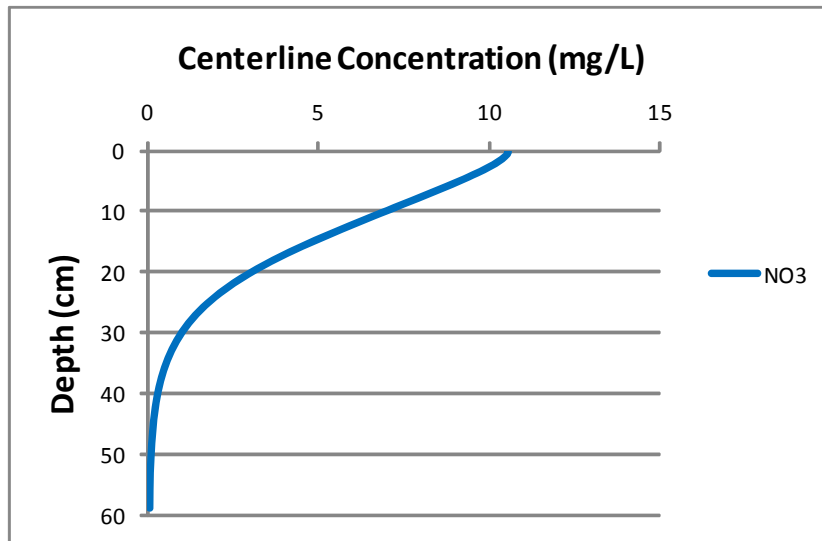


Figure VG-272. Scenario Output: Drip Dispersal, Silty Clay Soil, Nitrified Effluent, HLR = "High".

WASTEWATER UTILITY

Alabama

Montgomery Water Works & Sanitary Sewer Board

Alaska

Anchorage Water & Wastewater Utility

Arizona

Avondale, City of
Glendale, City of, Utilities Department
Mesa, City of
Peoria, City of
Phoenix Water Services Dept.
Pima County Wastewater Management
Tempe, City of

Arkansas

Little Rock Wastewater Utility

California

Central Contra Costa Sanitary District
Corona, City of
Crestline Sanitation District
Delta Diablo Sanitation District
Dublin San Ramon Services District
East Bay Dischargers Authority
East Bay Municipal Utility District
El Dorado Irrigation District
Fairfield-Suisun Sewer District
Fresno Department of Public Utilities
Inland Empire Utilities Agency
Irvine Ranch Water District
Las Gallinas Valley Sanitary District
Las Virgenes Municipal Water District
Livermore, City of
Los Angeles, City of
Los Angeles County, Sanitation Districts of
Napa Sanitation District
Novato Sanitary District
Orange County Sanitation District
Palo Alto, City of
Riverside, City of
Sacramento Regional County Sanitation District
San Diego Metropolitan Wastewater Department, City of
San Francisco, City & County of
San Jose, City of
Santa Barbara, City of
Santa Cruz, City of
Santa Rosa, City of
South Bayside System Authority
South Coast Water District

South Orange County Wastewater Authority
South Tahoe Public Utility District

Steger Sanitary District
Sunnyvale, City of
Union Sanitary District
West Valley Sanitation District

Colorado

Aurora, City of
Boulder, City of
Greeley, City of
Littleton/Englewood Water Pollution Control Plant
Metro Wastewater Reclamation District, Denver
Platte Canyon Water & Sanitation District

Connecticut

Greater New Haven WPCA
Stamford, City of

District of Columbia

District of Columbia Water & Sewer Authority

Florida

Broward, County of
Fort Lauderdale, City of
Jacksonville Electric Authority (JEA)
Loxahatchee River District
Miami-Dade Water & Sewer Authority
Orange County Utilities Department
Pinellas, County of
Reedy Creek Improvement District
St. Petersburg, City of
Tallahassee, City of
Toho Water Authority
West Palm Beach, City of

Georgia

Atlanta Department of Watershed Management
Augusta, City of
Clayton County Water Authority
Cobb County Water System
Columbus Water Works
Fulton County
Gwinnett County Department of Public Utilities
Savannah, City of

Hawaii

Honolulu, City & County of

Idaho

Boise, City of

Illinois

Decatur, Sanitary District of
Greater Peoria Sanitary District
Kankakee River Metropolitan Agency
Metropolitan Water Reclamation District of Greater Chicago

Wheaton Sanitary District

Indiana

Jeffersonville, City of

Iowa

Ames, City of
Cedar Rapids Wastewater Facility
Des Moines, City of
Iowa City

Kansas

Johnson County Wastewater Unified Government of Wyandotte County/
Kansas City, City of

Kentucky

Louisville & Jefferson County Metropolitan Sewer District
Sanitation District No. 1

Louisiana

Sewerage & Water Board of New Orleans

Maine

Bangor, City of
Portland Water District

Maryland

Anne Arundel County Bureau of Utility Operations
Howard County Bureau of Utilities
Washington Suburban Sanitary Commission

Massachusetts

Boston Water & Sewer Commission
Massachusetts Water Resources Authority (MWRA)
Upper Blackstone Water Pollution Abatement District

Michigan

Ann Arbor, City of
Detroit, City of
Holland Board of Public Works
Saginaw, City of
Wayne County Department of Environment
Wyoming, City of

Minnesota

Rochester, City of
Western Lake Superior Sanitary District

Missouri

Independence, City of
Kansas City Missouri Water Services Department
Little Blue Valley Sewer District
Metropolitan St. Louis Sewer District

Nebraska

Lincoln Wastewater & Solid Waste System

Nevada

Henderson, City of

New Jersey

Bergen County Utilities Authority
Ocean County Utilities Authority

New York

New York City Department of Environmental Protection

North Carolina

Charlotte/Mecklenburg Utilities
Durham, City of
Metropolitan Sewerage District of Buncombe County
Orange Water & Sewer Authority

Ohio

Akron, City of
Butler County Department of Environmental Services
Columbus, City of
Metropolitan Sewer District of Greater Cincinnati
Montgomery, County of
Northeast Ohio Regional Sewer District
Summit, County of

Oklahoma

Oklahoma City Water & Wastewater Utility Department
Tulsa, City of

Oregon

Albany, City of
Clean Water Services
Eugene, City of
Gresham, City of
Portland, City of
Bureau of Environmental Services
Lake Oswego, City of
Oak Lodge Sanitary District
Water Environment Services

Pennsylvania

Philadelphia, City of
University Area Joint Authority

South Carolina

Beaufort-Jasper Water & Sewer Authority
Charleston Water System
Mount Pleasant Waterworks & Sewer Commission
Spartanburg Water

Tennessee

Cleveland Utilities
Murfreesboro Water & Sewer Department
Nashville Metro Water Services

Texas

Austin, City of
Dallas Water Utilities
Denton, City of
El Paso Water Utilities
Fort Worth, City of
Houston, City of

San Antonio Water System
Trinity River Authority

Utah

Salt Lake City Corporation

Virginia

Alexandria Sanitation Authority
Fairfax, County of
Hampton Roads Sanitation
District
Hanover, County of
Henrico, County of
Hopewell Regional Wastewater
Treatment Facility
Loudoun Water

Lynchburg Regional
Wastewater Treatment Plant

Prince William County
Service Authority

Richmond, City of
Rivanna Water & Sewer
Authority

Washington

Everett, City of
King County Department of
Natural Resources
Seattle Public Utilities
Sunnyside, Port of
Yakima, City of

Wisconsin

Green Bay Metro
Sewerage District
Kenosha Water Utility
Madison Metropolitan
Sewerage District
Milwaukee Metropolitan
Sewerage District
Racine, City of
Sheboygan Regional
Wastewater Treatment
Wausau Water Works

**Water Services Association
of Australia**

ACTEW Corporation
Barwon Water
Central Highlands Water
City West Water
Coliban Water Corporation
Cradle Mountain Water
Gippsland Water
Gladstone Area Water Board
Gold Coast Water
Gosford City Council
Hunter Water Corporation
Logan Water
Melbourne Water
Onstream
Power & Water Corporation
Queensland Urban Utilities
South Australia Water
Corporation
Sydney Catchment Authority
Sydney Water
Unity Water
Wannon Regional Water
Corporation

Water Corporation
Water Distribution Brisbane
City Council
Western Water
Yarra Valley Water

Canada

Edmonton, City of/Edmonton
Waste Management Centre
of Excellence
Lethbridge, City of
Regina, City of,
Saskatchewan
Toronto, City of, Ontario
Winnipeg, City of, Manitoba

New Zealand

Watercare Services Limited

STORMWATER UTILITY

California

Fresno Metropolitan Flood
Control District
Los Angeles, City of,
Department of Public Works
Monterey, City of
San Francisco, City & County of
Santa Rosa, City of
Sunnyvale, City of

Colorado

Aurora, City of
Boulder, City of

Florida

Orlando, City of

Georgia

Griffin, City of

Iowa

Cedar Rapids Wastewater
Facility
Des Moines, City of

Kansas

Lenexa, City of
Overland Park, City of

Kentucky

Louisville & Jefferson County
Metropolitan Sewer District

Maine

Portland Water District

North Carolina

Charlotte, City of,
Stormwater Services

Pennsylvania

Philadelphia, City of

Tennessee

Chattanooga Stormwater
Management

Texas

Harris County Flood Control
District, Texas

Washington

Bellevue Utilities Department
Seattle Public Utilities

STATE

Connecticut Department of
Environmental Protection

Kansas Department of Health
& Environment
New England Interstate
Water Pollution Control
Commission (NEIWPC)
Ohio Environmental Protection
Agency
Ohio River Valley Sanitation
Commission
Urban Drainage & Flood
Control District, CO

CORPORATE

Advanced Data Mining
International
AECOM
Alan Plummer & Associates
Alpine Technology Inc.
American Cleaning Institute
Aqua-Aerobic Systems Inc.
Aquateam-Norwegian Water
Technology Centre A/S
ARCADIS
Associated Engineering
Bernardin Lochmueller &
Associates
Black & Veatch
Blue Water Technologies, Inc.
Brown & Caldwell
Burgess & Niple, Ltd.
Burns & McDonnell
CABE Associates Inc.
The Cadmus Group
Camp Dresser & McKee Inc.
Carollo Engineers Inc.
Carpenter Environmental
Associates Inc.
CET Engineering Services
CH2M HILL
CONTECH Stormwater
Solutions
CRA Infrastructure &
Engineering
CSIRO (Commonwealth
Scientific and Industrial
Research Organisation)
D&B/Guarino Engineers, LLC
Damon S. Williams
Associates, LLC
Ecovation
EMA Inc.
Environmental Operating
Solutions, Inc.
Environ International
Corporation
Fay, Spofford, & Thorndike Inc.
Freese & Nichols, Inc.
ftn Associates Inc.
Gannett Fleming Inc.
Garden & Associates, Ltd.
Geosyntec Consultants
GHD Inc.
Global Water Associates
Greeley and Hansen LLC
Hazen & Sawyer, P.C.
HDR Engineering Inc.
HNTB Corporation

Hydromantis Inc.
HydroQual Inc.
Inflico Degremont Inc.
Jacobs Engineering Group Inc.
Jason Consultants LLC Inc.
KCI Technologies Inc.
Kelly & Weaver, P.C.
Kennedy/Jenks Consultants
Larry Walker Associates
LimnoTech Inc.
The Low Impact Development
Center Inc.
Malcolm Pirnie Inc.
MaxWest Environmental
Systems, Inc.
McKim & Creed
MWH
Neotex Ltda
NTL Alaska, Inc.
O'Brien & Gere Engineers Inc.
Odor & Corrosion Technology
Consultants Inc.
Parametrix Inc.
Parsons
Post, Buckley, Schuh & Jernigan
Praxair, Inc.
RMC Water & Environment
Ross & Associates Ltd.
Siemens Water Technologies
Southeast Environmental
Engineering, LLC
Stone Environmental Inc.
Stratus Consulting Inc.
Synagro Technologies Inc.
Tetra Tech Inc.
Trojan Technologies Inc.
Trussell Technologies, Inc.
URS Corporation
Westin Engineering Inc.
Wright Water Engineers
Zoeller Pump Company

INDUSTRY

American Electric Power
American Water
Anglian Water Services, Ltd.
Bill & Melinda Gates
Foundation
Chevron Energy Technology
The Coca-Cola Company
Dow Chemical Company
DuPont Company
Eastman Chemical Company
Eli Lilly & Company
InsinkErator
Johnson & Johnson
Merck & Company Inc.
Procter & Gamble Company
Suez Environment
United Utilities North West
(UUNW)
United Water Services LLC
Veolia Water North America

WERF Board of Directors

Chair Alan H. Vicory, Jr., P.E., BCEE Ohio River Valley Water Sanitation Co	Patricia J. Anderson, P.E. Florida Department of Health Jeanette A. Brown, P.E., BCEE, D.WRE Stamford Water Pollution Control Authority Catherine R. Gerali Metro Wastewater Reclamation District Charles N. Haas, Ph.D., BCEEM Drexel University Stephen R. Maguin Sanitation Districts of Los Angeles County	Karen L. Pallansch, P.E., BCEE Alexandria Sanitation Authority Robert A. Reich, P.E. DuPont Company R. Rhodes Trussell, Ph.D., P.E. Trussell Technologies Inc. Rebecca F. West Spartanburg Water Brian L. Wheeler Toho Water Authority Joseph E. Zuback Global Water Advisors, Inc.	Executive Director Glenn Reinhardt
Vice-Chair William P. Dee, P.E., BCEE Malcolm Pirnie, Inc.			
Secretary William J. Bertera Water Environment Federation			
Treasurer Jeff Taylor Freese and Nichols, Inc.			

WERF Research Council

Chair Karen L. Pallansch, P.E., BCEE Alexandria Sanitation Authority	William J. Cooper, Ph.D. University of California- Irvine Ann Farrell, P.E. Central Contra Costa Sanitary District (CCCSD)	James A. Hanlon U.S. Environmental Protection Agency James A. Hodges, CPEng. Watercare Services Limited David Jenkins, Ph.D. University of California at Berkeley Lloyd W. Johnson, M.P.D., P.E. Aqua-Aerobic Systems, Inc.	Terry L. Johnson, Ph.D., P.E., BCEE Black & Veatch Corporation Beverley M. Stinson, Ph.D. AECOM Susan J. Sullivan New England Interstate Water Pollution Control Commission (NEIWPC)
Vice-Chair John B. Barber, Ph.D. Eastman Chemical Company	Robbin W. Finch Boise, City of Thomas Granato, Ph.D. Metropolitan Water Reclamation District of Greater Chicago		

WERF Product Order Form

As a benefit of joining the Water Environment Research Foundation, subscribers are entitled to receive one complimentary copy of all final reports and other products. Additional copies are available at cost (usually \$10). To order your complimentary copy of a report, please write "free" in the unit price column. WERF keeps track of all orders. If the charge differs from what is shown here, we will call to confirm the total before processing.

Name		Title		
Organization				
Address				
City	State	Zip Code	Country	
Phone	Fax	Email		

Stock #	Product	Quantity	Unit Price	Total

Method of Payment: (All orders must be prepaid.)

C check or Money Order Enclosed

Visa Mastercard American Express

Account No. _____ Exp. Date _____

Signature _____

Postage & Handling	
VA Residents Add 5% Sales Tax	
Canadian Residents Add 7% GST	
TOTAL	

Shipping & Handling:			
Amount of Order	United States	Canada & Mexico	All Others
Up to but not more than:	Add:	Add:	Add:
\$20.00	\$7.50*	\$9.50	50% of amount
30.00	8.00	9.50	40% of amount
40.00	8.50	9.50	
50.00	9.00	18.00	
60.00	10.00	18.00	
80.00	11.00	18.00	
100.00	13.00	24.00	
150.00	15.00	35.00	
200.00	18.00	40.00	
More than \$200.00	Add 20% of order	Add 20% of order	
* minimum amount for all orders			

To Order (Subscribers Only):

Log on to www.werf.org and click on "Publications."

Phone: 571-384-2100
 Fax : 703-299-0742

WERF
 Attn: Subscriber Services
 635 Slaters Lane
 Alexandria, VA 22314-1177

To Order (Non-Subscribers):

Non-subscribers may order WERF publications either through WERF or IWAP (www.iwapublishing.com). Visit WERF's website at www.werf.org for details.

Make checks payable to the Water Environment Research Foundation.



Water Environment Research Foundation
635 Slaters Lane, Suite G-110 ■ Alexandria, VA 22314-1177
Phone: 571-384-2100 ■ Fax: 703-299-0742 ■ Email: werf@werf.org
www.werf.org
WERF Stock No. DEC1R06c

Co-published by

IWA Publishing
Alliance House, 12 Caxton Street
London SW1H 0QS
United Kingdom
Phone: +44 (0)20 7654 5500
Fax: +44 (0)20 7654 5555
Email: publications@iwap.co.uk
Web: www.iwapublishing.co
IWAP ISBN: 978-1-84339-536-2/1-84339-536-3



Nov 2010